Fall 1-31-2000

Experiment, thermodynamic properties and modeling on combustion of methyl tert-butyl ether : isobutane and isobutene and thermodynamic properties of chloro alkanes and alkenes

Chiung-Ju Chen
New Jersey Institute of Technology

Recommended Citation

Chen, Chiung-Ju, "Experiment, thermodynamic properties and modeling on combustion of methyl tert-butyl ether : isobutane and isobutene and thermodynamic properties of chloro alkanes and alkenes" (2000). *Dissertations*. 425.
https://digitalcommons.njit.edu/dissertations/425

ABSTRACT

EXPERIMENT, THERMODYNAMIC PROPERTIES AND MODELING ON COMBUSTION OF METHYL *TERT*-BUTYL ETHER:
ISOBUTANE AND ISOBUTENE
AND
THERMODYNAMIC PROPERTIES OF CHLORO ALKANES AND ALKENES

by
Chiung-Ju Chen

The reaction systems: methyl *tert*-butyl ether (MTBE) unimolecular decomposition, MTBE radicals + O_2, *tert*-butyl radical + O_2, isobutene + HOO· (HO_2), isobutene + OH, isobutene-OH adducts + O_2, and allylic isobutenyl radical + O_2, are important systems in the understanding the oxidation chemistry of MTBE, tertiary butyl radical ($C_3C\cdot$), and isobutene, are analyzed. Thermochemical parameters are determined by *ab initio* - Mφller-Plesset (MP2(full)/6-31g(d)), complete basis set model chemistry (CBS-4 and CBS-q with MP2(full)/6-31g(d) and B3LYP/6-31g(d) optimized geometries), density functional (B3LYP/6-31g(d)), semi-empirical MOPAC (PM3) molecular orbital calculations, and by group additivity estimation. Thermochemical kinetic parameters are developed for each elementary reaction path in these complex systems; and a chemical activation kinetic analysis using quantum Rice-Ramsperger-Kassel (QRRK) theory for rate constant function of energy (*k(E)*) and master equation analysis for falloff is used to calculate rate constants as function of pressure and temperature.

Rate constants for HO_2 radical addition to carbon-carbon double bond calculated at CBS-q//MP2(full)/6-31G(d) and CBS-q//B3LYP/6-31G(d) levels of theory show similar trends to experimental data: HO_2 radical addition to tertiary carbon-carbon double bond (HO_2

addition at CD/C2 carbon atom of isobutene) has a lower activation energy than addition to secondary carbon-carbon double bond (CD/C/H), which is lower than addition to primary carbon-carbon bond (CD/H2). The E_a for addition to primary carbon-carbon double bonds of ethylene, propene and isobutene also show a decreasing trend.

The oxidation and pyrolysis of methyl *tert*-butyl ether in argon diluent has been studied in a flow reactor over the temperature range 873 to 973 K at atmospheric pressure with residence times between 0.5 - 2 sec. Three mixture compositions of MTBE and oxygen are studied in this MTBE oxidation as well as pyrolysis. Isobutene and methanol are observed as major products from both oxidation and pyrolysis of MTBE experiments.

A detailed kinetic model is developed for the pyrolysis and oxidation of MTBE. The mechanism includes oxidation and thermal decomposition of MTBE with major products and important intermediate. The computer code CHEMKINII is used for numerical integration.

Thermodynamic properties for representative multi-chloro alkanes and alkenes determined using the modified group additivity scheme are compared with literature data and show good agreement. The use of limited number of interaction groups provides improved accuracy in calculation of thermodynamic properties for multi-chloro alkanes and alkenes when chlorines are on adjacent carbon atoms. Three multi-chloro Benson-type groups plus five interaction groups for chloroalkanes; and two groups plus five interaction groups for chloroalkenes are developed.

EXPERIMENT, THERMODYNAMIC PROPERTIES AND MODELING ON COMBUSTION OF METHYL *TERT*-BUTYL ETHER: ISOBUTANE AND ISOBUTENE AND THERMODYNAMIC PROPERTIES OF CHLORO ALKANES AND ALKENES

by
Chiung-Ju Chen

A Dissertation
Submitted to the Faculty of
New Jersey Institute of Technology
in Partial Fulfillment of the Requirement for the Degree of
Doctor of Philosophy

Department of Chemical Engineering,
Chemistry and Environmental Science

January 2000

APPROVAL PAGE

EXPERIMENT, THERMODYNAMIC PROPERTIES AND MODELING ON COMBUSTION OF METHYL *TERT*-BUTYL ETHER: ISOBUTANE AND ISOBUTENE AND THERMODYNAMIC PROPERTIES OF CHLORO ALKANES AND ALKENES

Chiung-Ju Chen

Dr. Joseph W. Bozzelli, Dissertation Adviser — Date
Distinguished Professor of Chemistry, NJIT

Dr. Richard B. Trattner, Committee Member — Date
Professor of Environmental Science, NJIT

Dr. Lev N. Krasnoperov, Committee Member — Date
Professor of Chemistry, NJIT

Dr. James M. Grow, Committee Member — Date
Professor of Chemistry, NJIT

Dr. Jeffrey M. Grenda, Committee Member — Date
Exxon Research and Engineering Company

Dr. John Farrel, Committee Member — Date
Exxon Research and Engineering Company

BIOGRAPHYCAL SKETCH

Author: Chiung-Ju Chen

Degree: Doctor of Philosophy

Date: January 2000

Undergraduate and Graduate Education:

- Doctor of Philosophy in Environmental Science,
  New Jersey Institute of Technology, Newark, NJ, 2000

- Master of Environmental Science,
  New Jersey Institute of Technology, Newark, NJ, 1995

- Bachelor of Environmental Science,
  Tunghai University, Taiwan, 1991

Major: Environmental Science

Publications:

Chiung-Ju Chen; David K. Wong; Joseph W. Bozzelli,
"Standard Chemical Thermodynamic Properties of Multichloro Alkanes and Alkenes: A Modified Group Additivity Scheme,"
J. Phys. Chem. 1998, 102, 4551-4558.

Chiung-Ju Chen; Joseph W. Bozzelli,
"Analysis of Tertiary Butyl Radical + O_2, Isobutene +HO_2, Isobutene + OH and Isobutene-OH adducts + O_2: A Detailed Tertiary Butyl Oxidation Mechanism,"
J. Phys. Chem. 1999, 103, 9731 –9769.

Chiung-Ju Chen; Joseph W. Bozzelli,
"Kinetic Analysis for HO_2 Addition to Ethylene, Propene and Isobutene and Thermochemical Parameters for the Alkyl Hydroperoxides and Hydroperoxy Alkyl,"
Submitted to J. Phys. Chem. A 1999.

Chiung-Ju Chen; Joseph W. Bozzelli,
"Thermochemical Kinetic Analysis on the Reactions of Allylic Isobutenyl Radical with O_2: An Elementary Reaction Mechanism for Isobutene Oxidation,"
Submitted to J. Am. Chem. Soc. 1999.

Presentations:

Chiung-Ju Chen; Joseph W. Bozzelli,
"Reaction Pathways and Kinetic Analysis on Methyl *tert*-Butyl Ether Pyrolysis and Oxidation Reactions,"
Chemical and Physical Processes in Combustion, Proceedings of Eastern Section Combustion Institute Fall Technical Meeting, 2, pp. 37-40, North Carolina State University, Raleigh, NC, October 10-13, 1999.

Chiung-Ju Chen; Joseph W. Bozzelli,
"Kinetic and Thermodynamic Properties for HO_2 Addition to Ethylene, Propene and Isobutene Carbon-Carbon Double Bonds,"
First Joint Meeting of the U.S. Sections of the Combustion Institute: Western States, Central States, Eastern States, 36, pp. 144-147, The George Washington University Washington DC March 14-17, 1999.

Chiung-Ju Chen; Joseph W. Bozzelli,
"Thermochemical Kinetics Analysis on the Reaction of Allylic Isobutenyl Radical with O_2: An Elementary Reaction Mechanism for Isobutene Oxidation,"
Combustion, Proceedings of Eastern Section Combustion Institute Fall Technical ,118, pp. 519-522, Hilton Head Island, South Carolina, December 9-11, 1996.

Chiung-Ju Chen; Joseph W. Bozzelli,
"Thermochemical Kinetics Analysis on the Reaction of Tertiary Butyl Radical with O_2 and an Elementary Reaction Mechanism for Tertiary Butyl Oxidation Below 1200 K,"
Chemical and Physical Processes in Combustion, Proceedings of Eastern Section, Combustion Institute Fall Technical Meeting, 84, pp. 381-384, Worcester Polytechnic Institute, Worcester, MA, October 16-18, 1995.

Chiung-Ju Chen; Joseph W. Bozzelli,
"Thermodynamic Pathways and Kinetics Analysis on Methyl *tert*-Butyl Ether Oxidation,"
First Joint Meeting of the U.S. Sections of the Combustion Institute: Western States, Central States, Eastern States, The George Washington University Washington DC, March 14-17, 1999. Poster.

Chiung-Ju Chen; Joseph W. Bozzelli,
"Rate Constants for HO_2 Addition to Primary, Secondary, and Tertiary Carbon Double Bond: Ethylene, Propene and Isobutene Base on ab initio Calculation,"
27th Symposium (International) on Combustion, The Combustion Institute, University of Colorado at Boulder August 2-7, 1998. Poster.

To my beloved family

ACKNOWLEDGEMENT

I wish to express my appreciation to Professor Joseph W. Bozzelli, my adviser, not only for his professional advice but also his encouragement, patience, and kindness. I am deeply indebted to him for the opportunities that he made available to me.

I would also like to thank to my dissertation committee members, Dr. Richard B. Trattner, Dr. Lev N. Krasnoperov, Dr. James M. Grow, Dr. Sanjay V Malhotra, Dr. Jeffrey Grenda and Dr. John Farrel for their helpful corrections and productive comments.

It is my pleasure to thank Dr. Tsan H. Lay, who shared his knowledge with me. In addition, I would like to thank my coworkers at NJIT, Samuel Chern, Chad Sheng, Byung Ik Park, Li Zhu, Hongyan, Sun, Dawoon Jung, and Jongwoo Lee, for having dealt with me as a colleague, which has made my time at NJIT much more enjoyable and productive.

For love and inspiration I shall be eternally grateful to my parents. Without their constant support and encouragement, I truly believe all of this would not have been possible.

TABLE OF CONTENTS

TABLE OF CONTENTS
(Continued)

TABLE OF CONTENTS
(Continued)

TABLE OF CONTENTS
(Continued)

TABLE OF CONTENTS
(Continued)

TABLE OF CONTENTS
(Continued)

TABLE OF CONTENTS
(Continued)

Chapter **Page**

LIST OF TABLES

LIST OF TABLES

LIST OF TABLES
(Continued)

LIST OF TABLES
(Continued)

LIST OF TABLES
(Continued)

LIST OF TABLES
(Continued)

LIST OF TABLES
(Continued)

LIST OF FIGURES

Figure **Page**

LIST OF FIGURES
(Continued)

LIST OF FIGURES
(Continued)

LIST OF FIGURES
(Continued)

LIST OF FIGURES
(Continued)

LIST OF FIGURES
(Continued)

CHAPTER 1

THERMOCHEMICAL KINETICS

1.1 Introduction

Detail reaction kinetic models using mechanisms, based upon fundamental thermodynamic and kinetic principles are presently used and being developed by researchers attempting to optimize or more fully understand a number of systems comprised of many complex chemical reactions. These include combustion, and flame inhibition, ignition, atmospheric smog formation and transport, stratospheric ozone depletion, municipal and hazardous wastes incineration, chemical vapor deposition, semiconductor etching, rocket propulsion and other related fields.

One important requirement for modeling and simulation of these systems is accurate thermodynamic property data for molecular, intermediate radical and transition states. This data allow determination of equilibrium, and reverse rate constants from forward rate constant and equilibrium constant. *Ab initio* and density functional calculations with a reasonable computational resource provide an opportunity to accurately estimate thermodynamic properties of reactants, intermediate radicals, and products, plus estimate properties for transition states which is impossible to obtain through observation (experiment).

1.2 Computational Chemistry

Ab initio molecular orbital theory is concerned with predicting the properties of atomic and molecular systems. It is based upon the fundamental laws of quantum mechanics and uses a variety of mathematical transformation and approximation techniques to solve the fundamental equations, i.e. Schrödinger equation.

$$H\Psi = E\Psi$$

Here H is the *Hamiltonian*, a differential operator representing the total energy. E is the numerical value of the energy of the state, Ψ is the *wavefunction*.

Model chemistry is characterized by the combination of theoretical procedure and basis set. A basis set is a mathematical representation of the molecular orbitals within a molecule. The basis set can be interpreted as restricting each electron to a particular region of space. Large basis sets impose fewer constraints on electrons to a particular accurately approximate exact molecular orbital. They require correspondingly more computational resources. Standard basis sets for electronic structure calculation use linear combinations of gaussian functions to form the orbitals. Basis sets assign a group of basis functions to each atom within a molecule to approximate it orbitals. These basis functions themselves are composed of a linear combination of gaussian functions; such basis functions are refereed to as contracted functions, and the component gaussian functions are referred to as primitives. A basis function consisting of a single gaussian function is termed uncontracted. Digression on nomenclature of basis set 6-31G is:

6 primitive gaussian in the core function

1function in the valence region (one consisting of 3 primitive gaussians, one consisting of 1 primitive gaussian)

6-31+g(d) indicates it is the 6-31G basis set with d function added to heavy atoms. 6-311+g(3df,2p) is 3 d functions and 1 f function on heavy atoms (plus diffuse functions), and 2 p functions added on the hydrogen atoms.

Hartree-Fock calculation does not include a full treatment of the effects of electron correction: the energy contributions arising from electrons interacting with one another. A variety of theoretical methods, such as Møller-Plesset perturbation (MP2), have been developed which include some effects of electron correction. Traditionally, such methods are referred as post-SCF methods because they add correlation corrections to the basic Hartree-Fock model.

Recently, density functional (DFT) methods have been widely used. DFT methods compute electron correlation via general functional of the electron density. DFT functionals partition the electronic energy into several components which are computed separately: the kinetic energy, the electron-nuclear interaction, the coulomb repulsion, and an exchange-correlation term accounting for the remainder of the electron-electron interaction (which is itself divided into separate exchange and correlation components in most actual DFT functions). A variety of functionals have been defined, generally distinguished by the way that they treat exchange and correlation components:

> Local exchange and correlation functions involve only the values of the electron spin densities.
>
> Gradient-corrected functionals involve both the values of electron spin density and their gradients.

A popular gradient-corrected exchange functional is one proposed by Becke[1]; a widely used gradient-corrected correlation functional is the LYP functional of Lee, Yang and

Parr. The combination of the two forms the B-LYP method. B3LYP is Becke-style3-parameter density functional theory (using the Lee-Yang-Parr correlation functional).

1.3 Kinetics

1.3.1 RRK Theory

Most modern theories of unimolecular reaction rates, including the Slater theory, the RRK (Rice and Ramsperger and Kassel) theory and the RRKM (Marcus Rice) theory, are based on the fundamental Lindemann mechanism involving collision energization of the reactant molecules, and more specifically on Hinshelwood's development of the original treatment.

The Slater theory[2] is a dynamical theory concerned with the detailed treatment of molecular vibrations and the behavior of particular molecular coordinates as a function of time. Reaction is postulated to occur in Slater theory when a chosen coordinate achieves a critical extension by the phase-coincidence of certain modes of vibration. The rate constant of energized molecule dissociation to product(s) (k_a) is related to a "specific dissociation probability" L; this is the frequency with which a chosen coordinate in the molecule reaches a critical value, and can be calculated for the case in which the vibrations of the molecule are assumed to be harmonic. The specific dissociation probability (L) is actually a function of the energies in the individual oscillators and not simply of the total energy E of the molecule.

In RRK theory the assumption is made that the rate of conversion of energized molecules into products is related to the chance that the critical energy E_0 is concentrated in one part of the molecule, e.g. in one oscillator (Kassel theory) or in one squared term

(Rice-Ramsperger theory). This probability is clearly a function of the total energy E of the energized molecule.

The Marcus Rice theory, is known as RRKM theory since its basic model is RRK model. The main developments are the calculation of the rate constant of energization by quantum-statistical mechanisms and the application of ideas related to the Absolute Rate Theory for the calculation of the rate of conversion of energized molecules into products.

1.3.1.1 Lindemann-Hinshelwood Mechanism for Unimolecular Reactions: The theory known as Lindemann theory, which forms the basis for all modern theories of unimolecular reactions, has been developed from ideas published almost simultaneously by Lindemann[3] and Christiansen[4]. The concept is that: (a) by collision, a certain fraction of the molecules become energized, i.e. gain energy in excess of a critical quantity E_0. The rate of the energization process depends upon the rate of bimolecular collision. (b) energized molecules are de-energized by collision, which is a reverse reaction. This de-energized rate is taken to be energy-independent and is equated with the collision number Z_2 by assuming that every collision of A^* leads to a de-energized start. (c) there is a time-lag between the energization and unimolecular dissociation or isomerization of the energized molecules. This unimolecular dissociation also occurs with a rate constant k_3 independent of the energy content of A^*. The whole idea can be expressed by the following equations.

$A + M \rightarrow A^* + M$ (k_1)

$A^* + M \rightarrow A + M$ (k_2)

$A^* \rightarrow B + C$ (k_3)

where M can represent a product molecule, an added "inert" gas molecule, or a second molecule of reactant. In the simple Lindemann theory k_1, along with k_2 and k_3 are taken to be energy-independent and is calculated from the simple collision theory equation.

By application of the steady-state hypothesis to the concentration of A^*, the unimolecular rate constant and high pressure limit and low pressure limit rate and rate constants are then given as following:

High pressure limit rate $v_\infty = (k_1k_3/k_2)[A] = k_\infty[A]$

Low pressure limit rate $v_0 = v_{bim} = k_1[A][M] = k_{bim}[A][M]$

Unimolecular rate constant $k_{uni} = (k_1k_3/k_2)/\ (1 + k_3\ /k_2[M]) = k_\infty\ /\ (1 + k_\infty\ /k_1p)$

Fall-off $k_{uni}/\ k_\infty = 1\ /\ (1 + k_\infty\ /k_1p)$

One can expect that the Lindemann theory predict a change in the order of the initial rate of a unimolecular reaction with respect to concentration at low pressure.

The k_1 in original Lindemann theory is taken from the collision theory expression ($k_1 = Z_1\exp(-E_0/kT)$ with $Z_1 = (\sigma_d^2N_A/R)(8\pi N_Ak/\mu)^{1/2}(1/T)^{1/2}$, where Z_1 will be in Torr^{-1}-s^{-1} (consistent with [M] in Torr and k_3 in s^{-1}) when σ_d = collision diameter in cm; μ = reduced molar mass in g-mol^{-1} = $(1/M_A + 1/M_B)^{-1}$; T = temperature in K; $N_A = 6.0225 \times 10^{23}$ mol^{-1}; $R = 6.2326 \times 10^4$ cm^3-Torr-K^{-1}-mol^{-1}; $k = 1.3805 \times 10^{-16}$ erg-K^{-1}.

Based on the Lindemann's suggestion that k_1 could be increased by assuming that the required energy (energize molecules) could be drawn in part from the internal degrees of freedom (mainly vibration) of the reactant molecule, Hinshelwood[5] increases k_1 by using a much higher chance of a molecule possessing total energy $\geq E_0$ in s classical degrees of freedom, $(E_0/kT)^{s-1}\exp(-E_0/kT)/(s-1)!$, than one, $\exp(-E_0/kT)$ Lindemann used.

So the $k_1 = [Z_1/(s-1)!](E_0/kT)^{s-1}\exp(-E_0/kT)$ with k_1 a function of energy and replace k_1 and A^* as $k_{1(E\rightarrow E+\delta E)}$ and $A^*_{(E\rightarrow E+\delta E)}$ in mechanism above.

1.3.1.2 RRK Theory of Unimolecular Reactions: In order to make accurate quantitative predictions of the fall-off behavior of a unimolecular reaction it is essential to take into account the energy dependence of the rate constant k_a (k_3) for the conversion of energized molecules into activated complexes and hence products. One of accepted theories is the RRK theory, a statistical theory used in this thesis because it is more computable and needed parameters are readily obtained.

The RRK theory was developed virtually simultaneously by Rice and Ramsperger[6] and Kassel[7-9] with very similar approachs. Both consider that for reaction to occur a critical energy E_0 must become concentrated in one part of the molecule. They used the basic Lindemann-Hinshelwood mechanism of collision energization and de-energization, but assume more realistically that the rate constant of conversion of an energized molecule to products is proportional to a specific probability, a finite statistical probability that E_0 is be found in the relevant part of the energized molecule which contains E greater than E_0 since E of the molecule under consideration is assumed to be rapidly redistributed around the molecule. Obviously this probability will increase with E and make k_a a function of its energy content.

The difference between these two models is twofold. Firstly, Rice and Ramsperger used classical statistical mechanics throughout, while Kassel used classical method but also developed a quantum treatment; the latter is very much more realistic and accurate. Secondly, different assumptions were made about the part of the molecule into which the critical energy E_0 has to be concentrated. The Kassel's model seems slightly more realistic by assuming the energy had to be concentrated into one oscillator. The quantum version of the Kassel theory serves as a theoretical basis for calculation performed in this thesis. The mechanism of RRK theory is written as:

$A + M \Leftrightarrow A^*_{(E \to E+\delta E)} + M \qquad \delta k_{1(E \to E+\delta E)}/k_2$

$A^*_{(E)} \to \text{Products} \qquad k_a(E)$

The quantum version of version of Kassel's theory is based on the calculation of the probability that a system of s quantum oscillators, while the classical version considered s classical oscillators, with total energy E should have energy ≥ E_0 in one chosen oscillator. It assume that there are s identical quantum oscillators, all having frequencies ν and hence energy $h\nu$, and so the critical energy E_0 is expressed as the critical number of quanta being $m = E_0/h\nu$, and the energy E of energized molecule is expressed as a total of n quanta with $n = E/h\nu$. The probability of that one oscillator contains at least m quanta, probability (energy ≥ m quanta in one chosen oscillator) is then equal to:

$$\text{Probability (energy} \geq \text{ m quanta in one chosen oscillator)} = \frac{n!(n-m+s-1)!}{(n-m)!(n+s-1)!}$$

Hence,

$$k_a(nh\upsilon) = A\frac{n!(n-m+s-1)!}{(n-m)!(n+s-1)!}$$

where A is proportion constant here and actually the same as the classical one.

Corresponding $k_1(E)$ of Hinshelwood expression is derived, refereed to energization into a specific quantum state rather than into an energy range E to E+δE, as

$$k_1(nh\upsilon) = k_2\alpha^{\nu}(1-\alpha)^{s-1}\frac{(n+s-1)!}{n!(s-1)!}$$

where $\alpha = \exp(-h\nu/kT)$.

1.3.1.3 Chemical Activation Reactions: Molecules undergo thermal unimolecular reactions as a result of energization by molecular collision. This molecular collision at a given temperature produces energized molecules with an equilibrium distribution of energy which enables the fraction of molecules energized into a particular energy range or quantum state. The energization methods other than by molecular collision, such as photoactivation and chemical activation, may produce a non- equilibrium situation in which molecules acquire energies far in excess of the average thermal energy. This amount of excess of energy contained in energized adduct makes chemical activation reactions much more important in a particular system, and a much different treatment for the rate of conversion decomposition of energized adduct to product (including back to reactant) which is very competing with the rate of its collision stabilization.

A example of chemically activated reaction system is *tert*-butyl radical ($C_3C\cdot$) + O_2 system. As is discussed in chapter 3, $C_3C\cdot$ radical reacts with O_2 to form a chemically activated, energized adduct [$C_3COO\cdot^*$], this process of forming adduct is much more efficient than that by thermal molecular collision, and adduct contains excess energy from the chemical reaction. The energized adduct [$C_3COO\cdot^*$] could go back to reactant $C_3C\cdot$ + O_2, or could directly go to products C_2CyCCO (y = cyclic) + OH via a intramolecular H shift. The QRRK calculation shows that the chemical activation process is more important than thermal dissociation process.

The basic idea of the treatment of a chemical activation system is that a vibration excited molecule A^* by an association of reactants can reform reactants with a rate constant $k'_a(E)$, form decomposition products with a rate constant $k_a(E)$ or be de-energized to stable molecules A.

On the strong collision assumption the first order rate constant for de-energization is equal to the collision frequency, $\omega = Zp$ where p is the total pressure and Z is collision number (see "1.3.1.1 Lindemann-Hinshelwood Mechanism for Unimolecular Reactions" on page 5).

Suppose that the fraction of molecules which are energized per unit time into the energy range between E and $E+\delta E$ is $f(E)\delta E$. To simplify, one can consider only one decomposition path (back to reactant can be considered as one of decomposition paths), then the fraction of A^* decomposing (say path D) compared with those stabilized (say path S) is $k_a(E)/[k_a(E)+\omega]$. The fraction of molecules in the energy range between E and $E+\delta E$ decomposing to products is therefore $\{k_a(E)/[k_a(E)+\omega]\}f(E)\delta E$, and the total number of molecules decomposing per unit time (D), at all energies above the critical energy E_0, is:

$$D = \int_{E_0}^{\infty} \frac{k_a(E)}{k_a(E) + \omega} f(E) dE$$

corresponding, the total rate of stabilization (S) is:

$$S = \int_{E_0}^{\infty} \frac{\omega}{k_a(E) + \omega} f(E) dE$$

Considering an average rate constant $<k_a>$ for all energies above E_0, there have:

$$\frac{<k_a>}{\omega} = \frac{D}{S} = \frac{\text{No. molecules decomposing per unit time}}{\text{No. of molecules being stabilized per unit time}}$$

So,

$$< \mathrm{k_a} >= \omega \frac{\int_{\mathrm{E_0}}^{\infty} \{\mathrm{k_a}(E) / [\mathrm{k_a}(E) + \omega]\} f(E) \mathrm{dE}}{\int_{\mathrm{E_0}}^{\infty} \{\omega / [\mathrm{k_a}(E) + \omega]\} f(E) \mathrm{dE}}$$

The $f(E)$ is the distribution function of energized molecules in the energy range between E and E+δE. In the thermal energization systems, this distribution function is simply the thermal quantum Boltzmann distribution $K(E)$ and the rate of energization into the energy range between E and E+δE is $K(E)\delta\mathrm{E} = \delta\mathrm{k}_1/\mathrm{k}_2$. For the chemically activated system described here, the distribution function can be derived by applying the principle of detailed balancing to the reverse process to reactants. Consider a situation in which the processes D and S can be ignored and equilibrium is established between A^* and reactants, then the fraction of molecules with energy between E and E+δE is Boltzmann distribution $K(E)\delta\mathrm{E}$, so the rate of dissociation to reactants is then $\mathrm{K'}_a(E)K(E)\delta\mathrm{E}$, and by the principle of detailed balancing this also gives the rate of combination of reactants to give A^* in this energy range. The total rate of energization to all levels above the minimum energy $\mathrm{E_{min}}$ (the minimum energy of A^*) is:

$$\text{Total rate of energization} = \int_{\mathrm{E_0}}^{\infty} \mathrm{k'_a}(E)\mathrm{K}(E)\mathrm{dE}$$

Therefore, the distribution function is given by:

$$f(E)\delta\mathrm{E} = \frac{\mathrm{k'_a}(E)\mathrm{K}(E)\delta\mathrm{E}}{\int_{\mathrm{E_0}}^{\infty} \mathrm{k'_a}(E)\mathrm{K}(E)\mathrm{dE}}$$

The $f(E)\delta\mathrm{E}$ can be incorporated into QRRK theory for $\mathrm{k_a}(E)$ and $\mathrm{k_1}(E)$ (see "1.3.1.2 RRK Theory of Unimolecular Reaction on page 7) serves as a basis for the calculations for chemical activation reaction systems.

1.3.2 QRRK Analysis for Unimolecular and Chemical Activation Reactions

QRRK analysis, as initially presented by Dean[10-12] combined with the modified strong collision approach of Gilbert et al[13-15], are used to compute rate constants for both chemical activation and unimolecular reactions, over a range of temperature and pressure. The computer program CHEMDIS, based on the QRRK theory outlined as above, and unimolecular dissociation and chemical activation formalism carries out all unimolecular and chemical activation reactions involved in this thesis. The input parameters for CHEMDIS are: (1) High pressure limit rate constants (Arrhenius A factor and activation energy E_a) for each reaction included for analysis; (2) A reduced set of three vibration frequencies and their associated degeneracy; (3) Lennard-Jones transport parameters, (s (Angstroms) and e/k (Kelvin)), and (4) molecular weight of well species. All these input parameters are readily available or straightforward to estimate.

1.3.2.1 Input Information Requirements for QRRK Calculation: Pre-exponential factors (A_∞s), are calculated using canonical TST[16] along with MP2, DFT or PM3-determined entropies of intermediates and TSs for the reactions where thermodynamic properties of TS are available. High-pressure limit pre-exponential factors for combination reactions are obtained from the literature and from trends in homologous series of reactions. Activation energies come from complete basis model calculations CBS-q plus evaluated endothermicity of reaction ΔU_{rxn}, from analysis of Evans Polanyi relationships for abstractions plus evaluation of ring strain energy, and from analogy to similar reactions with known energies. Thermodynamic properties are provided for each system.

Reduced sets of three vibration frequencies and their associated degeneracies are computed from fits to heat capacity data, as described by Ritter and Bozzelli et al.[17-18]. These have been shown by Ritter to accurately reproduce molecular heat capacities, Cp(T), and by Bozzelli et al.[18] to yield accurate ratios of density of states to partition coefficient, $\rho(E)/Q$.

Lennard-Jones parameters, sigma (Angstroms) and ε/k (Kelvins), are obtained from tabulations[19] and from a calculation method based on molar volumes and compressibility[20].

When necessary, estimation is done in a consistent and uniform manner via use of generic reaction rate constants with reference to literature, experiment or theoretical calculation in each case. The QRRK calculation input parameters and their references are listed in the table associated with the respective reaction system.

1.3.2.2 Recent Modifications to the Quantum RRK Calculation: (a) Use of a manifold of three frequencies plus incorporation of one external rotation for the density of states, $\rho(E)/Q$ and in calculation of $k(E)$. (b) The Leonard-Jones collision frequency Z_{LJ} is now calculated by $Z_{LJ} = Z\ \Omega\ (2,2)$ integral[19, 20] obtained from fit of Reid et al.[20].

The QRRK analysis for $k(E)$ with modified strong collision and a constant F_E for falloff has been used previously to analyze a variety of chemical activation reaction systems, Westmoreland et al.[21,22], Dean et al.[23], and Bozzelli et al.[24, 25] There are a number of recent publications by other researchers that utilize the QRRK formalism with a more exact calculation F_E in modified strong collision analysis[26-31] or utilize just a QRRK formalism.[32, 33] It is shown to yield reasonable results in these applications, and provides a framework by which the effects of both temperature and pressure can be estimated for complex chemical activation or unimolecular dissociation reaction systems.

CHAPTER 2

KINETIC AND THERMODYNAMIC ANALYSIS ON METHYL *TERT*-BUTYL ETHER DISSOCIATION AND OXIDATION

2.1 Introduction

Methyl *tert*-butyl ether (MTBE) has been widely used as an oxygenate and octane enhancer in gasoline, because of its high octane number and low exhaust emissions[34] (NOx, CO, particles etc.). Recently it has been discovered as a contaminant of surface water and groundwater due to its high solubility in water. Its release to the environmental has generated great public and governmental concern because of the toxicity of MTBE and its degradation products.

To understand the impact of MTBE in both atmospheric and combustion environments, it is of considerable importance to understand the reaction pathways and kinetic mechanism of MTBE oxidation under combustion conditions. The kinetics of unimolecular decomposition reaction of MTBE

$$(CH_3)_3COCH_3 \rightarrow (CH_3)_2C{=}CH_2 + CH_3OH \qquad (1)$$

has been studied by several research groups. Daly and Wentrup[35] determined a rate constant, k_1, of $10^{14.4}\exp(-30970/T)$ s^{-1} over the temperature range 706 to 768 K. Choo et al.[36] reported $k_1 = 10^{13.9}\exp(-29700/T)$ s^{-1} in a very low-pressure pyrolysis reactor at 890-1160K. Brocard and Baronnet[37, 38] obtained k_1 in a Pyrex reactor of $10^{14.0}\exp(-29960/T)$ s^{-1}.

The rate constants for the gas-phase reaction of MTBE with OH[39-41], Cl[42] and NO_3[43] and the mechanism of the subsequent breakdown of isobutene and methanol in an oxidizing atmosphere[44] have been studied. The oxidation of MTBE has been investigated by Brocard et al.[45] from 573 to 773 K. They show isobutene and methanol are the major products, formation of methanol is via reaction (1) and their mechanism also includes the isomerization and decomposition of the two radicals, $(CH_3)_3COC{\cdot}H_2$ ($C_3{\cdot}COC$) and $(CH_3)_2C{\cdot}H_2COCH_3$ ($C_3COC{\cdot}$) with estimated rate constants. However O_2 reactions with these radicals, which are very important in this temperature range, are omitted.

Dunphy et al.[34] studied the high temperature oxidation of MTBE in reflected shock waves over the temperature range 1040 to 1850 K and with pressure of 3.5 bar in argon diluent. Norton et al.[46] have reported some preliminary observations on the high-temperature oxidation of MTBE in a flow-reactor. They note that isobutene is the major intermediate product. The concentration of isobutene is roughly equal to concentration of methanol at near-stoichiometric condition at1025 and 1110 K.

Although several experimental studies on the overall reaction have been reported for MTBE oxidation[34-46], analysis on the thermodynamic and kinetic reaction pathways has not been evaluated and is not well understood. *Ab initio* and density functional calculations with a reasonable computational resource provide an opportunity to accurately estimate thermodynamic properties of reactants, intermediate radicals, and products, plus estimate properties for transition states. One advantage of computational chemistry is that it provides thermodynamic data on some species which experiment can not easily produce (i.e. complex radical species and transition states).

In this chapter, thermodynamic properties ($\Delta H_f^\circ{}_{298}$, $S^\circ{}_{298}$, and Cp(T) $300 \leq T/K \leq 1500K$) of reactants, intermediate radicals, transition states, and final products are estimated using calculations at B3LYP/6-31g(d), B3LYP/6-311+g(3df,2p)

//B3LYP/6-31g(d) and CBS-q// B3LYP/6-31g(d) levels of theory. CBS-q calculations are chosen because Jungkamp et al.[47, 48], Petersson et al.[49] and our group[50] have shown that they result in reasonable accurate thermodynamic enthalpy data for these oxygenated molecular systems. Density function B3LYP is chosen to provide accurate geometries.

Reaction path analysis, reaction barrier, pre-exponential factor, and thermochemical properties of each elementary reaction step are evaluated for reactions of MTBE unimolecular decomposition and two radicals ($C_3{\cdot}COC$, $C_3COC{\cdot}$) plus O_2 reaction systems. Chemical activation kinetic analysis is performed using quantum Rice-Ramsperger-Kassel (QRRK) theory for k(E) and modified strong collision analysis for fall-off.

2.2 Method

2.2.1 Enthalpies of Formation ($\Delta H_f{}^\circ{}_{298}$)

Enthalpies of formation ($\Delta H_f{}^\circ{}_{298}$) for reactants, intermediate radicals, transition states and products are calculated using group balance isodesmic reactions and three levels of calculations: B3LYP/6-31g(d), B3LYP/6-311+g(3df,2p)//B3LYP/6-31g(d) and CBS-q//B3LYP/6-31g(d). The initial geometry of each compound or transition states is pre-optimized using UHF/PM3 in MOPAC[51] program, followed by optimization and vibrational frequency calculation at B3LYP/6-31G(d) level of theory using GAUSSIAN 94 programs[52]. The TS geometries are identified by the existence of only one imaginary frequency in the normal mode coordinate analysis, evaluation of the TS geometry, and TST reaction coordinate vibration information. Zero-point vibrational energies (ZPVE), vibrational frequencies and thermal contributions to enthalpy from harmonic frequencies are scaled with factors as recommended by Scott et al[53]. Single point energy calculations are carried out at the B3LYP/6-311+g(3df,2p)//B3LYP/6-31g(d). The CBS-q//B3LYP/6-31g(d) calculation modified from complete basis set (CBS-q) method of Petersson and coworkers[54-56] are used in determining enthalpies. Total energies, zero-point vibrational energies and thermal contributions to enthalpy calculated by B3LYP/6-31g(d), B3LYP/6-311+g(3df,2p)//B3LYP/6-31g(d) and CBS-q//B3LYP/6-31g(d) levels are listed in Table 1A.1. Total energies (at 298K) differences between TS and reactants, intermediates, and products determined at different theory levels are listed in Table 1A.2.

Nine group balance isodesmic reactions (IR1-IR9) are used to calculate enthalpies of these stable molecules C_3COC, $C_2C(CQ)OC$, C_2CCQ, C*C(C)CQ, C*(C)COC, C_3COCQ, and HOCOOH. (Q represents OOH group; Y represents cyclic group)

For C_3COC

$C_3COC + COH \rightarrow C_3COH + COC$ (IR1)

For $C_2C(CQ)OC$

$C_2C(CQ)OC + CC \rightarrow C_3COC + CCOOH$ (IR2)

For $C(OH)_2$

$COCOC + 2\ COH \rightarrow C(OH)_2 + 2\ COC$ (IR3)

For C_3COCQ

$C_3COCQ + CCOH + COH \rightarrow C_2C(CQ)OC + C(OH)_2 + CC$ (IR4)

For C_2CCQ

$C_2CCQ + COH \rightarrow C_2CCOH + COC$ (IR5)

For C*C(C)CQ

$C{*}C(C)CQ + C{*}CC + COH \rightarrow C_2C{*}C + C{*}CCOH + COOH$ (IR6)

For C*C(C)OC

C*C(C)OC + C=COH + CCOH → C=C(C)OH + C=COCC+COH (IR7)

For $C_2CYCCOCO$

$C_2CYCCOCO$ + COH → CYCCOCO + C_3COH (IR8)

For HOCOOH

HOCOOH + CC → CCOH + COOH (IR9)

Enthalpies of formation of the radicals: $C_3{\cdot}COC$, $C_3COC{\cdot}$, $C_2C(CQ{\cdot})OC$, $C_2C(CQ)OC{\cdot}$, $C_2{\cdot}C(CQ)OC$,$C_2C{\cdot}CQ$, $C_3COCQ{\cdot}$, $C_3{\cdot}COCQ$, and ·OCOOH are calculated from the following isodesmic reactions and bond enthalpies of DH°_{298} (CH_3CH_2-H) (101.1 kcal/mole), DH°_{298} (CH_3OCH_2-H) (96.69 kcal/mole), and DH°_{298} (CH_3OO-H) (86.3 kcal/mole).

For $C_3{\cdot}COC$

C_3COC + CC· → $C_3{\cdot}COC$ + CC (IR10)

For $C_3COC{\cdot}$

C_3COC + COC· → $C_3COC{\cdot}$ + COC (IR11)

For $C_2C(CQ{\cdot})OC$

$C_2C(CQ)OC$ + COO· → $C_2C(CQ{\cdot})OC$ + COOH (IR12)

For $C_2C(CQ)OC{\cdot}$

$C_2C(CQ)OC$ + COC· → $C_2C(CQ)OC{\cdot}$ + COC (IR13)

For $C_2{\cdot}C(CQ)OC$

$C_2C(CQ)OC$ + CC· → $C_2{\cdot}C(CQ)OC$ + CC (IR14)

For $C_2C{\cdot}CQ$

$C_2CCQ + CC{\cdot} \rightarrow C_2C{\cdot}CQ + CC$ (IR15)

For $C_3COCQ{\cdot}$

$C_3COCQ + COO{\cdot} \rightarrow C_3COCQ{\cdot} + COOH$ (IR16)

For $C_3{\cdot}COCQ$

$C_3COCQ + CC{\cdot} \rightarrow C_3{\cdot}COCQ + CC$ (IR17)

For ·OCOOH

$COCOOH + CO{\cdot} \rightarrow {\cdot}OCOOH + COH$ (IR18)

Group balance isodesmic reaction enthalpies (IR1-IR18) are calculated at CBS-q// B3LYP/6-31g(d), B3LYP/6-311+g(3df,2p)//B3LYP/6-31g(d), and B3LYP/6-31g(d) levels and listed in Table 1A.3. Enthalpies of formation of TSs are estimated from average value of $\Delta H_{298,\mathrm{reactants}}$ plus the reaction enthalpy ($\Delta H^{\neq}_{\mathrm{TS1\ -\ reactants}}$) and $\Delta H_{298,\mathrm{products}}$ plus reaction enthalpy ($\Delta H^{\neq}_{\mathrm{TS\ -\ products}}$) at B3LYP/6-31g(d), B3LYP/6-311+g(3df,2p)//B3LYP/6-31g(d) and CBS-q//B3LYP/6-31g(d) levels.

2.2.2 Entropy (S°_{298}) and Heat Capacity (Cp(300) to Cp(1500))

Contributions of translation, rotation, and vibration to entropies and heat capacities are calculated from scaled vibrational frequencies and moments of inertia of the optimized structures. The method of Pitzer and Gwinn[57] is used to calculate hindered internal rotational contribution to S and Cp(T). The number of optical isomers and spin degeneracy of unpaired electrons is also incorporated. Thermodynamic parameters - $\Delta H_f{}^\circ{}_{298}$, $S^\circ{}_{298}$, and Cp(300) to Cp(1500) for reactants, intermediates, and products are listed in Table 1A.4.

2.2.3 High-Pressure Limit A Factors (A_∞) and Rate Constants (k_∞) Determination

For the reactions where thermodynamic properties of TS are calculated by *ab initio* and density functional, k_∞s are fit by three parameters A_∞, n, and E_a over temperature range from 298 to 2000K:

$$k_\infty = A_\infty(T)^n \exp(-E_a/RT)$$

Entropy differences between reactant and TS are used to determine the Arrhenius pre-exponential factor, A, via conventional transition state theory (TST)[16]:

$$A = (k_bT/h_p)\exp(\Delta S^{\neq}/R) \text{ for unimolecular reaction}$$

$$A = (ek_bT/h_p)\exp(\Delta S^{\neq}/R) \text{ for bimolecular reactions}$$

Where h_p is Plank's constant, k_b is the Boltzmann constant.

Activation energy is determined as the difference in internal energy between reactant and TS.

2.2.4 Kinetics Analysis

Multi-frequency Quantum Rice-Rampsperger-Kassel (QRRK) analysis with modified strong collision analysis for fall-off calculation is used to estimate rate constants to products and stabilized adducts as a function of temperature and pressure. The QRRK code incorporates a temperature and pressure dependence output formalism for the rate constants, in form of an N x M (9 x 5) chebyshev polynomial expression. Those calculations utilize the potential energy surface and thermodynamic properties are determined in this study.

2.3 Results and Discussion

2.3.1 Unimolecular Dissociation of MTBE

The unimolecular decomposition reactions of MTBE include six product channels: these are the dissociation reaction in MTBE and are important reactions in initiation of MTBE oxidation at high temperature. The potential energy level diagram for these six reaction paths is shown in Figure 1B.1. The most important reaction channel proceeds through a four-center transition state (TSMTBE) to form isobutene and methanol products. Frequencies and moments of inertia for this transition state calculated from B3LYP/6-31g(d) are listed in Table 1A.5.

The TSMTBE structure represents a four-center transition state and is shown in Figure 1B.2. One of three methyl groups on the tetra carbon of MTBE (C_3COC) undergoes lose of one H attached on it. The leaving H on methyl group attacks the ether (oxygen), breaking the C---H bond and forming a H---O bond. The oxygen is also leaving the tetra carbon. The tetra carbon forms a π bond, C---C double bond, with carbon that loses the H atom.

In this four member transition ring (tC)==pC---H---O (tC means tetra C, pC means primary C), the bond length of forming carbon double bond is 1.422 Å. This bond length is longer than carbon double bond length, 1.334 Å, in isobutene, and shorter than single carbon bond, 1.538 Å, in MTBE. The bond length of forming O-H bond is 1.337Å; that is longer than O-H bond in methanol (0.949Å). The breaking C-O bond is 2.106Å, which is much longer than C-O bond, 1.442 Å, in MTBE. The breaking C---H bond length in the four member transition ring is 1.322Å which is longer than C-H bond in MTBE (1.09Å). The bond lengths in four member transition ring shows a loose transition structure which gives a relative high A factor (of 7.43 x 10^{13} at 800 K) for this reaction. All bonds other than ones involved in the reaction transition ring are only slightly different (<0.04 Å) between TS and MTBE.

Other reaction paths of MTBE dissociation have higher barriers then this molecular elimination to isobutene and methanol. Those reaction paths form intermediate radicals: $C_3COC.$, $C_3.COC$, $C_2C.OC$, $C_3CO.$, which can undergo further dissociation to stable molecular $C_2C=C$, $C_2C=O$, $CC=C$, CH_2O; to radicals $C_3C.$, CH_3, CH_3O, and other species.

Arrhenius pre-exponential factor, A_∞, is calculated via canonical TST. The high-pressure limit rate constants, fit by a three parameter (A, n, Ea) modified Arrhenius Equation over temperature range 300K to 2000K, are $2.15x10^{13}T^{0.19}exp(-61620\ cal\ /RT)$ ($cm^3\ mole^{-1}\ s^{-1}$) based on CBS-q//B3LYP/6-31g(d) calculation. Comparison of our calculated rate constant with experimental values for reaction (1), $C_3COC \rightarrow C_2C=C + CH_3OH$, is shown in Figure 1B.3. The symbols are from experimental data, Solid line is from QRRK calculation which based on CBS-q//B3LYP/6-31g(d) level. The results show good agreement between calculation with experimental data. Input parameters and references to specific high-pressure rate constants for the reaction of unimolecular dissociation of MTBE are listed in Table 1A.6. Parameters in Table 1A.6 are referenced to the ground (stabilized) level of the complex, as this is the formalism used in QRRK theory.

Figure 1B.4a and 1B.4b illustrate the predicted effect of temperature and pressure on MTBE decomposition reactions. Unimolecular elimination to isobutene and methanol channel has A of 7.42 x 10^{13} s^{-1} at 800 K, which is lower than other dissociation channels, but also has lower barrier by at least 20 kcal/mole then other channels. At high pressure (above 10 atm) and high temperature (above 1300 K) the $C_3CO. + CH_3$ channel competes with molecular elimination.

2.3.2 Unimolecular Dissociation of $C_3{\cdot}COC$ Radical

The $C_3{\cdot}COC$ radical is formed by abstraction H atom from one of three methyl groups attached to the tetra carbon of MTBE. Bond energy of $DH°_{298}(CH_3OC(CH_3)_2(CH_2)$-H)(103.26 kcal/mole) is determined to be 101.1 – (-2.16) = 103.29 kcal/mole, using $DH°_{298}(C_2H_3$-H) = 101.1 kcal/mole and the calculated reaction enthalpy ΔH_{rxn} = -2.16 kcal/mole at CBS-q//B3LYP/6-31g(d) levels for the isodesmic reaction (IR10).

The $C_3{\cdot}COC$ radical can undergo β-scission reaction, breaking a C-O bond and forming C=C double bond, to form isobutene (C_2C=C) and CH_3O radical. It can also undergo β-scission to form methyl isopropenyl ether (C=C(C)OC) and CH3 radical by breaking C-C bond. The reaction barrier for breaking C-O bond channel is ca. 12 kcal/mole lower than breaking C-C bond channel based on CBS-q//B3LYP/6-31g(d) calculation.

The high pressure limit rate constants, fit by a three parameters (A, n, Ea) modified Arrhenius Equation over a temperature range of 300K to 2000K, are $6.33 \times 10^{12}T^{0.02}\exp(-18290 \text{ cal }/RT)$ (cm^3 $mole^{-1}$ s^{-1}) and $1.90 \times 10^{12}T^{0.30}\exp(-30310 \text{ cal }/RT)$ (cm^3 $mole^{-1}$ s^{-1}) at CBS-q//B3LYP/6-31g(d) for $C_3{\cdot}COC \rightarrow (TS9) \rightarrow C_2C{=}C + CH_3O$ and $C_3{\cdot}COC \rightarrow (TS13) \rightarrow C{=}C(C)OC + CH_3$, respectively.

2.3.3 Unimolecular Dissociation of $C_3COC\cdot$ Radical

The $C_3COC\cdot$ radical is formed through abstraction of H atom from methyl group which attached to the on ether side of MTBE by a reactive radical, such as OH, HO_2, H, CH_3 etc. The bond energy, $DH°_{298}((CH_3)_3OCH_2\text{-}H)$(95.53 kcal/mole), is determined to be 101.1 – (-1.16) = 95.53 kcal/mole, using $DH°_{298}(H_3COCH_2\text{-}H)$ = 96.69 kcal/mole and the calculated reaction enthalpy ΔH_{rxn} = -1.16 kcal/mole at CBS-q//B3LYP/6-31g(d) levels for the isodesmic reaction (IR11). This bond energy is ca. 8 cal/mole lower than C-H bond of methyl group on tetra carbon of MTBE based on CBS-q//B3LYP/6-31g(d) calculation.

The $C_3COC\cdot$ radical can undergo β-scission to form *tert*-butyl radical and CH_2O. We find a barrier of 17.44 kcal/mole for forward reaction of $C_3COC\cdot \rightarrow C_3C\cdot + CH_2O$ based on CBS-q//B3LYP/6-31g(d) calculation ($\Delta H_{rxn,\,298}$ = 16.52 kcal/mole). The high-pressure limit rate constants are $1.68 \times 10^{12}T^{0.36}\exp(-18190\ \text{cal}/RT)$ ($cm^3\ mole^{-1}\ s^{-1}$) and $0.73\ T^{3.45}\exp(-6650\ \text{cal}/RT)$ ($cm^3\ mole^{-1}\ s^{-1}$) at CBS-q//B3LYP/6-31g(d) for forward and reverse reaction of $C_3COC\cdot \rightarrow (TS10) \rightarrow C_3C\cdot + CH_2O$, respectively.

2.3.4 $C_3\cdot COC + O_2$

The $C_3\cdot COC$ radicals once formed can undergo β-scission or react with molecular oxygen, which is abundant under atmosphere and troposphere conditions, to form the energized adducts $C_2C(COO\cdot)OC$ *. The potential energy level diagram for reaction paths $C_3\cdot COC$ unimolecular decomposition and addition with O_2 reactions is shown in Figure 1B.5. The reaction channels of $C_2C(COO\cdot)OC$* include dissociation back to reactants, stabilization to $C_2C(COO\cdot)OC$, and isomerization (H-shift) via seven-member ring transition state (TS1) to $C_2C(CQ)OC\cdot$ (Q=OOH) or via six-member ring transition (TS2) to $C_2\cdot C(CQ)OC$. The $C_2C(CQ)OC\cdot$* isomer can: undergo β-scission (via TS3) to $C_2C\cdot CQ$ radical + CH_2O, be stabilized to $C_2C(CQ)OC\cdot$ and isomerize back to $C_2C(COO\cdot)OC$ *. The $C_2\cdot C(CQ)OC$* isomer can: be stabilized to $C_2\cdot C(CQ)OC\cdot$or isomerize back to $C_2C(COO\cdot)OC$ *, and undergo β-scission via TS4 and TS5 to C*C(C)CQ + CH_3O radical and C=C(C)OC + C·H2OOH radical, respectively. Reaction of $C_2C(COO\cdot)OC$ * adduct to $C_2C(CO\cdot)OC$ + O is included for completeness, but it is only important at higher temperature (above 1500K). Input parameters and references to specific high-pressure rate constants for the reaction of $C_3\cdot COC$ and $C_3\cdot COC + O_2$ are listed in Table 1A.7.

An overall analysis of $C_3\cdot COC + O_2$ reaction system indicates: the initial reaction of $C_3\cdot COC + O_2 \rightarrow C_2C(COO\cdot)OC$ (stabilized adduct) has $\Delta H_{rxn,800K}$ = -38.0 kcal/mole and $\Delta U_{rxn,800K}$ = -36.41 kcal/mole with a reasonable high A factor for reverse reaction of 1.57×10^{15} s^{-1}, i.e. a moderately high A ; thus a loose transition state. The H-shift isomerization via seven-member ring TS1 has an E_a of 15.95 kcal/mole; which is lower than the E_a via six-member ring TS2 and lower than reverse reaction to $C_3\cdot COC + O_2$ from the stabilized adduct. The seven-member ring H-shift has a slightly lower A factor 2.26×10^9 s^{-1} at 800 K than six-member ring H-shift. Both H-shift isomerization TS's have barriers lower than dissociation to $C_3\cdot COC + O_2$; but also have lower A factors, i.e. they are tight TS's. The isomer from H-Shift via seven-member ring TST is $C_2C(CQ)OC\cdot$; its decomposition to $C_2C\cdot CQ$ radical + CH_2O (via TS3) has an A of 2.30×10^{13} s^{-1} at 800K, which is higher than reverse isomerization, 1.94×10^8 s^{-1}, but also has a higher barrier, 18.15 kcal/mole, than reverse isomerization (4.32 kcal/mole). Energy of

TS3 is lower than reactants (C_3·COC + O_2) 8 kcal/mole. The C_2C·CQ radical is discussed in the isobutene + HO_2 reaction system in chapter 3.

Reverse isomerization of C_2·C(CQ)OC radical has A of 3.61 x 10^{10} s^{-1}, which is lower than elimination to C=C(C)OC + C·H_2OOH (via TS4) 3.94 x 10^{12} s^{-1} and elimination to C=C(C)CQ + CH_3O (viaTS5) 8.43 x 10^{12} s^{-1}. Dissociation of C_2·C(CQ)OC to C=C(C)OC + C·H_2OOH has only a slightly higher E_a 2.29 kcal/mole than elimination to C=C(C)OC + C·H_2OOH, but much higher than reverse isomerization by 17.03 kcal/mole.

Figure 1B.6 illustrates the predicted effect of temperature and pressure for reactants to products and reactants to intermediates. The data illustrate that at low pressure (below 0.1 atm) and high temperature (above 1100 K) most of the energized complex reacts back to C_3·COC + O_2 than is stabilized; stabilization to C_2C(COO·)OC ·adduct is dominant at low temperature and high pressure. Product formation channel C=C(C)OC + C·H_2OOH dominate C=C(C)CQ + CH_3O channel by ca. 1 order of magnitude and complete with C_2C·CQ + CH_2O channel. C·H_2OOH rapidly decomposes to CH_2O + OH and will not be observed.

2.3.5 C_3COC· + O_2

The C_3COC· radical combines with O_2 to form the chemically activated C_3COCOO·* adduct. The reaction channels of C_3COCOO·* include dissociation back to reactants, stabilization to C_3COCOO·, and isomerization (H-shift) via seven-member ring transition state (TS8) to C_3·COCOOH*. The C_3·COCOOH * isomer can: undergo beta-scission to C_2C=C + O·COOH radical, and cyclize to C_2CYCOCOC + OH. Reaction of

$C_3COCOO\cdot$* adduct to $C_3CO\cdot + O$ is included for completeness, but it is only important at higher temperature (above 1500K). The potential energy level diagram of reaction paths for reaction path $C_3COC\cdot$ unimolecular decomposition and addition with O_2 reactions is shown in Figure 1B.7. Input parameters and references to specific high-pressure rate constants for the reaction of $C_3\cdot COC$ and $C_3\cdot COC + O_2$ are listed in Table 1A.8.

An overall analysis of the reaction system indicates: the initial reaction of $C_3COC\cdot + O_2 \rightarrow C_3COCQ\cdot$ has $\Delta H_{rxn,\ 800K} = -34.89$ kcal/mole and $\Delta U_{rxn,\ 800K} = -33.30$ kcal/mole with a reasonable high A factor for reverse reaction of $9.39 \times 10^{14}\ s^{-1}$, i.e. a moderately high A ; thus a loose transition state. The H-shift isomerization via six-member ring (via TS6) has an E_a of 20.34 kcal/mole; which is lower reverse reaction back to $C_3COC\cdot + O_2$ from the stabilized adduct. The six-member ring H-shift also has a lower A factor $9.57 \times 10^{9}\ s^{-1}$ at 800 K than reverse reaction ($9.39 \times 10^{14} s^{-1}$). This H-shift isomerization TS6 has barrier lower than dissociation to $C_3COC\cdot + O_2$; but tight TS. The $C_3COCQ\cdot$ decomposition to isobutene + O·COOH radical (via TS8) has an A of $4.86 \times 10^{13}\ s^{-1}$ at 800K, which is higher than reverse isomerization $1.46 \times 10^{8}\ s^{-1}$ and cyclization to $C_2YCCOCO + OH$ (via TS11) $4.38 \times 10^{9}\ s^{-1}$. Dissociation to isobutene + O·COOH also has higher E_a 17.95 kcal/mole than reverse isomerization (E_a = 5.18 kcal) and cyclization to $C_2YCCOCO + OH$ (E_a = 15.23 kcal). Both energy of transition states (TS8 and TS11) for product formation channel are lower than energy of reactants ($C_3COC\cdot + O_2$).

Figure 1B.8 illustrates the predicted effect of temperature and pressure for both reactants to products and reactants to intermediates. The data show that at low pressure (below 1 atm) and high temperature (above 800 K) most of the energized complex reacts back to reactants ($C_3COC\cdot + O_2$); stabilization to $C_3COCQ\cdot$ adduct is dominant at low temperature and high pressure. Figure 1B.8a indicates $C_3COCQ\cdot^*$ β-scission to isobutene + O·COOH radical dominates cyclization to $C_2YCCOCO$ + OH by ca. 2 orders of magnitude, but it is slower than reverse reaction by ca. 2 orders of magnitude at 1atm and above 1000K.

2.4 Summary

Thermodynamic proprieties of reactants, intermediates, transition states and products are calculated using density functional B3LYP/6-31g(d) and complete basis set (CBS-4 and CBS-q) model chemistries. Thermochemical and chemical activation reaction analysis are presented on MTBE unimolecular decomposition and two radicals ($C_3\cdot COC$, $C_3COC\cdot$) plus O_2 systems. Chemical activation kinetic analysis is preformed using quantum Rice-Ramsperger-Kassel (QRRK) theory for k(E) and modified strong collision analysis for fall-off. Calculated rate constant on unimolecular decomposition reaction of $(CH_3)_3COCH_3 \rightarrow (CH_3)_2C{=}CH_2 + CH_3OH$ are in good agreement with experimental data.

CHAPTER 3

ANALYSIS OF TERTIARY BUTYL RADICAL + O_2, ISOBUTENE + HO_2, ISOBUTENE + OH AND ISOBUTENE-OH ADDUCTS + O_2: A DETAILED TERTIARY BUTYL OXIDATION MECHANISM

3.1 Overview

The reaction systems: *tert*-butyl radical + O_2, isobutene + HO_2, isobutene + OH and isobutene-OH adducts + O_2, which are important to understanding the oxidation chemistry of tertiary butyl radical ($C_3C\cdot$), are analyzed. Thermochemical parameters are determined by *ab initio* - Mϕller-Plesset (MP2(full)/6-31g(d)), complete basis set model chemistry (CBS-4 and CBS-q with MP2(full)/6-31g(d) and B3LYP/6-31g(d) optimized geometries), density functional (B3LYP/6-31g(d)), semi-empirical MOPAC (PM3) molecular orbital calculations, and by group additivity estimation. Thermochemical kinetic parameters are developed for each elementary reaction path in these complex systems; and a chemical activation kinetic analysis using quantum Rice-Ramsperger-Kassel (QRRK) theory for *k(E)* and master equation analysis for falloff is used to calculate rate constants as function of pressure and temperature. An elementary reaction mechanism is constructed to model experimental data for oxidation of *tert*-butyl radical. Model predictions for the loss of the *tert*-butyl precursor, 2,2,3,3-tetramethylbutane (C_3CCC_3), production of isobutene and 2,2-dimethyloxirane are compared with experimental data reported in the literature[72]. Reaction of *tert*-butyl radical ($C_3C\cdot$) with O_2 forms an energized *tert*-butyl peroxy adduct $C_3COO\cdot^*$ which can dissociate back to reactants, dissociate to isobutene + HO_2 or isomerize to *tert*-butyl hydroperoxide

(C_3·COOH). This isomer can dissociate to either isobutene + HO_2 or 2,2-dimethyloxirane + OH, before it is stabilized. In the *tert*-butyl radical + O_2 reaction system, dissociation of the [C_3COO·]* adduct to isobutene + HO_2 via HO_2-molecular elimination is faster than the hydrogen-shift to C_3·COOH by a factor of 86 to 1 at 773K and 60 Torr. The reaction barrier (reaction enthalpy difference between TS4 and C_3·COOH) for the C_3·COOH reaction to 2,2-dimethyloxirane + OH is calculated as 17.98 (19.06) kcal/mole at CBS-q//MP2(full)/6-31g(d) level but is evaluated as 15.58 (18.06) kcal/mole by fitting experimental data. Data in parentheses are thermodynamic properties based on CBS-q//B3LYP/6-31g(d) calculation. Barriers for reactions of HO_2 + isobutene → C_3·COOH (HO_2 addition at CD/C2 carbon atom of isobutene, CD = carbon double bond) and HO_2 + isobutene → C_2C·COOH (HO_2 addition at CD/H2 carbon atom of isobutene) are respectively determined as 7.74 (7.38) and 10.69 (10.82) kcal/mole. 2,2-dimethyloxirane is formed primarily by HO_2 addition to isobutene. OH addition to isobutene results in adducts which further react with O_2 to form acetone, formaldehyde and the OH radical (Waddington mechanism) is also analyzed.

3.2 Introduction

Initial products from pyrolysis, oxidation, or photochemical reactions of saturated and unsaturated hydrocarbons are the corresponding radicals. Important reactions of these alkyl radicals in combustion and in atmospheric photochemistry are combination reactions with molecular oxygen to form peroxy adducts which can undergo further reaction in energized (chemical activation) or stabilized states. These reactions are complex, difficult to study experimentally and present a source of controversy with regard to both pathway and reaction rates. While these reactions comprise the principal reaction paths of the hydrocarbon radical conversion in most hydrocarbon oxidation, combustion and atmospheric photochemistry, they are relatively slow in the combustion environment and often a bottleneck to overall hydrocarbon conversion.

The C_2H_5 + O_2 reaction serves as an important reference in this study, as it has been studied the most extensively. It has been experimentally studied by Gutman et al.[59, 60], Kaiser et al.[61-66] and Pilling et al.[67] Kinetics of the ethyl system has been analyzed by Bozzelli and Dean[68] using quantum RRK theory, and by Wagner et al.[69] using variational RRKM theory for ethylene production and ethyl radical loss at pressures and temperatures relevant to the experimental data of Gutman's group[59, 60]. These analyses postulate the formation of a chemically activated peroxy radical adduct. This energized adduct can be stabilized to CCOO·, undergo unimolecular elimination to ethylene + HO_2, or isomerize through a cyclic five-member ring intermediate to a primary hydroperoxy alkyl radical (H shift). This hydroperoxy alkyl isomer can then react form to C_2H_4 + HO_2 or to cyclic epoxide + OH. The H-shift / HO_2-molecular elimination reaction in the ethyl system is analyzed by Bozzelli and Dean[68] to be a bottleneck to ethyl conversion; a result of the low Arrhenius A factor (tight transition state) and a barrier similar to the reaction reforming the C_2H_5 + O_2, which has a higher A factor. The activation energy for the C·COOH reaction to C_2H_4 + HO_2 was evaluated as ΔH_{rxn} + 8 kcal/mole. This is, however, in disagreement with the value of ΔH_{rxn} + 17 kcal/mole, reported by Baldwin et al.[70], and the range 12.7 - 14.1 kcal/mole reported by Gulati et al.[71] based on data from oxirane formation in larger molecules. Schaefer et al.[72] have recently reported a density functional (TZ2Pf UB3LYP) calculation value of 12.7 kcal/mole for reverse reaction

(C_2H_4 + HO_2 → C·COOH) barrier and they reported barriers of 27.1 kcal/mole for the direct HO_2-molecular elimination from the ethyl peroxy radical (CCOO·) to C_2H_4 + HO_2. They also report an activation energy of 37.0 kcal/mole to reach the 5 member ring intramolecular H-shift transition state from CCOO· to ethyl hydroperoxy radical (C·COOH). Jungkamp et al.[47] studied reactions in the atmospheric oxidation of *n*-butane and calculated reaction activation energies at various levels of theory. They report 0 K activation energies for intramolecular H-shift reactions of 2-butylperoxy radical abstracting primary, and 1-butylperoxy radical abstracting secondary hydrogen atoms by a peroxy group through a 6 member ring transition state as 24.3 and 20.3 kcal/mole, respectively, at CBS-q//B3LYP/6-31g(d,p) level of theory.

Few experimental studies on the *tert*-butyl radical reaction with O_2 have been reported. The research group of Atri and Baldwin[58, 73] studied the thermal decomposition of 2,2,3,3-tetramethylbutane in the presence of oxygen at temperatures from 673 to 815K and pressures from 50 to 600 Torr, in flow reactors (both KCl-coated and boric-acid coated vessels) - at slow flow - up to several minute reaction times. They report rate constants for C_3C--CC_3 bond cleavage and for HO_2 abstraction of hydrogen from the primary C-H bonds on the 2,2,3,3-tetramethylbutane. They also report concentration profiles for selected *tert*-butyl radical reaction products as well as 2,2,3,3-tetramethylbutane loss versus reaction time. Atri and Baldwin[58, 73] formulate a mechanism for kinetic evaluation using steady state approximations on the *tert*-butyl radical + O_2 reaction system. The model includes peroxy formation, reverse dissociation, isomerization (hydrogen atom transfer, non-reversible), and isomer decomposition to form a cyclic ether + OH from the alkyl hydroperoxide radical (isomer) plus abstraction reactions of HO_2 and OH radicals. Their interpretation of experimental data show that *tert*-butyl radicals are major products formed from the reaction of 2,2,3,3-tetramethylbutane decomposition and ~1% of *tert*-butyl radicals further react to cyclic ether + OH for their reaction times.

Evans et al.[74] studied the rate constants for the reaction of *tert*-butyl radicals formed from the decomposition of 2,2,3,3-tetramethylbutane in the presence of H_2 and O_2 in KCl-coated reaction vessels. They measured the relative yields of isobutene and isobutane in the early stages of reaction over the temperature range 713-813K, and analyzed the data using steady state and equilibrium relationships. They report rate constants of the reactions $C_3C\cdot + O_2 <=>$ isobutene + HO_2 and $C_3C\cdot + H_2 <=>$ isobutane + H, and make comparisons with rate constants for analogous reactions.

Lenhardt et al.[75] have studied rate constants for reactions of normal, secondary, tertiary and 3-hydroxy *s*-butyl radicals with O_2 at 300K and low pressure, 1 to 4 Torr. Butyl radicals were generated by flash photolysis of butyl iodides using a xenon flash lamp. Initial concentration of butyl radicals were low (below 10^{11} radicals cm^{-3}) to reduce importance of radical-radical combination. They monitored the pseudo-first-order decay of the butyl radicals as a function of oxygen using mass spectrometry. Their experimental results show no measurable pressure dependence for rate constants of butyl radical + O_2 recombination over the small pressure range of 1 to 4 Torr. They used adiabatic channel model calculations to interpret their results and report the high-pressure limit rate constant for combination of *tert*-butyl + O_2 as $k=1.41 \times 10^{13}$ cm^3 $mole^{-1}$ sec^{-1}.

Slagle et al.[76] studied the gas-phase equilibrium reaction of *tert*-butyl radical with molecular oxygen to form the peroxy radical over temperature range from 550 to 580K and pressures from 1 to 5 Torr. They monitored the reaction of *tert*-butyl radical + O_2 to equilibrium using photoionization mass spectrometry and reported the enthalpy change for $C_3C\cdot + O_2 <=> C_3COO\cdot$ equilibrium reaction by using a third law procedure combining the measured equilibrium constants with calculated or estimated entropy change for the reaction.

In this study, we perform a thermochemical analysis on the reaction of *tert*-butyl radical with O_2, in addition, to the analysis on a subset of reactions that relate to stable product formation from *tert*-butyl + O_2 reaction.

The reaction systems analyzed include:

tert-butyl radical + O_2 ⟶ Products

Isobutene + HO_2 ⟶ Products

Isobutene + OH ⟶ Products

Isobutene-OH + O_2 ⟶ Products

Reaction path analysis, reaction barrier, pre-exponential factor, and thermochemical properties of each elementary reaction step are evaluated for reactions of *tert*-butyl radical in an oxidizing atmosphere under moderate to low temperature combustion conditions. Important reaction pathways are shown in Figure 2B.1. We utilize a chemical activation kinetics treatment incorporating quantum Rice-Ramsperger-Kassel (QRRK) theory for *k(E)* and master equation analysis[13-15] as discussed by Gilbert and Gilbert's *UNIMOL* manual for falloff of the energized adduct. A similar multi-channel unimolecular quantum RRK and master equation falloff analysis are used for dissociation of the stabilized adducts. An elementary reaction mechanism is developed and used to model data of the Baldwin and Walker[58, 73] research group where tertiary butyl radical comes from the unimolecular decomposition of the 2,2,3,3-tetramethylbutane in presence of O_2. Calculations for loss of *tert*-butyl precursor, 2,2,3,3-tetramethylbutane, production of isobutene and 2,2-dimethyloxirane show good agreement with experimental data of Atri et al.[58] Data on the reaction $C_3C\cdot \rightarrow C_2C{=}C + H$ are in good agreement with data of Knyazev et al.[77]

3.3 Method

3.3.1 Thermodynamic Properties

Geometry optimizations and frequency calculations for reactants, intermediates and transition states in the *tert*-butyl radical + O_2 and isobutene + HO_2 reaction systems are performed using *ab initio* - Mϕller-Plesset (MP2) and B3LYP functional theory. Semi-empirical PM3 molecular orbital calculations are performed to evaluate entropy and heat capacity for important transition states and other relevant species of the isobutene-OH adducts + O_2 reaction system. The structures calculated from MP2(full)/6-31g(d), B3LYP/6-31g(d), and PM3 are provided as supporting information. Zero-point vibrational energies (ZPVE), vibrational frequencies and thermal contributions to enthalpy and entropy from harmonic frequencies are scaled with factors as recommended by Scott et al.[53] Entropies and heat capacities are calculated from scaled vibrational degrees of freedom. The method of Pitzer and Gwinn[57] is used for thermodynamic analysis of S and Cp(T) contribution from hindered internal rotors. The numbers of optical isomers and spin degeneracy of unpaired electrons are incorporated. Transition state (TS) geometries are identified by the existence of only one imaginary frequency in the normal mode coordinate analysis, evaluation TS geometry, and transition state theory

(TST[25]) reaction coordinate vibration information. *Ab initio* and semi-empirical (PM3) molecular orbital calculations were performed using the Gaussian94[52] and MOPAC 6.0[51] programs, respectively.

Total energies, zero-point vibrational energies and thermal contributions to enthalpy calculated by MP2(full)/ 6-31g(d), B3LYP/ 6-31g(d) and complete basis set (CBS-4 and CBS-q) model chemistries[54-56] for the species of *tert*-butyl radical ($C_3C\cdot$) + O_2 and isobutene ($C_2C{=}C$) + HO_2 reaction systems are listed in Table 2A.1. The CBS-4 and CBS-q calculations are performed using with geometry optimizations at MP2(full)/ 6-31g(d) and B3LYP/ 6-31g(d) levels of theory. Reaction enthalpies determined at different theory levels are listed in Table 2A.2. CBS-q results using either MP2(full)/ 6-31g(d) or B3LYP/ 6-31g(d) optimized geometries are similar, where differences are within 2.4 kcal/mole. We choose the CBS-q//MP2(full)/ 6-31g(d) calculation for discussion and kinetic analysis for $C_3C\cdot$ + O_2 and $C_2C{=}C$ + HO_2 reaction systems. CBS-q calculations are chosen because Jungkamp et al.[47, 48], Petersson et al.[49] and our group[50] have shown that they result in reasonable accurate thermodynamic enthalpy data for these molecular systems. CBS-q and G2(MP2) are probably the best methods for these (5 or 6 heavy atoms) systems and CBS-q requires ca. 2/3 the computation time of G2(MP2).

Thermodynamic parameters - $\Delta H_f{}^\circ{}_{298}$, $S^\circ{}_{298}$, and Cp(300) to Cp(1500) for species in the reaction schemes are listed in Table 2A.3. Thermodynamic parameters of molecular and radicals with the exception of species calculated from *ab initio* and PM3 are calculated from group additivity using THERM[78] with peroxy[79, 80], cyclic[81] and hydrogen bond increment (HBI) groups[82] parameters. We use heats of formation calculated from group additivity instead of those from PM3 calculations. The OO symbol is a group notation for peroxides. Peroxy groups were developed by Lay et al.[80, 81]. Hydrogen bond increment (HBI) groups are used to calculate thermodynamic properties of radicals[82]. The HBI group technique is based on known thermodynamic properties of the parent molecule and calculated changes that occur upon formation of radicals via loss of a H atom. The HBI group incorporates evaluated carbon hydrogen (C--H) bond energies for ΔH_f of the respective radical, and entropy and heat capacity changes that result from loss or changes in vibration frequencies, internal rotation, and spin degeneracy when a hydrogen atom is removed from the specific carbon site. HBI groups are described in ref.82 and listed in Table 2A.4. The thermochemical data allow calculation of reverse reaction rate constants by microscopic reversibility.

3.3.2 Kinetic Calculations

Unimolecular dissociation and isomerization reactions of the chemically activated and stabilized adducts resulting from addition or combination reactions are analyzed by first constructing potential energy diagrams for the reaction system. Thermodynamic parameters, $\Delta H_f°_{298}$, $S°_{298}$, Cp(T), reduced vibration frequency sets, and Lennard Jones parameters for species in each reaction path are presented.

High-pressure rate constants for each channel are obtained from literature or referenced estimation techniques. Kinetics parameters for unimolecular and bimolecular (chemical activation) reactions are then calculated using multi-frequency QRRK analysis for $k(E)$[21-23]. The master equation analysis[13-15] as discussed by Gilbert is used for falloff (β collision) with the steady state assumption on the energized adduct(s). $(\Delta E)°_{down}$ of 1000 cal/mole[83, 84] is used for master equation analysis, N_2 is used as the third body.

Reactions which involve a change in number of moles, such as unimolecular dissociation, have energy of activation calculated as delta U_{rxn} plus an E_a for the reverse addition, where U is internal energy (E_a reverse is usually 0.0 for simple association reactions). Enthalpies and E_a's, in the text and in potential energy diagrams are at 298 K, while those in the tables listing data input to the chemical activation reactions are for 800 K, which we select as representative of modeled combustion experiments.

3.3.3 Input Information Requirements for QRRK Calculation

Pre-exponential factors (A_∞s), are calculated using canonical TST[16] along with MP2, DFT or PM3-determined entropies of intermediates and transition states (TSs) for the reactions where thermodynamic properties of TS are available. High-pressure limit pre-exponential factors for combination reactions are obtained from the literature and from trends in homologous series of reactions. Activation energies come from complete basis model calculations CBS-q plus evaluated endothermicity of reaction ΔU_{rxn}, from analysis of Evans Polanyi relationships for abstractions plus evaluation of ring strain energy, and from analogy to similar reactions with known energies. Thermodynamic properties are provided for each system.

Reduced sets of three vibration frequencies and their associated degeneracies are computed from fits to heat capacity data, as described by Ritter and Bozzelli et al.[17, 18] These have been shown by Ritter to accurately reproduce molecular heat capacities, Cp(T), and by Bozzelli et al.[18] to yield accurate ratios of density of states to partition coefficient, $\rho(E)/Q$.

Lennard-Jones parameters, sigma (Angstroms) and ε/k (Kelvins), are obtained from tabulations[19] and from a calculation method based on molar volumes and compressibility [20]. When necessary, estimation is done in a consistent and uniform manner via use of generic reaction rate constants with reference to literature, experiment or theoretical calculation in each case. The QRRK calculation input parameters and their references are listed in the table associated with the respective reaction system.

3.3.4 Recent Modifications to the Quantum RRK Calculation

a; Use of a manifold of three frequencies plus incorporation of one external rotation for the density of states, $\rho(E)/Q$ and in calculation of $k(E)$.

b; The Leonard-Jones collision frequency Z_{LJ} is now calculated by $Z_{LJ} = Z\ \Omega\ (2,2)$ integral[16, 20] obtained from fit of Reid et al.[20].

The QRRK analysis for $k(E)$ with modified strong collision and a constant F_E for falloff has been used previously to analyze a variety of chemical activation reaction systems, Westmoreland et al.[21, 22], Dean et al.[23], and Bozzelli et al.[24, 25] There are a number of recent publications by other researchers that utilize the QRRK formalism with a more exact calculation F_E in modified strong collision analysis[26-31] or utilize just a QRRK formalism.[32, 33] It is shown to yield reasonable results in these applications, and provides a framework by which the effects of both temperature and pressure can be estimated for complex chemical activation or unimolecular dissociation reaction systems. The reaction channels resulting from O_2 addition to $C_2C{\cdot}COH$ adducts illustrated in Figure 2B.2 serve as an example of such complexity. The system incorporates 15 reactions: 8 forward, 4 reverse, 3 stabilizations, with 3 adducts in steady state and most barriers below $\Delta H_f{}^{o}{}_{298}$ of the reactants. We feel that QRRK analysis combined with either modified strong collision or master equation for falloff, is a reasonable method to estimate the rate constants as a function of temperature and pressure for these complex systems.

3.4 Experimental Data and Reaction Reactor Modeling

We use experimental data published by Atri et al.[58] for decomposition of 2,2,3,3-tetramethylbutane (C_3CCC_3) in presence of oxygen. This experimental study was carried out in a Pyrex flow reactor freshly coated with potassium chloride – at slow flow – up to several minutes reaction time and was conditioned at 773K and 60 torr.

In previous studies[73, 74, 85], Walker showed the $C_3CCC_3 + O_2 \Rightarrow$ isobutene + HO_2 reaction gives higher rate constants in KCl-coated vessels than in aged boric acid-coated vessels at temperatures greater than 723K. He postulated that HO_2 and H_2O_2 radicals are efficiently destroyed at the KCl-coated vessel surface at these temperatures. The basic mechanism postulated by Atri et al.[58] involves the overall reactions listed in (1)-(4) for conversion to stable molecules.

$$C_3C\text{-}CC_3 \longrightarrow 2\ C_3C\cdot \qquad (1)$$

$$C_3C\cdot + O_2 \longrightarrow C_2C{=}C + HO_2 \qquad (2)$$

$$HO_2 \xrightarrow{\text{surface}} 1/2\ H_2O + 3/4\ O_2 \qquad (3)$$

$$H_2O_2 \xrightarrow{\text{surface}} H_2O + 1/2\ O_2 \qquad (4)$$

For reactor modeling, two dummy molecules, X and Y, and four unidirectional reactions are added to our mechanism to simulate surface effects in the KCl-coated reactor (reaction 3 and 4 above). The points in Figure 2B.3 illustrate experimental data of the Walker and Baldwin research group.

3.5 Results and Discussion

3.5.1 Formation of *tert*-Butyl Radical ($C_3C\cdot$)

The *tert*-butyl radical is generated in our mechanism by the homogeneous decomposition of 2,2,3,3-tetramethylbutane in presence of O_2. Previous experiments[72-74, 85] on the oxidation C_3CCC_3 in a KCl-coated vessel have shown that homolysis of the central C-C bond (reaction 1) is the dominant reaction path over alternative initiation reactions, which include other CH_3-C scission reactions, C-H scissions and abstraction of a primary H atom by O_2, even at high pressures of O_2. The C_3C---CC_3 bond is 77.32 kcal/mole, weaker by 6.6 kcal/mole at 298K than other C-C bonds in the 2,2,3,3-tetramethylbutane molecule due to steric effects (repulsion of *tert*-butyl methyls - gauche interactions). Cleavage of the C_3CCC_3---H bond requires 101.1 kcal/mole and has a lower A factor than C_3C---CC_3 bond cleavage.

$$(CH_3)_3C\text{-}C(CH_3)_3 \longrightarrow 2\ C_3C\cdot \qquad (1)$$

We use the high-pressure limit $A_\infty = 6.0 \times 10^{16}\ S^{-1}$, $E_{a,\infty} = 69.47$ kcal/mole for C_3C---CC_3 fission from analysis of both Tsang's[86] and Arti's results[72].

3.5.2 Unimolecular Decay *tert*-Butyl Radical ($C_3C\cdot$)

The unimolecular decomposition of reaction (5) has been studied by Knyazev et al.[77] over a temperature range 712 - 779 K in He bath gas (2.35 - 17.36 torr).

$$C_3C\cdot \xrightarrow{(TS13)} C_2C{=}C + H \qquad (5)$$

Knyazev et al. used a heated tubular flow reactor and photoionization mass spectrometer for radical species detection. They create a transition-state model and calculate rate constants using master equation / RRKM calculation to determine a high-pressure limit rate constant for the decomposition reaction ($k_{5,\infty}=2.18\times10^{9}\times T^{1.48}\exp(-36000/RT)$ s^{-1}) and the reverse reaction ($k_{-5,\infty}=1.03\times10^{11}\times T^{0.25}\exp(-1460/RT)$ $cm^{3}molecule^{-1}s^{-1}$). Figures 2B.4a and 2B.4b compare the decomposition rate constants from experimental data of Knyazev et al. with our QRRK calculations using collision parameters of Knyazev et al. The high-pressure limit rate constants are from Knyazev et al. ($2.18\times10^{9}\times T^{1.48}\exp(-36000/RT)$ s^{-1}) and Tsang et al.[87] ($8.3\times10^{13}\exp(-38150/RT)$ s^{-1}), respectively. The agreement of our QRRK calculations using the rate constant parameters of Tsang with the experimental data is excellent; use of rate constant parameters of Knyazev in our calculations yield predictions that are ca. 10 % high.

Figure 2B.4c illustrates results from use of *ab initio* determined values for the reactant *tert*-butyl radical and the transition state structure, CBS-q//MP2(full)/6-31g(d) for energy with structure and frequencies determined at MP2(full)/6-31g(d) level. We use canonical transition state theory and obtain a high-pressure limit $A_{5,\infty}$ of $2.5\times10^{16}\times T^{-0.92}$ s^{-1}. Tunneling is taken into account using the Erwin-Henry computer code[89] (Eckart formalism) to determine high-pressure limit rate constants. The reaction barrier of H atom addition to isobutene is calculated to be 0.52 kcal/mole at CBS-q//MP2(full)/6-31g(d) level. MP2-calculated frequencies and moment of inertia for transition state (TS13) are described in Table 2A.5. A comparison of rate constants from QRRK calculation using the high-pressure limit rate constant $2.5\times10^{16}\times T^{-0.92}\exp(-37500/RT)$ s^{-1} with experimental data of Knyazev et al. is illustrated in Figure 2B.4c. Arrhenius pre-exponential factors for MP2 combined with the calculated β scission reaction barrier, $\Delta H_{rxn} + E_a$ for H addition at CBS-q//MP2(full)/6-31g(d) level, tunneling for the hydrogen atom elimination, and QRRK analysis yield good estimates of rate constants – in the falloff. These results from our QRRK analysis, canonical TST, tunneling, and *ab initio* calculated thermodynamic parameters are very similar, 1.1% higher, than data in Figure 2B.4b that use Tsang's parameters.

Overall kinetic analysis shows this unimolecular H atom elimination reaction is important, although it is slow on a scale relative to O_2 addition: $C_3C\cdot + O_2 \leftrightarrow C_3COO\cdot$. The reverse of oxygen addition, where $C_3C\cdot$ radical is regenerated, is however also important.

3.5.3 *tert*-Butyl Radical ($C_3C\cdot$) + O_2

The *tert*-butyl radical combines with O_2 to form the chemically activated $C_3COO\cdot^*$ adduct. The major reaction channels of $C_3COO\cdot^*$ include dissociation back to reactants, stabilization to $C_3COO\cdot$, molecular elimination to $C_2C{=}C + HO_2$, and isomerization (H-shift) to $C_3\cdot COOH^*$. The $C_3\cdot COOH^*$ isomer can: undergo beta-scission to $C_2C{=}C$ + HO_2, cyclize to C_2CYC_2O + OH, undergo beta-scission to C=C(C)OOH + CH_3, be stabilized to $C_3\cdot COOH$ or isomerize back to $C_3COO\cdot^*$. Reaction of $C_3COO\cdot^*$ adduct to $C_3CO\cdot$ + O is included for completeness, but it is only important at higher temperature (above 1500K). The potential energy level diagram for reaction paths is shown in Figure 2B.5.

$\Delta H_f°_{298}(C_3COO\cdot)$(-25.16 kcal/mole) is calculated by Lay et al.[88] using isodesmic reactions and *ab initio* calculations (MP4SDTQ/6-31g(d)//MP2/6-31g(d) and G2). Bond energy $DH°_{298}(HOOCC\text{-}H)$ is determined to be 101.1 + 1.77 = 102.87 kcal/mole, using $DH°_{298}(C_2H_5\text{-}H)$ = 101.1 kcal/mole and reaction enthalpy ΔH_{rxn} = -1.77 kcal/mole at G2 level for the isodesmic reaction (6).

$$CC + C{\cdot}COOH \rightarrow C{\cdot}C + CCOOH \qquad (6)$$

$DH°_{298}(C_2C(OOH)C\text{-}H)$(103.69 kcal/mole) is determined to be 102.87 – (-0.82) = 103.69 kcal/mole, using $DH°_{298}(HOOCC\text{-}H)$ = 102.87 kcal/mole and the calculated reaction enthalpy ΔH_{rxn} = -0.82 kcal/mole at CBS-q//MP2(full)/6-31g(d) and CBS-q//B3LYP/6-31g(d) levels for the isodesmic reaction (7).

$$C_3{\cdot}COOH + CCOOH \rightarrow C_3COOH + C{\cdot}COOH \qquad (7)$$

$\Delta H_f°_{298}(C_3{\cdot}COOH)$(-7.81 kcal/mole) is derived from $\Delta H_f°_{298}(C_3COOH)$ and $DH°_{298}(C_2C(OOH)C\text{-}H)$ using the following equation:

$$\Delta H_f°_{298}(C_3{\cdot}COOH) = DH°_{298}(C_2C(OOH)C\text{-}H) + \Delta H_f°_{298}(C_3COOH) - \Delta H_f°_{298}(H)$$

$$-7.81\text{kcal/mole} = (103.69\text{kcal/mole}) + (-59.4\text{kcal/mole}) - (52.1\text{kcal/mole})$$

Enthalpies of formation for transition states are calculated from reaction enthalpies (enthalpy differences between TS and reactants) in the exothermic direction plus enthalpies of formation of the reactants. $\Delta H_f°_{298}(TS1)$(2.29 kcal/mole) is determined from ($\Delta H_f°_{298}(C_2C{=}C)$+ $\Delta H_f°_{298}(HO_2)$)(-0.3 kcal/mole) plus reaction enthalpy ($\Delta H^{\neq}_{TS1\text{-}(C2C=C+HO2)}$)(2.59 kcal/mole). $\Delta H_f°_{298}(TS2)$(7.68 kcal/mole) is determined from $\Delta H_f°_{298}(C_3{\cdot}COOH)$(-7.81 kcal/mole) plus reaction enthalpy ($\Delta H^{\neq}_{TS2\text{-}C3.COOH}$)(15.49 kcal/mole). $\Delta H_f°_{298}(TS3)$(7.44 kcal/mole) is from ($\Delta H_f°_{298}(C_2C{=}C)$ + $\Delta H_f°_{298}(HO_2)$)(-0.3 kcal/mole) plus reaction enthalpy ($\Delta H^{\neq}_{TS3\text{-}(C2C=C+HO2)}$)(7.74 kcal/mole). All reaction enthalpies above are calculated at CBS-q//MP2(full)/6-31g(d) level. $\Delta H_f{}^{\circ}{}_{298}$ (TS4)(7.77 kcal/mole) is obtained from fitting experimental data, which results in downward adjustment of the calculated barrier of ca. 2.4 kcal/mole. This is the only barrier adjusted in this study.

High-pressure limit pre-exponential factors (A_∞) for *tert*-butyl peroxy ($C_3COO\cdot$) molecular elimination to isobutene + HO_2 (reaction 8), isomerization to *tert*-butyl hydroperoxide ($C_3{\cdot}COOH$) (reaction 9), hydroperoxide alkyl radical beta-scission to isobutene + HO_2 (reaction 10), and hydroperoxide alkyl radical cyclization to 2,2-dimethyloxirane + OH (reaction 11) are calculated using canonical TST along with MP2-determined entropies. High-pressure limit rate constants, k_∞, are fit to a three parameter modified Arrhenius Equation (A, n, E_a) over the temperature range 300K to 2000K. Input parameters for the chemical activation analysis of *tert*-butyl radical + O_2 reaction system is shown in Table 2A.6. Parameters in Table 2A.6 are referenced to the ground (stabilized) level of the complex, as this is the formalism used in QRRK theory. References to specific high-pressure rate constants and falloff parameters are also listed in Table 2A.6. The MP2-determined frequencies and moment of inertia for transition states, TS1-TS4, *tert*-butyl peroxy ($C_3COO\cdot$) and *tert*-butyl hydroperoxide ($C_3{\cdot}COOH$) are listed in Table 2A.7.

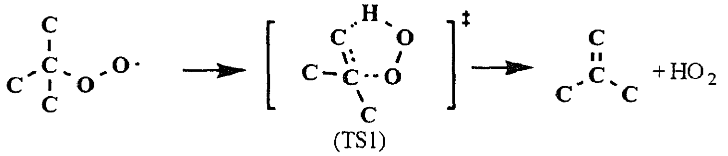

(8)

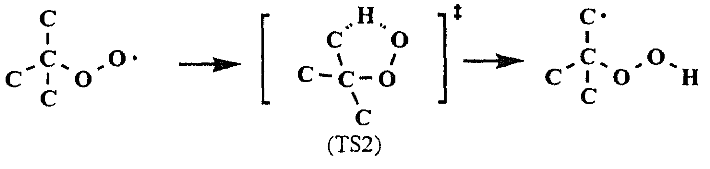

(9)

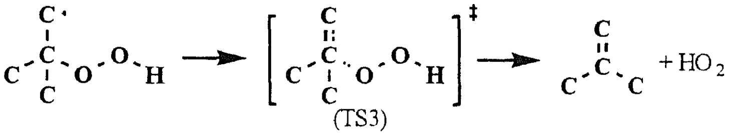

(10)

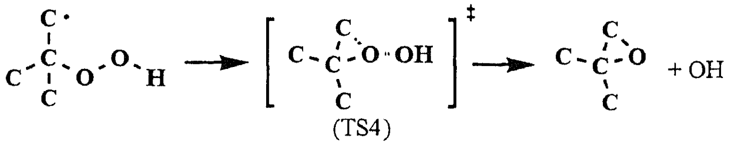

(11)

The rate constant for isomerization of $C_3COO\cdot \leftrightarrow TS2 \leftrightarrow C_3\cdot COOH$, reaction 9, includes Eckart calculation of H tunneling, as described in Schwartz et al.[89] The imaginary frequency of TS2, 1266 cm^{-1}, used in Eckart tunneling calculation is adjusted (down) from the MP2(full)/6-31g(d) determined imaginary frequency of 2876 cm^{-1} as recommended by Schwartz et al. This imaginary frequency (1266cm^{-1}) yields tunneling factors of $\Gamma = 1.3$ for reaction 9 at 773K. Other tunneling factors (Γs) at 500K, 600K, and 1000K are: 1.8, 1.5, and 1.2 for reaction 9, respectively. Schwartz et al. applied tunneling corrections with adjustment of the imaginary frequency and lowered barrier heights, to fit G2 calculated transition state parameters with experimental rate constants. The reactions were OH abstraction of hydrogen from CH_4, CH_3F, CH_2F_2, and CHF_3. An average decrease in barrier height of 1.12 kcal/mole from data obtained at the G2 level was used and the frequency was reduced by factors of 0.44 and 0.4 for MP2(full)/6-311g(d,p) and HF/6-31g(d) determined imaginary frequencies, respectively.

An overall analysis of the reaction system indicates: the initial reaction of $C_3C\cdot + O_2 \rightarrow C_3COO\cdot$ has $\Delta H_{rxn,800K} = 35.09$ kcal/mole and $\Delta U_{rxn,800K} = 33.50$ kcal/mol with a reasonable high A factor for reverse reaction of 6.83×10^{15} s^{-1}, i.e. a moderately high A ; thus a loose transition state. Molecular (HO_2) elimination from $C_3COO\cdot$ to isobutene + HO_2 (via TS1) has an E_a 27.43 kcal/mole with an A factor of 8.86×10^{12} s^{-1} at 773 K.

This elimination transition state is slightly looser than $C_3COO\cdot$ H-shift isomerization (via TS2) to $C_3\cdot COOH$. The H-shift isomerization has an E_a of 32.76 kcal/mole; which is higher than HO_2-molecular elimination and lower than reverse reaction to $C_3C\cdot + O_2$ from the stabilized adduct. The H-shift has a slightly lower A factor 3.11×10^{12} s^{-1} at 773 K than HO_2-molecular elimination. Both HO_2-molecular and H-shift isomerization through 5 member ring TS's, have barriers lower than dissociation to $C_3C\cdot + O_2$; but tight TS's. $C_3\cdot COOH$ decomposition to isobutene + HO_2 (via TS3) has an A of 5.33×10^{12} s^{-1} at 773K, which is lower than the elimination to C=C(C)Q + CH_3 9.21×10^{13} s^{-1} (Q represents OOH group), but higher than reverse isomerization 3.61×10^{10} s^{-1}, or 2,2-dimethyloxirane formation 8.17×10^{11} s^{-1}. Dissociation to isobutene + HO_2 has only a slightly higher E_a 15.89 kcal/mole than reverse isomerization $C_3COO\cdot$, 15.65 kcal/mole, but lower than E_a's for 2,2-dimethyloxirane formation, 16.13 kcal/mole, and C=C(C)Q + CH_3 elimination 35.49 kcal/mole. The rate constants listed above refer to 773K at high-pressure limits and are used for the QRRK input. The products isobutene + HO_2 are both relatively stable and build up in concentration so that reverse and further reactions of these species are important. The OH from the 2,2-dimethyloxirane formation reacts rapidly with other species; there is, effectively, no reverse reaction; OH addition to isobutene is, however, important.

Figure 2B.6 illustrates the predicted effect of temperature at 760 torr and at 60 torr on *tert*-butyl radical + O_2 reaction. The data illustrate that at low pressure and high temperature more of the energized complex reacts to $C_2C=C + HO_2$ than is stabilized (most reacts back to $C_3C\cdot + O_2$). At lower temperatures energized adduct stabilization is an important channel. The HO_2-molecular elimination reaction channel is faster than the

H-shift isomerization channel due to the lower barrier and similar A factor. The effects of pressure on rate constants are illustrated in Figure 2B.7 for temperatures of 300 and 1300 K. At 300 K, stabilization of the complex, $C_3COO\cdot$, is the dominant reaction channel above 0.0001 torr. At 1300 K dissociation of complex to reactants (reverse reaction) is the primary reaction of the energized adduct below 10 atm.

The rate of *tert*-butyl radical loss by reaction with O_2 increases with decease in temperature and increase in pressure as expected for reversible formation of the *tert*-butyl peroxy adduct. A significant fraction of this adduct, $C_3COO\cdot$, dissociates back to reactants at high temperature. This is a result of the high A for reverse reaction relative to the tight TST for isomerization or HO_2-molecular elimination where the reaction barriers are within 5.4 kcal/mole. The rate constants to stabilization decrease with decease in pressure and increase in temperature above 700K, due to the higher rate for dissociation of $C_3COO\cdot$ back to $C_3C\cdot + O_2$. Rate constants for direct (chemical activation) formation of 2,2-dimethyloxirane + OH and C=C(C)Q + CH_3 channels increase with increase in temperature and pressure.

The energized hydroperoxy radical $C_3\cdot COOH^*$, if formed, dissociates to $C_2C{=}C$ + HO_2 almost completely at low pressures and high temperature due to the higher A factor and similar barrier for this beta scission channel, relative to reverse isomerization. At higher pressures larger fractions of $C_3\cdot COOH$ are stabilized. Increased pressure, therefore, amplifies the importance of subsequent reactions of this hydroperoxide alkyl radical with O_2. At high temperature (above 1500K) the $C_3CO\cdot + O$ channel becomes important.

3.5.4 Isobutene ($C_2C{=}C$) + HO_2

Isobutene is formed by H atom elimination from $C_3C\cdot$ by HO_2-molecular elimination from $C_3COO\cdot$ and by HO_2 elimination from $C_3\cdot COOH$. The isobutene + HO_2 reaction system becomes important as a result of the relatively high yields of isobutene and high concentration of HO_2 in this intermediate temperature oxidation of *tert*-butyl radical. The addition of HO_2 radical to isobutene (addition at the isobutene CD/H2 carbon atom, CD = carbon double bond) proceeds through the sequence described below. Addition to the isobutene CD/C2 carbon atom is treated by reverse of reaction in the *tert*-butyl radical + O_2 system, as discussed above.

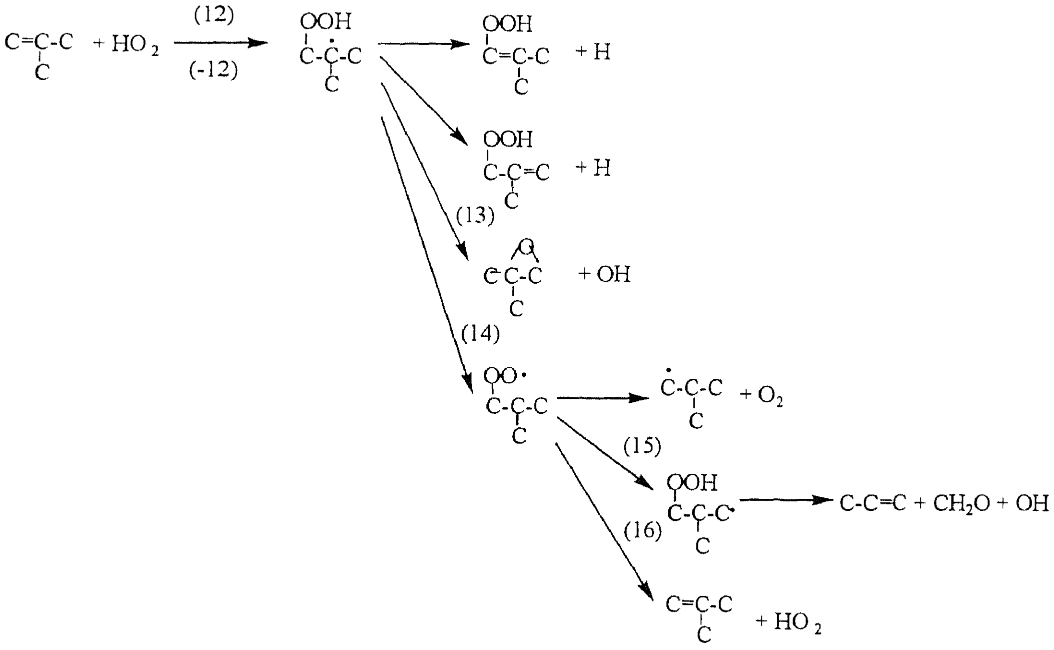

The reaction channels of the stabilized $C_2C\cdot COOH$ adduct include: dissociation back to isobutene + HO_2 (reaction -12, via TS5), H atom elimination (β-scission) to olefin-hydroperoxides, cyclization to form 2,2-dimethyloxirane product with OH radical (reaction 13, via TS6), and isomerization via five-member ring transition state (hydrogen shift) to form *iso*-butyl peroxy radical (reaction 14, via TS7). The *iso*-butyl peroxy radical can undergo β-scission to *iso*-butyl radical + O_2, HO_2-molecular elimination to isobutene (reaction 16, via TS9), and H-shift isomerization via a six-member ring transition state to hydroperoxide radical (reaction 15, via TS8) with subsequent β-scission to propene, formaldehyde and OH radical. The potential energy diagram for $C_2C{=}C$ + HO_2 (HO_2 addition at the CD/H2 carbon) reaction system is illustrated in Figure 2B.8.

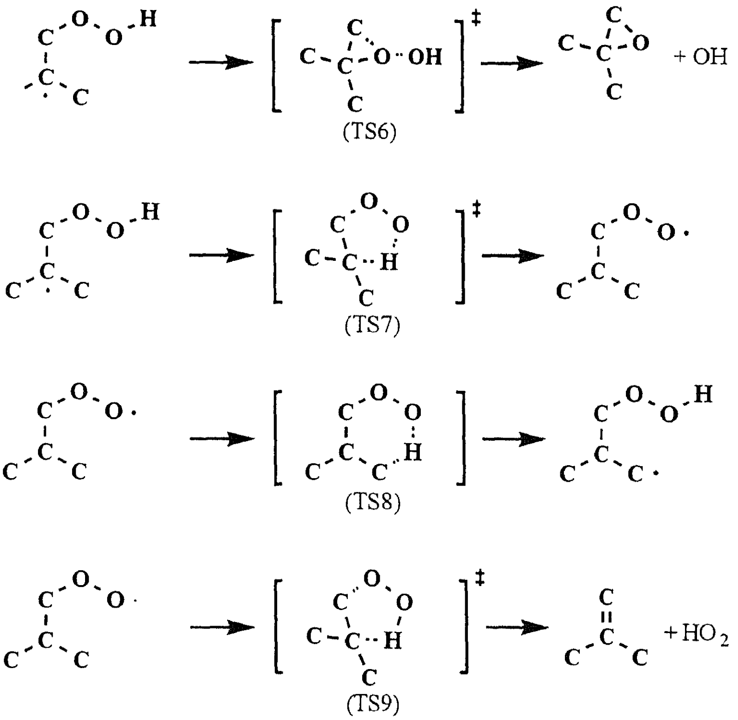

(13)

(14)

(15)

(16)

Enthalpies of formation of $C_2{\cdot}CCOOH$, $C_2C{\cdot}COOH$ and $C_2CCOO{\cdot}$ radicals are determined as –2.18, -8.37, and –19.07 kcal/mole, respectively, using calculated bond enthalpies (HOOCC(C)C-H, C_2 (COOH)C-H and C_2CCOO-H) and $\Delta H_f°_{298}$ (C_2CCOOH) (-52.71 kcal/mole). Bond enthalpies of HOOCC(C)C-H, C_2 (COOH)C-H and C_2CCOO-H are calculated from the following isodesmic reactions plus bond enthalpies of HOOCC-H (102.87 kcal/mole) and (COO-H (86.65 kcal/mole))[88].

$C_2{\cdot}CCOOH + CCOOH \rightarrow C_2CCOOH + C{\cdot}COOH$

$C_2C{\cdot}COOH + CCOOH \rightarrow C_2CCOOH + C{\cdot}COOH$

$C_2CCOO\cdot + COOH \rightarrow C_2CCOOH + COO\cdot$

$\Delta H_{rxn,298K}$ of these isodesmic reactions are determined to be 0.24, 6.43 and 0.56 kcal/mole, respectively, using the average value of two calculations: CBS-q//MP2(full)/6-31g(d) and CBS-q//B3LYP/6-31g(d).

$\Delta H_f°_{298}$(TS5)(10.39 kcal/mole) is determined from ($\Delta H_f°_{298}(C_2C{=}C)$ + $\Delta H_f°_{298}(HO_2)$)(-0.3 kcal/mole) plus reaction enthalpy ($\Delta H^{\neq}_{TS5\text{-}(C2C=C+HO2)}$)(10.69 kcal/mole). $\Delta H_f°_{298}$(TS6)(10.93 kcal/mole) is determined from ($\Delta H_f°_{298}(C_2C{=}C)$+ $\Delta H_f°_{298}(HO_2)$)(-0.3 kcal/mole) plus reaction enthalpy ($\Delta H^{\neq}_{TS6\text{-}(C2C=C+HO2)}$)(11.23 kcal/mole). $\Delta H_f°_{298}$(TS7)(9.31 kcal/mole) is from $\Delta H_f°_{298}$ ($C_2C\cdot COOH$)(-8.37 kcal/mole) plus reaction enthalpy ($\Delta H^{\neq}_{TS7\text{-}C2C\cdot COOH)}$)(17.68 kcal/mole). $\Delta H_f°_{298}$(TS8)(1.95 kcal/mole) is from $\Delta H_f°_{298}(C_2\cdot CCOOH)$(-2.18 kcal/mole) plus reaction enthalpy ($\Delta H^{\neq}_{TS8\text{-}C2\cdot CCOOH)}$)(4.13 kcal/mole). All reaction enthalpies above are calculated at CBS-q//MP2(full)/6-31g(d) level.

High-pressure limit pre-exponential factors (A_∞) for reactions 12-16 are calculated using canonical TST along with MP2-determined entropies. High-pressure limit rate constants, k_∞, are fit to a three parameters modified Arrhenius Equation (A, n, E_a) over the temperature range 300K to 2000K. The rate constants for isomerization of $C_2C\cdot COOH \leftrightarrow TS7 \leftrightarrow C_2CCOO\cdot$, reaction 14, and $C_2CCOO\cdot \leftrightarrow TS8 \leftrightarrow C_2\cdot CCOOH$, reaction 15, include Eckart calculation of H tunneling. The imaginary frequency of TS7 and TS8, 1193 and 953 cm^{-1}, used in Eckart tunneling calculation are adjusted (down) from MP2(full)/6-31g(d) determined imaginary frequency of 2710 and 2167 cm^{-1}. These reduced imaginary frequencies yield tunneling factors of Γ = 1.25 and 1.15 for reaction

14 and 15, respectively at 773K. The MP2-determined frequencies and moment of inertia for transition states, peroxy radicals and hydroperoxide radicals are listed in Table 2A.8. Input data for QRRK calculations, references to specific high-pressure limit rate constants and falloff parameters are listed in Tables 2A.9 and 2A.10 (HO_2 addition at the CD/C2 and CD/H2 carbon atoms, respectively).

Reaction barriers (reaction enthalpy difference between TS and reactants) for addition of HO_2 radical to isobutene at the CD/H2 and CD/C2 carbon atoms are calculated to be 7.74 and 10.69 kcal/mole, respectively, at CBS-q//MP2(full)/6-31g(d) level. The high-pressure limit rate constants are determined to be (1.31×10^4 $T^{2.10}$ cm^3/mole-s)exp(-7.54 kcal $mole^{-1}$/RT) and (5.6×10^4 $T^{1.89}$ cm^3/mole-s)exp(-10.56 kcal $mole^{-1}$/RT) for $C_2C{=}C + HO_2 \Rightarrow [C_3{\cdot}COOH]^*$ and $C_2C{=}C + HO_2 \Rightarrow [C_2C{\cdot}COOH]^*$, respectively. HO_2, electrophilic, radical addition to the CD/C2 carbon atom of isobutene has a lower activation energy than addition to the CD/H2 atom, resulting from partial electron donation from two $-CH_3$ groups. In the transition state, CH_3 groups donate electrons (ca. 0.22 to 0.26 Mulliken charge per CH_3, at MP2(full)/6-31g(d) level) to the olefinic carbon, which is undergoing bond formation with HO_2. Activation energies obtained from *ab initio* calculation show the same trend as experimental data of Gulati et al.[90]. The Walker group[90] report rate constants for the addition of HO_2 radicals to 2,3-dimethylbut-2-ene and hex-1-ene to be 4.79×10^{11}exp(-8390/RT) ($cm^3 mole^{-1} s^{-1}$) and 7.94×10^{11}exp(-13930/RT) ($cm^3 mole^{-1} s^{-1}$) at 673-703 K, respectively.

The calculated rate constants between 300-2000K at 760 torr from the QRRK / falloff analyses are illustrated in Figure 2B.9. The effects of pressure on rate constants are illustrated in Figure 2B.10 for temperature of 700K. Figures 2B.9 and 2B.10

illustrate that stabilization of $C_2C{\cdot}COOH$ adduct is the dominant reaction channel at low temperature and high pressure. At high temperature and low pressure energized complex dissociation back to reactants becomes more important. This reverse reaction (back to $C_2C{=}C + HO_2$) is faster than the 2,2-dimethyloxirane + OH formation channel by factors of 6 ~ 4 over temperature ranging from 300K to 3000K at 760 torr.

3.5.5 OH Addition to Isobutene and Isobutene-OH + O_2

The reactive hydroxy radical is formed mainly through reactions (17), (18) and (19).

$$C_3C\cdot + O_2 \longrightarrow C_2C{=}C + HO_2 \qquad (2)$$

$$HO_2 + HO_2 \longrightarrow H_2O_2 + O_2 \qquad (17)$$

$$H_2O_2 + M \longrightarrow 2\ OH + M \qquad (18)$$

$$R\cdot + HO_2 \longrightarrow RO\cdot + OH. \qquad (19)$$

OH will add to isobutene that is present at a relatively high concentration. Isobutene-OH adducts will then react with O_2. OH radicals add to isobutene at either the CD/H2 or CD/C2 carbon atom. We use the high-pressure limit rate constant for OH addition to isobutene as 8.5×10^{12} cm^3 $mole^{-1}$ s^{-1} exp(+0.3 kcal $mole^{-1}$/RT)[91].

In the presence of O_2, the isobutene-OH adducts will react with oxygen to form corresponding peroxy adducts and undergo further reactions (as below).

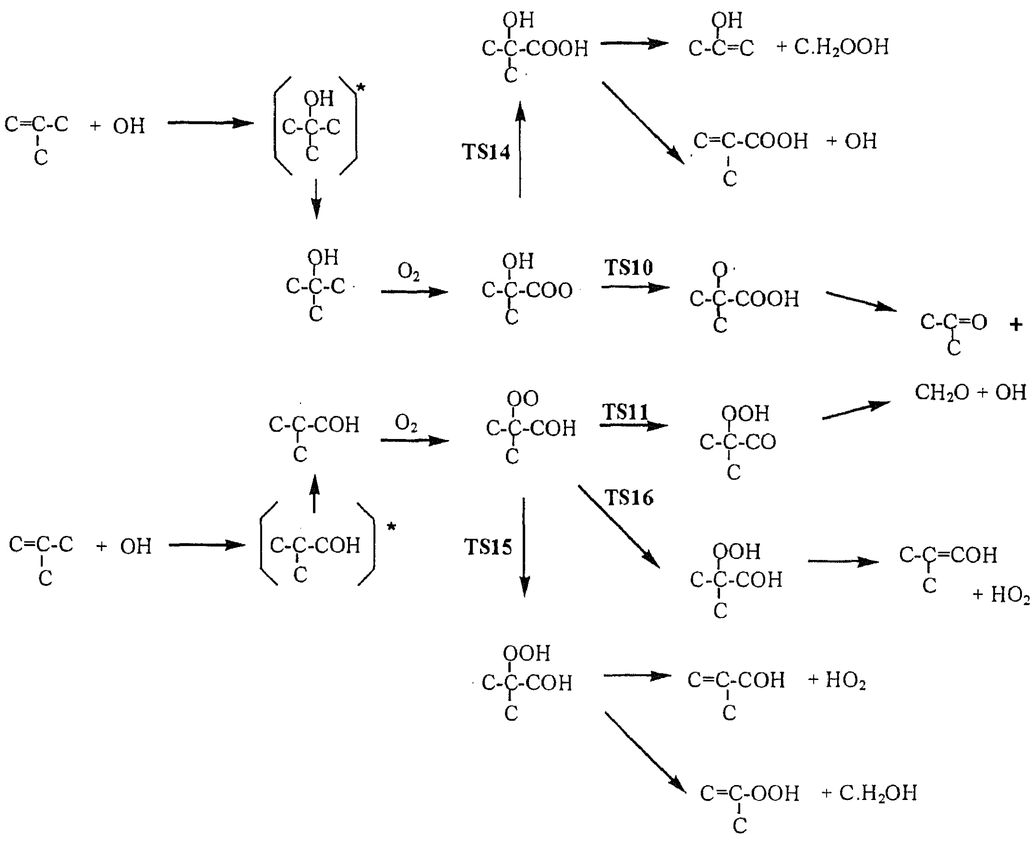

Where [ ]* indicates a energized intermediate.

The peroxy adducts undergo hydrogen transfer from hydroxyl group, -OH, to the peroxy group, -OO·, (via TS10 and TS11) leading to formation of hydroperoxy adducts with a 17.1 kcal/mole barrier that is mostly due to endothermicity. Cleavage of the RO--H bond requires ca. 104 kcal/mole and the formation of the OO---H bond returns only 88.5 kcal/mole. Hydrogen bonding in the ROO --- H --- OR' transition state reduces the barrier for this H shift isomerization by ca. 7 cal/mole. β-scission of the resulting oxy radicals form strong carbonyl bonds, C=O. The alkoxy radicals rapidly decompose to final products: formaldehyde, acetone and OH radicals after the isomerization. This detailed pathway explains the "Waddington mechanism"[90] for $C_2C=C + OH + O_2 \rightarrow$ Acetone + CH_2O + OH.

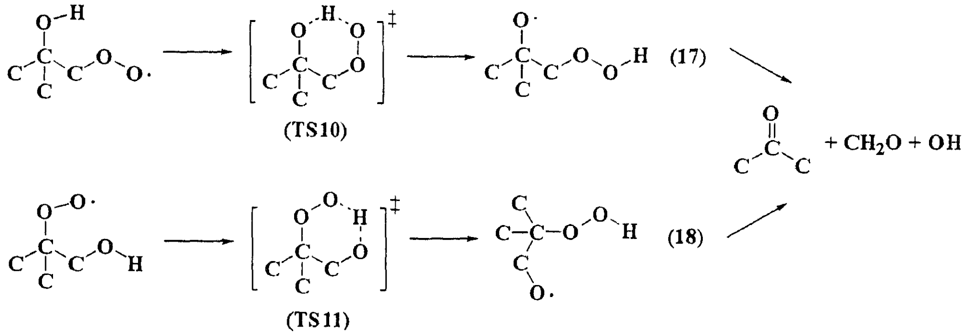

The high-pressure limit rate constants for intramolecular isomerizations-hydrogen transfer are calculated by canonical TST using PM3-determined entropies and fitting a three parameter (A, n, E_a) modified Arrhenius Equation between 300K to 2000K. The PM3-calculated frequencies and moment of inertia for intermediates and transition states are listed in Table 2A.11. Potential energy diagrams for the isobutene-OH + O_2 reaction systems are illustrated in Figures 2B.2 and 2B.11. High-pressure limit rate constants and references for the QRRK calculation input, and falloff parameters are listed in Tables 2A.12 and 2A.13. Calculated rate constants for isobutene-OH + O_2 → products over the range 300-2000K at 760 torr are illustrated in Figures 2B.12 and 2B.13. The isobutene-OH stabilization channel is dominant below 1000K and above 0.1 atm due to the relatively deep well (31.8 kcal/mole) and large (14-atom) molecule size. The stabilized isobutene-OH adduct rapidly combines with O_2, with the well depth of isobutene-OH + O_2 => isobutene-OH-OO· of ca. 35 kcal/mole[79]. This well depth indicates there is sufficient energy in the energized adduct for isomerization to the oxy radical with subsequent reaction (β-scission) to carbonyl products. These isomerization reactions compete with stabilization.

3.5.6 2,2-Dimethyloxirane (C_2CYC_2O) Formation

2,2-dimethyloxirane is formed via three paths: isomerization of $C_3COO\cdot$ to $C_3\cdot COOH$ which undergoes cyclization as discussed above; and from the two addition channels of HO_2 to isobutene. The 2,2-dimethyloxirane formation paths via the HO_2 addition to isobutene are:

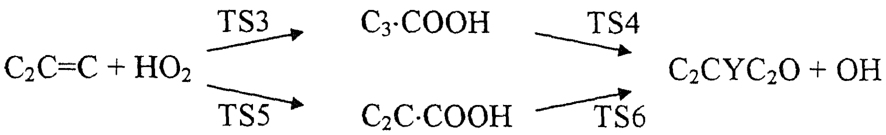

$$\begin{tikzcd}
 & C_3\cdot COOH \arrow[dr, "TS4"] & \\
C_2C{=}C + HO_2 \arrow[ur, "TS3"] \arrow[dr, "TS5"'] & & C_2CYC_2O + OH \\
 & C_2C\cdot COOH \arrow[ur, "TS6"'] &
\end{tikzcd}$$

The $C_2C\cdot COOH$ path is less important because TS3 is 3 kcal/mole lower than TS5. The barrier for 2,2-dimethyloxirane + OH formation from $C_2C\cdot COOH$ is calculated to be 19.3 kcal/mole which is obtained from the enthalpy difference between $C_2C\cdot COOH$ and TS6. The calculated barrier for $C_3\cdot COOH \rightarrow$ 2,2-dimethyloxirane + OH reaction is 17.98 kcal/mole (enthalpy difference between $C_3\cdot COOH$ and TS4). The calculated enthalpy of TS4 (10.17 kcal/mole) is determined from ($\Delta H_f{}^\circ{}_{298}(C_2C{=}C)+\Delta H_f{}^\circ{}_{298}(HO_2)$)(-0.3 kcal/mole) plus reaction enthalpy ($\Delta H^{\neq}_{TS4-(C2C=C+HO2)}$)(10.47 kcal/mole) at CBS-q//MP2(full)/6-31g(d). We need to adjust (reduce) the enthalpy of TS4 from 10.17 kcal/mole to 7.77 kcal/mole (barrier from 17.98 kcal/mole to 15.58 kcal/mole) in order to obtain agreement with experimental data of Atri et al.[58] Accuracy of these calculations for barrier is discussed in session 3.7 and we consider this reduction of 2.4 kcal/mole in one barrier reasonable. We further note that the mechanism results increase by only 0.2% and 1.07% in absolute concentration for isobutene and 2,2-dimethyloxirane formations, respectively, when this barrier is changed from 17.98 kcal/mole to 15.58 kcal/mole. The *tert*-butyl precursor, 2,2,3,3-tetramethylbutane is decreased by 0.8% in absolute concentration.

In Figure 2B.3 can been seen a comparison of our calculation with experimental data at 773K and 60 torr. Use of 15.58 and 17.98 kcal/mole barriers for the 2,2-dimethyloxirane + OH radical channel from $C_3{\cdot}COOH$ result in 1.62% and 0.55% yield of 2,2-dimethyloxirane at 210 seconds reaction, respectively. The corresponding data are illustrated via dash and dot lines in Figure 2B.3; and the Δ symbols are data of Atri et al.[58] which show a 1.6% yield at 210 seconds.

Sensitivity analysis shows that an increase in the A factor for the reaction $C_3COO{\cdot} \leftrightarrow TS1 \leftrightarrow C_2C{=}C + HO_2$ by 10 (direct HO_2-molecular elimination from $C_3COO{\cdot}$), both forward and reverse directions, results in a decrease of 2,2-dimethyloxirane formation by 47.67% at 15 seconds and 8.04% at 210 seconds. If the A factor of $C_3COO{\cdot} \leftrightarrow TS2$ is increased by 10 (H-shift isomerization to $C_3{\cdot}COOH$ which dissociates to $C_2C{=}C + HO_2$), the 2,2-dimethyloxirane formation is almost unchanged; it increases by only 2.43% at 15 seconds and 0.44% at 210 seconds. When the A factor for $C_2C{=}C + HO_2 \leftrightarrow [C_2C{\cdot}COOH]^* \leftrightarrow C_2C{\cdot}COOH$ is increased by 10, the 2,2-dimethyloxirane formation is again not changed significantly; it increases by 1.75% at 15 seconds and 3.93% at 210 seconds. Those results are at 60 Torr and 773K. Figure 2B.14 shows the relative contribution of specific reaction paths to 2,2-dimethyloxirane formation at 773K and 60 torr. At early times the primary path is via the $[C_3COO{\cdot}]^*$ adduct isomerization (H-shift) to $[C_3{\cdot}COOH]^*$ adduct then reaction to the 2,2-dimethyloxirane plus OH. This path decreases in importance as HO_2 radical and stable isobutene build up in concentration. After several seconds of reaction the primary path for 2,2-dimethyloxirane formation is from HO_2 addition to isobutene to form $[C_3{\cdot}COOH]^*$ (lower barrier addition) then reaction to 2,2-dimethyloxirane plus OH. The addition reactions of HO_2 + olefins in these moderate temperature hydrocarbon oxidation systems are clearly important. The O_2 and HO_2 addition reaction and isomerization reaction all have important reverse reaction paths; but due to the high reactivity of OH, the oxirane + OH channel does not.

3.5.7 Decomposition of 2,2-Dimethyloxirane (C_2CYC_2O)

C_2CYC_2O reacts with radicals, such as OH, $C_2{\cdot}C{=}C$, $C_3COO{\cdot}$, CH_3, $CH_3OO{\cdot}$and $C{=}CC{\cdot}$ to lose a H atom via abstraction.

$$C_2CYC_2O + OH \longrightarrow C_2CYCC{\cdot}O + H_2O$$

$$C_2CYC_2O + C_2{\cdot}C{=}C \longrightarrow C_2CYCC{\cdot}O + C_2C{=}C$$

$$C_2CYC_2O + C{=}CC{\cdot} \longrightarrow C_2CYCC{\cdot}O + C{=}CC$$

$$C_2CYC_2O + CH_3COO{\cdot} \longrightarrow C_2CYCC{\cdot}O + C_3COOH$$

$$C_2CYC_2O + CH_3OO{\cdot} \longrightarrow C_2CYCC{\cdot}O + CH_3OOH$$

$$C_2CYC_2O + CH_3 \longrightarrow C_2CYCC{\cdot}O + CH_4$$

The $C_2CYCC{\cdot}O$ once formed will rapidly break one of the C-O single bonds, releasing the relatively high ring strain (three member ring) and forming a strong carbonyl (C=O) bond. Subsequent elimination of a H atom to form methacrolein and dimethylketene products then occurs.

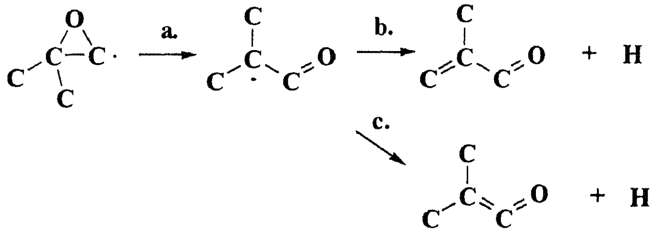

ΔH_{rxn} (a) = -23.93 kcal/mole

ΔH_{rxn} (b) = 38.26 kcal/mole

ΔH_{rxn} (c) = 37.54 kcal/mole

3.5.8 Reactions Important to $C_2C{=}C$ Formation

The research group of Walker[72-74, 83] has suggested that isobutene is a major and a primary product in the decomposition of 2,2,3,3-tetramethylbutane (C_3CCC_3) in the presence of O_2 in KCl-coated vessels. Our analysis indicates that it is formed mainly from $C_3C\cdot$ radicals with O_2 (described above).

The unimolecular decomposition reaction of $C_3C\cdot$ radicals is, on a relative base, slow at 773K, and isobutene formation by this path is slow. We use the high-pressure limit rate constant for $C_3C\cdot \rightarrow C_2C{=}C + H$ to be $(2.5\text{x}10^{16}T^{-0.92}s^{-1})\exp(-37500/RT)$; rate constants of Knyazev or of Tsang result in little or no change in relative rates.

3.5.9 Isobutene Reaction

Isobutene is consumed by slower reactions, such HO_2 addition then further reaction to 2,2-dimethyloxirane + OH, or addition with OH then reaction of this hydroxyl adduct with O_2. These reaction systems are discussed in the previous sections. Isobutene also reacts by abstraction (loss) of its allylic H atoms (allylic C--H bond energy only 88 kcal/mole) by HO_2, OH, O, O_2 and CC·DC radicals.

$$C_2C{=}C + HO_2 \rightarrow C_2{\cdot}C{=}C + H_2O_2$$

$$C_2C{=}C + OH \rightarrow C_2{\cdot}C{=}C + H_2O$$

$$C_2C{=}C + O_2 \rightarrow C_2{\cdot}C{=}C + HO_2$$

$$C_2C{=}C + O \rightarrow C_2{\cdot}C{=}C + OH$$

$$C_2C{=}C + CC{\cdot}{=}C \rightarrow C_2{\cdot}C{=}C + C{=}CC$$

3.5.10 Loss of 2,2,3,3-Tetramethylbutane (C_3CCC_3)

The *tert*-butyl radical is generated by the homogeneous decomposition of 2,2,3,3 tetramethylbutane in presence of O_2.

$$(CH_3)_3C\text{-}C(CH_3)_3 \longrightarrow 2\ C_3C^{\cdot} \qquad (1)$$

C_3CCC_3 can also undergo abstraction of H atom by HO_2, OH, $C_3C\cdot$ and $CC\cdot{=}C$ radicals.

$$C_3CCC_3 + HO_2 \longrightarrow C_3{\cdot}CCC_3 + H_2O_2$$

$$C_3CCC_3 + OH \longrightarrow C_3{\cdot}CCC_3 + H_2O$$

$$C_3CCC_3 + O \longrightarrow C_3{\cdot}CCC_3 + OH$$

$$C_3CCC_3 + C_3C{\cdot} \longrightarrow C_3{\cdot}CCC_3 + C_3C$$

$$C_3CCC_3 + CC{\cdot}{=}C \longrightarrow C_3{\cdot}CCC_3 + C{=}CC$$

The $C_3{\cdot}CCC_3$ radical undergoes a β-scission or further reacts with O_2. The β-scission reaction is more important above 1000K and is an added source of isobutene. (Q represents OOH group.)

$$C_3{\cdot}CCC_3 \longrightarrow C_3C{\cdot} + C_2C{=}C$$

$$\begin{tikzcd}
C_3{\cdot}CCC_3 + O_2 \arrow[d, leftrightarrow] & & \\
C_3CCC_3Q{\cdot} \arrow[r] \arrow[d] & C_3CC_2{\cdot}CQ \arrow[r] & C_3CC{=}C(C)\ {\cdot}{+}\ C{\cdot}H_2OOH \\
C_3{\cdot}CCC_3Q \arrow[r] & C_2C{=}C + C_2C{\cdot}COOH &
\end{tikzcd}$$

3.6 Model and Comparison to Experimental Data

A reaction mechanism includes the sub reaction systems discussed above is assembled, Table 2A.4. The CHEMKIN II interpreter and integrator, version 3.1, is used to model the reaction conditions of Atri et al.[58] for reaction time range (0 - 210 sec), 773 K and 60 torr. Wall loss reactions of Atri et al.[58] are included in the mechanism. Abstraction reactions are not considered pressure dependent, and therefore do not require any falloff analysis. Abstraction reactions of O, OH, HO_2 and R· radicals are taken from evaluated literature wherever possible. A procedure from Dean and Bozzelli[92] is used to estimate abstraction rate constants by H, O, OH and CH_3 radicals when no literature data available. A generic rate constant is utilized and adjusted for steric effects and reaction enthalpy for hydrogen abstractions by: C=CC· and HO_2 radicals.

The comparison of model calculations to experiments for loss of *tert*-butyl precursor, 2,2,3,3-tetramethylbutane, production of isobutene and 2,2-dimethyloxirane over the reaction time range (0 - 210 sec), 773 K and 60 torr is illustrated in Figure 2B.3. The model shows good agreement with experimental data of Atri et al.[58]

Rate constants at pressures of 0.076, 0.76, 7.6, 60, 760, and 7600 torr for the chemical activation and unimolecular reactions described above are listed in Table 2A.4.

3.7 Accuracy of *Ab Initio* and Density Functional CBS Calculations

The CBS-q calculation method suggests use of the HF/3-21g basis set optimized parameters. We select more accurate calculation level (B3LYP/6-31g(d) and MP2(full)/6-31g(d)) for geometry optimization and frequency calculation in the composite CBS-q calculations for analysis of energies of activation and Arrhenius pre-exponential factors.

Curtiss et al.[93] report that B3LYP/6-31g(d,p) provides highly accurate structures for compounds with elements up to atomic number 10. Curtiss et al.[93] further report average errors on a test set of 148 molecules of 1.58 kcal/mole for G2 energy calculation results with a maximum error of 8.4 kcal/mole.

J. Durant[94, 95] has compared density functional calculations BHandH and B3LYP with MP2 and Hartree-Fock methods for geometry and vibration frequencies. Durant[94, 95] reports that these density functional methods provide excellent (improved) geometries and vibration frequencies, relative to MP2 at reduced computation expense. Petersson et al.[96-98] currently recommends use of B3LYP or BLYP for geometries and frequencies in CBS calculations.

Jungkamp and Seinfeld[99] report rms errors for CBS-q//B3LYP/6-31g(d,p) calculated enthalpies of 1.7 kcal/mole for a test set of 10 transition state barriers. They also show DFT optimized geometries result in significantly improved structures, enthalpies and bond energies over the recommended HF/3-21g(d) level where a rms error of 4.1 kcal/mole was noted.

Mebel at al.[100] report use of B3LYP/6-31g(d,p) for geometries in their modified G2M(RCC,MP2) method as leading to improved accuracy for intermediates and transition states in application to vinyl radical reaction with O_2. They show several comparisons to experimental data where G2M(RCC,MP2) energy is underestimated by 2.5 kcal/mole for vinyl radical.

Jungkamp and Seinfeld[47] analyze the reaction system of primary and secondary butyl radicals with O_2 using CBS-q//B3LYP/6-31g(d,p) level calculations and show good agreement with group additivity calculated reaction enthalpies. Yamada et al.[49, 101, 102] show very good agreement between G2 and CBS-q//MP2(full)/6-31g(d,p) calculations, within 2 kcal/mole for stable and radical species in ethylene + OH and di-methyl ether radical + O_2 reaction systems. Yamada reports that Transition state energies show a maximum difference of 4.2 kcal/mole between the two composite methods for his two chemical activated systems with an average absolute difference of 1.6 kcal/mole for 8 transition state structures.

Wang and Brezinsky[103] implemented a B3LYP/6-31g(d) optimized structure into G2(MP2) calculation method and demonstrate accuracy of B3LYP/6-31g(d) structures. They compare calculated energies on the 55 molecules used in the original G2 study[93]. Their calculations resulted in improved energies over G2(MP2) with G2(B3LYP/MP2) average and maximum deviation of 1.32 and 3.7 kcal/mole, respectively.

It is difficult to accurately estimate error for TST species in these peroxy radical reaction systems. Our adjustment to match experimental data in this work is 2.4 kcal/mole- decrease in the calculated value for one transition state. A similar decrease in one calculated barrier was noted by Yamada et al.[49], 3 kcal/mole, in order to match calculated falloff data with experiment in the di-methyl ether radical + O_2 system.

3.8 Summary

A thermodynamic and chemical activation reaction analysis is done on the important reaction systems: *tert*-butyl radical + O_2, isobutene + HO_2, isobutene + OH and isobutene-OH + O_2. Thermodynamic proprieties, reaction paths and elementary reactions for these systems are presented versus temperature and pressure. An elementary reaction mechanism has been developed to model the experimental system - decomposition of 2,2,3,3 tetramethylbutane in the presence of oxygen, where reactions of *tert*-butyl radical and isobutene are of primary importance. Our modeling indicates the isobutene + HO_2

formation via HO_2-molecular elimination channel is faster than Hydrogen-shift channel at 773K and 60 Torr for $C_3C\cdot + O_2$ reaction. The reaction barrier for the $C_3\cdot COOH$ reaction to 2,2-dimethyloxirane + OH is evaluated as 15.58 (18.1) kcal/mole by fitting experimental data. Data in parentheses are thermodynamic properties based on CBS-q//B3LYP/6-31g(d) calculation. Barriers for reactions of HO_2 + isobutene → $C_3\cdot COOH$ (HO_2 addition at CD/C2 carbon atom of isobutene) and HO_2 + isobutene → $C_2C\cdot COOH$ (HO_2 addition at CD/H2 carbon atom of isobutene) are determined to be 7.74 (7.38) and 10.69 (10.82) kcal/mole, respectively. Detailed pathway explanations of the Waddington mechanism and rates constants for elementary steps are presented. Results from the mechanism are in good agreement with experimental data reported by Atri et al.[58]

CHAPTER 4

THERMOCHEMICAL KINETIC ANALYSIS ON THE REACTIONS OF ALLYLIC ISOBUTENYL RADICAL WITH O_2: AN ELEMENTARY REACTION MECHANISM FOR ISOBUTENE OXIDATION

4.1 Overview

Kinetics for the reactions of allylic isobutenyl radical ($C_2{\cdot}C{=}C$) with molecular oxygen are analyzed by using quantum Rice-Ramsperger-Kassel (QRRK) theory for *k(E)* and master equation analysis for falloff. Thermochemical properties and reaction path parameters are determined by *ab initio* - Mϕller-Plesset (MP2(full)/6-31g(d) and MP4(full)/6-31g(d,p)// MP2(full)/6-31g(d)), complete basis set model chemistry (CBS-4 and CBS-q with MP2(full)/6-31g(d) and B3LYP/6-31g(d) optimized geometries), and density functional (B3LYP/6-31g(d) and B3LYP/6-311+g(3df,2p)// B3LYP/6-31g(d)) calculations. An elementary reaction mechanism is constructed to model the experimental system - isobutene oxidation. The forward and reverse rate constants for initiation reaction $C_2C{=}C + O_2 \leftrightarrow C_2{\cdot}C{=}C + HO_2$ are determined to be $1.86 \times 10^9 T^{1.3} \exp(-40940\text{cal}/RT)$ ($\text{cm}^3\text{mole}^{-1}\text{s}^{-1}$) and $6.39 \times 10^8 T^{0.94} \exp(-120\text{cal}/RT)$ ($\text{cm}^3\text{mole}^{-1}\text{s}^{-1}$), respectively. Calculations on 2,5 dimethylhexa-1,5-diene, methacrolein, isobutene oxides and acetone product formation from reaction of isobutene oxidation mechanism are compared with experimental data. Reaction of allylic isobutenyl radical + O_2 forms an energized peroxy adduct $[C{=}C(C)COO{\cdot}]^*$ with a shallow well (ca. 21 kcal/mole), which predominantly dissociates back to reactants. The reaction channels of the $C{=}C(C)COO{\cdot}^*$ adduct include dissociation back to reactants, stabilization to

C=C(C)COO· radical, O-O bond fission to C=C(C)CO· + O, isomerization via hydrogen shift with subsequent β-scission or R·O-OH bond cleavage. The C=C(C)COO·* adduct

C=C(C)COO· radical, O-O bond fission to C=C(C)CO· + O, isomerization via hydrogen shift with subsequent β-scission or R·O-OH bond cleavage. The C=C(C)COO·* adduct

can also cyclize to four or five-member cyclic peroxide-alkyl radicals. All the product formation pathways of allylic isobutenyl radical with O_2 involve barriers that are above the energy of the initial reactants. This results in formation of isomers which exist in steady state concentration at early time in oxidation – at low to moderate temperatures. The primary reaction is reverse dissociation back to reactants, with slower reactions from the distributed isomers to new products. The concentration of allylic isobutenyl radical accumulates to relatively high levels and the radical is consumed mainly through radical-radical processes in moderate temperature isobutene oxidation. Reactions of C=C(C)COO· cyclization to four or five-member cyclic peroxides require relative high barriers due to the near complete loss of pi bond energy for the terminal double bond's twist needed in the transition states. These barriers are calculated as 28.02 (24.95) and 29.72 (27.98) kcal/mole at CBS-q//MP2(full)/6-31g(d) level with A factors of $2.42\text{x}10^{10}$ ($3.28\text{x}10^{10}$) and $3.88\text{x}10^{10}$ ($6.09\text{x}10^{10}$) s^{-1} at 743K, respectively, for four and five-member ring cyclization. Data in parentheses are calculation at B3LYP/6-311+g(3df,2p)//B3LYP/6-31g(d). A new reaction path is proposed: C=C(C·)COOH ↔ C=C(C·)CO· + OH ↔ C=Y(CCOC) + OH, which is responsible for methylene oxirane formation (Y=cyclic). The reaction barrier for the C=C(C·)COOH reaction to C=C(C·)CO· + OH is evaluated as 42.45 (41.90) kcal/mole with an A factor of $4\text{x}10^{15}s^{-1}$.

The reaction barrier of C=C(C·)COOH → TS5 → C=Y(CCOC) + OH is calculated as 42.14 (32.00) kcal/mole with an A factor of 6.95×10^{11} (1.03×10^{12}) s^{-1} at 743K.

4.2 Introduction

Alkenes are major initial products from pyrolysis, oxidation or photochemical reaction of alkanes. The double bond in alkenes allows both addition and abstraction reactions to occur which enhance complexity in studies on these compounds. The relatively high octane ratings for olefin blending suggest olefin reactions play an important role in pre-ignition chemistry related to engine knock. It is of value to try and understand the fundamental chemical pathways and reaction kinetics of olefin oxidation in this moderate to low temperature combustion chemistry for future model development and optimization. The oxidation reactions of olefins are also important in the atmosphere photochemistry of hydrocarbons, biochemical synthesis and metabolism.[104-108]

Brezinsky and Dryer[109] have studied the oxidation of isobutene and isobutene/n-octane mixture in a high temperature flow reactor. They attributed the inhibiting effect of isobutene on the progress of the n-octane oxidation to abstraction reactions of radicals with the isobutene which result in relatively unreactive isobutenyl radical and species, such as HO_2, CH_3, C=CC etc.

Ingham et al.[110] studied the oxidation of isobutene at temperature from 673 to 793 K and pressure at 60 torr, in flow reactor (aged boric-acid-coated vessels) - with slow flow - up to several minute reaction times. They report a rate constant for initiation reaction $C_2C{=}C + O_2 \leftrightarrow C_2{\cdot}C{=}C + HO_2$ to be $4.79 \times 10^{12}\exp(-38570/RT)$ $cm^3 mole^{-1} s^{-1}$. They also report concentration profiles for selected reaction products 2,5 dimethylhexa-

1,5-diene, methacrolein, isobutene oxide and acetone. Recently, Bauge et al.[111] have determined the global reactivity of isobutene ignition delays in shock-tube (at temperature from 1230 to 1930K and pressure from 9.5 to 10.5 atm). They also measured the product profiles in the perfectly stirred reactor (at temperature from 833 to 913K and 1 atm). They proposed a mechanism, which does not include the reactions of oxygen addition with $C_2 \cdot C=C$, to model the product profiles measured from stirred reactor.

In this study, thermochemical analysis is performed on the reactions of allylic isobutenyl radical with oxygen using thermodynamic properties ($\Delta H_f°_{298}$, $S°_{298}$, and Cp(300) to Cp(1500)) derived by *ab initio* and density functional calculations; and a chemical activation kinetic treatment incorporating quantum Rice-Ramsperger-Kassel (QRRK) theory for *k(E)* and master equation[13-15] of Gilbert et al. for falloff on the energized adduct. A multi-channel unimolecular Quantum RRK analysis is used for analysis of the stabilized adduct dissociations. Calculations for production of 2,5 dimethylhexa-1,5-diene, methacrolein, isobutene oxides and acetone from isobutene oxidation mechanism are compared to experimental data of Ingham et al.[110] Calculated reaction rates of allylic isobutenyl radical + O_2 are in agreement with the experimental value of Knyazev et al.[112]

4.3 Method

4.3.1 *Ab Initio* and Density Functional Calculations

The geometries of reactants, important intermediates, transition states and products in allylic isobutenyl radical + O_2 reaction system are pre-optimized using UHF/PM3

MOPAC[51] program, followed by optimizations and frequency calculations at MP2(full)/6-31g(d) and B3LYP/6-31g(d) levels of theory using the Gaussian94[52] program. Transition state (TS) geometries are identified by the existence of only one imaginary frequency in the normal mode coordinate analysis, evaluation of the TS geometry, and the reaction's coordinate vibration information.

Complete basis set (CBS-4 and CBS-q) model chemistry calculations[54-56] are also performed in this study on the MP2(full)/6-31g(d) and B3LYP/6-31g(d) determined geometries. They include single point calculation at the QCISD(T)/6-31g, MP4(SDQ)/6-31g(d'), MP2/6-31+d(d,p), and HF/CBSB1 levels of theory. CBS-q calculations are chosen because Jungkamp et al.[47, 48], Petersson et al.[49] and our group[50] have shown that they result in reasonable accurate thermodynamic enthalpy data for these (5 or 6 heavy atoms) oxyhydrocarbon molecular systems. CBS-q and G2(MP2) are probably the best composite methods for these 6 heavy atoms systems.

4.3.2 Thermodynamic Properties - $\Delta H_f°_{298}$, $S°_{298}$, and Cp (300) to Cp (1500)

Entropies and heat capacities are calculated based on frequencies and moments of inertia of the optimized MP2 (full)/6-31g(d) and B3LYP/6-31g(d) structures. Vibrational frequency contributions to entropies and heat capacities are scaled by 1.0228 and 1.0015 for MP2 (full)/6-31g(d) and B3LYP/6-31g(d) calculations, respectively, as recommended by Scott et al.[53] The method of Pitzer and Gwinn[57] is used for thermodynamic analysis of $S°_{298}$, and Cp (T) contribution from hindered internal rotors. The numbers of optical isomers and spin degeneracy of unpaired electrons are incorporated.

Zero-point vibrational energies (ZPVE) and thermal contributions to enthalpy are calculated at MP2 (full)/ 6-31g(d) and B3LYP/ 6-31g(d) levels. The vibrational frequency contributions to ZPVE are also scaled by 0.9661 and 0.9806 for MP2 (full)/6-31g(d) and B3LYP/6-31g(d) calculations, respectively. Total energies are calculated at MP2 (full)/ 6-31g(d), B3LYP/ 6-31g(d), MP4 (full)/ 6-31g(d, p)// MP2 (full)/ 6-31g(d), B3LYP/ 6-31g(d), B3LYP/ 6-311+g(3df,2p)// B3LYP/ 6-31g(d) and complete basis set (CBS-4 and CBS-q) model chemistry calculations[54-56] and listed in Table 3A.1. The CBS-4 and CBS-q calculations are performed using geometry optimizations at MP2(full)/ 6-31g(d) and B3LYP/ 6-31g(d) levels of theory. Total energies (at 298K) differences between TS and reactants, intermediates, and products determined at different theory levels are listed in Table 3A.2.

Reactions (IR1-IR15) are used to determine $\Delta H_f{}^\circ{}_{298}$ for reactant, intermediate radicals and products in the reaction systems of this study (target species). These reactions conserve both bond types (isodesmic) and groups. Calculations are performed on each species in the reaction to determine $\Delta H_{rxn,\,298}$. $\Delta H_f{}^\circ{}_{298}$ values of the needed species in a reaction are determined from the $\Delta H_{rxn,\,298}$ and evaluated literature $\Delta H_f{}^\circ{}_{298}$ values of the remaining species. These target species include: reactant, $C_2{\cdot}C{=}C$; intermediate radicals, C=C(C)COO·, C=C(C·)COOH, CY(C·COOC), $C_2{\cdot}Y(CCOO)$, $C(YC_2O)CO{\cdot}$, C=C(C)OOC· and C·OOH; and two products, C=Y(CCOC) and C=C(C)C=O.

For estimation of $C_2{\cdot}C{=}C$

$C_2{\cdot}C{=}C + C{=}C{-}C \longleftrightarrow C_2C{=}C + C{=}C{-}C{\cdot}$ (IR1)

For estimation of $\mathrm{C{=}C(C)COOH}$

$\mathrm{C{=}C(C)COOH + C{=}C\text{-}C + CH3OH \longleftrightarrow C{=}CCOH + C_2C{=}C + CH_3OOH}$ (IR2)

For estimation of $\mathrm{C{=}C(C)COO\cdot}$

$\mathrm{C{=}C(C)COO\cdot + CH_3OOH \longleftrightarrow C{=}C(C)COOH + CH_3OO\cdot}$ (IR3)

For estimation of $\mathrm{C{=}C(C\cdot)COOH}$

$\mathrm{C{=}C(C\cdot)COOH + C{=}C\text{-}C \longleftrightarrow C{=}C(C)COOH + C{=}C\text{-}C\cdot}$ (IR4)

For estimation of $\mathrm{CY(CCOOC)}$

$\mathrm{CY(CCOOC) + COCOC + CC \longleftrightarrow Y(CCOCO) + COOC + C_3C}$ (IR5)

For estimation of $\mathrm{CY(C\cdot COOC)}$

$\mathrm{CY(C\cdot COOC) + CC \longleftrightarrow CY(CCOOC) + CC\cdot}$ (IR6)

For estimation of $\mathrm{C_2Y(CCOO)}$

$\mathrm{C_2Y(CCOO){+}CCOC{+}CCC{+}CH_3OH \longleftrightarrow Y(COOC){+}C_3COH{+}COOC{+}CC}$ (IR7)

For estimation of $\mathrm{C_2\cdot Y(CCOO)}$

$\mathrm{C_2\cdot Y(CCOO) + CC \longleftrightarrow C_2Y(CCOO) + CC\cdot}$ (IR8)

For estimation of $\mathrm{C\cdot OOH}$

$\mathrm{C\cdot OOH + CH_3OH \longleftrightarrow CH_3OOH + CH_3O\cdot}$ (IR9)

For estimation of $\mathrm{C{=}C(C)OOC}$

$\mathrm{C{=}C(C)OOC + COOH \longleftrightarrow COOC + C{=}C(C)COOH}$ (IR10)

For estimation of $\mathrm{C{=}C(C)OOC\cdot}$

$\mathrm{C{=}C(C)OOC\cdot + COC \longleftrightarrow C{=}C(C)OOC + COC\cdot}$ (IR11)

For estimation of $\mathrm{CY(C_2O)COH}$

$\mathrm{CY(C_2O)COH + CC \longleftrightarrow Y(CCO) + C3COH}$ (IR12)

For estimation of $CY(C_2O)CO\cdot$

$CY(C_2O)CO\cdot + CH_3OH \longleftrightarrow CY(C_2O)COH + CH_3O\cdot$ (IR13)

For estimation of C=Y(CCOC)

$C{=}Y(CCOC) + 2CCCOH + 2C{=}CC \longleftrightarrow Y(CCCO) + 2C{=}CCOH + C_2C{=}C +$ (IR14)

CCC

For estimation of C=C(C)C=O

$C{=}C(C)C{=}O + C{=}CC \longleftrightarrow C_2C{=}C + C{=}C\text{-}C{=}O$ (IR15)

Group balance reaction enthalpies (IR1-IR15) are calculated at CBS-q//MP2(full)/6-31g(d), CBS-q// B3LYP/6-31g(d), MP4(full)/6-31g(d,p)//MP2(full)/6-31g(d), MP2(full)/6-31g(d), B3LYP/6-311+g(3df,2p)//B3LYP/6-31g(d), and B3LYP/6-31g(d) levels and listed in Table 3A.3a. $\Delta H_f{}^\circ{}_{298}$ of reactant, intermediate radicals and products calculated from the reactions are listed in Table 3A.3b. Enthalpies of formation of species adopted from literature, which are used to determine $\Delta H_f{}^\circ{}_{298}$ values of species studied in this work are listed in Table 3A.3c.

$\Delta H_f{}^0{}_{TS}$ Reaction Scheme

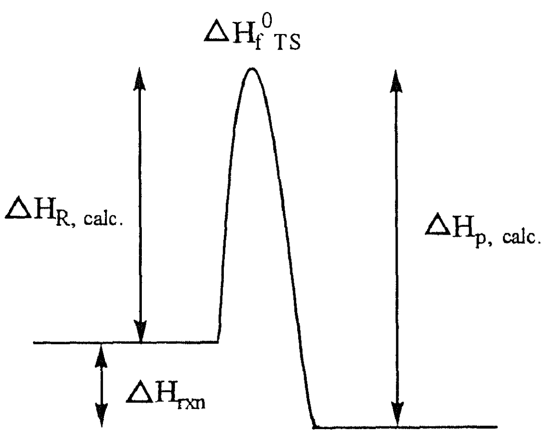

$\Delta H_{R,\ calc.} = \Delta H_{rxn}$ (reactant $\rightarrow$ TS)

$\Delta H_{P',\ calc.} = \Delta H_{rxn}$ (Product $\rightarrow$ TS) $+ \Delta H_{rxn}$

$$\Delta H_f{}^0{}_{TS} = \frac{\Delta H_{R,\ calc.} + \Delta H_{P',\ calc.}}{2}$$

Calculation of enthalpy of formation for transition states is illustrated in the $\Delta H_f{}^0{}_{TS}$ Reaction Scheme. $\Delta H_f{}^0{}_{TS}$ is calculated by an average of two values $\Delta H_{R,\ calc.}$ and $\Delta H_{P'}$,

$_{calc.}$. $\Delta H_{R,\ calc.}$ is the difference between the calculated energy of the TS and reactant(s). $\Delta H_{P',\ calc.}$ is the difference between the calculated energy of the TS and product(s) plus ΔH_{rxn} ($\Delta H_f^o{}_{product(s)} - \Delta H_f^o{}_{reactant(s)}$). $\Delta H_f{}^\circ{}_{298}$ of products and reactants are obtained from group balance isodesmic reactions (IR1-IR15). Thermodynamic parameters - $\Delta H_f{}^\circ{}_{298}$, $S^\circ{}_{298}$, and Cp(300) to Cp(1500) for species in allylic isobutenyl radical + O_2 reaction system are listed in Table 3A.4.

4.3.3 Kinetic Calculations

Unimolecular dissociation and isomerization reactions of the chemically activated and stabilized adducts resulting from addition or combination reactions are analyzed by first constructing potential energy diagrams for the reaction system. Thermodynamic parameters, $\Delta H_f{}^\circ{}_{298}$, $S^\circ{}_{298}$, Cp(T), reduced vibration frequency sets, and Lennard Jones parameters for species in each reaction path are presented.

High-pressure rate constants (k_∞) for each channel are obtained from *ab initio* calculation, literature, or referenced estimation techniques. Kinetics parameters for unimolecular and bimolecular (chemical activation) reactions are then calculated using multi-frequency QRRK analysis for *k*(*E*)[21-23] with the steady state assumption on the energized adduct(s). The master equation analysis[13-15] as discussed by Gilbert is used for falloff.

Reactions which incur a change in number of moles, such as unimolecular dissociation, have energy of activation calculated as delta U_{rxn} plus an E_a for the reverse addition, where U is internal energy (E_a reverse is usually 0.0 for simple association reactions).

4.3.4 Input Information Requirements for QRRK Calculation

Pre-exponential factors (A_∞s) are calculated using canonical TST[25] along with MP2 or DFT-determined entropies of intermediates and TSs for the reactions where thermodynamic properties of TS are available. High-pressure rate constants (k_∞) are represented using three parameters A, n and E_a over a temperature range of 300 to 2000K as expressed below.

$$k_\infty = A\,(T)^n \exp(-E_a/RT)$$

High-pressure limit pre-exponential factors for combination reactions are obtained from the literature and from trends in homologous series of reactions.

Reduced sets of three vibration frequencies and their associated degeneracies are computed from fits to heat capacity data, as described by Ritter and Bozzelli et al.[17, 18] These have been shown by Ritter to accurately reproduce molecular heat capacities, Cp(T), and by Bozzelli et al.[18] to yield accurate ratios of density of states to partition coefficient, $\rho(E)/Q$.

Lennard-Jones parameters, sigma (Angstroms) and ε/k (Kelvins), are obtained from tabulations[19] and from a calculation method based on molar volumes and compressibility.[20] When necessary, estimation is done in a consistent and uniform manner via use of generic reaction rate constants with reference to literature, experiment or theoretical calculation in each case. The QRRK calculation input parameters and their references are listed in the table associated with the respective reaction system.

4.3.5 Recent Modifications to the Quantum RRK Calculation

a; Use of a manifold of three frequencies plus incorporation of one external rotation for the density of states, $\rho(E)/Q$ and in calculation of $k(E)$.

b; The Leonard-Jones collision frequency Z_{LJ} is now calculated by $Z_{LJ} = Z\ \Omega\ (2,2)$ integral[19, 20] obtained from fit of Reid et al.[20]

The QRRK analysis for $k(E)$ with modified strong collision and a constant F_E for falloff has been used previously to analyze a variety of chemical activation reaction systems, Westmoreland et al.[21, 22], Dean et al.[23],and Bozzelli et al.[24, 25] There are a number of recent publications by other researchers that utilize the QRRK formalism with a more exact calculation F_E in modified strong collision analysis[26-31] or utilize just a QRRK formalism.[32, 33] It is shown to yield reasonable results in these applications, and provides a framework by which the effects of temperature and pressure can be evaluated for complex chemical activation or unimolecular dissociation reaction systems. The QRRK formalism used in this work is recently described by Chang et al.[10] The $C_2 \cdot C{=}C + O_2$ reaction system is complex and we suggest QRRK analysis with either modified strong collision or master equation for falloff as reasonable methods to estimate rate constants as a function of temperature and pressure for all channels in this complex system.

4.4 Results and Discussion

4.4.1 Formation of Allylic Isobutenyl Radical ($C_2 \cdot C{=}C$); Reaction Initiation

There are two reaction initiation processes: abstraction of hydrogen by O_2 and unimolecular dissociation. The resonance stabilized allylic isobutenyl radical is formed by abstraction the weakly bonded hydrogen atom (the allylic C-H bond is 88.1 kcal/mole) from isobutene. The endothermic initiation reaction (1) is a key rate-determining reaction in moderate temperature isobutene oxidation.

$$C_2C{=}C + O_2 \xleftrightarrow{TS10} C_2{\cdot}C{=}C + HO_2 \qquad (1)$$

$$\Delta H_{298} = 39.86 \text{ kcal/mole}$$

We find a small barrier of 0.28 kcal/mole based on CBS-q//MP2(full)/6-31g(d) calculation and no barrier based on B3LYP/6-311+g(3df,2p)//B3LYP/6-31g(d) calculation for reverse reaction (1).

Arrhenius pre-exponential factor, A_∞, is calculated via canonical TST. The high pressure limit rate constants, fit by a three parameter (A, n, Ea) modified Arrhenius Equation over temperature range 300K to 2000K, are $1.86 \times 10^9 T^{1.30} \exp(-40940 \text{ cal /RT})$ (cm^3 $mole^{-1}$ s^{-1}) and $6.39 \times 10^8 T^{0.94} \exp(-120 \text{ cal /RT})$ (cm^3 $mole^{-1}$ s^{-1}) for forward and reverse reaction (1), respectively, based on CBS-q//MP2(full)/6-31g(d) calculation. Comparison of our calculated rate constant with experimental values for the similar reaction of allyl radical, $C{=}C{-}C + O_2 \Rightarrow C{=}C{-}C{\cdot} + HO_2$, is shown in Figure 3B.1.

Sensitivity analysis shows that an increase in the A factor of reaction (1) by a factor of 2, results in an increase of acetone, methacrolein, 2,5-dimethylhexa-1,5-diene, and methylene oxirane formations by 7.13% (7.34%), 8.21% (8.74%), 7.81% (8.30%), and 11.70% (12.60%) respectively, at 743K and 60torr (reaction time = 210 sec). Results are based on thermodynamic properties calculated from CBS-q//MP2(full)/6-31g(d), data in parentheses are from B3LYP/6-311+g(3df,2p)//B3LYP/6-31g(d) calculation.

The unimolecular decomposition of isobutene to allylic isobutenyl radical with H atom is also included in mechanism.

$$C_2C{=}C \longleftrightarrow C_2{\cdot}C{=}C + H$$

We use high pressure limit rate constant 2×10^{15} exp(-87390 cal /RT) (s^{-1}) obtained from experimental data of Douhou et el[113].

The radicals, OH, HO_2 and $CH_3COCH_2\cdot$ ($C_2\cdot C{=}O$), can undergo abstraction reaction (2), (3), and (4) to form allylic isobutenyl radical under moderate temperature oxidation condition, with $CH_3C\cdot CH_2$ ($C\text{-}C\cdot{=}C$) having less importance.

$$C_2C{=}C + OH \longleftrightarrow C_2\cdot C{=}C + H_2O \qquad (2)$$

$$C_2C{=}C + HO_2 \longleftrightarrow C_2\cdot C{=}C + H_2O_2 \qquad (3)$$

$$C_2C{=}C + C_2\cdot C{=}O \longleftrightarrow C_2\cdot C{=}C + C_2C{=}O \qquad (4)$$

$$C_2C{=}C + CC\cdot{=}C \longleftrightarrow C_2\cdot C{=}C + CC{=}C \qquad (5)$$

We use rate constants $4.68 \times 10^6\, T^{2.0}$ exp(300 cal /RT) ($cm^3mole^{-1}s^{-1}$) and $1.93 \times 10^4\, T^{2.6}$ exp(-13910 cal /RT) ($cm^3mole^{-1}s^{-1}$) for reaction (2) and (3), respectively, following the analogous reaction of propene[114] and adjustment for steric effects. Rate constants of reaction (4) and (5) are $2.23 \times T^{3.5}$ exp(-6640 cal /RT) ($cm^3mole^{-1}s^{-1}$) and $4.42 \times T^{3.5}$ exp(-4680 cal /RT) ($cm^3mole^{-1}s^{-1}$). The radical $C\text{-}C\cdot{=}C$ arises from β-scission of $C{=}C(C)CO\cdot$, which is formed from cleavage of the weak (ca. 43 kcal/mole) O-O single bond of $C{=}C(C)COOH$. The $C{=}C(C)CO\cdot$ undergoes β-scission forming $C\text{-}C\cdot{=}C$ radical and CH_2O. (The $C{=}C(C)C{=}O$ + H reaction path is also included in our mechanism.)

4.4.2 Allylic Isobutenyl Radical ($C_2\cdot C{=}C$) + O_2 Reaction System

The potential energy diagrams for the chemical activation calculations of the O_2 + $C_2\cdot C{=}C$ combination reactions are shown in Figures 3B.2a and 3B.2b. The allylic isobutenyl radical undergoes addition with O_2 to form the chemically activated $C{=}C(C)COO\cdot^*$ adduct. The reaction channels of the $C{=}C(C)COO\cdot^*$ adduct include dissociation back to reactants, stabilization to C=C(C)COO· radical, isomerization via hydrogen shifts with subsequent β-scission or R·O-OH bond cleavage. The C=C(C)COO·* adduct can also cyclize to four or five-member cyclic peroxide-alkyl radicals. The reaction of C=C(C)COO·* adduct to C=C(C)CO· + O atom is included for completeness, but it is only important at high temperature (above 1500K). Figure 3B.2a shows isomerizations via H shift and the C=C(C)CO· + O reaction paths; while isomerization pathways to form cyclic adducts are shown in Figure 3B.2b.

4.4.2.1 Comparison of Thermodynamic Properties Determined by Different Calculation Methods: The optimized structures, frequencies and moments of inertia for reactant, important intermediates and transition states calculated from MP2(full)/6-31g(d) and B3LYP/6-31g(d) are listed in Table 3A.5. Comparison with stable molecules between MP2(full)/6-31g(d) and B3LYP/6-31g(d) optimized geometries are in agreement. Differences of bond length are within 0.019 Å, bond angles are within 1.8°, and dihedral angles are within 9.7°. Vibrational frequencies are within ±5% factor between MP2(full)/6-31g(d) and B3LYP/6-31g(d) calculations, with exception of two frequencies of C_2·Y(CCOC)(ν_6) and C=Y(CCOC)(ν_1). Comparison MP2 and DFT geometries on TS's show larger differences for active site bond lengths.

MP2(full)/6-31g(d) and B3LYP/6-31g(d) determined frequencies are listed in Table 3A.5. Torsion frequencies which correspond to internal rotors calculated from MP2(full)/6-31g(d) and B3LYP/6-31g(d) are not included in vibrational contributions for $S°_{298}$ and Cp(T)'s. Torsion frequency contributions to $S°_{298}$ and Cp(300) to Cp(1500) determined from method of Pitzer and Gwinn's for internal rotational contribution along with translational, rotational, and vibrational contribution calculated from MP2(full)/6-

31g(d) and B3LYP/6-31g(d) optimized geometries and frequencies. Comparison of the stable molecules indicates that MP2(full)/6-31g(d) and B3LYP/6-31g(d) determined $S°_{298}$ and Cp(T)'s are in agreement. Differences are within 1.06 cal/mole-K ($S°_{298}$ of CCYC·COOC) and 1.39 cal/mole-K (Cp(800K) of C=C(C)COOH) for $S°_{298}$ and Cp(T)'s, respectively. Differences of MP2 and B3LYP-determined $S°_{298}$ and Cp(T)'s of TS's are within 3.23 cal/mole-K ($S°_{298}$ of TS4) and 2.19 cal/mole-K (Cp(500K) of TS2) for $S°_{298}$ and Cp(T)'s, respectively.

Total energy (at 298K) differences between TS's and reactants, intermediates, and products calculated by MP2(full)/6-31g(d), MP4(full)/6-31g(d,p)//MP2(full)/6-31g(d), B3LYP/6-31g(d), B3LYP/6-311+g(3df,2p)// B3LYP/6-31g(d), and complete basis set (CBS-4 and CBS-q) model are listed in Table 3A.2. Comparison the results from our calculations show that the density functional calculated values at the B3LYP/6-31g(d) and B3LYP/6-311+g(3df,2p)// B3LYP/6-31g(d) levels are lower than MP2(full)/6-31g(d) values. CBS calculations based on MP2(full)/6-31g(d) and B3LYP/6-31g(d) optimized geometries have similar results, where differences are within 2 kcal/mole except in the reaction of allylic isobutenyl radical + O_2 → TS1 → C=C(C)COO·. Results of MP4(full)/6-31g(d,p)//MP2(full)/6-31g(d) calculations are between values of CBS-q//MP2(full)/6-31g(d) and MP2(full)/6-31g(d) calculations. We choose the values of CBS-q//MP2(full)/6-31g(d) and B3LYP/6-311+g(3df,2p)//B3LYP/6-31g(d) calculations for further discussion, data in parentheses are from B3LYP/6-311+g(3df,2p)//B3LYP/6-31g(d) calculations.

4.4.2.2 Formation of Allylic Isobutenyl Peroxy Radical (C=C(C)COO·): $\Delta H^\circ_{f,298}$ (C_2·C=C) is calculated to be 32.56 (32.81) kcal/mole from $\Delta H^\circ_{f,298}$ (C_2C=C) (-3.8 kcal/mole) and bond enthalpy (C=CC-H) (87.06 kcal/mole) using isodesmic reaction (IR1). $\Delta H^\circ_{f,298}$ (C=C(C)COO·) is determined to be 11.06 (10.79) kcal/mole using $\Delta H^\circ_{f,298}$ (C=C(C)COOH) (-24.51 (-23.85) kcal/mole from isodesmic reaction IR2) and bond enthalpy (C=C(C)COO-H) (87.66 (86.74) kcal/mole from isodesmic reaction IR3).

$$C_2\cdot C{=}C + O_2 \xleftrightarrow{TS1} C{=}C(C)COO\cdot \qquad (6)$$

The barriers of reaction (6) calculated from different levels show significant deviations. We find a small barrier of 1.47 kcal/mole based on CBS-q//MP2(full)/6-31g(d) calculation and no barrier based at B3LYP/6-311+g(3df,2p)//B3LYP/6-31g(d) for forward reaction (6). There is a ~0.4 Å difference between MP2(full)/6-31g(d) and B3LYP/6-31g(d) optimized geometries for the active site C---O bond length of TS1. There is also a factor ~7 difference between MP2(full)/6-31g(d) and B3LYP/6-31g(d) calculated imaginary frequency at TS1, 862 and 119 cm^{-1} respectively.

The Arrhenius pre-exponential factor, A_∞, is calculated via canonical TST. The high pressure limit rate constants, fit by a three parameters (A, n, Ea) modified Arrhenius Equation over a temperature range of 300K to 2000K, are $1.09 \times 10^{10} T^{0.57} \exp(-2290 \text{ cal } /RT)$ (cm^3 $mole^{-1}$ s^{-1}) and $4.65 \times 10^{8} T^{1.19} \exp(-530 \text{ cal } /RT)$ (cm^3 $mole^{-1}$ s^{-1}) at CBS-q//MP2(full)/6-31g(d) and B3LYP/6-311+g(3df,2p)//B3LYP/6-31g(d), respectively. The experimental rate constants reported by Jenkin et al.[115], 3.61×10^{11} (cm^3 $mole^{-1}$ s^{-1}) (at 296K), Slagle et al.[116], $<3.01 \times 10^{10}$ (cm^3 $mole^{-1}$ s^{-1}) (at 600K), and Ruiz et al.[117], 9.51×10^{10} (cm^3 $mole^{-1}$ s^{-1}) (at 348K) show no observed barrier for the similar reaction of allyl radical + O_2 → allylperoxy radical. These experimental evaluations do have low A factors suggesting a barriers may exists.

The shallow well depth for allylic isobutenyl radical + O_2 ⟷ C=C(C)COO· is due to loss of resonance stabilization and places the reaction barrier to new product channels 6.67 (2.97) kcal/mole or more higher than dissociation back to reactants. One exception is the C=C(C·)COOH adduct which can be formed with low barrier of 19.82 (19.60) kcal/mole relative to the stabilized C=C(C)COO· peroxy adduct via a six-member cyclic transition state structure, TS3. This isomer, however, has a significant barrier to further reactions. It requires 42.14 (32.00) kcal/mole, 51.25 (52.91) kcal/mole and 42.45 (41.90) kcal/mole (in addition to the 19.82 (19.60) kcal/mole for isomerization) for further reaction to methylene oxirane + OH, C=C=C + C·H_2OOH, and C=C(C·)CO· + OH, respectively. These reactions will be further discussed. The major reaction flux of C=C(C·)COOH is, therefore, back to the C=C(C)COO· peroxy radical or further reaction with O_2.

The major reaction channel of the C=C(C)COO· adduct is reaction back to allylic isobutenyl radical + O_2. Other reactions for the stabilized C=C(C)COO· adduct are isomerization (H-shift) pathways I, II and cyclization pathway IIIa and IIIb.

4.4.2.3 Isomerization (H-Shift) Pathways I and II: The first step of reaction paths I and II is intramolecular isomerization - hydrogen transfer - via TS2 and TS3 transition states, respectively. The H transfer step of reaction path I has a higher A factor of 1.33×10^{12} (2.14×10^{12}) s^{-1} at 743K but also a higher activation energy of 39.57 (38.27) kcal/mole than reaction path II (data below). This isomerization is the rate-determining step for reaction path I since the following β-scission forms a strong carbonyl bond, (C=O), which has a low barrier to products, 1-2 kcal/mole and slightly higher A factor. Reaction path I occurs through a four member-ring intramolecular H transfer and contributes to methacrolein product formation.

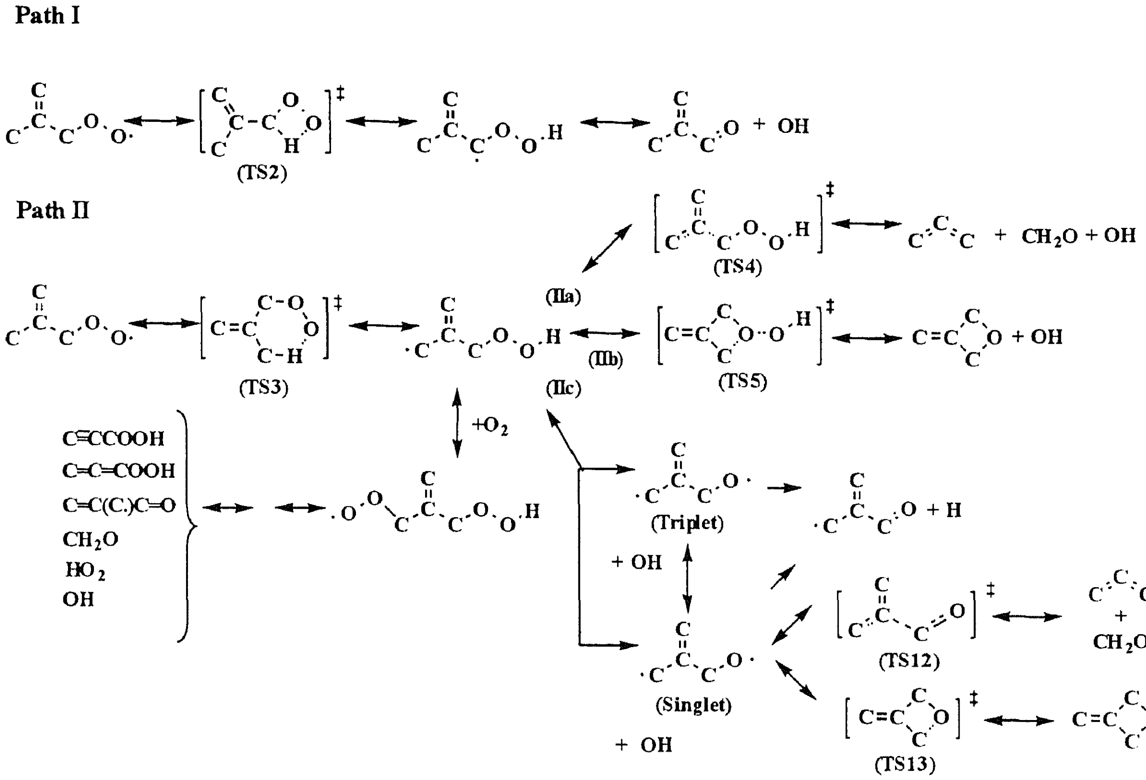

4.4.2.3.1 Reactions of C=C(C·)COOH Adduct: The first step of reaction path II has a low activation energy 19.82 (19.60) kcal/mole, but the following reactions all involve high barriers. Reaction IIa, β-scission to C=C=C + CH_2O + OH, requires 53.91 (55.09) kcal/mole of which 47.27 kcal/mole is from the endothermicity. Reaction path IIc is an important new, chain branching reaction path. It involves cleavage of the weak peroxide bond, C=C(C·)CO······OH (bond fission), to form C=C(C·)CO· biradical + OH. The C=C(C·)COOH → C=C(C·)CO· + OH channel has an A of 4×10^{15} s^{-1} and requires 42.45 (41.90) kcal/mole to break R·O—OH bond. The A factor is estimated from reactions of

ROOH → RO· + OH[118]. The barrier of 42.45 (41.90) kcal/mole is obtained from a best fit of our model to the experimental data; this value is close to experimental values of 41.4 ~ 42.92 kcal/mole for the reactions of ROOH → RO· + OH. Experimental rate constants for reactions of ROOH → RO· + OH are listed in Table 3A.6.

We consider this C=C(C·)COOH adduct dissociation to both triplet and singlet C=C(C·)CO· biradicals. The calculated barriers are 41.64 and 40.61 kcal/mole for C=C(C·)CO· (singlet) + OH and C=C(C·)CO· (triplet) + OH channels, respectively, using B3LYP/6-31g(d) level. The calculated difference in singlet versus triplet enthalpies is 1.03 kcal/mole at B3LYP/6-31g(d) level; triplet is lower. The A factor for dissociation to triplet vs. singlet ratio is 3:1. The singlet form is needed for reaction to methylene oxirane. Triplet to singlet conversion is included via collision with bath gas with a rate constant of 5×10^{13} s^{-1}, ca. one-tenth collision rate. Using the mechanism in CHEMKIN we observe almost no difference in product formation (overall conversion < 2%) between use of only one channel for the reaction, all reaction going to the singlet with E_a of 42.45 (41.90) kcal/mole ($A = 4 \times 10^{15}$ s^{-1}) versus use of reactions to both singlet and triplet with E_a of 42.22 (41.72) kcal/mole ($A = 3 \times 10^{15}$ s^{-1}) for triplet channel (E_a = 43.25 (42.75) kcal/mole and $A = 1 \times 10^{15}$ s^{-1} for the singlet channel). For modeling purposes a single channel can represent the C=C(C·)COOH ↔ C=C(C·)CO· + OH reaction.

It is also important to evaluate other dissociation reaction paths of singlet C=C(C·)CO· because this biradical can dissociate to two stable molecules (allene + CH_2O) or undergo intramolecular ring closure to methylene oxirane. Three reaction paths are considered and included in the mechanism for this singlet C=C(C·)CO· biradical.

i. Intramolecular ring closure (via TS13) to form a four member ring, methylene oxirane, product (ΔH = -40 kcal/mole). The reaction barrier of this singlet C=C(C·)CO· → TS13 is calculated to be 1.72 kcal/mole at the CBS-q//B3LYP/6-31g(d) level with A factor of 4.53×10^{11} s^{-1} at 800K.

ii. Dissociation (via TS12) to C=C=C + CH_2O (ΔH = -25.02 kcal/mole). The barrier for singlet C=C(C·)CO· → TS12 is determined as 6.41 kcal/mole at the CBS-q//B3LYP/6-31g(d) level with A factor of 2.93×10^{12} s^{-1} at 800K. This barrier results from rearrangement, (twist of methylene group), which involves loss of the allylic resonance.

iii. H atom elimination to C=C(C·)C=O radical form a carbonyl bond (C=O) (ΔH = 11.62 kcal/mole, E_a = 17.35 kcal/mole).

Triplet C=C(C·)CO· biradical β-scission to C=C(C·)C=O radical + H atom reaction path is also included.

An alternate and more conventional pathway to methylene oxirane is cyclization (reaction path IIb) via TS5 to form this oxirane + OH, which occurs via the alkyl carbon radical attack on the near peroxide oxygen atom (unimolecular) with concerted cleavage of the weak O-OH peroxide bond. This reaction via TS5 has an A of 6.95×10^{11} (1.03×10^{12}) s^{-1} (at 743K) and an E_a of 42.14 (32.00) kcal/mole. Comparison of geometries for TS5 calculated from MP2(full)/6-31g(d) and B3LYP/6-31g(d), show the MP2-determined TS5 is near planar in structure, while B3LYP-determined TS5 is a chair structure (dihedral angle d5234 = 0.6° in MP2 geometry and d5234 = 27° in B3LYP geometry) (see Table 3A.5). B3LYP-determined TS5 has longer bond lengths than MP2 at the active site bonds (bond length O4-C5=1.969 Å in B3LYP geometry (1.851Å in MP2 geometry) and O6-O4= 1.7384 Å in B3LYP geometry (1.5807Å in MP2 geometry)). The CBS-q calculated barriers based on MP2 and B3LYP geometries result in similar enthalpies, even though the geometries are different on these two levels. The calculated barrier is ca. 42 kcal/mole based on CBS-q//MP2(full)/6-31g(d) and CBS-q// B3LYP/6-31g(d) calculations. B3LYP/6-311+g(3df,2p)// B3LYP/6-31g(d) calculated barrier is ca 10 kcal/mole lower than the CBS-q value.

Separate calculations on the *tert* butyl + O_2 system[119, 120] to formation of 2,2-dimethyloxirane (3 member-ring ether) + OH from *tert* butyl hydroperoxy radical ($C_3 \cdot COOH$) and on formation oxirane (a 4 member ring) from methyl isopropyl hydroperoxy ether radical ($C_2COOHOC\cdot$), show barriers of 16 and 23 kcal/mole, respectively. These reactions in the *tert*-butyl system are 14 and 20 kcal/mole exothermic. The near thermoneutral reaction (ΔH_{rxn} = -0.67 kcal/mole) to form methylene oxirane from the allylic isobutenyl hydroperoxy radical in this allylic isobutenyl + O_2 system should have a 7 to 10 kcal/mole increase in the barrier (using an Evans Polanyi evaluation). An additional ca. 12 kcal/mole increase in the barrier is required for loss of resonance stabilization to form the TS. This thermochemical kinetic analysis yields:

(i) 14 + 10 + 12 = 36 or

(ii) 20 + 7 + 12 = 39 kcal/mole for the Ea of TS5.

The thermochemical analysis supports and we recommend the 42 kcal/mole: CBS-q calculated barrier.

CHEMKIN analysis with the reaction mechanism shows the two chemical activation reaction paths IIb (intramolecular ring formation/OH elimination) and IIc (biradical + OH) are primarily responsible for methylene oxirane formation. Sensitivity analysis using the mechanism shows that path IIc (C=C(C·)COOH ↔ C=C(C·)CO· + OH ↔ C=Y(CCOC) + OH) contributes 99.97% and 64.9% of methylene oxirane at 743K and 60 torr, based on properties calculated from CBS-q//MP2(full)/6-31g(d) and B3LYP/6-31g(3df,2p)// B3LYP/6-31g(d), respectively.

High sensitivity is observed on the barrier to reaction path IIc, methylene oxirane formation via biradical + OH, vs. IIb, intramolecular alkyl radical addition to the near peroxide oxygen and loss of OH radical, using results from B3LYP/6-31g(3df,2p)// B3LYP/6-31g(d) at 743K and 60 torr (reaction time = 210 sec), a decrease of 0.5 kcal/mole in E_a of C=C(C·)COOH → C=C(C·)CO· + OH, results an increase ~22% in total methylene oxirane formation via path IIc and a decrease ~0.5% via path IIb. When the E_a of path IIb, C=C(C·)COOH ↔ TS5 ↔ C=Y(CCOC) + OH, decreases by 0.5 kcal/mole, the overall formation of methylene oxirane increases by ~5% and decreases ~0.4% via path IIc.

Using CBS-q//MP2 values, sensitivity analysis at 743K and 60 torr (reaction time = 210 sec) shows that when E_a for C=C(C·)COOH → TS5 → C=Y(CCOC) + OH is adjusted by ±1 kcal/mole the methylene oxirane formation is not significantly changed (< ±0.005%). The reaction of C=C(C·)COOH ↔ C=C(C·)CO· + OH is much faster than C=C(C·)COOH ↔ TS5 ↔ C=Y(CCOC) + OH. A decrease 0.5 kcal/mole in the E_a of C=C(C·)COOH → C=C(C·)CO· + OH, results in ~14% increase in total methylene oxirane formation via path IIc; but no change for methylene oxirane formation via path IIb. These chemical activation paths are important in combustion systems.

4.4.2.4 Cyclization (Formation of Four and Five-Member Ring) Pathway III:

Reaction path III occurs via intramolecular addition of the terminal oxygen radical site to the C=C pi bond, forming four (reaction path IIIa) and five (reaction path IIIb) - member cyclic peroxide adducts. Reaction paths IIIa and IIIb are important to acetone formation. We note that the barriers for formation of the four and five member peroxides rings are higher by ca. 16 and 2 kcal/mole than reported earlier by Bozzelli and Dean[42] for the very similar allyl system. Activated energies for these two cyclizations are calculated as 28.20 (24.95) and 29.72 (27.98) kcal/mole with A factors of $2.42\text{x}10^{10}$ ($3.28\text{x}10^{10}$) and $3.88\text{x}10^{10}$ ($6.09\text{x}10^{10}$) s^{-1} at 743 K, respectively, for five and four-member ring cyclization. These high barriers 26-30 kcal/mole are required because the near complete loss of pi bond energy for the terminal C double bond's twist that is needed to form the transition states. The low A factors result from the loss of 2 rotors in transition states.

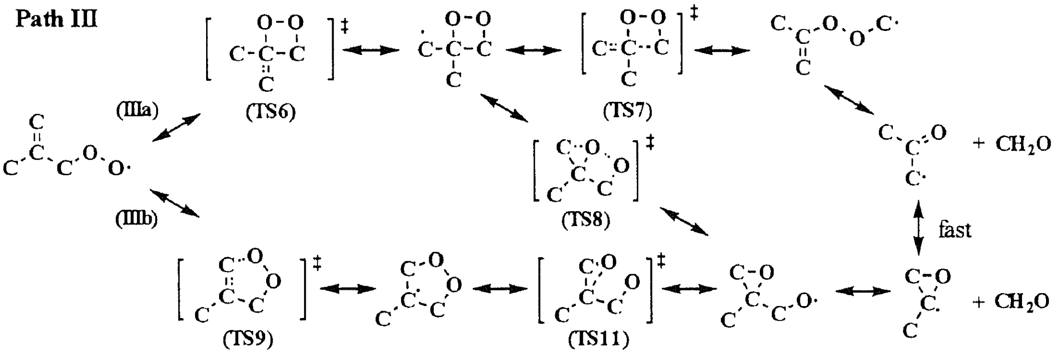

The reaction OH addition to isobutene, then reaction of the hydroxyl adducts with O_2 is also important in acetone formation. This OH + isobutene → adduct + (O_2) → products reaction system has been discussed in previous study[119].

4.4.3. $C_2 \cdot C{*}C + C_2 \cdot C{*}C$ Combination (Formation of 2,5-dimethylhexa-1,5-diene)

2,5-dimethylhexa-1,5-diene is one of major products in this moderate temperature isobutene oxidation. It is formed via combination reaction (7), which is a termination process. The overall reaction rate constant for allylic isobutenyl radical with O_2 is small, because of the very fast reverse reaction. The concentration of allylic isobutenyl radical accumulates to relatively high levels and the radical is consumed mainly through radical-radical processes. The behavior is in stark contrast to that of ethyl radicals and, in general, most alkyl radicals. For example, in the oxidation of propanal, which is an excellent source of ethyl radicals, oxidation at 673-793K yields only minute traces of butane[40]. We use 1.0×10^{13} ($cm^3\ mol^{-1}\ s^{-1}$)[12] for the high pressure limit rate constant of reaction (7).

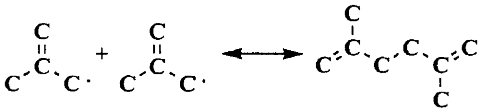

(7)

4.4.4 QRRK Analysis on Chemical Activation Reaction System

Input parameters and references to specific high pressure rate constants for the chemical activation calculations on the reaction of allylic isobutenyl radical + O_2 are listed in Table 3A.7. Parameters in Table 3A.7 are referenced to the ground (stabilized) level of the complex, as this is the formalism used in QRRK theory. Figures 3B.3a and 3B.3b illustrate the predicted effect of temperature and pressure on $C_2 \cdot C{=}C + O_2$ reactions based on CBS-q//MP2(full)/6-31g(d) calculations. The data show that at low pressure and high temperature most of the energized complex reacts back to reactants ($C_2 \cdot C{=}C + O_2$); stabilization to C=C(C)COO· and C=C(C·)COOH adducts are dominant at low temperature and high pressure. Figure 3B.3a indicates C=C(C)COO·* undergoes primarily reverse dissociation and O-O bond fission to biradical C=C(C·)CO· + OH above 1200K. Below 600K, the major reaction is stabilization to C=C(C)COO· and reverse reaction (back to reactants), which dominates stabilization to C=C(C·)COOH by ca. 2 orders of magnitude. The biradical C=C(C·)CO· + OH formation channel competes with the CY(C·CO) + CH_2O channel (C=C(C)COO· reaction through TS9, then through TS11), where CY(C·CO) can further react to acetone radical (C_2·C=O) + CH_2O. The concentration of C=C(C)COO· is controlled by equilibrium, not by formation rate. Rate constants for product formation channels increase with increasing temperature and decreasing pressure. The product formations are controlled by the slower reactions out of the equilibrium systems. The near steady state levels of C=C(C)COO· and C=C(C·)COOH make the reaction paths of C=C(C·)COOH with O_2 important and they need to be included in the mechanism.

All the reaction pathways of allylic isobutenyl radical with O_2 involve barriers, that are above the energy of the initial reactants, because of the shallow well (21.5 kcal/mole) resulting from loss of the resonance stabilized radical. Alkyl radical reactions have well depths of 32-37 kcal/mole and the activated complex initially formed has more energy for further reaction to products (chemical activation paths). This explains why the allylic isobutenyl radical shows very low reactivity towards O_2, and partially explains the high antiknock behavior in internal combustion engines of isobutene. Alkyl radicals plus isobutene react to alkanes plus allylic isobutenyl radical; capping the active alkyl radical and forming a non-reactive isobutenyl radical.

The rate constants k=AT^{n}exp(-Ea/RT) for QRRK calculated chemical activation and unimolecular dissociation at pressures of 0.076, 0.76, 7.6, 60, 760, and 7600 torr and temperature from 300 to 2000K are listed in Table 3A.8.

4.4.5 Model and Comparison to Experimental Data

An elementary reaction mechanism has been developed to model the experimental system – isobutene oxidation. The CHEMKIN II interpreter and integrator, version 3.1, is used to model the reaction conditions of Ingham et al.[110] for reaction time range (0 - 210 sec), 743 K and 60 torr (mole fractions of isobutene: O_2: N_2 = 0.067: 0.5: 0.433). Abstraction reactions are not considered pressure dependent, and therefore do not require falloff analysis. Abstraction reactions of O, OH, HO_2 and R· radicals are taken from evaluated literature wherever possible. A procedure from Dean and Bozzelli[92] is used to estimate abstraction rate constants by H, O, OH and CH_3 radicals when no literature data are available. A generic rate constant is utilized and adjusted for steric effects and reaction enthalpy for hydrogen abstractions by: C=CC· and HO_2 radicals[25] Table 3A.9 lists the reaction mechanism for conditions of 760 torr pressure and temperature range from 500 to 900K.

Figure 3B.4 shows that comparison of our calculation with experimental data for productions of 2,5 dimethylhexa-1,5-diene, methacrolein, isobutene oxides and acetone over the reaction time range (0-210 sec), 743K and 60 torr. Calculations based on thermodynamic parameters from CBS-q//MP2(full)/6-31g(d) and B3LYP/6-311+g(3df,2p)//B3LYP/6-31g(d) levels are illustrated in Figures 3B.4a and 3B.4b,respectively; and symbols are data of Ingham et al.[110] Calculated isobutene oxides are included 2,2-dimethyloxirane (3 member ring oxirane)(16%) and methylene oxirane(84.5%). 2,2-dimethyloxirane is formed primarily from $C_3 \cdot COOH$, which is from the HO_2 radical addition to isobutene. HO_2 addition to isobutene to form $C_3 \cdot COOH$ is the important path for oxirane formation and has been thoroughly discussed in our previously study[119]. Methacrolein forms via two major paths: (a.) Allylic isobutenyl radical combination with HO_2 forms a hydroperoxide adduct which will decompose via cleavage of the weak O-OH bond to produce methacrolein, H and OH radicals. (b) Reaction path I of allylic isobutentyl radical + O_2 reaction system. The results using CBS-q//MP2(full)/6-31g(d) calculation on 2,5 dimethylhexa-1,5-diene, methacrolein, and isobutene oxides product formation are in excellent agreement with experimental data of Ingham et al.[110] Acetone formation is overestimated based on B3LYP/6-311+g(3df,2p)//B3LYP/6-31g(d) calculation, but CBS-q values lead to good agreement.

This isobutene oxidation mechanism is also used to model the experimental conditions of Knyazev et al.[112] for the decay constant of the $C_2 \cdot C{=}C$ radical at 800K and 2.78 torr in He bath gas and varied $[O_2]$. The pseudo-first-order radical decay constants, k', are calculated at different concentration of O_2. Figure 3B.5 shows the radical decay k' vs. $[O_2]$ at 800K and 2.78 torr in He bath gas. The second-order rate constant of the reaction of $C_2 \cdot C{=}C$ radical with O_2 is calculated to be 1.05×10^7 s^{-1} $mole^{-1}$ cm^3 and 4.50×10^7 s^{-1} $mole^{-1}$ cm^3 based on thermodynamic parameters from CBS-q//MP2(full)/6-31g(d) and B3LYP/6-311+g(3df,2p)//B3LYP/6-31g(d) calculations, respectively. These small rate constants are consistent with experiment of Knyazev et al., $k < 10^8$ $s^{-1} mole^{-1} cm^3$, where no reaction of the allylic isobutenyl radical with molecule oxygen could be observed at 800K and 2.78 torr.

Figures 3B.6a and 3B.6b show the concentration of reactant ($C_2{\cdot}C{=}C$) and products vs. reaction time based on the CBS-q//MP2(full)/6-31g(d) mechanism at two different O_2 concentrations. OH, HO_2, H_2O, O, CO, CO_2, CH_2O, ketene (C=C=O), allene (C=C=C), 2,5-dimethylhexa-1,5-diene, methylene oxirane, methacrolein are primary products. Figure 3B.6a shows that the allylic isobutenyl radical undergoes association, reaction (7), to form 2,5-dimethylhexa-1,5-diene and dissociation to C=C=C + CH_3 radical at lower O_2 concentration ($[O_2] = 4.84\text{x}10^{14}$ molecules/cm^3 at 800K and 2.78 torr). Figure 3B.6b shows the allylic isobutenyl radical reacts with O_2 forming adducts and isomers, which rapidly dissociate (entropy driven) back to reactants showing a low rate constant to products, at high O_2 concentration ($[O_2] = 4.84\text{x}10^{16}$ molecules/cm^3 at 800K and 2.78 torr). The equilibrium concentrations of the adducts (from $R\cdot + O_2$) at high $[O_2]$ lowers the $C_2{\cdot}C{=}C$ concentration and therefore limit $C_2{\cdot}C{=}C + C_2{\cdot}C{=}C$ association to 2,5-dimethylhexa-1,5-diene. OH radical forms from reaction paths I and II. HO_2, H_2O and O are formed from further reactions of OH radical. CH_2O forms from reaction paths IIa and III. CO and CO_2 are from further reactions of CH_2O. Ketene (C=C=O) forms from $C_2{\cdot}C{=}O$ radical, which is formed from reaction path III. The $C_2{\cdot}C{=}O$ radical undergoes β-scission forming C=C=O and CH_3 radical. Allene (C=C=C) forms from reaction path IIa and via β-scission of $C_2{\cdot}C{=}C$ radical to form C=C=C and CH_3 radical.

4.5 Summary

A thermochemical and chemical activation reaction analysis is presented on the important reaction system: allylic isobutenyl radical + O_2. Thermodynamic proprieties, reaction paths and elementary reactions for this system are presented and kinetic parameters evaluated versus temperature and pressure. An elementary reaction mechanism has been developed to model the experimental system – isobutene oxidation. An important new reaction path, C=C(C·)COOH ↔ C=C(C·)CO· + OH ↔ C=Y(CCOC) + OH, for methylene oxirane formation is shown to be more important than C=C(C·)COOH ↔ TS5 ↔ C=Y(CCOC) + OH at 743K and 60 torr for the allylic isobutenyl radical + O_2 reaction. The reaction barrier for the C=C(C·)COOH reaction to C=C(C·)CO· + OH is evaluated as 42.45 (41.90) kcal/mole with an A factor of $4\text{x}10^{15}$ s^{-1}. Reaction barrier of C=C(C·)COOH → TS5 → C=YCCOC + OH is calculated as 42.14 (32.0) kcal/mole with an A factor of $6.95\text{x}10^{11}$ ($1.03\text{x}10^{12}$) s^{-1} at 743K. Other calculated barriers are as 28.02 (24.95) and 29.72 (27.98) kcal/mole with A factors of $4.27 \text{ x } 10^{10}$ $2.42\text{x}10^{10}$ ($3.28\text{x}10^{10}$) and $3.88\text{x}10^{10}$ ($6.09\text{x}10^{10}$) s^{-1} at 743K, respectively, for four and five-member ring cyclization. Results from the mechanism based on CBS-q calculation are in good agreement with experimental data reported by Ingham et al.[110] and by Knyazev et al.[112] Allylic isobutenyl radical reaction with O_2 form number of adducts which are shown to have no low energy product formation channels; thus reverse reaction to C_2·C=C + O_2 is the dominant adduct dissociation path. High [O_2] is shown lower C_2·C=C levels via formation of steady state peroxy and peroxide adducts. CBS-q calculations based on MP2(full)/ 6-31g(d) and B3LYP/6-31g(d) geometries result in reasonable accurate thermodynamic enthalpy data for C_2·C=C + O_2 reaction system that agree with results of Jungkamp et al.[47, 48] and Petersson et al.[49]

CHAPTER 5

KINETIC ANALYSIS FOR HO_2 ADDITION TO ETHYLENE, PROPENE AND ISOBUTENE AND THERMOCHEMICAL PARAMETERS FOR THE ALKYL HYDROPEROXIDES AND HYDROPEROXY ALKYL RADICALS

5.1 Overview

Thermochemical kinetic analysis for the reactions of HO_2 radical addition to the primary, secondary and tertiary carbon-carbon double bonds of ethylene, propene and isobutene are studied using canonical transition state theory (TST). Thermochemical properties of reactants, alkyl-hydroperoxides (ROOH), alkyl-hydroperoxy radicals (R·OOH), and transition states (TSs) are determined by *ab initio* and density functional calculations. Enthalpies of formation ($\Delta H_f°_{298}$) of product radicals (R·OOH) are determined using isodesmic reactions with group balance at MP4(full)/6-31G(d,p)//MP2(full)/6-31G(d), MP2(full)/6-31G(d), complete basis set model chemistry (CBS-q with MP2(full)/6-31g(d) and B3LYP/6-31g(d) optimized geometries), and density functional (B3LYP/6-31g(d) and B3LYP/6-311+g(3df,2p)//B3LYP/6-31g(d)) calculations. $\Delta H_f°_{298}$ of TS's are obtained from the $\Delta H_f°_{298}$ of reactants plus energies difference between reactants and TS's. Entropies ($S°_{298}$) and heat capacities (Cp(T) $300 \leq T/K \leq 1500$) contributions from vibrational, translational, and external rotational are calculated using the rigid-rotor-harmonic-oscillator approximation based on geometric parameters and vibrational frequencies obtained at MP2(full)/6-31G(d) and B3LYP/6-31G(d) levels of theory. Selected potential barriers of internal rotations for alkyl-hydroperoxy radicals and TS's are calculated at MP2(full)/6-31G(d) and CBS-Q//MP2(full)/6-31G(d) levels.

Contributions from hindered rotors of $S°_{298}$ and Cp(T) are calculated by method of Pitzer and Gwinn and by summation over the energy levels obtained by direct diagonalization of the Hamiltonian matrix of hindered internal rotations when the potential barriers of internal rotations are available. Calculated rate constants obtained at CBS-q//MP2(full)/6-31G(d) and CBS-q//B3LYP/6-31G(d) levels of theory show similar trends with experimental data: HO_2 radical addition to tertiary carbon-carbon double bond (HO_2 addition at CD/C2 carbon atom of isobutene) has a lower activation energy than addition to secondary carbon-carbon double bond CD/C/H, which is lower than addition to primary carbon-carbon bond CD/H2; the values are 12.11(11.56), 11.08(10.34) and 7.63(7.03) kcal/mole, respectively, at CBS-q//MP2 (full)/ 6-31G(d) level. Data in parentheses are calculation at CBS-q//B3LYP/6-31G(d) level. The E_a for addition to primary carbon-carbon double bonds of ethylene, propene and isobutene also show a decreasing trend 13.49(12.89), 12.16(11.20) and 10.70(10.59) kcal/mole, respectively. The high-pressure limit rate constants are (based on CBS-q//MP2(full)/6-31G(d) calculations) (Q=OOH):

$k_{1,\infty}(HO_2+C{=}C{\Rightarrow}C\cdot CQ)=4.13\times10^{4}T^{2.33}\exp(-13.49\text{kcal/mole}/RT)\text{cm}^3/\text{mole-s}$;

$k_{2,\infty}(HO_2+C{=}CC{\Rightarrow}CC\cdot CQ)=2.47\times10^{4}T^{2.13}\exp(-12.16\text{kcal/mole}^{-1}/RT)\text{cm}^3/\text{mole-s}$;

$k_{3,\infty}(HO_2+C{=}CC{\Rightarrow}C\cdot CQC)=7.74\times10^{3}T^{2.29}\exp(-11.08\text{kcal/mole}^{-1}/RT)\text{cm}^3/\text{mole-s}$;

$k_{4,\infty}(HO_2+C_2C{=}C{\Rightarrow}C\cdot CQ)=3.45\times10^{5}T^{1.77}\exp(-10.70\text{kcal/mole}^{-1}/RT)\text{cm}^3/\text{mole-s}$;

$k_{5,\infty}(HO_2+C_2C{=}C{\Rightarrow}C\cdot CQ)=2.78\times10^{4}T^{2.11}\exp(-7.63\text{kcal/mole}^{-1}/RT)\text{cm}^3/\text{mole-s}$.

Enthalpies of formation for alkyl-hydroperoxides are determined to be $\Delta H_f°_{298}$ (CCQ) = -39.70 ± 0.3 kcal/mole, $\Delta H_f°_{298}$ (CCCQ) = -44.77 ± 0.41 kcal/mole, $\Delta H_f°_{298}$ (CCQC) = -48.99 ± 0.32 kcal/mole, $\Delta H_f°_{298}$ (C_2CCQ) = -51.32 ± 0.38 kcal/mole, and $\Delta H_f°_{298}$

(C_3CQ) = -57.91 ± 0.47 kcal/mole. $\Delta H_f°_{298}$ of alkyl-hydroperoxy radicals are $\Delta H_f°_{298}$ ($C{\cdot}CQ$) = 10.96 ± 1.06 kcal/mole, $\Delta H_f°_{298}$ ($CC{\cdot}CQ$) = 2.62 ± 1.29 kcal/mole, $\Delta H_f°_{298}$ ($C{\cdot}CQC$) = 0.68 ± 1.54 kcal/mole, $\Delta H_f°_{298}$ ($C_2C{\cdot}CQ$) = -7.24 ± 1.25 kcal/mole, and $\Delta H_f°_{298}$ ($C_3{\cdot}CQ$) = -6.42 ± 1.28 kcal/mole.

5.2 Introduction

The addition of HO_2 radical to alkenes plays an important role in combustion kinetics and atmospheric chemistry. Hydroperoxides and alkyl hydroperoxides are also important in biochemical synthesis and metabolism.[104-108] HO_2 is a relative non reactive radical having weak HOO-H and HOO-CH_3 bonds of 88.2 and 70.1 kcal/mole respectively; it's low reactivity allow it to build up in concentration in atmospheric, photochemical and moderate temperature combustion systems. HO_2 radical addition to carbon-carbon double bond of alkenes to form alkyl-hydroperoxy radicals, can produce oxiranes (cyclic oxygenates) and OH radicals; isomerize to peroxy radicals which can dissociate to alkyl radicals + O_2; or be stabilized form stabilized adduct radicals that can further react with O_2. These alkyl-hydroperoxy radicals are also important products of alkyl + O_2 reactions (Scheme 1). The reactions of these stabilized adduct via isomerization, HO_2 elimination and additions with O_2 are important in controlling the negative temperature dependent in hydrocarbon oxidation.

SCHEME 1

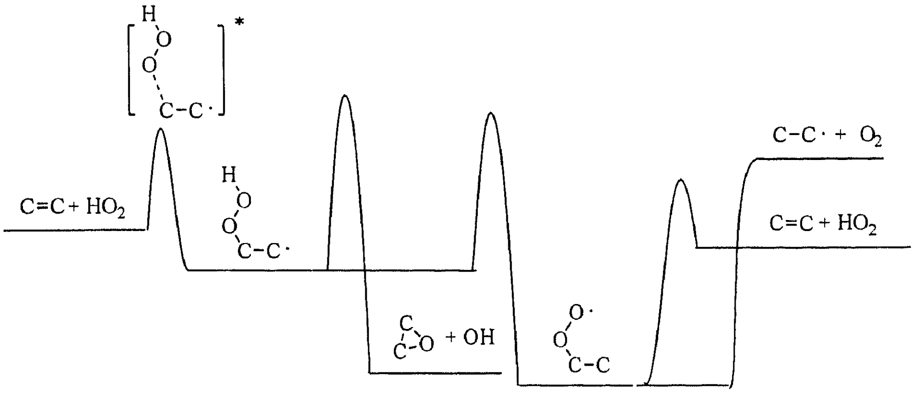

Energy vs. Reaction Pathways

The research group of Baldwin and Walker[121-125] has studied relative rate constants on the addition of HO_2 radicals to alkenes, and report Arrhenius parameters based on measurements of product-reactant ratios, i.e. [oxirane]/[reactants]. Accurate kinetic parameters are often difficult to derive from a complex reaction system using an overall, stable product slate resulting from several minutes of oxidation reaction. In this study we use *ab initio* calculations and isodesmic reactions with group balance to estimate thermochemical parameters and kinetic analysis on HO_2 radical addition to ethylene, propene and isobutene carbon-carbon double bonds forming the alkyl-hydroperoxy radicals.

5.3 Method

5.3.1 *Ab Initio* and Density Functional Calculations

The geometries of reactants, transition states, and product radicals are pre-optimized using UHF/PM3 in MOPAC[51] program, followed by optimization and vibrational frequency calculation at MP2(full)/6-31G(d) and B3LYP/6-31G(d) levels of theory using GAUSSIAN 94[52] program. Zero-point vibrational energies (ZPVE), vibrational frequencies and thermal contributions to enthalpy from harmonic frequencies are scaled as recommended by Scott et al.[53] Transition state (TS) geometries are identified by the existence of only one imaginary frequency in the normal mode coordinate analysis, evaluation of the TS geometry, and the reaction's coordinate vibration information.

5.3.2. Thermodynamic Properties - $\Delta H_f°_{298}$, $S°_{298}$, and Cp (300) to Cp (1500)

Total energy for all species are calculated at MP2(full)/6-31G(d), MP4(full)/6-31G(d,p)// MP2(full)/6-31G(d), B3LYP/6-31G(d), and B3LYP/6-311+G(3df,2p)//B3LYP/6-31G(d) levels of theory. Complete basis set (CBS-q) model chemistry[54-56] based on MP2(full)/6-31G(d) and B3LYP/6-31G(d) geometries are also calculated. CBS-q//MP2(full)/6-31G(d), CBS-q//B3LYP/6-31G(d), MP4(full)/6-31G(d,p)//MP2(full)/6-31G(d), and B3LYP/6-311+G(3df,2p)//B3LYP/6-31G(d) are abbreviated in the remainder of the text as CBSlqM, CBSlqB, MP4F, and B3LYP311, respectively.

Contributions of vibration, translation, and external rotation to entropies and heat capacities are calculated from scaled vibrational frequencies, molecular mass, and moments of inertia of the optimized structures. Potential barriers of internal rotations for 2-hydroperoxy-1-ethyl radical (C·-COOH, C·C-OOH, and C·CO-OH bonds) and TS1 (CC-OOH and CCO-OH bonds) are calculated at MP2(full)/6-31G(d) and CBS-Q//MP2(full)/6-31G(d) (abbreviated as CBSQM) levels. C·-COOH bond in other hydroperoxy radicals and C-C single bond in TS's are calculated at MP2(full)/6-31G(d) level. The geometries and harmonic vibrational frequencies are calculated for all rotational conformers at MP2(full)/6-31G(d) level.

Contributions from hindered rotors of $S°_{298}$ and Cp(T) are determined by method of Pitzer and Gwinn[57] and by direct integration over energy level of the intramolecular rotator potential energy curve.[126] The numbers of optical isomers and spin degeneracy of unpaired electrons are also incorporated for calculation of $S°_{298}$ and Cp(T).

A Fourier series is used represent the torsional potential calculated at discrete torsional angle:

$$V(\Phi) = a_0 + a_i \cos(i\Phi) + b_i \sin(i\Phi), \qquad i = 1,2,3\ldots \qquad \text{(F1)}$$

Where values of the coefficients are calculated to provide the true minima and maxima of the torsional potentials with allowance of a shift of the theoretical extrema angular positions.

Contributions from the internal rotors are determined by method of Lay et al.[127] They report evaluation of the matrix elements of individual sine and cosine terms in the basis of the free rotor wave functions is straightforward. The terms $\cos(i\Phi)$ and $b_i \sin(i\Phi)$ induce transitions with $\Delta K = \pm\, i$, where K is the rotational quantum number. Moreover, the matrix element does not depend on K, which leads to a simple form of the Hamiltonian matrix. The matrix has a band structure and consists of diagonal terms that are equal to those of the free rotor and subdiagonals of constant values that correspond to a different terms in the potential expansion.

The Hamiltonian matrix is then truncated to the size of $2K_{max} + 1$, where K_{max} is the maxium rotational quantum number considered. The choice of the size of the truncated maxtrix is made by checking the independence of the thermodynamic properties calculated on K_{max}. The truncated matrix (in reduced dimensionless form) is diagonalized, and the eigenvalues are used to calculate the partition function, entropy, heat capacity, etc. This is accomplished using direct summation over the calculated energy levels according to standard expressions of statistical thermodynamics.[74]

Reaction enthalpy $(\Delta H^{\neq}_{TS\text{ - reactants}})_{298}$ is obtained from the differences of total energies, ZPVE, and thermal correction for entropies between TS and reactants. Enthalpies of formation for TSs are estimated from experimental data of $\Delta H_f°_{298}$ of reactants plus the reaction enthalpy $(\Delta H^{\neq}_{TS\text{-reactants}})_{298}$. Two sets of isodesmic reactions with group balance, shown in Scheme 2 and 3, are used in this study and applied to accurately estimate the enthalpy of formation of alkyl-hydroperoxy radicals, $CH_2{\cdot}CH_2OOH$ (C·CQ), $CH_3CH{\cdot}CH_2OOH$ (CC·CQ), $CH_2{\cdot}CH(OOH)CH_3$ (C·CQC), $(CH_3)_2C{\cdot}CH_2OOH$ ($C_2C{\cdot}CQ$) and $CH_2{\cdot}\ C(OOH)(CH_3)_2$ ($C_3{\cdot}CQ$). An isodesmic reaction with group balance is characterized by conservation of both bonds and the number of groups of each group type in the reactants and products, where a group is defined as a polyvalent atom (ligancy≥2) in a molecule.[128] To obtain $\Delta H_f°_{298}$ of alkyl-hydroperoxy radicals, we also need the $\Delta H_f°_{298}$ of corresponding hydroperoxide alkanes (Scheme 2). Reactions in Scheme 2 are based on the reaction of CH_3OOH with the alcohols to form the desired hydroperoxides alkanes and CH3OH. The values of $\Delta H_f°_{298}$ (CH_3OOH) =-31.8 kcal/mole is obtained from Lay et al.[88] Enthalpies of formation for the alcohols used in reactions (IR1-IR5) are obtained from literature data.

SCHEME 2

CCQ + COH = CQ + CCOH (IR1)

CCCQ + COH = CQ + CCCOH (IR2)

CCQC + COH = CQ + CC(OH)C (IR3)

C_2CCQ + COH = CQ + C_2CCOH (IR4)

C_3CQ + COH = CQ + C_3COH (IR5)

(Q=OOH)

SCHEME 3

CCQ + C·C = C·CQ + CC (IR6)

CCCQ + C·CQ = CC·CQ + CCQ (IR7)

CCQC + C·CQ = C·CQC + CCQ (IR8)

C_2CCQ + C·CQ = C_2C·CQ + CCQ (IR9)

C_3CQ + C·CQ = C_3·CQ + CCQ (IR10)

Calculated enthalpies of formation of alkyl-hydroperoxy radicals, C·CQ, CC·CQ, C·CQC, C_2C·CQ and C_3·CQ are derived from the reactions in Scheme 3 and bond enthalpy of $DH°_{298}$ (QCC-H).

5.3.3 High-Pressure Limit A Factors (A_∞) and Rate Constants (k_∞) Determination

The high-pressure limit rate constant (k_∞) of HO_2 addition reactions are fit by three parameters A_∞, n, and E_a over temperature range from 298 to 2000K:

$k_\infty = A_\infty(T)^n \exp(-E_a/RT)$

Entropy differences between reactants and TS are used to determine the Arrhenius pre-exponential factor, A_∞, via canonical transition state theory[16] (TST) for unimolecular and bimolecular reactions $A_\infty = (kT/h)\exp(\Delta S^{\neq}/R)$ and $A_\infty = (ekT/h)\exp(\Delta S^{\neq}/R)$, respectively. Where *h* is Plank's constant, *k* is the Boltzmann constant. Activation energy is determined as the difference in internal energy between reactant and TS.

5.4 Results and Discussion

5.4.1 Geometries

Optimized structures and selected geometric parameters for reactants, transition states, and product radicals of ethylene, propene, and isobutene reactions with HO_2 radical are illustrated in Table 4A.1. Vibration frequencies and moments of inertia for all species are listed in Table 4A.2, the calculated vibrational frequencies are scaled by the factor 0.9427 and 0.9614 for MP2(full)/6-31G(d) and B3LYP/6-31g(d) theoretical frequencies, respectively, as recommended by Scott et al.[53] Torsion frequencies are not included in Table 4A.2.

5.4.1.1. Reactants and Product Radicals: Structures from the MP2(full)/6-31G(d) and B3LYP/6-31g(d) calculations are similar for both reactants and product radicals. C=C double bonds in MP2(full)/6-31G(d) geometries are slightly longer (~0.004Å) than B3LYP/6-31g(d) for olefin reactants only; other bond lengths in MP2(full)/6-31G(d) are slightly shorter (~0.006Å) than B3LYP/6-31g(d). The differences of bond length and angles for olefin reactants between MP2(full)/6-31G(d) and B3LYP/6-31g(d) are less than 0.006 Å and 1 degree, respectively. Both calculated reactant geometries are in good agreement with experimental results (Table 4A.1). Difference between the calculated and measured bond lengths and angles are within 0.015 Å and 1.2 degree, respectively.

Bond lengths of alkyl-hydroperoxy radicals in B3LYP/6-31g(d) geometries are longer than those in MP2(full)/6-31G(d) geometries except R·O-OH and R·OO-H bonds. The R·OO-H and R·O-OH bonds (except C_3·CQ radical) in MP2(full)/6-31G(d) geometries are longer than B3LYP/6-31g(d) by 0.003 Å and 0.021~0.003 Å, respectively.

The R·-COOH bond in alkyl-hydroperoxy radicals is ca. 0.16 Å longer than experimental C=C double bond in ethylene, propylene and isobutene (average value ca.1.329 Å[129]) and 0.04 Å shorter than experimental C-C single bond in ethanol (1.530 Å[77]). The new-formed R·C-OOH bond lengths in product radicals are between 1.434 Å (C·CQ) and 1.466 Å (C_3·CQ) in B3LYP/6-31g(d) geometries, while MP2(full)/6-31G(d) geometries yield slightly shorter bond length between 1.431 Å (C·CQ) and 1.459 Å (C_3·CQ). Differences of bond angles and dihedral angles are within 1.9° and 13.6° between B3LYP/6-31g(d) and MP2(full)/6-31G(d) geometries.

5.4.1.2. Transition States: Both of MP2(full)/6-31g(d) and B3LYP/6-31g(d) calculations show structures of the hydrocarbon in the transition states having a near planar-ethylene configuration with HO_2 addition perpendicular to the plane. The ∠CCO bond angle is varies from 96.1° (TS of HO_2 addition at CD/C2 carbon atom of isobutene) to 104.07° (TS of HO_2 addition at CD/H2 carbon atom of propene) for MP2(full)/6-31G(d) geometry. ∠CCO of B3LYP/6-31g(d) is 2.1~3.9° larger than those calculated by MP2(full)/6-31G(d). The forming RC---OOH bond lengths range from 1.9365 Å (TS of HO_2 addition ethylene) to 1.9743 Å (TS of HO_2 addition at CD/C2 carbon atom of isobutene) for MP2(full)/6-31G(d) geometry. RC---OOH bond lengths from B3LYP/6-31G(d) geometries are shorter than those of MP2(full)/6-31G(d) by 0.02~0.046 Å. The breaking C=C bond length is 1.35 Å and 1.38 Å from MP2(full)/6-31G(d) and B3LYP/6-31G(d) geometries, respectively (in case of HO_2 addition isobutene forming C_3·COOH, it is slightly longer than other TSs by 0.01 Å for both MP2 and DFT geometries). This distance is longer than average C=C double bonds, 1.33 Å, and shorter than average C-C single bonds 1.51 Å. The bond lengths of RO-OH in transition states are shorter than R·O-OH bond in alkyl-hydroperoxy radicals, but the ROO-H bond in TSs are slightly longer than R·OO-H bond in alkyl-hydroperoxy radicals.

5.4.2. Rotational Barriers

5.4.2.1 2-Hydroperoxy-1-Ethyl Radical and TS1: Potential barriers of internal rotations for 2-hydroperoxy-1-ethyl radical (C·-COOH, C·C-OOH, and C·CO-OH bonds) and TS1 (CC-OOH and CCO-OH bonds) are calculated at MP2(full)/6-31G(d) and CBSQM levels. Calculation of potential energy as function of dihedral angle is performed by varying torsion angle in 30° intervals and allowing other parameters to be optimized (except C·-COOH bond in C·CQ radical, the HCCH dihedral angle is fixed as 174°). The structures of minimum and maximum are full optimized for 2-hydroperoxy-1-ethyl radical. The geometries and harmonic vibrational frequencies are calculated for all rotational conformers and transition states at MP2(full)/6-31G(d) level. The barriers for internal rotations are calculated from the differences between the total energy of each conformation and that of the most stable conformer, where the zero point vibrational energy (ZPVE) and thermal correction to 298K are also included. Total energies, ZPVE, thermal correction to 298K and calculated rotation barriers for each rotational conformer of 2-hydroperoxy-1-ethyl radical and TS1 are listed in Table 4A.3. Potential barrier diagrams for internal rotations about C·-COOH, C·C-OOH and C·CO-OH bonds of 2-hydroperoxy-1-ethyl radical are shown in Figures 4B.1a, 4B.1b, and 4B.1c, respectively. Figures 4B.2a and 4B.2b show the diagrams about CC-OOH and CCO-OH bonds of TS1. Points are calculated values at MP2(full)/6-31g(d) (circles) and CBSQM (triangles).

Lines are results of Fourier expansions F1. Coefficients of the Fourier expansion components, a_i and b_i in equation F1 are listed in Table 4A.4.

Contributions from hindered rotors of $S°_{298}$ and Cp(T) calculated using the method of Pitzer and Gwinn and by direct integration over energy levels of the exact potential curve are listed in Table 4A.5. The differences of rotational barrier calculated at MP2(full)/6-31g(d) and CBSQM levels are less than 1.6 kcal/mole. Direct diagonalization of the Hamiltonian matrix of rotational potential energy and the Pitzer and Gwinn approximation method both lead to similar results in determination of hindered rotor contributions to $S°_{298}$ (difference within 0.58 cal/mole-K) and $Cp(T)_{298}$ (difference within 1.16 cal/mole-K).

5.4.2.2 Other Alkyl-Hydroperoxy Radicals and TSs: In TSs, -CH3 torsions are approximated by a symmetrical sinusoidal potential. The rotational barrier heights are calculated to be 1.34, 1.71, 1.63 and 2.15 kcal/mole for TS2A, TS2B, TS3A and TS3B, respectively, at MP2(full)/6-31G(d) level. Rotational barriers about CO-OH bond in other alkyl-hydroperoxy radicals (CC·CQ, C·CQC, C_2C·CQ, and C_3·CQ) and TS's (TS2A, TS2B, TS3A and TS3B) use the CBSQM values for the CO-OH bond in C·CQ radical and TS1, respectively. Table 4A.6 lists $S°_{298}$ and Cp(T) contributions from hindered rotors which are calculated using Pitzer and Gwinn approximation for hydroperoxy radicals and TSs (except 2-hydroperoxy-1-ethyl radical and TS1). Rotation barriers used in this study are also listed in Table 4A.6.

5.4.3. Thermodynamic Properties - $\Delta H_f°_{298}$, $S°_{298}$, and Cp (300) to Cp (1500)

Enthalpies of formation of the species used in the working reactions are adopted from literature data and are listed in Table 4A.7. Table 4A.8a lists reaction enthalpies in Scheme 2 using CBSlqM, CBSlqB, MP4F and B3LYP311 calculations. The very low, near zero, $\Delta H_{rxn,298}$ shows the reactions are thermoneutral which suggest good accuracy (cancellation of errors) for the calculated enthalpies. Table 4A.8b lists reaction enthalpies in Scheme 3 at various levels of theory. Enthalpy of reaction (IR6) indicates that the bond enthalpy $DH°_{298}$ (QCC-H) is about 1.67 kcal/mole (average value from CBSlqM, CBSlqB, MP4F and B3LYP311, CBSQ and G2 calculations) higher than $DH°_{298}$ (CH3CH2-H). Bond enthalpy of $DH°_{298}$ (QCC-H) is determined to be 101.1 + 1.67 = 102.77 kcal/mole, using $DH°_{298}$ (CH3CH2-H) = 101.1 kcal/mole.[130] $\Delta H_f°_{298}$ (C·CQ) is determined as 11.12 kcal/mole, using $DH°_{298}$ (QCC-H) = 102.77 kcal/mole and $\Delta H_f°_{298}$ (CCQ) = -39.52 kcal/mole which is derived from reaction IR1 in Scheme 2 at CBSlqM level.

Enthalpies of formation of other alkyl-hydroperoxy radicals can be also determined using $DH°_{298}$ (QCC-H) and $\Delta H_f°_{298}$ of corresponding hydroperoxide alkanes. $\Delta H_f°_{298}$ of alkyl-hydroperoxides and alkyl-hydroperoxy radicals determined in this work are listed in Table 4A.8c, with evaluated literature and our previous work reported by Lay et al.[76] Enthalpies of formation for alkyl-hydroperoxides are determined to be $\Delta H_f°_{298}$ (CCQ) = -39.70 ± 0.3 kcal/mole, $\Delta H_f°_{298}$ (CCCQ) = -44.77 ± 0.41 kcal/mole, $\Delta H_f°_{298}$ (CCQC) = -48.99 ± 0.32 kcal/mole, $\Delta H_f°_{298}$ (C_2CCQ) = -51.32 ± 0.38 kcal/mole, and $\Delta H_f°_{298}$ (C_3CQ) = -57.91 ± 0.57 kcal/mole based on average values from CBSlqM, CBSlqB, MP4F and B3LYP311 levels. The uncertainties in $\Delta H_f°_{298}$ are estimated as the sum of deviations between various levels of theory and the uncertainties of $\Delta H_f°_{298}$ of reference species in group balance isodesmic reactions. The deviations between various levels of theory (CBSlqM, CBSlqB, MP4F and B3LYP311 levels) are small and less than 0.58 kcal/mole. Enthalpies of formation of alkyl-hydroperoxy radicals are determined to be $\Delta H_f°_{298}$ (C·CQ) = 10.96 ± 1.06 kcal/mole, $\Delta H_f°_{298}$ (CC·CQ) = 2.62 ± 1.29 kcal/mole, $\Delta H_f°_{298}$ (C·CQC) = 0.68 ± 1.54 kcal/mole, $\Delta H_f°_{298}$ (C_2C·CQ) = -7.42 ± 1.25 kcal/mole, and $\Delta H_f°_{298}$ (C_3·CQ) = -6.42 ± 1.28 kcal/mole mole based on average values from CBSlqM, CBSlqB, MP4F and B3LYP311 levels.

Thermodynamic parameters of transition states and alkyl-hydroperoxy radicals based on CBSlqM and CBSlqB calculations are listed in Table 4A.9, with properties of reactants determined from THERM.[18] MP2(full)/6-31g(d) and B3LYP/6-31g(d) determined $S°_{298}$ and Cp(T)'s are in agreement; DFT-determined values are consistently higher than values of MP2 (one exception is $S°_{298}$ of C·CQ where MP2-determined entropy is higher than DFT value by 0.04 cal/mole-K). Differences are within 0.6 cal/mole-K ($S°_{298}$ of TS3B) and 1.22 cal/mole-K (Cp(800K) of C_3·CQ) for MP2 and DFT-determined $S°_{298}$ and Cp(T)'s, respectively. $S°_{298}$ of alkyl-hydroperoxy radicals are determined to be: $S°_{298}$ (C·CQ) = 82.23 cal/mole-K, $S°_{298}$ (CC·CQ) = 91.39 cal/mole-K, $S°_{298}$ (C·CQC) = 88.15 cal/mole-K, $S°_{298}$ (C_2C·CQ) = 97.93 cal/mole-K, and $S°_{298}$ (C_3·CQ) = 93.02 cal/mole-K based on average values from MP2(full)/6-31g(d) and B3LYP/6-31g(d) calculations. C_p(300) of alkyl-hydroperoxy radical are determined to be: C_p(300) (C·CQ) = 20.17 cal/mole-K, C_p(300) (CC·CQ) = 24.48 cal/mole-K, C_p(300)

(C·CQC) = 26.16 cal/mole-K, $C_p(300)$ (C_2C·CQ) = 30.32 cal/mole-K, and $C_p(300)$ (C_3·CQ) = 32.02 cal/mole-K.

5.4.4. High-Pressure Rate Constants (k_∞)

Table 4A.10 lists the total energy, ZPVE, thermal correction to enthalpies, and spin contamination (S^2) of reactants, transition states and product radicals calculated using MP2(full)/6-31G(d) and B3LYP/6-31G(d) geometries. The ZPVE are scaled by the factor 0.9661 and 0.9804 for MP2(full)/6-31G(d) and B3LYP/6-31g(d) frequencies, respectively. Table 4A.11 lists reaction enthalpies (energy differences between reactants and TSs) obtained from various levels of theory. Reaction enthalpy $(\Delta H^{\neq}_{TS\ -\ reactants})_{298}$ for HO_2 addition to the primary, secondary and tertiary carbon double bonds are 12.20 (11.85), 11.32 (10.78) and 7.74 (7.38) kcal/mole, respectively, at CBSlqM level. Data in parentheses are calculation at CBSlqB level. The value of 12.20 (11.85) kcal/mole is average value of HO_2 addition to primary carbon-carbon double of ethylene, propene and isobutene.

Table 4A.12 lists Mulliken charge for all species calculated at MP2(full)/6-31g(d) level. In the transition state, CH_3 groups donate electrons (ca. 0.22 to 0.26 Mulliken charge per CH_3, at MP2(full)/6-31g(d) level) to the olefinic carbon, which is undergoing bond formation with HO_2. Partial electron donation from two -CH_3 groups in the HO_2, electrophilic, radical addition to the CD/C2 carbon atom of isobutene results in a lower activation energy than addition to the CD/H2 atom, 7.63 vs.13.49 kcal/mole at CBSlqM level.

Table 4A.13 lists rate constants k_∞ determined from TST and fit by three parameters A_∞, n, and E_a over temperature range from 298 to 2000K. Calculated rate constants obtained at CBSlqM and CBSlqB levels of theory show similar trends with experimental data (in Table 4A.11b): HO_2 radical addition to the tertiary carbon double bond (HO_2 addition at CD/C2 carbon atom of isobutene) has a lower activation energy than addition to secondary carbon double bond CD/C/H, which is lower than addition to primary double bonds; the values are 12.11(11.56), 11.08(10.34) and 7.63(7.03) kcal/mole, respectively. The E_a's for addition to primary double bonds of ethylene, propene and isobutene also show a respective decreasing trend 13.49(12.89), 12.16(11.20) and 10.70(10.59) kcal/mole, respectively. Values reported by Walker's research group[121-125] from experiments on overall cyclic ether product formation rates show the E_a for HO_2 addition to carbon double bond CD/H2 (HO_2 + ethylene), CD/C/H (HO_2 + (E)-but–2-ene) and CD/C2 (HO_2 + 2,3-dimethylbut-2-ene) to be 17.85, 11.95 and 8.46 kcal/mole, respectively. These values from cyclic ether formation result from a kinetic analysis which often incorporates equilibrium and thermochemical properties significantly different from data in this study or our previously published evaluations.[80, 88, 126]

Comparison of calculated A_∞ factors for HO_2 radical addition to the primary, secondary and tertiary carbon double bonds indicates they are all similar, within one order of magnitude. Calculated values are also in agreement with experimental data, 1.92×10^{12}, 2.04×10^{11}, 1.90×10^{11} cm^3/mole-s (temperature range from 653K to 793K) for addition to carbon double bond CD/H2, CD/C/H and CD/C2, respectively. Those experimental A factors have been divided by two from reported values for adjustment steric effects. Reaction of HO_2 radical addition to tertiary carbon double bond has higher rate constant than HO_2 radical addition to primary and secondary, resulting from the lower E_a and similar A_∞ factor.

5.5 Summary

Thermodynamic properties of product radicals and transition states are calculated for HO_2 addition to primary, secondary and tertiary carbon-carbon double bond of ethylene, propene and isobutene using *ab initio* and density functional calculations. $\Delta H_f°_{298}$ for the alkyl-hydroperoxy radicals, C·CQ, CC·CQ, C·CQC, C_2C·CQ and C_3·CQ, are estimated using total energies derived from CBSlqM, CBSlqB, MP4F and B3LYP311 calculations and group balance isodesmic reactions with ZPVE and thermal correction to 298.15K. $\Delta H_f°_{298}$ are determined to be $\Delta H_f°_{298}$ (C·CQ) = 10.96 ± 1.06 kcal/mole, $\Delta H_f°_{298}$ (CC·CQ) = 2.62 ± 1.29 kcal/mole, $\Delta H_f°_{298}$ (C·CQC) = 0.68 ± 1.54 kcal/mole, $\Delta H_f°_{298}$ (C_2C·CQ) = -7.24 ± 1.25 kcal/mole, and $\Delta H_f°_{298}$ (C_3·CQ) = -6.42 ± 1.28 kcal/mole.

$S°_{298}$ and Cp(T) ($300 \leq T/K \leq 1500$) contributions from vibrational, translational, and external rotational are calculated using the rigid-rotor-harmonic-oscillator approximation based on geometric parameters and vibrational frequencies obtained at MP2(full)/6-31G(d) and B3LYP/6-31G(d) levels of theory. Contributions from hindered rotors of $S°_{298}$ and Cp(T) for C·CQ radical and TS1 are calculated by summation over the energy levels obtained by direct diagonalization of the Hamiltonian matrix of hindered internal rotations, while other radicals and TSs are calculated by method of Pitzer and Gwinn.

Activation energy based on CBSlqM and CBSlqB calculations show similar trends with experimental data. Calculated E_a's for HO_2 radical addition to the tertiary, secondary, and primary carbon double bond are 12.11(11.56), 11.08(10.34) and 7.63(7.03) kcal/mole, respectively. The Arrhenius pre-exponential factor, A_{800}, calculated from TST along with MP2 and DFT determined entropy, $1.00\text{x}10^{12}$ ($1.67\text{x}10^{12}$), $1.19\text{x}10^{11}$ ($2.37\text{x}10^{11}$) and $1.09\text{x}10^{11}$ ($2.54\text{x}10^{11}$) cm^3/mole-s for addition to CD/H2, CD/C/H and CD/C2 carbon-carbon double bonds, respectively, are also in agreement with experiment. Data in parentheses are calculation at CBSlqB level.

The high-pressure limit rate constants are (based on CBSlqB calculations):

$k_{1,\infty}(HO_2\text{+C=C}\Rightarrow\text{C·CQ})=6.97\text{x}10^3T^{2.63}\exp(-12.89\text{cal/mole/RT})\text{cm}^3\text{/mole-s}$;

$k_{2,\infty}(HO_2\text{+C=CC}\Rightarrow\text{CC·CQ})=2.30\text{x}10^3T^{2.51}\exp(-11.20\text{kcal/mole/RT})\text{cm}^3\text{/mole-s}$;

$k_{3,\infty}(HO_2\text{+C=CC}\Rightarrow\text{C·CQC})=7.40\text{x}10^2T^{2.68}\exp(-10.34\text{kcal/mole/RT})\text{cm}^3\text{/mole-s}$;

$k_{4,\infty}(HO_2\text{+}C_2\text{C=C}\Rightarrow\text{C·CQ})=2.62\text{x}10^4T^{2.20}\exp(-10.59\text{kcal/mole/RT})\text{cm}^3\text{/mole-s}$;

$k_{5,\infty}(HO_2\text{+}C_2\text{C=C}\Rightarrow\text{C·CQ})=1.59\text{x}10^3T^{2.58}\exp(-7.03\text{ kcal/mole/RT})\text{cm}^3\text{/mole-s}$.

Reverse (hydroperoxide alkyl radical unimolecular dissociation) rate constants are also reported:

$k_{-1,\infty}=1.80\text{x}10^{10}T^{0.63}\exp(-18.21\text{kcal/mole/RT})\text{cm}^3\text{/mole-s}$;

$k_{-2,\infty}=6.52\text{x}10^9T^{0.68}\exp(-17.45\text{kcal/mole/RT})\text{ cm}^3\text{/mole-s}$;

$k_{-3,\infty}=1.35\text{x}10^{12}T^{0.11}\exp(-17.79\text{kcal/mole/RT})\text{cm}^3\text{/mole-s}$;

$k_{-4,\infty}=1.15\text{x}10^{10}T^{0.61}\exp(-17.97\text{kcal/mole/RT})\text{cm}^3\text{/mole-s}$;

$k_{-5,\infty}=6.02\text{x}10^{13}T^{-0.35}\exp(-14.79\text{kcal/mole/RT})\text{ cm}^3\text{/mole-s}$.

CHAPTER 6

METHYL *TERT*-BUTYL ETHER OXIDATION AND PYROLYSIS EXPERIMENT: COMPARISON WITH MODEL

6.1 Overview

The oxidation and pyrolysis of methyl *tert*-butyl ether in argon diluent has been studied in a flow reactor over the temperature range 873 to 973 K and at atmospheric pressure and residence times between 0.5 - 2 sec. Three mixture compositions of MTBE and oxygen are studied in this MTBE oxidation study: equivalence ratios of 1.5 for a fuel-rich, 1.0 for a stoichiometric, and 0.75 for a fuel-lean as well as pyrolysis. The major products are analyzed by on line gas chromatography with flame ionization detectors and gas chromatography / mass spectrometry is used to identify and confirm gas species on batch samples. An elementary reaction mechanism including 1500 reactions is assembled. The CHEMKIN II interpreter and integrator, version 3.1, is used to model experimental data for MTBE profile and major product formations.

6.2 Experimental Approach

Reactant MTBE is HPLC grade supplied by Fisher Co. Argon and helium gases are reagent grade supplied by Liquid Carbonic Co. and filtered (activated carbon and molecular sieve) of O_2, H_2O, and hydrocarbon impurities before entering the reactor system. Argon flow is used as make-up gas to achieve the 0.5 % methyl *tert*-butyl ether concentration.

A diagram of the experimental apparatus is shown in Figure 5B.1. A 10.5mm ID quartz tube by 100 cm in length is employed as the reactor, which is housed within 63.5 cm length of a three-zone Clamshell 3.2 cm ID electric tube furnace equipped with three independent Omega Model CN-310 digital temperature controllers. Temperature profile versus reactor length are obtained at each flow using a type K thermocouple probe moved axially within the 100 cm length reactor. Temperature control results in temperature profiles isothermal to within ± 5 °C over 60 % of the furnace length for each temperature. The temperature profiles are shown in Figure 5B.2.

A bypass line for reactant gas flow around the heated reactor is used to determine the initial concentration of reactants without passing through the high temperature reactor zone. A temperature range from 873 to 973 K is covered at points of 873, 898, 923, 948, and 973 K. Reaction times (V/Q with V = volume of the reactor and Q = inlet flow rate under conditions of the reactor) ranges from 0.5 to 2.0 seconds with data points at 0.5, 1.0, 1.25, 1.5, 1.75 and 2.0 seconds. Four fuel to oxygen reaction ratios: pyrolysis ($\phi = \infty$), fuel rich ($\phi = 1.5$), stoichiometry ($\phi = 1.0$) and fuel lean ($\phi = 0.75$) are studied. The equivalence ratio ϕ is defined as : $\phi = 7.5\ (\%_{MTBE}/\%_{oxygen})$ by using the total reaction

$$(CH_3)_3COCH_3 + 7.5\ O_2 = 5\ CO_2 + 6\ H_2O$$

as a reference.

The inlet gas mixtures are preheated to about 150°C to insure mixing and improve the reactor temperature control. The reactants can either flow through the reactor or flow directly to GC sampling valve via a bypass line. The reactor effluent gas passes to the GC gas sampling valve through a heated line (~150°C) in order to limit condensation.

Gas samples are drawn through the sampling line by a mechanical vacuum pump with a constant flow rate of 30 mL/min. The bulk of the reactor effluent passes through a sodium bicarbonate (NaHCO3) flask for neutralization before bring released to a fume hood. A Varian-3270 Gas Chromatograph with two parallel columns and flame ionization detectors is used, on-line, to determine the concentration of reactants and products. Two six port VALCO gas sampling valves are employed to introduce the gas samples into the GC columns. Gas samples are passed through two sampling loops (1.0 cm^3 volume) in parallel at a constant flow rate of 30 cm^3/min, and then the valves are switched and the gases in the loop are injected into packed columns on the GC.

Two packed columns, 1.5m x 2.16mm ID, stainless steel column packed with 1% Alltech AT-1000 on Graphpac GB and 2.13m x 2.16mm ID stainless steel column packed with 80/100 Poropak Q, are used to perform separations of the hydrocarbonds, oxy-hydrocarbons, CO and CO_2. In order to quantitative analyze of CO and CO_2, a catalytic converter containing 5% of 80/100 ruthenium on alumna catalyst with constant flow (24.4 mL/min) of H_2 which is connected in series after the packed column and held at ~ 300 C°. This catalytic converter is used to convert the CO and CO_2 to methane after Poropak Q column separation, for amplified sensitivity on a FID.

The optimized conditions for the 1% Alltech AT-1000 on Graphpac GB column is: flow-rate of He carrier gas, 29.6 mL/min; detector temperature, 230 °C; and over temperature, maintained at 45 °C for 4 min, ramped to 150 °C at 12 °C/min for 45 min.

Signal from the two FIDs, with 1% Alltech AT-1000 on Graphpac GB and Poropak Q, are integrated by Varian 4270 and Spectra-Physics SP4270 integrators respectively. Calibration for obtaining appropriate molar response factors and retention times of relevant compounds is performed by injecting known concentrations of standard gases. The retention times vs. relative response factors are shown in Tables 5A.1 and 5A.2 for 1% Alltech AT-1000 on Graphpac GB column and Poropak Q column respectively.

Products identification was also performed in GC/MS (Hewlett Packard 5988) with a 50 m length, 0.22 mm I.D. methyl-silicone capillary column on batch sample. Gas sample is collected (trapped) by passing reactor effluent through a empty 2.16mm ID stainless column in liquid N2 bath for GC/MS analysis.

6.3 Experimental Results

Figure 5B.3 shows the GC peaks (from 1% Alltech AT-1000 on Graphpac GB column) on results of MTBE oxidation products (reactor temperature = 898 K, pressure = 1atm, fuel equivalence ratio = 0 75 and reaction time = 2.0 sec). The GC/MS peaks from 50m length, 0.22 mm I.D. methyl-silicone capillary column are shown in Figure 5B.4. The mass spectra at column reaction times of: 8.32, 8.55, 9.43, 9.99, 10.31, 10.58, and 15.53 minutes are show in Figures 5B.5-11 along with reference mass spectra. The carbon containing products analyzed by GC/MS are CO, CO_2, CH_4, C_2H_4, C_2H_6, CH_3OH, CH_2O, propene, acetone, acrolein (C=C-C=O), methyl acetate (CC(=O)OC), isobutyraldehyde (C_2CC=O), methacrolein (C=C(C)C=O), isopropenyl methyl ether (C=C(C)OC), and 2,5 dimethylhexa-1,5-diene.

6.3.1 Pyrolysis

Experimental results on MTBE pyrolysis are shown in Figures 5B.37a-37e for the temperatures of 873, 898, 923, 948, and 973 K respectively. Little or no MTBE decay is observed below 823 K. 41.6% ~ 96.1% of MTBE decay (2.9×10^{-3} to 2.0×10^{-4} in mole fraction) within reaction time (0.4 to 2 sec) at 923 K. The major products are isobutene and methanol. The concentrations of isobutene and methanol increase with increasing temperature (between 873 and 948 K) and reaction time (RT = 0.4 to 2.0 sec). The maximum concentrations of isobutene and methanol are 5.2×10^{-3} and 6.1×10^{-3} (in mole fraction) at RT = 1.25 sec and 1.5 sec, respectively, then decrease with increasing reaction time to 2.0 sec at 973 K. The concentrations of CH_4, CO, CH_2O and C=C-C increase with with increasing temperature (between 873 and 973 K) and reaction time (0.4 to 2 sec). Concentrations of those products are at the same order of magnitude (10^{-6} to 10^{-4} in mole fraction) between temperature range from 873 to 973 K and reaction time range from 0.4 to 2.0 sec. The concentrations of C_2H_2, isobutane, acetone, and $C_2CC{=}O$ are at the same order of magnitude (10^{-7} to 10^{-6} in mole fraction) while concentrations of C_2H_4, C_2H_6, and C=C(C)C=O are also at the same order of magnitude (10^{-7} to 10^{-5} in mole fraction) between temperature range from 873 to 973 K and reaction time range from 0.4 to 2.0 sec. No formation of C=C(C)OC product is observed under MTBE pyrolysis condition.

6.3.2 Fuel Rich Condition ($\phi = 1.5$)

Experimental results on oxidation reaction under fuel rich condition are shown in Figures 5B.38a-38e for the temperatures of 873, 898, 923, 948, and 973 K respectively. Little or no MTBE decay is observed below 823 K. 24.2% ~ 88.1% of MTBE decay (3.8×10^{-3} to 6.0×10^{-4} in mole fraction) within reaction time (0.4 to 2 sec) at 898 K. The major products are isobutene and methanol. The concentrations of isobutene and methanol increase with increasing reaction time (0.4 to 1.25 sec) at 898 K, the maximum concentrations of 3.3 × 10^{-3} and 4.4 × 10^{-3} (in mole fraction), respectively, at 898 K and 1.25 sec, then decrease with increasing reaction time. The concentrations of CH_4, CO, CO_2, C_2H_6, C_2H_4, C_2H_2, CH_2O, C=C-C and C=C(C)C=O increase with increasing reaction time (0.4 to 2 sec) at 898 K. The concentrations of acetone, C=C(C)OC, and C_2CC=O increase with increasing reaction time (0.4 to 1.5 sec) at 898 K , the maximum concentrations of 1.1 × 10^{-5} , 3.5 × 10^{-5} and 1.1 × 10^{-4} (in mole fraction), respectively, at 898 K and 1.75 sec, then decrease with reaction time.

Concentrations of isobutene and methanol increase with increasing temperature (between 873 and 923 K) and reaction time (0.4 to 2.0 sec), the maximum concentrations are 4.6 × 10^{-3} (at 973 K and RT = 0.75 sec) and 4.5 × 10^{-3} (at 973 K and RT = 0.5 sec) for isobutene and methanol, then decrease with temperature at 948 and 973 K. CO_2 concentration increases with increasing temperature (between 873 and 923 K) and reaction time (0.4 to 2.0 sec). Its concentration dramatically increases with reaction time (0.4 to 2.0 sec), 1.2 × 10^{-4} to 2.4 × 10^{-3} at 973 K. CO_2 shows a maximum concentration (2.4× 10^{-3}) at 973 K and 2 sec. CO concentration increases with increasing temperature (between 873 and 923 K) and reaction time (0.4 to 2.0 sec), the maximum concentration of CO is 2.2 × 10^{-2} at 973 K and reaction time of 1.5 sec, then slight decreases to 2.1 × 10^{-2} at 973 K and reaction time of 2.0 sec.

The maximum concentrations of CH_4, C_2H_4 and C_2H_2 are 2.4 × 10^{-3}, 1.3 × 10^{-3} and 1.1 × 10^{-4}, respectively, at 948 K and reaction time of 1.75 sec. The maximum concentration of C_2H_6 is 1.2 × 10^{-4} at 973 K and reaction time of 0.5 sec. No formations of C_2H_6 and C_2H_2 are observed at temperature 873 K.

Concentrations of acetone increases with increasing reaction time (0.4 to 2.0sec) at 873, 898 and 923 K, the maximum concentration is 1.3×10^{-5} (at 948 K and RT = 0.75 sec), then decrease with increasing reaction time to 2 sec at 973 K. Concentrations of C=C(C)OC and C_2CC=O increase with increasing reaction time (0.4 to 2.0 sec) at 873 and 898 K, while both concentrations increase with reaction time to 1.3×10^{-3} and 1.1×10^{-4}, respectively, at 1.25 sec and 948 K then decrease with reaction time at 973K. The concentration of C=C(C)C=O increases with increasing reaction time (0.4 to 2.0 sec) at 873 and 898 K. The maximum concentration is 4.3×10^{-4} (mole fraction) at 923 K and reaction time of 1.5 sec. The concentration of C=C(C)C=O decreases with increasing temperature (above 948 K) and reaction time (1.0 to 2.0 sec).

6.3.3 Stoichiometric Condition ($\phi = 1.0$)

Experimental results on oxidation reaction under stoichiometric condition are shown in Figures 5B.39a-39e for the temperatures of 873, 898, 923, 948, and 973 K respectively. Little or no MTBE decay is observed below 823 K. 19.6% ~ 83.3% of MTBE decay (4.0×10^{-3} to 8.4×10^{-4} in mole fraction) within reaction time (0.4 to 2 sec) at 898 K. The major products are isobutene and methanol. The concentration of isobutene and methanol increase with increasing reaction time (0.4 to 1.25 sec) at 873 and 898 K. The maximum concentration of isobutene is 4.5×10^{-3} at 923 K and 0.75 sec while the maximum concentration of methanol is 4.2×10^{-3} at 923 K and 0.5 sec. The concentrations of isobutene and methanol decrease with increasing reaction time (0.4 to 2.0 sec) at 948 and 973 K. The difference of MTBE decay is less than 5% between equivalence ratio of 1.5 and 1.0.

The concentrations of acetone, C=C(C)OC, $C_2CC=O$, C=C(C)C=O, C=C-C and CH_2O are increase with increasing reaction time (0.4 to 2.0 sec) at 873 and 898K while concentrations are decrease with increasing reaction time (0.4 to 2.0 sec) at 973K. At 923 K, those products have the maximum concentrations between reaction time at 0.75 and 1 sec while maximum formations at reaction time of 0.75 sec at 948 K.

The concentrations of CH_4, CO, CO_2, C_2H_6, C_2H_4 and C_2H_2 increase with increasing reaction time (0.4 to 2 sec) at 873, 898 and 923 K. The concentrations of CH_4, CO, CO_2, C_2H_6, C_2H_4 and C_2H_2 increase with reaction time to 1.75 sec at 923 K and decrease at 2.0 sec. At 973 K, concentrations of CH_4, CO and C_2H_4 reach the maximum amount at 1.0 sec then decrease with increasing reaction time to 2.0 sec while the maximum concentrations of C_2H_6 and C_2H_4 are at 0.5 sec. No formation of C_2H_6 and C_2H_4 are observed below 873 K.

6.3.4 Fuel Lean Condition ($\phi = 0.75$)

Experimental results on oxidation reaction under fuel lean condition are shown in Figures 5B.40a-40e for the temperatures of 873, 898, 923, 948, and 973 K respectively. Little or no MTBE decay is observed below 823 K. 25.2% ~ 86.4% of MTBE decay (3.7×10^{-3} to 6.8×10^{-4} in mole fraction) within reaction time (0.4 to 2 sec) at 898 K. The major products are isobutene and methanol. The concentration of isobutene and methanol increase with increasing reaction time (0.4 to 1.25 sec) at 898 K. The maximum concentration of isobutene and methanol are 4.4×10^{-3} at 923 K and 0.5 sec. The concentrations of isobutene and methanol decrease with increasing reaction time (0.4 to 2 sec) at 948 and 973 K. The differences of MTBE decay are less than 5% between different equivalence ratio of 0.5, 1.0 and 1.5.

The concentrations of acetone, $C_2CC=O$, C=C(C)C=O and C=C-C increase with increasing reaction time (0.4 to 2 sec) at 873 and 898K. At 973 K, the concentrations of acetone, C=C(C)OC, $C_2CC=O$, C=C(C)C=O, C=C-C and CH2O decrease with increasing reaction time (0.4 to 2 sec). Those products have the maximum concentrations between reaction time 1.0 and 1.5 sec. At 948 K, concentrations of C=C(C)OC, $C_2CC=O$ and C=C(C)C=O decrease with increasing reaction time (0.4 to 2 sec) while acetone, C=CC and CH2O have maximum formations between reaction time 0.75 and 1.25 sec.

The concentrations of CH_4, CO, C_2H_6, C_2H_4 and C_2H_2 increase with increasing reaction time (0.4 to 2 sec) at 873, 898 and 923 K. The concentration of CH_4, CO, and C_2H_4 increase with reaction time (0.4 to 1.25 sec) at 948 K then decrease between 1.25 and 2.0 sec. At 973 K, concentrations of CH_4, CO and C_2H_2 reach the maximum at 0.6 sec then decrease with increasing reaction time to 2.0 sec while the maximum concentration of C_2H_4 is at 0.5 sec. All MTBE are converted to CO and CO_2 at reaction time above 1.25 sec and 973 K.

6.4 Overall Mechanism

The mechanism which is developed in the CHEMKIN II format and includes three parts: (i) A Primary mechanism containing reactions in which MTBE, isobutene, *tert*-butyl radical and oxygen are considered as reactants; (ii) A secondary mechanism including reactions whose reactants are the molecular products formed by the primary mechanism (acetone ($C_2C=O$), methyl acetate ($CC(=O)OC$), isobutyraldehyde ($C_2CC=O$), methacrolein ($C=C(C)C=O$) and isopropenyl methyl ether ($C=C(C)OC$) are included); (iii) hydrogen, oxygen and C_1 –C_3 reactions obtained from previous studies. The types of reaction systems in overall mechanism are considered: H atom abstraction by O, H, OH, HO_2, O_2, CH_3 and $CH_3O\cdot$ radicals; addition with HO_2 and O_2; OH radicals addition to carbon carbon double bond and further react of these OH-adducts with O_2; OH radical addition to carbonyl bonds ($C=O$).

The reaction systems include:

MTBE → Products (Chapter 2)

$C_3{\cdot}COC$ → Products (Chapter 2)

$C_3{\cdot}COC + O_2$ → Products (Chapter 2)

$C_3COC\cdot$ → Products (Chapter 2)

$C_3COC\cdot + O_2$ → Products (Chapter 2)

Tert-butyl radical + O_2 → Products (Chapter 3)

Isobutene + HO_2 → Products (Chapter 3)

Isobutene + OH → Products (Table 5A.8 & Figure 5B.12)

Isobutene-OH + O_2 → Products (Chapter 3)

Allylic isobutenyl radical + O_2 → Products (Chapter 4)

$C_2C{\cdot}OC + O_2$ → Products (Table 5A.9 & Figure 5B.13)

$C=C(C)OC\cdot + O_2$ → Products (Table 5A.11 & Figure 5B.17)

$C=C(C\cdot)OC + O_2$ → Products (Table 5A.12 & Figures 5B.18-19)

$C{\cdot}=C(C)OC + O_2$ → Products (Table 5A.13 & Figure 5B.20)

C=C(C)OC + OH → Products (Table 5A.14 & Figure 5B.21)

HOCC· (C)OC + O_2 → Products (Table 5A.15 & Figure 5B.22)

C·C(OH)(C)OC + O_2 → Products (Table 5A.16 & Figure 5B.23)

C=C(C)OC + HO_2 → Products (Table 5A.17 & Figure 5B.24)

C·C(=O)OC + O_2 → Products (Table 5A.18 & Figure 5B.25)

CC(=O)OC· + O_2 → Products (Table 5A.19 & Figure 5B.26)

C_2·CC=O + O_2 → Products (Table 5A.20 & Figure 5B.27)

C_2C·C=O + O_2 → Products (Table 5A.21 & Figure 5B.28)

C_2CC·=O + O_2 → Products (Table 5A.22 & Figure 5B.29)

C=C(C·)C=O + O_2 → Products (Table 5A.23 & Figure 5B.30)

C=C(C)C·=O + O_2 → Products (Table 5A.24 & Figure 5B.31)

C=C(C)C=O + OH → Products (Table 5A.25 & Figure 5B.32)

C·C(OH)(C)C=O + O_2 → Products (Table 5A.26 & Figure 5B.33)

HOCC· (C)C=O + O_2 → Products (Table 5A.27 & Figure 5B.34)

CC(=O)C·=O + O_2 → Products (Table 5A.28 & Figure 5B.35)

C·C(=O)C=O + O_2 → Products (Table 5A.29 & Figure 5B.36)

OH addition to carbonyl bonds (C=O) of C=C(C)CO, C_2CC=O and

CC(C=O)C=O (Table 5A.10 & Figures 5B.14-16)

$R\cdot + HO_2 \longrightarrow ROOH^* \longrightarrow RO\cdot + OH$

Input parameters and references to specific high-pressure rate constants for those reaction systems are listed in Tables as describe above. Parameters in those Tables are referenced to the ground (stabilized) level of the complex, as this is the formalism used in QRRK theory. The potential energy diagrams are show in Figures as describe above. Reaction systems of $C_2{\cdot}COC + O_2$, $C_2C{=}C + OH$, C=C(C)OC + OH and OH addition to carbonyl bonds (C=O) of C=C(C)CO, $C_2CC{=}O$ and CC(C=O)C=O are performed at CBS-q//B3LYP/6-31g(d) calculation. The reaction enthalpies of group balance isodesmic reactions and total energies different between TSs and reactants and products are listed in Tables 5A.3-5A.6. Thermodynamic properties of TSs for those reaction systems are listed in Table 5A.7. Table 5A.30 lists group balance isodesmic reactions for determination $\Delta H^0_{f,\ 298}$ of CC(=O)OC, C=C(C)OC, $C_2CC{=}O$, and CC(=O)C=O stable molecules, and corresponding radicals. Reference high-pressure rate reactions used in Tables 5A.8-5A.29 for estimating A factor and Ea are listed in Table 5A.31. Those estimating high-pressure rate constants are obtained from fit with three parameter modified Arrhenius equation using canonical TST along with B3LYP-determined entropies for A factor and E_a evaluated from CBS-q// B3LYP/6-31g(d) calculation. Comparison experimental results and model under pyrolysis and stoichiometric condition are shown in Figures 5B.41 and 5B.42 for the temperatures of 873, 898, 923, 923, and 973 K. MTBE decay and major products isobutene and methanol formations are in good agreements between model calculation and experimental data under pyrolysis at 873, 898, 923, 948, and 973 K are showed in Figures 5B.34 – 38. MTBE decay is in good agreement between model prediction and experimental data under fuel lean, fuel rich and stoichiometric conditions at 873, 898, 948 and 973 K, while model prediction overestimate at 923 K. At 837 K, isobutene and methanol formations are in good agreements between model prediction and experimental data, but model prediction underestimate at high temperature. Model prediction for pyrolysis condition underestimate product formations of CH_4, C_2H_2, C_2H_4, C_2H_6, C=CC, C_3C, $C_2CC=O$ and C=C(C)C=O while overestimate product formations of CO, CH_2O and acetone. Model prediction for stoichiometric condition underestimate product formations of CH_4, C_2H_4, C_2H_6, C=CC and C=C(C)OC while overestimate product formations of CO, CO_2, C_2H_2, CH_2O, acetone, C_3C, $C_2CC=O$ and C=C(C)C=O.

6.6 Conclusion

Experimental data have been studied at 1 atm, temperatures of 873 K to 973 K and reaction time of 0.4 sec to 2.0 sec. The major products from both oxidation and pyrolysis of MTBE are isobutene and methanol, with C=C(C)OC, $C_2CC=O$, C=C(C)C=O, C=CC and CH_2O as important minor species at relative low temperatures. Small hydrocarbons, C_3H_6, C_2H_4, CH_4, are dominate at low [O_2] and high temperature conditions. CO_2 is produced with more O_2 in reactant fuel mixture and there is no CO_2 observed in pyrolysis environment. CO is observed in all environments and its concentration level is dependent on [O_2] and temperatures. Important secondary products are $C_2C=O$, CH_2O, CH_4, C_2H_4, C_3H_6, C=C(C)C=O, $C_2CC=O$, C=C(C)COH, C_2CCOH, CO and CO_2. More isobutene than methanol is produced under the conditions of high O_2 levels and relative lower temperatures, more formation of CH_3OH products than isobutene formation at high temperature. The difference between the amount of isobutene and methanol products is smaller in pyrolysis environment than oxidation condition. The differences of MTBE decay are less than 5% between different equivalence ratio of 0.5, 1.0 and 1.5. Isobutene formation are close between different equivalence ratio (Φ = 0.5, 1.0 and 1.5) at 873 K and more isobutene decay under Φ = 0.5 condition at 923, 948 and 973 K.

CHAPTER 7

STANDARD CHEMICAL THERMODYNAMIC PROPERTIES OF MULTI-CHLORO ALKANES AND ALKENES: A MODIFIED GROUP ADDITIVITY SCHEME

7.1 Overview

Chlorinated hydrocarbon groups plus non-next-nearest neighbor interaction terms, which combine with the Benson group additivity method for accurate estimation of thermodynamic properties ($\Delta H_f°$, S° and Cp(T)300-1500K) on multi-chloro alkanes and alkenes, are developed. New chlorocarbon alkane and alkene Benson type group values are derived from molecule systems where no chlorines are on the carbon adjacent to the carbon atom bonded to chlorine(s). A set of interaction terms for $\Delta H_f°$, S° and Cp(T)(300-1500K) is derived to account for non-next-nearest neighbor chlorine-chlorine interactions. These are derived from the experimental thermodynamic property data on 28 chlorinated hydrocarbons species and current hydrocarbon groups. Thermodynamic properties for representative multi-chloro alkanes and alkenes determined using this modified group additivity scheme are compared with literature data and show good agreement ($\Delta H_f°{}_{,298}=\pm0.29$ kcal/mole, $S°_{298}=\pm0.68$ cal/mole-K and Cp(T)=±0.23 cal/mole-K). The use of limited number of interaction groups provides improved accuracy in calculation of thermodynamic properties for multi-chloro alkanes and alkenes when chlorines are on adjacent carbon atoms. We develop three multi-chloro Benson groups plus five interaction groups for chloroalkanes; and two groups plus five interaction groups for chloroalkenes. This non-next-nearest neighbor interaction group approaches accounts 13.6 kcal/mole in standard enthalpy for hexachloro-ethane and 2.7 cal/mole-K in standard entropy for tetrachloro-ethylene. The multi-chloro groups combined with the interaction groups, allow estimation of thermodynamic properties ($\Delta H_f°$, S° and Cp(T) 300-1500K) on larger multi-chlorocarbon species, where no thermodynamic property data or accurate estimation techniques are available.

7.2 Introduction

Chlorocarbons are widely used chemicals or solvents in synthesis and in chemical industry, as starting materials and intermediates in synthesis of polymers, pesticides and other products. Many chlorocarbons are present in the atmosphere and chlorinated organic species are present in both municipal and hazardous wastes. Thermodynamic properties of chlorocarbons are important to industries utilizing them, in analysis of environmental effects and in evaluation of kinetics or thermodynamic equilibrium for both destruction and synthesis processes. These properties are also needed as input in some kinetic modeling and in equilibrium codes.

The presence of chlorocarbon is known to slow the overall oxidation rate of hydrocarbons through studies of flame velocity, temperature, and flame stability[131]. Reports of studies under varied condition sets indicate that both acceleration and inhibition effects can be observed in hydrocarbon reaction systems with a chlorinated hydrocarbon present.[132-134] It would be of significant value to have knowledge of their fundamental thermodynamic properties for equilibria calculations and for an accurate and fundamental understanding of the reaction pathways relating to chlorocarbon formation, destruction and interactions in synthesis, combustion and other environmental degradation/transformation processes.

Several techniques are available for estimation of thermodynamic properties data. *Ab initio* methods may be precise at higher levels but they are computationally time-intensive. They have difficulty treating large systems, and are untested for large chlorocarbon molecules. Semiempirical molecular orbital calculations are faster, require less memory or disk capacity than *ab initio*, but are not of sufficient accuracy for ΔH_f°'s. Dewar et al.[135] compared AM1 calculation results with the experimental data for 157 halogen-containing molecules. The AM1 error in heats of formation for more than 60 compounds were larger than ± 5 kcal/mole and the average error for organic halides was 4.39 kcal/mole. Li Zhu et al.[136] found similar or larger errors for MOPAC6 PM3 calculations[27] on chlorocarbon and chloro hydrocarbon compounds.

Benson's group method[128, 137-139] has been widely used to estimate enthalpies of formation and Gibbs free energies of reactions for many organic species. Group additivity is easy to use, it is based on experimental data and known to be accurate for hydrocarbons.[140, 141] Benson's group values do not, however, fully account for the steric or electrostatic interactions between adjacent bulky groups or atoms such as methyls, chlorines or other halogens on aromatics or alkyl chains when used for the estimation of thermodynamic properties (ΔH_f°, S° and Cp(T)(300-1500K)) of these molecules. These interactions are termed non-next-nearest neighbor interactions because they arise from the substituents on two adjacent central atoms: a central atom is defined by Benson[137] as an atom bonded to 2 or more substituents.

7.3 Procedure

Selection (definition) of the initial groups is critical to development of a group additivity scheme for accurate property estimation. It is also important to note that previous group additivity approaches for chlorocarbons did not incorporate effects of non-next-nearest neighbors. Consider the two molecules 1,1 dichloro-ethane and 1,2 dichloro-ethane and the groups that are used to estimate the thermodynamic properties.

	1,1 dichloro-ethane	1,2 dichloro-ethane
	CH_3-$CHCl_2$	CH_2Cl-CH_2Cl
Groups		
	$C/C/Cl_2/H$	$C/C/Cl/H_2$
	$C/C/H_3$	$C/C/Cl/H_2$

In the 1,1 dichloro-ethane isomer, the $C/C/Cl_2/H$ group incorporates polar and steric interactions between the two chlorines as well as adjacent hydrogens and carbons on the central carbon atom. The 1,2 dichloro-ethane isomer $C/C/Cl/H_2$ groups do not include or incorporate any interactions (polar, steric, ...etc.) between the two chlorines.

We derive a new set of groups for chlorocarbon alkanes and alkenes from the experimental thermodynamic property data on respective chlorinated hydrocarbons. The groups are derived from literature data on molecules where there are only carbon or hydrogen atoms on carbons which are adjacent to the carbon atom bonded to chlorine(s). The $C/C/Cl/H_2$, $C/C/Cl_2/H$ or $C/C/Cl_3$ groups are derived from chloro-ethane (CH_3CH_2Cl); 1,1 dichloro-ethane (CH_3CHCl_2); and 1,1,1 trichloro-ethane (CH_3CCl_3), respectively. There are no chlorines, other halogens, or bulky groups/fragments on the carbon atom(s) adjacent to the carbon atom containing the chlorines in the defining group. The C/C/Cl_3 group, for example, is defined from the parent 1,1,1 trichloro-ethane, and the C/C/H_3 group from hydrocarbon properties. Similarly CD/Cl/H and CD/Cl_2 groups are derived from chloro-ethylene (CH_2=CHCl) and 1,1 dichloro-ethylene (CH_2=CCl_2), respectively. Thermodynamic properties of chlorocarbons with no Cl on the carbon atoms adjacent a carbon with Cl are now accurately predicted; but an adjustment needs to be made for chlorocarbon species where there is a Cl (or other halogen) on an adjacent carbon, such as 1,2 dichloro-ethane, or 1,1,2 trichloro-ethylene. This adjustment comes in the form of an interaction group to count the total number of Cl atoms (that interact) on each of the two adjacent carbon atoms. There is no interaction group when the Cl atoms are only on one of the carbons. We choose an additive scheme for number of chlorines, thus CCl_3-CCl_3 has 6 interactions, not 9.

Our assumption is based on the known accuracy and validity of group additivity for hydrocarbon and oxyhydrocarbons[80, 128, 140, 141] with gauche interactions. Conventional group additivity does not, however, work for chlorocarbons. This is readily observed in comparison of enthalpies estimated by published Benson group values with experimental data illustrated in the enthalpy sections of Table 6A.1.

One alternate method to correct for non-next-nearest neighbor effects on adjacent carbons is use of gauche interactions.[138] This method is not, however, appropriate for chlorocarbon species. 1,2 dichloro-ethane, for example, has no Cl-Cl gauche interaction, but needs a correction (interaction term) of 2.54 kcal/mole to obtain the correct $\Delta H^\circ_{f,298}$ by group additivity using the C/C/Cl/H_2 group determined in this study (see below).

In our previous work, interaction terms for multiple Br, Cl, F, CH3 and OH substituents on aromatic compounds[142] and a set of groups for mono-chloroalkanes[143] have been developed. In this paper, we derive new chlorocarbon groups which can be used with the Benson group additivity scheme for calculation of the thermodynamic properties of multi-chloro alkanes and alkenes. Our method requires the inclusion of non-next-neighbor interaction terms (groups) when chlorine atoms are on carbons adjacent to a carbon bonded to one or more chlorine(s).

A multi-chloro group is derived by choosing representative molecules and their literature[144-146] thermodynamic properties $\Delta H_f°$, S° and Cp(T)(300-1500K). The molecules contain the same multi-chloro groups with no chlorines or other halogens on adjacent carbons. Average deviations in thermodynamic values determined by group additivity and the literature are obtained.

$X_{\text{ClC group}} = X_{\text{expt}} - \Sigma X_{\text{HC group}}$

where X represents the specific enthalpy, entropy, or heat capacity property.

$X_{\text{ClC group}}$ is the chlorocarbon group.

X_{expt} is the corresponding experimental or literature value.

$\Sigma X_{\text{HC group}}$ is the sum of the hydrocarbon groups in the molecule.

Deviations between group additivity values and literature values are minimized when more than one molecule with known thermodynamic properties is available for the group derivation. The multi-chlorocarbon groups result from minimization of the average deviations. The multi-chlorocarbon groups developed for use with the respective Benson/Cohen hydrocarbon groups (HC) are listed in Table 6A.2a. We choose the recent hydrocarbon (HC) group values published by Benson and Cohen[138, 141] for use in the derivation of our new HClC group data. The hydrocarbon (HC) group values of Benson and Cohen are listed in Table 6A.2b. Rln(σ) where σ is symmetry of the parent chloro hydrocarbon, is subtracted from the S value of the molecule in order to obtain the intrinsic entropy group value.

Thermodynamic properties of multi-chloro alkanes and alkenes with chlorine on adjacent carbons such as 1,2 dichloro-ethane are then further corrected by use of interaction terms which account for non-next-nearest neighbor interactions between the Cl substituents. Molecules having the same number (total) of these type of interactions are grouped together. $X_{INT} = X_{expt} - X_{Ga}$

X_{INT} is the interaction group.

The interaction group is based on the average thermo-value deviations for molecules in the grouping (same # of interactions). The nomenclature used is in terms of a general interaction: abbreviation (INT). For example, INT/Cl_2 indicates two adjacent Cl interactions, as in 1, 2 dichloro-ethane. Interaction groups developed for use with the respective Benson/Cohen hydrocarbon groups (HC) are listed in Table 6A.2c.

7.4 Discussion

Table 6A.1 shows the comparisons of $\Delta H_f^\circ{}_{,298}$ and $S^\circ{}_{298}$ in use of the original Benson and the newly derived (this work) groups using group additivity with literature data of Stull[146], TRC[144], and Pedley[145] for the relevant chlorocarbons. Tables 6A.3 and 6A.4 compare the heat capacity with the data from TRC[144] for the temperature at 300, 400, 500, 600, 800 and 1000K. In each table, the compounds selected for calculation of the group value are followed by the compounds which require interaction terms. While the data in each table are presented to two significant decimal places, they are not accurate to this degree. They are meant only for inclusion in developing computer codes for use in calculating molecule and radical thermodynamic properties and other applications where rounding off can be effected at the end of the summation.

Enthalpies, entropies and heat capacities as a function of temperature for any species can be easily determined manually or by THERM[78]. THERM also extrapolates data to 5000K and calculates ΔG_{rxn} and equilibrium constants. The groups, interaction terms, symmetry correction, and number of number internal rotors for the 28 reference species are listed in the appendix (internal rotors are used to adjust Cp $T=\infty$)[18]. Table 6A.5 estimates and gives example calculations for 6 larger and more complex multi-chloro species.

Figures 6B.1a and 6B.1c illustrate the deviations between values by using published Benson groups and literature values for $\Delta H_f°_{,298}$ (kcal/mole) and $S°_{298}$ (cal/mole-K), respectively, for the 24 reference multi-chloro alkanes and alkenes. Deviations range from -3.95, 1,2,3 trichloro-ethane, to 6.01 kcal/mole, 1,1,1 trichloro-ethane, in $\Delta H_f°_{,298}$ and from -1.43, 1,1 dichloro-hexane, to 2.96 cal/mole-K, 1,2 dichloro-ethane for entropy. Figures 6B.1b and 6B.1d illustrate the deviations for $\Delta H_f°_{,298}$ and $S°_{298}$, respectively, between values from our multi-chloro group values with interaction terms and literature measurements. Deviations are less than 1.06 kcal/mole, 1,1,2,2, tetrachloro-ethane, for $\Delta H_f°_{,298}$ and 1.67 cal/mole-K, 1,2 dichloro-propane for $S°_{298}$.

The interaction of chlorines across a carbon-carbon bond is accounted for by an interaction (correction) term. Figure 6B.2 illustrates that higher chlorinated species have stronger or increased interactions and that the correction increase is near quadratic with the number of interactions. For example, heat of formation for C_2Cl_6 using only nearest neighbor groups (groups derived in this work with no interaction group) is ca. 13

kcal/mole lower than the experimental data; the C_2Cl_6 molecule has six Cl interactions. Table 6A.6 lists the enthalpy interaction corrections on a per chlorine base. The corrections are near constant for the alkanes through 4 at 1.28 / Cl atom; but increase rapidly above 4, where number of gauche interaction increase 2 fold for each Cl added.

Contributions to entropy and heat capacities are from translation, rotations, vibrations and internal rotations. Changes in vibration and internal rotation with increased number of Cl's will affect the interaction (correction) terms. For chloro alkenes interaction terms (groups), INT/CD/Cl_2, INT/CD/Cl_3 and INT/CD/Cl_4, have no intramolecular rotation effect. As the number of chlorines across double bond increase, some vibrational frequencies decrease and lead to increase entropy and heat capacities at low temperature. Interaction terms (groups) for chloro alkanes, INT/Cl_2, INT/Cl_3, INT/Cl_4 INT/Cl_5 and INT/Cl_6, are more complex and are affected by both vibration and internal rotation. As the number of chlorines on second carbon increase, the internal rotation barrier increases but some vibrational frequencies decrease. A combined effect results in an initial decrease then an increase for entropies and heat capacities, with increase chlorine substitution.

Comparison of $\Delta H_f°_{,298}$ and $S°_{298}$ data in Table 6A.1 indicates that use of multi-chloro groups and interaction terms of this study provide good agreement with literature values. Deviations (group additivity values of this study vs. TRC values) are less than 1.08 kcal/mole for $\Delta H_f°_{,298}$. Data on entropies and heat capacities are also in good agreement with experimental data; deviations are less than 1.67 cal/(mole-K) for $S°_{298}$ and 1.25 cal/(mole-K) for Cp(T)(300-1500K).

We do not know if the cis/trans energies utilized by Benson are significant relative to the Cl/Cl interactions. Calculations of these interactions at the semiempirical molecular orbital level (MOPAC 6 AM1 and PM3)[51, 136] suggest very small or no difference in the thermodynamic properties of cis/trans isomers. Differences in $\Delta H_f°_{,298}$ are less than 0.4 kcal/mole, $S°_{298}$ and all heat capacity values are within 0.1 and 0.35 cal/mole-K respectively. We term this a CIS/Cl/Cl, and note that the correction is small relative to uncertainties. We therefore suggest that omission of this cis correction for simplicity is reasonable.

Estimation of Thermodynamic Properties for Larger (Greater than C2) Chlorocarbons

An important correction in larger chlorocarbons is use of the Cl/Cl interaction term values for gauche interactions where a chlorine is gauche to a methyl that contains a Cl. For example, 1,1,2,3 tetrachloro-propane would then have one INT/Cl3 for the 3 Cl/Cl interactions plus the one gauche-Cl interaction across the C1-C2 carbons; and one INT/Cl2 interaction for 2 Cl/Cl interactions across the C2-C3 carbons. Examples are provided in the estimations in Table 6A.5. The use of gauche-Cl interaction results from comparison of our group additivity estimation with limited literature data[137] on C3 and C4 chlorocarbons and comparisons of empirically corrected MOPAC6 PM3 calculated results on larger chlorocarbon systems.

We provide a further example of chlorine-chlorine interactions and describe one additional, important, interaction term for use in unsaturated chlorocarbons. MOPAC6 PM3 and AM1 calculations suggest reasons for the comparatively high enthalpies of formation for the following chlorinated 1,3-butadienes.

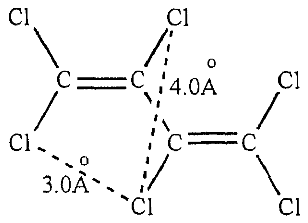

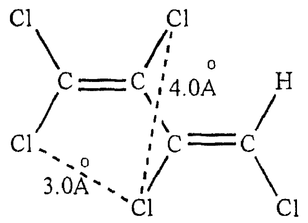

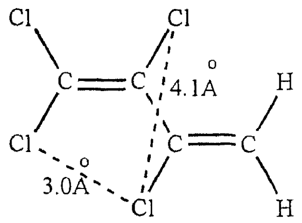

The distance between Cl atoms attached to the two CD/CD/Cl carbons is about 4.0Å while distance between the Cl atom on the CD/CD/Cl carbons and the Cl's cis(Z) to the ethylene groups is only ca. 3.0Å. The result of this close interaction between the two chlorines (cis like interaction across 3 bonds) is to twist the CD-CD single bond so the molecule is non planar and the π resonance is lost. We term this a Z/Cl/CD3 interaction (group) and calculate a correction value of 18.01cal/mole from 3 molecules in the literature[16] for $\Delta H_f^{\circ}{}_{,298}$ and 0.65 cal/(mole-K) for S°_{298}.

We have derived 5 chlorohydrocarbon groups and 10 interaction terms from a total of 28 molecules in literature. It is proposed that this set of groups and interaction terms be used to estimate higher carbon number chlorohydrocarbons until higher level calculations and or experimental data are available for development of an improved estimation scheme. At present limited results from an empirically derived correction applied to semiempirical calculations suggests the accuracy of this group additivity scheme is reasonable[80].

7.5 Summary

Three multi-chloro groups plus five interaction terms for chloroalkanes and two groups plus five interaction terms for chloroalkenes for use in group additivity are developed. The multi-chloro groups combined with the interaction groups, yield an improved estimation method for thermodynamic properties (ΔH_f°, S° and Cp(T) 300-1500K) for larger and more complex multi-chlorocarbon species, where no literature thermodynamic property data are available.

APPENDIX 1A

TABLES IN THE KINETIC AND THERMODYNAMIC ANALYSIS ON METHYL *TERT*-BUTYL ETHER DISSOCIATION AND OXIDATION

Table 1A.1 Total Energies, Zero-Point Energies And Thermal Corrections to Enthalpies

	Total Energy 0 K (Hartree)				ZPVE[a]	Thermal corr[b].
	B3LYP /6-31G(d,p)	B3LYP /6-31G(3df,2p)	CBS4 Energy	CBS-q Energy	(Hartree)	(kcal/mole)
Based on B3LYP/6-31G(d,p) Geometries						
OH	-75.7284818	-75.7655307	-75.6564577	-75.6655811	0.0084120	2.07
CH_3	-39.8428791	-39.8577461	-39.7587197	-39.7675895	0.0297420	2.54
CH_3OH	-115.7239626	-115.7729054	-115.5616179	-115.5773506	0.0513920	2.67
$CH_3O\cdot$	-115.0545946	-115.0991965	-114.8917400	-114.9093786	0.0365420	2.48
CH_2O	-114.5031976	-114.5492467	-114.3592600	-114.3759095	0.0267180	2.39
C_2H_6	-79.8387446	-79.8615270	-79.6614036	-79.6777145	0.0749520	2.77
C_2H_5	-79.1652067	-79.1900054	-78.9982882	-79.0144245	0.0594340	3.07
C_2H_4	-78.5938067	-78.6210956	-78.4394715	-78.4561889	0.0511190	2.50
COC	-155.0329666	-155.0885304	-154.7847603	-154.8072095	0.0799050	3.29
$COC\cdot$	-154.3689591	-154.4263307	-154.1283719	-154.1512037	0.0660470	3.35
CCOH	-155.0462071	-155.1049509	-154.8044251	-154.8273972	0.0801340	3.29
C=COH	-153.8160552	-153.8766023	-153.5922289	-153.6156268	0.0567680	2.86
$C_2{=}COH$	-193.1415846	-193.2120396	-192.8409632	-192.8715003	0.0848630	3.63
C(OH)2	-190.9497822	-191.0320988	-190.7202809	-190.7431883	0.0574530	2.95
C=COCC	-232.4423693	-232.5202449	-232.0555434	-232.0928983	0.1139650	4.35
$C_2C{=}O$	-192.8599962	-192.8915819	-193.1642116	-193.2307601	0.0837150	4.00
$C_3C\cdot$	-157.4842749	-157.5147029	-157.8092737	-157.8534737	0.1156470	3.97
C_2COH	-194.3687326	-194.4364068	-194.0485824	-194.0790207	0.1082580	3.99
C_3COH	-233.6891708	-233.7668666	-233.2951755	-233.3328053	0.1358040	4.82
CCOC	-194.3550837	-194.420442	-194.0279640	-194.0576084	0.1084460	4.06
C_2COC	-233.6745954	-233.7495869	-233.2711845	-233.3082164	0.1364220	4.87
$C_2\cdot COC$	-232.9977198	-233.074013	-232.6032942	-232.6401113	0.1215080	5.02
$C_2C\cdot OC$	-233.0160041	-233.0922067	-232.6184318	-232.6557597	0.1226680	5.03
$C_2COC\cdot$	-233.0091505	-233.0854648	-232.6132076	-232.6506884	0.1226240	4.88
C_3COC	-272.9914817	-273.0761333	-272.5146416	-272.5588638	0.1641400	5.69
$C_3\cdot COC$	-272.3152331	-272.4015987	-271.8473998	-271.8913696	0.1486800	5.52
$C_3COC\cdot$	-272.3294424	-272.4157665	-271.8600329	-271.9046192	0.1502200	5.69
COOH	-190.8563041	-190.9322544	-190.6158969	-190.6416999	0.0547400	3.30
HOCOOH	-266.0794992	-266.1890779	-265.7727837	-265.8059749	0.0605780	3.68
$O\cdot COOH$	-265.4098431	-265.515307	-265.1012325	-265.1367493	0.0458550	3.49
C=CC	-117.9165469	-117.9535785	-117.6819799	-117.7054810	0.0798180	3.16
C=CCOH	-193.120848	-193.1938519	-192.8216887	-192.8519727	0.0848850	3.77
$C_2C{=}C$	-157.2388352	-157.2885553	-156.9261782	-156.9565204	0.1080830	3.92
C_2CCOH	-233.6804196	-233.7588227	-233.2843792	-233.3215348	0.1368700	4.85
C_2CCQ	-308.8119007	-308.917536	-308.3388372	-308.3861500	0.1400520	5.68
$C_2\cdot CCQ$	-308.1365983	-308.2439247	-307.6732626	-307.7202907	0.1248030	5.95
$C_2C\cdot CQ$	-308.1505861	-308.2565517	-307.6827151	-307.7303010	0.1252160	5.97
C=C(C)OC	-232.4476539	-232.5258033	-232.0641655	-232.1013077	0.1134710	4.43
C=C(C)CQ	-307.5770887	-307.6854766	-307.1239823	-307.1714635	0.1165370	5.29
C=COHOC	-268.3494707	-268.451387	-267.9758848	-268.0128109	0.0896600	4.32
C_2CCOC	-272.9872283	-273.0718444	-272.5063246	-272.5503100	0.1652860	5.65
TS9	-272.2899862	-272.3780372	-271.8072407	-271.8633420	0.1474530	5.95
TS10	-272.3031521	-272.3905237	-271.8213709	-271.8776076	0.1458900	6.18
TS13	-272.2678617	-272.3575192	-271.7902639	-271.8442630	0.1459830	6.02
Based on B3LYP/6-31G(d) Geometries						
OH	-75.7234543	-75.7654943	-75.6565131	-75.6656518	0.0083060	2.07
CH_3OH	-115.7144039	-115.7728491	-115.5615065	-115.5772655	0.0514520	2.66
$CH_3O\cdot$	-115.0504618	-115.0991947	-114.8915237	-114.9091613	0.0367730	2.48
C_2H_6	-79.8304208	-79.8614843	-79.6610854	-79.6774113	0.0752520	2.77
C_2H_5	-79.1578671	-79.1899782	-78.9980592	-79.0142090	0.0596450	3.08
COC	-155.0250451	-155.0885161	-154.7844018	-154.8068463	0.0803050	3.28
$COC\cdot$	-154.3618207	-154.4262618	-154.1280481	-154.1508759	0.0663630	3.34

Table 1A.1 (Continued)

	Total Energy 0 K (Hartree)				ZPVE [a]	Thermal corr [b].
	B3LYP /6-31G(d,p)	B3LYP /6-31G(3df,2p)	CBS4 Energy	CBS-q Energy	(Hartree)	(kcal/mole)
			Based on B3LYP/6-31G(d) Geometries			
COOH	-190.8472708	-190.9322151	-190.6157444	-190.6415612	0.0548740	3.29
COO·	-190.2152293	-190.2914205	-189.9750368	-190.0052633	0.0432600	3.01
CCOH	-155.0337984	-155.1048856	-154.8041980	-154.8272042	0.0802950	3.27
CCOOH	-230.1665214	-230.263758	-229.8576881	-229.8909312	0.0836400	3.97
$C(OH)_2$	-190.9364343	-191.0320383	-190.7202165	-190.7431599	0.0574080	2.93
COCOC	-269.5522496	-269.6589669	-269.1636606	-269.2000961	0.1142170	4.67
CH_2O	-114.5004711	-114.5492502	-114.3591643	-114.3758137	0.0268190	2.39
C·OOH	-190.1817231	-190.2668064	-189.9564129	-189.9828907	0.0404460	3.34
O·COOH	-265.4021446	-265.5152889	-265.1011577	-265.1366687	0.0459640	3.49
$C_2C=C$	-157.2272862	-157.2854882	-156.9257269	-156.9561072	0.1084940	3.92
C=C(C·)OC	-232.4361834	-232.5257551	-232.0636894	-232.1008549	0.1139260	4.42
C=C(C·)COOH	-307.5620754	-307.6854094	-307.1235851	-307.1711028	0.1168590	5.28
C_2C·COOH	-308.1343836	-308.2564912	-307.6822240	-307.7298523	0.1256230	5.97
C·COCQ	-344.0173117	-344.158088	-343.5690418	-343.6161954	0.1023200	5.45
YCOCOC	-268.3440911	-268.4471326	-267.9744164	-268.0090806	0.0933570	3.57
$C_2CYCCOCO$	-346.9829881	-347.110695	-346.4681881	-346.5175100	0.1493390	5.15
C_3COH	-233.6709556	-233.7667589	-233.2947504	-233.3324340	0.1361480	4.82
C_3COC	-272.9747731	-273.0760524	-272.5139251	-272.5581776	0.1648420	5.68
C_3COCQ	-423.3224832	-423.487986	-422.7229902	-422.7846199	0.1733130	6.93
C_3·COCQ	-422.6508191	-422.8160003	-422.0584716	-422.1198575	0.1582660	7.08
C_3COCQ·	-422.6885646	-422.8458848	-422.0811579	-422.1473230	0.1614830	6.70
$C_2CICQOC$	-423.3065992	-423.4725135	-422.7075227	-422.7688731	0.1727810	7.19
C_2·CICQOC	-422.6353186	-422.8011587	-422.0431871	-422.1044996	0.1578850	7.24
C_2CICQ·OC	-422.6768738	-422.8345332	-422.0709618	-422.1366158	0.1614890	6.78
$C_2CICQOC$·	-422.6450989	-422.8116007	-422.0525551	-422.1143343	0.1587660	7.19
TS1	-422.6407061	-422.80141	-422.0415631	-422.1069231	0.1559880	6.01
TS2	-422.6269484	-422.7893265	-422.0323358	-422.0966102	0.1550520	6.25
TS3	-422.6355618	-422.8022278	-422.0442230	-422.1065468	0.1587020	6.66
TS3	-422.6218329	-422.7893795	-422.0159358	-422.0888577	0.1546920	7.64
TS4	-422.6039657	-422.7713399	-421.9984426	-422.0703752	0.1565600	7.00
TS5	-422.6078418	-422.7757379	-421.9995090	-422.0735298	0.1563140	7.35
TS6	-422.6450609	-422.8057865	-422.0470561	-422.1111334	0.1555870	5.96
TS8	-422.6306016	-422.7978215	-422.0207222	-422.0945795	0.1571210	6.99
TS11	-422.6299973	-422.7965409	-422.0126974	-422.0968764	0.1573450	6.74

a. Unscaled zero-point vibrational energies in Hartrees. In the calculation of reaction enthalpies, ZPVE is scaled by 0.9661 and 0.9806 for MP2(full)/6-31g(d) and B3LYP/6-31g(d) levels, respectively.

b. Thermal corr. in kcal/mole: Thermal corrections are calculated as follows for T=298.15 K: $H°_T - H°_0 = H_{trans}(T) + H_{rot}(T) + \Delta H_{vib}(T) + RT$; $H_{trans}(T) = (3/2)RT$, $H_{rot}(T) = (3/2)RT$, $\Delta H_{vib}(T) = N_A h \Sigma \nu_i / (\exp(h\nu_i/kT) - 1)$, where N_A is the Avogadro constant, h is the Plant constant, k is the Boltzman constant, and ν_i is vibrational frequencies.

Table 1A.2 Reaction Enthalpies

Reactions Enthalpies^a	CBS-4	CBS-q	B3LYP /6-31g(d)	B3LYP /6-311+g(3df,2p)
			//B3LYP/6-31g(d)	
C_3COC → TSMTBE	64.76	61.36	57.16	55.39
$C_2C{=}C{+}CH_3OH$ → TSMTBE	47.01	44.78	41.13	46.27
$C_3{\cdot}COC$ → TS9^b	25.63	18.02	23.31	22.23
$C_2C{*}C + CH_3O$ → TS9^b	6.24	1.15	3.44	5.49
$C_3{\cdot}COC$ → TS13^b	36.35	30.06	28.57	26.50
$C{*}(C)COC + CH_3$ → TS13^b	19.52	14.51	14.98	17.09
$C_2ClCQ{\cdot}OC$ → TS1	17.68	17.86	18.54	16.63
$C_2ClCQOC{\cdot}$ → TS1	5.72	3.47	-0.13	3.51
$C_2ClCQ{\cdot}OC$ → TS2	23.70	24.57	26.83	23.87
$C_2{\cdot}ClCQOC$ → TS2	5.81	3.96	2.51	4.69
$C_2ClCQOC{\cdot}$ → TS3	23.42	16.43	12.54	11.88
$C_2C{\cdot}CQ + CH_2O$ → TS3	15.25	9.82	8.83	10.93
$C_2{\cdot}ClCQOC$ → TS4	27.84	21.17	18.62	17.66
$C{*}C(C)OC + C{\cdot}H_2OOH$ → TS4	12.84	7.63	9.34	13.91
$C_2{\cdot}ClCQOC$ → TS5	27.52	19.54	16.38	15.09
$C{*}C(C)COOH + CH_3O$ → TS5	9.38	3.82	4.19	6.81
$C_3COC{\cdot}$ → TS10^b	24.75	17.44	14.32	13.67
$C_3C{\cdot} + CH_2O$ → TS10^b	13.73	7.98	7.84	9.64
$C_3COCQ{\cdot}$ → TS6	20.65	21.96	22.93	20.79
$C_3{\cdot}COCQ$ → TS6	6.04	4.35	0.84	3.64
$C_3{\cdot}COCQ$ → TS8	23.60	15.78	11.90	10.62
$C_2C{*}C + O{\cdot}COOH$ → TS8	3.45	-1.55	0.49	3.08
$C_3{\cdot}COCQ$ → TS11	28.39	14.09	12.17	11.31
$C_2YCOCOC + OH$ → TS11	69.80	53.67	47.31	49.32

UNIT: kcal/mole

a. Reaction enthalpies include thermal correction and zero-point energy correction

b. Based on B3LYP/6-31g(d,p) geometries

Table 1A.3 Reaction Enthalpies for Group Balance Isodesmic Reaction

Group Balance Isodesmic Reactions[a]	CBS-4	CBS-q	B3LYP /6-31g(d)	B3LYP /6-311+g(3df,2p)
			//B3LYP/6-31g(d)	
C_3COC + COH = C_3COH + COC[b]	-2.55	-2.63	-4.34	-4.13
C_3COC + COC· = **C_3COC·** + COC[b]	-1.17	-1.16	-1.33	-1.25
C_3COCQ + CCOH + COH = $C_2CICQOC$ + $C(OH)_2$ + CC	-0.06	-0.20	-1.48	0.06
COCOC + $2CH_3OH$ = **$C(OH)_2$** + 2COC	-1.96	-1.89	-3.37	-2.70
C_3COCQ + CH_3OO· = **C_3COCQ·** + CH_3OOH	0.76	0.68	1.10	0.74
C_3COCQ + CC· = **C_3·COCQ** + CC	0.77	0.81	-0.38	0.48
$C_2CYCCOCO$ + CH_3OH = CYCCOCO + C_3COH	1.98	1.97	0.98	0.94
$C_2CYCCOCO$ + CC· = **C_2CYCC·OCO** + CC	-5.72	-6.17	-7.21	-6.64
$C_2CYCCOCO$ + COC· = **$C_2CYCCOC$·O** + COC	-4.11	-4.37	-4.61	-3.73
$C_2CYCCOCO$ + CC· = **C_2·CYCCOCO** +CC	2.36	2.29	1.18	1.58
HOCOOH + CH_3OH = $C(OH)_2$ + CH_3OOH[b]	-1.22	-1.09	-1.62	-1.46
HOCOOH + CH_3O· = **O·COOH** + CH_3OH[b]	1.05	0.78	0.25	0.11

Group Balance Isodesmic Reactions	CBS-4	CBS-q	B3LYP /6-31g(d)	B3LYP /6-311+g(3df,2p)
			//B3LYP/6-31g(d)	
C_3COC + COH = C_3COH + COC[b]	-2.55	-2.63	-4.34	-4.13
C_3COC + CC· = **C_3·COC** + CC[b]	2.11	2.16	1.26	1.45
$C_2CICQOC$ + CC = C_3COC + CCOOH	-2.20	-2.08	-2.72	-3.68
$C_2CICQOC$ + CH_3OO· = **C_2CICQ·OC** + CH_3OOH	-2.72	-2.65	-1.37	-1.68
$C_2CICQOC$ + COC· = **$C_2CICQOC$·** + COC	-0.92	-0.95	-1.17	-0.93
$C_2CICQOC$ + CC· = **C_2·CCQOC** + CC	0.57	0.48	-0.62	0.09
C*C(C)CQ + C*CC + CH_3OH = C_2C*C + C*CCOH + CH_3OOH[b]	2.27	2.45	0.87	-1.84
C*C(C)OC + C*COH + CCOH = C_2*COH + C*COCC + COH[b]	1.77	1.70	1.24	1.35
C_2CCQ + CH_3OH = C_2CCOH + CH_3OOH[b]	-0.09	-0.03	-0.64	-0.50
C_2CCQ + CC· = **C_2·CCQ** + CC[b]	1.50	1.57	1.23	1.43

UNIT: kcal/mole

c. Reaction enthalpies include thermal correction and zero-point energy correction

d. Based on B3LYP/6-31g(d,p) geometries

Table 1A.4 Thermodynamic Properties

SPECIES	ΔH°_{f298}	S°_{298}	Cp_{300}	Cp_{400}	Cp_{500}	Cp_{600}	Cp_{800}	Cp_{1000}	Cp_{1500}
O	59.51	38.4	5	5	5	5	5	5	5
OH	9.5	43.8	6.79	6.86	6.93	7	7.14	7.28	
O_2	0	49	6.86	7.1	7.33	7.54	7.89	8.18	8.7
HO_2	3.5	54.7	8.28	8.78	9.26	9.71	10.5	11.16	12.24
H_2O	-57.8	43.72	8.17	8.88	9.56	10.2	11.3	12.1	12.98
CH_3	34.8	46.3	9.12	9.91	10.68	11.41	12.75	13.9	16
CH_4	-17.9	44.4	8.71	9.82	10.99	12.19	14.52	16.6	20.17
CH_2O	-26	50.92	8.47	9.38	10.46	11.52	13.37	14.81	
$CH_3O\cdot$	3.96	55.84	9.51	11.04	12.61	14.13	16.67	18.58	21.43
$C\cdot H_2OH$	-3.6	60.41	11.77	13.27	14.42	15.47	17.22	18.61	20.85
CH_3OH	-48	57.3	10.49	12.34	14.22	16.02	19.05	21.38	25.02
O·C=O	-38.3	65.04	9.52	11	12.3	13.29	15.12	16.26	
$C\cdot H_2OOH$	14.6	68.25	16.55	18.4	19.87	21.44	23.2	24.93	
O·COOH	-23.05	74.21	16.93	20.21	22.98	25.16	28.11	29.96	32.47
$C_2C{=}C$	-3.8	69.99	21.58	26.65	31.3	35.34	41.91	46.89	54.71
$C_2\cdot C{=}C$	32.56	70.99	20.96	26.09	30.52	34.22	40.07	44.43	51.22
$C_3C\cdot$	11.7	75.67	22.33	27.04	31.82	36.27	43.62	49.34	58.53
$C_2C\cdot COOH$	-6.77	97.77	28.62	34.89	40.86	46.01	53.99	59.71	68.42
C_3COC	-68.02	85.62	32.2	40.3	47.7	53.97	63.75	70.95	82.25
$C_3COC\cdot$	-24.59	89.17	32.82	40.53	47.31	52.93	61.53	67.86	77.86
$C_3\cdot COC$	-16.36	93.12	33.38	40.57	47	52.45	60.99	67.38	77.58
C_3COCQ	-94.67	103.1	40.18	49.98	58.43	65.29	75.39	82.43	93.14
$C_3COCQ\cdot$	-59.79	102.11	38.48	47.46	55.2	61.52	71	77.83	88.38
$C_3\cdot COCQ$	-44.36	109.89	41.12	50.1	57.65	63.73	72.63	78.88	88.49
$C_2CICQOC$	-85.81	106.95	40.12	49.32	57.47	64.23	74.39	81.62	92.66
$C_2CICQ\cdot OC$	-54.26	105.57	38.01	46.49	54	60.27	69.92	76.96	87.88
$C_2CICQOC\cdot$	-42.17	110	40.76	49.57	57.1	63.21	72.22	78.56	88.31
$C_2\cdot CICQOC$	-35.83	111.42	40.99	49.4	56.66	62.63	71.63	78.06	88.03
C=C(C)OC	-36.03	81.44	23.46	28.62	33.52	37.82	44.79	50.08	58.49
C=C(C)CQ	-24.53	90.51	28.25	34.76	40.48	45.18	52.22	57.19	64.77
$C_2YCCOCO$	-91.71	80.03	29.02	37.95	45.96	52.65	62.73	69.88	80.67
$C_2CICO\cdot OC$	-54.44	97.21	34.61	43.46	50.66	56.64	66.41	73.29	
$C_3COCO\cdot$	-61.57	94.65	35.12	43.56	50.61	56.56	66.37	73.3	
$C_2C\cdot COC{=}O$	-60.29	102.72	32.07	38.23	44.14	49.43	58.23	64.9	
$C_3\cdot COCO$	-62.49	99.21	33.07	40.53	46.96	52.19	60.62	66.81	
TSMTBE	-6.84	88.67	31.21	38.42	45.47	51.76	61.98	69.66	81.65
TS1	-37.55	89.06	35.49	45.45	54.08	61.17	71.72	79.11	90.21
TS2	-30.78	95.76	35.93	45.25	53.41	60.2	70.5	77.86	89
TS3	-24.35	110.71	39.57	48.14	55.66	61.83	71.04	77.51	87.39
TS4	-14.23	108.77	38.68	47.2	54.6	60.71	69.93	76.53	86.73
TS5	-16.52	110.39	38.36	46.76	54.23	60.46	69.85	76.54	86.8
TS6	-38.92	88.45	35.49	45.68	54.4	61.49	71.96	79.28	90.28
TS8	-26.85	107.54	37.95	47.13	55.01	61.4	70.77	77.31	87.27
TS9	1.49	91.89	30.46	37.73	44.43	50.17	59.17	65.85	76.38
TS10	-6.74	89.54	31.58	39	45.74	51.47	60.32	66.82	76.99
TS11	-29.41	94.39	37.04	46.44	54.44	60.95	70.7	77.69	88.58
TS13	13.49	92.65	32.46	39.54	45.8	51.08	59.47	65.85	76.16

Units: Hf: Kcal/mole; S & Cp(T): cal/mole

Table 1A.5 Frequencies and Moments of Inertia for Transition State (TSMTBE) Calculated at B3LYP/6-31g(d, p) Level

Molecule	Frequencies	Moments of inertia[a]
TSMTBE	(-1748.37), 70.91, 121.28, 155.15, 197.96, 223.46, 235.24, 300.92, 372.09, 419.39, 433.44, 539.25, 573.96, 815.64, 913.95, 927.42, 991.11, 1034.30, 1050.88, 1069.62, 1127.87, 1172.72, 1178.90, 1324.73, 1383.44, 1411.38, 1420.25, 1426.67, 1476.56, 1479.75, 1487.43, 1491.51, 1503.15, 1507.87, 1515.26, 1535.79, 1650.67, 2933.19, 2987.64, 3012.52, 3023.45, 3030.96, 3104.49, 3113.46, 3122.21, 3146.22, 3157.53, 3205.35	425.74293 780.66853 806.21650

Unit: amu-Bohr^2

Table 1A.6 Input Parameters and High-Pressure Limit Rate Constants (k_∞) for QRRK Calculation $C_3COC \rightarrow$ Products

Reaction	A (s-1 or cm^3/mol-s)	n	Ea (kcal/mol)	ref.
$C_3COC \rightarrow C_2C{*}C + CH_3OH$	2.15×10^{13}	0.19	58.72	a.
$C_3COC \rightarrow C_3C\cdot + CH_3O$	4.98×10^{17}	0.	79.61	b.
$C_3COC \rightarrow C_3CO\cdot + CH_3$	2.92×10^{15}	0.	81.17	c.
$C_3COC \rightarrow C_2C\cdot OC + CH_3$	8.66×10^{16}	0.	81.91	d.
$C_3COC \rightarrow C_3\cdot COC + H$	2.48×10^{16}	0.	103.31	e.
$C_3COC \rightarrow C_3COC\cdot + H$	1.37×10^{15}	0.	95.30	f.

Geometric mean frequency
C_3COC: 359.6 cm^{-1} (9.831), 1312.5 cm^{-1} (13.523), 3164.2 cm^{-1} (8.146)
Lennard-Jones parameters: $\sigma = 5.5471$ A°, $\varepsilon/k = 584.86$ K

a. Fit with three parameter modified Arrhenius equation; A estimated using canonical TST and B3LYP-determined entropies, Ea evaluated from CBS-q// B3LYP/6-31g(d) calculation.
b. k via <MR>; $A_r = 9.04 \times 10^{12}$, 90 TSA. $E_{a,f} = \Delta U_{rxn}$
c. k via <MR>; $A_r = 1.21 \times 10^{13}$, 86 TSA/HAM for $CH_3O + CH_3 \rightarrow COC$. $E_{a,f} = \Delta U_{rxn}$
d. k via <MR>;$A_r = 1.63 \times 10^{13}\ T^{-0.596}$, 90 TSA for C3C. + $CH_3 \rightarrow$ neo-C5. $E_{a,f} = \Delta U_{rxn}$
e. k via <MR>;$A_r = 3.61 \times 10^{13}$, 90 TSA for C3C. + H → Prod.. $E_{a,f} = \Delta U_{rxn}$
f. k via <MR>;$A_r = 1.30 \times 10^{13}$, for CCC. + H → CCC. $E_{a,f} = \Delta U_{rxn}$

Table 1A.7 Input Parameters and High-Pressure Limit Rate Constants (k_∞) for QRRK Calculation $C_3COC\cdot \rightarrow C_3C\cdot + CH_2O$

Reaction	A (s-1 or cm^3/mol-s)	n	Ea (kcal/mol)	ref.
$C_3COC\cdot \rightarrow C_3C\cdot + CH_2O$	1.68×10^{12}	0.36	18.19	a.

Geometric mean frequency
$C_3COC\cdot$: 359.6 cm^{-1} (9.831), 1312.5 cm^{-1} (13.523), 3164.2 cm^{-1} (8.146)
Lennard-Jones parameters: σ = 5.5471A°, ε/k = 584.86 K

a. Fit with three parameter modified Arrhenius equation; A estimated using canonical TST and B3LYP-determined entropies, Ea evaluated from CBS-q// B3LYP/6-31g(d) calculation.

Input Parameters and High-Pressure Limit Rate Constants (k_∞) for RRK Calculation $C_3COC\bullet + O_2 \rightarrow$ Product

Reaction	A (s-1 or cm^3/mol-s)	N	Ea (kcal/mol)	ref.
$C_3COC\cdot + O_2 \rightarrow C3COCQ\cdot$	3.60×10^{12}	0.	0.	b.
$C_3COCQ\cdot \rightarrow C_3COC\cdot + O_2$	9.39×10^{14}	0.	32.63	c.
$C_3COCQ\cdot \rightarrow C_3\cdot COCQ$	2.00×10^{6}	1.27	20.34	a.
$C_3COCQ\cdot \rightarrow C_3COCO\cdot + O$	3.57×10^{14}	0.	56.20	d.
$C_3\cdot COCQ \rightarrow C_3COCQ\cdot$	5.49×10^{6}	0.49	5.18	a.
$C_3\cdot COCQ \rightarrow C_2C{*}C + \cdot OCOOH$	4.01×10^{12}	0.003	17.95	a.
$C_3\cdot COCQ \rightarrow C2YCCOCO + OH$	3.66×10^{9}	0.03	15.23	a.

Geometric mean frequency
$C3COCQ\cdot$: 359.6 cm^{-1} (9.831), 1312.5 cm^{-1} (13.523), 3164.2 cm^{-1} (8.146)
$C_3\cdot COCQ$: 359.6 cm^{-1} (9.831), 1312.5 cm^{-1} (13.523), 3164.2 cm^{-1} (8.146)
Lennard-Jones parameters: σ = 5.5471A°, ε/k = 584.86 K

b. Estimated from $CCC\cdot + O_2 \rightarrow CCCQ\cdot$
c. <MR>
d. Estimated from $O + CH_3O$

Table 1A.8 Input Parameters and High-Pressure Limit Rate Constants (k_∞) for QRRK Calculation $C_3\cdot COC \rightarrow$ Products

Reaction	A (s-1 or cm^3/mol-s)	N	Ea (kcal/mol)	Ref.
$C_3\cdot COC \rightarrow C_2C{*}C + CH_3O$	6.33×10^{12}	0.02	18.29	a.
$C_3\cdot COC \rightarrow C{*}C(C)OC + CH_3$	1.90×10^{12}	0.30	30.31	a.

Geometric mean frequency
$C_3\cdot COC$: 359.6 cm^{-1} (9.831), 1312.5 cm^{-1} (13.523), 3164.2 cm^{-1} (8.146)
Lennard-Jones parameters: σ = 5.5471A°, ε/k = 584.86 K

a. Fit with three parameter modified Arrhenius equation; A estimated using canonical TST and B3LYP-determined entropies, Ea evaluated from CBS-q// B3LYP/6-31g(d) calculation.

Input Parameters and High-Pressure Limit Rate Constants (k_∞) for RRK Calculation $C_3\bullet COC + O_2 \rightarrow$ Product

Reaction	A (s-1 or cm^3/mol-s)	N	Ea (kcal/mol)	Ref.
$C_3\cdot COC + O_2 \rightarrow C_2CICQ\cdot OC$	3.60×10^{12}	0.	0.	b.
$C_2CICQ\cdot OC \rightarrow C_3\cdot COC + O_2$	1.57×10^{15}	0.	36.65	c.
$C_2CICQ\cdot OC \rightarrow C_2CICQOC\cdot$	3.56×10^{4}	1.65	15.95	a.
$C_2CICQ\cdot OC \rightarrow C_2\cdot CICQOC$	3.84×10^{7}	1.14	23.14	a.
$C_2CICQ\cdot OC \rightarrow C_2CICO\cdot OC + O$	3.26×10^{14}	0.	58.33	d.
$C_2CICQOC\cdot \rightarrow C_2CICQ\cdot OC$	3.93×10^{6}	0.58	4.32	a.
$C_2CICQOC\cdot \rightarrow C_2C\cdot CQ + CH_2O$	1.62×10^{12}	0.40	18.15	a.
$C_2\cdot CICQOC \rightarrow C_2CICQ\cdot OC$	4.12×10^{8}	0.30	5.00	a.
$C_2\cdot CICQOC \rightarrow C{*}C(C)OC + C\cdot H_2OOH$	1.67×10^{12}	0.13	22.04	a.
$C_2\cdot CICQOC \rightarrow C{*}C(C)CQ + CH_3O\cdot$	5.62×10^{12}	0.06	19.75	a.

Geometric mean frequency
$C_2CICQ\cdot OC$: 359.6 cm^{-1} (9.831), 1312.5 cm^{-1} (13.523), 3164.2 cm^{-1} (8.146)
$C_2CICQOC\cdot$: 359.6 cm^{-1} (9.831), 1312.5 cm^{-1} (13.523), 3164.2 cm^{-1} (8.146)
$C_2\cdot CICQOC$: 359.6 cm^{-1} (9.831), 1312.5 cm^{-1} (13.523), 3164.2 cm^{-1} (8.146)
Lennard-Jones parameters: σ = 5.5471A°, ε/k = 584.86 K

b. Estimated from $CCC\cdot + O_2 \rightarrow CCCQ\cdot$
c. <MR>
d. Estimated from $O + CH_3O$

APPENDIX 1B

FIGURES IN THE KINETIC AND THERMODYNAMIC ANALYSIS ON METHYL *TERT*-BUTYL ETHER DISSOCIATION AND OXIDATION

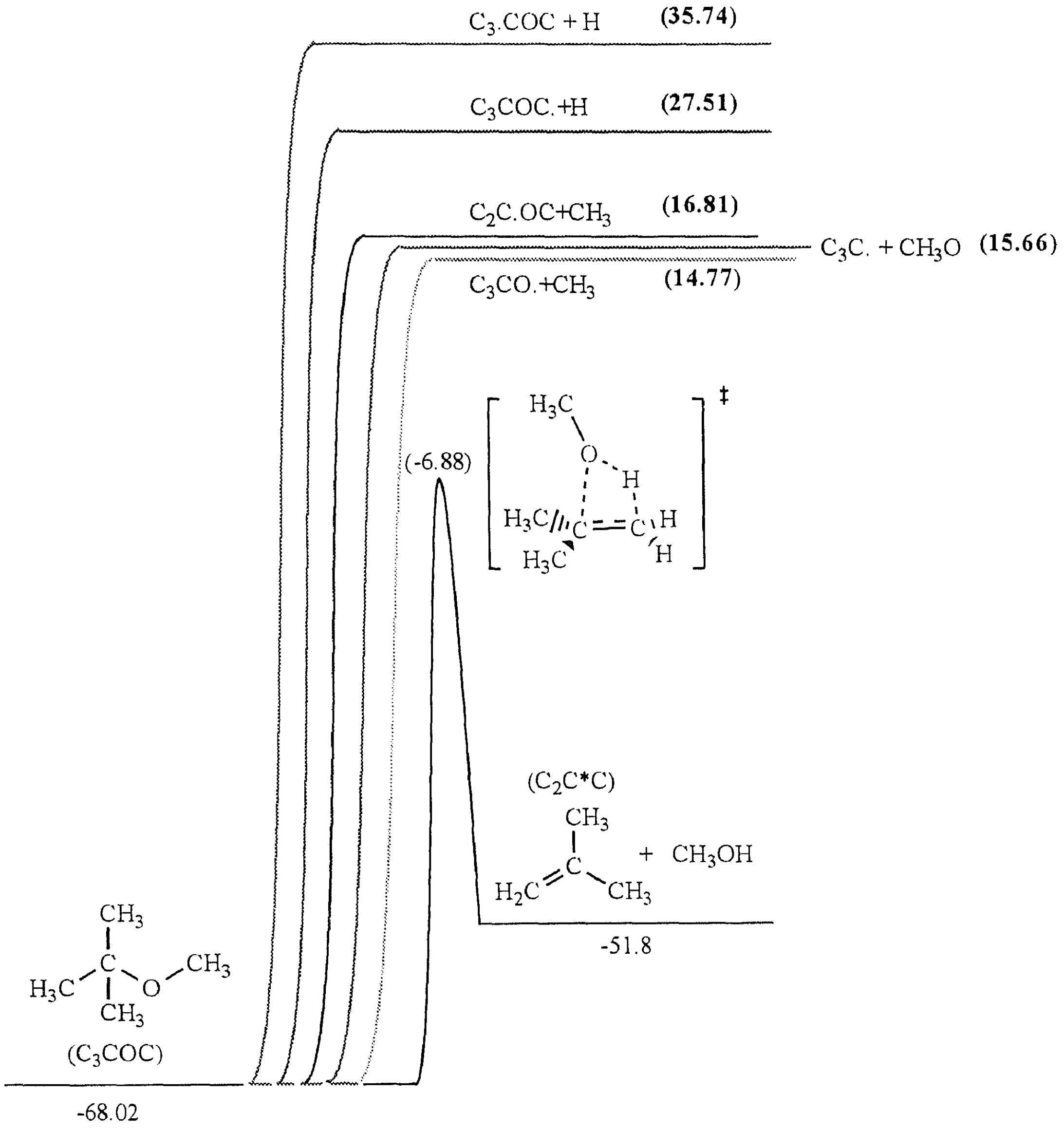

Figure 1B.1 The potential energy level diagram for MTBE dissociation

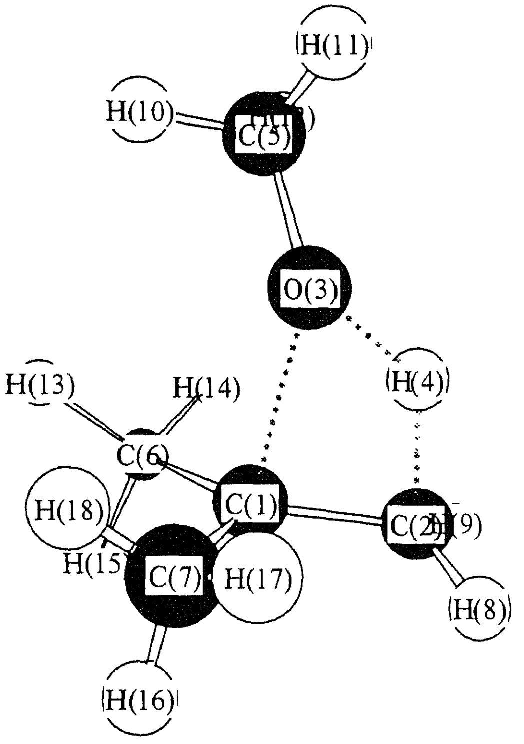

Bond Length (Å)		Bond Angle (degree)		Dihedral Angle (degree)	
r21	1.4250	a312	86.23	d4312	3.33
r31	2.0635	a431	59.09	d5312	117.82
r43	1.3190	a531	128.30	d6123	101.43
r53	1.3978	a612	120.33	d7123	263.90
r61	1.4999	a712	120.19	d8213	105.44
r71	1.5008	a821	117.59	d9213	249.40
r82	1.0881	a921	117.36	d10531	73.38
r92	1.0886	a1053	110.70	d11531	191.66
r105	1.1026	a1153	111.00	d12531	312.48
r115	1.1019	a1253	113.58	d13612	210.12
r125	1.1061	a1361	112.08	d14612	333.08
r136	1.0931	a1461	111.64	d15612	91.46
r146	1.0922	a1561	108.37	d16712	273.41
r156	1.0991	a1671	108.63	d17712	32.07
r167	1.0997	a1771	110.94	d18712	154.11
r177	1.0913	a1871	112.00		
r187	1.0921				

Figure 1B.2 Structure of transition state for reaction $C_3COC \leftrightarrow C_2C=C + CH_3OH$

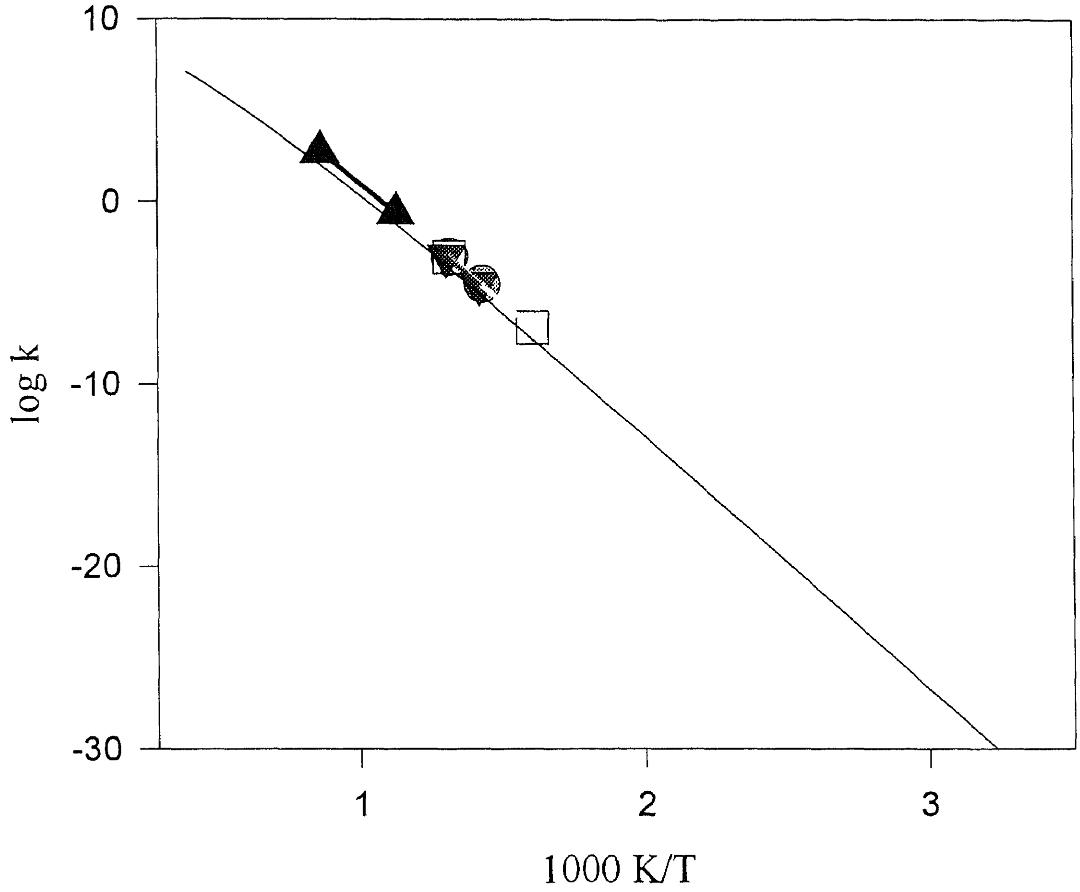

Figure 1B.3 Comparison of CBS-q//B3LYP/6-31g(d) calculated rate constant with experimental values for reaction $C_3COC \rightarrow C_2C{=}C + CH_3OH$

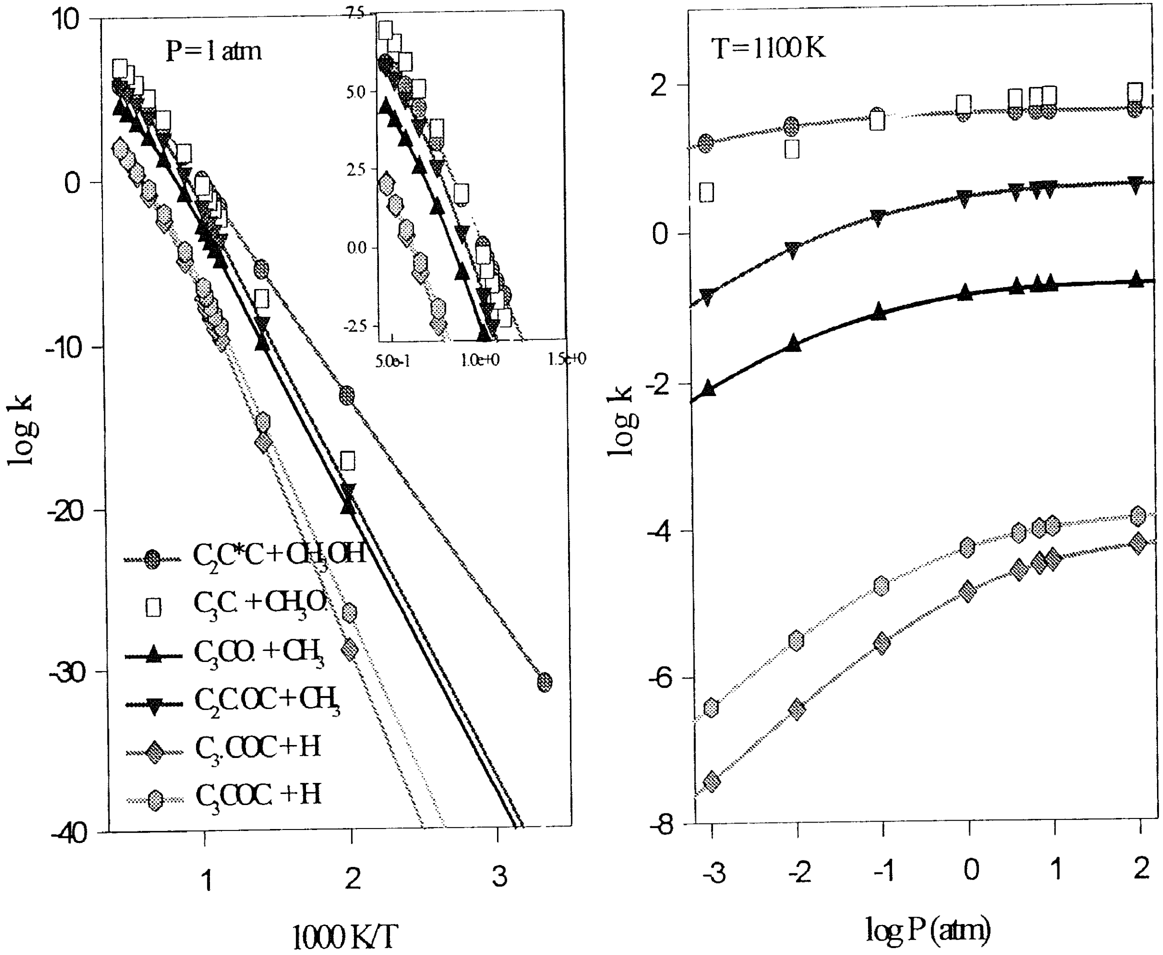

Figure 1B.4 QRRK calculated rate constants for C_3COC -> products

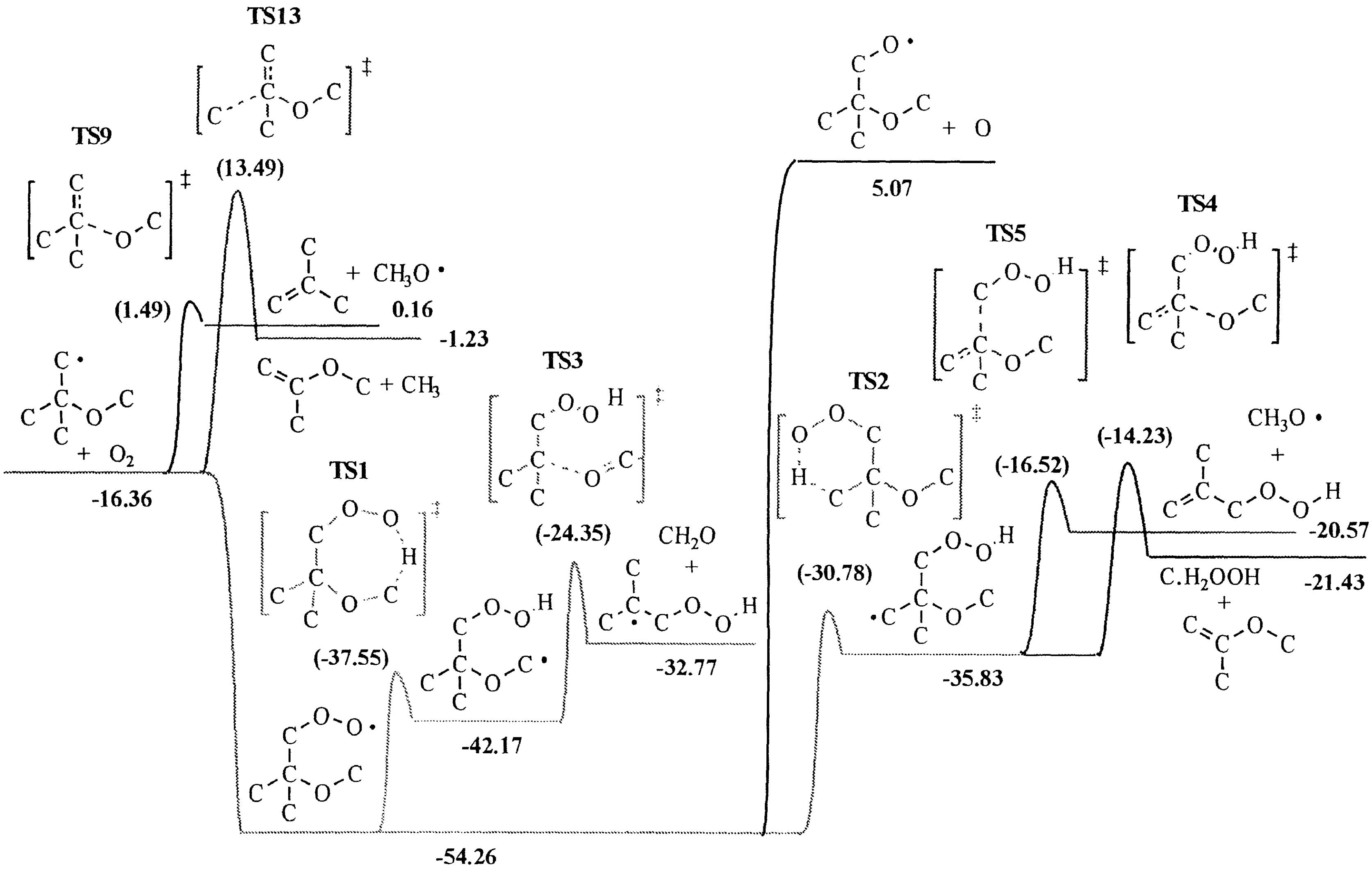

Figure 1B.5 The potential energy level diagram for $C_3 \cdot COC + O_2$ -> products

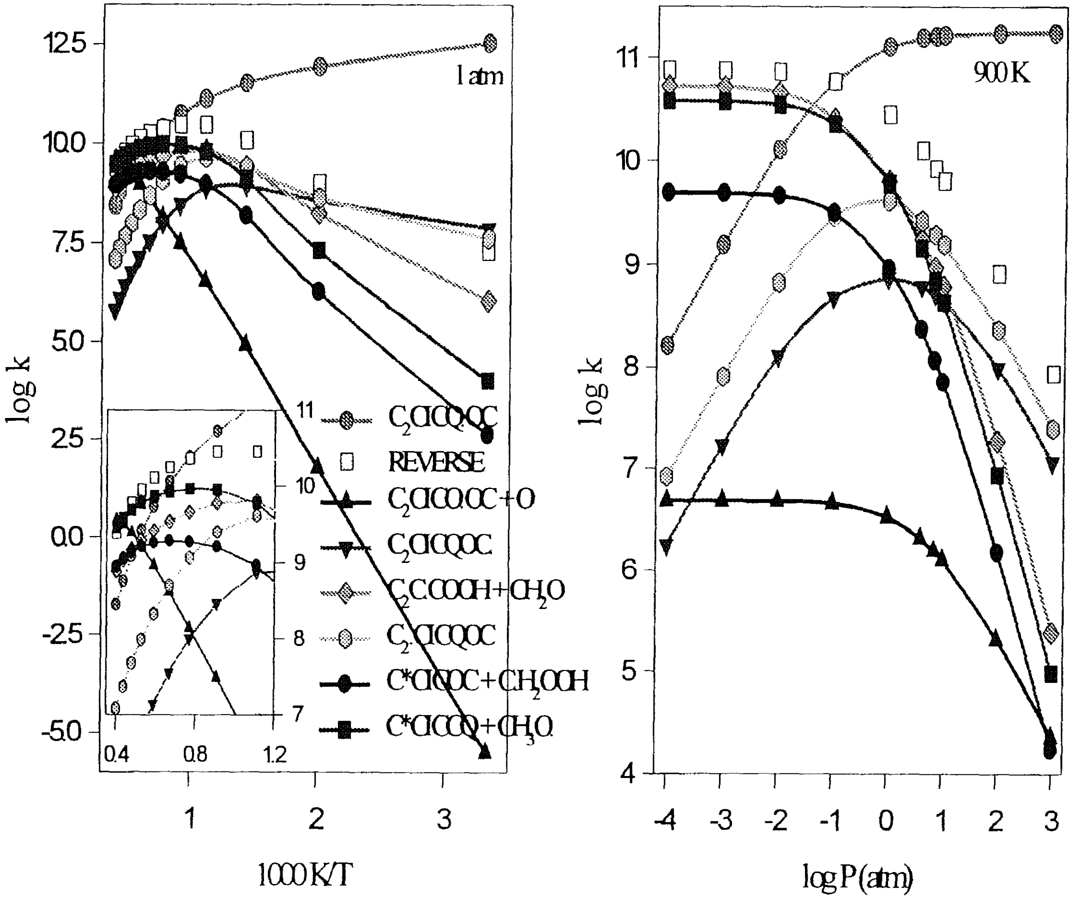

Figure 1B.6 QRRK calculated rate constants for $C_3{\cdot}COC + O_2$ -> $[C_2ClCQ{\cdot}OC]^*$ -> products

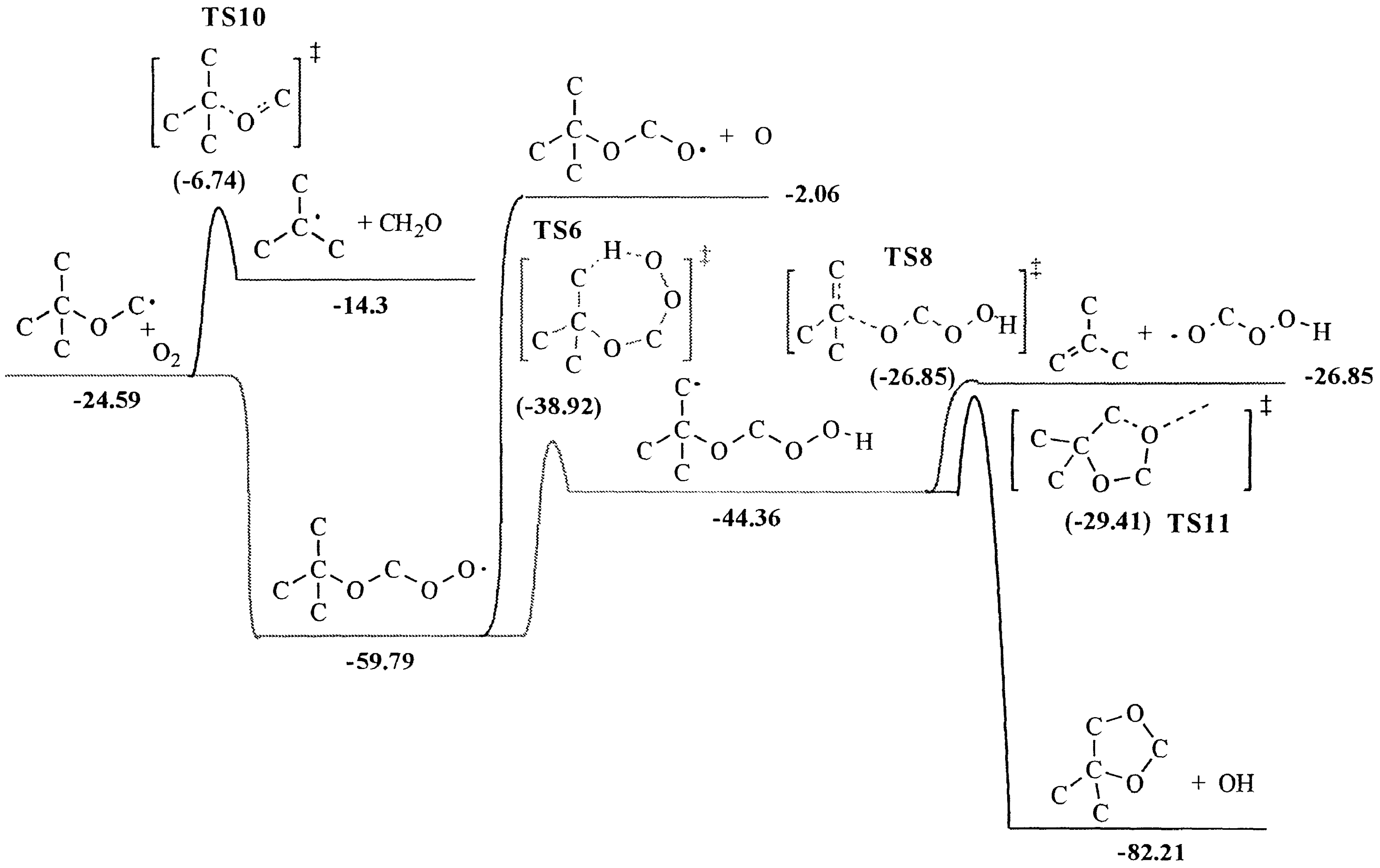

Figure 1B.7 The potential energy level diagram for $C_3COC\cdot + O_2$ -> products

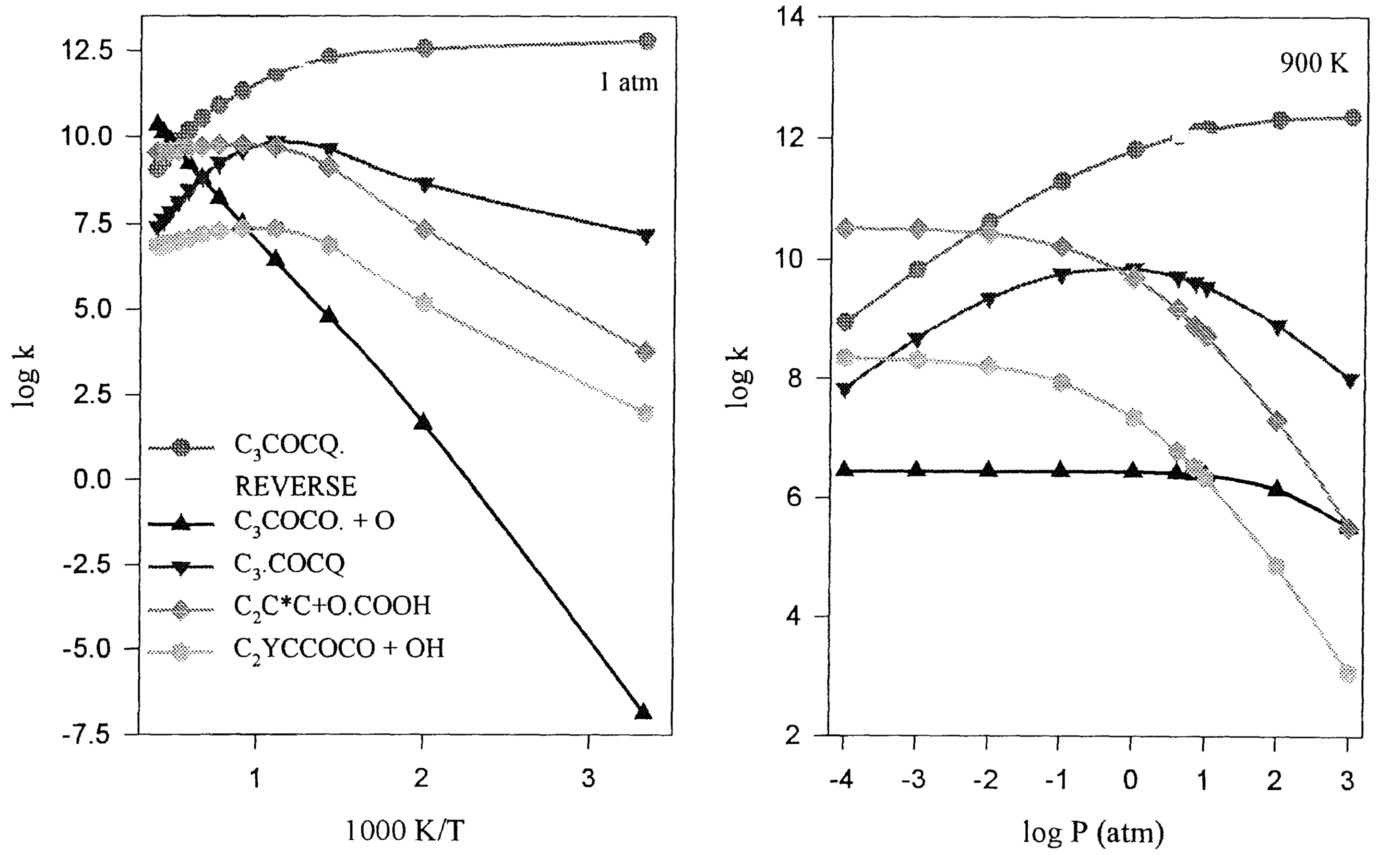

Figure 1B.8 QRRK calculated rate constants for $C_3COC\cdot + O_2$ -> $[C_3COCQ\cdot]^*$ -> products

APPENDIX 2A

TABLES IN THE ANALYSIS OF TERTIARY BUTYL RADICAL + O_2, ISOBUTENE + HO_2, ISOBUTENE + OH AND ISOBUTENE-OH ADDUCTS + O_2: A DETAILED TERTIARY BUTYL OXIDATION MECHANISM

Table 2A.1 Total Energies (E, Hartree), Zero-Point Energies (ZPE, Hartree, unscaled) and Thermal Corrections to Enthalpies ($H_{thermal}$, Kcal/mole)

	Geometry [a]	Total Energy 0 K (Hartree)	CBS4 Energy 0 K (Hartree)	CBS-q Energy 0 K (Hartree)	ZPVE [b] (Hartree)	Thermal corr [c]. (kcal/mole)
O_2	B3LYP	-150.3200379	-150.1712192	-150.1894687	0.0037790	2.08
	MP2	-149.9543197	-150.1698796	-150.1886165	0.0032180	2.08
HO_2	B3LYP	-150.8991541	-150.7471229	-150.7692372	0.0140230	2.38
	MP2	-150.5023650	-150.7472364	-150.7691685	0.0143970	2.38
$C_3C\cdot$	B3LYP	-157.7983253	-157.4847320	-157.5152719	0.1172620	4.60
	MP2	-157.1957939	-157.4840491	-157.5143749	0.1208430	4.42
$C_3COO\cdot$	B3LYP	-308.1729037	-307.7123770	-307.7647070	0.1278390	5.32
	MP2	-307.2013203	-307.7124269	-307.7640157	0.1313710	5.13
$C_3\cdot CQ$	B3LYP	-308.1277093	-307.6813989	-307.7295115	0.1243930	5.85
	MP2	-307.1674984	-307.6804133	-307.7279854	0.1284340	5.69
$C_2C{=}C$	B3LYP	-157.2272862	-156.9257269	-156.9561072	0.1084940	3.92
	MP2	-156.6463970	-156.9258866	-156.9561746	0.1106620	3.90
TS1	B3LYP	-308.1235557	-307.6641159	-307.7186974	0.1215310	5.33
	MP2	-307.1436192	-307.6661269	-307.7193443	0.1252530	5.12
TS2	B3LYP	-308.1044353	-307.6542136	-307.7043273	0.1213150	4.92
	MP2	-307.1288762	-307.6517572	-307.7017197	0.1260070	4.71
TS3	B3LYP	-308.1107498	-307.6536277	-307.7126306	0.1237190	5.70
	MP2	-307.1231334	-307.6534212	-307.7117598	0.1277380	5.50
TS4	B3LYP	-308.1121421	-307.6392894	-307.7058520	0.1228820	5.62
	MP2	-307.1188941	-307.6460046	-307.7071357	0.1268270	5.33
$C_2C\cdot COOH$	B3LYP	-308.1343836	-307.6822240	-307.7298523	0.1256230	5.97
	MP2	-307.1666503	-307.6819361	-307.7294981	0.1286010	5.90
$C_2CCOO\cdot$	B3LYP	-308.1632657	-307.6984653	-307.7503242	0.129112	5.24
	MP2	-307.1881332	-307.6979195	-307.7490726	0.1324170	5.16
$C_2\cdot CCOOH$	B3LYP	-308.1200886	-307.6729020	-307.7199649	0.125108	5.95
	MP2	-307.1576780	-307.6725188	-307.7195564	0.1278980	5.86
TS5	B3LYP	-308.1137740	-307.6483930	-307.7073561	0.124175	5.83
	MP2	-307.1220775	-307.6494883	-307.7073123	0.1281360	5.66
TS6	B3LYP	-308.1164419	-307.6360605	-307.7035120	0.123276	6.0
	MP2	-307.1158846	-307.6455639	-307.7064356	0.1273560	6.65
TS7	B3LYP	-308.1066583	-307.6514605	-307.7027579	0.122524	4.98
	MP2	-307.1262664	-307.6473950	-307.6994882	0.1271550	4.77
TS8	B3LYP	-308.1145911	-307.6608680	-307.7111833	0.122972	4.68
	MP2	-307.1360371	-307.6590087	-307.7108057	0.1270320	4.51
TS9	B3LYP	-308.1097740	-307.6443304	-307.7021652	0.121833	5.29
	MP2	-307.1310841	-307.6468554	-307.6988988	0.1271380	5.05
TS12	B3LYP	-308.0809123	-307.6204060	-307.6782392	0.123323	5.55
	MP2	-307.0955402	-307.6208411	-307.6774771	0.1265470	5.46
TS13	MP2	-157.126503	-157.4189205	-157.4551846	0.1133000	4.30

a. Using 6-31g* basis set

b. Unscaled zero-point vibrational energies in Hartree. In the calculation of reaction enthalpies, ZPVE is scaled by 0.9661 and 0.9806 for MP2(full)/6-31g(d) and B3LYP/6-31g(d) levels, respectively.

c. Thermal corr. in kcal/mole: Thermal corrections are calculated as follows for T=298.15 K: $H°_T - H°_0 = H_{trans}(T) + H_{rot}(T) + \Delta H_{vib}(T) + RT$; $H_{trans}(T) = (3/2)RT$, $H_{rot}(T) = (3/2)RT$, $\Delta H_{vib}(T) = N_A h \Sigma v_i/(\exp(hv_i/kT)-1)$, where N_A is the Avogadro constant, h is the Plant constant, k is the Boltzman constant, and v_i is vibrational frequencies.

Table 2A.2 Reaction Enthalpies

	CBS-4[a]	CBS-q	CBS-4	CBS-q
	//MP2(full)/6-31g(d)		//B3LYP/6-31g(d)	
$C_3\cdot COOH + CCOOH \Leftrightarrow C_3COOH + C\cdot COOH$	-1.06	**-1.10**	-0.68	**-0.52**
$C_2\cdot CCOOH + CCOOH \Leftrightarrow C_2CCOOH + C\cdot COOH$	0.27	**0.27**	0.28	**0.23**
$C_2C\cdot COOH + CCOOH \Leftrightarrow C_2CCOOH + C\cdot COOH$	6.16	**6.46**	6.13	**6.41**
$C_2CCOO\cdot + COOH \Leftrightarrow C_2CCOOH + COO\cdot$	0.44	**0.43**	0.64	**0.70**
$C_2C{=}C + HO_2 \Leftrightarrow TS1$	2.90	**2.59**	3.86	**3.20**
$C_3\cdot COOH \Leftrightarrow TS2$	15.88	**15.49**	15.20	**14.88**
$C_2C{=}C + HO_2 \Leftrightarrow TS3$	6.30	**7.74**	5.42	**7.38**
$C_2C{=}C + HO_2 \Leftrightarrow TS4$	8.15	**10.47**	8.49	**11.55**
$C_2C{=}C + HO_2 \Leftrightarrow TS5$	9.11	**10.69**	8.89	**10.82**
$C_2C{=}C + HO_2 \Leftrightarrow TS6$	9.11	**11.23**	10.31	**13.40**
$C_2C\cdot COOH \Leftrightarrow TS7$	19.42	**17.68**	17.13	**16.01**
$C_2\cdot CCOOH \Leftrightarrow TS8$	6.18	**4.13**	5.65	**4.24**
$C_2C{=}C + HO_2 \Leftrightarrow TS9$	14.71	**15.31**	12.42	**13.54**
$C_2\cdot CCOOH \Leftrightarrow TS12$	27.03	**26.00**	26.86	**25.79**

a. Reaction enthalpies include thermal correction and zero-point energy correction

Table 2A.3 Thermodynamic Properties

SPECIES	$\Delta H°_{f298}$	$S°_{298}$	Cp_{300}	Cp_{400}	Cp_{500}	Cp_{600}	Cp_{800}	Cp_{1000}	Cp_{1500}
N_2	0	45.7	6.65	6.86	6.99	7.1	7.31	7.61	7.98
H	52.1	27.3	4.9	4.9	4.9	4.9	4.9	4.9	4.9
H_2	0	31.2	6.89	6.97	7.05	7.13	7.27	7.4	7.69
X	59.52	38.4	5	5	5	5	5	5	5
Y	9.5	43.8	6.79	6.86	6.93	7	7.14	7.28	7.61
O	59.52	38.4	5	5	5	5	5	5	5
O_2	0	49	6.82	7.15	7.36	7.51	7.82	8.24	8.69
OH	9.5	43.8	6.79	6.86	6.93	7	7.14	7.28	7.61
H_2O	-57.8	43.72	8.21	8.91	9.59	10.21	11.29	12.07	12.96
HO_2	3.5	54.7	8.29	8.77	9.23	9.67	10.47	11.13	12.23
H_2O_2	-32.6	55.71	10.69	11.84	12.77	13.51	14.6	15.34	16.57
CH_3	34.8	46.3	9.13	9.94	10.71	11.44	12.78	13.93	16.01
CH_4	-17.9	44.4	8.8	9.87	11	12.16	14.43	16.48	20.08
CO	-26.4	47.2	6.71	6.89	7.06	7.23	7.53	7.79	8.29
CO_2	-94.02	51	9.18	9.81	10.44	11.04	12.11	12.93	13.79
			Using THERM Group Additivity						
CH_2O	-26	50.92	8.48	9.49	10.51	11.51	13.33	14.82	16.98
HCO	10.4	53.6	8.65	9	9.39	9.8	10.6	11.33	12.49
CH_3OH	-48	57.31	10.51	12.46	14.31	16.04	19.06	21.46	25.11
$CH_3O\cdot$	3.96	55.85	9.62	11.19	12.7	14.14	16.7	18.74	21.69
$C\cdot H_2OH$	-3.6	60.42	11.68	13.25	14.58	15.69	17.44	18.74	20.94
CH_3OOH	-31.8	64.97	15.91	18.35	20.48	22.34	25.36	27.62	31.05
CH_3OO	4.3	65.19	13.92	15.49	16.95	18.29	20.66	22.62	25.95
$C\cdot H_2OOH$	14.6	68.26	16.57	18.39	19.95	21.27	23.36	24.86	27.04
C*C*O	-11.74	57.83	12.7	14.79	16.45	17.78	19.68	20.95	22.96
CC*O	-39.18	63.14	13.17	15.83	18.26	20.47	24.19	27.06	31.22
CC·*O	-2.28	64.26	12.29	14.4	16.32	18.07	21.02	23.31	26.64
CCC	-25.33	64.51	17.88	22.74	27.05	30.86	37.13	41.91	49.28
CC·C	21.02	70.32	16.26	20.4	24.15	27.51	33.17	37.53	44.14
C*CC	4.65	63.82	15.45	19.32	22.74	25.75	30.72	34.51	40.34
CC·*C	61.56	65.63	15.09	18.09	20.8	23.24	27.37	30.59	35.58
C*CC·	40.75	63.44	14.87	18.65	21.88	24.63	28.95	32.09	36.77
C*C*C	45.92	58.31	14.19	17.22	19.8	21.99	25.46	28.02	32.03
C#CC	44.28	59.29	13.98	16.64	19.07	21.28	25	27.86	31.94
C#CC·	81.59	60.96	13.76	16.1	18.09	19.79	22.47	24.42	27.31
CCC*O	-44.5	72.74	19.37	23.37	26.92	30.06	35.25	39.19	45.2
CC·C*O	-4.7	70.37	18.07	21.88	25.19	28.06	32.66	36.06	41.08
C_2C*O	-51.56	70.1	17.92	22.13	25.92	29.3	34.92	39.19	45.45
C_2·C*O	-9.26	72.5	18.29	22.29	25.76	28.75	33.51	36.93	41.75
C*C(C)OH	-38.81	72.63	19.11	23.28	26.94	30.15	35.36	39.24	45
CCYCCO	-21.87	68.17	17.37	22.57	26.94	30.62	36.3	40.32	46.31
CCYC·CO	24.48	72.61	15.77	20.22	24.03	27.29	32.38	35.96	40.98
C_2COOH	-49.98	81.34	26.32	32.11	37.07	41.3	47.94	52.75	59.86
C_2C·OOH	-8.48	87.32	26.46	30.82	34.68	38.09	43.69	47.96	54.55
C*C(C)Q	-15.57	82.85	23.54	28.17	32.12	35.49	40.8	44.66	50.41
C*C(C)Q·	20.53	83.07	21.57	25.29	28.54	31.38	36.05	39.68	45.58
C*C*CQ	26.6	77.13	22.32	26.43	29.8	32.55	36.58	39.26	42.98
CC*OCOOH	-70.32	90.59	27.1	31.82	35.98	39.62	45.54	49.93	56.2
CC*OCOO·	-34.21	90.81	25.06	28.94	32.44	35.57	40.86	44.96	51.11
C·C*OCOOH	-28.01	91.61	27.09	31.55	35.38	38.67	43.82	47.46	52.31

Table 2A.3 (Continued)

SPECIES	ΔH°_{f298}	S°_{298}	Cp_{300}	Cp_{400}	Cp_{500}	Cp_{600}	Cp_{800}	Cp_{1000}	Cp_{1500}
C_3C	-32.5	70.44	23.17	29.65	35.33	40.29	48.37	54.46	63.76
$C_3C\cdot$	11.7	75.68	22.31	27.25	31.87	36.14	43.55	49.44	58.37
$C_3\cdot C$	16.5	77.41	22.4	28.27	33.42	37.91	45.22	50.71	59.11
$C_2C{*}C$	-3.8	70	21.58	26.74	31.3	35.31	41.9	46.91	54.64
$C_2\cdot C{*}C$	32.3	71	20.99	26.11	30.47	34.2	40.1	44.44	51.16
$C_2C{*}C\cdot$	55.3	72.76	21.39	25.94	29.92	33.4	39.09	43.41	50.12
C_3COH	-75.11	78.02	27.23	34.24	40.21	45.29	53.3	59.19	68.35
$C_3CO\cdot$	-23.14	76.56	26.25	32.93	38.6	43.4	50.92	56.39	64.77
$C_3\cdot COH$	-26.1	84.99	26.46	32.86	38.29	42.9	50.15	55.45	63.71
C_2CCOH	-68.31	83.26	26.19	33.12	39.1	44.25	52.49	58.58	67.92
$C_2C\cdot COH$	-24.1	88.5	25.35	30.72	35.64	40.09	47.66	53.56	62.54
$C_2CCO\cdot$	-16.34	81.8	25.2	31.81	37.49	42.37	50.11	55.78	64.35
$C_2CC{*}O$	-51.2	79.66	23.57	29.64	34.9	39.43	46.67	51.96	59.79
$C_2C\cdot C{*}O$	-13.5	77.95	24.14	29.29	33.76	37.63	43.86	48.51	55.61
$C_2C{*}COH$	-45.93	79.06	25.53	31.3	36.21	40.39	46.98	51.82	59.37
$C{*}C(C)COH$	-38.26	82.02	24.73	30.24	35.07	39.28	46.1	51.2	58.91
$C{*}C(C)CO\cdot$	13.7	80.56	23.77	28.96	33.49	37.42	43.74	48.41	55.37
$C{*}CICC{*}O$	-27.34	74.65	23.18	28.32	32.61	36.2	41.71	45.61	51.52
$C{*}CICC\cdot{*}O$	3.56	73.26	22.96	27.39	31.02	34.01	38.52	41.7	46.8
$C_2C{*}C{*}O$	-28.06	73.98	24.27	28.96	32.92	36.26	41.48	45.29	51.24
C_2CYC_2O	-31.47	71.09	23.1	29.9	35.6	40.38	47.73	52.94	60.74
$C_2CYCC\cdot O$	10.43	73.61	22.97	29.14	34.26	38.5	44.93	49.44	56.23
$CCYCOCC$	-28.54	73.69	20.89	27.95	33.95	39.03	46.94	52.59	60.95
$CCYC\cdot COC$	17.99	78.24	19.07	24.75	29.81	34.29	41.66	47.21	55.35
$C{*}CYCCOC$	4.97	69	18.72	24.34	29.23	33.47	40.21	45.08	52.01
$C_2\cdot CYC_2O$	17.53	77.26	22.33	28.51	33.68	37.99	44.57	49.2	56.09
$C{*}CIC\cdot C{*}O$	8.76	74.27	22.59	27.68	31.8	35.1	39.91	43.14	48.02
C_3COOH	-59.40	84.24	32.35	39.67	45.85	51.06	59.16	65.01	73.96
C_2CCOOH	-52.70	91.92	31.02	38.56	45.04	50.56	58.93	65.33	74.18
$C_2C{*}CQ$	-23.92	87.27	29.8	36.03	41.35	45.88	53	58.11	65.6
$C{*}C(C)CQ$	-24.38	90.11	30.26	36.22	41.32	45.67	52.56	57.59	65.2
$CC(CO\cdot)CO$	-35.04	90.22	25.71	31.8	37.01	41.44	48.37	53.35	60.64
$C{*}CICOOC\cdot$	31	95.08	27.92	33.77	38.76	43	49.67	54.48	61.45
$C_2CYCCOO$	-16.51	76.71	25.37	32.93	39.26	44.54	52.61	58.23	66.4
$C_2\cdot CYCCOO$	32.49	81.51	24.6	31.55	37.34	42.16	49.45	54.49	61.77
$CCYCCOOC$	-28.68	75.42	23.82	31.85	38.55	44.14	52.62	58.5	66.98
$CCYC\cdot COOC$	15.22	77.14	23.78	31.27	37.4	42.41	49.81	54.82	62.17
$CCYCC\cdot OOC$	17.32	77.14	23.78	31.27	37.4	42.41	49.81	54.82	62.17
$C{*}C(C)CQ\cdot$	11.72	92.51	28.23	33.32	37.74	41.57	47.79	52.52	60.03
$C{*}C(C\cdot)CQ$	11.72	89.73	29.75	35.65	40.57	44.64	50.83	55.15	61.48
$C{*}C(C)C\cdot Q$	9.12	88.48	28.7	34.38	39.22	43.34	49.77	54.38	61.06
C_2CQCOH	-95.49	97.06	35.53	43.15	49.55	54.91	63.19	69.12	78.27
C_2COHCQ	-96.3	98.46	35.62	43.24	49.67	55.09	63.53	69.59	78.76
$C_2C(Q)C{*}O$	-75.44	94.38	32.5	39.72	45.81	50.91	58.71	64.1	71.51
C_3QCQ	-80.88	104.68	40.79	48.67	55.29	60.82	69.33	75.33	84.23
$C_2CQCQ\cdot$	-44.77	104.9	38.72	45.76	51.72	56.76	64.63	70.34	79.13
$C_2CQ\cdot CQ$	-44.77	104.9	38.72	45.76	51.72	56.76	64.63	70.34	79.13
$C_2\cdot CQCQ$	-31.87	109.63	40.14	47.37	53.42	58.46	66.17	71.58	79.57
$C_2CQC\cdot Q$	-36.97	108.5	40.91	47.81	53.64	58.55	66.14	71.53	79.54
CYC_6H_6	19.8	64.25	19.53	26.69	32.68	37.67	45.3	50.6	58.17

Table 2A.3 (Continued)

SPECIES	ΔH°_{f298}	S°_{298}	Cp_{300}	Cp_{400}	Cp_{500}	Cp_{600}	Cp_{800}	Cp_{1000}	Cp_{1500}
C*CCCC*C	20.18	88.59	28.69	36.57	43.28	48.98	57.91	64.37	74.28
C_2C*CC_2	-20.12	90.51	32.93	40.7	47.58	53.65	63.65	71.26	82.94
$C_2*CCCC*C$	11.73	98.33	34.84	43.99	51.83	58.52	69.09	76.81	88.57
$C*C(C)CC_3$	-22.52	90.93	37.93	48.53	57.51	65.1	76.92	85.37	98.01
C_3CCC_2	-49.2	91.79	39.91	51.57	61.5	69.95	83.18	92.74	107.06
$C_3CC\cdot C_2$	-4.8	97.03	39.09	49.18	58.04	65.79	78.36	87.71	101.67
C_3CCQC_2	-74.79	106.96	49.25	61.61	71.97	80.63	93.91	103.28	117.35
$C_3\cdot CCQC_2$	-25.78	113.94	48.46	60.22	70.05	78.24	90.75	99.54	112.69
$C_3CCQ\cdot C_2$	-38.68	107.18	47.17	58.7	68.4	76.56	89.21	98.29	112.25
C_3CCC_3	-53.92	93.43	45.88	59.59	71.13	80.81	95.69	106.16	121.6
$C_3\cdot CCC_3$	-4.92	101.78	45.11	58.21	69.21	78.42	92.53	102.42	116.95
$DIC_2\cdot C*C$	3.28	104.51	40.98	51.42	60.39	68.07	80.26	89.21	102.88
C_3CCC_3Q	-75	115.25	54.37	68.61	80.57	90.57	105.9	116.63	132.29
$C_3CCC_3Q\cdot$	-38.89	115.47	52.33	65.71	77	86.51	101.2	111.64	127.2
$C_3CCC_2\cdot CQ$	-25.99	120.59	53.87	67.3	78.57	88	102.45	112.57	127.43
C_3COOCC_3	-83.45	112.76	53.76	67.89	79.81	89.85	105.43	116.59	133.14
$C_2CCOOTB$	-78.67	120.83	52.77	66.78	78.7	88.8	104.59	115.98	132.79
$C_2C\cdot COOTB$	-34.46	125.42	52.18	64.69	75.55	84.94	100	111.11	127.48
Using PM3 Molecular Orbital Calculation for Key Reaction Species and Transition States[a]									
$C_2COHCQ\cdot$	-60.19	96.02	32.85	40.56	47.20	52.53	60.33	65.80	74.22
TS10		84.30	30.26	38.86	46.23	52.17	60.82	66.77	75.57
$C_2CO\cdot CQ$	-44.33	96.60	33.58	41.37	47.90	53.09	60.55	62.65	73.37
$C_2CQ\cdot COH$	-59.38	96.14	33.23	40.71	47.14	52.34	60.06	65.55	74.06
TS11		84.71	30.51	39.07	46.39	52.29	60.90	66.83	75.61
$C_2CQCO\cdot$	-43.52	95.17	34.49	42.65	49.60	55.14	62.98	68.18	75.80
$C_2\cdot COHCQ$	-47.29	100.36	34.66	42.21	48.50	53.47	60.69	65.74	73.58
$C_2\cdot CQCOH$	-46.48	103.99	35.12	42.76	49.13	54.19	61.48	66.47	74.10
$C_2CQC\cdot OH$	-53.58	100.10	35.47	42.78	49.03	54.07	61.39	66.40	74.06
TS14		86.75	30.94	39.46	46.65	52.39	60.75	66.53	75.23
TS15		91.89	32.04	40.16	46.96	52.41	60.40	66.00	74.47
TS16		89.51	32.70	40.83	47.69	53.15	61.06	66.52	74.75
Using CBS-q//MP2(full)/6-31G* Calculation for Species and Transition States of $C_3C.$ + O_2 and $C_2C{=}C$ + HO_2 Reaction Systems									
$C_3COO\cdot$	-25.16[b]	82.98	28.7	35.43	41.42	46.43	54.08	59.63	68.43
TS1	2.29	82.16	27.41	34.31	40.52	45.78	53.84	59.65	68.63
TS2	7.68	79.83	26.54	33.86	40.34	45.75	53.92	59.73	68.67
$C_3\cdot COOH$	-7.81[c]	91.60	30.28	37.07	43.05	47.99	55.34	60.49	68.49
TS3	7.44	89.35	28.18	34.8	40.67	45.57	52.98	58.32	66.75
TS4	7.77[d]	85.61	28.48	35.3	41.17	45.98	53.25	58.56	67.15
TS5	10.39	89.59	27.47	34.03	39.97	44.97	52.59	58.06	66.66
TS6	10.93	87.24	27.69	34.06	39.9	44.85	52.49	58.09	67.02
$C_2C\cdot COOH$	-8.37[c]	97.15	27.75	33.69	39.52	44.63	52.63	58.44	67.54
$C_2CCOO\cdot$	-19.07[c]	89.20	27.69	34.29	40.26	45.28	53.08	58.84	67.99
TS7	9.31	80.20	25.61	32.68	39.21	44.76	53.24	59.29	68.52
TS8	1.95	78.60	24.75	32.18	38.96	44.7	53.43	59.67	69.15
TS9	15.01	82.00	26.54	33.42	39.68	45.02	53.24	59.19	68.38
$C_2\cdot CCOOH$	-2.18[c]	95.98	30.27	36.83	42.72	47.61	54.91	60.11	68.26
TS12	23.82	94.86	27.91	34.69	40.68	45.68	53.22	58.64	67.09
TS13	48.82	74.88	22.96	28.09	32.85	37.04	43.85	49.04	57.38

Table 2A.3 (Continued)

SPECIES	$\Delta H°_{f298}$	$S°_{298}$	Cp_{300}	Cp_{400}	Cp_{500}	Cp_{600}	Cp_{800}	Cp_{1000}	Cp_{1500}
Using CBS-q//B3LYP/6-31G* Calculation for Species and Transition States of $C_3C\cdot + O_2$ and $C_2C{=}C + HO_2$ Reaction Systems									
$C_3COO\cdot$	-25.16[b]	83.85	29.84	36.86	42.97	47.99	55.55	60.99	69.43
TS1	2.9	83.88	28.73	35.85	42.16	47.43	55.39	61.06	69.66
TS2	7.07	81.11	28.37	36.09	42.66	47.98	55.86	61.40	69.81
$C_3\cdot COOH$	-7.81[c]	92.50	31.67	38.84	44.92	49.82	56.99	61.96	69.55
TS3	7.08	89.67	28.61	35.35	41.27	46.19	53.59	58.90	67.21
TS4	10.25[d]	87.24	30.11	37.08	42.92	47.65	54.74	59.90	68.14
TS5	10.52	90.63	28.69	35.58	41.64	46.65	54.15	59.49	67.72
TS6	13.1	92.04	29.08	35.64	41.53	46.45	53.99	59.47	68.06
$C_2C\cdot COOH$	-8.37[c]	97.77	28.62	34.89	40.86	46.01	53.99	59.71	68.42
$C_2CCOO\cdot$	-19.07[c]	89.89	28.73	35.68	41.80	46.85	54.57	60.21	69.01
TS7	7.64	81.61	27.18	34.67	41.32	46.85	55.13	60.95	69.68
TS8	2.06	79.79	26.43	34.25	41.09	46.75	55.23	61.21	70.21
TS9	13.24	83.71	28.61	35.79	42.14	47.43	55.38	61.03	69.62
$C_2\cdot CCOOH$	-2.18[c]	96.62	31.12	37.97	43.97	48.89	56.15	61.29	69.18
TS12	23.61	95.32	28.65	35.52	41.51	46.47	53.94	59.29	67.58

Units: Hf: Kcal/mole; S & Cp(T): cal/mole

a $\Delta H°_{f298}$ from THERM; b. ref.46; c. calculated from average values of ΔH_{rxn} of isodesmic reactions (list in Table 2) at CBS-q//MP2(full)/6-31g* and CBS-q//B3LYP/6-31g* levels; d. best fit with experimental data

Table 2A.4 Hydrogen Atom Bond Increments Group for Hydrocarbon Radicals

	D°(R-H)	$\Delta S^{\circ}_{int,298}$[a]	ΔCp_{300}	ΔCp_{400}	ΔCp_{500}	ΔCp_{600}	ΔCp_{800}	ΔCp_{1000}	ΔCp_{1500}
P[b]	101.1	2.61	-0.77	-1.36	-1.91	-2.4	-3.16	-3.74	-4.66
S[c]	98.45	4.44	-1.5	-2.33	-3.1	-3.39	-3.75	-4.45	-5.2
Tertalkyl	96.5	5.24	-0.78	-2.48	-3.55	-4.15	-4.75	-5.02	-5.39
CCJC	98.45	4.51	-1.3	-2.36	-3.02	-3.44	-3.98	-4.36	-4.99
Neopentyl	101.1	3.03	-0.59	-1.32	-2.05	-2.65	-3.5	-4.06	-4.87
VIN	111.2	1.39	-0.19	-0.75	-1.36	-1.92	-2.82	-3.49	-4.53
VIN_S	109	1.81	-0.34	-1.21	-1.94	-2.52	-3.34	-3.91	-4.76
ALLYL_P	88.2	-2.56	-0.62	-0.56	-0.78	-1.12	-1.84	-2.46	-3.49
ALLYL_S	85.6	-3.81	-1.54	-1.82	-2.08	-2.32	-2.75	-3.14	-3.85
C≡CCJ	89.4	-0.51	-0.84	-1.17	-1.56	-1.95	-2.7	-3.31	-5.31
CYC_4	98.45	1.68	-0.35	-0.6	-1.02	-1.51	-2.45	-3.2	-4.12
CYC_5H_9	98.1	1.72	-0.06	-0.52	-1.11	-1.74	-2.85	-3.69	-4.83
$CYCJC_3O_2$	96	1.72	-0.06	-0.52	-1.11	-1.74	-2.85	-3.69	-4.83
ROJ	104.06	-1.46	-0.98	-1.3	-1.61	-1.89	-2.38	-2.8	-3.59
RC=COJ	88	-1.11	-1.34	-1.99	-2.48	-2.79	-3.13	-3.33	-3.79
CJOH	96.5	0.93	1.28	0.93	0.2	-0.55	-1.83	-2.77	-4.17
CCJOH	94	0.78	0.33	-0.3	-1.02	-1.67	-2.67	-3.39	-4.49
CCJOR	94	1.15	-0.13	-0.67	-1.31	-1.89	-2.82	-3.49	-4.54
C_2CJOR	92.8	2.46	-1.49	-2.88	-3.9	-4.51	-5.09	-5.32	-5.58
CCJCHO	91.9	-2.37	-1.36	-1.57	-1.73	-1.89	-2.66	-3.11	-3.5
C_2CJCHO	89.8	-1.71	0.62	-0.2	-1.23	-1.82	-2.87	-3.47	
ROOJ	88.2	0.22	-2.05	-2.84	-3.55	-4.09	-4.72	-4.97	-5.08
CJOOH	98.5	1.11	0.62	0.09	-0.53	-1.09	-2.01	-2.75	-4.01
CCJOOH	96	3.82	0.14	-0.84	-1.66	-2.3	-3.18	-3.79	-4.7
C_2CJOOH	93.6	5.98	0.22	-1.31	-2.45	-3.21	-4.13	-4.62	-5.24
CJCOOH	102.87	2.73	-0.66	-1.28	-1.86	-2.35	-3.14	-3.72	-4.65
C_2JCOOH	101.1	2.76	-0.65	-1.28	-1.88	-2.38	-3.16	-3.75	-4.67
$C_2CJCOOH$	96.44	4.59	-0.49	-2.12	-3.22	-3.88	-4.53	-4.87	-5.31
C_2JC*O	94.4	-1.16	0.32	0.19	-0.15	-0.57	-1.43	-2.22	-3.67
CCJ*O	89	1.12	-0.83	-1.43	-1.96	-2.42	-3.16	-3.73	-4.64
C*CCJ*O	83	-1.39	-0.19	-0.85	-1.59	-2.21	-3.21	-3.89	-4.6
OJC=O	104	0.79	-1.31	-1.87	-2.32	-2.69	-3.28	-3.74	-4.56
C_3COOJ	85.3[d]	0.22	-2.05	-2.84	-3.55	-4.09	-4.72	-4.97	-5.08
C_3JCOOH	103.69	3.15	-0.48	-1.24	-2	-2.6	-3.47	-4.04	-4.87

Units: D°(R-H) kcal/mole ; $\Delta S^{\circ}_{int,298}$ & ΔCp(T): cal/mole

a. Includes electronic spin degeneracy

b. The general group for all kinds of primary alkyl radicals

c. The general group for all kinds of secondary alkyl radicals

d. From ref. 46

Table 2A.5 Frequencies and Moments of Inertia for Transition State (TS13) Calculated at MP2(full)/6-31g(d) Level

Molecule	Frequencies	Moments of inertia[a]
TS13	(-1209.96), 160.71, 187.62, 310.47, 351.78, 389.62, 456.41, 566.92, 849.08, 880.50, 1000.67, 1024.42, 1075.10, 1082.60, 1118.11, 1150.19, 1359.67, 1465.27, 1471.77, 1493.69, 1532.27, 1548.17, 1549.51, 1563.43, 1718.82, 3086.30, 3089.62, 3157.77, 3159.55, 3203.61, 3204.92, 3216.43, 3307.31	220.62451 224.58246 401.49206

Unit: amu-Bohr^2

Table 2A.6 Input Parameters and High - Pressure Limit Rate Constants (k_∞) for QRRK Calculation: $C_3C\cdot + O_2 \rightarrow$ Products

	Reaction	A (s-1 or cm^3/mol-s)	n	E_a (kcal/mol)	ref.
k_1	$C_3C\cdot + O_2 \rightarrow C_3COO\cdot$	6.62×10^{12}	0.	0.0	61.
k_{-1}	$C_3COO\cdot \rightarrow C_3C\cdot + O_2$	6.83×10^{15}	0.	33.50	a.
k_2	$C_3COO\cdot \rightarrow C_3CO\cdot + O$	1.70×10^{15}	0.	59.01	85.
k_3	$C_3COO\cdot \rightarrow C_2C{*}C{+}HO_2$	$3.70 \times 10^{10} (4.93 \times 10^{10})$	0.82 (0.85)	27.43 (28.04)	b.
k_4	$C_3COO\cdot \rightarrow C_3\cdot COOH.$	$1.44 \times 10^{10} (3.97 \times 10^{9})$	0.81 (1.04)	32.76 (32.06)	b.
k_{-4}	$C_3.COOH \rightarrow C_3COO\cdot$	$7.21 \times 10^{9} (3.33 \times 10^{9})$	0.24 (0.39)	15.65 (14.80)	c.
k_5	$C_3\cdot COOH \rightarrow C_2C{*}C{+}HO_2$	$1.21 \times 10^{13} (2.63 \times 10^{14})$	-0.12 (-0.63)	15.89 (15.81)	b.
k_6	$C_3\cdot COOH \rightarrow C_2CYC2O{+}OH$	$5.89 \times 10^{11} (4.11 \times 10^{9})$	0.05 (0.80)	16.13 (17.96)	d.
k_7	$C_3\cdot COOH \rightarrow C{*}C(C)Q{+}CH_3$	9.21×10^{13}	0.	35.49	62.

L.J. Parameters: $\sigma = 5.55$ A; e/k = 585 K
Geometric mean frequency
$C_3\cdot COOH$ 250.1cm^{-1} (10.789), 1090.9cm^{-1} (16.285), 2881.2cm^{-1} (9.417)
$C_3COO\cdot$ 368cm^{-1} (12.104), 1230.1cm^{-1} (16.899), 3157.5cm^{-1} (7.998)
* Data in parentheses are from B3LYP-determined entropies and CBS-q// B3LYP/6-31g* calculation.

a. Via k_{-1} and <MR>, $E_{a\,-1} = \Delta U_{rxn}$

b. fitting with three parameter modified Arrhenius equation; A estimated using TST and MP2-determined entropies, E_a evaluated from CBS-q//MP2(full)/6-31G* calculation plus endothermicity of reaction enthalpy.

c. fitting with three parameter modified Arrhenius equation; A estimated using TST and MP2-determined entropies, E_a evaluated from CBS-q// MP2(full)/6-31G* calculation.

d. fitting with three parameter modified Arrhenius equation; A estimated using TST and MP2-determined entropies, E_a best fit experimental data in this study.

Table 2A.7 Frequencies and Moments of Inertia for Intermediates and Transition States of $C_3C\cdot + O_2$ Reaction System Calculated at MP2(full)/6-31g(d) Level

Molecule	Frequencies	moments of inertia[a]
$C_3COO\cdot$	129.64, 217.46, 268.16, 273.05, 286.26, 346.92, 376.52, 415.53, 455.19, 565.71, 763.56, 870.63, 970.60, 973.12, 998.18, 1080.04, 1089.89, 1245.28, 1309.86, 1326.36, 1352.84, 1453.60, 1457.53, 1479.70, 1533.11, 1548.05, 1548.93, 1559.77, 1559.88, 1581.36, 3112.08, 3114.13, 3117.49, 3203.72, 3205.34, 3210.33, 3211.69, 3225.47, 3228.10	398.87628 616.98629 617.41482
TS1	(-1261.40), 134.30, 179.70, 219.72, 223.72, 241.76, 387.53, 441.56, 526.71, 558.48, 593.16, 695.08, 849.14, 983.21, 1011.75, 1045.85, 1061.96, 1108.40, 1146.51, 1252.23, 1364.17, 1462.48, 1469.71, 1489.72, 1533.33, 1542.86, 1543.72, 1552.50, 1564.24, 1658.17, 1714.68, 3092.18, 3095.40, 3176.79, 3178.48, 3184.52, 3208.74, 3211.02, 3276.42	410.73702 711.77631 714.82995
TS2	(-2876.70), 217.20, 227.15, 265.66, 313.11, 357.38, 407.36, 421.95, 524.03, 625.78, 681.05, 817.15, 902.73, 955.77, 979.79, 1015.81, 1069.36, 1103.91, 1233.33, 1245.49, 1304.27, 1319.61, 1345.61, 1453.88, 1467.02, 1505.61, 1539.47, 1549.05, 1555.60, 1570.87, 1827.28, 3109.60, 3113.34, 3171.19, 3200.77, 3205.41, 3213.61, 3223.94, 3270.48	378.17489 589.09898 613.33608
$C_3\cdot COOH$	74.77, 151.87, 247.28, 258.62, 270.51, 285.52, 354.23, 361.16, 397.82, 470.20, 537.23, 569.03, 777.74, 916.46, 950.41, 985.38, 1036.53, 1062.73, 1215.97, 1315.91, 1340.47, 1360.49, 1397.58, 1447.16, 1461.52, 1519.40, 1540.58, 1556.29, 1560.93, 1575.49, 3110.12, 3115.33, 3199.99, 3206.33, 3218.34, 3224.71, 3233.46, 3349.63, 3718.98	395.14592 624.04899 633.96915
TS3	(-775.53), 96.01, 163.16, 189.74, 219.70, 239.37, 308.20, 396.81, 403.49, 449.38, 479.88, 663.38, 836.26, , 891.92, 994.48, 1012.61, 1046.61, 1062.66, 1117.39, 1168.90, 1362.65, 1418.99, 1452.66, 1467.74, 1494.20, 1533.91, 1545.87, 1547.47, 1563.70, 1640.61, 3108.35, 3113.14, 3195.40, 3201.12, 3219.70, 3225.07, 3231.87, 3326.24, 3681.71	404.16563 708.21527 734.08415
TS4	(-1325.33), 151.04, 211.92, 218.36, 234.31, 265.59, 365.52, 370.62, 426.77, 435.40, 509.57, 644.44, 789.84, 792.74, 925.43, 958.60, 991.17, 1066.23, 1072.66, 1129.12, 1210.86, 1331.97, 1408.74, 1457.99, 1468.67, 1526.72, 1535.88, 1551.63, 1563.20, 1571.37, 3111.27, 3114.77, 3203.59, 3208.15, 3218.90, 3221.32, 3256.00, 3379.64, 3770.68	430.34696 605.93921 628.62574

Unit: amu-Bohr^2

Table 2A.8 Frequencies and Moments of Inertia for Intermediates and Transition States of $C_2C^*C + HO_2$ Reaction System Calculated at MP2(full)/6-31g(d) Level

Molecule	Frequencies	moments of inertia[a]
$C_2C\cdot COOH$	54.16, 112.67, 145.54, 165.79, 190.59, 265.22, 313.30, 367.31, 410.95, 573.06, 812.86, 867.16, 963.93, 976.30, 1010.90, 1040.97, 1068.46, 1121.40, 1281.29, 1327.47, 1360.54, 1382.34, 1428.06, 1463.00, 1474.71, 1523.72, 1538.09, 1545.33, 1553.98, 1563.03, 3045.98, 3047.52,, 3050.83, 3138.54, 3140.57, 3142.38, 3188.03, 3198.07, 3700.57	318.82942 807.06745 903.69160
TS5	(-782.49), 53.48, 133.55, 136.83, 153.89, 187.04, 302.56, 390.14, 450.19, 462.72, 485.10, 848.65, 903.55, 992.14, 1003.08, 1031.10, 1071.85, 1119.88, 1135.23, 1182.05, 1366.39, 1417.35, 1462.56, 1469.71, 1484.15, 1531.13, 1540.90, 1548.20, 1560.27, 1692.60, 3089.15, 3093.27, 3165.24, 3167.89, 3203.79, 3209.97, 3219.66, 3312.89, 3666.89	380.31285 762.51238 878.64915
TS6	(-1369.21), 113.32, 131.51, 138.47, 162.95, 219.41, 278.79, 325.38, 403.28, 419.28, 491.55, 788.57, 975.60, 1006.54, 1013.10, 1057.56, 1094.56, 1115.71, 1161.45, 1199.28, 1300.27, 1370.07, 1434.50, 1471.11, 1473.56, 1528.97, 1542.99, 1543.66, 1564.90, 1595.45, 3078.58, 3081.06, 3112.69, 3159.34, 3160.89, 3186.07, 3212.61, 3217.28, 3772.37	296.28913 825.73071 947.98193
TS7	(-2710.41), 141.63, 213.25, 249.26, 277.02, 310.90, 372.95, 425.20, 574.73, 688.46, 851.99, 965.42, 982.12, 1007.18, 1007.68, 1058.32, 1186.23, 1200.10, 1227.86, 1296.86, 1322.53, 1344.43, 1392.47, 1455.88, 1470.03, 1537.43, 1543.40, 1551.41, 1556.49, 1563.09, 1847.04, 3083.72, 3086.47, 3094.77, 3167.71, 3169.32, 3175.44, 3202.24, 3213.34	342.49651 689.30912 764.77772
$C_2CCOO\cdot$	81.45, 95.76, 233.29, 254.80, 269.59, 353.72, 422.97, 448.35, 561.76, 850.59, 945.68, 955.56, 968.78, 1013.25, 1016.79, 1187.25, 1219.23, 1243.23, 1285.26, 1326.80, 1364.14, 1421.40, 1438.38, 1463.23 ,1481.75 ,1533.80, 1551.64, 1558.38, 1568.80, 1574.86, 3099.47, 3103.00, 3107.32, 3126.74, 3186.03, 3190.46, 3198.22, 3205.87, 3216.72	268.22031 810.52556 977.48312
TS9	(-1354.46), 127.47, 188.28, 206.02, 217.18, 243.12, 369.74, 432.99, 570.60, 649.47, 713.36, 856.13, 878.30, 990.66, 1007.61, 1076.21, 1079.97, 1120.73, 1187.41, 1225.14, 1338.14, 1466.34, 1473.79, 1495.17, 1541.59, 1553.90, 1563.81, 1571.97, 1589.76, 1740.15, 1894.37, 3092.39, 3094.32, 3171.45, 3171.70, 3192.02, 3192.92, 3217.16, 3305.93	371.65782 796.94415 839.07288
TS8	(-2166.99), 129.66, 250.39, 303.38, 323.59, 438.15, 453.57, 489.91, 560.17, 703.74, 869.47, 957.77, 985.79, 993.22, 1021.88, 1064.72, 1171.39, 1208.60, 1209.36, 1244.44, 1305.30, 1321.56, 1352.93, 1413.99, 1416.09, 1462.95, 1514.10, 1535.27, 1559.39, 1564.55, 1616.79, 3099.97, 3102.94, 3126.44, 3158.28, 3182.70, 3191.81, 3202.37, 3253.87	276.71800 696.43767 882.06318
$C_2\cdot CCOOH$	96.62, 115.52, 133.07, 168.77, 201.03, 247.34, 346.74, 385.37, 402.61, 454.92, 626.06, 859.28, 911.59, 977.78, 1004.88, 1013.33, 1042.51, 1113.93, 1207.26, 1220.27, 1279.39, 1368.56, 1383.57, 1397.07, 1428.99, 1466.37, 1525.55, 1558.70, 1566.86, 1586.31, 3008.25, 3081.39, 3110.15, 3141.29, 3193.38, 3222.02, 3231.18, 3341.56, 3721.14	280.46147 859.03050 966.76821
TS12	(-652.21), 57.76, 135.73, 172.72, 196.11, 251.24, 390.20, 432.22, 446.31, 503.10, 601.77, 631.09, 874.59, , 878.88, 924.61, 972.56, 1001.29, 1083.07, 1098.90, 1166.39, 1227.12, 1238.02, 1326.49, 1444.96, 461.35, 1490.91, 1494.54, 1550.80, 1561.28, 1636.71, 3113.56, 3166.87, 3196.51, 3205.41, 3211.77, 3223.73, 3301.18, 3308.67, 3569.12	371.83682 759.37160 918.60184

Unit: amu-Bohr^2

Table 2A.9 Input Parameters and High - Pressure Limit Rate Constants (k_∞) for QRRK Calculation: $C_2C^*C + HO_2 \Leftrightarrow [C_3{\cdot}COOH]^*$ and $C_2C^*C + HO_2 \Leftrightarrow [C_3COO{\cdot}]^*$

	Reaction	**A** (s-1 or cc/mol-s)	n	**E_a** (kcal/mol)	ref.
k_1	$C_2C^*C + HO_2 \rightarrow C_3{\cdot}COOH$	1.31×10^4 (2.20×10^3)	2.10 (2.39)	7.54 (7.00)	a.
k_{-1}	$C_3{\cdot}COOH \rightarrow C_2C^*C + HO_2$	$1.21 \times 10^{13}(2.63 \times 10^{14})$	-0.12(-0.63)	15.89(15.81)	a.
k_2	$C_2C^*C + HO_2 \rightarrow C_3COO{\cdot}$	2.01×10^1 (3.45×10^{-1})	2.48 (3.22)	19.60 (21.47)	a.
k_{-2}	$C_3COO{\cdot} \rightarrow C_2C^*C + HO_2$	$3.70 \times 10^{10}(4.93 \times 10^{10})$	0.82 (0.85)	27.43 (28.04)	a.

Geometric mean frequency
$C_3{\cdot}COOH$ 250.1cm^{-1} (10.789), 1090.9cm^{-1} (16.285), 2881.2cm^{-1} (9.417)
$C_3COO{\cdot}$ 368cm^{-1} (12.104), 1230.1cm^{-1} (16.899), 3157.5cm^{-1} (7.998)
Lennard-Jones parameters: σ = 5.55A°, ε/k = 585 K

- Data in parentheses are from B3LYP-determined entropies and CBS-q// B3LYP/6-31g* calculation

a. fitting with two parameter modified Arrhenius equation; A estimated using TST and MP2-determined entropies, E_a evaluated from CBS-q//MP2(full)/6-31G* calculation. (Data in parentheses are from B3LYP-determined entropies and CBS-q// B3LYP/6-31g* calculation.)

Input Parameters and High - Pressure Limit Rate Constants (k_∞) for QRRK Calculation: $C^*C(C)Q \rightarrow C_2{\cdot}C^*O + OH$

	Reaction	A (s-1 or cc/mol-s)	E_a (kcal/mol)
k_1	$C^*C(C)Q \rightarrow C_2{\cdot}C^*O + OH$	4.05E15	14.47

geometric mean frequency
$C^*C(C)Q$ 526.0cm^{-1} (12.851), 1827.0cm^{-1} (10.334), 2881.2cm^{-1} (2.315)
Lennard-Jones parameters: σ = 5.1983A°, ε/k = 533.08 K

k_1 A_1=4.05E+15, from CCOOH → CCO·+OH (ref.64); $E_{a1} = \Delta U_{rxn} - RTm$

Input Parameters and High - Pressure Limit Rate Constants (k_∞) for QRRK Calculation: $C2{\cdot}C^*O \rightarrow C^*C^*O + CH_3$

	Reaction	A (s-1 or cc/mol-s)	Ea (kcal/mol)
k_1	$C_2{\cdot}C^*O \rightarrow C^*C^*O + CH_3$	1.11E13	39.44

geometric mean frequency
$C_2{\cdot}C^*O$ 372.4cm^{-1} (5.286), 1158.0cm^{-1} (9.242), 2500.5cm^{-1} (5.471)
Lennard-Jones parameters: σ =4.8034A°, ε/k = 481.73 K

k_1 A_1 via A_{-1} and MR, $E_{a1} = \Delta U_{rxn} + E_{a-1}$

k_{-1} Base on C=C-C + CH_3, A_{-1} =1.19E11, E_{a-1}=8.191 (ref.63)

Table 2A.10 Input Parameters and High - Pressure Limit Rate Constants (k_∞) for QRRK Calculation: $C_2C*C+HO_2 \Leftrightarrow [C_2C\cdot COOH]* \Leftrightarrow$ Products

	Reaction	A (s^{-1} or cc/mol-s)	n	Ea (kcal/mol)
k_1	$C_2C*C + HO_2 \rightarrow C_2C\cdot COOH$	5.60×10^4 (6.46×10^2)	1.89 (2.64)	10.56 (10.26)
k_{-1}	$C_2C\cdot COOH \rightarrow C_2C*C + HO_2$	6.50×10^8 (3.80×10^8)	0.96 (1.08)	18.83 (18.91)
k_2	$C_2C\cdot COOH \rightarrow C_2C*CQ + H$	7.51×10^{12}		41.26
k_3	$C_2C\cdot COOH \rightarrow C*C(C)CQ + H$	3.14×10^{13}		40.77
k_4	$C_2C\cdot COOH \rightarrow C_2CyC_2O + OH$	1.92×10^8 (2.32×10^7)	0.97 (1.56)	19.37 (21.05)
k_5	$C_2C\cdot COOH \rightarrow C_2CCOO\cdot$	1.02×10^6 (2.54×10^5)	1.18 (1.46)	17.33 (15.54)
k_{-5}	$C_2CCOO\cdot \rightarrow C_2C\cdot COOH$	3.67×10^8 (1.44×10^8)	0.91 (1.11)	28.18 (26.46)
k_6	$C_2CCOO\cdot \rightarrow C_2C*C + HO_2$	5.47×10^8 (1.30×10^8)	0.97 (1.30)	33.97 (32.06)
k_7	$C_2CCOO\cdot \rightarrow C_2\cdot CCOOH$	8.23×10^7 (3.63×10^7)	0.97 (1.15)	20.71 (20.77)
k_{-7}	$C_2\cdot CCOOH \rightarrow C_2CCOO\cdot$	5.98×10^8 (1.28×10^8)	0.13 (0.42)	4.16 (4.15)
k_8	$C_2CCOO\cdot \rightarrow C_3\cdot C + O_2$	8.21×10^{14}		33.94
k_9	$C_2\cdot CCOOH \rightarrow C*CC + C\cdot H_2OOH$	3.10×10^{12} (1.43×10^{13})	0.15 (-0.09)	26.42 (26.37)

geometric mean frequency

$C_2C\cdot COOH$ 250.1cm^{-1} (11.469), 1329.2cm^{-1} (17.070), 2792.5cm^{-1} (7.961)

$C_2CCOO\cdot$ 250.2cm^{-1} (9.560), 1119.2cm^{-1} (16.494), 2788.5cm^{-1} (10.946)

$C_2\cdot CCOOH$ 250.6cm^{-1} (10.626), 1179.9cm^{-1} (17.723), 3081.5cm^{-1} (9.151)

Lennard-Jones parameters: σ = 5.5471A°, ε/k = 584.86 K

* Data in parentheses are from B3LYP-determined entropies and CBS-q// B3LYP/6-31g* calculation

k_1	fitting with three parameter modified Arrhenius equation; A_1 estimated using TST and MP2-determined entropies, E_{a1} evaluated from CBS-q// MP2(full)/6-31G* calculation.
k_{-1}	fitting with three parameter modified Arrhenius equation; A_{-1} estimated using TST and MP2-determined entropies, $E_{a-1}=E_{a1} + \Delta Urxn$
k_2	Via k_{-2} and <MR>
k_{-2}	Estimated A_{-2}=1.0e13, E_{a-2}=3.
k_3	Via k_{-3} and <MR>
k_{-3}	Estimated A_{-3}=1.0e13, E_{a-3}=3.
k_4	fitting with three parameter modified Arrhenius equation, A_4 estimated using TST and MP2-determined entropies, E_{a4} best fit experimental data in this study
k_5	fitting with three parameter modified Arrhenius equation; A_5 estimated using TST and MP2-determined entropies, E_{a5} evaluated from CBS-q// MP2(full)/6-31G* calculation.
k_{-5}	fitting with three parameter modified Arrhenius equation; A_4 estimated using TST and MP2-determined entropies, $E_{a-5}=Ea_5 + \Delta Urxn$
k_6	fitting with three parameter modified Arrhenius equation; A_6 estimated using TST and MP2-determined entropies, E_{a6} evaluated from CBS-q// MP2(full)/6-31G* calculation.
k_7	fitting with three parameter modified Arrhenius equation; A_7 estimated using TST and MP2-determined entropies, E_{a7} evaluated from CBS-q// MP2(full)/6-31G* calculation.
k_{-7}	fitting with three parameter modified Arrhenius equation; A_4 estimated using TST and MP2-determined entropies, $E_{a-7}=E_{a7} - \Delta U_{rxn}$
k_8	Via k_{-8} and <MR>
k_{-8}	A_{-8}=3.60E12, Ea_{-8}=0, from C*CC· +O_2 (ref.61)
k_9	fitting with three parameter modified Arrhenius equation; A_1 estimated using TST and MP2-determined entropies, E_{a1} evaluated from CBS-q// MP2(full)/6-31G* calculation.

Table 2A.10 (Continued)

Input Parameters and High - Pressure Limit Rate Constants (k_∞) for QRRK Calculation: C_2C*CQ → Products

	Reaction	A (s^{-1} or cc/mol-s)	Ea (kcal/mol)
k_1	C_2C*CQ → C_2C·C*O+ OH	4.05E15	21.40

geometric mean frequency

C_2C*CQ 337.9cm^{-1} (11.813), 1223.0cm^{-1} (14.753), 2824.6cm^{-1} (7.434)

Lennard-Jones parameters: σ = 5.5471A°, ε/k = 584.86 K

k_1 A_1=4.05E15, from CCOOH → CCO· + OH (ref.64)

Input Parameters and High - Pressure Limit Rate Constants (k_∞) for QRRK Calculation: C2C*CO· → Products

	Reaction	A (s^{-1} or cc/mol-s)	Ea (kcal/mol)
k_1	C_2C*CO· → C_2C*C*O + H	5.14E13	37.39

geometric mean frequency

C_2C*CO· 419.1cm^{-1} (10.253), 1349.8cm^{-1} (11.776), 3014.7cm^{-1} (6.971)

Lennard-Jones parameters: σ = 5.1983A°, ε/k = 533.08 K

k_1 Via k_{-1} and MR, estimated A_{-1}=1.0E13, E_{a-1}=3.

Table 2A.11 PM3-Determined Frequencies and Moments of Inertia for Intermediates and Transition States of Isobutene-OH + O_2 Reaction System

Molecule	Frequencies	moments of inertia[a]
C$_2$CQ·COH	60.86, 103.69, 158.53, 183.01, 230.69, 296.93, 321.99, 338.98, 377.67, 419.30, 558.70, 605.58, 804.94, 892.16, 912.64, 963.78, 979.97, 995.75, 1049.09, 1133.33, 1215.58, 1245.41, 1312.80, 1339.81, 1371.14, 1383.77, 1397.78, 1398.46, 1399.68, 1406.14, 1407.08, 1408.85, 1443.12, 2936.80, 3020.89, 3082.73, 3083.73, 3084.26, 3085.13, 3177.23, 3178.80, 3887.40	291.233533 338.436954 436.864864
TS11	(-870.22), 122.88, 145.99, 173.57, 221.05, 302.57, 349.92, 421.59, 439.56, 504.40, 570.32, 635.27, 855.92, 886.16, 922.66, 933.43, 962.62, 980.44, 989.31, 1018.70, 1105.31, 1190.50, 1218.27, 1271.67, 1311.30, 1328.82, 1382.78, 1395.51, 1397.16, 1399.46, 1403.39, 1406.40, 1407.82, 1776.33, 2957.14, 3020.26, 3084.76, 3086.99, 3087.50, 3088.52, 3179.70, 3180.55	230.297465 355.352881 397.562299
C$_2$CQCO·	54.47, 97.29, 129.86, 158.54, 189.09, 240.47, 263.69, 340.85, 386.70, 422.76, 487.77, 578.44, 631.62, 815.34, 849.08, 939.24, 955.82, 964.23, 995.88, 1036.87, 1186.38, 1236.21, 1256.68, 1272.55, 1325.83, 1394.38, 1398.83, 1401.63, 1405.58, 1412.77, 1413.23, 1440.19, 1518.69, 2994.59, 3015.48, 3085.29, 3086.26, 3087.24, 3087.58, 3180.59, 3181.66, 3988.34	304.681126 325.430673 440.567673
C$_2$COHCQ·	36.08, 91.57, 156.17, 185.65, 240.81, 311.90, 339.68, 357.74, 429.62, 481.13, 515.13, 586.82, 866.24, 920.04, 960.03, 965.31, 988.35, 989.68, 1011.51, 1093.82, 1160.90, 1255.92, 1289.90, 1336.94, 1346.73, 1384.22, 1398.84, 1400.74, 1407.78, 1408.69, 1409.29, 1415.55, 1433.80, 2973.53, 3025.28, 3084.46, 3086.98, 3088.75, 3089.47, 3181.50, 3183.73, 3895.54	196.005571 480.429104 489.709306
TS15	(-2699.96), 83.12, 113.77, 166.77, 261.04, 325.90, 339.30, 372.53, 415.87, 428.74, 534.43, 563.65, 579.07, 699.49, 883.28, 899.63, 950.74, 968.44, 990.09, 1036.01, 1060.54, 1114.18, 1137.37, 1235.03, 1265.49, 1314.17, 1332.82, 1372.93, 1388.84, 1395.80, 1399.89, 1407.07, 1452.82, 1547.68, 2937.18, 3027.79, 3085.43, 3087.35, 3088.69, 3135.66, 3181.51,3836.21	252.014028 378.006671 458.428245
C$_2$.CQCOH	77.96, 107.91, 125.09, 146.08, 174.05, 252.13, 267.58, 284.74, 344.79,384.55, 422.48, 486.95, 574.14, 630.94, 741.62, 853.82, 911.53, 918.94,979.38, 993.96, 1062.11, 1126.20, 1194.53, 1250.03, 1307.41, 1316.46, 1360.40, 1389.27, 1392.65, 1401.02, 1412.60, 1412.92, 1432.07, 2921.81, 2971.71, 3089.22, 3092.06, 3153.12, 3184.81, 3201.21, 3909.39, 3968.50	301.509221 319.436628 435.630709
TS16	(-2758.61), 100.58, 146.50, 188.97, 197.93, 269.13, 284.43, 307.43, 357.69, 457.29, 477.74, 516.96, 585.68, 655.65, 844.61, 856.07, 924.92, 958.80, 978.47, 988.17, 1023.13, 1080.86, 1231.85, 1250.57, 1275.71, 1325.66, 1388.94, 1394.25, 1398.06, 1402.21, 1404.98, 1410.68, 1413.95, 1445.47, 2947.24, 3085.15, 3086.06, 3088.93, 3090.62, 3180.94, 3181.85, 3901.61	292.899823 331.689037 434.464659
C$_2$CQC·OH	59.34, 87.46, 125.99, 175.54, 190.05, 206.86, 238.31, 288.86, 309.44, 367.02, 380.12, 432.66, 495.69, 585.83, 808.82, 872.52, 946.25, 958.06, 989.41, 1001.08, 1119.06, 1231.77, 1271.73, 1299.54, 1380.57, 1388.28, 1399.78, 1404.43, 1407.78, 1410.03, 1411.12, 1520.49, 1550.43, 3059.09, 3086.21, 3087.66, 3090.52, 3092.04, 3182.66, 3183.67, 3910.57, 3988.73	187.656693 492.738857 499.571646
TS10	(-700.41), 90.74, 148.25, 173.19, 261.74, 325.20, 336.43, 425.65, 465.66, 490.94, 562.46, 651.24, 872.72, 881.67, 943.12, 956.38, 974.11, 983.14, 1007.53, 1035.84, 1108.00, 1153.78, 1251.65, 1270.83, 1304.00, 1349.97, 1364.17, 1394.55, 1397.65, 1398.02, 1403.60, 1407.46, 1411.64, 1722.69, 2971.84, 3045.88, 3086.95, 3088.74, 3089.65, 3090.03, 3181.43, 3183.70	202.977381 399.814918 419.935328
C$_2$CO·CQ	11.85, 84.46, 159.34, 169.02, 177.65, 192.94, 271.86, 340.54, 358.98, 468.82, 493.17, 547.30, 796.54, 882.81, 915.16, 962.28, 964.11, 989.82, 998.32, 1090.04, 1141.33, 1243.22, 1300.61, 1353.74, 1367.08, 1380.11, 1401.22, 1405.51, 1410.87, 1411.26, 1417.46, 1489.81, 2282.70, 2937.54, 2991.52, 3087.46, 3087.82, 3089.55, 3091.30, 3182.50, 3184.55, 3987.46	183.451362 560.883182 564.527788
TS14	(-2791.09), 75.29, 175.28, 259.62, 287.05, 312.80, 346.26, 424.64, 455.67, 480.99, 519.85, 557.56, 681.00, 717.80, 873.68, 953.99, 960.47, 975.89, 995.65, 1058.17, 1092.98, 1122.80, 1129.32, 1162.99, 1232.23, 1324.36, 1334.85, 1355.01, 1363.29, 1392.75, 1396.42, 1403.59, 1412.82, 1418.98, 2960.87, 3038.66, 3083.71, 3088.47, 3114.66, 3137.46, 3182.17, 3898.15	202.873387 429.133131 454.272972

Table 2A.11 (Continued)

C_2·COHCQ	24.96, 83.47, 117.67, 159.19, 169.76, 183.42, 285.55, 328.97, 347.86, 364.18, 441.14, 503.07, 553.85, 646.46, 795.63, 916.00, 922.30, 934.47, 976.84, 988.25, 1087.09, 1140.73, 1162.62, 1229.96, 1312.11, 1331.87, 1347.02, 1376.73, 1395.64, 1405.07, 1408.16, 1474.32, 1490.67, 2926.68, 2982.85, 3086.49, 3091.84, 3154.06, 3184.32, 3205.03,3897.33, 3989.37	181.191039 556.802137 569.411493

Unit: 10 E-40 g*cm^2

Table 2A.12 Input Parameters and High - Pressure Limit Rate Constants (k_∞) for QRRK Calculation: $C_2C{*}C + OH \rightarrow C_3{\cdot}COH$

	Reaction	A (s−1 or cc/mol-s)	Ea (kcal/mol)
k_1	$C_2C{*}C + OH \rightarrow C_3{\cdot}COH$	8.5×10^{12}	-0.3
k_{-1}	$C_3{\cdot}COH \rightarrow C_2C{*}C + OH$	1.02×10^{14}	30.16

geometric mean frequency
$C_3{\cdot}COH$ 439.7cm^{-1} (11.660), 1274.0cm^{-1} (13.717), 3014.7cm^{-1} (8.624)
Lennard-Jones parameters: σ = 5.1983A°, ε/k = 553.08 K

k_1	ref. 63; k_{-1} via k_1 and <MR>

Input Parameters and High - Pressure Limit Rate Constants (k_∞) for QRRK Calculation: $C_3{\cdot}COH + O_2 \rightarrow$ Products

	Reaction	A (s−1 or cc/mol-s)	n	Ea (kcal/mol)
k_1	$C_3{\cdot}COH + O_2 \rightarrow C_2COHCQ{\cdot}$	3.6×10^{12}		0.0
k_{-1}	$C_2COHCQ{\cdot} \rightarrow C_3{\cdot}COH + O_2$	8.25×10^{14}		32.23
k_2	$C_2COHCQ{\cdot} \rightarrow C_2CO{\cdot}CQ$	7.56×10^{7}	1.06	17.83
k_{-2}	$C_2CO{\cdot}CQ \rightarrow C_2COHCQ{\cdot}$	9.16×10^{6}	1.34	0.99
k_3	$C_2CO{\cdot}CQ \rightarrow C_2C{*}O + C{\cdot}H_2OOH$	7.80×10^{14}		12.41
k_4	$C_2COHCQ{\cdot} \rightarrow C_2{\cdot}COHCQ$	2.53×10^{8}	1.08	8.06
k_{-4}	$C_2{\cdot}COHCQ \rightarrow C_2COHCQ{\cdot}$	8.47×10^{7}	0.85	21.68
k_5	$C_2{\cdot}COHCQ \rightarrow C{*}C(C)CQ + OH$	8.89×10^{13}		32.10
k_6	$C_2{\cdot}COHCQ \rightarrow C{*}C(C)OH + C{\cdot}H_2OOH$	1.90×10^{14}		28.83

geometric mean frequency
$C_2COHCQ{\cdot}$ 270.0cm^{-1} (12.085), 1109.5cm^{-1} (16.601), 2859.8cm^{-1} (10.814)
$C_2CO{\cdot}CQ$ 277.7cm^{-1} (12.704), 1121.3cm^{-1} (17.851), 2824.5cm^{-1} (8.945)
$C_2{\cdot}COHCQ$ 298.6cm^{-1} (13.666), 1139.6cm^{-1} (15.948), 2851.4cm^{-1} (9.386)
Lennard-Jones parameters: σ = 5.8569A°, ε/k = 632.06 K

k_1	A_1=3.6E12, , from Atkinson et al. for CCC· + O_2; E_{a1}=0 (ref. 61)
k_{-1}	Via k_1 and <MR>, $E_{a\text{-}1}$= ΔU_{rxn}
k_2	A_2 estimated using TST, PM3-determined entropies and fitting with three parameter modified Arrhenius equation, Ea_2 evaluated from ring strain (0.1) + ΔH_{rxn} (16.84) + Ea abstraction (6.89)-6 (H-bond)
k_{-2}	A_{-2} estimated using TST, PM3-determined entropies and fitting with three parameter modified Arrhenius equation, $E_{a\text{-}2}$ = E_{a2} - ΔU_{rxn}
k_3	Via k_{-3} and <MR>, A_{-3} = 3.3E11, estimated from (C_2H_4 + CH_3), $E_{a\text{-}3}$ = 7.7 (ref. 62)
k_4	A_4 estimated using TST, PM3-determined entropies and fitting with three parameter modified Arrhenius equation, E_{a4} evaluated from ring strain (0.1) + Ea abstraction (7.96)
k_{-4}	A_{-4} estimated using TST, PM3-determined entropies and fitting with three parameter modified Arrhenius equation, $E_{a\text{-}4}$ = E_{a4} + ΔU_{rxn}
k_5	k_5 via k_{-5} and <MR>, A_5 = 2.7E12, estimated from 1/2(C_2H_4 + OH), $E_{a\text{-}5}$=1.0 (ref. 66)
k_6	k_6 via k_{-6} and <MR>, A_6 = 3.3E11, estimated from 1/2(C_2H_4 + CH_3), $E_{a\text{-}6}$=7.7 (ref. 62)

Input Parameters and High - Pressure Limit Rate Constants (k_∞) for QRRK Calculation: $C{\cdot}H_2OOH \rightarrow CH_2O + OH$

	Reaction	A (s−1 or cc/mol-s)	Ea (kcal/mol)
k_1	$C{\cdot}H_2OOH \rightarrow CH_2O + OH$	2.90E12	1.0

geometric mean frequency
$C{\cdot}H_2OOH$ 100.3cm^{-1} (3.429), 986.7cm^{-1} (4.763), 2506.4cm^{-1} (2.808)
Lennard-Jones parameters: σ = 4.3451A°, ε/k = 422.61 K

k_1	A_1 via A_{-1} and <MR>, A_{-1} = 2.70E12, estimated from 1/2(C_2H_4 + OH), $E_{a\text{-}1}$ =1.0 (ref. 66)

Table 2A.13 Input Parameters and High - Pressure Limit Rate Constants (k_∞) for QRRK Calculation: $C_2C*C + OH \rightarrow C_2C\cdot COH$

	Reaction	A (s–1 or cc/mol-s)	Ea (kcal/mol)
k_1	$C_2C*C + OH \rightarrow C_2C\cdot COH$	8.5×10^{12}	-0.3
k_{-1}	$C_2C\cdot COOH \rightarrow C_2C*C + OH$	5.54×10^{13}	29.39

geometric mean frequency

C2C·COH 389.3cm^{-1} (10.799), 1475.6cm^{-1} (15.383), 3185.2cm^{-1} (7.818)

Lennard-Jones parameters: σ = 5.1983A°, ε/k = 553.08 K

k_1 ref. 63; k_{-1} via k_1 and <MR>

Input Parameters and High - Pressure Limit Rate Constants (k_∞) for QRRK Calculation: $C_2C\cdot COH + O_2 \rightarrow$ Products

	Reaction	A (s–1 or cc/mol-s)	n	Ea (kcal/mol)
k_1	$C_2C\cdot COH + O_2 \rightarrow C_2CQ\cdot COH$	3.6×10^{12}		0.0
k_{-1}	$C_2CQ\cdot COH \rightarrow C_2C\cdot COH + O_2$	3.3×10^{15}		32.28
k_2	$C_2CQ\cdot COH \rightarrow C_2CQCO\cdot$	5.06×10^{7}	1.15	17.83
k_{-2}	$C_2CQCO\cdot \rightarrow C_2CQ\cdot COH$	6.93×10^{10}	-0.02	0.99
k_3	$C_2CQCO\cdot \rightarrow C_2C\cdot OOH + CH_2O$	1.23×10^{15}		13.87
k_4	$C_2CQ\cdot COH \rightarrow C_2\cdot CQCOH$	4.61×10^{9}	1.04	27.94
k_{-4}	$C_2\cdot CQCOH \rightarrow C_2CQ\cdot COH$	2.30×10^{9}	0.44	14.23
k_5	$C_2\cdot CQCOH \rightarrow C*C(C)Q + C\cdot H_2OH$	3.68×10^{14}		33.22
k_6	$C_2\cdot CQCOH \rightarrow C*C(C)COH + HO_2$	1.30×10^{13}		16.37
k_7	$C_2CQ\cdot COH \rightarrow C_2CQC\cdot OH$	2.80×10^{8}	1.33	23.47
k_{-7}	$C_2CQC\cdot OH \rightarrow C_2CQ\cdot COH$	8.34×10^{8}	0.75	16.47
k_8	$C_2CQC\cdot OH \rightarrow C_2C*COH + HO_2$	2.67×10^{13}		15.93

geometric mean frequency

C2CQ·COH 291.4cm^{-1} (12.538), 1135.9cm^{-1} (16.437), 2997.8cm^{-1} (10.525)

C2CQCO· 295.9cm^{-1} (13.107), 1144.8cm^{-1} (17.750), 2992.0cm^{-1} (8.643)

C2·CQCOH 311.9cm^{-1} (13.953), 1174.6cm^{-1} (16.498), 3055.0cm^{-1} (8.348)

C2CQC·OH 309.2cm^{-1} (14.390), 1147.0cm^{-1} (15.883), 3022.3cm^{-1} (8.727)

Lennard-Jones parameters: σ = 5.8569A°, ε/k = 632.06 K

k_1 A_1 =3.6E12, , from Atkinson et al. for CCC· + O_2; E_{a1} =0 (ref. 61)

k_{-1} Via k_1 and <MR>, $E_{a-1} = \Delta U_{rxn}$

k_2 A_2 estimated using TST, PM3-determined entropies and fitting with three parameter modified Arrhenius equation, Ea_2 evaluated from ring train (0.1) + ΔH_{rxn} (16.84) + Ea abstraction (6.89)- 6 (H-bond)

k_{-2} A_{-2} estimated using TST, PM3-determined entropies and fitting with three parameter modified Arrhenius equation, $E_{a-2} = E_{a2} - \Delta U_{rxn}$

k_3 Via k_{-3} and <MR>, A_{-3} = 1.67E11, estimated from ½($C_2H_4 + CH_3$), E_{a-3} = 7.7 (ref. 62)

k_4 A_4 estimated using TST, PM3-determined entropies and fitting with three parameter modified Arrhenius equation, E_{a4} evaluated from ring strain (6.3) + ΔH_{rxn} (13.71) + E_a abstraction (7.93)

k_{-4} A_{-4} estimated using TST, PM3-determined entropies and fitting with three parameter modified Arrhenius equation, $E_{a-4} = E_{a4} - \Delta U_{rxn}$

k_5 k_5 via k_{-5} and <MR>, A_5 = 9.64E10, estimated from (C=C-C + CH_3), E_{a-5} =8.006 (ref.65)

k_6 Via k_{-6} and <MR>, A_{-6} = 2.8E11, estimated from 1/2($C_2H_4 + HO_2$), E_{a-6} = 8.46 (ref.66)

k_7 A_7 estimated using TST, PM3-determined entropies and fitting with three parameter modified Arrhenius equation, E_{a4} evaluated from ring strain (6.3) + ΔH_{rxn} (10.17) + E_a abstraction (7.0)

k_{-7} A_{-7} estimated using TST, PM3-determined entropies and fitting with three parameter modified Arrhenius equation, $E_{a7} = E_{a-7}$ - ΔUrxn

k_8 Via k_{-8} and <MR>, A_{-8} = 2.8E11 estimated from 1/2($C_2H_4 + HO_2$), E_{a-8} = 8.46 (ref.66)

Input Parameters and High - Pressure Limit Rate Constants (k_∞) for QRRK Calculation: $C_2C\cdot OOH \rightarrow C_2C*O + OH$

	Reaction	A (s–1 or cc/mol-s)	Ea (kcal/mol)
k_1	$C_2C\cdot OOH \rightarrow C_2C*O + OH$	1.54E12	1.0

geometric mean frequency

C2C·OOH 100.3cm^{-1} (7.507), 1069.9cm^{-1} (12.133), 2730.8cm^{-1} (8.360)

Lennard-Jones parameters: σ = 5.1983A°, ε/k = 533.08 K

k_1 A_1 via A_{-1} and <MR>, A_{-1} = 2.70E12, estimated from 1/2(C_2H_4 + OH), E_{a1}=1.0 (ref. 66)

APPENDIX 2B

FIGURES IN THE ANALYSIS OF TERTIARY BUTYL RADICAL + O_2, ISOBUTENE + HO_2, ISOBUTENE + OH AND ISOBUTENE-OH ADDUCTS + O_2: A DETAILED TERTIARY BUTYL OXIDATION MECHANISM

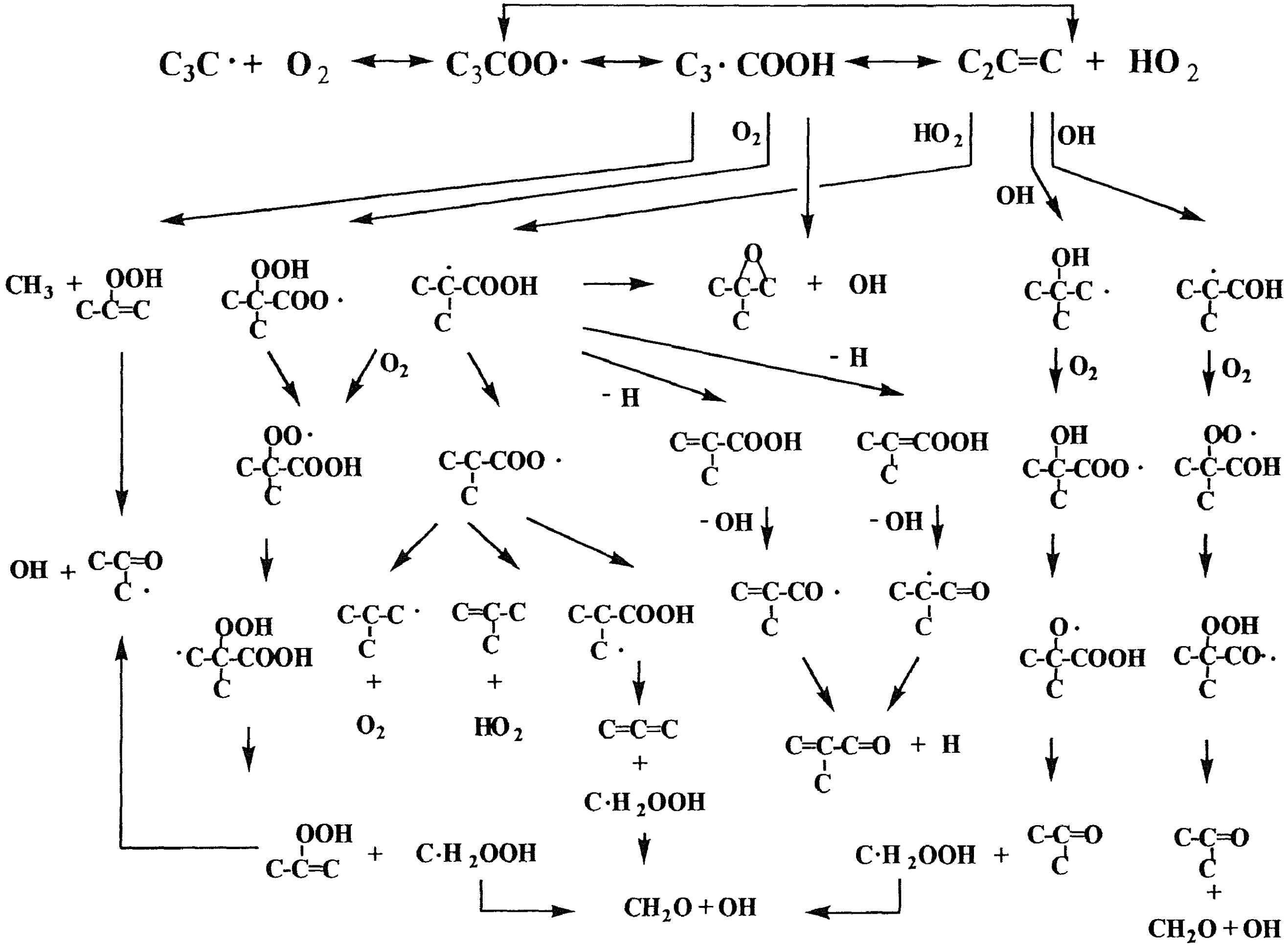

Figure 2B.1 Important reaction pathways for *tert*-butyl radical oxidation

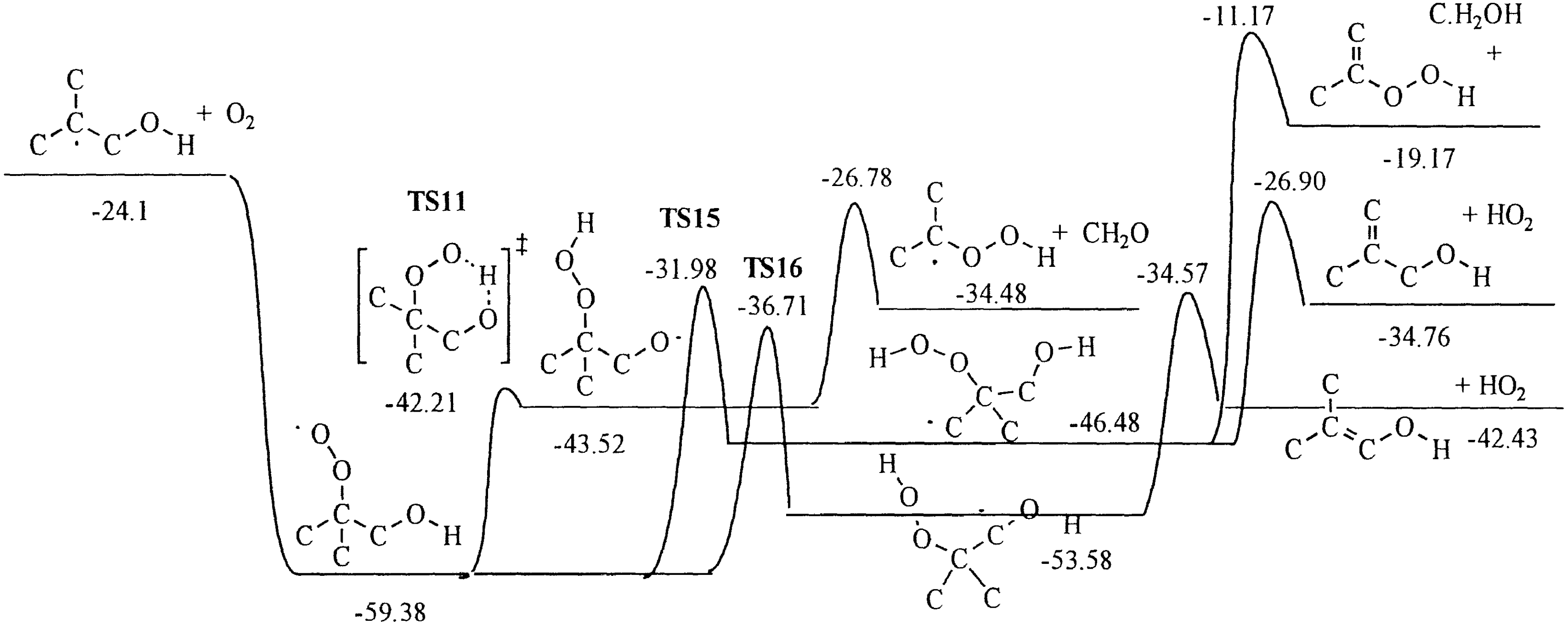

unit in kcal/mole

Figure 2B.2 Potential energy diagram for $C_2C{\cdot}COH + O_2$ => products

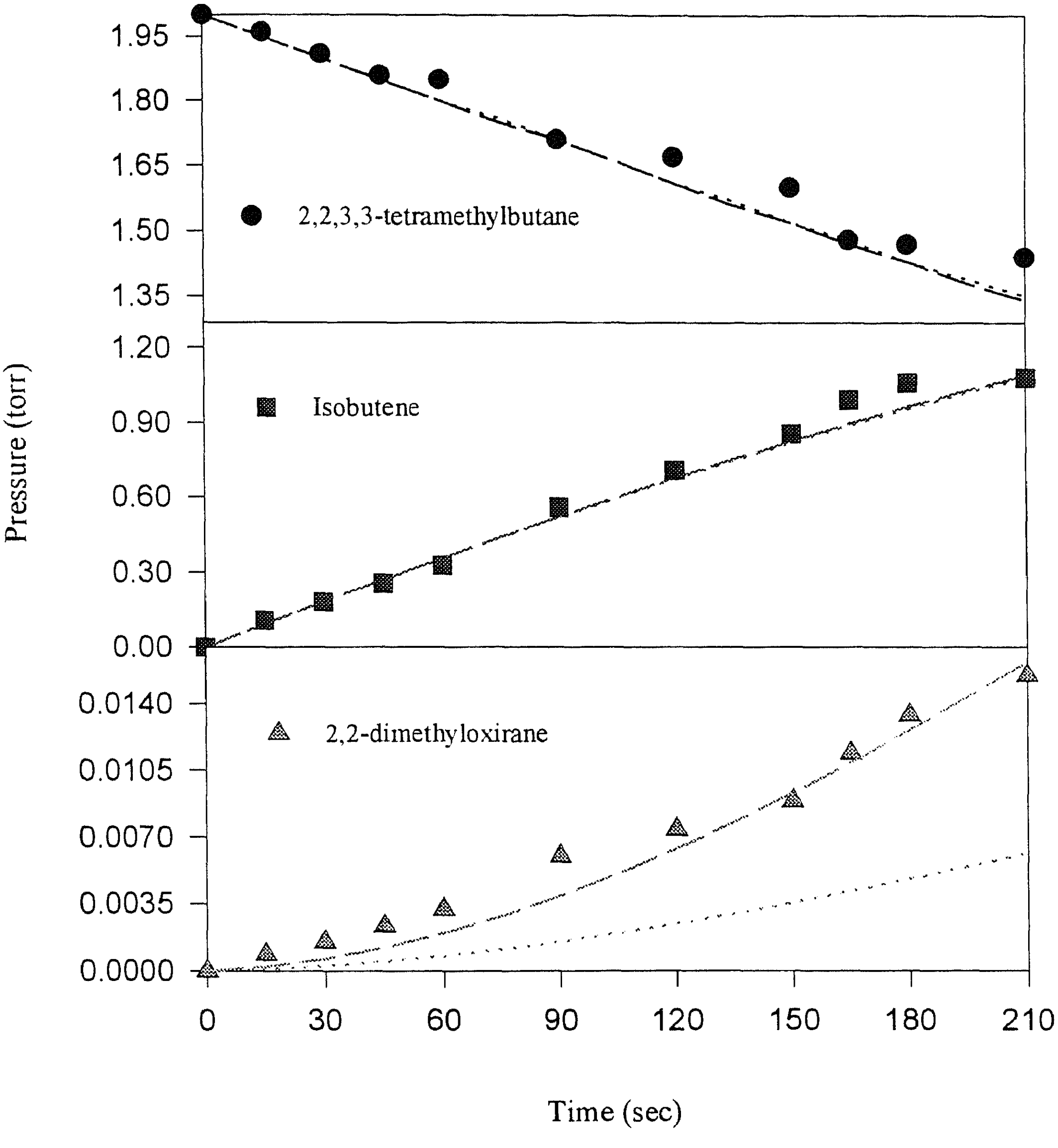

Figure 2B.3 Comparison of model prediction and experimental data. Symbols are experimental data from Arti et al.[11], 773K and 60 torr. Dash lines are model prediction using of barrier 16.13 kcal/mole for C_3·COOH -> 2,2-dimethyloxirane + OH. Dot lines are model prediction using of barrier 17.98 kcal/mole for C_3·COOH -> 2,2-dimethyloxirane + OH

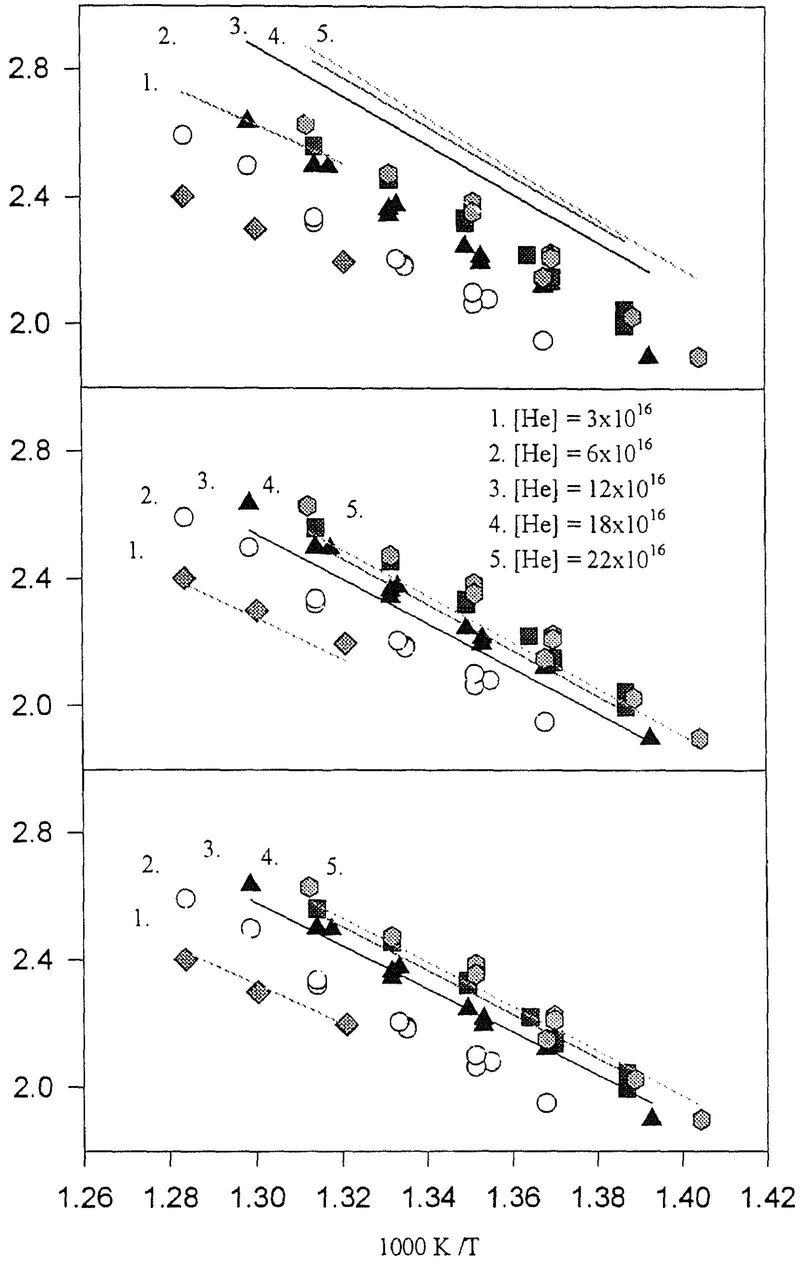

Figure 2B.4 Plot of the *tert*-butyl radical unimolecular rate constants (log k vs. 1000K/T) for different He densities (atom cm^{-3}). Symbols are experimental data from Knyazev et al.[77] a. Lines represent the results of QRRK calculation using the high-pressure limit rate constants from Knyazev et al.[77] ($2.18 \times 10^9 T^{1.48} \exp(-36000/RT)$). b. Lines represent the results of QRRK calculation using the high-pressure limit rate constants from Tsang et al.[87] ($8.3 \times 10^{13} \exp(-38150/RT)$). c. Lines represent the results of QRRK calculation using the high-pressure limit rate constants from *ab initio* calculation of transition state structure, canonical TST, and tunneling ($2.5 \times 10^{16} T^{-0.92} \exp(-37500/RT)$).

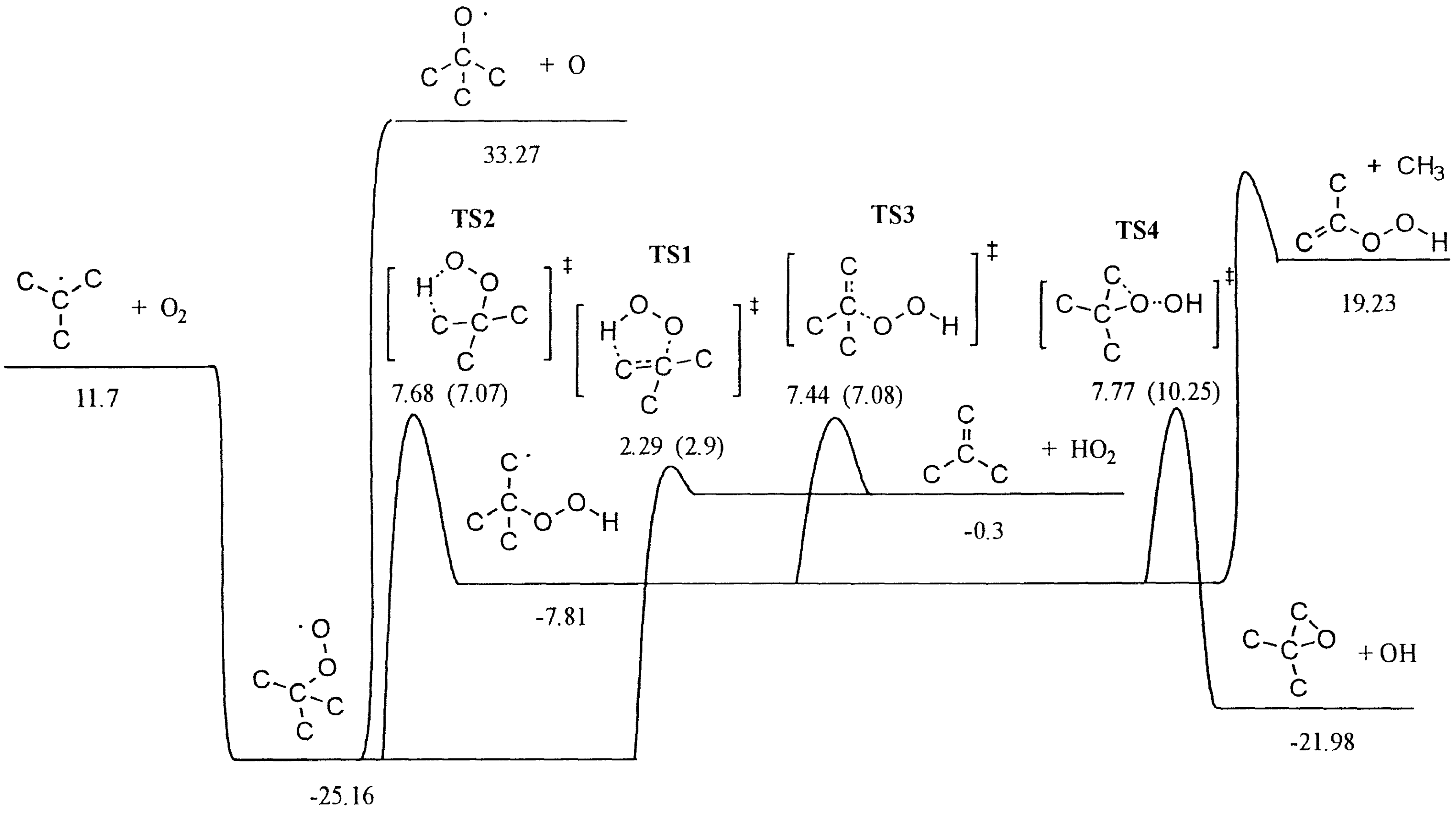

unit in kcal/mole

Figure 2B.5 Potential energy diagram of *tert*-butyl radical addition with O_2 reaction based on CBS-q//MP2(full)/6-31g*. Data in parentheses are from CBS-q// B3LYP/6-31g* calculation.

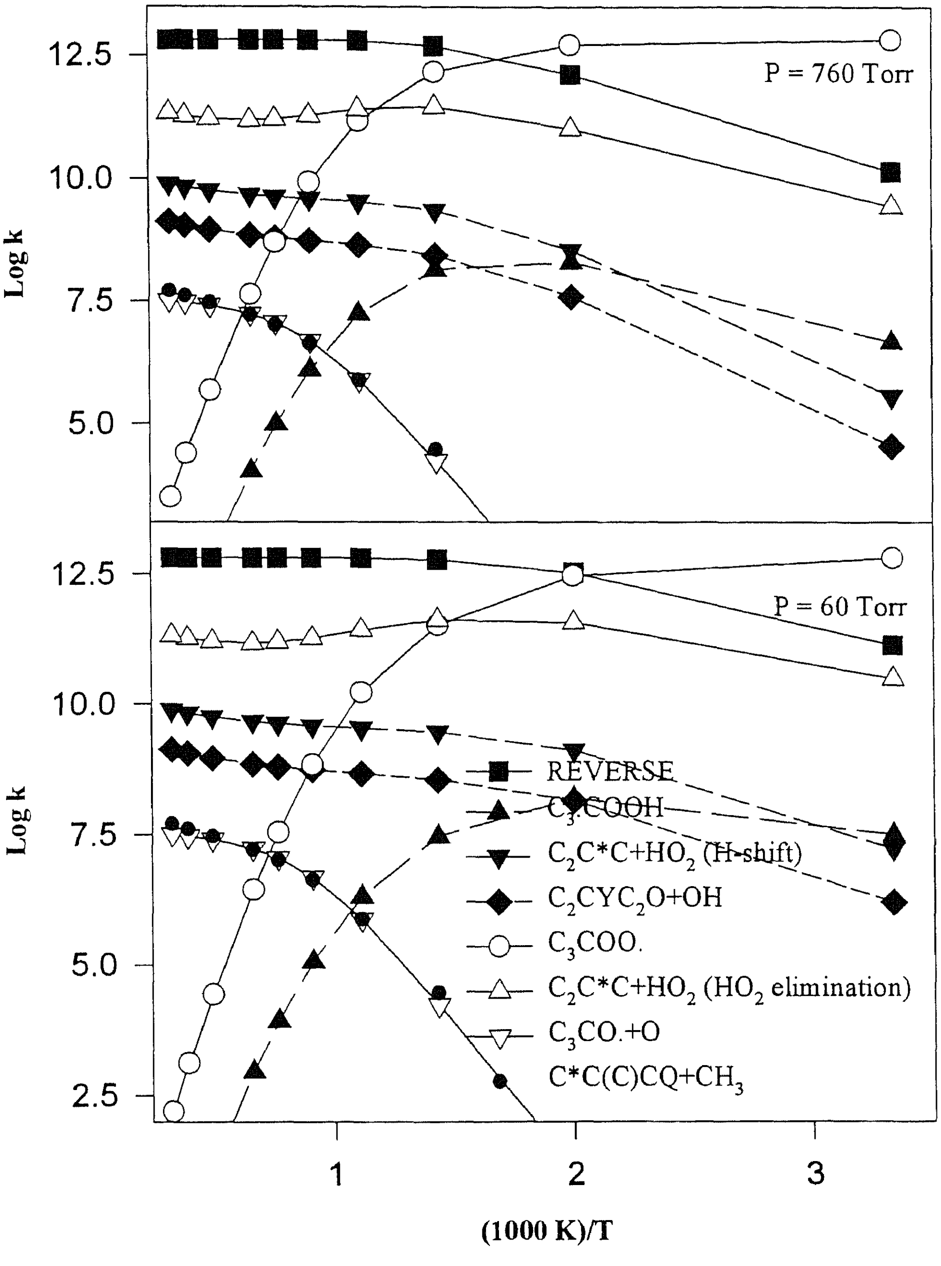

]

Figure 2B.6 Calculated rate constants at different temperature for chemically activated reactions: *tert* -butyl radical + O_2 => $[C_3COO\cdot]^*$ => products. a. pressure at 760 torr; b. pressure at 60 torr. Based on CBS-q//MP2(full)/6-31g* calculation.

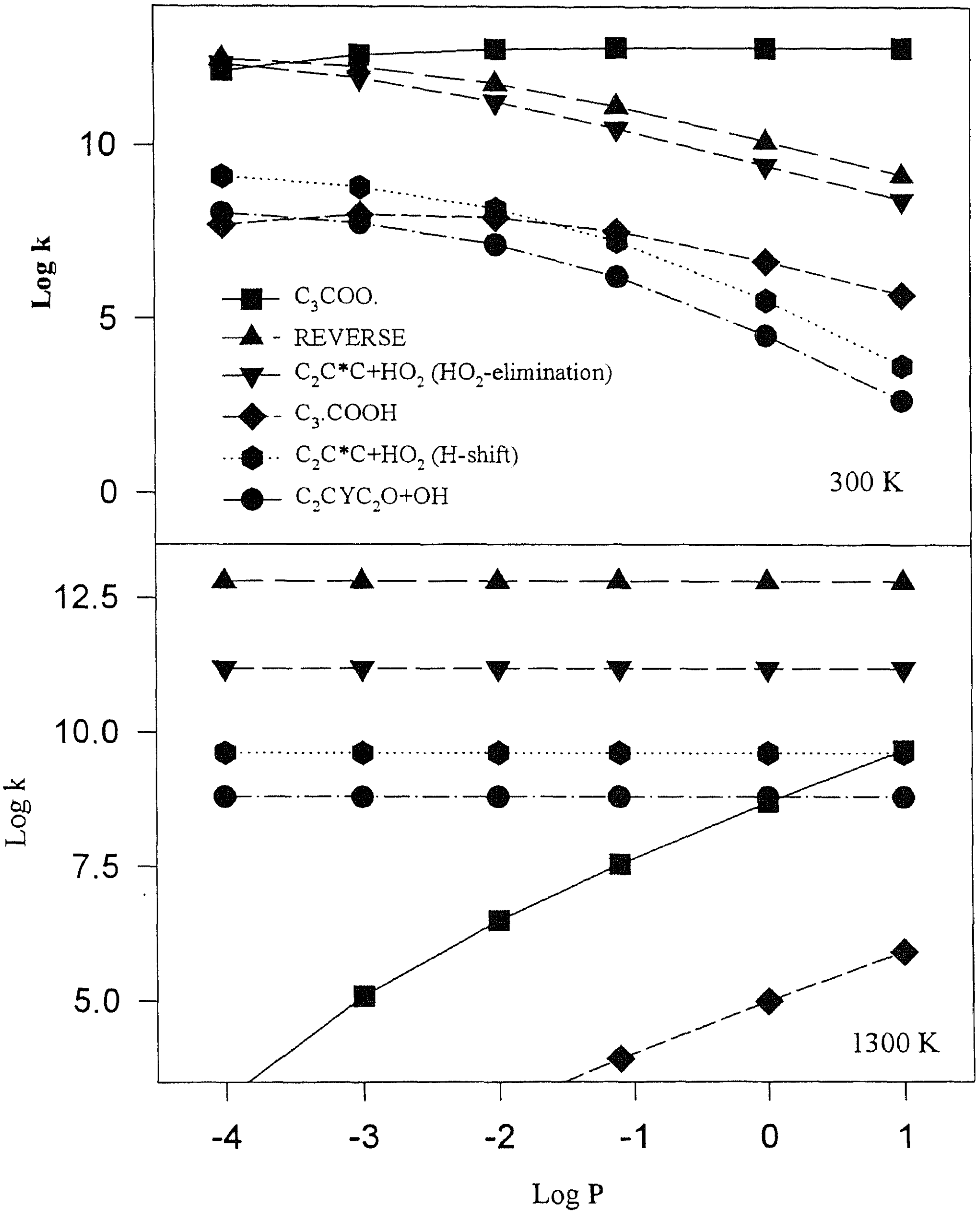

Figure 2B.7 Calculated rate constants at different pressure for chemically activated reactions: *tert* -butyl radical + O_2 => $[C_3COO\cdot]^*$ => products. a. 300K; b. 1300K. Based on CBS-q//MP2(full)/6-31g* calculation.

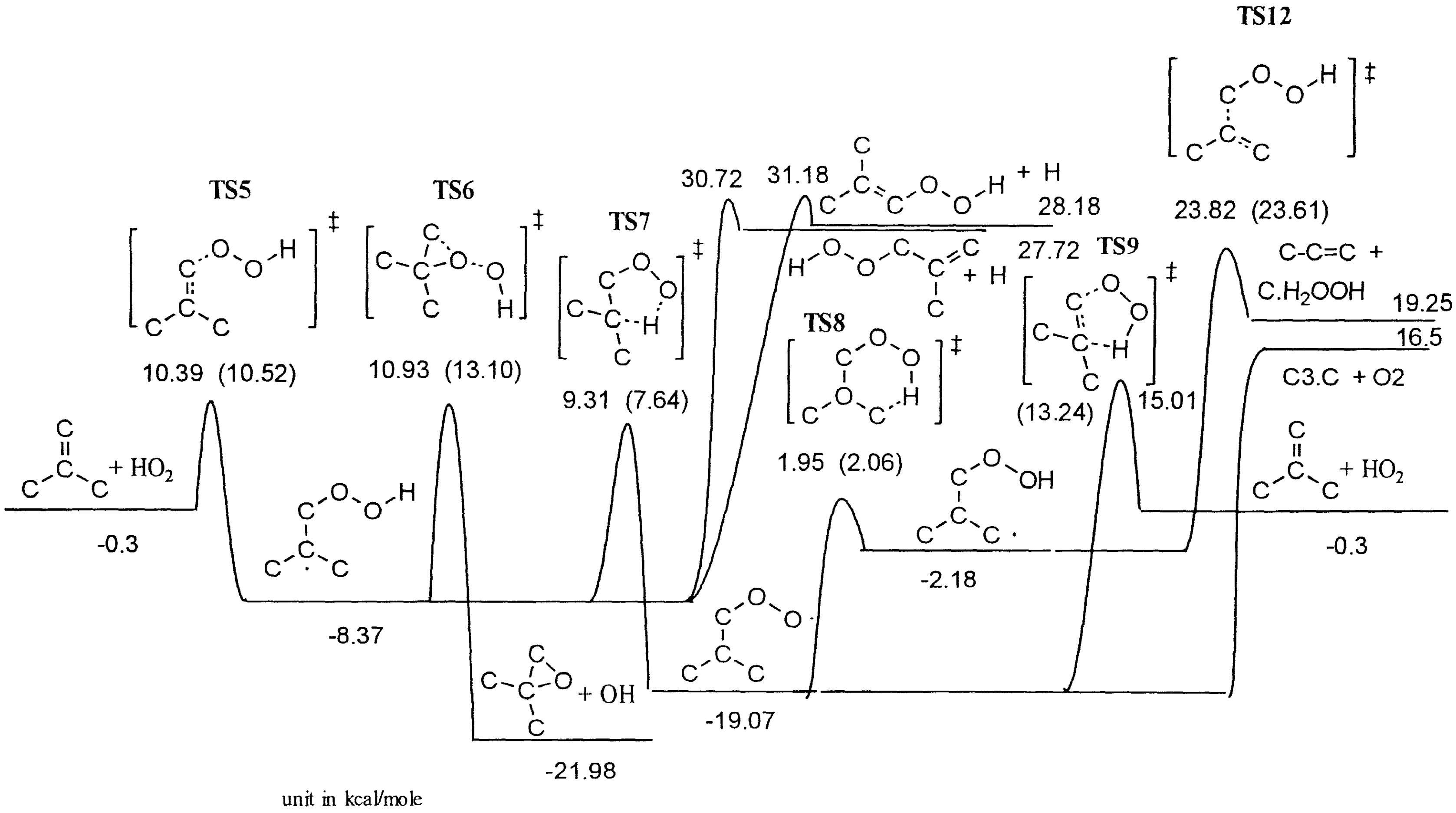

Figure 2B.8 Potential energy diagram for $C_2C{*}C + HO_2$ => $[C_2C{\cdot}COOH]{*}$ => products based on CBS-q//MP2(full)/6-31g*. Data in parentheses are from CBS-q// B3LYP/6-31g* calculation

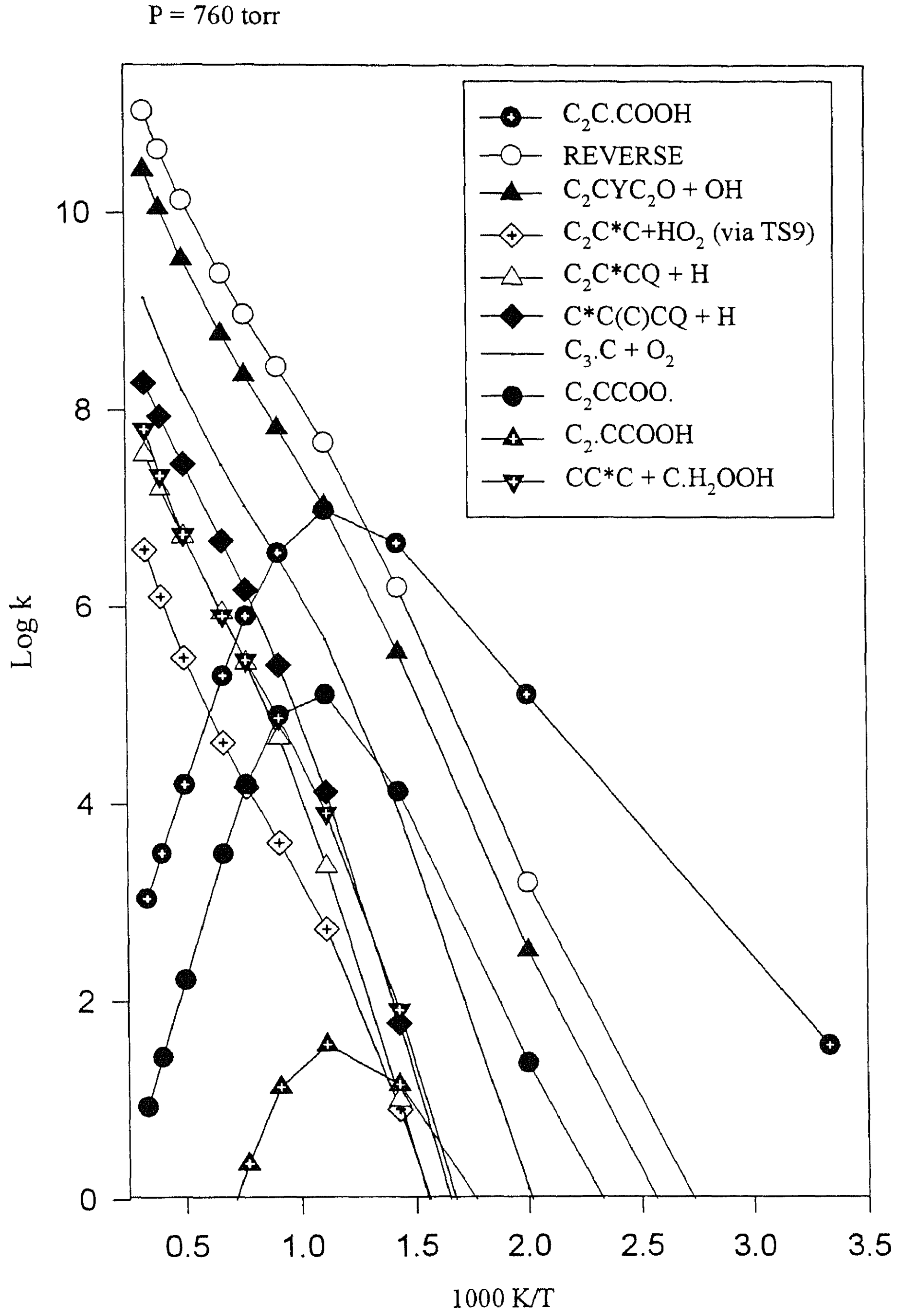

Figure 2B.9 Calculated rate constants at different temperature and 760 torr for chemically activated reactions: $C_2C*C + HO_2 \Rightarrow [C_2C{\cdot}COOH]* \Rightarrow$ products. Based on CBS-q//MP2(full)/6-31g* calculation.

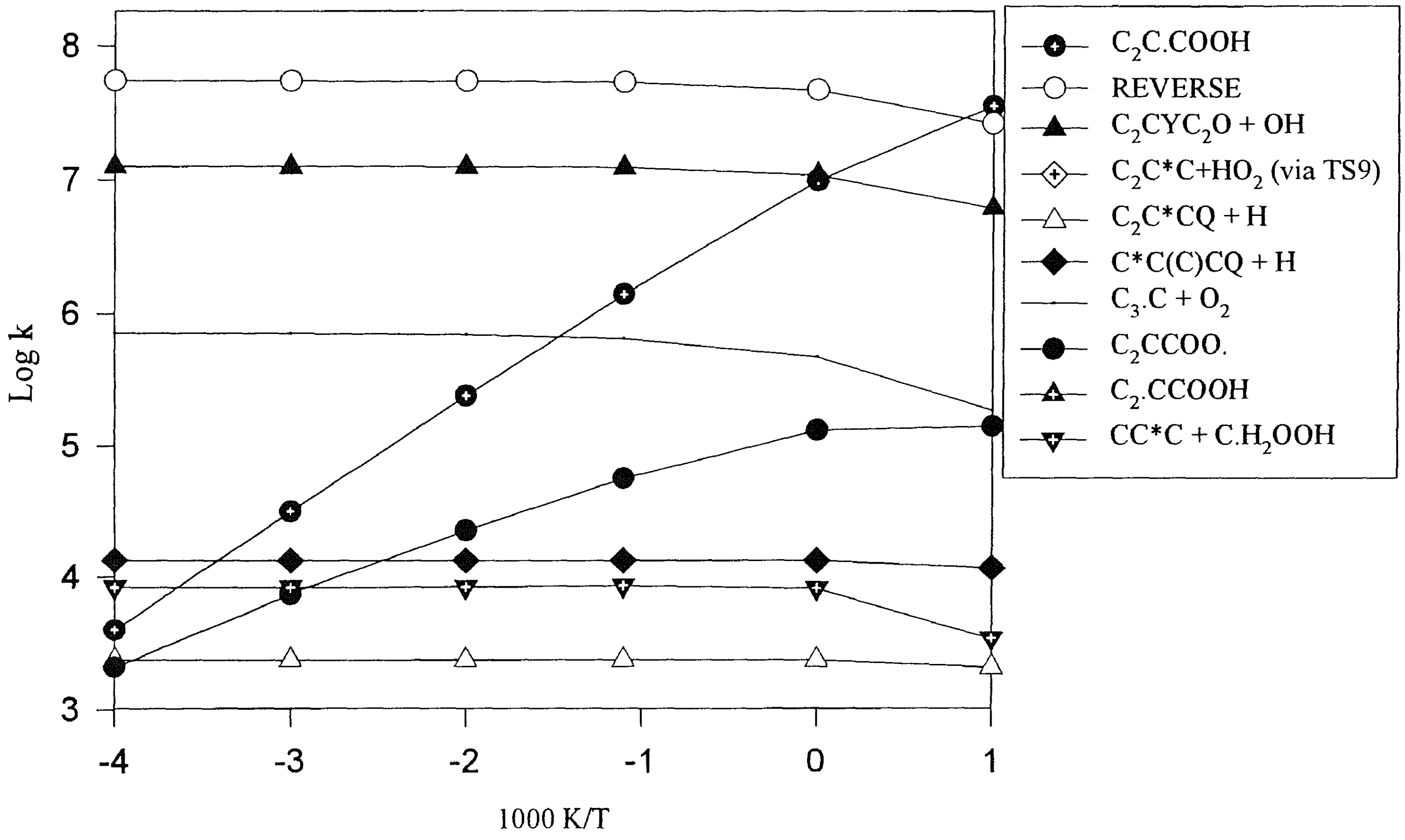

Figure 2B.10 Calculated rate constants at different pressure and 700K for chemically activated reactions: $C_2C{*}C + HO_2 \Rightarrow [C_2C{\cdot}COOH]^* \Rightarrow$ products. Based on CBS-q//MP2(full)/6-31g* calculation.

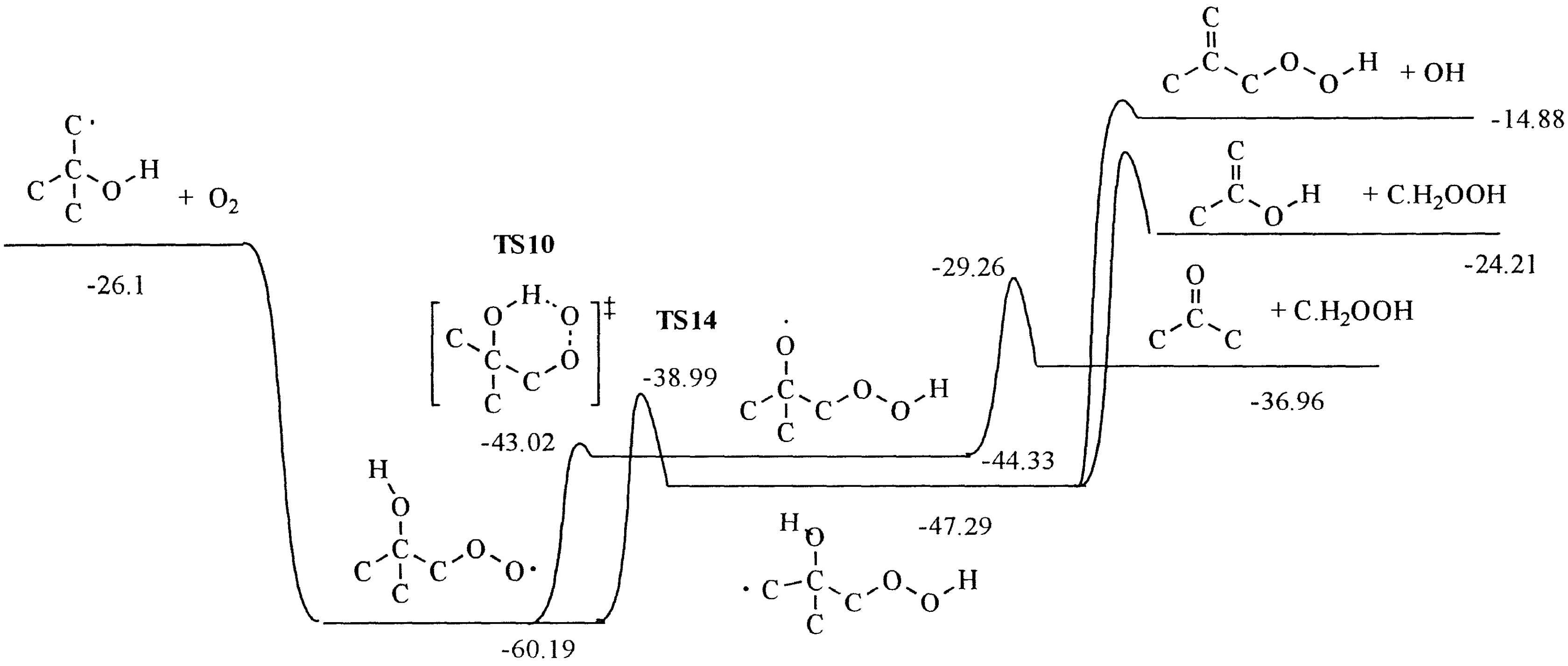

unit in kcal/mole

Figure 2B.11 Potential energy diagram for $C_3{\cdot}COH + O_2 \Rightarrow$ Products.

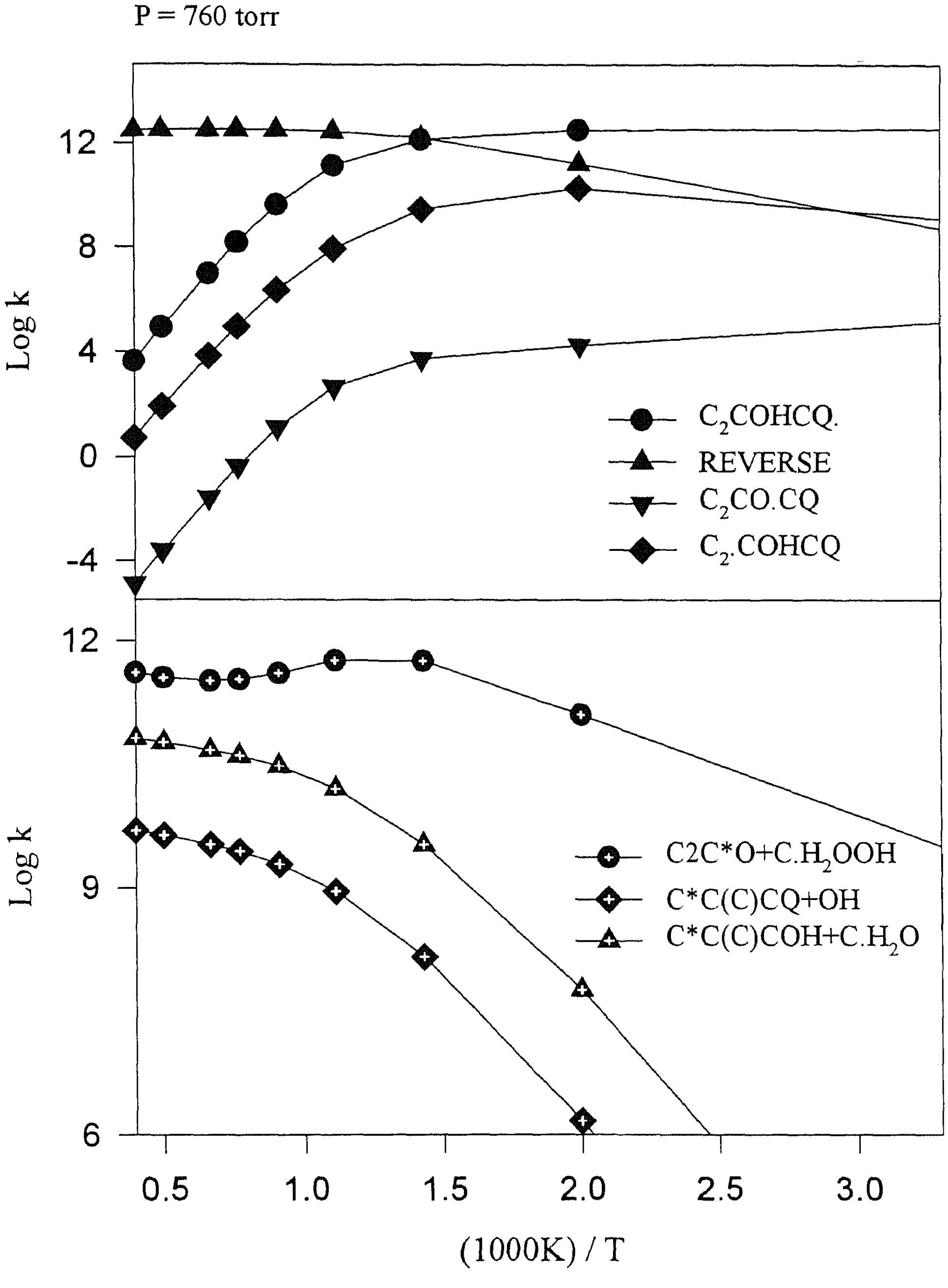

Figure 2B.12 Calculated rate constants at different temperature and 760 torr for chemically activated reactions: $C_3{\cdot}COH + O_2 \Rightarrow [C_2OHCQ{\cdot}]^* \Rightarrow$ products.

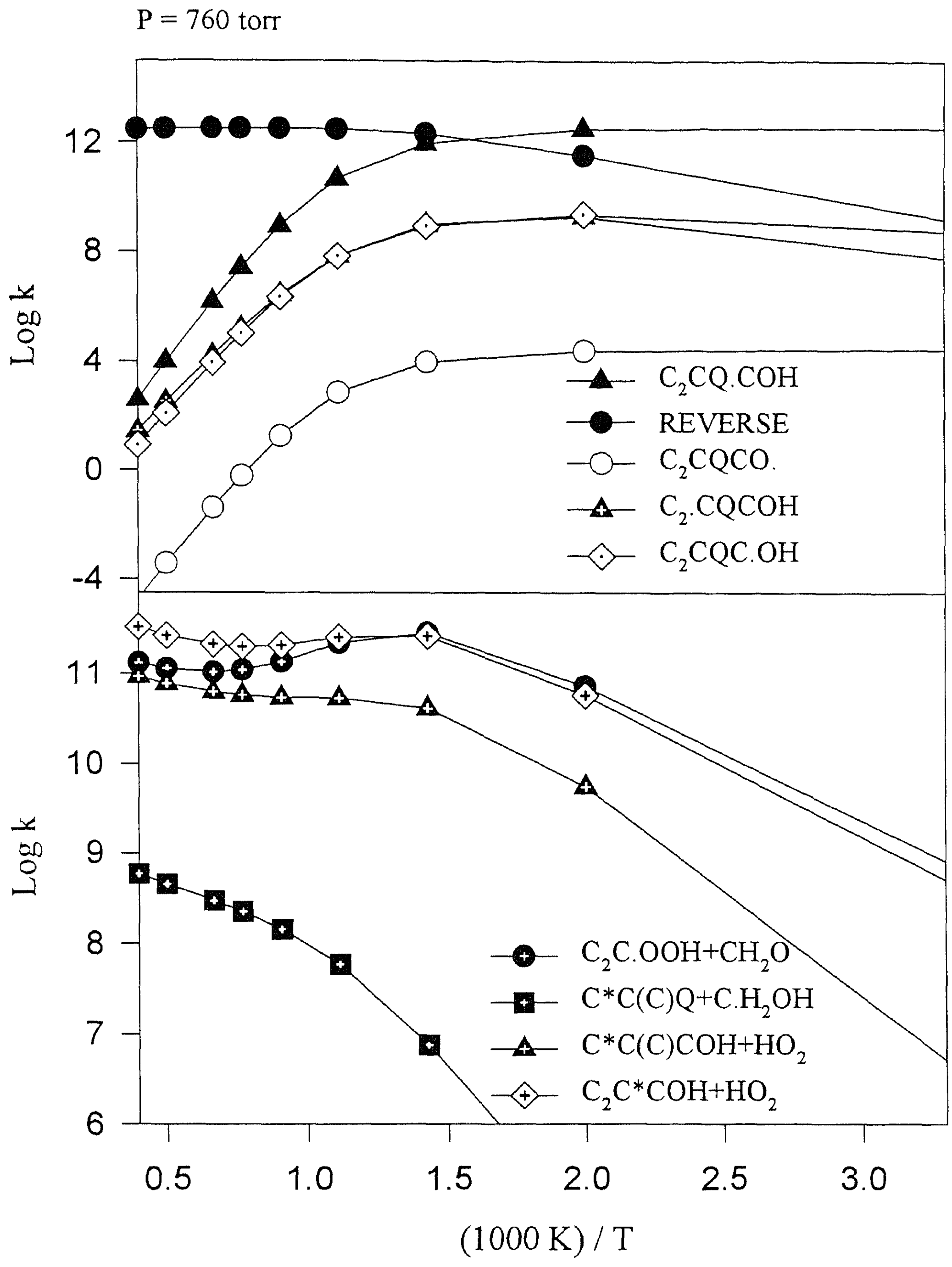

Figure 2B.13 Calculated rate constants at different temperature and 760 torr for chemically activated reactions: $C_2C{\cdot}COH + O_2$ => $[C_2CQ{\cdot}COH]^*$ => products.

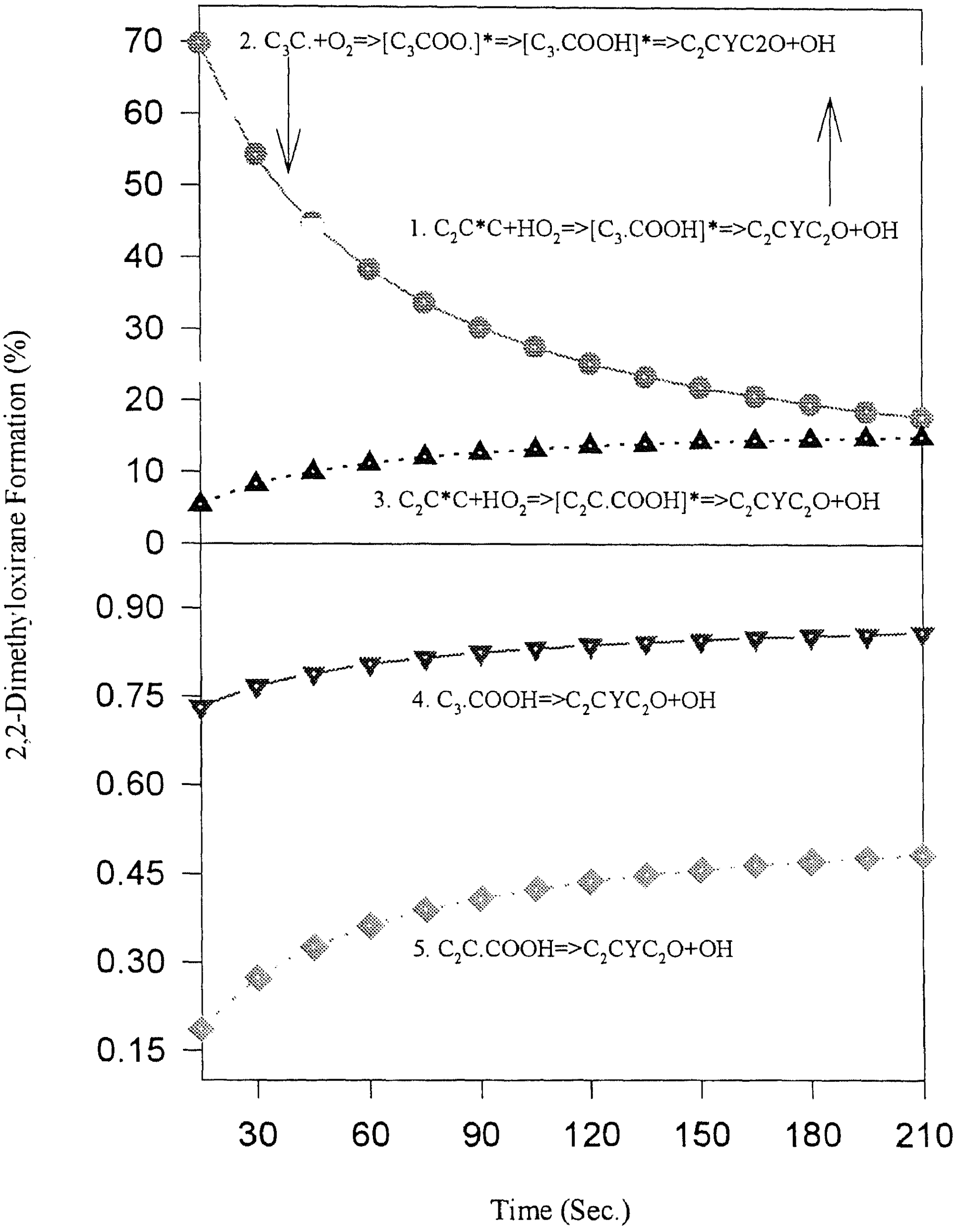

Figure 2B.14 Relative contribution of specific reaction paths to 2,2-dimethyloxirane formation at 773K and 60 torr.

APPENDIX 3A

TABLES IN THE THERMOCHEMICAL KINETIC ANALYSIS ON THE REACTIONS OF ALLYLIC ISOBUTENYL RADICAL WITH O_2: AN ELEMENTARY REACTION MECHANISM FOR ISOBUTENE OXIDATION

Table 3A.1a Total Energies, Zero-Point Vibrational Energies (ZPVE, unscaled) And Thermal Corrections to Enthalpies ($H_{thermal}$) Based on MP2(full)/6-31g(d) Geometry

	MP2(full)/6-31g(d)	MP4(full)/6-31g(d,p)	CBS-4	CBS-q	ZPVE [a]	$H_{thermal}$ [b].
	//MP2(full)/6-31g(d) (0 K in Hartree)			(in Hartree)		(in kcal/mole)
OH	-75.5232063	-75.5496631	-75.6855787	-75.6656062	0.0085200	2.07
O_2	-149.9543197	-149.9690146	-150.2486844	-150.1886013	0.0032180	2.08
C_2·C=C	-155.9975739	-156.1241910	-156.3117742	-156.3108738	0.0965490	3.87
C=C(C)CCOO·	-305.9843357	-306.1289445	-306.5075572	-306.5297530	0.1111330	4.91
C=C(C·)CCOOH	-305.9692885	-306.1136883	-306.5080257	-306.5241740	0.1051600	4.92
CY(C·CCOO)	-305.9897145	-306.1281088	-306.5076315	-306.5244330	0.1080340	4.52
C_2·Y(CCOO)	-305.9653543	-306.0950638	-306.4789331	-306.5007222	0.1059580	4.73
C=(C)COOC·	-305.9627393	-306.1033664	-306.4891129	-306.5083455	0.1044360	5.22
C·OOH	-189.6450008	-189.7099425	-189.9847751	-189.9822373	0.0418930	3.21
C=C=C	-116.2485221	-116.3287995	-116.4492943	-116.4733126	0.0563250	2.96
C=Y(CCOC)	-230.4557534	-230.5735122	-230.8321433	-230.8677875	0.0930530	3.64
C=C(C)C=O	-230.5073408	-230.6256125	-230.8776803	-230.9161439	0.0914170	4.14
TS1	-305.9269172	-306.0749718	-306.4896278	-306.4955498	0.1055970	4.95
TS2	-305.9004963	-306.0484941	-306.4472297	-306.4674437	0.1050600	4.67
TS3	-305.9272923	-306.0747215	-306.4720526	-306.4928868	0.103798	4.16
TS4	-305.8661903	-306.0146123	-306.4265353	-306.4475823	0.103157	5.38
TS5	-305.8867488	-306.0392506	-306.4405368	-306.4617081	0.1071070	4.83
TS6	-305.9224260	-306.0698360	-306.4618599	-306.4818575	0.1077110	4.38
TS7	-305.9133756	-306.0571896	-306.4548455	-306.4727446	0.1065940	4.37
TS8	-305.9032901	-306.0564589	-306.4586297	-306.4726205	0.103944	4.64
TS9	-305.9241391	-306.0720794	-306.4634331	-306.4827719	0.1079770	4.26
TS10	-306.4930034		-307.0176902	-307.0783845	0.110347	5.54

Table 3A.1b Total Energies, Zero-Point Vibrational Energies (ZPVE, unscaled) And Thermal Corrections to Enthalpies ($H_{thermal}$) Based on B3LYP/6-31g(d) Geometry

	MP2(full)/6-31g(d)	MP4(full)/6-31g(d,p)	CBS-4	CBS-q	ZPVE [a]	$H_{thermal}$ [b].
	//MP2(full)/6-31g(d) (0 K in Hartree)			(in Hartree)		(in kcal/mole)
OH	-75.7234543	-75.7654940	-75.6856046	-75.6656518	0.0083060	2.07
O_2	-150.3200379	-150.3792854	-150.2499238	-150.1894687	0.0037790	2.08
C_2·C=C	-156.5772530	-156.6356096	-156.3124918	-156.3117605	0.0943890	3.94
C=C(C)CCOO·	-306.9293266	-307.0443548	-306.5117148	-306.5352796	0.1051800	5.01
CY(C·CCOO)	-306.9239203	-307.0361847	-306.5093648	-306.5261640	0.1051620	4.66
C_2·Y(CCOO)	-306.8941809	-307.0069888	-306.4850343	-306.5032407	0.1035240	4.81
C=C(C·)CCOOH	-306.9129603	-307.0360513	-306.5086455	-306.5247914	0.1031790	5.01
C=(C)COOC·	-306.8991391	-307.0166137	-306.4880397	-306.5073736	0.1012380	5.10
CY(C_2O)CO·	-306.9684759	-307.0836231	-306.5609202	-306.5766734	0.1046030	4.64
C·OOH	-190.1817231	-190.2668064	-189.9856582	-189.9828907	0.0404460	3.34
C=C=C	-116.6576755	-116.7037789	-116.4495647	-116.4735384	0.0554790	2.95
C=Y(CCOC)	-231.1847129	-231.2706597	-230.8323142	-230.8679382	0.0914480	3.62
C=C(C)C=O	-231.2335248	-231.3207250	-230.8779444	-230.9163186	0.0900240	4.17
C=C(C·)CO· (singlet)	-231.1156204		-231.0246530	-231.0306430	0.0849770	3.76
C=C(C·)CO· (triplet)	-231.1171747		-231.0254140	-231.0321800	0.0849770	4.25
TS1	-306.9009817	-307.0163989	-306.4940383	-306.4806888	0.1007720	5.34
TS2	-306.8590108	-306.9775092	-306.4504668	-306.4748138	0.0986740	4.88
TS3	-306.8850734	-307.0035274	-306.4771657	-306.4965087	0.099803	4.23
TS4	-306.8282664	-306.9557059	-306.4287835	-306.4503604	0.097714	5.88
TS5	-306.8599891	-306.9853313	-306.4436928	-306.4641314	0.1007730	5.05
TS6	-306.8811393	-306.9949396	-306.4656203	-306.4857780	0.1028710	4.62
TS7	-306.8674006	-306.9820584	-306.4538930	-306.4746787	0.1008750	4.69
TS8	-306.8735957	-306.9868416	-306.4548531	-306.4717148	0.1026050	4.50
TS9	-306.8848599	-306.9994651	-306.4668307	-306.4861556	0.1037450	4.44
TS10	-307.4821547	-307.6036883	-307.0224450	-307.0815849	0.1069	5.77
TS11	-306.8882338	-307.0101781	-306.4752159	-306.5026421	0.0979440	4.77
TS12	-231.1171769	-231.2042921	-230.7075770	-230.7630097	0.0833265	4.26
TS13	-231.1027288	-231.1928672	-230.7195225	-230.7697227	0.0832235	4.15

a. Unscaled zero-point vibrational energies in Hartree. In the calculation of reaction enthalpies, ZPVE is scaled by 0.9661 and 0.9806 for MP2(full)/6-31g(d) and B3LYP/6-31g(d) levels, respectively.

b. Thermal corr. in kcal/mole: Thermal corrections are calculated as follows for T=298.15 K: $H°_T - H°_0 = H_{trans}(T) + H_{rot}(T) + \Delta H_{vib}(T) + RT$; $H_{trans}(T) = (3/2)RT$, $H_{rot}(T) = (3/2)RT$, $\Delta H_{vib}(T) = N_A h \Sigma \nu_i/(\exp(h\nu_i/kT)-1)$, where N_A is the Avogadro constant, h is the Plant constant, k is the Boltzman constant, and ν_i is vibrational frequencies.

Table 3A.2 Total energy (at 298K) Differences Between TS's and Reactants, Intermediates and Products

	CBS-4[a]	CBS-q	MP2(full) /6-31g(d)	MP4(full) /6-31g(d)	CBS-4	CBS-q	B3LYP /6-31g(d)	B3LYP /6-311+g(3df,2p)
	//MP2(full)/6-31g(d)				// B3LYP /6-31g(d)			
C_2·C=C+O_2 ⇒ TS1	-4.78	1.47	18.21	13.98	-6.0	12.22	-1.39	-0.01
C=C(C)COO· ⇒ TS1	11.30	21.51	32.72	30.56	11.42	34.59	15.41	15.16
C=C(C)COO· ⇒ TS2	37.62	38.86	48.69	46.56	38.30	37.81	39.99	37.81
C=C(C)COO· ⇒ TS3	21.54	22.39	30.61	28.84	20.90	23.55	23.69	21.54
C=C(C·)CQ ⇒ TS3	21.82	18.88	24.77	22.87	18.98	16.97	14.64	17.55
C=C(C·)CQ ⇒ TS4	51.59	48.52	63.94	61.41	50.98	47.57	50.65	47.92
C=C=C+C·OOH ⇒ TS4	3.93	4.21	19.35	17.34	3.63	3.40	7.67	10.02
C=C(C·)CQ ⇒ TS5	42.26	39.11	52.88	47.80	40.79	38.10	31.79	30.38
C=Y(CCOC)+OH ⇒ TS5	47.55	44.10	60.34	55.14	45.93	42.94	30.21	31.87
C=C(C)COO· ⇒ TS6	28.15	29.53	36.25	34.50	28.53	30.67	28.43	29.20
C_2·Y(CCOO) ⇒ TS6	10.37	11.50	27.66	16.55	11.99	10.77	7.59	6.97
C_2·Y(CCOO) ⇒ TS7	14.76	17.20	32.65	23.80	19.43	17.81	15.06	13.90
C=C(C)OOC· ⇒ TS7	20.65	21.49	31.43	29.43	21.02	20.11	19.29	21.05
C_2·Y(CCOO) ⇒ TS8	12.66	17.55	37.64	22.92	18.63	19.48	12.05	11.77
CCY(CCO)CO· ⇒ TS8					66.41	65.72	58.16	59.36
C=C(C)COO· ⇒ TS9	27.05	28.84	35.22	33.13	27.60	30.26	26.45	26.72
CY(C·CCOO) ⇒ TS9	27.48	25.89	40.86	34.87	26.47	24.88	23.42	21.95
C_2C=C+O_2 ⇒ TS10	48.20	40.88	64.99		46.53	39.93	37.37	34.80
C_2·C=C+HO_2 ⇒ TS10	2.33	0.28	3.27		-0.33	-0.92	-5.09	-1.75
CY(C·CCOO) ⇒ TS11					21.54	14.87	18.07	11.99
CCY(C_2O)CO· ⇒ TS11					53.91	46.59	46.39	42.12

a. Reaction enthalpies include thermal correction and zero-point energy correction
Unit: in kcal/mole

Table 3A.3a Group Balance Reaction Enthalpies

Reactions	CBS-4	CBS-q	MP2(full) /6-31g(d)	MP4(full) /6-31g(d,p)	CBS-4	CBS-q	B3LYP /6-31g(d)	B3LYP /6-311+g(3df,2p)
	//MP2(full) /6-31g(d)				//B3LYP/6-31g(d)			
C_2·C=C + C=CC ⇔ C_2C=C + C=CC·	-1.38	-1.40	-2.08	-1.75	-1.45	-1.46	-1.72	-1.65
C=C(C)COOH + C=CC + CH_3OH ⇔ C=CCOH + C_2C=C + CH_3OOH	0.59	0.72	0.73	0.72	2.27	2.45	0.89	0.06
C=C(C)COO· + CH_3OOH ⇔ C=C(C)COOH +CH_3OO·	-1.22	-1.06	-2.27	-2.19	-0.44	0.28	-0.42	-0.14
C=C(C·)COOH +C=CC⇔ C=C(C)COOH + C=CC·	-0.61	-0.74	-0.87	-0.37	-2.26	-2.40	-1.12	-1.29
CY(CCOOC) + COCOC + CC ⇔ Y(CCOCO) + COOC + C_3C	3.14	3.63	3.19	3.57	2.37	2.89	2.26	1.57
CY(CCOOC) + CC· ⇔ CY(C·COOC) + CC	-2.30	-2.53	-2.50	-2.87	-2.99	-3.24	-6.08	-5.17
C_2Y(CCOO) + CCOC + CCC + COH ⇔ Y(CCCO) + C_3COH + COOC + CC	-1.30	-0.22	-0.08	0.75	-1.72	-0.77	-0.86	-0.75
C_2Y(CCOO) + CC· ⇔ C_2·Y(CCOO) + CC	6.79	0.36	1.34	6.77	-0.07	-0.91	0.31	0.80
C·OOH + CH_3OH ⇔ COOH + C·OH	-2.43	-2.13	-3.12	-2.87	-2.21	-1.93	-1.75	-1.54
C=C(C)OOC + COOH ⇔ COOC + C=C(C)OOH	0.83	1.03	0.50	0.64	0.32	0.51	-0.57	-0.70
C=C(C)OOC + COC· ⇔ C=C(C)OOC· + COC	2.14	2.01	2.64	2.58	3.14	2.79	2.87	3.06
CY(C_2O)COH + CC ⇔ Y(CCO) + C_3COH	3.44	3.60	4.47	4.73	3.43	3.54	5.92	3.48
CY(C_2O)COH + CH_3O• ⇔ CY(C_2O)CO· + CH_3OH					4.11	3.99	3.06	1.67
C=CY(CCOC) + $_2$CCCOH + $_2$C=CC ⇔ Y(CCCO) + $_2$C=CCOH + C_2C=C + CCC	2.97	3.59	1.00	1.55	3.21	3.81	2.53	1.04
C=C(C)C=O + C=CC ⇔ C_2C=C + C=CC=O	1.26	1.22	1.31	1.27	1.19	1.24	1.09	0.95

Unit: in kcal/mole

Table 3A.3b Enthalpies (at298K) of Reactant, Intermediates, And Products Calculated from Isodesmic Reactions (IR1-IR15)

$\Delta H^{\circ}_{f,298}$	CBS-4	CBS-q	MP2(full) /6-31g(d)	MP4(full) /6-31g(d,p)	CBS-4	CBS-q	B3LYP /6-31g(d)	B3LYP /6-311+g(3df,2p)
(kcal/mole)	//MP2(full)/6-31g(d)				//B3LYP/6-31g(d)			
C_2·C=C	32.54	**32.56**	33.24	32.91	32.61	32.62	32.88	**32.81**
C=C(C)COOH	-24.38	**-24.51**	-24.52	-24.51	-26.06	-26.24	-24.68	**-23.85**
C=C(C)COO·	11.34	**11.06**	12.25	12.18	8.88	7.98	10.24	**10.79**
C=C(C·)COOH	11.19	**11.19**	11.30	10.82	11.16	11.12	11.40	**12.40**
CY(CCOOC)	-33.82	**-34.31**	-33.87	-34.25	-33.05	-33.57	-32.94	**-32.25**
CY(C·COOC)	13.39	**12.66**	13.12	12.37	13.46	12.68	10.48	**12.07**
C_2Y(CCOO)	-19.06	**-20.14**	-20.28	-21.11	-18.64	-19.59	-19.50	**-19.61**
C_2·Y(CCOO)	37.23	**29.73**	30.56	35.16	30.79	29.01	30.31	**30.69**
C·OOH	15.03	**14.73**	15.72	15.47	14.81	14.53	14.35	**14.14**
C=C(C)OOC	-19.94	**-20.14**	-19.61	-19.75	-19.43	-19.62	-18.54	**-18.41**
C=C(C)OOC·	26.79	**26.46**	27.63	27.42	28.29	27.76	28.92	**29.24**
CY(C_2O)COH	-70.17	**-70.33**	-71.20	-71.46	-70.16	-70.27	-72.65	**-70.21**
CY(C_2O)CO·					-13.98	-14.20	-17.51	**-16.46**
C=CY(CCOC)	1.64	**1.02**	3.61	3.06	1.40	0.80	2.08	**3.57**
C=C(C)C=O	-28.39	**-28.35**	-28.44	-28.40	-28.32	-28.37	-28.22	**-28.08**

Table 3A.3c Enthalpy and Bond Dissociation Energy Used in Isodesmic Reaction to Determine $\Delta H°_{f,\,298}$ of Species Studied in This Work

Compound	$\Delta H°_{f,\,298}$ in kcal/mole	source
CC	-20.54	Ref. 43
C_3C	-32.27	Ref. 44
C*CC	4.71	Ref. 44
C_2C*C	-3.8	Ref. 43
C*CCOH	-31.52	Ref. 44
C*C(C)OOH	-19.91	a.
C_3COH	-74.69	Ref. 45
COOH	-31.8	Ref. 46
CCCOH	-61.85	Ref. 43
COOC	-31.00	Ref. 46
CCOC	-51.74	Ref. 45
COCOC	-83.27	Ref. 45
C=CC=O	-18.61	b.
Y(CCO)	-12.58	Ref. 47
Y(CCCO)	-19.24	Ref. 45
Y(CCOCO)	-71.22	Ref. 45

Compound	$DH_f°_{298}$ in kcal/mole	source
CC-H	101.6	Ref. 48
C=CC-H	87.06	Ref. 48
COO-H	86.6	Ref. 46
CH_3O-H	104.8	Ref. 46
H-CH_2OH	96.5	Ref. 48
COC-H	96.69	c.

a. Based on CBS-q//B3LYP/6-31g(d) calculation
b. Average value of ref. 43, ref. 44 and ref. 49
c. Based on G2 and CBSQ calculations

Table 3A.4 Thermodynamic Properties

SPECIES	$\Delta H^\circ_{f,298}$	S°_{298}	Cp_{300}	Cp_{400}	Cp_{500}	Cp_{600}	Cp_{800}	Cp_{1000}	Cp_{1500}
N_2	0	45.7	6.65	6.86	6.99	7.1	7.31	7.61	7.98
O	59.52	38.4	5	5	5	5	5	5	5
O_2	0	49	6.82	7.15	7.36	7.51	7.82	8.24	8.69
OH	9.5	43.8	6.79	6.86	6.93	7	7.14	7.28	7.61
CH_2O	-26	50.92	8.48	9.49	10.51	11.51	13.33	14.82	16.98
Using THERM Group Additivity									
C*C*C	45.92	58.31	14.19	17.22	19.8	21.99	25.46	28.02	32.03
CC·C*O	-4.7	70.37	18.07	21.88	25.19	28.06	32.66	36.06	41.08
C$_2$·C*O	-9.26	72.5	18.29	22.29	25.76	28.75	33.51	36.93	41.75
CCYC·CO	24.48	72.61	15.77	20.22	24.03	27.29	32.38	35.96	40.98
C*C(C)CO.	11.52	80.05	23.92	29.37	34.05	37.95	44.03	48.55	55.62
CC(CO·)CO	-35.04	90.22	25.71	31.8	37.01	41.44	48.37	53.35	60.64
CCYCC·OOC	9.02	77.14	23.78	31.27	37.4	42.41	49.81	54.82	62.17
C*C(C)C·Q	9.12	88.48	28.7	34.38	39.22	43.34	49.77	54.38	61.06
DIC$_2$·C*C	3.28	104.51	40.98	51.42	60.39	68.07	80.26	89.21	102.88
Using CBS-q//MP2(full)/6-31G(d) Calculations									
C·H$_2$OOH	14.73	68.26^a	16.57	18.39	19.95	21.27	23.36	24.86	27.04
C$_2$.C*C	32.56	70.99^a	20.96	26.09	30.52	34.22	40.07	44.43	51.22
C*C(C)CQ.	11.06	89.72	25.26	30.42	35.17	39.27	45.8	50.78	58.76
C*C(C.)CQ	11.19	90.07	26.72	33.27	38.79	43.22	49.64	54.07	60.8
CCYC.COOC	12.66	78.38	23.71	30.14	35.9	40.73	48.11	53.42	61.47
C$_2$.CYCCOO	29.73	79.36	25.03	31.53	37.13	41.71	48.54	53.40	60.87
C*CYCCOC	1.02	69.51	18.66	24.29	29.35	33.59	40.06	44.71	51.79
C*CICC*O	-28.22	75.91^a	21.55	26.46	30.84	34.59	40.51	44.84	51.3
C*CICOOC.	26.46	95.07^a	29.09	34.87	39.37	43.28	50	54.82	
C=C(C.)CO.(singlet)	44.94	77.22^b	23.15	28.46	32.83	36.38	41.77	45.71	51.86
C=C(C.)CO.(triplet)	43.91	79.11^b	23.11	28.49	32.88	36.44	41.84	45.76	51.89
TS1	34.03	90.96	25.13	30.15	34.74	38.72	45.03	49.82	57.43
TS2	49.92	85.16	24.28	29.86	34.93	39.27	46.08	51.1	58.82
TS3	31.76	78.39	23.01	29.68	35.55	40.43	47.81	53.03	60.85
TS4	62.17	96.19	29.54	35.14	39.85	43.64	49.23	53.2	59.39
TS5	52.46	83.44	25.31	31.15	36.15	40.28	46.6	51.31	58.93
TS6	40.91	78.4	23.29	28.98	34.24	38.77	45.86	51.06	59.14
TS7	47.44	78.29	24.19	30.09	35.28	39.65	46.43	51.42	59.26
TS8	47.28	79.92	25.32	31.05	36.14	40.43	47.07	51.95	59.59
TS9	39.23	77.66	22.41	28.35	33.83	38.51	45.77	51.05	59.18
TS10	36.71	96.11	26.22	32.23	37.63	42.16	48.95	53.59	60.16
Using B3LYP/6-31G(3df,2p) //B3LYP/6-31G* Calculations									
C·H$_2$OOH	14.14	68.26^a	16.57	18.39	19.95	21.27	23.36	24.86	27.04
C$_2$.C*C	32.81	70.99^a	20.96	26.09	30.52	34.22	40.07	44.43	51.22
C*C(C)CQ.	10.79	90.11	25.99	31.41	36.34	40.56	47.19	52.12	59.76
C*C(C.)CQ	12.4	90.33	27.21	33.78	39.27	43.66	50.05	54.45	61.08
CCYC.COOC	12.07	79.44	24.18	30.71	36.5	41.35	48.72	53.99	61.91
C$_2$.CYCCOO	30.69	79.60	25.45	32.09	37.73	42.30	49.09	53.91	61.25
C*CYCCOC	3.57	69.02	18.84	24.57	29.68	33.94	40.42	45.06	52.06
C*CICC*O	-28.08	75.91^a	21.55	26.46	30.84	34.59	40.51	44.84	51.3
CCY(C$_2$O)CO.	-16.46	86.14^a	25.42	32.21	38.41	42.71	49.74	54.51	
C*CICOOC.	29.24	95.07^a	29.09	34.87	39.37	43.28	50	54.82	
C=C(C.)CO.(singlet)	45.65	77.22	23.15	28.46	32.83	36.38	41.77	45.71	51.86
C=C(C.)CO.(triplet)	44.62	79.11	23.11	28.49	32.88	36.44	41.84	45.76	51.89
TS1	32.81	92.67	26.8	31.88	36.38	40.21	46.25	50.81	58.05
TS2	48.6	86.3	25.87	31.91	37.12	41.43	47.96	52.65	59.77
TS3	31.14	78.22	24.08	31.07	37.01	41.84	49	54	61.45
TS4	65.16	92.96	27.7	33.39	38.24	42.18	48	52.15	58.68
TS5	43.86	84.54	26.92	32.87	37.89	41.98	48.19	52.72	59.91
TS6	38.83	79.39	24.77	30.71	35.97	40.38	47.18	52.14	59.81
TS7	47.44	79.93	26.25	32.27	37.38	41.57	47.98	52.68	60.03

Table 3A.4 (Continued)

SPECIES	$\Delta H^\circ_{f,298}$	S°_{298}	Cp_{300}	Cp_{400}	Cp_{500}	Cp_{600}	Cp_{800}	Cp_{1000}	Cp_{1500}
TS8	41.97	78.46	24.85	30.92	36.21	40.61	47.36	52.28	59.88
TS9	35.77	78.41	23.56	29.74	35.24	39.83	46.88	51.98	59.78
TS10	36.13	96.87	27.64	33.72	39.04	43.42	49.93	54.37	60.64
TS11	28.54	80.42	24.94	30.73	36.09	40.72	47.92	53.08	60.70
TS12	52.06	73.99	21.64	26.64	30.97	34.58	40.15	44.25	50.61
TS13	47.37	70.54	19.71	25.22	29.94	33.81	39.67	43.9	50.42

a. S & Cp(T) from THERM[43]

b. S & Cp(T) from B3LYP/6-31G(3df,2p)//B3LYP/6-31G* Calculations

Table 3A.5a Structures and Frequencies for Important Intermediates and Products of C=C(C)C· + O_2 Reaction System Calculated at MP2(full)/6-31g(d) and B3LYP/6-31g(d)

Molecule	Bond Length			Bond Angle			Dihedral Angle			Frequencies B3LYP / 6-31g*			Frequencies MP2 / 6-31g*			Moments of inertia	
		B3LYP	MP2		B3LYP	MP2		B3LYP	MP2							B3LYP	MP2
C_2·C=C 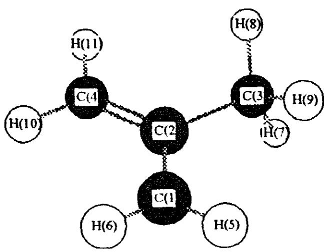 	r21	1.3901	1.3794	a321	119.29	119.41	d4213	178.96	178.56	*21.1*[a]	974.9	1512.5	*23.2*	1004.8	1557.2	182.1	179.2
	r32	1.5194	1.5117	a421	121.42	121.17	d5123	1.65	1.90	407.9	1030.6	1548.5	417.6	1026.4	1604.9	205.5	203.5
	r42	1.3901	1.3794	a512	121.73	121.82	d6123	181.73	181.77	430.7	1053.2	3044.7	442.8	1092.6	3111.6	376.3	371.5
	r51	1.0857	1.0834	a612	121.13	121.09	d7321	89.49	89.29	481.9	1061.7	3107.0	495.8	1104.1	3195.2		
	r61	1.0862	1.0839	a732	110.84	110.66	d8321	209.09	209.02	547.3	1345.1	3129.0	578.6	1307.7	3208.9		
	r73	1.0973	1.0940	a832	111.45	111.14	d9321	329.90	329.57	556.5	1381.5	3155.7	592.0	1437.1	3225.7		
	r83	1.0948	1.0923	a932	111.45	111.14	d10421	359.31	359.67	760.9	1429.2	3163.0	787.2	1483.2	3233.4		
	r93	1.0948	1.0923	a1042	121.13	121.09	d11421	179.39	179.54	791.7	1497.1	3253.1	810.0	1534.3	3329.2		
	r104	1.0862	1.0839	a1142	121.73	121.82				853.2	1507.7	3255.2	888.4	1557.1	3331.0		
	r114	1.0857	1.0834														
C=C(C)COO· 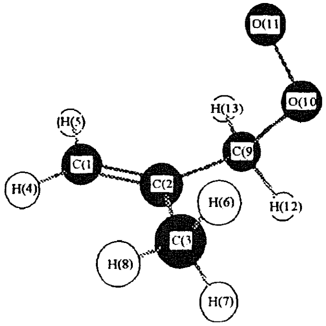 	r21	1.3360	1.3239	a321	123.59	123.99	d4123	359.09	358.96	*52.9*	947.0	1497.1	*53.0*	1000.1	1535.0	315.1	315.2
	r32	1.5072	1.5004	a412	121.59	121.63	d5123	179.10	178.91	*89.2*	989.8	1510.6	*99.0*	1012.2	1544.8	726.5	704.7
	r41	1.0870	1.0857	a512	121.82	121.79	d6321	238.62	239.48	*182.2*	999.1	1526.4	*189.3*	1038.2	1560.5	836.4	804.4
	r51	1.0867	1.0855	a632	110.78	110.43	d7321	120.11	120.78	235.5	1074.3	1740.0	246.2	1113.4	2969.6		
	r63	1.0967	1.0936	a732	111.16	110.87	d8321	359.25	0.03	390.1	1098.9	3038.8	403.7	1141.3	3102.7		
	r73	1.0987	1.0956	a832	111.41	111.07	d9213	179.35	179.00	420.6	1166.2	3071.4	430.2	1234.7	3125.4		
	r83	1.0936	1.0919	a921	120.06	119.99	d10921	121.27	124.83	448.5	1276.9	3093.3	457.9	1297.3	3182.4		
	r92	1.5037	1.4962	a1092	111.72	111.13	d11109	284.56	288.85	586.0	1319.9	3137.0	609.2	1360.4	3205.0		
	r109	1.4718	1.4666	a11109	111.14	110.11	2	235.64	239.09	721.9	1373.0	3149.0	765.6	1410.4	3211.1		
	r1110	1.3224	1.3149	a1292	112.06	112.09	d12921	0.57	4.04	832.1	1441.7	3164.2	879.1	1471.1	3304.3		
	r129	1.0962	1.0949	a1392	112.62	112.67	d13921			879.0	1473.0	3242.7	942.5	1516.4	3370.1		
	r139	1.0918	1.0917														

Table 3A.5a (Continued)

Molecule	Bond Length			Bond Angle			Dihedral Angle			Frequencies B3LYP / 6-31g*			Frequencies MP2 / 6-31g*			Moments of inertia	
		B3LYP	MP2		B3LYP	MP2		B3LYP	MP2							B3LYP	MP2
C=C(C·)COOH 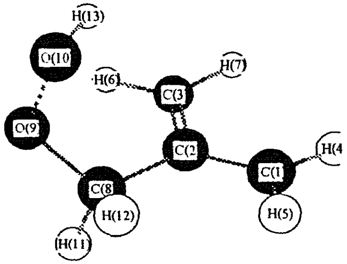	r21	1.3867	1.3742	a321	122.90	122.82	d4123	357.54	357.81	*60.2*	804.5	1427.8	*61.1*	832.8	1465.6	299.2	302.6
	r32	1.3912	1.3822	a412	121.23	121.20	d5123	177.85	177.91	*134.9*	863.8	1489.9	*146.3*	869.0	1528.1	736.1	718.4
	r41	1.0860	1.0840	a512	121.58	121.71	d6321	178.59	178.72	*257.0*	890.2	1511.2	*264.5*	905.8	1530.8	805.7	779.1
	r51	1.0857	1.0834	a632	121.14	121.26	d7321	359.26	359.28	319.6	986.8	1550.8	320.9	1004.6	1597.9		
	r63	1.0851	1.0830	a732	121.06	121.04	d8213	178.98	178.79	392.4	1016.1	3047.4	407.1	1038.6	3107.1		
	r73	1.0857	1.0837	a821	118.66	119.00	d9821	145.06	141.86	420.5	1048.7	3095.7	428.8	1084.8	3171.2		
	r82	1.5254	1.5150	a982	113.57	112.62	d10982	290.67	291.96	459.9	1076.5	3167.4	467.2	1093.5	3228.2		
	r98	1.4218	1.4242	a1098	107.21	105.62	d11821	259.94	256.63	555.0	1289.0	3175.0	589.0	1276.1	3235.7		
	r109	1.4523	1.4641	a1182	110.54	110.82	d12821	20.47	18.11	571.4	1335.4	3257.9	601.3	1324.9	3331.4		
	r118	1.0980	1.0960	a1282	110.99	111.15	d13109	89.82	89.72	604.1	1377.4	3266.4	624.9	1395.3	3338.6		
	r128	1.0964	1.0948	a13109	100.67	99.60	8			776.1	1403.6	3657.9	802.6	1407.1	3679.1		
	r1310	0.9767	0.9795														
C_2·CYCCOC 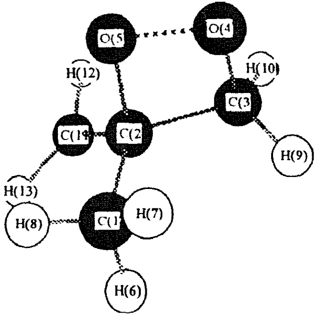	r21	1.5232	1.5133	a321	114.44	113.85	d4321	264.31	269.62	*133.3*	892.5	1485.7	*140.0*	935.1	1519.8	327.5	326.4
	r32	1.5409	1.5222	a432	90.31	89.99	d5432	345.92	341.00	*172.8*	938.3	1516.2	*181.2*	965.9	1548.8	528.2	520.8
	r43	1.4401	1.4495	a543	89.90	88.10	d6123	281.62	281.80	247.7	966.1	1522.8	272.5	986.3	1556.2	591.7	584.8
	r54	1.4925	1.4866	a612	110.59	110.59	d7123	42.07	42.30	304.1	1000.1	1543.8	313.6	1036.7	1570.5		
	r61	1.0969	1.0947	a712	110.15	109.42	d8123	161.75	161.68	349.1	1037.8	3042.6	358.5	1044.2	3105.1		
	r71	1.0936	1.0916	a812	110.26	109.87	d9321	19.44	24.17	393.6	1124.1	3053.7	401.5	1168.7	3108.7		
	r81	1.0950	1.0928	a932	117.10	118.01	d10321	150.37	156.53	436.5	1165.7	3104.1	450.3	1184.4	3181.7		
	r93	1.0956	1.0940	a1032	113.85	113.46	d11213	140.23	140.37	580.4	1265.0	3122.6	533.6	1310.6	3200.6		
	r103	1.0973	1.0955	a1121	114.17	114.31	d12112	177.63	175.72	663.7	1310.0	3145.3	675.2	1348.4	3221.0		
	r112	1.4736	1.4743	a12112	119.62	119.51	1	2.93	1.42	829.5	1350.6	3173.4	843.8	1393.4	3240.3		
	r1211	1.0851	1.0824	a13112	121.57	121.54	d13112			858.3	1434.1	3278.2	896.2	1460.6	3357.1		
	r1311	1.0850	1.0822				1										

Table 3A.5a (Continued)

Molecule	Bond Length			Bond Angle			Dihedral Angle			Frequencies B3LYP / 6-31g*			Frequencies MP2 / 6-31g*			Moments of inertia	
		B3LYP	MP2		B3LYP	MP2		B3LYP	MP2							B3LYP	MP2
CCYC·COOC	r21	1.4966	1.4930	a312	126.33	124.53	d4123	163.96	154.31	***82.1***	971.1	1506.3	***91.2***	992.6	1538.7	254.5	255.5
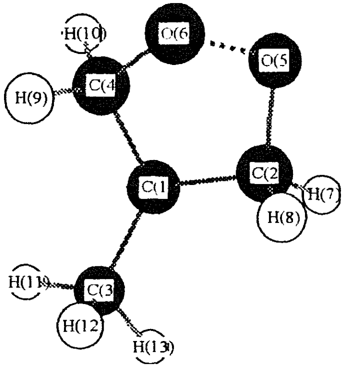	r31	1.4871	1.4859	a412	105.25	104.78	d5213	179.83	188.00	***102.0***	993.3	1508.0	***143.6***	1015.2	1543.7	575.9	568.9
	r41	1.4993	1.4969	a521	104.29	104.11	d6412	348.87	347.58	219.6	1016.1	1514.4	258.2	1039.9	1547.9	775.8	761.5
	r52	1.4284	1.4313	a641	104.65	104.45	d7213	64.52	73.01	290.1	1065.5	1516.2	297.6	1099.2	1551.4		
	r64	1.4312	1.4360	a721	114.27	114.42	d8213	300.27	307.77	298.1	1184.7	2936.9	320.0	1208.3	3032.6		
	r72	1.0986	1.0959	a821	112.61	112.31	d9412	233.52	232.82	569.7	1209.2	2957.9	585.0	1237.4	3054.3		
	r82	1.1070	1.1030	a941	114.00	113.85	d10412	109.43	107.52	691.2	1266.8	2966.3	687.8	1295.7	3061.0		
	r94	1.0992	1.0964	a1041	112.61	112.74	d11312	200.29	194.78	823.2	1284.3	3046.6	818.2	1322.5	3138.8		
	r104	1.1050	1.1001	a1131	111.58	111.32	d12312	80.66	75.03	837.6	1316.9	3054.4	845.3	1340.9	3142.1		
	r113	1.0970	1.0937	a1231	112.27	111.50	d13312	320.84	315.20	953.5	1410.8	3061.4	977.6	1438.5	3149.2		
	r123	1.1052	1.1009	a1331	111.67	111.32				962.2	1440.3	3104.1	984.0	1470.3	3193.7		
	r133	1.0967	1.0937														
C=C(C)OOC·	r21	1.3322	1.3345	a321	126.56	127.03	d4213	180.22	180.19	***42.0***	829.9	1456.3	***68.6***	817.1	1487.7	234.5	240.8
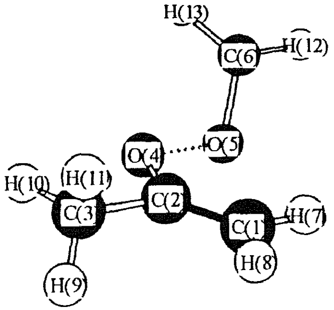	r32	1.5115	1.4959	a421	126.07	125.93	d5421	2.17	1.69	***52.1***	840.1	1512.6	***95.6***	872.6	1532.9	766.5	741.6
	r42	1.3831	1.3884	a542	110.97	110.17	d6542	243.53	254.92	***77.3***	885.2	1516.0	***163.0***	926.9	1555.8	923.3	885.0
	r54	1.4645	1.4631	a654	107.97	106.70	d7123	179.47	179.34	***89.2***	958.7	1746.0	***135.9***	981.1	1777.2		
	r65	1.3611	1.3743	a712	122.47	122.52	d8123	359.93	359.90	302.3	1022.0	3065.5	332.8	1051.0	3114.6		
	r71	1.0810	1.0794	a812	119.09	118.79	d9321	300.07	240.12	372.8	1059.7	3130.5	385.4	1108.6	3197.1		
	r81	1.0840	1.0819	a932	110.78	110.54	d10321	180.17	120.58	463.0	1140.2	3143.6	462.7	1169.9	3209.8		
	r93	1.0946	1.0932	a1032	110.60	110.68	d11321	60.23	0.35	510.5	1201.9	3145.9	506.5	1225.3	3224.1		
	r103	1.0934	1.0934	a1132	110.73	109.73	d12654	174.82	183.76	523.7	1283.4	3203.5	547.0	1312.2	3258.8		
	r113	1.0946	1.0910	a1265	110.29	109.45	d13654	320.96	326.25	683.1	1429.7	3281.9	754.9	1451.8	3356.9		
	r126	1.0849	1.0831	a1365	117.50	116.46				741.7	1448.3	3297.4	814.6	1480.3	3363.3		
	r136	1.0864	1.0832														

Table 3A.5a (Continued)

Molecule	Bond Length			Bond Angle			Dihedral Angle			Frequencies B3LYP / 6-31g*			Frequencies MP2 / 6-31g*			Moments of inertia	
		B3LYP	MP2		B3LYP	MP2		B3LYP	MP2							B3LYP	MP2
CY(C$_2$O)CO·	r21	1.5101	1.5011	a321	121.45	121.18	d4321	104.22	103.80	***90.1***	933.7	1449.9	***95.6***	965.1	1488.0	314.1	313.1
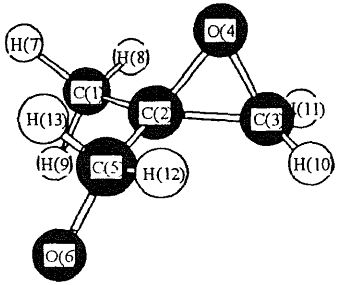	r32	1.4719	1.4646	a432	59.22	59.50	d5213	204.25	203.70	***194.1***	1025.4	1513.7	***207.6***	1045.7	1546.1	611.3	606.8
	r43	1.4366	1.4435	a521	115.99	116.19	d6521	54.69	57.16	238.9	1084.8	1526.5	241.8	1089.6	1560.1	749.0	739.5
	r52	1.5285	1.5115	a652	115.08	113.86	d7123	217.98	216.88	353.6	1094.6	1558.5	366.6	1113.3	1586.1		
	r65	1.3659	1.3848	a712	110.44	110.11	d8123	337.90	336.51	370.4	1139.1	2878.2	380.3	1152.6	3014.3		
	r71	1.0969	1.0944	a812	110.88	110.36	d9123	98.77	97.36	383.9	1165.7	2970.8	393.3	1184.3	3093.4		
	r81	1.0936	1.0917	a912	110.07	110.11	d10321	207.54	207.02	502.4	1169.2	3055.5	514.4	1193.2	3110.7		
	r91	1.0945	1.0927	a1032	120.12	120.02	d11321	0.68	0.42	729.1	1269.4	3103.7	749.0	1343.7	3167.0		
	r103	1.0907	1.0885	a1132	119.50	119.36	d12521	183.93	183.51	774.4	1315.8	3122.2	782.4	1377.0	3199.0		
	r113	1.0901	1.0878	a1252	111.05	111.03	d13521	298.30	300.37	834.7	1382.4	3146.1	865.6	1452.8	3219.6		
	r125	1.1058	1.1001	a1352	108.31	109.56				933.2	1418.3	3187.1	951.1	1462.4	3264.0		
	r135	1.1140	1.1057														
C=C(C)C=O	r21	1.3414	1.3436	a321	125.17	125.23	d4213	180.00	180.00	***121.0***	983.6	1519.0	***146.7***	1001.9	1552.3	210.0	208.6
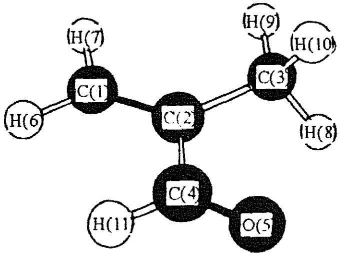	r32	1.5035	1.4970	a421	117.74	117.83	d5421	180.00	179.97	***182.3***	1021.8	1716.0	***172.7***	1022.2	1719.8	411.5	410.6
	r42	1.4832	1.4764	a542	124.08	123.54	d6123	180.00	180.00	262.4	1048.8	1797.8	266.4	1069.8	1761.7	610.4	608.1
	r54	1.2160	1.2273	a612	121.08	121.08	d7123	0.00	0.00	400.7	1088.4	2910.0	402.4	1103.1	2985.0		
	r61	1.0881	1.0869	a712	122.30	122.20	d8321	238.66	238.86	437.5	1340.4	3056.7	427.0	1378.9	3113.0		
	r71	1.0865	1.0855	a832	110.55	110.36	d9321	359.97	0.00	627.2	1414.6	3112.5	633.4	1428.3	3196.2		
	r83	1.0960	1.0933	a932	111.52	111.16	d10321	121.28	121.12	705.7	1440.9	3141.0	715.4	1467.9	3206.0		
	r93	1.0935	1.0920	a1032	110.55	110.36	d11421	0.00	0.03	834.8	1478.0	3160.2	857.1	1501.9	3213.6		
	r103	1.0960	1.0933	a1142	114.91	115.64				969.8	1502.8	3242.3	948.4	1537.0	3299.3		
	r114	1.1129	1.1096														

Table 3A.5a (Continued)

Molecule	Bond Length			Bond Angle			Dihedral Angle			Frequencies B3LYP / 6-31g*			Frequencies MP2 / 6-31g*			Moments of inertia	
																B3LYP	MP2
		B3LYP	MP2		B3LYP	MP2		B3LYP	MP2								
C=Y(CCOC) 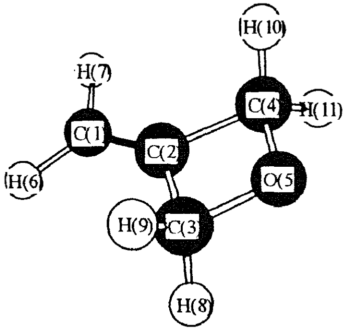	r21	1.3259	1.3295	a321	136.49	136.25	d4213	180.00	180.00	124.1	1006.3	1522.6	102.6	1013.9	1558.1	151.4	151.2
	r32	1.5141	1.5076	a421	136.49	136.25	d5321	180.00	180.00	349.5	1028.0	1550.6	349.8	1046.3	1582.7	385.7	385.1
	r42	1.5141	1.5076	a532	90.54	90.48	d6123	0.00	0.00	391.8	1089.0	1791.9	379.4	1109.7	1798.8	514.0	513.2
	r53	1.4501	1.4550	a612	121.62	121.49	d7123	180.00	180.00	663.6	1143.1	3014.6	677.7	1161.8	3083.5		
	r61	1.0871	1.0854	a712	121.62	121.49	d8321	64.95	65.30	702.1	1147.5	3027.1	708.9	1162.9	3092.0		
	r71	1.0871	1.0854	a832	116.11	116.13	d9321	295.05	294.70	883.1	1240.0	3056.5	893.7	1272.1	3142.4		
	r83	1.0993	1.0969	a932	116.11	116.13	d10421	64.95	65.30	911.7	1308.5	3056.5	901.4	1332.3	3142.6		
	r93	1.0993	1.0969	a1042	116.11	116.13	d11421	295.05	294.70	916.5	1360.9	3160.7	938.5	1376.4	3213.7		
	r104	1.0993	1.0969	a1142	116.11	116.13				983.9	1474.1	3236.9	1006.1	1493.5	3304.3		
	r114	1.0993	1.0969														
C=C(C·)CO· (singlet) 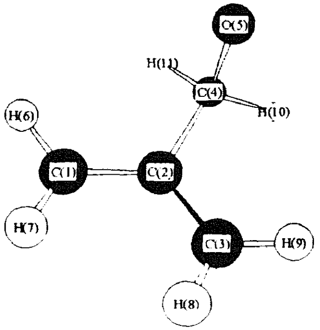	r21	1.3880		a321	123.11		d4213	181.61		*6.4*	817.1	1424.5				216.9	
	r32	1.3866		a421	118.38		d5421	86.31		255.8	882.0	1520.7				441.9	
	r42	1.5225		a542	114.87		d6123	179.55		378.2	989.0	1557.5				581.7	
	r54	1.3694		a612	121.45		d7123	0.24		413.7	1056.0	2908.8					
	r61	1.0857		a712	121.42		d8321	0.49		442.0	1081.9	2933.0					
	r71	1.0863		a832	121.42		d9321	180.83		542.4	1112.9	3164.8					
	r83	1.0863		a932	121.47		d10421	209.86		580.9	1323.1	3171.6					
	r93	1.0857		a1042	110.99		d11421	324.52		632.6	1375.6	3256.3					
	r104	1.1092		a1142	110.59					784.8	1390.6	3258.5					
	r114	1.1102															

Table 3A.5a (Continued)

Molecule	Bond Length			Bond Angle			Dihedral Angle			Frequencies B3LYP / 6-31g*			Frequencies MP2 / 6-31g*	Moments of inertia	
		B3LYP	MP2		B3LYP	MP2		B3LYP	MP2					B3LYP	MP2
C=C(C·)CO· (triplet)	r21	1.3899		a321	123.58		d4213	179.02		*46.7*	809.1	1403.8		191.3	
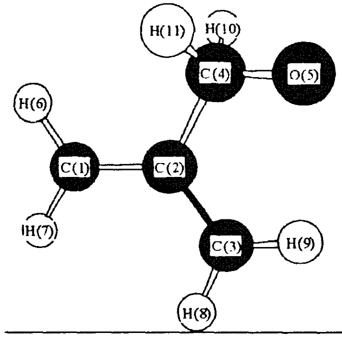	r32	1.3854		a421	117.71		d5421	168.43		281.8	838.4	1509.6		444.9	
	r42	1.5295		a542	117.80		d6123	179.08		396.5	988.5	1546.7		623.0	
	r54	1.3611		a612	121.72		d7123	359.09		406.9	1043.6	2878.4			
	r61	1.0867		a712	121.22		d8321	359.55		529.6	1106.0	2934.7			
	r71	1.0854		a832	120.99		d9321	180.47		553.0	1139.2	3164.7			
	r83	1.0855		a932	120.68		d10421	287.93		573.1	1298.6	3181.1			
	r93	1.0837		a1042	109.28		d11421	40.66		634.2	1362.8	3253.8			
	r104	1.1139		a1142	111.11					756.1	1383.8	3278.9			
	r114	1.1087													

Table 3A.5b Structures and Frequencies for Transition States of C=C(C)C· + O_2 Reaction System Calculated at MP2(full)/6-31g(d) and B3LYP/6-31g(d) Levels

Molecule	Bond Length			Bond Angle			Dihedral Angle			Frequencies B3LYP / 6-31g*			Frequencies MP2 / 6-31g*			Moments of inertia	
		B3LYP	MP2		B3LYP	MP2		B3LYP	MP2							B3LYP	MP2
TS1	r21	1.3755	1.3303	a321	121.01	122.80	d4123	358.01	355.90	(-118.7)	851.1	1516.6	(-862.4)	902.5	1547.6	356.0	335.5
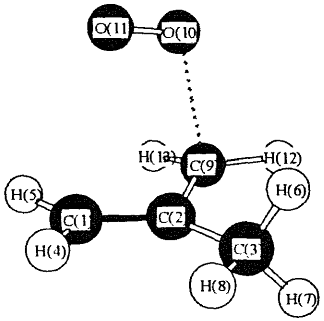	r32	1.5156	1.5050	a412	121.80	122.05	d5123	180.69	178.70	***62.8***	862.2	1520.5	***91.4***	972.3	1566.3	757.6	695.2
	r41	1.0859	1.0847	a512	121.29	121.58	d6321	246.06	249.22	***89.5***	876.6	1544.9	***112.0***	1010.2	1703.8	832.4	773.5
	r51	1.0850	1.0835	a632	110.83	110.42	d7321	126.76	129.78	***104.4***	984.2	1582.7	***156.1***	1038.9	1774.6		
	r63	1.0967	1.0946	a732	111.24	111.21	d8321	6.27	9.21	144.7	1048.1	3049.2	189.4	1061.1	3105.2		
	r73	1.0963	1.0939	a832	111.50	111.03	d9213	188.34	192.53	347.6	1067.9	3104.8	400.7	1113.8	3185.1		
	r83	1.0939	1.0919	a921	119.03	117.45	d10921	70.78	71.43	402.2	1080.7	3132.3	428.5	1134.5	3209.5		
	r92	1.3986	1.4192	a1092	92.80	99.83	d11109	329.51	328.07	439.9	1379.0	3175.6	471.4	1367.8	3225.4		
	r109	2.3636	1.9739	a11109	106.62	112.27	2	174.91	177.54	507.7	1420.1	3181.6	578.4	1465.5	3237.1		
	r1110	1.2350	1.2175	a1292	121.67	120.78	d12921	345.62	332.93	625.7	1448.9	3265.1	764.3	1508.4	3327.8		
	r129	1.0858	1.0850	a1392	120.97	119.31	d13921			662.2	1484.0	3271.3	826.4	1545.9	3330.0		
	r139	1.0842	1.0837														
TS2	r21	1.3488	1.3104	a321	123.22	124.54	d4213	181.41	180.30	(-1857.7)	889.7	1454.2	(-2459.9)	1002.9	1541.8	250.6	251.1
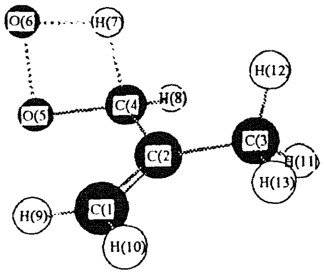	r32	1.5102	1.5021	a421	120.63	120.43	d5421	351.16	359.66	***103.5***	919.8	1510.5	***97.4***	1007.4	1558.4	808.2	773.5
	r42	1.4651	1.4800	a542	118.26	117.46	d6542	119.36	113.90	***130.9***	943.5	1522.2	***147.0***	1061.6	1814.6	946.0	908.0
	r54	1.3910	1.3944	a654	90.35	88.45	d7421	89.81	97.40	139.0	986.1	1648.8	175.4	1080.5	1945.4		
	r65	1.4929	1.4378	a742	113.48	85.05	d8421	208.55	218.86	262.0	1030.6	1928.5	275.3	1136.6	2170.7		
	r74	1.3142	1.294	a842	117.96	118.19	d9123	178.79	179.51	372.3	1084.5	3042.6	386.8	1152.3	3102.1		
	r76	1.329	1.2867	a912	120.86	121.20	d10123	358.25	359.43	451.8	1130.2	3080.1	479.1	1221.4	3154.3		
	r84	1.0966	1.0950	a1012	121.23	121.27	d11321	120.89	121.22	537.1	1182.8	3092.9	547.4	1299.2	3178.1		
	r91	1.0844	1.0830	a1132	111.33	111.11	d12321	240.10	240.54	624.8	1274.1	3138.2	697.9	1414.6	3213.1		
	r101	1.0860	1.0848	a1232	111.29	110.92	d13321	0.35	0.80	690.1	1405.9	3180.0	790.1	1467.6	3237.4		
	r113	1.0975	1.0949	a1332	111.08	110.68				849.8	1433.8	3272.7	926.4	1499.3	3333.8		
	r123	1.0976	1.0949														
	r133	1.0933	1.0915														

Table 3A.5b (Continued)

Molecule	Bond Length			Bond Angle			Dihedral Angle			Frequencies B3LYP / 6-31g*			Frequencies MP2 / 6-31g*			Moments of inertia	
		B3LYP	MP2		B3LYP	MP2		B3LYP	MP2							B3LYP	MP2
TS3 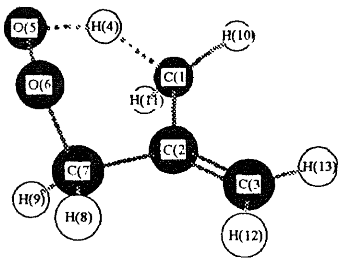	r21	1.4516	1.4749	a321	124.69	124.67	d4123	230.05	219.03	(-1871.5)	905.2	1453.8	(-2334.4)	967.2	1498.9	292.1	281.0
	r32	1.3552	1.3120	a412	95.76	98.28	d5412	315.87	318.73	133.6	912.9	1491.8	104.3	1019.6	1518.8	604.5	600.4
	r41	1.3899	1.3129	a541	146.47	145.99	d6541	51.65	53.67	291.5	992.8	1510.8	301.5	1040.1	1538.0	786.9	793.9
	r54	1.2069	1.2145	a654	101.16	101.45	d7654	306.95	303.74	381.0	996.8	1586.6	388.1	1072.0	1634.9		
	r65	1.4041	1.4074	a765	107.80	106.17	d8765	187.54	187.92	419.0	1010.6	1627.2	415.9	1124.7	1946.5		
	r72	1.514	1.507	a876	105.16	105.59	d9765	306.20	306.98	478.8	1066.5	3055.8	474.1	1136.0	3106.9		
	r76	1.4426	1.4365	a976	109.30	109.36	d10123	351.12	337.46	518.2	1089.0	3106.9	518.0	1207.4	3164.7		
	r87	1.0929	1.0924	a1012	117.61	116.43	d11123	132.67	114.64	611.5	1246.7	3140.9	626.9	1288.0	3197.9		
	r97	1.0971	1.0964	a1112	116.90	115.31	d12321	352.77	357.15	664.8	1263.6	3165.7	692.1	1341.7	3222.8		
	r101	1.0896	1.0890	a1232	121.43	121.91	d13321	174.54	178.38	691.2	1315.6	3196.7	800.0	1345.1	3262.2		
	r111	1.0926	1.0912	a1332	121.64	121.70				872.6	1359.8	3250.6	909.2	1388.9	3309.7		
	r123	1.0865	1.0854														
	r133	1.0865	1.0855														
TS4 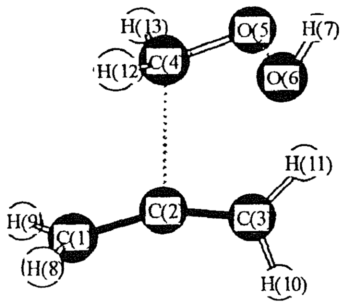	r21	1.3399	1.3227	a321	157.15	159.82	d4213	178.27	179.03	(-438.7)	753.4	1457.7	(-736.5)	821.2	1479.9	288.9	303.1
	r32	1.3152	1.2839	a421	103.96	101.71	d5421	166.14	172.80	***46.2***	802.9	1463.6	***62.3***	858.6	1491.5	889.4	937.4
	r42	2.3339	2.2327	a542	113.81	113.48	d6542	285.15	282.44	***89.0***	847.7	1505.5	***114.9***	961.1	1543.4	1015.8	1059.3
	r54	1.3649	1.3792	a654	107.27	106.00	d7654	215.08	223.97	***140.1***	898.3	1922.1	***169.0***	1011.0	2357.8		
	r65	1.4664	1.4741	a765	98.32	97.69	d8123	98.37	94.63	164.9	912.3	3127.1	226.8	1060.0	3184.8		
	r76	0.9749	0.9780	a812	121.24	120.87	d9123	268.85	266.66	186.5	1030.1	3140.8	292.1	1076.7	3238.2		
	r81	1.0881	1.0830	a912	121.38	120.99	d10321	357.31	359.49	265.0	1038.7	3146.0	318.5	1109.9	3249.6		
	r91	1.0883	1.0832	a1032	119.76	118.62	d11321	178.30	179.89	341.7	1073.5	3214.3	401.8	1132.9	3321.8		
	r103	1.0895	1.0861	a1132	122.95	123.72	d12421	40.74	48.32	368.3	1126.6	3234.5	457.0	1188.7	3329.9		
	r113	1.0852	1.0821	a1242	102.19	103.08	d13421	279.30	286.63	439.0	1213.5	3256.6	473.0	1242.9	3341.6		
	r124	1.0879	1.0859	a1342	96.17	99.16				558.3	1419.5	3708.0	643.7	1405.0	3715.0		
	r134	1.0865	1.0855														

Table 3A.5b (Continued)

Molecule	Bond Length			Bond Angle			Dihedral Angle			Frequencies B3LYP / 6-31g*			Frequencies MP2 / 6-31g*			Moments of inertia	
		B3LYP	MP2		B3LYP	MP2		B3LYP	MP2							B3LYP	MP2
TS5 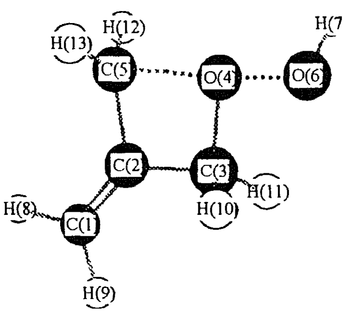 	r21	1.3397	1.3022	a321	129.90	131.29	d4321	220.41	180.52	(-815.4)	880.4	1463.8	(-1568.9)	931.2	1499.8	204.5	188.3
	r32	1.5000	1.4979	a432	93.99	95.53	d5213	197.20	179.88	***98.0***	897.3	1505.7	***79.9***	961.7	1524.9	856.7	815.5
	r43	1.4471	1.4556	a521	128.65	130.48	d6432	179.58	176.93	160.4	928.6	1540.3	128.1	1001.1	1562.9	1000.3	977.4
	r52	1.4625	1.4873	a643	101.14	100.21	d7643	214.84	138.89	179.0	967.1	1706.1	199.5	1037.8	2753.6		
	r54	1.969	1.851	a764	92.73	97.45	d8123	171.36	180.05	234.1	971.8	3034.6	261.9	1053.7	3118.0		
	r64	1.7384	1.5807	a812	121.43	121.61	d9123	350.27	0.10	341.4	985.0	3109.7	415.6	1057.9	3178.3		
	r76	0.9743	0.9734	a912	121.47	121.63	d10321	337.03	295.60	389.3	1064.9	3151.9	453.9	1143.9	3229.4		
	r81	1.0866	1.0851	a1032	115.92	115.48	d11321	106.20	65.08	406.3	1088.3	3166.1	474.6	1196.8	3278.2		
	r91	1.0863	1.0860	a1132	114.79	115.49	d12521	232.64	284.28	614.0	1174.5	3247.0	649.1	1235.3	3306.0		
	r103	1.0943	1.0943	a1252	119.88	119.19	d13521	31.24	75.67	641.7	1286.6	3248.2	723.5	1310.1	3341.3		
	r113	1.0990	1.0943	a1352	121.05	119.29				690.9	1331.9	3729.5	763.8	1363.6	3780.6		
	r125	1.0854	1.0841														
	r135	1.0886	1.0837														
TS6 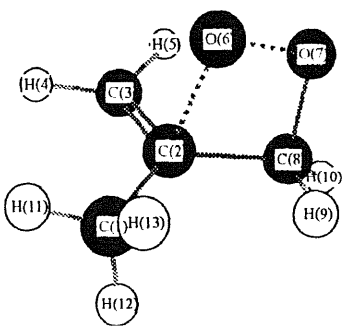 	r21	1.5051	1.4962	a321	120.38	122.06	d4321	18.29	12.62	(-658.5)	858.5	1504.8	(-1060.6)	1000.8	1537.9	330.6	319.4
	r32	1.3939	1.3549	a432	120.83	121.13	d5321	189.16	185.37	***127.4***	974.5	1517.8	***159.2***	1017.7	1554.4	562.3	554.9
	r43	1.0855	1.0834	a532	120.93	120.89	d6213	114.70	110.48	174.4	997.4	1537.1	200.4	1052.0	1578.4	610.3	603.0
	r53	1.0851	1.0829	a621	106.51	107.92	d7621	131.77	136.49	252.9	1022.0	1551.8	266.3	1073.6	1657.5		
	r62	1.8499	1.9002	a762	84.47	82.96	d8762	343.25	337.76	321.8	1049.2	3027.3	323.4	1107.8	3090.6		
	r76	1.4484	1.4177	a876	95.13	94.93	d9876	262.99	271.68	386.3	1070.1	3045.4	400.5	1230.5	3108.7		
	r82	1.534	1.524	a987	111.67	111.46	d10876	141.13	149.19	411.2	1202.0	3093.4	435.3	1320.2	3167.6		
	r87	1.4284	1.4261	a1087	109.84	110.03	d11123	329.56	340.19	517.8	1297.1	3112.9	637.5	1414.7	3196.0		
	r98	1.0992	1.0975	a1112	111.39	111.39	d12123	89.22	100.33	640.5	1387.1	3144.6	686.7	1453.2	3222.1		
	r108	1.0958	1.0944	a1212	110.08	109.78	d13123	208.46	219.09	788.3	1404.5	3174.6	877.5	1489.9	3238.5		
	r111	1.0943	1.0918	a1312	110.39	109.67				850.8	1443.1	3268.6	925.9	1510.7	3344.2		
	r121	1.0985	1.0952														
	r131	1.0937	1.0919														

Table 3A.5b (Continued)

Molecule	Bond Length			Bond Angle			Dihedral Angle			Frequencies B3LYP / 6-31g*			Frequencies MP2 / 6-31g*			Moments of inertia	
		B3LYP	MP2		B3LYP	MP2		B3LYP	MP2							B3LYP	MP2
TS7 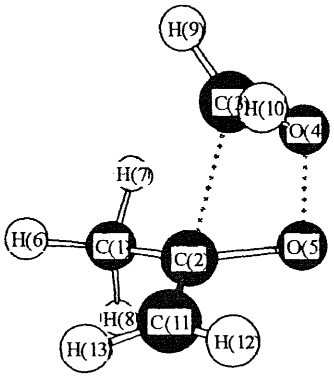	r21	1.5183	1.5054	a321	104.57	103.18	d4321	271.14	274.58	(-874.2)	805.0	1506.1	(-1013.7)	878.6	1536.7	335.2	331.2
	r32	1.9673	2.0153	a432	81.15	77.09	d5213	277.97	282.12	***196.9***	826.6	1511.0	***198.3***	953.4	1560.7	549.6	536.4
	r43	1.3744	1.3997	a521	113.78	113.91	d6123	271.50	268.99	218.6	924.9	1524.3	242.8	992.1	1602.0	618.0	607.5
	r52	1.4340	1.4386	a612	110.70	110.28	d7123	32.68	30.35	250.0	975.6	1558.7	271.5	1060.1	1792.6		
	r61	1.0946	1.0921	a712	110.89	110.89	d8123	151.71	149.38	293.8	1032.9	3059.5	341.2	1070.9	3120.1		
	r71	1.0924	1.0898	a812	109.69	109.10	d9321	23.72	23.00	371.8	1072.4	3088.3	406.5	1101.8	3160.4		
	r81	1.0961	1.0935	a932	118.46	125.70	d10321	156.05	161.39	440.4	1094.8	3125.3	473.4	1205.6	3208.1		
	r93	1.0906	1.0880	a1032	104.67	103.19	d11213	134.19	133.02	467.6	1187.6	3152.5	610.3	1284.8	3233.8		
	r103	1.0915	1.0885	a1121	121.76	123.67	d12112	165.92	166.52	568.2	1235.8	3180.1	626.8	1430.4	3243.8		
	r112	1.3753	1.3482	a12112	120.43	120.67	1	342.50	341.89	648.6	1390.1	3197.0	720.6	1467.0	3290.1		
	r1211	1.0844	1.0823	a13112	121.14	120.78	d13112			665.8	1433.6	3274.8	832.0	1523.9	3348.8		
	r1311	1.0853	1.0829				1										
TS8 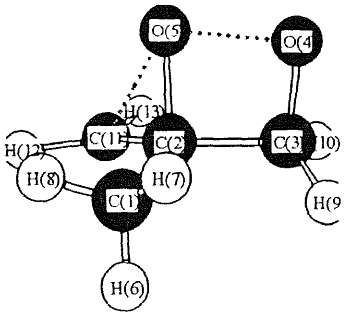	r21	1.5189	1.5146	a321	115.41	113.36	d4321	264.00	272.49	(-809.6)	880.0	1491.7	(-627.7)	931.8	1520.7	338.4	336.5
	r32	1.5332	1.5176	a432	93.79	93.78	d5213	255.47	257.27	***154.9***	940.7	1515.0	***195.7***	970.4	1548.1	511.6	529.6
	r43	1.4291	1.4331	a521	113.26	110.88	d6123	283.93	284.38	237.9	967.5	1523.0	226.5	992.8	1558.6	597.0	592.0
	r52	1.4444	1.4528	a612	110.62	110.68	d7123	43.93	45.01	316.3	1026.9	1542.7	254.9	1038.9	1569.4		
	r54	1.764	1.808	a712	109.56	109.34	d8123	163.46	164.15	346.1	1038.7	3018.0	280.8	1043.8	3098.6		
	r61	1.0966	1.0942	a812	110.67	109.78	d9321	19.84	27.43	376.8	1127.7	3053.7	354.4	1169.7	3110.8		
	r71	1.0939	1.0917	a932	116.50	116.41	d10321	148.00	157.20	404.9	1171.7	3075.1	377.8	1190.2	3168.0		
	r81	1.0949	1.0928	a1032	112.96	113.08	d11213	151.81	140.52	492.7	1284.1	3123.2	454.4	1313.0	3203.6		
	r93	1.0976	1.0954	a1121	116.94	114.22	d12112	21.65	27.40	638.8	1325.5	3142.1	601.2	1343.3	3221.3		
	r103	1.0995	1.0958	a12112	120.71	119.97	1	191.45	190.06	728.9	1369.3	3181.9	615.8	1402.3	3238.6		
	r112	1.4637	1.4791	a13112	120.02	119.64	d13112			815.7	1434.8	3292.3	814.9	1460.9	3355.0		
	r115	2.071	1.808				1										
	r1211	1.0855	1.0827														
	r1311	1.0839	1.0827														

Table 3A.5b (Continued)

Molecule	Bond Length			Bond Angle			Dihedral Angle			Frequencies B3LYP / 6-31g*			Frequencies MP2 / 6-31g*			Moments of inertia	
		B3LYP	MP2		B3LYP	MP2		B3LYP	MP2							B3LYP	MP2
TS9 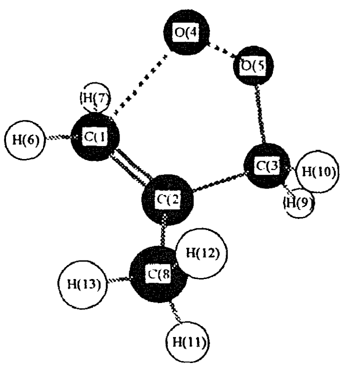	r21	1.3910	1.3576	a321	112.06	112.61	d4123	324.55	320.33	(-662.3)	959.2	1498.3	(-887.6)	1001.3	1535.5	272.9	272.7
	r32	1.5173	1.5100	a412	89.24	87.23	d5412	54.52	58.43	***97.5***	969.9	1509.0	***121.6***	1032.4	1548.4	595.2	579.6
	r41	1.9669	1.9625	a541	90.79	89.90	d6123	203.65	199.16	144.1	990.0	1516.4	160.3	1055.5	1553.2	746.0	717.5
	r53	1.428	1.429	a612	119.37	119.50	d7123	46.77	38.70	321.4	998.3	1558.8	330.9	1085.1	1658.2		
	r54	1.4175	1.4089	a712	121.53	122.34	d8213	159.93	160.08	359.2	1022.1	3000.9	376.2	1113.7	3074.1		
	r61	1.0894	1.0878	a821	124.89	125.02	d9321	250.87	254.96	396.8	1079.2	3019.2	433.5	1200.9	3090.2		
	r71	1.0833	1.0804	a932	115.68	116.15	d10321	128.15	131.13	508.2	1241.4	3060.0	535.9	1288.2	3145.6		
	r82	1.4948	1.4906	a1032	108.83	108.85	d11821	130.44	134.74	612.0	1276.2	3064.6	634.7	1329.6	3162.7		
	r93	1.0984	1.0962	a1182	111.10	110.60	d12821	248.73	253.19	837.3	1363.2	3128.6	878.8	1414.1	3208.6		
	r103	1.1018	1.0993	a1282	111.21	110.65	d13821	10.24	14.49	864.5	1415.1	3156.5	926.5	1461.0	3224.8		
	r118	1.0997	1.0957	a1382	111.78	111.53				885.2	1437.7	3247.5	1000.4	1481.2	3333.2		
	r128	1.1001	1.0964														
	r138	1.0940	1.0917														
TS10 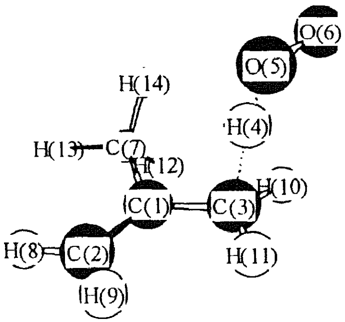	r21	1.3693	1.3363	a312	121.14	120.71	d4312	258.47	253.74	(-1308.4)	852.5	1508.1	(-2564.6)	883.8	1530.3	306.1	300.0
	r31	1.4278	1.4417	a431	105.59	104.63	d5431	238.64	258.77	***23.1***	871.7	1514.6	***40.8***	984.5	1544.7	1160.1	1049.5
	r43	1.5250	1.3820	a543	170.69	166.38	d6541	256.65	272.92	***56.4***	952.7	1533.9	***65.9***	997.8	1556.9	1291.8	1189.0.
	r54	1.1130	1.1752	a654	107.01	106.35	d7123	182.19	182.68	***92.8***	994.6	1548.3	***116.3***	1020.8	1566.0		
	r65	1.2990	1.2818	a712	120.86	122.25	d8213	178.51	178.86	122.7	1022.9	1585.2	163.6	1042.3	1678.2		
	r71	1.5140	1.5045	a821	121.67	121.82	d9213	358.28	358.36	180.0	1076.5	3050.0	195.6	1120.2	3110.1		
	r82	1.0857	1.0844	a921	121.33	121.52	d10312	161.34	154.03	399.5	1086.2	3105.2	404.0	1129.7	3154.7		
	r92	1.0865	1.0849	a1031	119.07	117.46	d11312	11.19	10.33	428.1	1121.3	3115.0	437.3	1195.5	3192.2		
	r103	1.0919	1.0924	a1131	118.72	117.36	d12712	239.71	238.64	482.4	1320.9	3137.3	497.6	1339.8	3215.6		
	r113	1.0892	1.0886	a1271	110.85	110.56	d13712	0.52	359.57	539.5	1396.5	3168.3	582.4	1462.8	3225.6		
	r127	1.0968	1.0941	a1371	111.75	111.42	d14712	121.16	120.32	616.2	1430.1	3209.6	699.8	1478.3	3263.2		
	r137	1.0935	1.0915	a1471	110.70	110.18				675.8	1450.0	3255.8	717.0	1502.2	3321.4		
	r147	1.0966	1.0938														

Table 3A.5b (Continued)

Molecule	Bond Length			Bond Angle			Dihedral Angle			Frequencies B3LYP / 6-31g*			Frequencies MP2 / 6-31g*	Moments of inertia	
		B3LYP	MP2		B3LYP	MP2		B3LYP	MP2					B3LYP	MP2
TS11 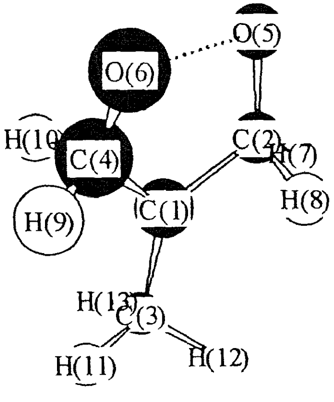	r21	1.4638		a312	123.89		d4123	181.29		(-837.5)	975.8	1424.7		339.7	
	r31	1.4921		a412	111.41		d5213	163.52		***84.8***	1014.1	1457.8		549.0	
	r41	1.4630		a521	119.42		d6412	348.97		181.8	1099.5	1500.4		846.1	
	r52	1.3157		a641	119.21		d7213	21.42		233.4	1121.2	1511.5			
	r64	1.3155		a721	113.92		d8213	279.28		291.7	1182.9	2314.0			
	r72	1.1084		a821	84.70		d9412	207.30		329.5	1211.6	2328.0			
	r82	1.1809		a941	113.35		d10412	105.11		384.6	1253.0	2938.1			
	r94	1.1084		a1041	85.27		d11312	160.98		523.1	1255.3	2944.3			
	r104	1.1794		a1131	112.27		d12312	39.93		557.3	1320.6	3049.3			
	r113	1.0936		a1231	109.77		d13312	282.73		620.5	1351.2	3108.6			
	r123	1.0958		a1331	110.61					907.2	1372.9	3143.7			
	r133	1.0978													
TS12 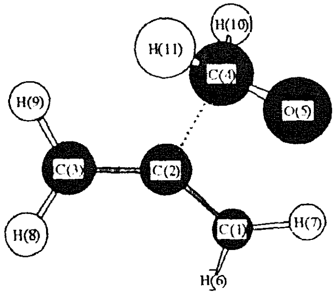	r21	1.3492		a321	136.00		d4213	175.25		(-795.3)	907.3	1521.2		213.3	
	r32	1.3661		a421	111.68		d5421	325.47		***115.7***	938.2	1571.8		429.1	
	r42	1.7914		a542	104.31		d6123	21.82		266.7	1018.6	1661.3		600.4	
	r54	1.2834		a612	120.96		d7123	196.12		304.5	1030.7	2897.4			
	r61	1.0871		a712	119.73		d8321	37.62		388.0	1059.9	2959.8			
	r71	1.0843		a832	121.45		d9321	208.80		420.7	1211.3	3152.7			
	r83	1.0879		a932	121.48		d10421	87.05		519.7	1275.0	3169.3			
	r93	1.0872		a1042	97.23		d11421	200.73		677.1	1374.9	3235.6			
	r104	1.1100		a1142	104.31					857.0	1447.1	3272.3			
	r114	1.1054													

Table 3A.6 Experimental Rate Constants for the Reactions of ROOH → RO· + OH

$CH_3OOH = CH_3O\cdot + OH$	6x10^{14}exp(-42320 /RT) s^{-1}	Ref. 152.
$CH_3OOH = CH_3O\cdot + OH$	4x10^{15}exp(-42920 /RT) s^{-1}	Ref. 148.
$CH_3OOH = CH_3O\cdot + OH$	6.31x10^{14}exp(-42300 /RT) s^{-1}	Ref. 153.
$CH_3CH_2OOH = CH_3CH_2O\cdot + OH$	4x10^{15}exp(-42920 /RT) s^{-1}	Ref. 152.
$CH_3CH_2OOH = CH_3CH_2O\cdot + OH$	4x10^{15}exp(-42920 /RT) s^{-1}	Ref. 148.
$(CH_3)_2CHOOH = i\text{-}C_3H7O\cdot + OH$	1.58x10^{15}exp(-39990 /RT) s^{-1}	Ref. 154.
tert-$C_4H_9OOH = (CH_3)_3CO\cdot + OH$	5.01x10^{15}exp(-42520 /RT) s^{-1}	Ref. 155.
tert-$C_4H_9OOH = (CH_3)_3CO\cdot + OH$	2x10^{15}exp(-41400 /RT) s^{-1}	Ref. 156.

Table 3A.7 Input Parameters and High-Pressure Limit Rate Constants (k_∞) for QRRK Calculation C_2·C*C + O_2 → Product

Reaction	A (s-1 or cm^3/mol-s)	n	Ea (kcal/mol)	ref.
C_2·C*C + O_2 → C*C(C)CQ·	1.09×10^{10} (4.65×10^{8})	0.57 (1.19)	2.29 (0.53)	a.
C*C(C)CQ· → C_2·C*C + O_2	6.07×10^{11} (1.42×10^{12})	0.61 (0.61)	23.29 (22.45)	a.
C*C(C)CQ· → C*C(C)CO· + O	1.82×10^{14}	0.0	60.62	b.
C*C(C)CQ· → C*CICC*O + OH	1.52×10^{9} (3.96×10^{8})	1.03 (1.30)	39.46 (37.62)	a.
C*C(C)CQ· → C*C(C·)CQ	1.41×10^{5} (1.94×10^{5})	1.84 (1.77)	19.82 (19.60)	a.
C*C(C·)CQ → C*C(C)CQ·	1.1×10^{10} (8.23×10^{8})	0.15 (0.51)	20.76 (18.75)	a.
C*C(C·)CQ → C*CYCCOC + OH	6.82×10^{12} (2.29×10^{11})	-0.35 (0.23)	42.14 (32.00)	a.
C*C(C·)CQ → C*C(C·)CO· + OH	4.0×10^{15}		42.72	
C*C(C·)CQ → C*C*C + C·H_2OOH	1.18×10^{12} (8.06×10^{11})	0.91 (0.66)	51.39 (53.01)	a.
C*C(C)CQ· → CCYC·COOC	1.19×10^{8} (2.56×10^{8})	0.80 (0.73)	28.02 (24.95)	a.
CCYC·COOC → C*C(C)CQ·	3.15×10^{13} (4.88×10^{12})	-0.13 (0.14)	27.32 (24.33)	a.
CCYC·COOC → CCYCC·OOC	3.56×10^{13}	0.0	38.82	c.
CCYCC·OOC → CCYC·COOC	8.10×10^{13}	0.0	44.18	d.
CCYCC·OOC → CC(CO·)CO	3.19×10^{14}	0.0	3.0	d.
CC(CO·)CO → CCYCC·OOC	4.66×10^{11}	0.0	55.56	e.
CC(CO·)CO → CC·C*O + CH_2O	4.30×10^{12}	0.0	9.78	f.
CCYC·COOC → CCY(C_2O)CO·	4.56×10^{11} (4.56×10^{11})	0.93 (0.64)	17.47 (16.81)	g.
CCY(C_2O)CO· → CCYC·COOC	6.92×10^{11}	0.062	44.77 (47.04)	d.
CCY(C_2O)CO· → CCYC·CO + CH_2O	1.74×10^{13}	0.0	18.15	f.
C*C(C)CQ· → C_2·CYCCOO	1.07×10^{8} (1.30×10^{8})	0.89 (0.93)	29.72 (27.99)	a.
C_2·CYCCOO → C*C(C)CQ·	3.36×10^{14} (7.41×10^{12})	-0.54 (0.12)	12.09 (8.72)	a.
C_2·CYCCOO → C*CICOOC·	4.41×10^{13} (5.97×10^{11})	-0.23 (0.56)	18.50 (17.17)	a.
C*CICOOC· → C_2·CYCCOO	1.58×10^{11} (2.14×10^{9})	-0.58 (0.20)	21.83 (18.69)	a.
C*CICOOC· → C_2·C*O + CH_2O	1.41×10^{10}	0.0	1.0	h.
C_2·CYCCOO → CCY(C_2O)CO·	1.21×10^{13} (2.59×10^{12})	0.10 (0.21)	20.32 (12.52)	a.
CCY(C_2O)CO·→ C_2·CYCCOO	6.18×10^{12} (1.32×10^{12})	-0.27 (-0.16)	64.55 (59.97)	a.

Geometric mean frequency (from CPFIT ref.26)
C*C(C)CQ.: 359.6 cm^{-1} (9.831), 1312.5 cm^{-1} (13.523), 3164.2 cm^{-1} (8.146)
C*C(C.)CQ: 250.1 cm^{-1} (7.359), 1046.9 cm^{-1} (16.965), 2873.1 cm^{-1} (6.677)
CCYC.COOC: 447.7 cm^{-1} (9.694), 1289 cm^{-1} (15.604), 3077.4 cm^{-1} (7.201)
C_2.CYCCOO: 437.4 cm^{-1} (10.563), 1233.5 cm^{-1} (14.718), 3142.2 cm^{-1} (6.718)
Lennard-Jones parameters: σ = 5.5471A°, ε/k = 584.86 K (ref.28)

a. Fit with three parameter modified Arrhenius equation; A estimated using canonical TST and MP2-determined entropies, Ea evaluated from CBS-q//MP2(full)/6-31G(d) calculation. (Data in parentheses are from B3LYP-determined entropies and B3LYP/6-311+g(3df/2p)// B3LYP/6-31g(d) calculation.)
b. Estimated from O + CH_3O
c. A estimated using TST, four equivalent H's, Ea evaluated from ring strain (28.0) + Ea abstraction (10.8)
d. <MR>
e. A estimated using TST, loss of two rotors, symmetry; one equivalent H's, Ea evaluated from ring train (3.0) + ΔH_{rxn} (52.56)
f. Estimated from C_2H_4 + CH_3
g. A estimated using canonical TST and B3LYP-determined entropies. Ea evaluated from CBS-q//B3LYP/6-31G(d) calculation. (Data in parentheses are from B3LYP-determined entropies and B3LYP/6-311+g(3df/2p)//B3LYP/6-31g(d) calculation.)
h. Estimated from CO + CH_3O

Table 3A.8 QRRK Calculated Rate Constants for $C_2{\cdot}C{=}C{+}O_2$ Reaction System (Based on CBS-q//MP2(full)/6-31g(d))

Reactions			A	n	Ea	atm
C_2.C*C+O_2	⇔	C*C(C)CQ.	1.97E+73	-21.34	15.21	0.0001
C_2.C*C+O_2	⇔	C*C(C)CQ.	6.40E+75	-21.72	16.97	0.001
C_2.C*C+O_2	⇔	C*C(C)CQ.	7.90E+77	-21.98	18.87	0.01
C_2.C*C+O_2	⇔	C*C(C)CQ.	1.86E+78	-21.76	20.17	0.079
C_2.C*C+O_2	⇔	C*C(C)CQ.	1.50E+78	-21.69	20.27	0.1
C_2.C*C+O_2	⇔	C*C(C)CQ.	2.66E+75	-20.5	20.63	1
C_2.C*C+O_2	⇔	C*C(C)CQ.	7.96E+68	-18.2	19.59	10
C_2.C*C+O_2	⇔	C*ClCC*O+OH	8.62E+15	-1.7	21.02	0.0001
C_2.C*C+O_2	⇔	C*ClCC*O+OH	8.66E+15	-1.7	21.03	0.001
C_2.C*C+O_2	⇔	C*ClCC*O+OH	8.71E+15	-1.7	21.03	0.01
C_2.C*C+O_2	⇔	C*ClCC*O+OH	1.60E+16	-1.78	21.18	0.079
C_2.C*C+O_2	⇔	C*ClCC*O+OH	2.12E+16	-1.82	21.26	0.1
C_2.C*C+O_2	⇔	C*ClCC*O+OH	2.64E+19	-2.7	23.16	1
C_2.C*C+O_2	⇔	C*ClCC*O+OH	6.30E+22	-3.63	25.91	10
C_2.C*C+O_2	⇔	C*C(C.)CQ	6.82E+71	-20.45	18.51	0.0001
C_2.C*C+O_2	⇔	C*C(C.)CQ	6.83E+73	-20.66	21.30	0.001
C_2.C*C+O_2	⇔	C*C(C.)CQ	2.89E+73	-20.15	23.63	0.01
C_2.C*C+O_2	⇔	C*C(C.)CQ	4.78E+70	-19	24.95	0.079
C_2.C*C+O_2	⇔	C*C(C.)CQ	1.72E+70	-18.84	25.05	0.1
C_2.C*C+O_2	⇔	C*C(C.)CQ	3.62E+64	-16.86	25.45	1
C_2.C*C+O_2	⇔	C*C(C.)CQ	1.72E+55	-13.85	24.36	10
C_2.C*C+O_2	⇔	C*CYCCOC+OH	2.64E+27	-5.73	26.14	0.0001
C_2.C*C+O_2	⇔	C*CYCCOC+OH	1.38E+28	-5.93	26.52	0.001
C_2.C*C+O_2	⇔	C*CYCCOC+OH	1.61E+32	-7.09	29.04	0.01
C_2.C*C+O_2	⇔	C*CYCCOC+OH	1.38E+34	-7.59	31.35	0.079
C_2.C*C+O_2	⇔	C*CYCCOC+OH	1.16E+34	-7.55	31.53	0.1
C_2.C*C+O_2	⇔	C*CYCCOC+OH	1.10E+31	-6.54	32.90	1
C_2.C*C+O_2	⇔	C*CYCCOC+OH	1.22E+24	-4.35	33.42	10
C_2.C*C+O_2	⇔	C*ClC.CO.+OH	5.62E+29	-5.46	27.23	0.0001
C_2.C*C+O_2	⇔	C*ClC.CO.+OH	1.72E+30	-5.6	27.48	0.001
C_2.C*C+O_2	⇔	C*ClC.CO.+OH	1.45E+34	-6.73	29.84	0.01
C_2.C*C+O_2	⇔	C*ClC.CO.+OH	3.54E+36	-7.36	32.27	0.079
C_2.C*C+O_2	⇔	C*ClC.CO.+OH	3.36E+36	-7.34	32.47	0.1
C_2.C*C+O_2	⇔	C*ClC.CO.+OH	6.90E+33	-6.42	33.89	1
C_2.C*C+O_2	⇔	C*ClC.CO.+OH	1.51E+27	-4.32	34.51	10
C_2.C*C+O_2	⇔	C*ClC.CO.T+OH	1.16E+30	-5.38	26.21	0.0001
C_2.C*C+O_2	⇔	C*ClC.CO.T+OH	5.83E+30	-5.59	26.59	0.001
C_2.C*C+O_2	⇔	C*ClC.CO.T+OH	6.71E+34	-6.74	29.09	0.01
C_2.C*C+O_2	⇔	C*ClC.CO.T+OH	6.24E+36	-7.25	31.41	0.079
C_2.C*C+O_2	⇔	C*ClC.CO.T+OH	5.29E+36	-7.22	31.60	0.1
C_2.C*C+O_2	⇔	C*ClC.CO.T+OH	5.31E+33	-6.21	32.96	1
C_2.C*C+O_2	⇔	C*ClC.CO.T+OH	6.17E+26	-4.02	33.50	10
C_2.C*C+O_2	⇔	C*C*C+C.H_2OOH	1.52E+28	-5.21	35.50	0.0001
C_2.C*C+O_2	⇔	C*C*C+C.H_2OOH	1.01E+28	-5.16	35.38	0.001
C_2.C*C+O_2	⇔	C*C*C+C.H_2OOH	1.72E+29	-5.52	35.95	0.01
C_2.C*C+O_2	⇔	C*C*C+C.H_2OOH	6.96E+33	-6.84	38.66	0.079
C_2.C*C+O_2	⇔	C*C*C+C.H_2OOH	2.08E+34	-6.97	39.00	0.1
C_2.C*C+O_2	⇔	C*C*C+C.H_2OOH	6.45E+35	-7.31	41.55	1
C_2.C*C+O_2	⇔	C*C*C+C.H_2OOH	7.77E+31	-5.99	42.96	10
C_2.C*C+O_2	⇔	CCYC.COOC	3.12E+52	-18.36	15.97	0.0001
C_2.C*C+O_2	⇔	CCYC.COOC	7.76E+53	-18.49	15.40	0.001
C_2.C*C+O_2	⇔	CCYC.COOC	2.44E+60	-20.07	16.52	0.01
C_2.C*C+O_2	⇔	CCYC.COOC	7.74E+70	-22.69	20.02	0.079
C_2.C*C+O_2	⇔	CCYC.COOC	2.26E+72	-23.05	20.63	0.1
C_2.C*C+O_2	⇔	CCYC.COOC	8.06E+84	-25.93	27.59	1
C_2.C*C+O_2	⇔	CCYC.COOC	2.92E+88	-26.08	32.96	10
C_2.C*C+O_2	⇔	CC.C*O+CH_2O	1.20E+11	-1.38	20.51	0.0001
C_2.C*C+O_2	⇔	CC.C*O+CH_2O	1.21E+11	-1.38	20.51	0.001
C_2.C*C+O_2	⇔	CC.C*O+CH_2O	1.23E+11	-1.39	20.51	0.01
C_2.C*C+O_2	⇔	CC.C*O+CH_2O	2.49E+11	-1.47	20.69	0.079
C_2.C*C+O_2	⇔	CC.C*O+CH_2O	3.40E+11	-1.51	20.77	0.1
C_2.C*C+O_2	⇔	CC.C*O+CH_2O	1.46E+15	-2.55	22.98	1
C_2.C*C+O_2	⇔	CC.C*O+CH_2O	2.93E+21	-4.32	27.43	10
C_2.C*C+O_2	⇔	CCYC.CO+CH_2O (via TS8)	1.27E+08	0.2	7.51	0.0001
C_2.C*C+O_2	⇔	CCYC.CO+CH_2O (via TS8)	3.31E+08	0.08	7.76	0.001

Table 3A.8 (Continued)

Reactions			A	N	Ea	atm
C_2.C*C+O_2	<=>	CCYC.CO+CH_2O (via TS8)	5.89E+10	-0.57	9.11	0.01
C_2.C*C+O_2	<=>	CCYC.CO+CH_2O (via TS8)	3.26E+14	-1.63	11.50	0.079
C_2.C*C+O_2	<=>	CCYC.CO+CH_2O (via TS8)	9.76E+14	-1.77	11.82	0.1
C_2.C*C+O_2	<=>	CCYC.CO+CH_2O (via TS8)	8.48E+19	-3.15	15.49	1
C_2.C*C+O_2	<=>	CCYC.CO+CH_2O (via TS8)	9.27E+23	-4.21	19.79	10
C_2.C*C+O_2	<=>	C_2.CYCCOO	4.44E+56	-17.79	18.11	0.0001
C_2.C*C+O_2	<=>	C_2.CYCCOO	1.14E+58	-17.91	18.38	0.001
C_2.C*C+O_2	<=>	C_2.CYCCOO	4.64E+61	-18.64	20.19	0.01
C_2.C*C+O_2	<=>	C_2.CYCCOO	1.55E+66	-19.63	23.13	0.079
C_2.C*C+O_2	<=>	C_2.CYCCOO	5.16E+66	-19.74	23.51	0.1
C_2.C*C+O_2	<=>	C_2.CYCCOO	2.72E+71	-20.72	27.48	1
C_2.C*C+O_2	<=>	C_2.CYCCOO	8.08E+73	-21.02	31.16	10
C_2.C*C+O_2	<=>	C_2.C*O+CH_2O	5.66E+11	-0.9	16.78	0.0001
C_2.C*C+O_2	<=>	C_2.C*O+CH_2O	5.70E+11	-0.9	16.78	0.001
C_2.C*C+O_2	<=>	C_2.C*O+CH_2O	6.24E+11	-0.91	16.81	0.01
C_2.C*C+O_2	<=>	C_2.C*O+CH_2O	7.81E+12	-1.23	17.46	0.079
C_2.C*C+O_2	<=>	C_2.C*O+CH_2O	1.58E+13	-1.31	17.64	0.1
C_2.C*C+O_2	<=>	C_2.C*O+CH_2O	1.33E+18	-2.72	20.79	1
C_2.C*C+O_2	<=>	C_2.C*O+CH_2O	5.65E+23	-4.27	25.38	10
C_2.C*C+O_2	<=>	CCYC.CO+CH_2O (via TS11)	7.98E+11	-0.81	18.73	0.0001
C_2.C*C+O_2	<=>	CCYC.CO+CH_2O (via TS11)	8.03E+11	-0.81	18.73	0.001
C_2.C*C+O_2	<=>	CCYC.CO+CH_2O (via TS11)	8.21E+11	-0.82	18.73	0.01
C_2.C*C+O_2	<=>	CCYC.CO+CH_2O (via TS11)	3.36E+12	-0.99	19.10	0.079
C_2.C*C+O_2	<=>	CCYC.CO+CH_2O (via TS11)	5.56E+12	-1.05	19.23	0.1
C_2.C*C+O_2	<=>	CCYC.CO+CH_2O (via TS11)	1.14E+17	-2.28	21.93	1
C_2.C*C+O_2	<=>	CCYC.CO+CH_2O (via TS11)	6.45E+22	-3.88	26.40	10
C*C(C)CQ.	<=>	C*CICC*O+OH	5.21E-29	8.48	25.60	0.0001
C*C(C)CQ.	<=>	C*CICC*O+OH	8.27E-59	18.18	13.61	0.001
C*C(C)CQ.	<=>	C*CICC*O+OH	1.17E-81	25.74	2.87	0.01
C*C(C)CQ.	<=>	C*CICC*O+OH	4.36E-35	11.79	16.34	0.079
C*C(C)CQ.	<=>	C*CICC*O+OH	1.24E-31	10.83	17.65	0.1
C*C(C)CQ.	<=>	C*CICC*O+OH	1.12E+60	-16.42	50.02	1
C*C(C)CQ.	<=>	C*CICC*O+OH	7.04E+55	-14.3	51.43	10
C*C(C)CQ.	<=>	C*C(C.)CQ	2.25E+04	1.25	16.79	0.0001
C*C(C)CQ.	<=>	C*C(C.)CQ	1.17E-02	3.3	14.85	0.001
C*C(C)CQ.	<=>	C*C(C.)CQ	5.53E-03	3.49	14.90	0.01
C*C(C)CQ.	<=>	C*C(C.)CQ	1.44E+06	0.96	17.84	0.079
C*C(C)CQ.	<=>	C*C(C.)CQ	2.71E+06	0.9	18.01	0.1
C*C(C)CQ.	<=>	C*C(C.)CQ	2.33E+30	-6.36	26.58	1
C*C(C)CQ.	<=>	C*C(C.)CQ	3.54E+25	-4.7	25.66	10
C*C(C)CQ.	<=>	CCYC.COOC	2.28E-25	8.88	14.03	0.0001
C*C(C)CQ.	<=>	CCYC.COOC	3.26E-33	11.58	9.87	0.001
C*C(C)CQ.	<=>	CCYC.COOC	8.36E-23	8.71	13.09	0.01
C*C(C)CQ.	<=>	CCYC.COOC	2.10E+00	2.03	20.89	0.079
C*C(C)CQ.	<=>	CCYC.COOC	2.47E+01	1.75	21.41	0.1
C*C(C)CQ.	<=>	CCYC.COOC	1.36E+45	-11.44	37.25	1
C*C(C)CQ.	<=>	CCYC.COOC	1.56E+39	-9.25	36.64	10
C*C(C)CQ.	<=>	C_2.CYCCOO	3.92E-25	8.55	16.11	0.0001
C*C(C)CQ.	<=>	C_2.CYCCOO	5.36E-43	14.4	8.25	0.001
C*C(C)CQ.	<=>	C_2.CYCCOO	7.96E-31	11.02	11.61	0.01
C*C(C)CQ.	<=>	C_2.CYCCOO	9.09E-04	2.97	20.92	0.079
C*C(C)CQ.	<=>	C_2.CYCCOO	1.88E-02	2.62	21.55	0.1
C*C(C)CQ.	<=>	C_2.CYCCOO	3.41E+47	-12.21	39.40	1
C*C(C)CQ.	<=>	C_2.CYCCOO	3.90E+41	-9.97	38.97	10
C*C(C.)CQ	<=>	C*CYCCOC+OH	8.59E-44	13.43	14.83	0.0001
C*C(C.)CQ	<=>	C*CYCCOC+OH	2.62E-08	3.72	27.81	0.001
C*C(C.)CQ	<=>	C*CYCCOC+OH	2.01E+61	-16.65	53.30	0.01
C*C(C.)CQ	<=>	C*CYCCOC+OH	6.14E+57	-15	54.11	0.079
C*C(C.)CQ	<=>	C*CYCCOC+OH	1.22E+57	-14.74	54.04	0.1
C*C(C.)CQ	<=>	C*CYCCOC+OH	4.14E+49	-12.13	52.72	1
C*C(C.)CQ	<=>	C*CYCCOC+OH	4.24E+40	-9.17	50.47	10
C*C(C.)CQ	<=>	C*CIC.CO.+OH	1.43E-45	14.82	14.57	0.0001
C*C(C.)CQ	<=>	C*CIC.CO.+OH	6.77E-09	4.78	27.68	0.001
C*C(C.)CQ	<=>	C*CIC.CO.+OH	3.06E+64	-16.71	54.45	0.01
C*C(C.)CQ	<=>	C*CIC.CO.+OH	2.09E+61	-15.13	55.47	0.079

Table 3A.8 (Continued)

Reactions	A	n	Ea	atm
C*C(C.)CQ <=> C*CIC.CO.+OH	4.35E+60	-14.87	55.42	0.1
C*C(C.)CQ <=> C*CIC.CO.+OH	1.70E+53	-12.26	54.20	1
C*C(C.)CQ <=> C*CIC.CO.+OH	1.08E+44	-9.22	51.93	10
C*C(C.)CQ <=> C*CIC.CO.T+OH	2.10E-41	13.84	14.82	0.0001
C*C(C.)CQ <=> C*CIC.CO.T+OH	7.14E-06	4.12	27.79	0.001
C*C(C.)CQ <=> C*CIC.CO.T+OH	1.03E+64	-16.33	53.38	0.01
C*C(C.)CQ <=> C*CIC.CO.T+OH	3.33E+60	-14.69	54.21	0.079
C*C(C.)CQ <=> C*CIC.CO.T+OH	6.62E+59	-14.43	54.14	0.1
C*C(C.)CQ <=> C*CIC.CO.T+OH	2.27E+52	-11.82	52.82	1
C*C(C.)CQ <=> C*CIC.CO.T+OH	2.24E+43	-8.85	50.57	10
C*C(C.)CQ <=> C*C*C+C.H$_2$OOH	1.53E-73	22.17	14.60	0.0001
C*C(C.)CQ <=> C*C*C+C.H$_2$OOH	5.26E-37	12.28	25.48	0.001
C*C(C.)CQ <=> C*C*C+C.H$_2$OOH	3.75E+66	-18.2	61.71	0.01
C*C(C.)CQ <=> C*C*C+C.H$_2$OOH	1.18E+67	-17.43	64.62	0.079
C*C(C.)CQ <=> C*C*C+C.H$_2$OOH	4.61E+66	-17.23	64.74	0.1
C*C(C.)CQ <=> C*C*C+C.H$_2$OOH	5.66E+60	-14.87	64.70	1
C*C(C.)CQ <=> C*C*C+C.H$_2$OOH	7.63E+50	-11.49	62.69	10
CCYC.COOC <=> CC.C*O+CH$_2$O	3.29E-02	-0.9	34.02	0.0001
CCYC.COOC <=> CC.C*O+CH$_2$O	1.45E-07	1.55	32.99	0.001
CCYC.COOC <=> CC.C*O+CH$_2$O	2.37E-46	14.17	18.94	0.01
CCYC.COOC <=> CC.C*O+CH$_2$O	1.08-112	35.5	-4.86	0.079
CCYC.COOC <=> CC.C*O+CH$_2$O	2.05-119	37.72	-7.20	0.1
CCYC.COOC <=> CC.C*O+CH$_2$O	2.53E-80	25.54	-1.32	1
CCYC.COOC <=> CC.C*O+CH$_2$O	8.84E+66	-18.83	48.30	10
CCYC.COOC <=> CCYC.CO+CH$_2$O	5.87E+10	-0.82	13.02	0.0001
CCYC.COOC <=> CCYC.CO+CH$_2$O	7.90E+05	1.34	12.89	0.001
CCYC.COOC <=> CCYC.CO+CH$_2$O	2.20E-08	5.76	8.45	0.01
CCYC.COOC <=> CCYC.CO+CH$_2$O	7.74E-11	6.78	8.18	0.079
CCYC.COOC <=> CCYC.CO+CH$_2$O	3.89E-11	6.92	8.24	0.1
CCYC.COOC <=> CCYC.CO+CH$_2$O	1.55E-03	4.54	10.16	1
CCYC.COOC <=> CCYC.CO+CH$_2$O	5.63E+35	-7.25	23.46	10
C$_2$.CYCCOO <=> C2.C*O+CH$_2$O	1.38E+16	-2.87	21.50	0.0001
C$_2$.CYCCOO <=> C2.C*O+CH$_2$O	1.26E+17	-2.85	21.49	0.001
C$_2$.CYCCOO <=> C2.C*O+CH$_2$O	4.46E+17	-2.71	21.37	0.01
C$_2$.CYCCOO <=> C2.C*O+CH$_2$O	2.83E-18	8.83	10.98	0.079
C$_2$.CYCCOO <=> C2.C*O+CH$_2$O	7.33E-17	8.6	12.20	0.1
C$_2$.CYCCOO <=> C2.C*O+CH$_2$O	7.45E+07	1.01	17.93	1
C$_2$.CYCCOO <=> C2.C*O+CH$_2$O	2.71E+42	-9.7	28.34	10
C$_2$.CYCCOO <=> CCYC.CO+CH$_2$O	5.44E+14	-2.49	21.48	0.0001
C$_2$.CYCCOO <=> CCYC.CO+CH$_2$O	4.94E+15	-2.48	21.47	0.001
C$_2$.CYCCOO <=> CCYC.CO+CH$_2$O	1.64E+16	-2.32	21.34	0.01
C$_2$.CYCCOO <=> CCYC.CO+CH$_2$O	9.13E-24	10.51	9.77	0.079
C$_2$.CYCCOO <=> CCYC.CO+CH$_2$O	1.83E-22	10.34	11.06	0.1
C$_2$.CYCCOO <=> CCYC.CO+CH$_2$O	1.23E+04	2.14	17.18	1
C$_2$.CYCCOO <=> CCYC.CO+CH$_2$O	7.39E+40	-9.25	28.35	10

Rate Constants in Form AT^n exp(-Ea/RT)

Units: A factor: bimolecular: cm^3 mol^{-1} s^{-1}; unimolecular: s^{-1}; Ea: kcal/mol

Table 3A.9 Detail Mechanism

Reactions	A	n	Ea	Atm	a.
$C_3CCC_3=2C_3C.$	2.61E+23	-2.07	71.92	1	a.
$C_3CCC_3=C_3CC.C_2+CH_3$	2.34E+41	-7.11	89.42	1	a.
$C_3CC.C_2=C_2C*CC_2+CH_3$	1.13E+75	-19.14	45.41	1	a.
$C_3CC.C_2+O_2=C_3CCQ.C_2$	7.80E+171	-49.82	57.09	1	a.
$C_3CC.C_2+O_2=C_3.CCQC_2$	1.90E+63	-14.68	30.40	1	a.
$C_3CC.C_2+O_2=C_2C*C+C_2C.OOH$	1.16E+94	-29.08	14.84	1	a.
$C_3CCQ.C_2=C_3.CCQC_2$	8.83E+70	-17.56	31.16	1	a.
$C_3.CCQC_2=C_2C*C+C_2C.OOH$	2.09E+52	-12.64	35.98	1	a.
$C_3.CCC_3=C_3C.+C_2C*C$	3.38E+48	-11.64	23.84	1	a.
$C_3.CCC_3+O_2=C_3CCC_3Q.$	2.57E+181	-52.61	61.69	1	a.
$C_3.CCC_3+O_2=C_3CCC_2.CQ$	6.08E+117	-36.23	25.08	1	a.
$C_3.CCC_3+O_2=C_3CC*C(C)+C.H_2OOH$	9.48E+80	-19.82	44.83	1	a.
$C_3CCC_3Q.=C_3CCC_2.CQ$	6.42E+63	-16.32	39.90	1	a.
$C_3CCC_2.CQ=C_3CC*C(C)+C.H_2OOH$	2.95E+59	-14.65	37.00	1	a.
$C_3C.=C_2C*C+H$	5.98E+26	-4.18	41.14	1	a.
$C_3C.+O_2=C_3COO.$	1.11E+80	-21.37	21.98	1	a.
$C_3C.+O_2=C_3CO.+O$	4.74E+24	-3.89	30.00	1	a.
$C_3C.+O_2=C_2C*C+HO_2$ (via TS1)	1.08E+45	-10.02	16.78	1	a.
$C_3C.+O_2=C_3.COOH$	1.52E+114	-32.79	39.76	1	a.
$C_3C.+O_2=C_2C*C+HO_2$ (via TS_2)	4.73E+49	-11.71	22.56	1	a.
$C_3C.+O_2=C_2CYC_2O+OH$	6.03E+47	-11.37	22.43	1	a.
$C_3C.+O_2=C*C(C)Q+CH_3$	2.14E+14	-1.01	22.07	1	a.
$C_3COO.=C_3CO.+O$	1.59E+88	-25.87	74.26	1	a.
$C_3COO.=C_2C*C+HO_2$	2.15E+51	-12.05	41.26	1	a.
$C_3COO.=C_3.COOH$	2.40E+63	-16.13	50.02	1	a.
$C_3.COOH=C_2C*C+HO_2$	1.27E+65	-16.54	35.47	1	a.
$C_3.COOH=C_2CYC_2O+OH$	4.62E+63	-16.35	35.46	1	a.
$C_3.COOH=C*C(C)Q+CH_3$	3.85E+66	-18.58	45.14	1	a.
$C_3C.+HO_2=C_3COOH$	4.40E+91	-25.31	23.62	1	a.
$C_3C.+HO_2=C_3CO.+OH$	1.49E+27	-4.12	7.00	1	a.
$C_3COOH=C_3CO.+OH$	8.57E+35	-6.37	51.46	1	a.
$C_3C.+C_3COO.=C_3COOCC_3$	8.81E+197	-59.25	58.28	1	a.
$C_3C.+C_3COO.=C_3CO.+C_3CO.$	4.52E+27	-4.4	6.83	1	a.
$C_3COOCC_3=C_3CO.+C_3CO.$	1.31E+75	-18.54	54.98	1	a.
$C_2C*C+C_3COO.=C_2C.COOTB$	1.44E+228	-70.36	69.39	1	a.
$C_2C*C+C_3COO.=C_2CYC_2O+C_3CO.$	5.07E+33	-6.89	29.54	1	a.
$C_2C.COOTB=C_2CYC_2O+C_3CO.$	8.85E+55	-14.82	34.29	1	a.
$C_2C*C=CC.*C+CH_3$	2.71E+26	-2.56	92.52	1	a.
$C_2C*C=C_2.C*C+H$	1.32E+21	-1.82	89.44	1	a.
$C_2C*C+OH=C_3.COH$	3.25E+54	-13.013	14.07	1	a.
$C_2C*C+OH=C_3CO.$	1.43E+27	-6.366	11.85	1	a.
$C_2C*C+OH=C_2C*O+CH_3$	1.32E+30	-5.435	16.34	1	a.
$C_3.COH=C_3CO.$	2.13E+46	-12.816	37.35	1	a.
$C_3.COH=C_2C*O+CH_3$	1.93E+52	-12.907	43.14	1	a.
$C_3CO.=C_2C*O+CH_3$	6.13E+54	-14.308	18.53	1	a.
$C_3.COH+O_2=C_2COHCQ.$	7.96E+50	-12.12	12.95	1	a.
$C_3.COH+O_2=C_2CO.CQ$	1.13E+45	-10.57	16.54	1	a.
$C_3.COH+O_2=C_2C*O+C.H_2OOH$	1.80E+45	-9.89	19.03	1	a.
$C_3.COH+O_2=C_2.COHCQ$	9.26E+48	-11.24	19.85	1	a.
$C_3.COH+O_2=C*C(C)CQ+OH$	7.78E+54	-12.47	33.78	1	a.
$C_3.COH+O_2=C*C(C)OH+C.H_2OOH$	5.61E+57	-13.54	33.40	1	a.
$C_2COHCQ.=C_2CO.CQ$	4.63E+35	-8.24	25.08	1	a.
$C_2COHCQ.=C_2C*O+C.H_2OOH$	4.23E+40	-8.88	33.72	1	a.
$C_2COHCQ.=C_2.COHCQ$	1.38E+36	-7.68	31.10	1	a.
$C_2COHCQ.=C*C(C)CQ+OH$	6.45E+75	-19.2	65.49	1	a.
$C_2COHCQ.=C*C(C)OH+C.H_2OOH$	4.89E+75	-19.33	63.49	1	a.
$C_2CO.CQ=C_2C*O+C.H_2OOH$	7.51E+25	-4.76	9.60	1	a.
$C_2.COHCQ=C*C(C)CQ+OH$	9.66E+25	-4	32.48	1	a.
$C_2.COHCQ=C*C(C)OH+C.H_2OOH$	2.06E+24	-3.76	29.12	1	a.
$C.H_2OOH=CH_2O+OH$	4.24E-58	21.27	-26.06	1	a.
$C_2C*C+OH=C_2C.COH$	1.13E+49	-11.283	12.26	1	a.
$C_2C*C+OH=C_2CCO.$	5.67E+24	-5.31	11.42	1	a.
$C_2C*C+OH=C_2CC*O+H$	6.84E+18	-2.332	16.88	1	a.
$C_2C*C+OH=CC.C+CH_2O$	9.27E+24	-3.874	15.33	1	a.
$C_2C*C+OH=C_2.CCOH$	7.12E+42	-10.561	24.88	1	a.
$C_2C*C+OH=C*CC+C.H_2OH$	3.65E+27	-5.167	26.95	1	a.

Table 3A.9 (Continued)

Reactions	A	n	Ea	Atm	a.
$C_2C.COH=C_2CCO.$	2.64E+39	-10.433	34.85	1	a.
$C_2C.COH=C_2CC*O+H$	2.00E+42	-10.269	44.99	1	a.
$C_2C.COH=CC.C+CH_2O$	2.31E+42	-9.908	40.21	1	a.
$C_2C.COH=C_2.CCOH$	1.17E+49	-13.052	46.91	1	a.
$C_2C.COH=C*CC+C.H_2OH$	1.34E+46	-11.582	54.65	1	a.
$C_2CCO.=C_2CC*O+H$	5.69E+20	-3.645	19.29	1	a.
$C_2CCO.=CC.C+CH_2O$	2.19E+47	-11.775	17.53	1	a.
$C_2CCO.=C_2.CCOH$	2.65E+27	-6.435	20.20	1	a.
$C_2CCO.=C*CC+C.H_2OH$	2.00E+16	-2.102	30.15	1	a.
$C_2.CCOH=C*CC+C.H_2OH$	4.08E+67	-18.856	38.49	1	a.
$C_2C.COH+O_2=C_2CQ.COH$	2.03E+66	-17.11	17.40	1	a.
$C_2C.COH+O_2=C*C(C)COH+HO_2$	5.29E+57	-13.79	21.54	1	a.
$C_2C.COH+O_2=C_2C*COH+HO_2$	4.94E+54	-13.15	21.45	1	a.
$C_2C.COH+O_2=C_2CQCO.$	4.79E+56	-15.03	20.74	1	a.
$C_2C.COH+O_2=C_2C.OOH+CH_2O$	8.34E+55	-13.4	21.59	1	a.
$C_2C.COH+O_2=C_2.CQCOH$	1.51E+66	-16.83	26.47	1	a.
$C_2C.COH+O_2=C*C(C)Q+C.H_2OH$	9.14E+53	-12.4	32.09	1	a.
$C_2C.COH+O_2=C*C(C)COH+HO_2$	2.53E+68	-16.94	33.07	1	a.
$C_2C.COH+O_2=C_2CQC.OH$	2.22E+69	-18.1	24.42	1	a.
$C_2C.COH+O_2=C_2C*COH+HO_2$	1.59E+66	-16.26	28.92	1	a.
$C_2CQ.COH=C*C(C)COH+HO_2$	1.00E+43	-9.63	31.92	1	a.
$C_2CQ.COH=C_2C*COH+HO_2$	6.41E+47	-11.35	36.15	1	a.
$C_2CQ.COH=C_2CQCO.$	3.03E+54	-14.97	27.91	1	a.
$C_2CQ.COH=C_2C.OOH+CH_2O$	2.42E+37	-8.1	29.05	1	a.
$C_2CQ.COH=C_2.CQCOH$	1.95E+61	-15.38	44.85	1	a.
$C_2CQ.COH=C*C(C)Q+C.H_2OH$	1.73E+76	-19.55	63.72	1	a.
$C_2CQ.COH=C*C(C)COH+HO_2$	5.44E+77	-19.95	58.41	1	a.
$C_2CQ.COH=C_2CQC.OH$	4.67E+62	-15.96	41.01	1	a.
$C_2CQ.COH=C_2C*COH+HO_2$	6.41E+77	-19.85	54.66	1	a.
$C_2CQCO.=C_2C.OOH+CH_2O$	4.20E+16	-2.14	2.66	1	a.
$C_2.CQCOH=C_2C.OOH+CH_2O$	2.35E+83	-24.53	41.04	1	a.
$C_2.CQCOH=C*C(C)Q+C.H_2OH$	8.43E+75	-20.81	33.06	1	a.
$C_2CQC.OH=C_2C*COH+HO_2$	1.26E+54	-13.22	29.57	1	a.
$C_2C.OOH=C_2C*O+OH$	5.56E+16	-1.02	6.21	1	a.
$C_2C*C.+O_2=C_2C*CQ.$	5.52E+49	-11.74	12.64	1	a.
$C_2C*C.+O_2=C_2C.C*O+O$	9.65E+35	-6.64	16.50	1	a.
$C_2C*C.+O_2=C_2.C*CQ$	3.03E+28	-6.5	15.53	1	a.
$C_2C*C.+O_2=C*ClCC*O+OH$	4.96E+30	-5.85	15.79	1	a.
$C_2C*C.+O_2=C*C*CQ+CH_3$	1.31E-09	4.6	17.01	1	a.
$C_2C*C.+O_2=C_2C.CYCOO$	1.50E+24	-4.24	7.04	1	a.
$C_2C*C.+O_2=C_2C*O+HCO$	9.31E+33	-6.78	17.98	1	a.
$C_2C*C.+O_2=C_2CYCOOC.$	1.36E+29	-6.48	9.92	1	a.
$C_2C*C.+O_2=C_2C*O+HCO$	1.70E+34	-6.83	15.51	1	a.
$C_2C*CQ.=C_2C.C*O+O$	8.17E+38	-7.67	44.65	1	a.
$C_2C*CQ.=C_2.C*CQ$	2.31E+26	-6.02	40.49	1	a.
$C_2C*CQ.=C*ClCC*O+OH$	4.11E+28	-5.39	40.80	1	a.
$C_2C*CQ.=C*C*CQ+CH_3$	3.95E+33	-8.88	65.11	1	a.
$C_2C*CQ.=C_2C.CYCOO$	1.24E+15	-2	19.72	1	a.
$C_2C*CQ.=C_2C*O+HCO$	5.92E+50	-12.02	53.87	1	a.
$C_2C*CQ.=C_2CYCOOC.$	5.66E+28	-6.51	33.48	1	a.
$C_2C*CQ.=C_2C*O+HCO$	1.35E+30	-5.77	38.93	1	a.
$C_2.C*CQ=C*ClCC*O+OH$	1.11E+12	-0.83	-0.26	1	a.
$C_2.C*CQ=C*C*CQ+CH_3$	2.52E+12	-0.93	55.48	1	a.
$C_2C.CYCOO=C_2C*O+HCO$	8.21E+03	1.9	19.31	1	a.
$C_2CYCOOC.=C_2C*O+HCO$	5.42E+45	-11.15	18.87	1	a.
$C_2C*C+HO_2=C*C(C)Q+CH_3$	1.46E+11	0.29	29.41	1	a.
$C_2C*C+HO_2=C_2CYC_2O+OH$	4.62E+30	-6.02	21.90	1	a.
$C*C(C)Q=C_2.C*O+OH$	1.98E-316	101.12	-115.25	1	a.
$C_2C*C+HO_2=C_2C.COOH$	3.57E+48	-11.82	26.16	1	a.
$C_2C*C+HO_2=C_2C*CQ+H$	1.00E+40	-8.49	47.83	1	a.
$C_2C*C+HO_2=C*C(C)CQ+H$	1.02E+40	-8.28	47.24	1	a.
$C_2C*C+HO_2=C_2CYC_2O+OH$	1.48E+14	-0.41	25.01	1	a.
$C_2C*C+HO_2=C_2CCOO.$	1.38E+40	-9.1	33.13	1	a.
$C_2C*C+HO_2=C_2C*C+HO_2$	1.50E+33	-7.09	41.05	1	a.
$C_2C*C+HO_2=C_3.C+O_2$	2.20E+39	-8.05	41.04	1	a.
$C_2C*C+HO_2=C_2.CCOOH$	3.85E+94	-27.76	48.55	1	a.

Table 3A.9 (Continued)

Reactions	A	n	Ea	Atm	a.
C$_2$C*C+HO$_2$=C*CC+C.H$_2$OOH	4.99E+49	-11.45	51.77	1	a.
C$_2$C.COOH=C$_2$C*CQ+H	1.87E+81	-21.82	63.26	1	a.
C$_2$C.COOH=C*C(C)CQ+H	5.52E+80	-21.44	62.45	1	a.
C$_2$C.COOH=C$_2$CYC$_2$O+OH	1.30E+32	-6.48	28.01	1	a.
C$_2$C.COOH=C$_2$CCOO.	6.60E+30	-6.5	26.98	1	a.
C$_2$CCOO.=C$_2$C*C+HO$_2$ (via TS9)	1.01E+47	-11.09	47.04	1	a.
C$_2$CCOO.=C$_3$.C+O$_2$	1.31E+53	-12.05	46.99	1	a.
C$_2$CCOO.=C$_2$.CCOOH	1.02E+20	-2.81	25.05	1	a.
C$_2$.CCOOH=C*CC+C.H$_2$OOH	2.60E+35	-7.29	31.54	1	a.
C$_2$C*CQ=C$_2$C.C*O+OH	2.11E+57	-14.27	29.91	1	a.
C$_3$.C+HO$_2$=C$_2$CCOOH	7.50E+86	-23.74	22.29	1	a.
C$_3$.C+HO$_2$=C$_2$CCO.+OH	1.01E+29	-4.66	8.02	1	a.
C$_2$CCOOH=C$_2$CCO.+OH	1.33E+34	-5.8	51.57	1	a.
C$_2$CCO.=CC.C+CH$_2$O	1.29E+40	-9.19	20.16	1	a.
C$_2$C.COOH+O$_2$=C$_2$CQ.CQ	1.39E+30	-5.51	6.25	1	a.
C$_2$C.COOH+O$_2$=C$_2$CQC.Q	1.22E-15	3.5	0.62	1	a.
C$_2$C.COOH+O$_2$=C$_2$C*CQ+HO$_2$	3.05E-17	7.36	-0.30	1	a.
C$_2$C.COOH+O$_2$=C$_2$C(Q)C*O+OH	1.37E-14	8.53	-2.52	1	a.
C$_2$C.COOH+O$_2$=C$_2$.CQCQ	5.54E+104	-29.57	35.19	1	a.
C$_2$C.COOH+O$_2$=C*C(C)Q+C.H$_2$OOH	9.37E-13	3.9	7.56	1	a.
C$_2$C.COOH+O$_2$=C*C(C)CQ+HO$_2$	1.89E+10	1.15	9.62	1	a.
C$_2$CQ.CQ=C$_2$.CQCQ	2.40E+56	-15.53	35.04	1	a.
C$_3$.COOH+O$_2$=C$_2$CQCQ.	1.50E+150	-42.93	49.93	1	a.
C$_3$.COOH+O$_2$=C$_2$.CQCQ	3.25E+23	-5.96	-5.86	1	a.
C$_3$.COOH+O$_2$=C*C(C)Q+C.H$_2$OOH	1.99E-02	2.76	9.73	1	a.
C$_3$.COOH+O$_2$=C*C(C)CQ+HO$_2$	2.29E+04	3.28	7.03	1	a.
C$_3$.COOH+O$_2$=C$_2$CQ.CQ	1.75E+142	-40.33	53.01	1	a.
C$_3$.COOH+O$_2$=C$_2$CQC.Q	2.47E+23	-7.51	25.59	1	a.
C$_3$.COOH+O$_2$=C$_2$C*CQ+HO$_2$	2.06E-57	20.31	-8.55	1	a.
C$_3$.COOH+O$_2$=C$_2$C(Q)C*O+OH	2.84E-49	19.67	-8.19	1	a.
C$_2$CQCQ.=C$_2$.CQCQ	8.20E+62	-16.44	37.42	1	a.
C$_2$CQCQ.=C$_2$CQ.CQ	2.90E+47	-12.36	24.09	1	a.
C$_2$.CQCQ=C*C(C)Q+C.H$_2$OOH	1.67E+68	-19.81	42.90	1	a.
C$_2$.CQCQ=C*C(C)CQ+HO$_2$	1.25E+52	-12.74	26.95	1	a.
C$_2$CQ.CQ=C$_2$CQC.Q	5.15E+48	-13.07	29.98	1	a.
C$_2$CQC.Q=C$_2$C*CQ+HO$_2$	2.10E-66	20.13	-6.45	1	a.
C$_2$CQC.Q=C$_2$C(Q)C*O+OH	1.08E-53	19.52	-22.06	1	a.
C$_2$C(Q)C*O=C$_2$C.C*O+HO$_2$	1.55E+76	-19.47	82.07	1	a.
C$_2$C(Q)C*O=C$_2$C(O.)CO+OH	3.51E+36	-6.56	51.38	1	a.
C$_2$.C*C+O$_2$=C*C(C)CQ.	1.59E+72	-19.14	22.94	1	a.
C$_2$.C*C+O$_2$=C*ClCC*O+OH	4.70E+12	-0.59	20.86	1	a.
C$_2$.C*C+O$_2$=C*C(C.)CQ	5.96E+41	-9.4	21.14	1	a.
C$_2$.C*C+O$_2$=C*CYCCOC+OH	4.15E+22	-3.7	32.04	1	a.
C$_2$.C*C+O$_2$=C*ClC.CO.+OH	4.65E+26	-3.97	33.49	1	a.
C$_2$.C*C+O$_2$=C*ClC.CO.T+OH	2.50E+25	-3.4	32.14	1	a.
C$_2$.C*C+O$_2$=C*C*C+C.H$_2$OOH	3.24E+36	-7.32	43.75	1	a.
C$_2$.C*C+O$_2$=CCYC.COOC	2.29E+91	-27.74	31.62	1	a.
C$_2$.C*C+O$_2$=CC.C*O+CH$_2$O	1.86E+01	1.76	17.99	1	a.
C$_2$.C*C+O$_2$=CCYC.CO+CH$_2$O (via TS8)	2.16E+30	-6.32	19.75	1	a.
C$_2$.C*C+O$_2$=C$_2$.CYCCOO	1.13E+82	-23.83	32.99	1	a.
C$_2$.C*C+O$_2$=C$_2$.C*O+CH$_2$O	3.36E+15	-1.92	19.78	1	a.
C$_2$.C*C+O$_2$=CCYC.CO+CH$_2$O (via TS11)	1.46E+11	-0.47	19.73	1	a.
C*C(C)CQ.=C*ClCC*O+OH	6.62E+81	-23.12	58.32	1	a.
C*C(C)CQ.=C*C(C.)CQ	1.69E+41	-9.59	31.85	1	a.
C*C(C)CQ.=CCYC.COOC	1.13E+63	-16.87	44.92	1	a.
C*C(C)CQ.=C$_2$.CYCCOO	3.33E+66	-17.98	47.37	1	a.
C*C(C.)CQ=C*CYCCOC+OH	1.74E+43	-9.92	52.62	1	a.
C*C(C.)CQ=C*ClC.CO.+OH	6.78E+47	-10.35	54.50	1	a.
C*C(C.)CQ=C*ClC.CO.T+OH	1.13E+46	-9.63	52.75	1	a.
C*C(C.)CQ=C*C*C+C.H$_2$OOH	2.71E+62	-15.13	67.70	1	a.
CCYC.COOC =CC.C*O+CH$_2$O	1.70E+64	-19.71	42.96	1	a.
CCYC.COOC =CCYC.CO+CH$_2$O	2.08E+52	-12.73	27.98	1	a.
C$_2$.CYCCOO =C$_2$.C*O+CH$_2$O	2.24E+58	-15.12	32.40	1	a.
C$_2$.CYCCOO =CCYC.CO+CH$_2$O	8.17E+56	-14.73	32.39	1	a.
C*ClC.CO.=C*C*C+CH$_2$O	1.38E+15	-1.633	6.64	1	a.
C*ClC.CO.=C*ClC.C*O+H	7.67E+14	-1.347	16.93	1	a.

Table 3A.9 (Continued)

Reactions	A	n	Ea	Atm	a.
C*CIC.CO.=C*CYCCOC	2.42E+16	-2.321	1.78	1	a.
C*CIC.CO.T=C*CIC.CO.	1.57E+11	-0.07	0.26	1	a.
C*CIC.CO.T=C*CIC.C*O+H	1.73E+02	0.39	16.38	1	a.
C*C(C.)CQ+O$_2$=C*CICQ.CQ	6.18E+142	-41.77	42.25	1	a.
C*C(C.)CQ+O$_2$=C*C(C.)CQ+O$_2$	7.43E+45	-10.2	16.72	1	a.
C*C(C.)CQ+O$_2$=C.*CICQCQ	2.78E+83	-25.51	26.16	1	a.
C*C(C.)CQ+O$_2$=C#CCQ+C.H$_2$OOH	2.71E+39	-7.81	46.33	1	a.
C*C(C.)CQ+O$_2$=C*CIC.QCQ	2.47E+83	-28.57	31.98	1	a.
C*C(C.)CQ+O$_2$=C*C*CQ+C.H$_2$OOH	5.11E+30	-6.49	44.69	1	a.
C*C(C.)CQ+O$_2$=C*CICQCO+OH	2.84E+28	-5.63	14.73	1	a.
C*CICQ.CQ=C.*CICQCQ	1.52E+57	-15.4	36.23	1	a.
C*CICQ.CQ=C*CIC.QCQ	1.18E+48	-12.58	28.89	1	a.
C*CICQ.CQ=C#CCQ+C.H$_2$OOH	2.96E-255	80.16	-81.57	1	a.
C*CICQ.CQ=C*CICQ.CQ	6.58E-147	48.72	-49.69	1	a.
C*CIC.QCQ=C*C*CQ+C.H$_2$OOH	1.36E+09	-1.79	69.43	1	a.
C*CIC.QCQ=C*CICQCO+OH	1.57E+10	0.53	-0.02	1	a.
CCYC.CO=C$_2$.C*O	3.51E+25	-3.72	10.12	1	a.
CCYC.CO=C*C*O+CH$_3$	2.08E+15	-0.02	15.50	1	a.
C$_2$.C*O=C*C*O+CH$_3$	1.51E+24	-3.47	43.16	1	a.
C$_2$CYC$_2$O=CCYC.CO+CH$_3$	7.25E+18	-0.19	88.88	1	a.
C$_2$CYCC.O=C$_2$C.C*O	2.04E+28	-4.58	11.16	1	a.
C$_2$CYCC.O=C$_2$C*C*O+H	2.79E+23	-2.34	25.42	1	a.
C$_2$CYCC.O=C*CICC*O+H	8.68E+23	-2.49	25.96	1	a.
C$_2$C.C*O=C$_2$C*C*O+H	3.05E+41	-8.8	50.11	1	a.
C$_2$C.C*O=C*CICC*O+H	2.92E+42	-9.1	50.96	1	a.
C$_2$.CYC$_2$O=C*C(C)OC.	9.28E+16	-1.37	16.53	1	a.
C$_2$.CYC$_2$O=CC.*C+CH$_2$O	5.42E+22	-2.02	38.07	1	a.
C*C(C)OC.=CC.*C+CH$_2$O	5.56E+37	-7.69	40.49	1	a.
C$_2$.CYC$_2$O=C*C(C)CO.	4.95E+21	-3.75	4.45	1	a.
C$_2$.CYC$_2$O=CC.*C+CH$_2$O	9.28E+21	-2.23	26.23	1	a.
C$_2$.CYC$_2$O=C*CICC*O+H	8.38E+14	-0.23	19.67	1	a.
C*C(C)CO.=CC.*C+CH$_2$O	6.10E+17	-2.01	23.64	1	a.
C*C(C)CO.=C*CICC*O+H	6.41E+11	-0.34	17.16	1	a.
C$_2$.C*O+O$_2$=CC*OCOO.	1.43E+70	-18.51	18.00	1	a.
C$_2$.C*O+O$_2$=C.C*OCOOH	3.57E+103	-29.05	32.03	1	a.
C$_2$.C*O+O$_2$=C*C*O+C.H$_2$OOH	1.24E+15	-0.7	23.69	1	a.
CC*OCOO.=C.C*OCOOH	1.75E+46	-10.94	29.46	1	a.
C.C*OCOOH=C*C*O+C.H$_2$OOH	1.45E+56	-15.58	44.30	1	a.
C$_2$.C*C+HO$_2$=C*C(C)CQ	6.26E+62	-16.027	16.32	1	a.
C$_2$.C*C+HO$_2$=C*C(C)CO.+OH	4.59E+29	-4.946	10.77	1	a.
C*C(C)CQ=C*C(C)CO.+OH	8.69E+38	-7.345	50.94	1	a.
C*CICC.*O=CC.*C+CO	6.94E+12	0.04	33.22	1	a.
C$_2$.C*C+OH=C*C(C)COH	1.02E+12	0	0.00	1	a.
C$_2$.C*C+OH=C*C(C)CO.+H	8.63E-32	13.2	17.44	1	a.
C*C(C)COH=C*C(C)CO.+H	5.90E+13	-0.02	103.54	1	a.
C$_3$CCC$_3$+OH=H$_2$O+C$_3$.CCC$_3$	9.99E+06	2	0.18		b.
C$_3$CCC$_3$+HO$_2$=H$_2$O$_2$+C$_3$.CCC$_3$	1.00E+12	0	17.30		c.
C$_3$CCC$_3$+O=OH+C$_3$.CCC$_3$	3.90E+14	0	7.68		d.
C$_3$.CCC$_3$+C*CC=C*CC.+C$_3$CCC$_3$	2.23	3.5	6.64		e.
C$_3$.CCC$_3$+C$_2$C*C=C$_2$.C*C+C$_3$CCC$_3$	4.46	3.5	6.64		f.
C$_3$C.+C$_3$CCC$_3$=C$_3$C+C$_3$.CCC$_3$	1.12E-05	5.17	9.07		g.
C$_3$C.+HO$_2$=C$_3$C+O$_2$	3.01E+11	0	0.00		h.
C$_3$C.+C$_2$C*C=C$_3$C+C$_2$.C*C	84.4	3.3	17.17		i.
C$_3$C+H=C$_3$C.+H$_2$	2.40E+08	1.5	4.28		d.
C$_3$C+OH=C$_3$C.+H$_2$O	1.20E+06	1.5	-1.54		d.
C$_3$C+HO$_2$=C$_3$C.+H$_2$O$_2$	3.61E+03	2.55	10.53		j.
C$_3$C+O=C$_3$C.+OH	1.70E+08	1.5	2.27		d.
C$_3$C+CH$_3$=C$_3$C.+CH$_4$	8.10E+05	1.87	17.48		d.
CH$_3$+C*C*C=C$_2$.C*C	4.57E+13	0	54.19		k.
C$_2$C*C+O=C$_2$.C*C+OH	7.54E+10	0.7	7.63		l.
C$_2$C*C+OH=C$_2$.C*C+H$_2$O	3.90E+06	2	-0.30		m.
C$_2$C*C+OH=C$_2$C*C.+H$_2$O	1.61E+06	2	2.78		n.
C$_2$C*C+HO$_2$=C$_2$.C*C+H$_2$O$_2$	1.21E+04	2.6	13.91		o.
C$_2$C*C+O$_2$=C$_2$.C*C+HO$_2$	1.86E+09	1.3	40.94		p.
C$_2$CYC$_2$O+OH=C$_2$CYCC.O+H$_2$O	2.40E+06	2	-2.19		d.
C$_2$CYC$_2$O+C$_2$.C*C=C$_2$CYCC.O+C$_2$C*C	7.80E+01	3.3	18.17		q.

Table 3A.9 (Continued)

Reactions	A	n	Ea	Atm	a.
$C_2CYC_2O+C*CC.=C_2CYCC.O+C*CC$	7.80E+01	3.3	18.17		q.
$C_2CYC_2O+C_3COO.=C_2CYCC.O+C_3COOH$	7.20E+03	2.55	12.45		r.
$C_2CYC_2O+CH_3OO=C_2CYCC.O+CH_3OOH$	7.20E+03	2.55	12.45		r.
$C_2CYC_2O+CH_3=C_2CYCC.O+CH_4$	1.62E+06	1.87	6.64		d.
$C_2C*O+O_2=C_2.C*O+HO_2$	8.00E+13	0	46.80		s.
$C_2C*O=CH_3+CC.*O$	2.70E+16	0	81.74		t.
$CC.*O =CH_3+CO$	2.50E+13	0	16.38		u.
$C_2C*O+OH=C_2.C*O+H_2O$	1.02E+12	0	1.19		v.
$C_2C*O+O=C_2.C*O+OH$	1.00E+13	0	5.96		w.
$C_2C*O+H=C_2.C*O+H_2$	1.86E+13	0	6.36		x.
$C_2C*O+CH_3=CH_4+C_2.C*O$	3.29E+11	0	9.60		y.
$C_2.C*O+H=C_2C*O$	1.00E+13	0	0.00		a.
$C_2.C*O+C_2C*C=C_2.C*C+C_2C*O$	2.23	3.5	6.64		z.
$CCYC.COC+C_2C*C=CCYCOCC+C_2.C*C$	6.02E-05	4.98	8.36		aa.
CCYC.COC+C*CC=C*CC.+CCYCOCC	3.01E-05	4.98	8.36		ab.
$CCYC.COOC+C_2C*C=CCYCCOOC+C_2.C*C$	1.34E-01	4	8.07		aa.
CCYC.COOC+C*CC=CCYCCOOC+C*CC.	6.62E-02	4	8.07		ab.
$C_2.C*C+C_2.C*C=DIC_2.C*C$	2.00E+13	0	0.00		ac.
$C_2.C*C+C*CC.=C_2*CCCC*C$	1.00E+13	0	0.00		ac.
$C*C(C)CO.+C_2C*C=C_2.C*C+C*C(C)COH$	1.80E+02	2.95	11.98		ad.
C*C(C)CO.+C*CC=C*C(C)COH+C*CC.	9.00E+01	2.95	11.98		ae.
$C*ClCC*O+CH_3=CH_4+C*ClCC.*O$	8.10E+05	1.87	-1.17		d.
$C*ClCC*O+OH=H_2O+C*ClCC.*O$	1.20E+06	2	1.31		d.
$C*ClCC*O+HO_2=H_2O_2+C*ClCC.*O$	3.01E+12	0	11.92		af.
C*ClCC*O+C*CC.=C*CC+C*ClCC.*O	3.08E+11	0	7.22		ag.
$C*ClCC*O+C_2.C*C=C_2C*C+C*ClCC.*O$	3.08E+11	0	7.22		ag.
C*ClCC.*O=CC.*C+CO	1.50E+11	0	4.81		ah.
$C_3.CCC_3+C*C(C)COH=C*C(C)CO.+C_3CCC_3$	10.5	3.1	8.96		ai.
$C*C(C)COH=C_2.C*C+OH$	3.69E+12	0.09	32.93		a.
$C*C(C)COH+HO_2=C*C(C)CO.+H_2O_2$	3.34E+03	2.55	18.86		aj.
$C*C(C)OH+HO_2=C_2.C*O+H_2O_2$	1.93E+04	2.6	13.91		ak.
$C_2C*COH+HO_2=C_2C.C*O+H_2O_2$	9.64E+03	2.6	13.91		al.
C*CC+O=C*CC.+OH	6.03E+10	0.7	7.63		i.
$CC.*C+C_2C*C=C*CC+C_2.C*C$	4.42	3.5	4.68		am.
$CC.*C+C_3CCC_3=C_3.CCC_3+C*CC$	2.72	3.65	5.17		an.
C*CC.+C*CC.=C*CCCC*C	1.03E+13	0	-0.26		i.
C*C*C+C*CC.=C#CC.+C*CC	1.26E+08	1.9	18.19		ao.
$C*C*C+C_2.C*C=C\#CC.+C_2C*C$	1.26E+08	1.9	18.19		ao.
C#CC.+C#CC.=CYC6H6	3.40E+13	0	0.00		ap.
$O+CH_4=CH_3+OH$	6.92E+08	1.56	8.49		aq.
$CH_3+C_2C*C=CH_4+C_2.C*C$	1.86E+06	1.87	1.22		d.
$CH_3+C_3CCC_3=C_3.CCC_3+CH_4$	1.46E+07	1.87	10.60		d.
$CH_3+O_2=CH_3OO$	1.99E+31	-6.72	4.21		a.
$CH_3+O_2=CH_2O+OH$	2.61E+08	1.01	12.49		a.
$CH_3+CH_2O=HCO+CH_4$	5.54E+03	2.81	5.86		ar.
$CH_3+HO_2=CH_3O.+OH$	1.81E+13	0	0.00		aq.
$CH_3O.=CH_2O+H$	6.13E+28	-5.65	31.35		a.
$CH_3O.+HO_2=CH_2O+H_2O_2$	3.01E+11	0	0.00		ar.
$CH_2O+O=OH+HCO$	1.81E+13	0	3.08		ar.
$CH_2O+H=H_2+HCO$	2.29E+10	1.05	3.28		aq.
$CH_2O+OH=H_2O+HCO$	3.44E+09	1.18	-0.45		aq.
$HCO+O_2=CO+HO_2$	6.25E+15	-1.15	2.02		as.
$HCO+O_2=CO_2+OH$	5.45E+14	-1.15	2.02		as.
$CO+O=CO_2$	6.17E+14	0	3.00		ar.
CO+H+M=HCO+M	6.31E+20	-1.82	3.69		aq.
$CO+OH=CO_2+H$	6.32E+06	1.5	-0.50		ar.
$CO+HO_2=CO_2+OH$	1.51E+14	0	23.65		ar.
$CO+O_2=CO_2+O$	2.53E+12	0	47.69		ar.
$H+O_2=OH+O$	1.99E+14	0	16.80		aq.
$H+O_2+M=HO_2+M$	1.41E+18	-0.8	0.00		aq.
$H_2/3.41/N_2/1.0/H_2O/2.53/$					
$OH+HO_2=H_2O+O_2$	1.45E+16	-1	0.00		ar.
$H+HO_2=OH+OH$	1.69E+14	0	0.87		ar.
$H+HO_2=H_2+O_2$	6.62E+13	0	2.13		ar.
$O+HO_2=O_2+OH$	1.75E+13	0	-0.40		at.
$OH+OH=O+H_2O$	1.51E+09	1.14	0.10		aq.

Table 3A.9 (Continued)

Reactions	A	n	Ea	Atm	a.
$O+H_2=OH+H$	5.12E+04	2.67	6.29		aq.
$O+O+M=O_2+M$	1.89E+13	0	-1.8		ar.
$H+H+M=H_2+M$	5.44E+18	-1.3	0		ar.
$N_2/1.0/$					
$H+OH+M=H_2O+M$	2.21E+22	-2	0		aq.
$N_2/1.0/\ H_2O/16.96/$					
$HO_2+HO_2=H_2O_2+O_2$	1.87E+12	0	1.54		aq.
$H_2O_2+M=OH+OH+M$	1.21E+17	0	45.51		aq.
$N_2/1.0/$					
$H_2O_2+H=H_2+HO_2$	4.82E+13	0	7.95		ar.
$H_2O_2+OH=HO_2+H_2O$	1.75E+12	0	0.32		at.
$CH_4+HO_2=H_2O_2+CH_3$	9.04E+12	0	24.64		aq.
$HO_2+C*CC=C*CC.+H_2O_2$	9.64E+03	2.6	13.91		i.
$H_2+OH=H_2O+H$	1.02E+08	1.6	3.30		aq.
$_2HO_2=_2OH+O_2$	1.00E+12	0	11.5		as.
$H+O+M=OH+M$	4.71E+18	-1	0		ar.
$HO_2+H=H_2O+O$	3.01E+13	0	1.72		aq.
$H_2O_2+H=H_2O+OH$	2.41E+13	0	3.97		ar.
$H_2O_2+O=OH+HO_2$	9.63E+06	2	3.97		ar.

Rate Constants in Form AT^n exp(-Ea/RT)

Units: A factor: bimolecular: $cm^3\ mol^{-1}\ s^{-1}$; unimolecular: s^{-1}; Ea: kcal/mol

a. from QRRK calculations; **b.** ref. 37; **c.** ref. 70; **d.** ref.71; **e.** $C*CC+C_3.C=C*CC.+C_3C$(ref.33); **f.** 2x $C*CC+C_3.C=C*CC.+C_3C$(ref.33); **g.** 2x $C_3C.+C_3C=C_3C+C_3.C$(ref.66); **h.** $C_2H5+HO_2=C_2H6+O_2$(ref.67); **i.** ref.33; **j.** ref.66; **k.** ref.71; **l.** 1.25x $C*CC+O=C*CC.+OH$(ref.33); **m.** .1.25x $C*CC+OH=C*CC.+H_2O$(ref.33); **n.** 0.75x $C*CC+OH=CC*C.+H_2O$(ref.33); **o.** 1.25x $C*CC+OH=C*CC.+H_2O$(ref.33); **p.** study in this work; **q.** A factor from $C*CC.+CCC=C*CC+CC.C$, Ea = $\Delta U+8.066$(ref.33); **r.** A factor from 2x $C_3C+CH_3OO=C_3C.+CH_3OOH$; Ea = $\Delta U+0.5$(ref.66); **s.** estimate A=8e13, Ea = $\Delta U+1.0$; **t.** ref.74; **u.** ref.67; **v.** ref.68; **w.** ref.69; **x.** ref.75; **y.** ref. 37; **z.** $C_2H5+C*CC=C_2H6+C*CC.$(ref.33); **aa.** 2x $CC.C+C*CC=CCC+C*CC.$(ref.33); **ab.** $CC.C+C*CC=CCC+C*CC.$(ref.33); **ac.** $C*CC.+ C*CC.=C*CCCC*C$(ref.33); **ad.** 2x $CH_3O.+C*CC=CH_3OH+C*CC.$(ref.33); **ae.** $CH_3O.+C*CC=CH_3OH+C*CC.$(ref.33); **af.** $CC*O+HO_2=CC.*O+H_2O_2$(ref.51); **ag.** $C*CC.+ CC*O =C*CC+ CC.*O$(ref.72); **ah.** $C_2H_3+CO=CH_2CHC.*O$(ref.67) and <MR>; **ai.** $C_3.C+CH_3OH=C_3C+CH_3O.$(ref.66); **aj.** A factor from 1/9($C_3C+HO_2=C_3.C+H_2O_2$) and Ea =$\Delta U+3$(ref.66); **ak.** 2x $C*CC+HO_2=C*CC.+H_2O_2$(ref.33); **al.** $C*CC+HO_2=C*CC.+H_2O_2$(ref.33); **am.** 2x $C_2H_3+C*CC=C_2H_4+C*CC.$(ref.33); **an.** 2x $C_2H_3+C_3C=C_2H_4+C_3.C$(ref.33); **ao.** $C*CC.+CH_2O=C*CC+HCO$(ref.33); **ap.** ref.73; **aq.** ref.51; **ar.** ref.67; **as.** ref.38, **at.** ref.74.

APPENDIX 3B

FIGURES IN THE THERMOCHEMICAL KINETIC ANALYSIS ON THE REACTIONS OF ALLYLIC ISOBUTENYL RADICAL WITH O_2: AN ELEMENTARY REACTION MECHANISM FOR ISOBUTENE OXIDATION

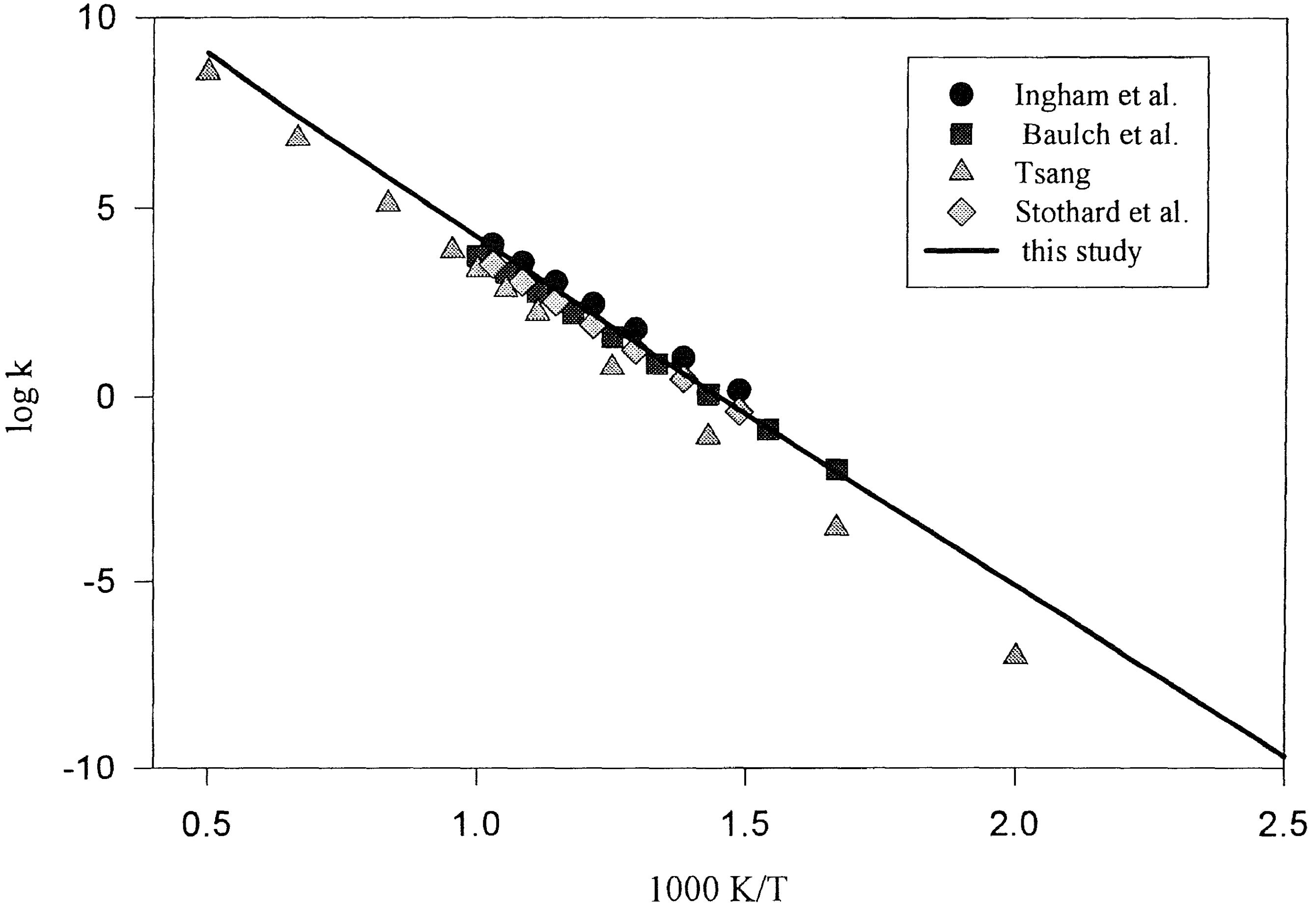

Figure 3B. 1 Comparsion calculated rate constant of $C_2C{=}C + O_2$ -> $C_2.C{=}C + HO_2$ with experimental values for similar reaction of $C{=}C\text{-}C + O_2$ -> $C{=}C\text{-}C. + O_2$

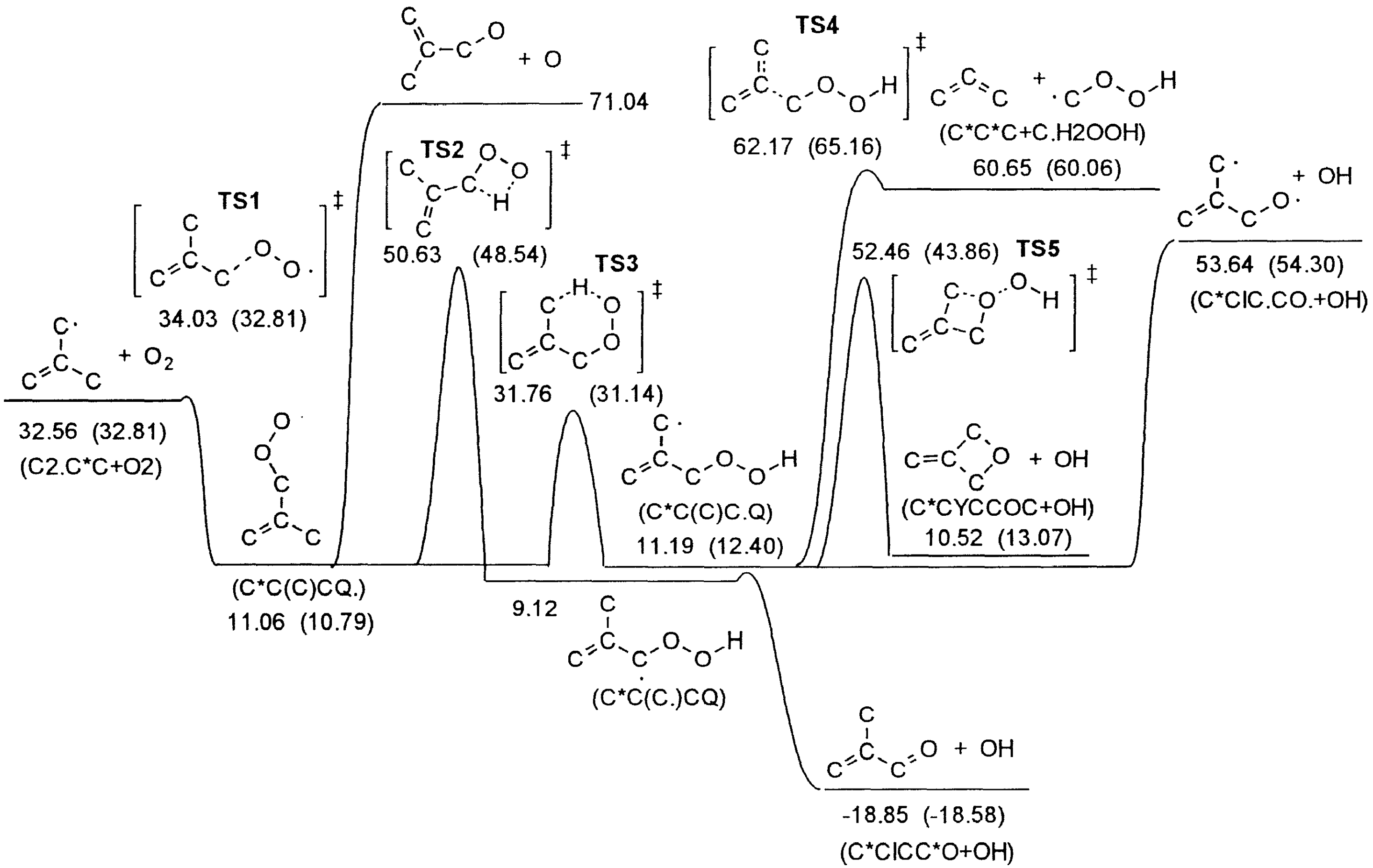

Figure 3B.2a The potential energy diagrams for allylic isobutenyl radical ($C_2 \cdot C=C$) + O_2 -> products. Isomerizations via H shifts and C=C(C)CO· + O atom paths.

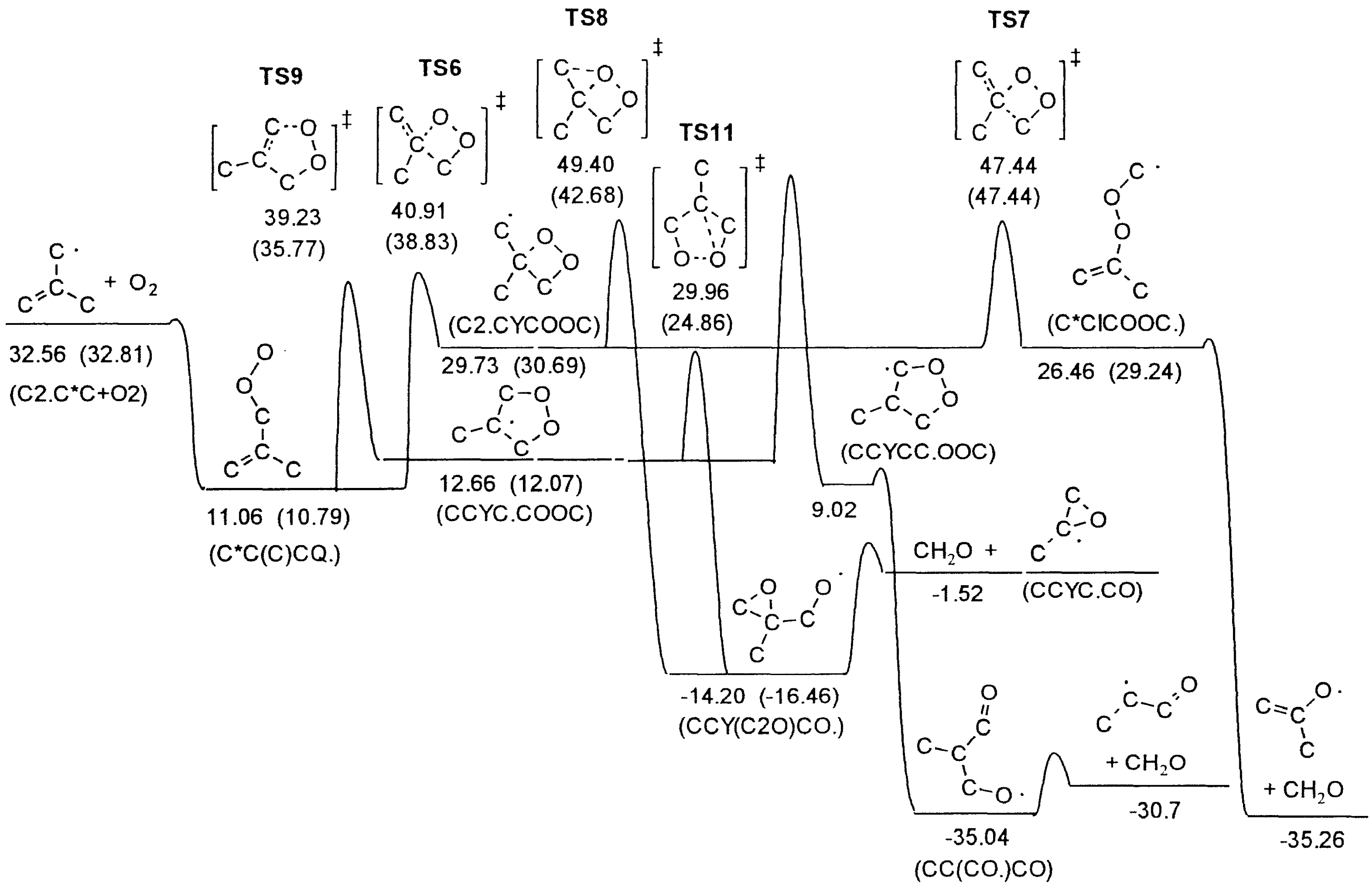

Figure 3B.2b The potential energy diagrams for allylic isobutenyl radical ($C_2 {\cdot} C{=}C$) + O_2 -> products. Cyclization pathways to form cyclic adducts and further reactions.

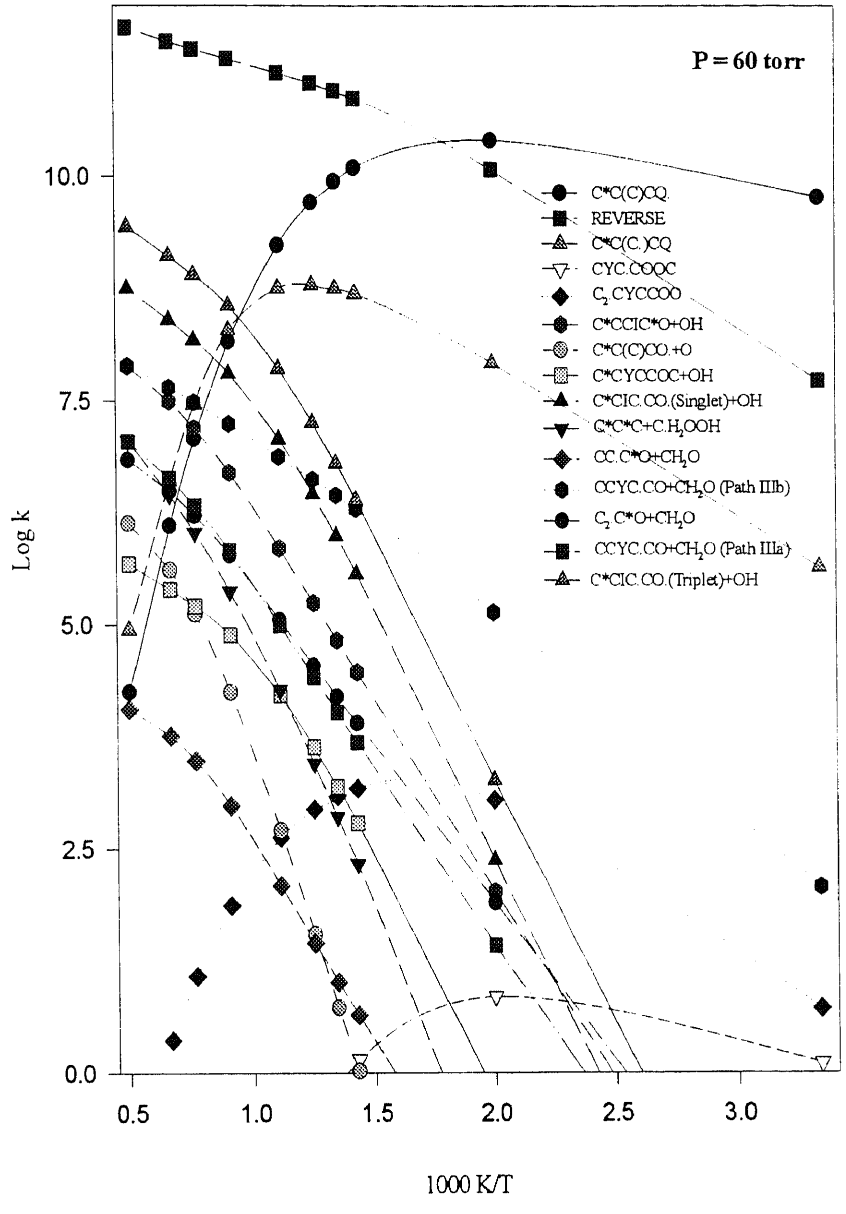

Figure 3B.3a Calculated rate constants at different temperature and 60torr for $C_2 \cdot C{=}C + O_2 \Rightarrow [C{=}C(C)COO \cdot {}^*] \Rightarrow$ products.

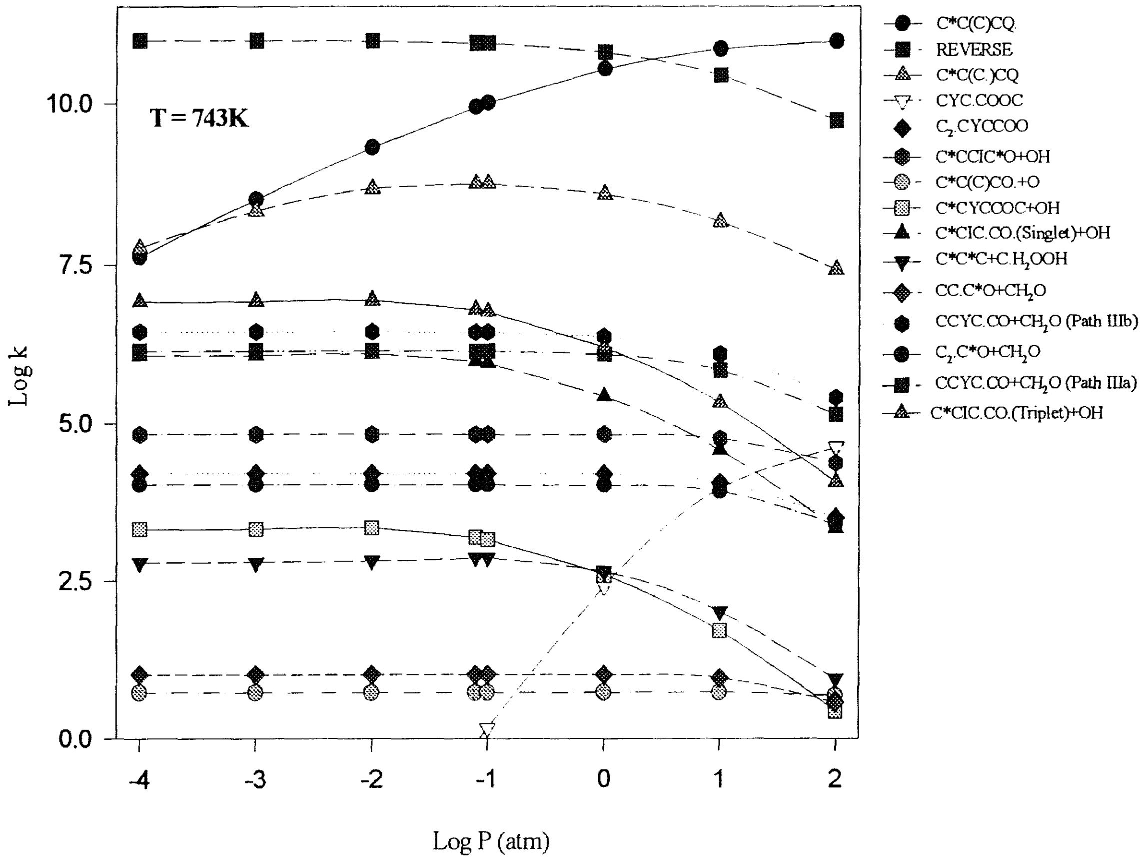

Figure 3B.3b Calculated rate constants at different pressures and 743 K for $C_2{\cdot}C{=}C + O_2 \Rightarrow [C{=}C(C)COO{\cdot}*] \Rightarrow$ products.

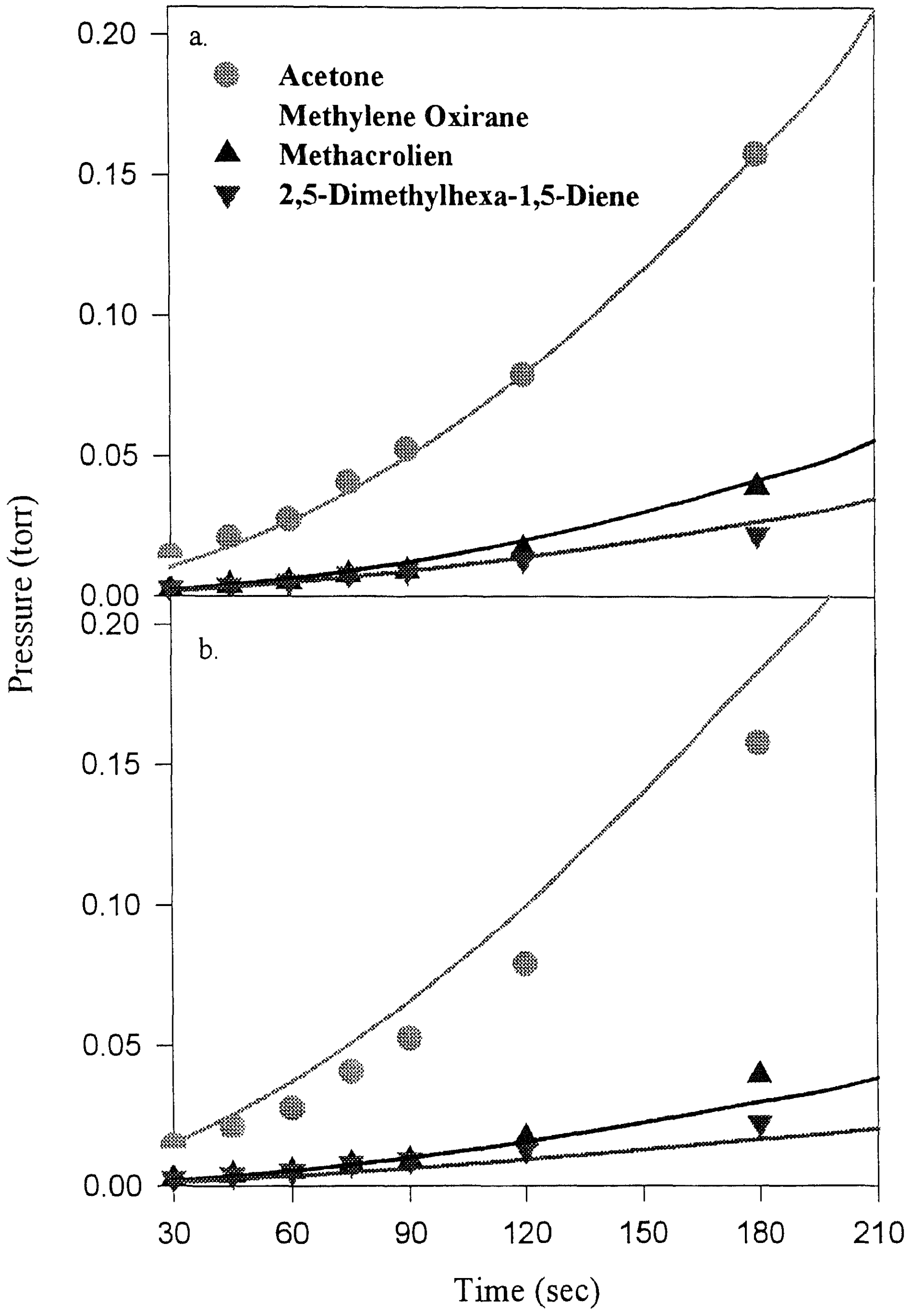

Figure 3B.4 Comparison model prediction and experimental data. Symbols are experimental data from Ingham et al.[7] for reaction time range (0 - 210 sec), 743 K and 60 torr (molar fraction of isobutene: O_2: N_2 = 0.067: 0.5: 0.433). Lines are calculations base on thermodynamic. a. isomerizations via H shifts and C=C(C)CO· + O atom paths parameters from CBS-q//MP2(full)/6-31g(d) and B3LYP/6-311+g(3df,2p)//B3LYP/6-31g(d) levels and illustrated in Figure 4a and Figure 4b, respectively.

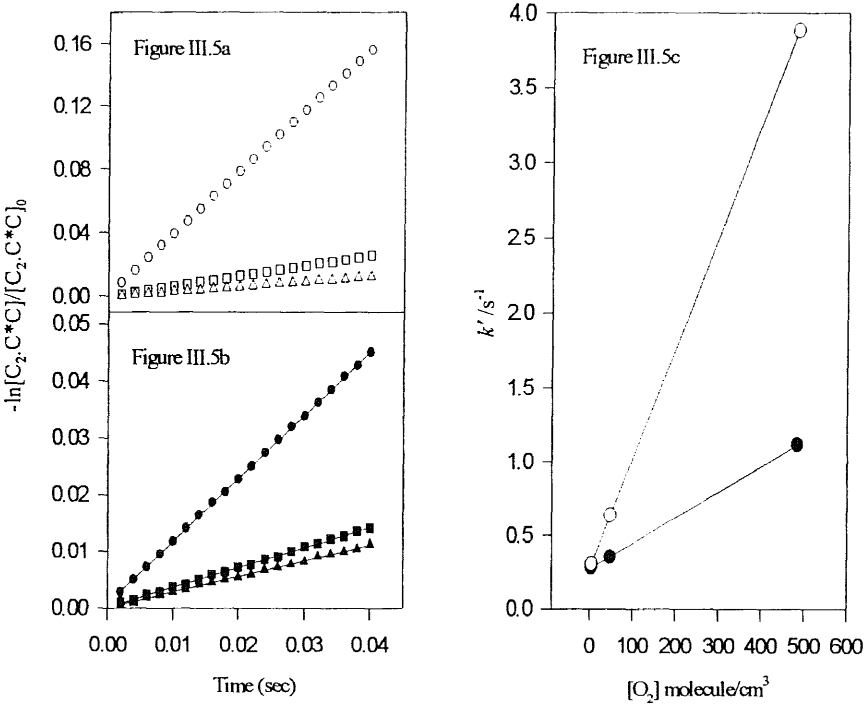

Figure 3B.5 First-order $C_2{\cdot}C{=}C$ radical decay rate *k'* vs. $[O_2]$ at 800K and 2.78 torr in He bath gas. $[C_2{\cdot}C{=}C\ ] = 2\text{x}10^{10}$ molecules cm^{-3}. Circles: $[O_2] = 4.84\text{x}10^{16}$ molecules cm^{-3}; Squares: $[O_2] = 4.84\text{x}10^{15}$ molecules cm^{-3}; Triangles: $[O_2] = 4.84\text{x}10^{14}$ molecules cm^{-3} b. The second-order rate constant of the reaction of $C_2{\cdot}C{=}C$ radical with O_2 is calculated to be $1.05\text{x}10^7$ s^{-1} $mole^{-1}$ cm^3 and $4.50\text{x}10^7$ s^{-1} $mole^{-1}$ cm^3 based on thermodynamic parameters from CBS-q//MP2(full)/6-31g(d) (solid points) and B3LYP/6-311+g(3df,2p)//B3LYP/6-31g(d) (open points) calculations, respectively.

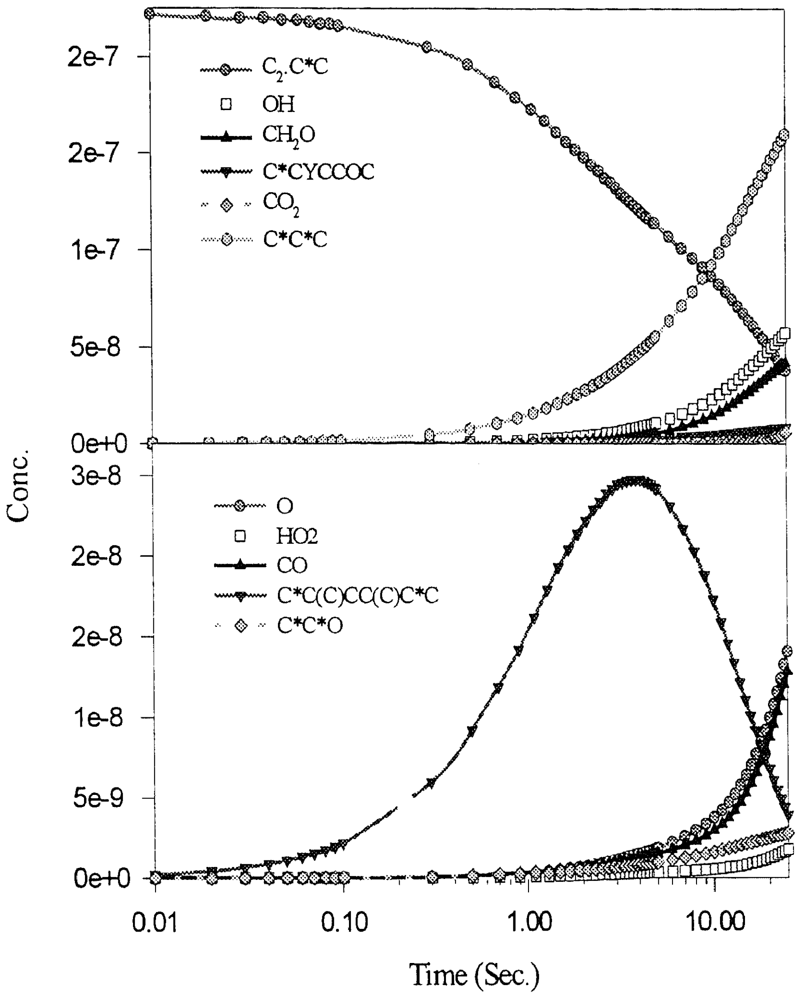

Figure 3B.6a Concentration of reactant ($C_2{\cdot}C{=}C$ radical) and products vs. reaction time based on CBS-q//MP2(full)/6-31g(d) mechanism at 800K, 2.78 torr in He bath gas and [$C_2{\cdot}C{=}C$] = $2x10^{10}$ molecules cm^{-3}. a. [O_2] = $4.84x10^{14}$ molecules cm^{-3}

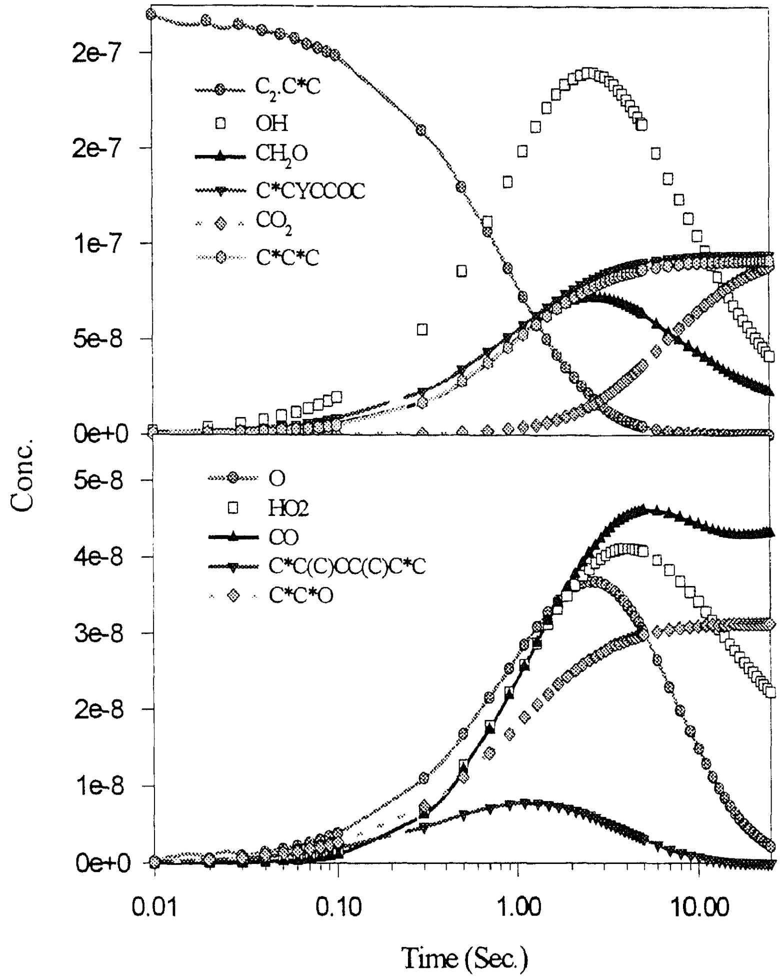

Figure 3B.6b Concentration of reactant ($C_2 \cdot C{=}C$ radical) and products vs. reaction time based on CBS-q//MP2(full)/6-31g(d) mechanism at 800K, 2.78 torr in He bath gas and [$C_2 \cdot C{=}C$] = 2×10^{10} molecules cm^{-3}. b. [O_2] = 4.84×10^{16} molecules cm^{-3}

APPENDIX 4A

TABLES IN KINETIC ANALYSIS FOR HO_2 ADDITION TO ETHYLENE, PROPENE AND ISOBUTENE AND THERMOCHEMICAL PARAMETERS FOR THE ALKYL HYDROPEROXIDES AND HYDROPEROXY ALKYL RADICALS

Table 4A.1a Geometrical Parameters (Distances in Å, Angles in Deg.) for the Reactants: Enthylene, Propene and Isobutene

		Bond Length				Bond Angle				Dihedral Angle	
		B3LYP	MP2	EXPT[17]		B3LYP	MP2	EXPT[17]		B3LYP	MP2
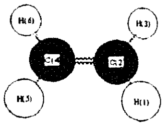	r21	1.087	1.085	1.085	a321	116.3	116.6	117.8	d4213	180.0	180.0
	r32	1.087	1.085		a421	121.9	121.7		d5421	0.0	0.0
	r42	1.331	1.335	1.339	a542	121.9	121.7		d6421	180.0	180.0
	r54	1.087	1.085		a642	121.9	121.7				
	r64	1.087	1.085								
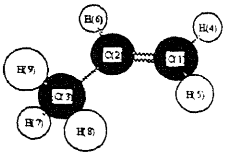	r21	1.333	1.337	1.318	a321	125.2	124.6	124.3	d4123	180.0	180.0
	r32	1.502	1.498		a412	121.8	121.7		d5123	0.0	360.0
	r41	1.087	1.085		a512	121.6	121.5		d6213	180.0	180.0
	r51	1.089	1.086		a621	118.9	119.0		d7321	239.3	239.5
	r62	1.091	1.089		a732	111.2	111.1		d8321	0.0	360.0
	r73	1.099	1.095		a832	111.5	111.0		d9321	120.7	120.4
	r83	1.095	1.093		a932	111.2	111.1				
	r93	1.099	1.095								
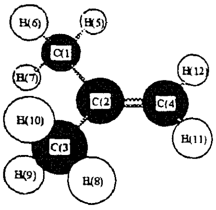	r21	1.509	1.503	1.507	a321	115.8	115.8		d4213	180.0	180.0
	r32	1.509	1.503		a421	122.1	122.1	122.4	d5123	180.0	180.0
	r42	1.337	1.339	1.330	a512	111.9	111.6		d6123	59.1	59.2
	r51	1.094	1.093		a612	111.0	110.8		d7123	300.9	300.8
	r61	1.099	1.096		a712	111.0	110.8		d8321	180.0	180.0
	r71	1.099	1.096		a832	111.9	111.6		d9321	59.1	59.3
	r83	1.094	1.093		a932	111.0	110.8		d10321	300.9	300.8
	r93	1.099	1.096		a1032	111.0	110.8		d11421	180.0	180.0
	r103	1.099	1.096		a1142	121.8	121.7		d12421	0.0	0.0
	r114	1.087	1.086		a1242	121.8	121.7				
	r124	1.087	1.086								

Table 4A.1b Geometrical Parameters (Distances in Å, Angles in Deg.) for the Product Radicals Corresponding to HO_2 Addition to Enthylene, Propene and Isobutene

	Bond Length			Bond Angle			Dihedral Angle		
		B3LYP	MP2		B3LYP	MP2		B3LYP	MP2
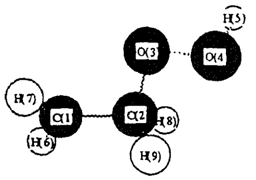	r21	1.484	1.483	a321	107.1	106.2	d4321	169.9	171.9
	r32	1.434	1.431	a432	106.4	104.9	d5432	112.7	120.5
	r43	1.457	1.467	a543	99.8	98.5	d6123	137.7	147.4
	r54	0.974	0.977	a612	121.2	120.8	d7123	314.9	317.8
	r61	1.084	1.081	a712	119.6	119.5	d8213	238.8	239.6
	r71	1.084	1.081	a821	111.8	111.9	d9213	118.2	118.3
	r82	1.100	1.097	a921	111.8	112.2			
	r92	1.104	1.100						
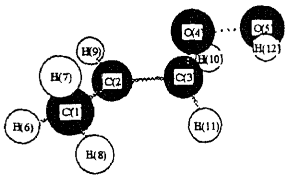	r21	1.491	1.488	a321	121.9	119.9	d4321	283.7	293.9
	r32	1.488	1.486	a432	106.9	106.4	d5432	181.3	179.5
	r43	1.445	1.442	a543	106.6	105.2	d6123	206.8	199.4
	r54	1.461	1.464	a612	111.7	111.6	d7123	87.6	79.3
	r61	1.097	1.093	a712	111.5	111.2	d8123	328.3	320.4
	r71	1.104	1.099	a812	111.6	110.9	d9213	194.4	197.3
	r81	1.097	1.095	a921	118.6	119.2	d10321	164.4	174.3
	r92	1.087	1.084	a1032	112.0	112.4	d11321	42.5	52.1
	r103	1.097	1.094	a1132	111.4	111.3	d12543	250.4	244.0
	r113	1.101	1.099	a1254	99.9	98.9			
	r125	0.974	0.977						
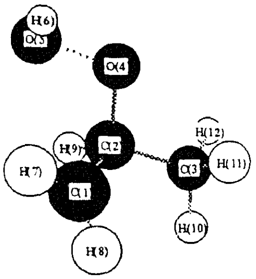	r21	1.492	1.489	a321	113.1	113.1	d4213	243.7	244.3
	r32	1.534	1.525	a421	111.5	111.1	d5421	291.3	291.3
	r42	1.445	1.439	a542	107.8	106.4	d6542	96.2	98.9
	r54	1.452	1.465	a654	100.7	99.6	d7123	245.2	258.8
	r65	0.975	0.977	a712	122.0	121.6	d8123	61.5	66.8
	r71	1.085	1.082	a812	119.4	118.9	d9213	123.6	124.1
	r81	1.087	1.084	a921	110.4	110.5	d10321	62.5	61.6
	r92	1.097	1.096	a1032	110.0	109.9	d11321	302.7	302.0
	r103	1.094	1.092	a1132	110.6	110.0	d12321	182.6	181.9
	r113	1.095	1.092	a1232	110.1	110.1			
	r123	1.095	1.092						
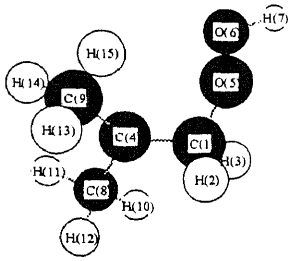	r21	1.104	1.103	a312	108.5	108.1	d4123	123.6	123.6
	r31	1.097	1.096	a412	112.0	111.9	d5123	245.2	244.7
	r41	1.497	1.493	a512	101.9	101.5	d6512	169.2	169.6
	r51	1.436	1.433	a651	105.6	104.9	d7651	96.1	95.0
	r65	1.454	1.465	a765	99.7	97.8	d8412	253.2	265.3
	r76	0.975	0.978	a841	119.0	117.6	d9412	59.0	61.7
	r84	1.495	1.491	a941	117.7	118.2	d10841	332.7	321.7
	r94	1.498	1.493	a1084	111.5	111.6	d11841	211.5	200.8
	r108	1.096	1.094	a1184	111.1	110.9	d12841	92.9	81.8
	r118	1.099	1.095	a1284	111.8	111.9	d13941	265.8	273.2
	r128	1.105	1.102	a1394	111.1	111.4	d14941	147.1	154.3
	r139	1.105	1.102	a1494	111.4	110.9	d15941	25.6	32.7
	r149	1.098	1.095	a1594	111.2	110.9			
	r159	1.095	1.093						
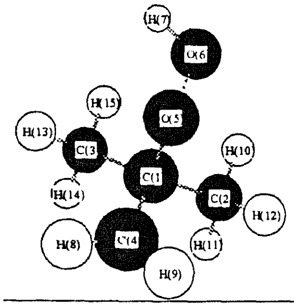	r21	1.533	1.522	a312	112.2	112.1	d4123	125.9	125.3
	r31	1.533	1.522	a412	111.6	111.2	d5123	237.7	237.7
	r41	1.496	1.494	a512	109.5	109.4	d6512	61.2	60.3
	r51	1.466	1.459	a651	109.1	107.7	d7651	110.1	114.0
	r65	1.467	1.458	a765	99.6	98.9	d8412	205.8	206.2
	r76	0.974	0.977	a841	120.7	120.5	d9412	35.9	39.3
	r84	1.085	1.083	a941	120.2	119.9	d10213	60.1	58.6
	r94	1.085	1.083	a1021	110.3	110.3	d11213	299.8	298.1
	r102	1.093	1.091	a1121	110.6	110.2	d12213	179.7	178.2
	r112	1.096	1.094	a1221	110.2	109.7	d13312	181.1	182.7
	r122	1.095	1.093	a1331	110.4	109.9	d14312	61.3	63.1
	r133	1.096	1.094	a1431	110.6	110.3	d15312	301.4	303.2
	r143	1.095	1.093	a1531	110.4	110.4			
	r153	1.094	1.091						

Table 4A.1c Geometrical Parameters (Distances in Å, Angles in Deg.) for the Transition states Corresponding to HO_2 Addition to Enthylene, Propene and Isobutene

	Bond Length			Bond Angle			Dihedral Angle		
		B3LYP	MP2		B3LYP	MP2		B3LYP	MP2
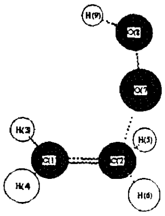 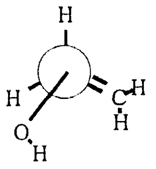 TS1	r21	1.379	1.352	a312	121.3	121.3	d4123	186.8	185.7
	r31	1.086	1.083	a521	120.1	120.7	d5213	343.1	346.2
	r52	1.085	1.082	a721	105.6	103.5	d7213	87.7	87.7
	r72	1.909	1.937	a872	109.2	108.7	d8721	273.5	280.8
	r87	1.393	1.387	a987	102.5	102.2	d9872	106.3	102.9
	r98	0.976	0.978						
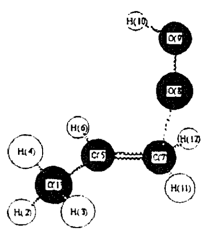 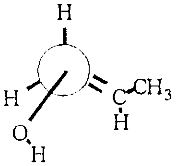 TS2A	r21	1.099	1.095	a312	108.2	108.5	d4123	244.4	243.7
	r31	1.095	1.092	a412	106.3	106.9	d5123	123.0	122.3
	r41	1.100	1.096	a512	111.2	111.0	d6512	57.3	58.0
	r51	1.496	1.492	a651	116.9	117.0	d7512	230.7	231.9
	r65	1.090	1.088	a751	124.3	124.0	d8751	275.1	275.0
	r75	1.381	1.351	a875	106.1	103.1	d9875	272.3	278.8
	r87	1.918	1.943	a987	109.1	108.6	d10987	104.7	102.5
	r98	1.396	1.390	a1098	102.5	102.2	d11751	16.8	13.9
	r109	0.976	0.977	a1175	119.3	120.2	d12751	170.4	173.1
	r117	1.087	1.085	a1275	120.1	120.8			
	r127	1.085	1.082						
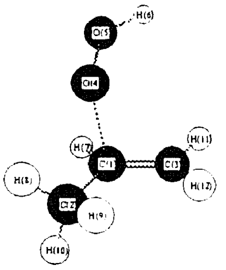 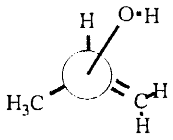 TS2B	r21	1.506	1.498	a312	121.7	122.6	d4123	250.9	254.7
	r31	1.384	1.353	a412	97.8	95.9	d5412	209.8	200.5
	r41	1.920	1.954	a541	109.3	109.8	d6541	251.0	254.3
	r54	1.396	1.388	a654	102.4	102.2	d7123	154.0	159.9
	r65	0.976	0.978	a712	115.7	116.1	d8213	152.9	146.2
	r71	1.087	1.085	a821	110.6	110.4	d9213	32.1	25.5
	r82	1.093	1.091	a921	111.2	110.8	d10213	272.5	265.7
	r92	1.095	1.092	a1021	110.1	109.9	d11312	169.4	172.1
	r102	1.098	1.094	a1131	121.3	121.3	d12312	342.2	346.2
	r113	1.086	1.083	a1231	121.1	121.2			
	r123	1.087	1.084						
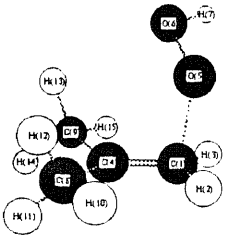 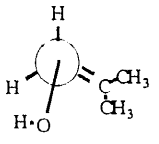 TS3A	r21	1.086	1.085	a312	115.3	115.7	d4123	154.4	159.9
	r31	1.087	1.085	a412	119.9	120.7	d5123	262.5	262.9
	r41	1.382	1.349	a512	91.2	90.1	d6512	170.4	179.4
	r51	1.933	1.953	a651	110.4	110.8	d7651	275.2	274.8
	r65	1.399	1.394	a765	102.8	102.4	d8412	17.6	15.4
	r76	0.977	0.978	a841	121.2	121.3	d9412	187.5	184.9
	r84	1.501	1.495	a941	120.8	121.2	d10841	350.3	349.6
	r94	1.500	1.494	a1084	112.1	111.7	d11841	228.8	228.0
	r108	1.094	1.092	a1184	111.2	110.9	d12841	110.6	109.7
	r118	1.099	1.096	a1284	110.7	109.9	d13941	261.9	259.5
	r128	1.100	1.096	a1394	110.1	109.3	d14941	143.2	140.6
	r139	1.101	1.097	a1494	111.6	111.2	d15941	21.2	18.9
	r149	1.098	1.095	a1594	112.1	111.8			
	r159	1.095	1.092						

Table 4A.1c (Continued)

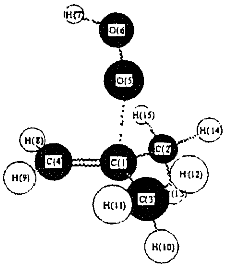

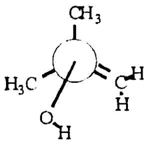

TS3B

Bond Length			Bond Angle			Dihedral Angle		
	B3LYP	MP2		B3LYP	MP2		B3LYP	MP2
r21	1.511	1.503	a312	116.0	115.9	d4123	206.9	200.3
r31	1.512	1.504	a412	119.4	120.6	d5123	100.0	98.2
r41	1.392	1.357	a512	100.1	98.3	d6512	46.1	48.4
r51	1.928	1.974	a651	111.9	111.8	d7651	107.0	107.0
r65	1.399	1.391	a765	102.2	102.0	d8412	341.8	345.5
r76	0.975	0.978	a841	121.1	121.1	d9412	168.8	171.5
r84	1.086	1.085	a941	121.1	121.3	d10312	296.2	296.8
r94	1.086	1.084	a1031	110.0	109.6	d11312	176.2	176.6
r103	1.098	1.095	a1131	111.5	111.3	d12312	55.4	55.8
r113	1.094	1.092	a1231	110.4	110.1	d13213	73.2	71.3
r123	1.094	1.092	a1321	110.0	109.5	d14213	313.6	311.9
r132	1.098	1.095	a1421	110.7	110.3	d15213	193.3	191.6
r142	1.094	1.092	a1521	111.1	110.9			
r152	1.093	1.091						

Table 4A.2a Harmonic Vibrational Frequencies (cm^{-1}) for Transition States Corresponding to HO_2 Addition to Ethylene, Propene and Isobutene

	Frequencies (Based on MP2(full)/6-31g(d) level)												moments of inertia (amu-Bohr^2)
TS1	-783.7	287.0	422.3	476.4	807.5	867.6	955.2	1048.7	1110.1	1210.3	1276.0	1347.3	103.12
	3052.6	3058.4	3139.6	3158.9	3470.9	1438.5	1546.5						411.98
													445.73
TS2A	-774.1	200.4	336.7	417.5	431.7	696.0	897.5	921.6	954.9	1019.3	1039.0	1110.0	175.62
	1169.3	1267.5	1341.5	1379.4	1413.1	1451.5	1466.6	1565.5	2917.5	2984.8	3019.5	3046.7	723.33
	3049.4	3143.4	3471.9										757.92
TS2B	-759.2	275.3	297.1	419.5	433.1	575.2	853.4	891.6	925.8	990.4	1029.1	1105.3	224.42
	1169.2	1262.2	1343.6	1371.2	1417.0	1453.9	1468.9	1546.4	2935.0	3015.6	3037.2	3044.9	541.32
	3070.7	3141.5	3471.6										689.78
TS3A	-737.7	176.3	285.2	367.8	424.4	436.2	457.3	800.0	851.8	935.3	945.6	972.0	380.31
	1010.4	1055.7	1070.2	1114.3	1288.1	1336.1	1378.8	1385.5	1399.1	1443.4	1452.6	1459.5	762.51
	1470.9	1595.6	2912.1	2916.0	2983.9	2986.4	3020.2	3026.0	3035.2	3123.1	3456.8		878.65
TS3B	-731.2	227.0	291.0	375.3	380.8	424.3	453.6	626.1	784.7	841.2	936.6	954.9	395.48
	987.1	1001.8	1053.0	1103.0	1282.5	1337.5	1368.7	1382.3	1407.3	1446.2	1457.5	1458.9	703.31
	1474.1	1541.4	2927.4	2931.9	3009.5	3014.9	3032.3	3037.5	3043.7	3133.1	3469.5		731.38
C·CQ	286.7	417.8	475.2	801.5	895.7	979.7	1059.4	1122.9	1186.6	1299.8	1344.4	488.4	54.08
	1483.4	2880.5	2939.5	3070.8	3181.7	3510.6							411.55
													444.29
CC·CQ	252.2	348.4	445.6	507.5	883.2	920.5	950.0	984.2	1117.2	1123.4	1135.3	1207.1	125.71
	1297.4	1326.3	1368.8	1393.4	1453.3	1465.2	1489.3	2897.9	2900.6	2971.0	2974.8	3011.5	708.19
	3083.9	3505.9											768.60
C·CQC	269.0	317.2	442.0	453.6	532.5	809.8	879.8	900.7	930.0	1040.5	1134.8	1149.1	218.65
	1281.9	1302.3	1343.3	1370.6	1428.3	1459.5	1470.3	2938.5	2941.3	3031.3	3033.7	3046.9	459.88
	3158.0	3496.3											611.80
C_2C·CQ	250.0	295.4	346.3	387.4	540.2	766.3	817.5	908.7	920.4	953.0	981.3	1007.2	333.11
	1057.1	1207.9	1251.4	1282.6	1303.1	1346.2	1379.2	1390.2	1436.4	1450.0	1456.8	1464.9	802.70
	1473.5	2871.5	2872.9	2876.0	2958.7	2960.6	2962.3	3005.4	3014.8	3488.5			896.31
C_3C·CQ	269.2	333.9	340.5	375.0	443.3	506.5	536.4	733.2	864.0	896.0	928.9	977.1	395.15
	1001.8	1146.3	1240.5	1263.7	1282.5	1317.5	1364.2	1377.8	1432.3	1452.3	1467.1	1471.5	624.05
	1485.2	2931.9	2936.8	3016.6	3022.6	3033.9	3039.9	3048.2	3157.7	3505.9			633.97

Table 4A.2b Harmonic Vibrational Frequencies (cm^{-1}) for Transition States Corresponding to HO_2 Addition to Ethylene, Propene and Isobutene

	Frequencies (Based on B3LYP/6-31g(d) level)												moments of inertia (amu-Bohr^2)
TS1	-496.8	291.8	404.5	455.9	786.4	790.7	897.8	995.4	1041.5	1202.4	1229.8	1354.5	103.12
	1430.7	1514.8	3044.6	3049.7	3119.2	3141.3	3501.8						411.98
													445.73
TS2A	-483.0	210.6	333.3	396.9	415.4	671.1	877.3	885.2	912.4	977.7	1006.1	1027.7	165.13
	1158.8	1236.5	1348.0	1373.1	1397.7	1445.2	1459.3	1515.9	2903.2	2943.1	2998.4	3037.5	768.75
	3042.0	3129.2	3502.7										795.53
TS2B	-476.0	280.6	300.8	400.8	422.2	507.9	765.2	869.4	913.5	932.3	992.9	1045.6	231.02
	1155.7	1230.3	1350.5	1364.2	1398.6	1449.8	1464.4	1500.0	2932.0	2992.0	3020.6	3041.9	546.88
	3060.3	3129.4	3508.7										696.66
TS3A	-466.4	166.1	285.4	362.0	407.6	426.6	442.8	778.0	835.5	889.0	939.0	959.1	368.34
	988.9	1010.1	1039.9	1046.3	1272.6	1347.1	1362.8	1379.0	1386.3	1439.6	1447.3	1454.5	818.37
	1467.0	1522.0	2900.5	2906.5	2945.6	2952.8	3001.2	3007.3	3032.9	3112.2	3483.2		953.73
TS3B	-457.9	231.0	300.6	364.6	378.9	409.0	431.4	516.5	743.9	769.2	911.7	922.6	404.17
	947.3	993.3	1032.4	1051.4	1265.2	1342.8	1348.3	1376.2	1390.0	1444.2	1452.1	1454.9	708.22
	1472.5	1493.7	2929.7	2934.0	2994.1	2999.4	3019.7	3029.5	3041.3	3128.1	3512.4		734.08
C·CQ	287.6	443.3	490.3	791.3	895.8	965.0	1037.5	1115.3	1190.9	1326.9	1344.0	459.0	53.85
	1469.9	2857.1	2910.9	3063.3	3166.3	3555.2							415.46
													445.78
CC·CQ	260.9	346.8	455.3	518.0	858.2	869.8	917.4	927.5	971.0	1121.9	1125.1	1203.4	118.22
	1311.1	1327.5	1367.2	1380.9	1445.3	1456.1	1482.4	2871.6	2890.3	2943.6	2957.0	2984.5	748.63
	3067.2	3549.4											795.50
C·CQC	269.5	320.4	436.2	460.7	541.5	807.6	881.1	896.3	916.8	1010.9	1122.9	1141.2	220.61
	1281.0	1334.7	1341.3	1367.5	1423.0	1453.9	1467.1	2941.1	2942.2	3015.2	3018.2	3040.4	464.00
	3144.3	3542.2											618.78
C_2C·CQ	234.8	293.8	350.0	384.4	534.6	750.7	835.2	911.0	917.1	946.0	971.6	982.7	343.72
	1028.2	1203.9	1254.4	1269.4	1331.4	1342.2	1372.4	1387.3	1429.0	1442.3	1448.1	1457.8	805.43
	1466.8	2848.3	2853.0	2866.2	2926.7	2934.3	2955.8	2985.6	2993.1	3540.6			903.20
C_3C·CQ	258.7	328.6	336.2	372.8	439.7	505.1	556.6	724.0	826.3	843.2	879.4	926.9	401.54
	966.5	998.1	1123.1	1220.0	1255.6	1309.4	1363.2	1377.0	1427.2	1448.4	1463.1	1467.7	633.34
	1481.6	2936.5	2943.2	3002.2	3008.1	3018.3	3027.0	3047.1	3148.3	3560.5			643.22

Table 4A.3 Total Energy, Zero-Point Vibrational Energies, Thermal Correction, And Internal Rotation Barriers of TS1 and 2-Hydroperoxy-1-Ethyl Radical

Torsion angle		Total energy (hartree)		ZPVE[a]	$H_{thermal}$[b]	Rotational barrier (kcal/mole)[c]	
		MP2(full)/6-31g(d)	CBS-Q[d]	Kcal/mole		MP2(full)/6-31g(d)	CBS-Q[d]
TS1	**CC-OOH**						
	-5	-228.7621645	-229.1274687	3.41	42.18	2.71	3.43
	0	-228.7620629	-229.1272540	3.41	42.18	2.77	3.56
	5	-228.7620359	-229.1271514	3.41	42.18	2.78	3.63
	30	-228.7628320	-229.1281435	3.42	42.17	2.28	3.02
	60	-228.7644161	-229.1303841	3.44	42.18	1.33	1.52
	75.20	-228.7647060	-229.1311215	3.44	42.23	1.19	1.05
	90	-228.7644496	-229.1307296	3.43	42.28	1.38	1.31
	115	-228.7634505	-229.1297802	3.41	42.29	2.01	1.98
	120	-228.7632756	-229.1297161	3.41	42.28	2.11	2.02
	125	-228.7631293	-229.1297196	3.41	42.27	2.19	2.02
	150	-228.7628813	-229.1303355	3.42	42.20	2.28	1.64
	175	-228.7630742	-229.1300503	3.42	42.16	2.13	1.78
	180	-228.7630975	-229.1296801	3.42	42.16	2.11	2.01
	210	-228.7633215	-229.1293380	3.41	42.21	2.01	2.26
	240	-228.7647700	-229.1301744	3.40	42.32	1.21	1.73
	270	-228.7665092	-229.1323222	3.42	42.33	0.14	0.27
	280.70	-228.7666916	-229.1327393	3.43	42.30	0.00	0.00
	300	-228.7660909	-229.1322836	3.43	42.23	0.31	0.29
	330	-228.7636625	-229.1297477	3.41	42.19	1.77	2.01
	360	-228.7620629	-229.1272616	3.41	42.18	2.77	3.56
	CCO-OH						
	0	-228.7474757	-229.1151436	3.75	42.09	12.17	11.51
	30	-228.7517307	-229.1191947	3.72	41.65	9.03	8.93
	60	-228.7609838	-229.1274317	3.44	42.04	3.34	3.35
	90	-228.7661446	-229.1322706	3.43	42.23	0.27	0.29
	103.01	-228.7666916	-229.1327375	3.43	42.30	0.00	0.00
	120	-228.7657577	-229.1317874	3.43	42.36	0.66	0.61
	150	-228.7600745	-229.1264396	3.55	42.33	4.31	4.07
	180	-228.7523517	-229.1180858	3.77	42.37	9.42	9.68
	190	-228.7509029	-229.1156923	3.81	42.39	10.38	11.22
	195	-228.7507782	-229.1160681	3.83	42.31	10.41	11.01
	200	-228.7511861	-229.1151786	3.85	42.16	10.01	11.58
	210	-228.75318	-229.1188890	3.84	41.92	8.51	9.24
	240	-228.7605883	-229.1273410	3.54	42.08	3.73	3.53
	270	-228.7645911	-229.1310102	3.45	42.22	1.26	1.12
	275.73	-228.764706	-229.1311229	3.44	42.23	1.19	1.05
	300	-228.7626601	-229.1287587	3.44	42.22	2.46	2.53
	330	-228.755464	-229.1244116	3.58	42.01	6.91	5.40
	360	-228.7474757	-229.1151436	3.75	42.09	12.17	11.51
C·CQ	**C·-COOH**						
	0	-228.8124851	-229.1598939	41.82	3.93	0.46	0.27
	0.28	-228.8124854	-229.1598863	41.83	3.93	0.46	0.27
	30	-228.8129459	-229.1598838	41.87	3.90	0.19	0.10
	42.24	-228.8130662	-229.1597073	41.97	3.89	0.20	0.16
	60	-228.8128063	-229.1592828	42.30	3.85	0.65	0.57
	90	-228.8121396	-229.1584321	42.59	3.82	1.33	1.07
	92.31	-228.8121347	-229.1584197	42.59	3.82	1.33	1.08
	120	-228.8127581	-229.1590216	42.46	3.83	0.82	0.71
	147.35	-228.8134071	-229.1599021	42.02	3.86	0.00	0.00
	180	-228.8126679	-229.1599364	41.84	3.93	0.36	0.23
	197.04	-228.8124388	-229.1597525	41.83	3.93	0.49	0.35
	210	-228.8125460	-229.1597816	41.84	3.92	0.43	0.32
	240	-228.8129126	-229.1592929	42.39	3.84	0.66	0.53
	248.92	-228.8129302	-229.1591378	42.53	3.82	0.78	0.63
	263.58	-228.8129203	-229.1589532	42.66	3.81	0.91	0.74
	270	-228.8129270	-229.1589273	42.69	3.81	0.92	0.75
	300	-228.8131254	-229.1592107	42.55	3.82	0.67	0.58
	308.86	-228.8131546	-229.1592939	42.42	3.83	0.53	0.47
	330	-228.8129498	-229.1596399	41.98	3.89	0.28	0.25
	360	-228.8124854	-229.1598902	41.83	3.93	0.46	0.27

Table 4A.3 (Continued)

Torsion angle	Total energy (hartree)		ZPVE[a]	$H_{thermal}$[b]	Rotational barrier (kcal/mole)[c]	
	MP2(full)/6-31g(d)	CBS-Q[d]	Kcal/mole		MP2(full)/6-31g(d)	CBS-Q[d]
C·C-OOH						
-1.02	-228.8037463	-229.1498706	42.03	3.80	6.83	6.48
30	-228.8071461	-229.1542549	41.80	3.37	3.68	3.76
66.98	-228.813076	-229.1589102	41.77	3.41	0.58	0.62
90	-228.8111734	-229.1577259	41.79	3.42	1.51	1.54
116.52	-228.8090495	-229.1559429	42.06	3.77	3.02	2.70
150	-228.8119317	-229.1589051	41.77	3.44	0.67	0.68
172.03	-228.8134071	-229.1597629	41.81	3.45	0.00	0.00
210	-228.8095028	-229.1567332	41.99	3.78	2.95	2.63
239.16	-228.8087762	-229.1558283	41.99	3.84	3.34	2.95
240	-228.8083101	-229.1553129	41.99	3.78	3.60	3.27
270	-228.8123781	-229.1585331	42.11	3.72	1.39	1.12
300	-228.813511	-229.1592246	42.22	3.75	1.04	0.74
289.36	-228.8141222	-229.159871	42.14	3.74	0.52	0.23
330	-228.8067175	-229.1541645	41.90	3.88	4.42	4.00
358.98	-228.8037463	-229.1498706	42.03	3.80	6.83	6.48
C·CO-OH						
0	-228.8016037	-229.1517770	41.97	3.93	7.42	5.84
0.17	-228.8016036	-229.1517754	41.97	3.93	7.42	5.84
30	-228.8044058	-229.1539892	41.90	3.94	5.61	4.45
60	-228.8095432	-229.1570267	42.06	3.77	2.38	1.94
90	-228.8126289	-229.1594660	42.09	3.77	0.47	0.41
120	-228.8134069	-229.1601160	42.02	3.86	0.00	0.00
120.49	-228.8134071	-229.1601187	42.02	3.86	0.00	0.00
150	-228.8131274	-229.1610336	42.03	3.90	0.23	0.03
180	-228.8128132	-229.1606958	42.06	3.90	0.46	0.25
191.07	-228.8127838	-229.1605611	42.05	3.91	0.47	0.33
210	-228.8128679	-229.1605997	42.01	3.92	0.39	0.31
238.88	-228.8130701	-229.1598785	41.97	3.90	0.21	0.15
238.99	-228.8130699	-229.1598915	41.97	3.90	0.20	0.14
240	-228.8130694	-229.1598873	41.97	3.89	0.20	0.15
270	-228.8123060	-229.1593540	42.06	3.79	0.66	0.49
300	-228.8092943	-229.1705722	42.03	3.78	2.52	1.92
330	-228.8043895	-229.1541411	41.87	3.94	5.59	4.36
360	-228.8016037	-229.1517764	41.97	3.93	7.42	5.84

a. ZPVE with the frequency of the torsion motion about CC-OOH bond excluded.

b. Thermal Correction to 298K with the frequency of the torsion motion about CC-OOH bond excluded.

c. Rotational barriers are calculated as the difference in total energies + scaled (0.9661) zero-point vibrational energies + thermal correction to 298K, where the corresponding torsional frequencies are excluded in the calculation of ZPVE and Thermal correction.

d. Base on MP2(full)/6-31g(d) geometry.

Table 4A.4 Coefficients (kcal/mole) of Truncated Fourier Series Representation Expansions[c] for Internal Rotation Potentials

Rotors	*a0*	*a1*	*a2*	*a3*	*a4*	*a5*	*a6*	*a7*	*b1*	*b2*	*b3*	*b4*	*b5*	*b6*	*b7*
C·CQ															
C·-COOH	0.5618[a]	0.0138	-0.3985	0.0419	0.2054	-0.0005	0.0414	-0.0058	0.0429	0.0268	-0.1603	0.0806	0.0036	0.0349	0.0018
	0.4464[b]	0.0065	-0.3657	0.0212	0.1355	-0.0028	0.0348	-0.0058	0.0372	0.0007	-0.1373	0.0565	-0.0091	0.0281	0.0034
C·CO-OH	2.4806[a]	1.2368	1.1111	2.0146	-0.1030	-0.1342			-0.2974	0.1828	-0.5166	0.1677	-0.1514		
	2.4924[b]	1.3292	1.0178	1.8799	0.0279	0.0285			-0.3355	0.2506	-0.5356	0.1788	-0.1043		
C·CO-OH	2.1674[a]	3.1012	1.7196	0.3747					-0.0878	0.0332	0.0064				
	1.6856[b]	2.4781	1.3244	0.3076					-0.0366	0.0694	-0.0218				
TS1															
CC···OOH	1.6413[a]	-0.0636	0.8428	0.3880	-0.0419	0.0025			0.5474	0.0520	-0.0785	0.0187	-0.0044		
	1.8005[b]	0.2684	0.9549	0.6074	-0.0229	-0.0645			0.4226	0.3646	-0.1058	0.1127	-0.0206		
CCO-OH	5.1966[a]	0.9758	4.9889	0.1881	0.6336	0.1109			-0.6566	1.5190	-0.2362	0.3780	-0.0645		
	4.0687[b]	-0.8364	3.2036	-0.9274					-0.7771	1.1543	-0.8809				

a. Rotational bonds is calculated at MP2(full)/6-31g(d) level of theory

b. Rotational bonds is calculated at CBS-Q//MP2(full)/6-31g(d) level of theory

c. $V(\Phi)=a_0+a_i\cos(i\Phi)+b_i\sin(i\Phi)$, $i = 1,2,3\ldots$

Table 4A.5 Calculation of S°_{298} and Cp(T) Contribution from Internal Rotor for 2-Hydroperoxy-1-Ethyl Radical and TS1

Rotors			S°_{298} cal/mole K	Cp_{300} cal/mole K	Cp_{400}	Cp_{500}	Cp_{600}	Cp_{800}	Cp_{1000}	Cp_{1500}	Ir[e] amu-Å^2	V_{mean}[f] kcal/mole	N[g]
C·CQ													
	C--COOH	P&G[a]	4.92	1.38	1.25	1.17	1.12	1.07	1.04	1.02	1.70	0.91	3
		P&G[b]	5.00	1.26	1.16	1.10	1.07	1.04	1.02	1.01	1.70	0.73	3
		ROT[c]	4.92	1.37	1.24	1.17	1.12	1.07	1.05	1.02			
		ROT[d]	4.97	1.30	1.19	1.13	1.09	1.05	1.03	1.01			
	C·CO-OH	P&G[a]	5.41	2.18	2.29	2.32	2.25	2.03	1.81	1.45	15.55	4.48	3
		P&G[b]	5.50	2.21	2.31	2.29	2.20	1.95	1.73	1.40	15.55	4.15	3
		ROT[c]	5.49	2.30	2.32	2.26	2.14	1.83	1.54	0.98			
		ROT[d]	5.42	2.83	2.57	2.34	2.13	1.76	1.46	0.93			
	C·CO-OH	P&G[a]	2.92	1.96	2.14	2.16	2.08	1.86	1.66	1.36	0.91	3.95	2
		P&G[b]	3.20	2.07	2.11	2.01	1.88	1.63	1.45	1.23	0.91	3.09	2
		ROT[c]	3.50	1.32	1.35	1.39	1.43	1.48	1.49	1.43			
		ROT[d]	3.57	1.34	1.39	1.44	1.48	1.50	1.47	1.36			
TS1													
	CC···OOH	P&G[a]	6.03	2.30	2.13	1.93	1.75	1.49	1.35	1.16	13.93	2.53	2
		P&G[b]	5.97	2.31	2.17	1.97	1.79	1.53	1.37	1.18	13.93	2.64	2
		ROT[c]	5.65	3.50	2.87	2.32	1.94	1.45	1.15	0.72			
		ROT[d]	5.41	3.37	2.53	1.85	1.38	0.83	0.55	0.25			
	CCO-OH	P&G[a]	1.99	1.26	1.57	1.78	1.91	2.11	2.23	2.22	0.91	11.29	2
		P&G[b]	2.03	1.30	1.61	1.81	1.94	2.14	2.24	2.19			
		ROT[c]	1.71	2.33	2.35	2.29	2.23	2.18	2.14	2.00	0.91	10.59	2
		ROT[d]	1.93	2.09	2.29	2.42	2.46	2.39	2.23	1.83			

a. Use of Pitzer and Gwinn approximation and rotational barrier based on MP2(full)/6-31g(d) level of theory.
b. Use of Pitzer and Gwinn approximation and rotational barrier based on CBS-Q//MP2(full)/6-31g(d) level of theory.
c. Using direct integration over energy levels of the exact potential energy curve of the rotational barriers which are calculated at MP2(full)/6-31g(d) level of theory.
d. Using direct integration over energy levels of the exact potential energy curve of the rotational barriers which are calculated at CBS-Q//MP2(full)/6-31g(d) level of theory.
e. Reduced moments of inertia are calculated about the rotational bonds based on MP2(full)/6-31g(d) level of theory.
f. Arithmetic mean of rotational barriers.
g. Number of potential maxima

Table 4A.6 Internal Rotor Contribution to Entropies and Heat Capacities Obtained Using Pitzer and Gwinn Approximation

	Rotors[a]	S°_{298}	Cp_{300}	Cp_{400}	Cp_{500}	Cp_{600}	Cp_{800}	Cp_{1000}	Cp_{1500}	Ir[b]	V_{mean}[c]	n[d]
		cal/mole K				cal/mole K				amu-Å^2	kcal/mole	
CC·CQ												
	C-C.COOH	5.49	1.29	1.18	1.12	1.08	1.04	1.03	1.01	2.83	0.74	3
	CC.-COOH	6.92	1.91	1.63	1.45	1.34	1.20	1.13	1.06	18.52	1.5	3
	CC.C-OOH	5.82	2.23	2.32	2.30	2.21	1.95	1.73	1.40	21.55	4.15	3
	CC.CO-OH	3.20	2.07	2.12	2.02	1.88	1.63	1.45	1.23	0.92	3.09	2
	Total int.rotors	**21.43**	**7.50**	**7.24**	**6.88**	**6.50**	**5.82**	**5.34**	**4.70**			
C·CQC												
	C.-C(C)OOH	4.79	1.57	1.39	1.28	1.20	1.12	1.07	1.03	1.72	1.2	3
	C-C(C.)OOH	4.08	2.06	2.20	2.19	2.09	1.85	1.65	1.35	3.06	3.87	3
	C(C.)C-OOH	5.43	2.10	2.22	2.30	2.33	2.23	2.06	1.66	21.67	5.76	3
	C(C.)CO-OH	3.20	2.07	2.11	2.02	1.88	1.63	1.45	1.23	0.92	3.09	2
	Total int.rotors	**17.50**	**7.81**	**7.93**	**7.78**	**7.50**	**6.83**	**6.24**	**5.27**			
C_2C·CQ												
	C-C.(C)COOH (x2)	10.31	3.66	3.18	2.85	2.64	2.38	2.25	2.11	3.03	1.5	3
	C2C.COOH	6.94	2.21	1.96	1.74	1.58	1.37	1.25	1.11	27.47	2.1	3
	C2C.C-OOH	5.92	2.23	2.32	2.30	2.21	1.96	1.73	1.40	23.91	4.15	3
	C2C.CO-OH	3.20	2.07	2.12	2.02	1.88	1.63	1.45	1.23	0.92	3.09	2
	Total int.rotors	**26.37**	**10.17**	**9.57**	**8.91**	**8.30**	**7.33**	**6.68**	**5.85**			
C_3·CQ												
	C-C(C.)(C)OOH (x2)	7.71	3.90	4.31	4.46	4.42	4.08	3.66	2.96	3.06	4.7	3
	C.-C(C2)OOH	4.63	1.75	1.55	1.40	1.31	1.18	1.12	1.05	1.73	1.5	3
	C2C(C.)-OOH	5.32	2.05	2.15	2.24	2.30	2.32	2.22	1.85	24.15	7.0	3
	C2C(C.)O-OH	3.19	2.07	2.11	2.01	1.88	1.63	1.45	1.23	0.91	3.09	2
	Total int.rotors	**20.85**	**9.77**	**10.12**	**10.12**	**9.91**	**9.21**	**8.46**	**7.09**			
TS2A												
	C-CCQ	5.21	1.77	1.52	1.37	1.27	1.16	1.10	1.04	2.95	1.34	2
	CCC-OOH	6.25	2.32	2.17	1.97	1.79	1.53	1.37	1.18	18.51	2.64	2
	CCCO-OH	2.03	1.30	1.61	1.81	1.95	2.14	2.24	2.19	0.89	10.59	2
	Total int.rotors	**13.50**	**5.39**	**5.30**	**5.15**	**5.01**	**4.83**	**4.72**	**4.41**			
TS2B												
	C-C(OOH)C	5.05	1.94	1.70	1.52	1.40	1.24	1.16	1.07	3.03	1.71	3
	CC(C)-OOH	6.30	2.32	2.17	1.97	1.79	1.53	1.37	1.18	19.49	2.64	2
	CC(C)O-OH	2.03	1.30	1.61	1.81	1.95	2.14	2.24	2.19	0.89	10.59	2
	Total int.rotors	**13.39**	**5.56**	**5.49**	**5.30**	**5.13**	**4.92**	**4.77**	**4.44**			
TS3A												
	C-C(C)COOH (x2)	10.13	3.79	3.32	2.97	2.73	2.44	2.29	2.13	2.95	1.63	3
	C2CC-OOH	6.37	2.32	2.17	1.97	1.79	1.53	1.37	1.18	20.93	2.64	2
	C2CCO-OH	2.04	1.30	1.61	1.81	1.95	2.15	2.24	2.19	0.90	10.59	2
	Total int.rotors	**18.54**	**7.41**	**7.10**	**6.75**	**6.47**	**6.12**	**5.90**	**5.50**			
TS3B												
	C-C(C)2OOH (x2)	9.59	4.19	3.83	3.44	3.13	2.73	2.50	2.23	3.05	2.15	3
	C3C-OOH	6.41	2.32	2.17	1.97	1.79	1.53	1.37	1.18	21.76	2.64	2
	C3CO-OH	2.04	1.30	1.61	1.81	1.95	2.15	2.24	2.19	0.90	10.59	2
	Total int.rotors	**18.03**	**7.82**	**7.61**	**7.22**	**6.87**	**6.41**	**6.11**	**5.60**			

a. Reduced moments of inertia are calculated about the rotational bonds based on MP2(full)/6-31g(d) level of theory.

b. Arithmetic mean of rotational barriers.

c. Number of potential maxima

Table 4A.7 Enthalpy Data Used in Isodesmic Reactions to Determine $\Delta H_f{}^\circ{}_{298}$ of Other Species

Compound	$\Delta H_f{}^\circ{}_{298}$ in kcal/mole	source
COOH	-31.8	Ref. 15
COH	-48.08	Ref. 21
CCOH	-56.21	Ref. 22
CCCOH	-60.97	Ref. 22
C_2COH	-65.20	Ref. 22
C_2CCOH	-67.85	Ref. 22
C_3COH	-74.69	Ref. 22
HOO·	3.5	Ref. 23

Table 4A.8a Reaction Enthalpies of Group Isodesmic Reactions Used in SCHEME 2

	CBS-q[a]	MP2(full) /6-31g(d)	MP4(Full) /6-31G(d,p)	CBS-q	B3LYP /6-31g(d)	B3LYP /6-311+g(3df,2p)
	//MP2(Full)/6-31G(d)			//B3LYP/6-31G(d)		
CCQ+COH=+CCOH+COOH	-0.41	0.12	0.23	-0.42	-0.10	-0.32
CCCQ+COH=CCCOH+COOH	0.50	-0.34	-0.46	0.52	-0.74	-0.24
C$_2$CQ+COH=C$_2$COH+COOH	0.19	0.19	0.16	0.30	-0.59	-0.35
C$_2$CCQ+COH=C$_2$CCOH+COOH	-0.15	-0.34	-0.34	-0.03	-0.62	-0.49
C$_3$CQ+COH=C$_3$COH+COOH	-0.42	-0.18	-0.08	-0.30	-1.16	-1.20

Table 4A.8b Reaction Enthalpies of Group Isodesmic Reactions Used in SCHEME 3

	CBS-q[a]	MP2(full) /6-31g(d)	MP4(Full) /6-31G(d,p)	CBS-q	B3LYP /6-31g(d)	B3LYP /6-311+g(3df,2p)
	//MP2(Full)/6-31G(d)			//B3LYP/6-31G(d)		
CCQ+C·C=C·CQ+CC[b]	1.64	1.90	1.84	1.79	1.45	1.37
CCCQ+ C·CQ =CC·CQ+CCQ	-2.53	-3.08	-3.26	-3.04	-4.79	-4.29
C_2CQ+ C·CQ =C·CQC+ CCQ	-1.88	-2.00	-2.21	0.13	-0.28	-0.03
C_2CCQ+ C·CQ =C_2C·CQ+ CCQ	-6.25	-5.78	-6.16	-6.41	-8.89	-7.54
C_3CQ+ C·CQ =C_3·CQ+ CCQ	1.10	1.66	1.15	0.52	-0.03	0.49

Table 4A.8c Calculated Enthalpies of Formation[a] for Alkyl-Hydroperoxides and Alkyl-Hydroperoxy Radicals Using Group Isodesmic Reactions in SCHEME 2 and SCHEME 3

	CBS-q	MP2(full) /6-31g(d)	MP4(Full) /6-31G(d,p)	CBS-q	B3LYP /6-31g(d)	B3LYP /6-311+g(3df,2p)		
	//MP2(Full)/6-31G(d)			//B3LYP/6-31G(d)				
CCQ	-39.52	-40.05	-40.16	-39.51	-39.83	-39.61	-39.9	-39.71[d]; -38.9[c]; -41.92[j]
CCCQ	-45.19	-44.35	-44.23	-45.21	-43.95	-44.45		
CCQC	-49.11	-49.11	-49.08	-49.22	-48.33	-48.57	-49.0	-49.0[f]; -49.3[g]; -47.5[h];-43.5[c]; -51.0[j]
C$_2$CCQ	-51.42	-51.23	-51.23	-51.54	-50.95	-51.08		
C$_3$CQ	-57.99	-58.23	-58.33	-58.11	-57.25	-57.21	-58.4	-58.8[i]; -57.1[f]; -57.6[h]; -57.4[c]; -59.63[j]
C·CQ	11.12	10.85	10.69	11.27	10.62	10.77		
CC·CQ	2.96	3.24	3.18	2.43	1.92	1.93		
C·CQC	-0.32	-0.45	-0.62	1.59	2.06	2.07		
C$_2$C·CQ	-6.99	-6.35	-6.72	-7.29	-9.17	-7.95		
C$_3$·CQ	-6.22	-5.91	-6.51	-6.92	-6.60	-6.05		

a. in kcal/mole; b Calculated reaction enthalpies are 1.40 (kcal/mole) and 1.77 (kcal/mole) based on CBS-Q and G2 calculations; c.ref.15; d.ref.24; e.ref.25; f.ref.26; g.ref.27; h.ref.5; i.ref.28; j.ref.29

Table 4A.9 Ideal Gas Phase Thermodynamic Properties

Species[a]		Hf^{o}_{298}[b]	S^{o}_{298}[c]	Cp(300)[c]	Cp(400)	Cp(500)	Cp(600)	Cp(800)	Cp(1000)	Cp(1500)
					THERM					
ETHYLENE		12.50	52.30	10.34	12.72	14.86	16.76	19.94	22.37	26.10
PROPENE		4.65	63.81	15.45	19.23	22.72	25.79	30.74	34.49	40.39
ISOBUTENE		-3.80	69.99	21.58	26.65	31.30	35.34	41.91	46.89	54.71
					CBS-q//MP2(full)/6-31g(d)					
C·CQ	TVR[d]		68.29	14.62	18.06	21.19	23.84	27.98	31.07	36.07
	Internal Rotor[e]		13.96	5.47	5.15	4.91	4.7	4.31	3.96	3.3
	Total	11.12	82.25	20.09	23.21	26.1	28.54	32.29	35.03	39.37
CC·CQ	TVR		69.9	16.69	21.51	26.11	30.12	36.46	41.18	48.66
	Internal Rotor		21.43	7.5	7.24	6.88	6.5	5.82	5.34	4.7
	Total	2.96	91.33	24.19	28.75	32.99	36.62	42.28	46.52	53.36
CCQC·	TVR		70.6	18.18	23.11	27.56	31.35	37.28	41.71	48.85
	Internal Rotor		17.5	7.81	7.93	7.78	7.5	6.83	6.24	5.27
	Total	-0.32	88.1	25.99	31.04	35.34	38.85	44.11	47.95	54.12
$C_2C{\cdot}CQ$	TVR		71.41	19.9	26.2	32.17	37.38	45.66	51.83	61.53
	Internal Rotor		26.37	10.17	9.57	8.91	8.3	7.33	6.68	5.85
	Total	-6.99	97.78	30.07	35.77	41.08	45.68	52.99	58.51	67.38
$C_3{\cdot}CQ$	TVR		71.95	21.77	28.01	33.7	38.59	46.35	52.18	61.54
	Internal Rotor		20.85	9.77	10.12	10.12	9.91	9.21	8.46	7.09
	Total	-6.22	92.8	31.54	38.13	43.82	48.5	55.56	60.64	68.63
TS1	TVR		68.9	14.66	18.1	21.2	23.82	27.89	30.94	35.93
	Internal Rotor		7.34	5.46	4.82	4.27	3.84	3.22	2.78	2.08
	Total	29.57	76.24	20.12	22.92	25.47	27.66	31.11	33.72	38.01
TS2A	TVR		71.24	17.62	22.41	26.87	30.71	36.79	41.35	48.67
	Internal Rotor		13.5	5.39	5.3	5.15	5.01	4.83	4.72	4.41
	Total	20.50	84.74	23.01	27.71	32.02	35.72	41.62	46.07	53.08
TS2B	TVR		70.96	18	22.81	27.22	31.01	36.98	41.47	48.71
	Internal Rotor		13.39	5.56	5.49	5.3	5.13	4.92	4.77	4.44
	Total	19.47	84.35	23.56	28.3	32.52	36.14	41.9	46.24	53.15
TS3A	TVR		72.8	21.03	27.16	32.91	37.91	45.88	51.88	61.44
	Internal Rotor		18.54	7.41	7.1	6.75	6.47	6.12	5.9	5.5
	Total	10.39	91.34	28.44	34.26	39.66	44.38	52	57.78	66.94
TS3B	TVR		72.59	21.75	27.93	33.59	38.48	46.25	52.11	61.51
	Internal Rotor		18.03	7.82	7.61	7.22	6.87	6.41	6.11	5.6
	Total	7.44	90.62	29.57	35.54	40.81	45.35	52.66	58.22	67.11
					CBS-q/B3LYP/6-31g(d)					
C·CQ	TVR		68.25	14.78	18.32	21.49	24.15	28.29	31.37	36.31
	Internal Rotor		13.96	5.47	5.15	4.91	4.7	4.31	3.96	3.3
	Total	11.27	82.21	20.25	23.47	26.40	28.85	32.60	35.33	39.61
CC·CQ	TVR		70.02	17.27	22.31	26.96	30.94	37.19	41.82	49.11
	Internal Rotor		21.43	7.5	7.24	6.88	6.5	5.82	5.34	4.7
	Total	2.43	91.45	24.77	29.55	33.84	37.44	43.01	47.16	53.81
CCQC·	TVR		70.7	18.51	23.54	28.02	31.81	37.72	42.13	49.17
	Internal Rotor		17.5	7.81	7.93	7.78	7.5	6.83	6.24	5.27
	Total	1.59	88.20	26.32	31.47	35.80	39.31	44.55	48.37	54.44
$C_2C{\cdot}CQ$	TVR		71.7	20.39	26.84	32.87	38.09	46.35	52.47	62.02
	Internal Rotor		26.37	10.17	9.57	8.91	8.3	7.33	6.68	5.85
	Total	-7.29	98.07	30.56	36.41	41.78	46.39	53.68	59.15	67.87
$C_3{\cdot}CQ$	TVR		72.39	22.72	29.22	34.95	39.79	47.37	53.05	62.12
	Internal Rotor		20.85	9.77	10.12	10.12	9.91	9.21	8.46	7.09
	Total	-6.92	93.24	32.49	39.34	45.07	49.70	56.58	61.51	69.21
TS1	TVR		69.22	15.31	18.87	21.97	24.53	28.48	31.44	36.27
	Internal Rotor		7.34	5.46	4.82	4.27	3.84	3.22	2.78	2.08
	Total	29.12	76.56	20.77	23.69	26.24	28.37	31.70	34.22	38.35
TS2A	TVR		71.54	18.35	23.3	27.79	31.6	37.57	42.03	49.14
	Internal Rotor		13.5	5.39	5.3	5.15	5.01	4.83	4.72	4.41
	Total	19.75	85.04	23.74	28.60	32.94	36.61	42.40	46.75	53.55
TS2B	TVR		71.41	18.87	23.81	28.21	31.93	37.77	42.14	49.16
	Internal Rotor		13.39	5.56	5.49	5.3	5.13	4.92	4.77	4.44
	Total	18.93	84.80	24.43	29.30	33.51	37.06	42.69	46.91	53.60
TS3A	TVR		73.39	21.83	28.16	33.96	38.94	46.81	52.7	62.02
	Internal Rotor		18.54	7.41	7.1	6.75	6.47	6.12	5.9	5.5
	Total	10.52	91.93	29.24	35.26	40.71	45.41	52.93	58.60	67.52

Table 4A.9 (Continued)

Species		Hf°_{298}[b]	S°_{298}[c]	Cp(300)[c]	Cp(400)	Cp(500)	Cp(600)	Cp(800)	Cp(1000)	Cp(1500)
				CBS-q/B3LYP/6-31g(d)						
TS3B	TVR		73.15	22.86	29.15	34.79	39.6	47.21	52.93	62.08
	Internal Rotor		18.03	7.82	7.61	7.22	6.87	6.41	6.11	5.6
	Total	7.08	91.18	30.68	36.76	42.01	46.47	53.62	59.04	67.68

a. Thermodynamic properties are referred to a standard state of an ideal gas of pure enantiometer at 1 atm.
b. In kcal mole^{-1}.
c. In cal mole^{-1}K^{-1}.
d. The sum of contributions from translation, external rotation, vibration, optical isomer, and spin degeneracy.
e. S°_{298} and Cp(T) contributions from hindered rotors.

Table 4A.10a Total Energies (0K, Hartree), Zero-Point Vibrational Energies (ZPVE, kcal/mole) and Thermal Corrections to Enthalpies ($H_{thermal}$, kcal/mole). Based on MP2(full)/6-31g(d) Geometries

	CBS-q	MP2(full)/6-31g(d)	MP4(full)/6-31g(d,p)	ZPVE	$H_{thermal}$	Spin Contamination (S^2)	
		// MP2(full)/6-31g(d)				MP2	CBS-q
HO_2	-150.7691008	-150.502365	-150.5380066	9.03	2.38		
C_2H_4	-78.456045	-78.294286	-78.363698	32.69	2.50		
C=CC	-117.7049391	-117.4696584	-117.5715729	51.23	3.14		
C_2C=C	-156.9556433	-156.6463965	-156.7808087	69.45	3.90		
TS1	-229.2019201	-228.7666916	-228.872815	43.93	3.88	1.004	0.761
TS2a	-268.4531959	-267.9432248	-268.0822207	62.25	4.80	0.993	0.761
TS2b	-268.4547135	-267.9442604	-268.0831538	62.10	4.72	0.994	0.761
TS3a	-307.7067101	-307.1220775	-307.2938753	80.41	5.66	0.982	0.761
TS3b	-307.7111594	-307.1231334	-307.2948341	80.16	5.50	0.988	0.761

Table 4A.10b Total Energies (0K, Hartree), Zero-Point Vibrational Energies (ZPVE, kcal/mole) and Thermal Corrections to Enthalpies ($H_{thermal}$, kcal/mole). Based on B3LYP/6-31g(d) Geometries

	CBS-q	B3lyp/6-31g(d)	B3lyp/6-311+g(3df,2p)	ZPVE	$H_{thermal}$	Spin Contamination (S^2)	
	// B3lyp/6-31g(d)					MP2	CBS-q
HO_2	-150.7692372	-150.8991541	-150.9676579	2.39	8.80		
C_2H_4	-78.45610003	-78.5874573	-78.6210637	2.50	32.14		
C=CC	-117.7052425	-117.9075542	-117.9535269	3.15	50.24		
C_2C=C	-156.9561062	-157.2272862	-157.285488	3.92	68.08		
TS1	-229.2029457	-229.471956	-229.5712395	3.95	42.46	0.782	0.763
TS2a	-268.454965	-268.7930636	-268.9051628	4.89	60.27	0.779	0.763
TS2b	-268.4562084	-268.7919922	-268.9039991	4.84	60.12	0.781	0.763
TS3a	-307.7073561	-308.113774	-308.2383777	5.83	77.92	0.778	0.763
TS3b	-307.7126306	-308.1107498	-308.2351148	5.71	77.63	0.782	0.763

Table 4A.11a Reaction Enthalpies for HO_2 Addition to Ethylene, Propene and Isobutene, at 298 K

	Ethylene	Propene		Isobutene	
Computation Level	CD/H2 (P)	CD/H2 (P)	CD/C/H (S)	CD/H2 (P)	CD/C2 (T)
B3LYP/6-31g(d)	9.75	9.12	9.60	8.50	9.99
B3LYP/6-311+g(3df,2p)// B3LYP/6-31g(d)	11.52	10.62	11.15	9.82	11.46
* CBS-q// B3LYP/6-31g(d)	13.12	11.60	10.78	10.82	7.38
MP2(full)/6-31g(d)	19.93	19.26	18.39	17.98	16.92
MP4(full)/6-31g(d,p)//MP2(full)/6-31g(d)	19.26	18.35	17.55	16.89	15.88
* CBS-q// MP2(full)/6-31g(d)	13.57	12.35	11.32	10.69	7.74

* choose
unit: kcal/mole
include thermal correction and zero-point energy correction

Table 4A.11b Experimental Rate[a] Constants for Reactions of HO_2 Addition with Olefins

		A (s−1 or cc/mol-s)	E_a (kcal/mol)	T (K)
Ethylene	CD/H2 (P)	3.80×10^{12}	17.85	653-793
(E)-but−2-ene	CD/C/H (S)	4.07×10^{11}	11.95	673-793
2,3-dimethylbut-2-ene	CD/C2 (T)	3.80×10^{11}	8.46	653-793

a. Ref. 6a-e.

Table 4A.12 Mulliken Charge for All Species Calculated at MP2(full)/6-31g(d) Level

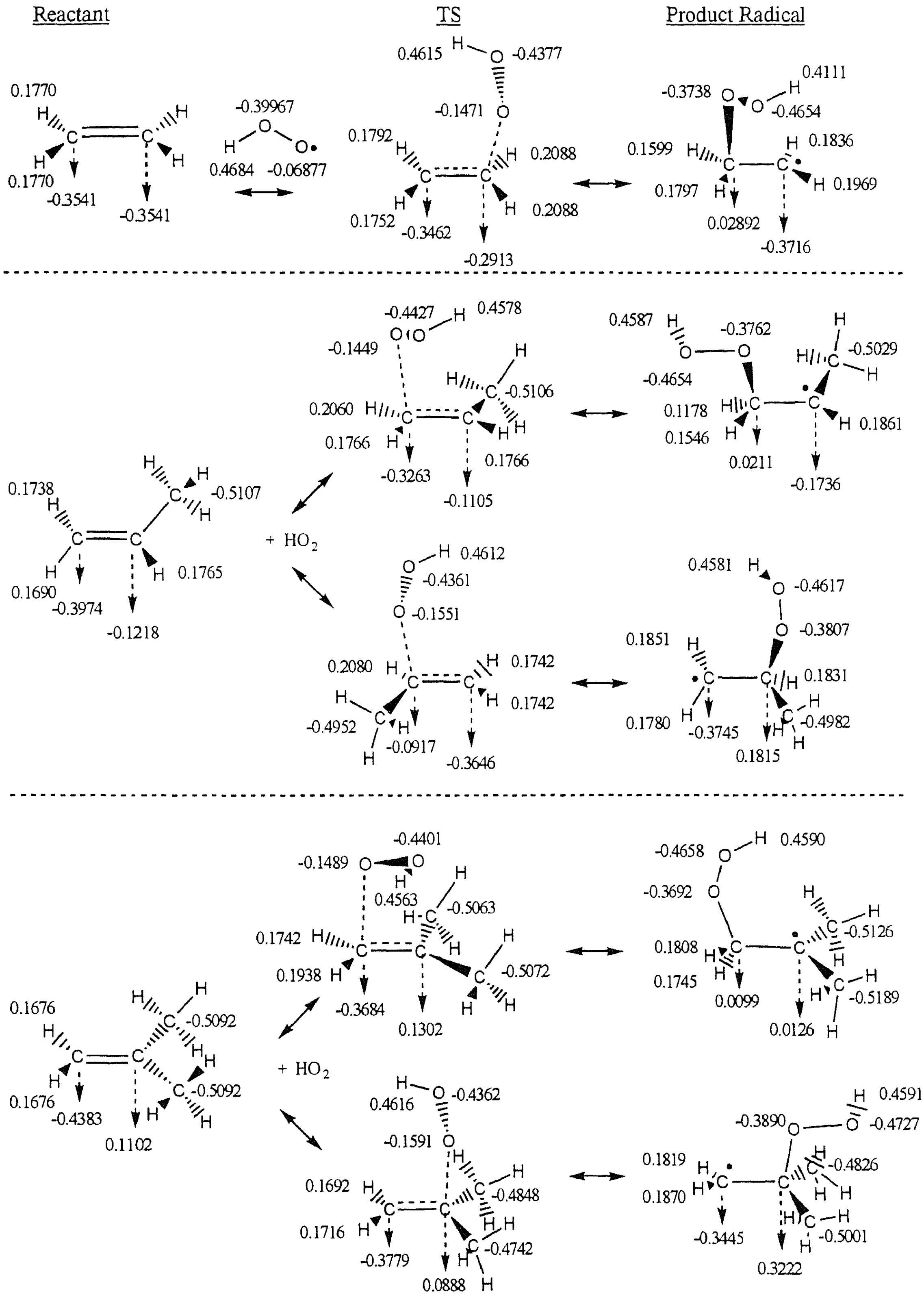

Table 4A.13a Rate Constants k_∞ determined from TST and Reaction Enthalpies Using CBSq//MP2(full)/6-31g(d)

Reaction	A (s^{-1} or cm^3/mol-s)	n	Ea (kcal/mole)
Forward			
C_2H_4+HO_2=TS1	4.13E+04	2.3323	13.49
C_3H_6+HO_2=TS2A	2.47E+04	2.1322	12.16
C_3H_6+HO_2=TS2B	7.74E+03	2.2849	11.08
i-C_4H_8+HO_2=TS3A	3.45E+05	1.7648	10.70
i-C_4H_8+HO_2=TS3B	2.78E+04	2.1061	7.63
Reverse			
C·CQ=TS1	3.89E+10	0.4809	18.87
CC·CQ=TS2A	7.33E+09	0.6457	17.68
C·CQC=TS2B	3.65E+12	-0.0771	20.32
C_2C·CQ=TS3A	2.00E+10	0.5005	17.58
C_3·CQ=TS3B	4.89E+13	-0.3253	14.43

Reaction	A_{300}	A_{800}	A_{1500}	K_{300}	K_{800}	K_{1500}
		(s^{-1} or cm^3/mol-s)			(s^{-1} or cm^3/mol-s)	
Forward						
C_2H_4+HO_2=TS1	7.95E+10	1.00E+12	3.70E+12	3.71E+00	5.05E+07	1.15E+10
C_3H_6+HO_2=TS2A	1.74E+10	1.15E+11	4.66E+11	6.52E+00	1.82E+07	2.47E+09
C_3H_6+HO_2=TS2B	1.43E+10	1.19E+11	5.08E+11	3.00E+01	3.13E+07	3.40E+09
i-C_4H_8+HO_2=TS3A	2.14E+10	9.32E+10	3.14E+11	1.31E+02	5.49E+07	3.85E+09
i-C_4H_8+HO_2=TS3B	1.49E+10	1.09E+11	4.09E+11	1.27E+04	2.98E+08	1.05E+10
Reverse						
C·CQ=TS1	3.04E+11	6.02E+11	7.45E+11	1.08E-02	6.77E+06	2.33E+09
CC·CQ=TS2A	2.26E+11	3.73E+11	5.96E+11	3.81E-02	8.09E+06	2.18E+09
C·CQC=TS2B	9.40E+11	6.80E+11	7.68E+11	3.69E-03	6.12E+06	2.27E+09
C_2C·CQ=TS3A	2.43E+11	3.27E+11	4.94E+11	5.40E-02	8.92E+06	2.13E+09
C_3·CQ=TS3B	2.07E+12	1.39E+12	1.27E+12	2.36E+02	6.36E+08	3.58E+10

Table 4A.13b Rate Constants k_∞ Determined from TST and Reaction Enthalpies Using CBSq//B3LYP/6-31g(d)

Reaction	A	n	Ea
	(s^{-1} or cm^3/mol-s)		(kcal/mole)
Forward			
C_2H_4+HO_2=TS1	6.97E+03	2.6280	12.89
C_3H_6+HO_2=TS2A	2.30E+03	2.5130	11.20
C_3H_6+HO_2=TS2B	7.40E+02	2.6762	10.34
i-C_4H_8+HO_2=TS3A	2.62E+04	2.1984	10.59
i-C_4H_8+HO_2=TS3B	1.59E+03	2.5839	7.03
Reverse			
C·CQ=TS1	1.80E+10	0.6306	18.21
CC·CQ=TS2A	6.52E+09	0.6781	17.45
C·CQC=TS2B	1.35E+12	0.1047	17.79
C_2C·CQ=TS3A	1.15E+10	0.6102	17.97
C_3·CQ=TS3B	6.02E+13	-0.3446	14.79

Reaction	A_{300}	A_{800}	A_{1500}	K_{300}	K_{800}	K_{1500}
		(s^{-1} or cm^3/mol-s)			(s^{-1} or cm^3/mol-s)	
Forward						
C_2H_4+HO_2=TS1	9.36E+10	1.67E+12	7.17E+12	9.23E+00	8.95E+07	2.05E+10
C_3H_6+HO_2=TS2A	2.02E+10	2.04E+11	1.01E+12	2.66E+01	3.95E+07	5.14E+09
C_3H_6+HO_2=TS2B	1.80E+10	2.37E+11	1.23E+12	9.24E+01	6.51E+07	7.28E+09
i-C_4H_8+HO_2=TS3A	2.89E+10	2.03E+11	8.59E+11	1.41E+02	8.09E+07	7.21E+09
i-C_4H_8+HO_2=TS3B	1.99E+10	2.54E+11	1.21E+12	3.05E+04	6.09E+08	2.43E+10
Reverse						
C·CQ=TS1	3.65E+11	8.93E+11	1.18E+12	3.53E-02	1.29E+07	4.02E+09
CC·CQ=TS2A	2.47E+11	4.26E+11	6.93E+11	6.03E-02	1.04E+07	2.66E+09
C·CQC=TS2B	1.12E+12	1.04E+12	1.26E+12	2.67E-01	3.75E+07	7.43E+09
C_2C·CQ=TS3A	2.83E+11	4.45E+11	6.98E+11	3.04E-02	8.40E+06	2.41E+09
C_3·CQ=TS3B	2.20E+12	1.47E+12	1.33E+12	1.41E+02	5.47E+08	3.39E+10

APPENDIX 4B

FIGURES IN THE KINETIC ANALYSIS FOR HO_2 ADDITION TO ETHYLENE, PROPENE AND ISOBUTENE AND THERMOCHEMICAL PARAMETERS FOR THE ALKYL HYDROPEROXIDES AND HYDROPEROXY ALKYL RADICALS

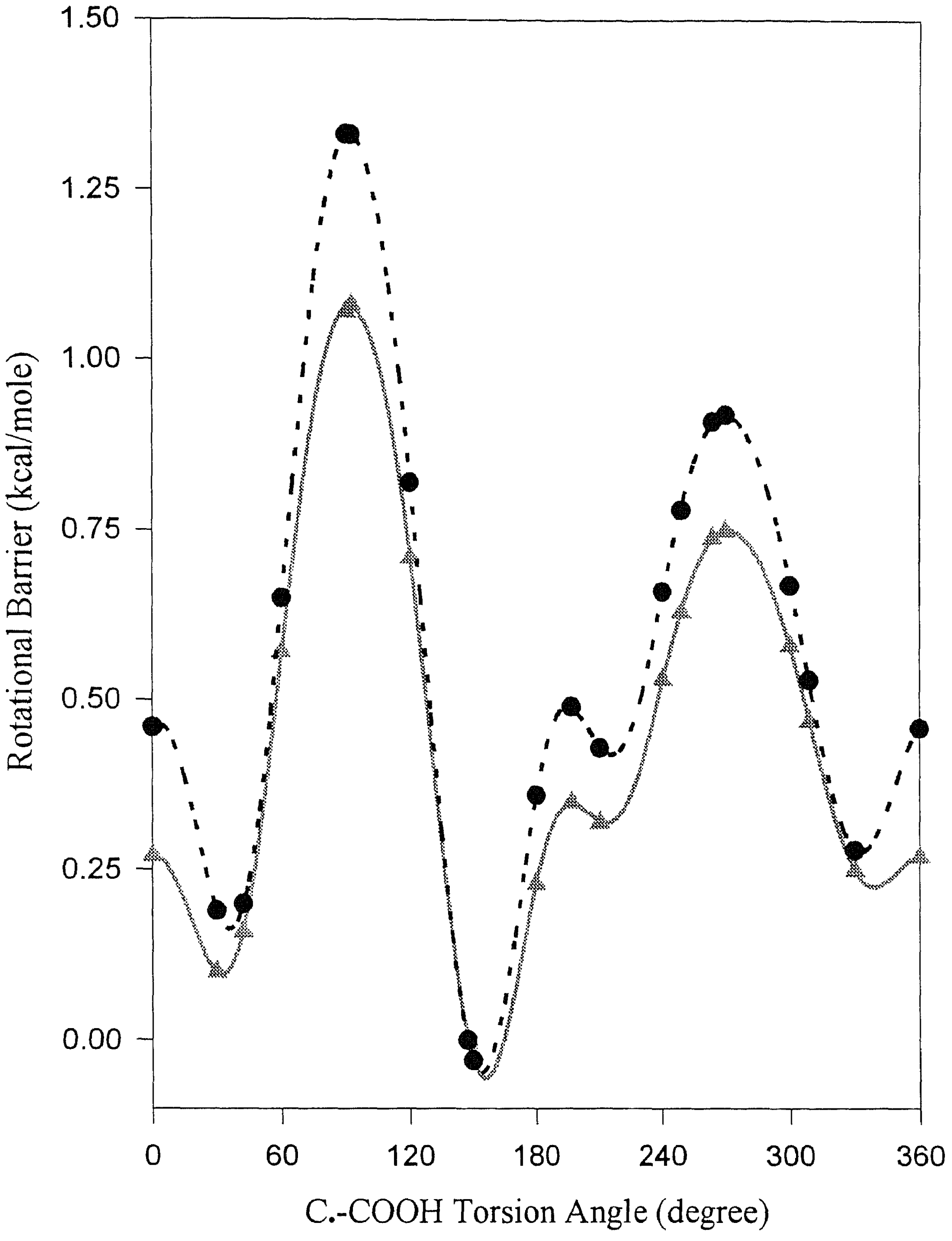

Figure 4B.1a Potential barriers for internal rotations about C·-COOH bonds in 2-hydroperoxy-1-ethyl radical. Points are calculated values at MP2(full)/ 6-31g(d) and CBS-Q// MP2(full)/6-31g(d) levels of theory, in circles and triangles, respectively. Lines are results of Fourier expansion equation, F1, with the coefficients listed in Table 4B.4.

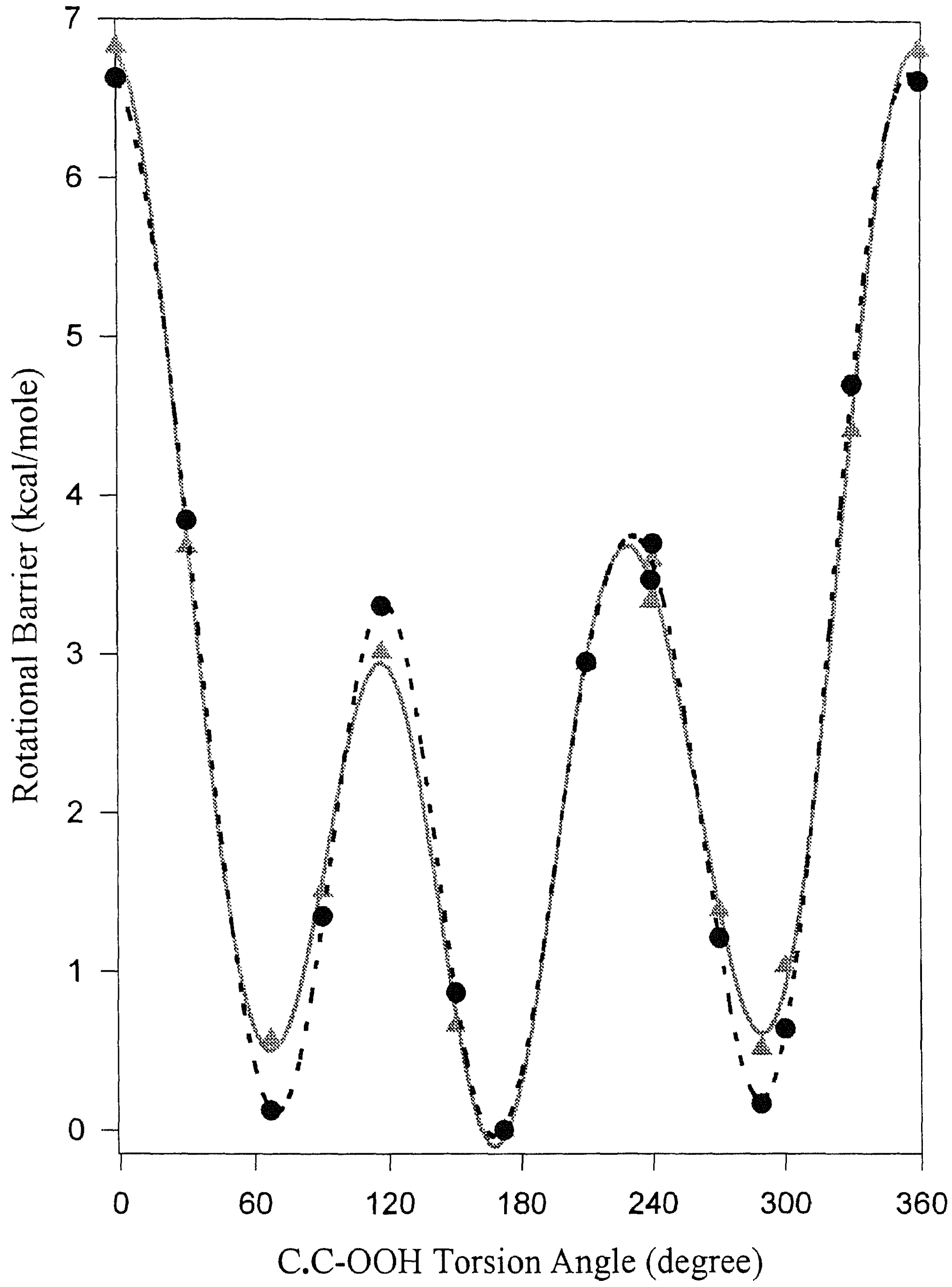

Figure 4B.1b Potential barriers for internal rotations about C-C-OOH bonds in 2-hydroperoxy-1-ethyl radical. Points are calculated values at MP2(full)/ 6-31g(d) and CBS-Q// MP2(full)/6-31g(d) levels of theory, in circles and triangles, respectively. Lines are results of Fourier expansion equation, F1, with the coefficients listed in Table 4B.4.

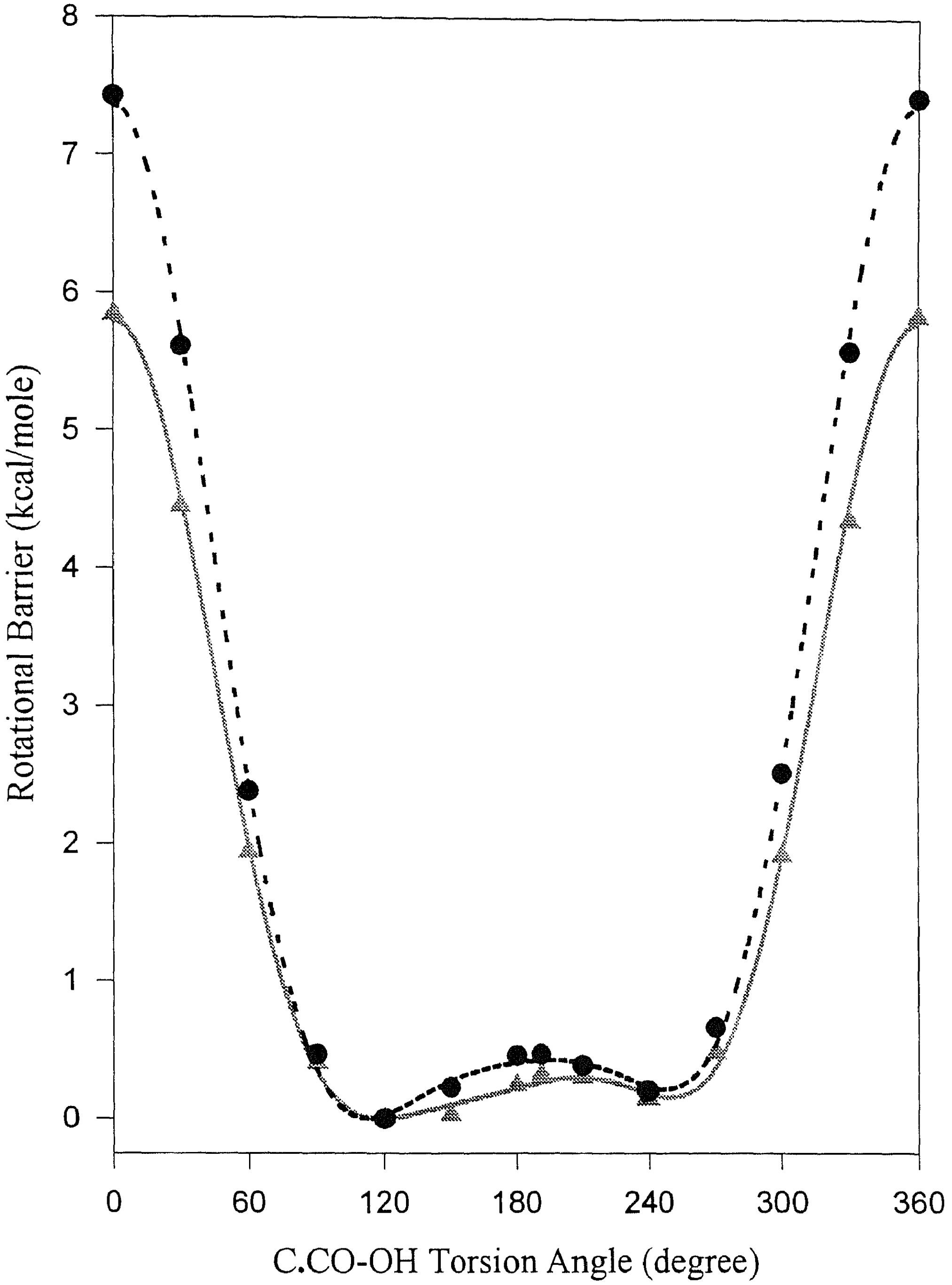

Figure 4B.1c Potential barriers for internal rotations about C·CO-OH bonds in 2-hydroperoxy-1-ethyl radical. Points are calculated values at MP2(full)/ 6-31g(d) and CBS-Q// MP2(full)/6-31g(d) levels of theory, in circles and triangles, respectively. Lines are results of Fourier expansion equation, F1, with the coefficients listed in Table 4B.4.

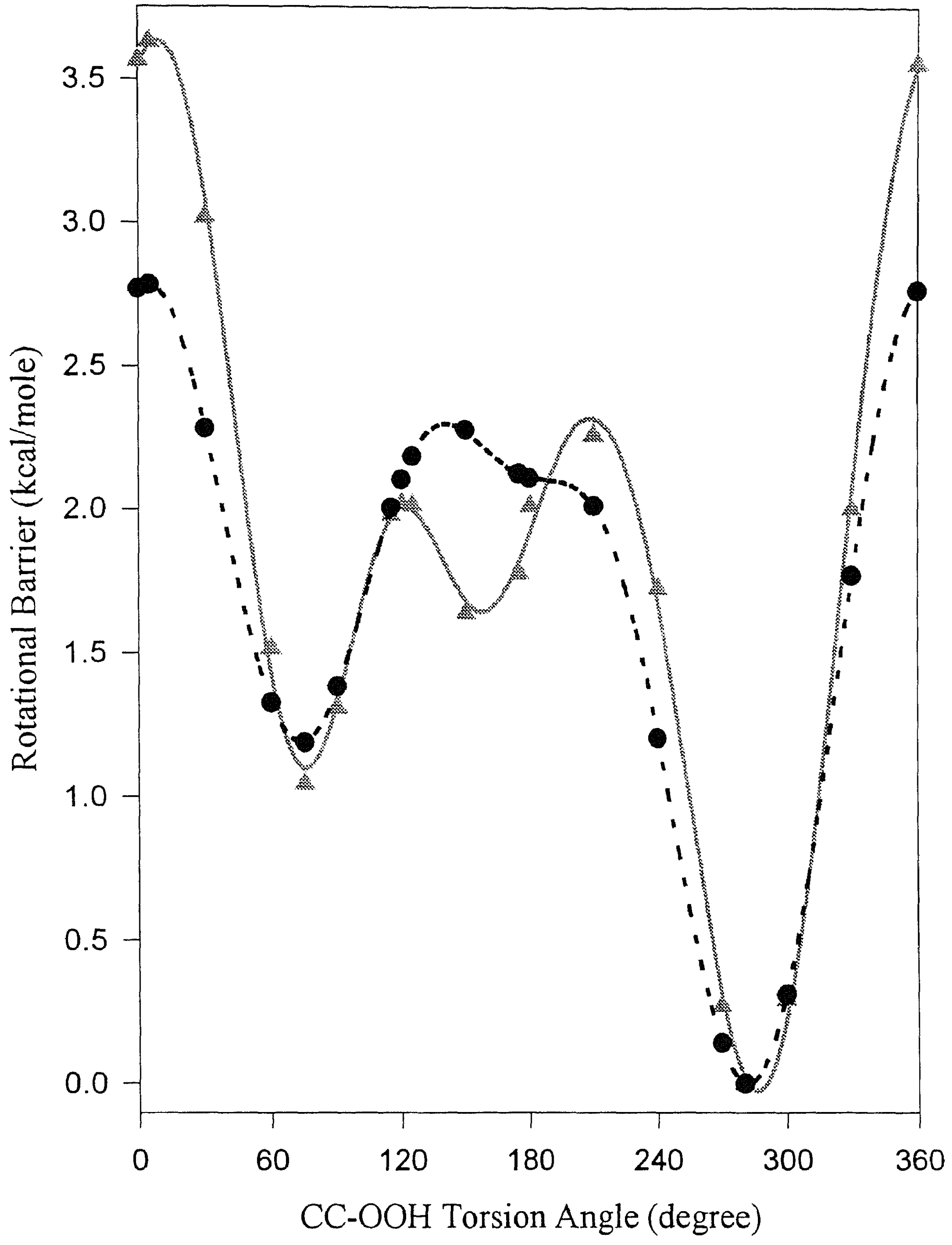

Figure 4B.2a Potential barriers for internal rotations about CC-OOH bonds in TS1. Points are calculated values at MP2(full)/6-31g(d) and CBS-Q// MP2(full)/6-31g(d) levels of theory, in circles and triangles, respectively. Lines are results of Fourier expansion equation, F1, with the coefficients listed in Table 4B.4.

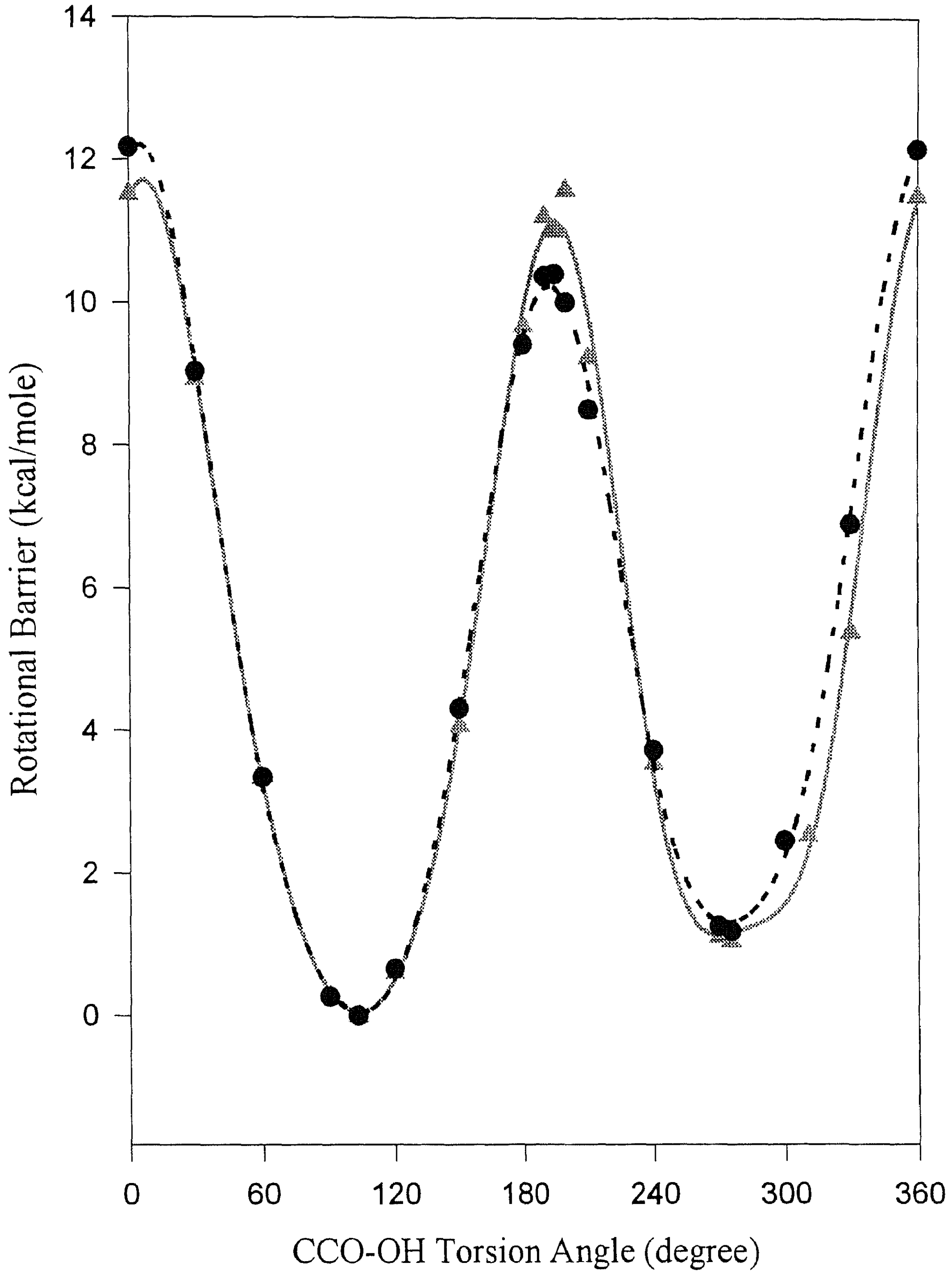

Figure 4B.2b Potential barriers for internal rotations about CCO-OH bonds in TS1. Points are calculated values at MP2(full)/6-31g(d) and CBS-Q// MP2(full)/6-31g(d) levels of theory, in circles and triangles, respectively. Lines are results of Fourier expansion equation, F1, with the coefficients listed in Table 4B.4.

APPENDIX 5A

TABLES IN THE METHYL *TERT*-BUTYL ETHER OXIDATION AND PYROLYSIS EXPERIMENT: COMPARISON WITH MODEL

Table 5A.1 Average Retention Time and Relative Response Factors for 1% Alltech AT-1000 on Graphpac GB column

Compound	Retention Time (min)	Relative Response Factor (RRF)
CH_4	1.3	0.22
C_2H_2	1.83	0.35
C_2H_4	2.09	0.43
C_2H_6	2.45	0.44
$CHCCH_3$ (C#CC)	5.99	0.60
Propene (C=CC)	6.37	0.64
Propane (CCC)	6.58	0.64
Iso-butane (C_3C)	10.89	0.84
Acrolein (C=C-C=O)	11.36	0.6
Iso-Butene (C_2C=C)	11.81	0.82
Acetone (C_2C=O)	13.37	0.65
Methyl Acetate (CC=OOC)	14.22	0.8
Isobutyraldehyde (C_2CC=O)	15.09	0.79
Methacrolein (C=C(C)C=O)	16.98	0.86
MTBE	19.49	1.00
2,5 Dimethylhexa-1,5-diene (DIC_2.C*C)	29.74	1.6

Table 5A.2 Average Retention Time and Relative Response Factors for Poropak Q Column

Compound	Retention Time (min)	Relative Response Factor (RRF)
CO	0.94	0.18
CH_4	1.16	0.19
CO_2	3.9	0.18
C_2H_4 (C=C)	4.56	0.36
C_2H_6 (CC)	5.26	0.37
C_2H_2 (C#C)	7.6	0.26
Propane (CCC)	10.86	0.51
Propene (C=CC)	10.94	0.50
CH_2O	11.91	0.17
CHCCH3 (C#CC)	12.88	0.56
Iso-butane (C_3C)	14.54	0.66
CH_3OH	15.4	0.216
Iso-Butene (C_2C=C)	15.48	0.63
MTBE		1

Table 5A.3 Reaction Enthalpies for $C_2C{\cdot}OC + O_2$ Reaction System

Group Balance Isodesmic Reactions[a]	CBS-4	CBS-q	B3LYP /6-31g(d)	B3LYP /6-311+g(3df,2p)
			//B3LYP/6-31g(d)	
C_2COC + CCOH = CCOC + C_2COH[b]	-2.18	-2.12	-3.23	-2.86
C_2COC + $COC{\bullet}$ = **$C_2C{\bullet}OC$** + COC[b]	-2.18	-2.12	-3.23	-2.86
C_2CQOC + COC + CCOH = $C_2C(OC)_2$ + CCOOH + COH	2.13	2.15	3.24	2.77
C_2COOH + COH = C_2COH + COOH	0.30	0.30	-0.59	-0.35
C*C(C)Q + COH = C*C(C)OH + COOH	-2.55	-2.66	-4.03	-3.60
C2CYCOCO + COH + CCCOH + COC = CC + CH2(OH)2 + C2C(OC)2 + YCCOC	2.96	3.19	3.46	4.74
C_2CQOC + $COO{\bullet}$ = **$C_2CQ{\bullet}OC$** + COOH	-1.58	-1.88	-0.34	-0.74
C_2CQOC + $COC{\bullet}$ = **$C_2CQOC{\bullet}$** + COC	-0.16	-0.10	-0.33	-0.34
C_2CQOC + $CC{\bullet}$ = **$C_2{\bullet}CQOC$** + CC	2.54	2.41	1.19	1.84
C_2COOH + $CC{\bullet}$ = **$C_2C{\bullet}OOH$** + CC	-51.12	-51.39	-51.08	-51.52
C_2COOH + $C{\bullet}OOH$ = **$C_2C{\bullet}OOH$** + COOH	-48.54	-48.28	-47.14	-48.15

Reactions	CBS-4	CBS-q	B3LYP /6-31g(d)	B3LYP /6-311+g(3df,2p)
			//B3LYP/6-31g(d)	
$C_2CQ{\bullet}OC$ -> TSC2COC1	18.37	18.49	21.20	18.74
$C_2CQOC{\bullet}$ -> TSC2COC1	6.79	4.01	2.71	5.97
$C_2CQOC{\bullet}$ -> TSC2COC2	23.20	16.62	12.13	12.09
$C_2C{\bullet}OOH + CH_2O$ -> TSC2COC2	55.48	50.41	45.58	50.12
$C_2CQ{\bullet}OC$ -> TSC2COC4	26.93	25.51	22.63	19.23
C*C(C)OC + HO_2 -> TSC2COC4	4.38	2.74	-2.10	3.42
$C_2{\bullet}CQOC$ -> TSC2COC5	19.26	12.20	12.71	10.77
C*C(C)OC + HO_2 -> TSC2COC5	15.44	11.20	13.08	14.97
$C_2{\bullet}CQOC$ -> TSC2COC6	28.61	20.25	16.34	15.68
C*C(C)Q + CH_3O -> TSC2COC6	7.07	0.80	-0.29	3.67
$C_2C{\bullet}OC$ -> TSC2COC7[b]	27.46	20.07	17.59	16.87
$C_2C{*}O{+}CH_3$ -> TSC2COC7[b]	26.13	20.70	16.16	18.70
$C_2CQ{\bullet}OC$ -> TSC2COC8	36.84	21.63	36.75	31.19
$C_2CYCOCO$ + OH -> TSC2COC8	62.15	45.09	37.61	40.37

UNIT: kcal/mole

a. Reaction enthalpies include thermal correction and zero-point energy correction

b. Based on B3LYP/6-31g(d,p) geometries

Table 5A.4 Reaction Enthalpies for C$_2$C*C + OH Reaction System

Group Balance Isodesmic Reactions[a]	CBS-4	CBS-q	B3LYP /6-31g(d, p)	B3LYP /6-311+g(3df,2p)
			//B3LYP/6-31g(d,p)	
C$_2$CCOH + CC = CCOH + C3C	0.07	0.09	0.04	-0.46
C$_2$CCOH + CC• = **C$_2$C•COH** + CC	-3.80	-4.03	-7.50	-6.17
C$_2$CCOH + CH$_3$O = **C$_2$CCO•** + CH$_3$OH	0.27	0.07	-0.85	-0.55
C$_2$CCOH + CC• = **C$_2$•CCOH** + CC	0.65	0.58	-0.19	0.31
C$_3$COH = C$_2$CCOH	6.81	7.11	6.18	5.74
C$_3$COH + CC• = **C$_3$•COH** + CC	1.58	1.61	0.80	1.11
C$_3$COH + CH$_3$O• = **C$_3$CO•** + CH$_3$OH	3.50	3.50	1.64	1.48
C$_2$CC*O + CC = CH$_3$C*O + C3C	-0.89	-0.85	-0.77	-0.86
C$_2$CC*O + CC• = **C$_2$•CC*O** + CC	0.25	0.00	-0.46	-0.18
C$_2$CC*O + CC• = **C$_2$C•C*O** + CC	-14.07	-17.85	-20.69	-18.97
C$_2$CC*O + CC• = **C$_2$CC•*O** + CC	-11.93	-12.36	-13.08	-12.05

Reactions	CBS-4	CBS-q	B3LYP /6-31g(d, p)	B3LYP /6-311+g(3df,2p)
			//B3LYP/6-31g(d, p)	
C$_3$•COH -> TSC2YCCHO	31.02	28.68	24.99	27.37
C$_3$CO• -> TSC2YCCHO	25.34	24.34	26.84	25.71
C$_3$CO• -> TSC3COJ	14.83	10.67	14.29	11.64
C$_2$C*O + CH$_3$ -> TSC3COJ	12.30	8.71	10.67	12.91
C$_2$C•COH -> TSC2YCCOH	30.83	28.35	29.89	31.37
C$_2$CCO• -> TSC2YCCOH	23.00	21.80	25.92	24.46
C$_2$CCO• -> TSC2CCDOXH	23.08	19.93	25.62	23.17
C$_2$CC*O+H -> TSC2CCDOXH	7.76	3.62	2.88	3.59
C$_2$CCO• -> TSC2CXCH2O	7.50	9.38	11.89	9.07
CC•C + CH$_2$O -> TSC2CXCH2O	-2.62	-0.36	1.54	3.16
C$_2$CCO• -> TSCYCCOHC	19.93	19.17	20.00	19.11
C$_2$•CCOOH -> TSCYCCOHC	23.31	21.11	16.65	19.54
C$_2$•CCOOH -> TSC2DCXCOH	31.96	25.64	23.52	21.87
C*CC + C.H$_2$OH -> TSC2DCXCOH	10.87	6.05	6.61	9.36

UNIT: kcal/mole

a. Reaction enthalpies include thermal correction and zero-point energy correction

Table 5A.5 Reaction Enthalpies for C*C(C)OC + OH Reaction System

Group Balance Isodesmic Reactions[a]	CBS-4	CBS-q	B3LYP /6-31g(d)	B3LYP /6-311+g(3df,2p)
			//B3LYP/6-31g(d)	
COCICCOH + CC = C_2COC + CCOH	-0.86	-0.69	-0.01	-1.74
COCICCOH + CC• = **COCI•CCOH** + CC	-7.65	-8.01	-9.42	-9.55
COCICCOH + COC• = **C•OCICCOH** + COC	-0.78	-0.74	-0.75	-0.83
COCICCOH + CC• = **COCIC•COH** + CC	1.06	1.13	0.23	0.67
CCCOH + CC• = **CC•COH** + CC	-2.29	-2.35	-3.80	-3.28
C_2COHOC + COC = $C_2C(OC)_2$ + CH_3OH	2.34	2.35	4.36	4.00
C_2COHOC + CH_3O = **C_2CO•OC** + CH_3OH	3.16	2.67	1.92	1.48
C_2COHOC + COC• = **C_2COHOC•** + COC	-0.40	-0.40	-0.80	-0.67
C_2COHOC + CC• = **C_2•COHOC** + CC	1.90	1.87	0.63	
C_2COH + CC• = **C_2C•OH** + CC	-8.13	-8.33	-9.83	-9.09

Reactions	CBS-4	CBS-q	B3LYP /6-31g(d)	B3LYP /6-311+g(3df,2p)
			//B3LYP/6-31g(d)	
COCI•CCOH -> TCOYCCOHYC	35.18	32.16	30.26	33.00
CC•OC + CH_2O -> TCH2OCCJOC	1.62	-2.13	0.42	0.77
COCIC•COH -> TCOYCCOHC	23.83	21.31	17.76	20.51
COCIC•COH -> TCH3OXCDCCOH	28.41	20.22	15.38	14.47
C*CCOH + CH_3O -> TCH3OXCDCCOH	6.20	0.66	5.21	1.46
COCIC•COH -> TCJH2OHXCDCOC	29.41	23.92	21.44	19.55
C*COC + C•H2OH -> TCJH2OHXCDCOC	11.66	7.61	7.03	10.90
C•CICCOH -> TCYCCOHCO	10.58	7.60	4.44	8.13
C•OCICCOH->TCH2OCCJCOH	30.14	22.42	19.80	18.43
CC•COH+CH_2O-> TCH2OCCJCOH	19.07	12.96	12.42	12.57
C_2•COHOC -> TCH3OXC2DCOH	28.67	21.23	17.30	58439.42
C*C(C)OH + CH_3O ->TCH3OXC2DCOH	8.39	3.33	11.19	5.37
C_2•COHOC->TCOYCCHOYC	30.95	28.48	26.72	58452.65
C_2CO•OC->TCOYCCHOYC	25.79	25.07	30.75	27.38
C_2CO•OC->TCH3OXC2DO	16.06	10.86	10.94	10.11
C_2C*O+CH_3O-> TCH3OXC2DO	12.38	8.33	9.78	13.32
C_2CO•OC->TC2YCOHCO	17.02	15.17	17.71	15.55
C_2COHOC•->TC2YCOHCO	28.90	25.62	20.19	24.18
C_2COHOC•->TCH2OXC2CJOH	23.99	16.81	12.92	12.10
C_2C•OH+CH2O-> TCH2OXC2CJOH	12.10	6.42	5.79	6.23

UNIT: kcal/mole

b. Reaction enthalpies include thermal correction and zero-point energy correction

Table 5A.6 Reaction Enthalpies for C*C(C)C*O + OH Reaction System

Group Balance Isodesmic Reactions[a]	CBS-4	CBS-q	B3LYP /6-31g(d)	B3LYP /6-311+g(3df,2p)
	//B3LYP/6-31g(d)			
$C_2DCC(OH)_2$ + CC = $CC(OH)_2$ + C_2C*C	1.75	1.87	1.43	-0.25
$CC(OH)_2$ + 2COC = $CC(OC)_2$ + 2COH	0.00	-0.10	2.20	1.83
$C_2DCC(OH)_2$ + CH_3O = **$C_2DCCOHO$•** + CH_3OH	6.25	4.33	5.69	4.69
$C_2CC(OH)_2$ + 2COC + CC = $CC(OC)_2$ + C_3C + $2CH_3OH$	-0.50	-0.59	1.75	0.20

Reactions	CBS-4	CBS-q	B3LYP /6-31g(d)	B3LYP /6-311+g(3df,2p)
	//B3LYP/6-31g(d)			
OH+ C*CICC*O -> TSOHCDCICCDO	4.60	3.56	2.04	4.79
$C_2DCCOHO$• -> TSOHCDCICCDO	15.93	16.05	14.43	14.25
$C_2DCCOHO$• -> TSC2DJCXCO2H	2.54	3.17	2.36	1.18
CC•*C + O*COH -> TSC2DJCXCO2H	4.30	4.87	6.26	8.67

C_2CC*O + OH Reaction System

Group Balance Isodesmic Reactions	CBS-4	CBS-q	B3LYP /6-31g(d)	B3LYP /6-311+g(3df,2p)
	//B3LYP/6-31g(d)			
$C_2CC(OH)_2$ + 2COC + CC = $CC(OC)_2$ + C_3C + $2CH_3OH$	-0.50	-0.59	1.75	0.20
C_2CCOH_2 + CH_3O = **C_2CCOHO•** + C_3OH	-1.69	-3.17	-4.27	-4.64

Reactions	CBS-4	CBS-q	B3LYP /6-31g(d)	B3LYP /6-311+g(3df,2p)
	//B3LYP/6-31g(d)			
OH + C_2CC*O -> TSOHADC2CCDO	2.47	1.79	-0.80	2.35
C_2CCOHO• -> TSOHADC2CCDO	22.51	22.54	23.84	22.92
C_2CCOHO• -> TSC2CJXCO2H	-0.13	0.47	2.36	1.02
CC•C + O=COH -> TSC2CJXCO2H	6.74	7.05	10.09	12.77

CC*OC*O + OH Reaction System

Group Balance Isodesmic Reactions	CBS-4	CBS-q	B3LYP /6-31g(d)	B3LYP /6-311+g(3df,2p)
	//B3LYP/6-31g(d)			
$CCOH_2CDO$ + CC = CCHO + $C_2C(OH)_2$	-4.20	-3.95	-1.74	-3.37
$C_2C(OH)_2$ + 2COC = $C_2C(OC)_2$ + 2C H_3OH	7.49	7.58	11.43	10.33
$CCOH_2CDO$ + CH_3O = **CCOHO•CDO** + CH_3OH	2.45	-0.95	-1.66	-3.25
$OCICC(OH)_2$ + CC = $CC(OH)_2$ + C_2C*O	-0.47	-0.01	1.91	-0.73
$OICC(OH)_2$ + CH_3O = **OICCOHO•** + CH_3OH	0.62	-2.60	-2.81	-4.75

Reactions	CBS-4	CBS-q	B3LYP /6-31g(d)	B3LYP /6-311+g(3df,2p)
	//B3LYP/6-31g(d)			
OH + CC*OC*O -> TSOHADCCDOCDO	3.73	2.07	1.99	5.00
CCOHO•CDO -> TSOHADCCDOCDO	23.32	24.31	27.88	28.31
CCOHO•CDO -> TSHCOXCCO2H	4.66	4.06	3.71	4.01
HCO + CCO_2H -> TSHCOXCCO2H	21.36	18.34	15.39	19.26
OH + CC*OC*O -> TSOHADCCDOCDOP	3.22	1.37	1.37	4.33
OCICCOHO• -> TSOHADCCDOCDOP	26.45	27.02	31.34	32.10
OCICCOHO• -> TSCCJDOXCO2H	-4.91	-3.03	-0.35	-1.03
CC•*O + O*COH -> TSCCJDOXCO2H	8.06	7.79	8.16	10.82

UNIT: kcal/mole

c. Reaction enthalpies include thermal correction and zero-point energy correction

Table 5A.7 Thermodynamic Properties of Transition States for $C_2C{\cdot}OC + O_2$ Reaction System

SPECIES	ΔH°_{f298}	S°_{298}	Cp_{300}	Cp_{400}	Cp_{500}	Cp_{600}	Cp_{800}	Cp_{1000}	Cp_{1500}
TSC2COC1	-41.77	84.32	30.95	39.27	46.37	52.13	60.61	66.51	75.35
TSC2COC2	-30.31	99.33	32.79	40.37	46.83	52.05	59.72	65.06	73.13
TSC2COC3	-23.54[a]	91.47	31.66	39.26	45.82	51.23	59.42	65.26	74.14
TSC2COC4	-31.69	94.3	31.97	38.94	45.24	50.59	58.85	64.82	73.9
TSC2COC5	-24.32	101.46	32.47	39.38	45.41	50.38	57.99	63.49	72.06
TSC2COC6	-15.15	99.96	32.01	39.3	45.66	50.9	58.75	64.27	72.67
TSC2COC7	2.99	82.91	26.49	32.54	37.81	42.17	48.99	54.12	62.38
TSC2COC8	-23.44	90.62	32.93	40.58	47	52.16	59.8	65.27	73.83

$C_2C{*}C$ + OH Reaction System

SPECIES	ΔH°_{f298}	S°_{298}	Cp_{300}	Cp_{400}	Cp_{500}	Cp_{600}	Cp_{800}	Cp_{1000}	Cp_{1500}
TC2YCCHO	4.25	76.36	25.37	32.18	38.03	42.84	50.18	55.51	63.8
TC3CO.	-8.73	81.27	26.68	32.75	37.96	42.26	48.99	54.07	62.3
TC2YCCOH	5.39	76.38	24.06	30.75	36.73	41.75	49.48	55.08	63.67
TC2CCDOXH	4.1	83.33	27.29	33.4	38.73	43.18	50.1	55.24	63.26
TC2CXCH2O	-4.98	85.13	25.05	30.95	36.33	40.91	48.19	53.64	62.28
TCYCCOHC	2.76	74.73	23.09	30.1	36.39	41.65	49.73	55.54	64.39
TC2DCXCOH	7.19	87.49	25.42	31.12	36.24	40.61	47.59	52.89	61.54

C*C(C)OC + OH Reaction System

SPECIES	ΔH°_{f298}	S°_{298}	Cp_{300}	Cp_{400}	Cp_{500}	Cp_{600}	Cp_{800}	Cp_{1000}	Cp_{1500}
TCH3OXC2DCOH	-34	92.9	28.67	34.63	40.08	44.73	52.1	57.63	66.48
TCOYCCHOYC	-28.06	86.34	28.24	35.02	41.04	46.12	53.93	59.61	68.33
TCH3XC2CDO	-40.78	89.68	27.99	34.18	39.95	44.87	52.55	58.19	67
TC2YCOHCO	-38.03	79.43	27.74	35.25	41.8	47.2	55.27	60.97	69.61
TCH2OXC2CJOH	-45.64	91.92	30.58	36.51	41.77	46.22	53.25	58.53	67
TCOYCCOHYC	-22.26	86.44	26.97	33.58	39.71	44.98	53.18	59.11	68.14
TCH2OXCCJOC	-33.27	93.97	28.42	34.02	39.37	44.07	51.69	57.47	66.59
TCOYCCOHC	-23.97	85.25	26.26	33.13	39.47	44.89	53.32	59.45	68.75
TCH3OXCDCCOH	-25.13	95.62	28.02	33.89	39.36	44.06	51.6	57.27	66.32
TCH2OHXCDCOC	-21.45	95.46	29.24	35.12	40.38	44.87	52.03	57.47	66.29
TCYCCOHCO	-44.46	76.41	25.72	33.29	40.12	45.87	54.62	60.81	70.06
TCH2OXCCJCOH	-28.73	96.66	30.11	35.97	41.28	45.79	52.93	58.31	66.9

C*C(C)C*O + OH Reaction System

SPECIES	ΔH°_{f298}	S°_{298}	Cp_{300}	Cp_{400}	Cp_{500}	Cp_{600}	Cp_{800}	Cp_{1000}	Cp_{1500}
TSOHCDCICCDO	-15.07	90.79	24.55	30.06	34.94	39.06	45.49	50.24	57.72
TSC2DCJXCO2H	-26.12	90.31	25.11	30.43	35.19	39.25	45.61	50.34	57.78

C2CC*O + OH Reaction System

SPECIES	ΔH°_{f298}	S°_{298}	Cp_{300}	Cp_{400}	Cp_{500}	Cp_{600}	Cp_{800}	Cp_{1000}	Cp_{1500}
TSOHC2CCDO	-41.61	92.10	27.85	34.40	40.15	44.96	52.41	57.94	66.72
TSC2CJXCO2H	-64.08	89.77	28.17	34.63	40.35	45.12	52.55	58.04	66.76

CC*OC*O + OH Reaction System

SPECIES	ΔH°_{f298}	S°_{298}	Cp_{300}	Cp_{400}	Cp_{500}	Cp_{600}	Cp_{800}	Cp_{1000}	Cp_{1500}
TSOHCCDOCDO	-55.30	88.36	24.82	29.10	32.79	35.85	40.50	43.88	49.11
TSHCOXCCO2H	-76.24	85.37	24.09	28.73	32.59	35.75	40.48	43.86	49.09
TSOHCCDOCDOP	-52.32	89.65	24.45	28.42	31.92	34.90	39.63	43.14	48.68
TSCCJDOXCO2H	-83.18	88.21	23.16	27.26	30.95	34.11	39.08	42.75	48.46

UNIT: ΔH°_{f298}: kcal/mole; S & Cp(T) : cal/mole/K

Table 5A.8 Input Parameters and High-Pressure Limit Rate Constants (k_∞) for QRRK Calculation: $C_2C*C + OH \rightarrow C_3{\cdot}COH \rightarrow$ Products

Reaction	A (s-1 or cm^3/mol-s)	N	Ea (kcal/mol)	ref.
$C_2C*C + OH \rightarrow C_3{\bullet}COH$	1.81×10^{13}	0.	0.	a.
$C_3{\bullet}COH \rightarrow C_2C*C + OH$	1.60×10^{14}	0.	27.81	b.
$C_3{\bullet}COH \rightarrow C_3CO{\bullet}$	8.03×10^{8}	0.82497	28.65	c.
$C_3CO{\bullet} \rightarrow C_3{\bullet}COH$	2.59×10^{12}	0.47988	24.59	c.
$C_3CO{\bullet} \rightarrow C_2C*O + CH_3$	8.45×10^{14}	0.03757	12.10	c.

Geometric mean frequency
$C_3{\bullet}COH$: 373.9 cm^{-1} (11.05), 1245.2 cm^{-1} (14.775), 3253.7 cm^{-1} (8.175)
$C_3CO{\bullet}$: 362.3 cm^{-1} (9.329), 1181.0 cm^{-1} (17.093), 3149.7 cm^{-1} (8.078)
Lennard-Jones parameters: σ = 5.1983A°, ε/k = 533.08 K

a. 90TSA.
b. <MR>
c. Fit with three parameter modified Arrhenius equation; A estimated using canonical TST and B3LYP-determined entropies, Ea evaluated from CBS-q// B3LYP/6-31g(d) calculation.

Input Parameters and High-Pressure Limit Rate Constants (k_∞) for QRRK Calculation: $C_2{\bullet}C*C + OH \rightarrow C_2C{\bullet}COH \rightarrow$ Products

Reaction	A (s-1 or cm^3/mol-s)	n	Ea (kcal/mol)	Ref.
$C_2C*C + OH \rightarrow C_2C{\bullet}COH$	1.81×10^{13}	0.	0.	a.
$C_2C{\bullet}COH \rightarrow C_2C*C + OH$	8.53×10^{13}	0.	27.54	b.
$C_2C{\bullet}COH \rightarrow C_2CCO{\bullet}$	1.26×10^{6}	1.55556	27.87	c.
$C_2CCO{\bullet} \rightarrow C_2C{\bullet}COH$	8.84×10^{9}	0.6744	21.84	c.
$C_2CCO{\bullet} \rightarrow C_2{\bullet}CCOH$	1.84×10^{9}	0.75423	19.06	c.
$C_2CCO{\bullet} \rightarrow C_2CC*O + H$	2.39×10^{10}	1.11279	20.58	c.
$C_2CCO{\bullet} \rightarrow CC{\bullet}C + CH_2O$	2.90×10^{13}	0.16774	11.97	c.
$C_2{\bullet}CCOH \rightarrow C_2CCO{\bullet}$	9.01×10^{6}	1.0599	20.76	c.
$C_2{\bullet}CCOH \rightarrow C*CC + C{\bullet}H_2OH$	2.45×10^{12}	0.2468	26.09	c.

Geometric mean frequency
$C_2C{\bullet}COH$: 343.7 cm^{-1} (10.08), 1368.2 cm^{-1} (15.166), 3131.9 cm^{-1} (8.754)
$C_2CCO{\bullet}$: 398.8 cm^{-1} (10.14), 1258.1 cm^{-1} (15.506), 3037.5 cm^{-1} (8.853)
$C_2{\bullet}CCOH$: 387.2 cm^{-1} (10.673, 1275.0 cm^{-1} (14.578), 3188.2 cm^{-1} (8.749)
Lennard-Jones parameters: σ = 5.1983A°, ε/k = 533.08 K

Table 5A.9 Input Parameters and High-Pressure Limit Rate Constants (k_∞) for QRRK Calculation: $C_2C{\cdot}OC \rightarrow C_2C{*}O + CH_3$

Reaction	A (s-1 or cm^3/mol-s)	n	Ea (kcal/mol)	ref.
$C_2C\bullet OC \rightarrow C_2C{*}O + CH_3$	1.82×10^8	1.22014	20.98	a.

Geometric mean frequency
$C_2C\bullet OC$: 435.1 cm^{-1} (12.04), 1443.5 cm^{-1} (12.622), 2813.5 cm^{-1} (9.388)
Lennard-Jones parameters: σ = 5.1983A°, ε/k = 533.08 K

a. Fit with three parameter modified Arrhenius equation; A estimated using canonical TST and B3LYP-determined entropies, Ea evaluated from CBS-q// B3LYP/6-31g(d) calculation.

Input Parameters and High-Pressure Limit Rate Constants (k_∞) for QRRK Calculation: $C_2\bullet COC + O_2 \rightarrow$ Product

Reaction	A (s-1 or cm^3/mol-s)	n	Ea (kcal/mol)	ref.
$C_2C\bullet OC + O_2 \rightarrow C_2CQ\bullet OC$	3.60×10^{12}	0.	0.	b.
$C_2CQ\bullet OC \rightarrow C_2C\bullet OC + O_2$	4.5×10^{15}	0.	38.06	c.
$C_2CQ\bullet OC \rightarrow C_2CQOC\bullet$	9.49×10^5	1.53649	16.72	a.
$C_2CQ\bullet OC \rightarrow C_2\bullet CQOC$	1.11×10^9	1.05347	35.39	d.
$C_2CQ\bullet OC \rightarrow C_2CO\bullet OC + O$	2.45×10^{14}	0	63.72	d.
$C_2CQ\bullet OC \rightarrow C{*}C(C)OC{+}HO_2$	2.46×10^{10}	0.81234	25.51	a.
$C_2CQOC\bullet \rightarrow C_2CQ\bullet OC$	1.11×10^8	0.50141	5.03	a.
$C_2CQOC\bullet \rightarrow C_2C\bullet OOH + CH_2O$	3.76×10^{12}	0.14199	17.00	a.
$C_2CQOC\bullet \rightarrow C_2CYCOCO + OH$	2.10×10^{10}	0.25788	23.79	a.
$C_2\bullet CQOC \rightarrow C_2CQ\bullet OC$	3.75×10^9	0.40592	16.06	a.
$C_2\bullet CQOC \rightarrow C{*}C(C)OC + HO_2$	5.08×10^{13}	-0.21234	12.88	a.
$C_2\bullet CQOC \rightarrow C{*}C(C)Q{+}\ CH_3$	3.18×10^{12}	0.06684	24.79	a.

Geometric mean frequency
$C_2CQ\bullet OC$: 379.5 cm^{-1} (13.49), 978.8 cm^{-1} (11.982), 2393.6 cm^{-1} (14.03)
$C_2CQOC\bullet$: 353.4 cm^{-1} (13.83), 991.4 cm^{-1} (12.520), 2298.8 cm^{-1} (12.65)
$C_2\bullet CQOC$: 361.1 cm^{-1} (13.57), 955.7 cm^{-1} (12.689), 2297.8 cm^{-1} (12.75)
Lennard-Jones parameters: σ = 5.8569A°, ε/k = 632.06 K

b. Estimated from $CCC\bullet + O_2 \rightarrow CCCQ\bullet$
c. <MR>
d. Estimated from $O + CH_3O$

Input Parameters and High-Pressure Limit Rate Constants (k_∞) for QRRK Calculation: $C_2CO\bullet OC \rightarrow$ Product

Reaction	A (s-1 or cm^3/mol-s)	n	Ea (kcal/mol)	ref.
$C_2CO\bullet OC \rightarrow C_2C{*}O + CH_3O$	2.20×10^{13}	0.	9.19.	e.
$C_2CO\bullet OC \rightarrow CC{*}OOC{+}CH_3$	4.53×10^{14}	0.	12.01	f.

Geometric mean frequency
$C_2CO\bullet OC$: 542.7 cm^{-1} (18.31), 1810.1 cm^{-1} (18.293), 4000.0 cm^{-1} (3.402)
Lennard-Jones parameters: σ = 5.5471A°, ε/k = 584.86 K

e. k via <MR>; A_r estimated using canonical TST and B3LYP-determined entropies, Ea,r evaluated from CBS-q// B3LYP/6-31g(d) calculation.

f. k via <MR>; k_r estimated from rate constant of $CH_3 + C_2C{*}O \rightarrow C_3CO\bullet$ which A estimated using canonical TST and B3LYP-determined entropies, Ea evaluated from CBS-q// B3LYP/6-31g(d) calculation.

Table 5A.9 (Continued)

Input Parameters and High-Pressure Limit Rate Constants (k_∞) for QRRK Calculation: $C_2C{\cdot}OC + HO_2 \rightarrow$ Product

Reaction	A (s-1 or cm^3/mol-s)	n	Ea (kcal/mol)	ref.
$C_2C{\bullet}OC + HO_2 \rightarrow C_2CQOC$	1.00×10^{12}	0.	0.	b.
$C_2CQOC \rightarrow C_2C{\bullet}OC + HO_2$	5.40×10^{15}	0.	72.63	c.
$C_2CQOC \rightarrow C_2CO{\bullet}OC + OH$	2.31×10^{14}	0.	43.07	g.

Geometric mean frequency
C_2CQOC: 354.9 cm^{-1} (14.22), 1239.0 cm^{-1} (19.799), 3231.4 cm^{-1} (7.984)
Lennard-Jones parameters: σ = 5.8569A°, ε/k = 632.06 K

g. k via <MR>; $A_r = 1.0 \times 10^{13}$, Benson et al. $E_{a,r} = 0$.

Table 5A.10 Input Parameters and High-Pressure Limit Rate Constants (k_∞) for QRRK Calculation: C*CICC*O + OH → Products

Reaction	A (s-1 or cm^3/mol-s)	N	Ea (kcal/mol)	Ref.
C*CICC*O + OH → C_2DCCOHO•	1.04×10^{9}	0.89078	4.03	a.
C_2DCCOHO• → C*CICC*O + OH	1.16×10^{14}	0.01846	16.82	a.
C_2DCCOHO• → CC•*C+O*COH	5.66×10^{13}	0.009838	5.76	a.

Geometric mean frequency
C_2DCCOHO•: 412.8 cm^{-1} (10.83), 1301.7 cm^{-1} (13.675), 3184.0 cm^{-1} (6.993)
Lennard-Jones parameters: $\sigma = 5.5471$A°, $\varepsilon/k = 584.86$ K

a. Fit with three parameter modified Arrhenius equation; A estimated using canonical TST and B3LYP-determined entropies, Ea evaluated from CBS-q// B3LYP/6-31g(d) calculation.

Input Parameters and High-Pressure Limit Rate Constants (k_∞) for QRRK Calculation: C_2CC*O + OH → Products

Reaction	A (s-1 or cm^3/mol-s)	n	Ea (kcal/mol)	Ref.
C_2CC*O + OH → C_2CCOHO•	1.99×10^{7}	1.32462	0.	a.
C_2CCOHO• → C_2CC*O + OH	6.30×10^{14}	-0.30169	25.26	a.
C_2CCOHO• → CC•C+O*COH	1.27×10^{14}	-0.23326	2.77	a.

Geometric mean frequency
C_2CCOHO•: 377.1 cm^{-1} (12.74), 1237.7 cm^{-1} (15.609), 3164.9 cm^{-1} (8.653)
Lennard-Jones parameters: $\sigma = 5.5471$A°, $\varepsilon/k = 584.86$ K

Input Parameters and High-Pressure Limit Rate Constants (k_∞) for QRRK Calculation CC*OC*O + OH → CCOHO•CDO → Products

Reaction	A (s-1 or cm^3/mol-s)	n	Ea (kcal/mol)	Ref.
CC*OC*O + OH → CCOHO•CDO	1.90×10^{6}	1.64335	-0.21	a.
CCOHO•CDO → C_2CC*O + OH	1.00×10^{15}	-0.35165	27.43	a.
CCOHO•CDO → HCO + CC*OOH	1.13×10^{13}	0.0732	6.16	a.

Geometric mean frequency
CCOHO•CDO: 371.6 cm^{-1} (10.89), 1223.1 cm^{-1} (10.206), 3307.2 cm^{-1} (4.407)
Lennard-Jones parameters: $\sigma = 5.5471$A°, $\varepsilon/k = 584.86$ K

Input Parameters and High-Pressure Limit Rate Constants (k_∞) for QRRK Calculation: CC*OC*O + OH → OCICCOHO• → Products

Reaction	A (s-1 or cm^3/mol-s)	n	Ea (kcal/mol)	Ref.
CC*OC*O + OH → OCICCOHO•	3.15×10^{7}	1.32253	2.96	a.
OCICCOHO• → C_2CC*O + OH	5.92×10^{12}	0.23597	32.12	a.
OCICCOHO• → CC•*O + O*COH	5.87×10^{12}	0.11366	1.26	a.

Geometric mean frequency
OCICCOHO•: 335.5 cm^{-1} (10.29), 1353.4 cm^{-1} (10.055), 3197.4 cm^{-1} (5.152)
ennard-Jones parameters: $\sigma = 5.5471$A°, $\varepsilon/k = 584.86$ K

Table 5A.11 Input Parameters and High-Pressure Limit Rate Constants (k_∞) for QRRK Calculation C*C(C)OC· → CC·*C + CH$_2$O

Reaction	A (s-1 or cm^3/mol-s)	n	Ea (kcal/mol)	ref.
C*C(C)OC• → CC•*C + CH$_2$O	1.48×10^{15}	-0.51431	33.17	a.

Geometric mean frequency
C*C(C)OC•: 386.4 cm^{-1} (8.938), 939.7 cm^{-1} (8.979), 2346.7 cm^{-1} (10.583)
Lennard-Jones parameters: σ = 5.1983A°, ε/k = 533.08 K

a. Fit with three parameter modified Arrhenius equation; A estimated using canonical TST and B3LYP-determined entropies, Ea evaluated from CBS-q// B3LYP/6-31g(d) calculation.

Input Parameters and High-Pressure Limit Rate Constants (k_∞) for QRRK Calculation: C*C(C)OC• + O$_2$ → Product

Reaction	A (s-1 or cm^3/mol-s)	n	Ea (kcal/mol)	ref.
C*C(C)OC• + O$_2$ → C*ClCOCQ•	4.82×10^{12}	0.	0.	b.
C*ClCOCQ• → C*C(C)OC• + O$_2$	1.0×10^{15}	0.	34.79	c.
C*ClCOCQ• → C•*ClCOCQ	1.85×10^{5}	1.76064	27.22	d.
C*ClCOCQ• → C*ClC•OCQ	2.72×10^{3}	2.24232	11.50	d.
C*ClCOCQ• → C*ClCOCO• + O	1.91×10^{14}	0.	59.11	e.
C•*ClCOCQ → C*ClCOCQ•	2.76×10^{8}	0.5573	4.82	c.
C•*ClCOCQ → C#CC +O•COOH	1.56×10^{13}	0.	28.15	f.
C*ClC•OCQ → C*ClCOCQ•	1.64×10^{8}	0.64123	12.43	c.
C*ClC•OCQ → C*C*C + O•COOH	3.63×10^{12}	0.	52.05	g.

Geometric mean frequency
C*ClCOCQ•: 320.4 cm^{-1} (9.753), 800.1 cm^{-1} (9.8992), 2172.0 cm^{-1} (14.349)
C•*ClCOCQ: 204.6 cm^{-1} (4.927), 595.0 cm^{-1} (15.260), 2000.0 cm^{-1} (13.313)
C*ClC•OCQ: 512.8 cm^{-1} (12.515), 507.4 cm^{-1} (7.411), 1874.3 cm^{-1} (13.574)
Lennard-Jones parameters: σ = 5.8569A°, ε/k = 632.06 K

b. Estimated from COC• + O$_2$ → COCQ•

c. <MR>

d. Fit with three parameter modified Arrhenius equation; A estimated using canonical TST and PM3-determined entropies, Ea evaluated from $E_a = E_{abst} + \Delta U_{rxn}$.

e. Estimated from O + CH$_3$O

f. k via <MR>; k_r estimated from rate constant of CH$_3$O + C#CC → (via transition state BT2) → C•*C(C)OC which A estimated using canonical TST and B3LYP-determined entropies, Ea evaluated from CBS-q// B3LYP/6-31g(d) calculation.

g. k via <MR>; k_r estimated from rate constant of CH$_3$O + C*C*C → (via transition state BT1) → C*C(C•)OC which A estimated using canonical TST and B3LYP-determined entropies, Ea evaluated from CBS-q// B3LYP/6-31g(d) calculation.

Table 5A.12 Input Parameters and High-Pressure Limit Rate Constants (k_∞) for QRRK Calculation: C*C(C·)OC → C*C*C + CH_3O

Reaction	A (s-1 or cm^3/mol-s)	n	Ea (kcal/mol)	ref.
C*C(C•)OC → C*C*C + CH_3O	3.75×10^{16}	-0.76471	53.10	a.

Geometric mean frequency
C*C(C•)OC: 370.8 cm^{-1} (8.938), 800.9 cm^{-1} (8.979), 2188.2 cm^{-1} (10.583)
Lennard-Jones parameters: σ = 5.1983A°, ε/k = 533.08 K

a. Fit with three parameter modified Arrhenius equation; A estimated using canonical TST and B3LYP-determined entropies, Ea evaluated from CBS-q// B3LYP/6-31g(d) calculation.

Input Parameters and High-Pressure Limit Rate Constants (k_∞) for QRRK Calculation: C*C(C•)OC + O_2 → Product

Reaction	A (s-1 or cm^3/mol-s)	n	Ea (kcal/mol)	ref.
C*C(C•)OC + O_2 → C*CICQ•OC	4.48×10^{11}	0.	0.	b.
C*CICQ•OC → C*C(C•)OC + O_2	7.11×10^{12}	0.	19.97	c.
C*CICQ•OC → C*CICQOC•	2.48×10^{4}	1.87514	17.22	d.
C*CICQ•OC → C•*CICQOC	4.53×10^{5}	1.74526	27.15	d.
C*CICQ•OC → COYC•COOC	5.12×10^{7}	0.89293	29.10	e.
C*CICQ•OC → COYCCOOC•	8.25×10^{7}	0.94384	29.77	f.
C*CICQ•OC → C*CICO•OC + O	1.33×10^{14}	0.	58.79	g.
C*CICQOC• → C*CICQ•OC	9.94×10^{6}	0.71540	9.53	c.
C*CICQOC• → C*C•CQ + CH_2O	1.09×10^{13}	0.38	28.54	h.
C*CICQOC• → CDYCOCOC + OH	1.41×10^{9}	0.	15.23	i.
C•*CICQOC → C*CICQ•OC	1.73×10^{8}	0.76319	4.69	c.
C•*CICQOC → C#CCQ + CH_3O	2.35×10^{13}	0.	27.72	j.
C•*CICQOC → C#COC + C•H_2OOH	1.20×10^{14}	0.	41.36	k.
COYC•COOC → C*CICQ•OC	3.60×10^{8}	1.57505	25.70	c.
COYC•COOC → COYC•OC + CH_2O	1.00×10^{13}	0.	21.0	l.
COYCCOOC• → C*CICQ•OC	4.98×10^{10}	0.87256	18.40	c.
COYCCOOC• → COYC•OC + CH_2O	3.34×10^{11}	0.49026	13.67	m.
COYCCOOC• → C•C*OOC + CH_2O	1.01×10^{13}	0.	18.50	n

Geometric mean frequency
C*CICQ•OC: 343.7 cm^{-1} (11.28), 800.0 cm^{-1} (8.3052), 2136.7 cm^{-1} (14.414)
C*CICQOC•: 100.0 cm^{-1} (3.396), 581.1 cm^{-1} (17.411), 2015.2 cm^{-1} (12.693)
C•*CICQOC: 100.2 cm^{-1} (3.776), 604.7 cm^{-1} (16.85), 2010.3 cm^{-1} (12.875)
COYC•COOC: 520.0 cm^{-1} (14.570), 1657.0cm^{-1} (17.01), 3606.5 cm^{-1} (3.419)
COYCCOOC•: 511.6 cm^{-1} (15.162), 1416. cm^{-1} (13.23), 2828.8 cm^{-1} (6.105)
Lennard-Jones parameters: σ = 5.8569A°, ε/k = 632.06 K

d. Estimated from C2•C*C + O_2 → C*CICCQ•

e. <MR>

f. Fit with three parameter modified Arrhenius equation; A estimated using canonical TST and PM3-determined entropies, Ea evaluated from $E_a = E_{abst} + \Delta U_{rxn}$.

g. Fit with three parameter modified Arrhenius equation; A estimated using canonical TST and PM3-determined entropies, Ea evaluated from reaction barrier of C*CICCQ• -> CCYC•COOC (Ea=28.84, based on CBS-q//MP2(full)/6-31g(d))

h. Fit with three parameter modified Arrhenius equation; A estimated using canonical TST and PM3-determined entropies, Ea evaluated from from reaction barrier of C*CICCQ• -> C2•CYCCOO (Ea=29.53, based on CBS-q//MP2(full)/6-31g(d))

i. Estimated from O + CH_3O

j. k via <MR>; k_r estimated from rate constant of CH_2O + CC•*C → (via transition state BT3A) → C*C(C)OC• which A estimated using canonical TST and B3LYP-determined entropies, Ea evaluated from CBS-q// B3LYP/6-31g(d) calculation.

k. k estimated from rate constant of C_3•OCOCQ → (via transition state TS1 in chapter 2) → C_2CYCCOCO + OH which A estimated using canonical TST and B3LYP-determined entropies, Ea evaluated from CBS-q// B3LYP/6-31g(d) calculation.

l. k via <MR>; k_r estimated from rate constant of CH_3O + C#CC → (via transition state BT2) → C•*C(C)OC which A estimated using canonical TST and B3LYP-determined entropies, Ea evaluated from CBS-q// B3LYP/6-31g(d) calculation

Table 5A.12 (Continued)

m. k via <MR>; k_r estimated from rate constant of CH_3 + C#CC → C_2C*C (NIST)

n. k estimated from reaction of CCYC•COOC → CCYC•OC + CH2O which A estimated using canonical TST and MP2-determined entropies, Ea evaluated from CBS-q//MP2(full)/6-31g(d) calculation. (chapter 4)

o. k estimated from reaction of C_2•CYCCOO → CCYC•OC + CH2O which A estimated using canonical TST and MP2-determined entropies, Ea evaluated from CBS-q//MP2(full)/6-31g(d) calculation. (chapter 4)

p. k estimated from reaction of C_2•CYCCOO → C*CICOOC• which A estimated using canonical TST and MP2-determined entropies, Ea evaluated from CBS-q//MP2(full)/6-31g(d) calculation. (chapter 4)

Table 5A.13 Input Parameters and High-Pressure Limit Rate Constants (k_∞) for QRRK Calculation C·*C(C)OC → C#CC + CH_3O

Reaction	A (s-1 or cm^3/mol-s)	n	Ea (kcal/mol)	ref.
C•*C(C)OC → C#CC + CH_3O	6.46×10^{17}	-1.24151	29.19	a.

Geometric mean frequency
C•*C(C)OC: 410.4 cm^{-1} (9.302), 1003.6 cm^{-1} (8.713), 2355.0 cm^{-1} (10.485)
Lennard-Jones parameters: σ = 5.1983A°, ε/k = 533.08 K

a. Fit with three parameter modified Arrhenius equation; A estimated using canonical TST and B3LYP-determined entropies, Ea evaluated from CBS-q// B3LYP/6-31g(d) calculation.

Input Parameters and High-Pressure Limit Rate Constants (k_∞) for QRRK Calculation: C•*C(C)OC + O_2 → Product

Reaction	A (s-1 or cm^3/mol-s)	n	Ea (kcal/mol)	ref.
C•*C(C)OC + O_2 → Q•C*ClCOC	6.00×10^{12}	0.	0.	b.
Q•C*ClCOC → C*C(C•)OC + O_2	2.80×10^{14}	0.	41.70	c.
Q•C*ClCOC → QC*ClC•OC	6.05×10^{9}	0.3541	11.86	d.
Q•C*ClCOC → QC*ClCOC•	1.21×10^{7}	1.17812	17.70	d.
Q•C*ClCOC → CC*OOC + HCO	2.36×10^{10}	0.40177	29.42	e.
Q•C*ClCOC → O•C*ClCOC + O	1.89×10^{14}	0.	34.88	f.
QC*ClC•OC → Q•C*ClCOC	3.60×10^{12}	-0.4443	15.00	c.
QC*ClC•OC → C*C*CQ + CH_3O	1.97×10^{14}	0.	54.05	g.
QC*ClCOC• → Q•C*ClCOC	1.84×10^{9}	0.15204	9.88	c.
QC*ClCOC• → CC•*COOH + CH_2O	1.08×10^{13}	0.	28.55	h.

Geometric mean frequency
Q•C*ClCOC: 382.2 cm^{-1} (12.134), 921.4 cm^{-1} (10.335), 2391.1 cm^{-1} (11.531)
QC*ClC•OC: 404.1 cm^{-1} (11.68), 809.6 cm^{-1} (10.289), 2065.5 cm^{-1} (11.526)
QC*ClCOC•: 356.1 cm^{-1} (12.343), 845.3 cm^{-1} (11.05), 2272.8 cm^{-1} (10.106)
Lennard-Jones parameters: σ = 5.8569A°, ε/k = 632.06 K

b. Estimated from C=C• + O_2 → C=CQ•
c. <MR>
d. Fit with three parameter modified Arrhenius equation; A estimated using canonical TST and PM3-determined entropies, Ea evaluated from $E_a = E_{abst} + \Delta U_{rxn}$.
e. Fit with three parameter modified Arrhenius equation; A estimated using canonical TST and PM3-determined entropies, Ea evaluated from reaction barrier of C*CQ• → C•CYCOO (Ea=29.12)
f. Estimated from O + CH_3O
g. k via <MR>; k_r estimated from rate constant of CH_3O + C*C*C →(via transition state BT1) → C*C(C•)OC which A estimated using canonical TST and B3LYP-determined entropies, Ea evaluated from CBS-q// B3LYP/6-31g(d) calculation.
h. k estimated from rate constant of CH_2O + CC•*C →(via transition state BT3A) → C*C(C)OC• which A estimated using canonical TST and B3LYP-determined entropies, Ea evaluated from CBS-q// B3LYP/6-31g(d) calculation.

Table 5A.14 Input Parameters and High-Pressure Limit Rate Constants (k_∞) for QRRK Calculation: C*C(C)OC + OH → C_2·COHOC → Products

Reaction	A (s-1 or $\mathrm{cm^3}$/mol-s)	N	Ea (kcal/mol)	ref.
C*C(C)OC + OH → C_2•COHOC	1.81×10^{13}	0.	0.	a.
C_2•COHOC → C*C(C)OC + OH	3.43×10^{14}	0.	26.91	
C_2•COHOC → C_2CO•OC	3.76×10^{9}	0.68225	28.55	
C_2•COHOC → C*C(C)OH + CH_3O	2.50×10^{13}	-0.09522	23.26	
C_2CO•OC → C_2•COHOC	1.02×10^{12}	0.33848	25.47	b.
C_2CO•OC → C_2COHOC•	6.05×10^{8}	0.89637	15.03	c.
C_2CO•OC → C_2C*O + CH_3O	4.51×10^{14}	-0.30036	13.21	c.
C_2COHOC• → C_2CO•OC	4.29×10^{7}	0.87532	25.42	
C_2COHOC• → C_2C•OH+CH_2O	6.09×10^{12}	0.14239	18.68	c.

Geometric mean frequency
C_2•COHOC: 530.2 $\mathrm{cm^{-1}}$ (18.08), 1816.7 $\mathrm{cm^{-1}}$ (14.797), 3999.3 $\mathrm{cm^{-1}}$ (3.620)
C_2CO•OC: 542.7 $\mathrm{cm^{-1}}$ (18.31), 1810.1$\mathrm{cm^{-1}}$ (15.288), 4000.0 $\mathrm{cm^{-1}}$ (3.402)
C_2COHOC•: 521.2 $\mathrm{cm^{-1}}$ (18.90), 1843.0 $\mathrm{cm^{-1}}$ (14.053), 3999.1 $\mathrm{cm^{-1}}$ (3.548)
Lennard-Jones parameters: $\sigma = 5.5471$A°, $\varepsilon/k = 584.86$ K

b. 90TSA.
c. <MR>
d. Fit with three parameter modified Arrhenius equation; A estimated using canonical TST and B3LYP-determined entropies, Ea evaluated from CBS-q// B3LYP/6-31g(d) calculation.

Input Parameters and High-Pressure Limit Rate Constants (k_∞) for QRRK Calculation: C*C(C)OC + OH → COCI•CCOH → Products

Reaction	A (s-1 or $\mathrm{cm^3}$/mol-s)	n	Ea (kcal/mol)	Ref.
C*C(C)OC + OH → COCI•CCOH	1.81×10^{13}	0.	0.	a.
COCI•CCOH → C*C(C)OC + OH	3.05×10^{14}	0.	25.91	b.
COCI•CCOH → COCICCO•	2.72×10^{7}	1.27279	31.82	c.
COCICCO• → COCI•CCOH	6.41×10^{11}	0.0916	22.96	c.
COCICCO• → C•OCICCOH	5.33×10^{7}	0.68467	0.16	c.
COCICCO• → COCIC•COH	2.09×10^{11}	0.14719	21.12	c.
COCICCO• → CC•OC + CH_2O	1.71×10^{15}	-0.46395	12.52	c.
C•OCICCOH → COCICCO•	3.70×10^{6}	0.66574	7.32	c.
C•OCICCOH → CC•COH+ CH_2O	8.28×10^{12}	0.14173	23.95	c.
COCIC•COH → COCICCO•	7.54×10^{8}	0.49357	21.35	c.
COCIC•COH → C*COC + C•H_2OH	2.45×10^{12}	0.08287	24.55	c.
COCIC•COH → C*CCOH + CH_3O	2.14×10^{13}	-0.18061	20.93	c.

Geometric mean frequency
COCI•CCOH: 507.2 $\mathrm{cm^{-1}}$ (16.072), 1722.0 $\mathrm{cm^{-1}}$ (13.913), 3234.3 $\mathrm{cm^{-1}}$ (6.516)
COCICCO•: 566.8 $\mathrm{cm^{-1}}$ (18.50), 1797.4 $\mathrm{cm^{-1}}$ (14.528), 3850.1 $\mathrm{cm^{-1}}$ (3.972)
C•OCICCOH: 545.4 $\mathrm{cm^{-1}}$ (19.14), 1848.6 $\mathrm{cm^{-1}}$ (13.495), 3982.4 $\mathrm{cm^{-1}}$ (3.870)
COCIC•COH: 555.9 $\mathrm{cm^{-1}}$ (18.34), 1820.6 $\mathrm{cm^{-1}}$ (14.195), 3967.7 $\mathrm{cm^{-1}}$ (3.968)
Lennard-Jones parameters: $\sigma = 5.5471$A°, $\varepsilon/k = 584.86$ K

Table 5A.15 Input Parameters and High-Pressure Limit Rate Constants (k_∞) for QRRK Calculation: COCI·CCOH + O_2 → Products

Reaction	A (s-1 or cm^3/mol-s)	Ea (kcal/mol)	ref.
COCI•CCOH + O_2 → COCTCQ•CK	3.6×10^{12}	0.	a.
COCTCQ•CK → COCI•CCOH + O_2	3.36×10^{14}	32.4	b.
COCTCQ•CK → COCTC•QCK	3.14×10^{12}	31.84	c.
COCTCQ•CK → COCTCQCO•	1.20×10^{11}	18.24	d.
COCTCQ•CK → C•OCTCQCK	3.61×10^{11}	19.17	e.
COCTC•QCK → COCTCQ•CK	1.80×10^{11}	18.20	b.
COCTC•QCK → C*CQCOH + CH_3O	1.63×10^{12}	28.24	f.
COCTC•QCK → C*CICOHOC + HO_2	7.21×10^{9}	6.78	g.
COCTC•QCK → C*C(Q)OC + C•H_2OH	4.27×10^{13}	28.99	h.
COCTCQCO• → COCTCQ•CK	1.29×10^{11}	1.21	b.
COCTCQCO• → COC•(Q)C + CH_2O	7.51×10^{12}	4.73	i.
COCTCQ•CK → COCTCQ•CK	2.80×10^{10}	9.73	b.
COCTCQ•CK → CC•(Q)COH + CH_2O	4.16×10^{13}	15.57	j.

Geometric mean frequency

COCTCQ•CK: 370.6 cm^{-1} (15.29), 995.1 cm^{-1} (12.689), 2445.1 cm^{-1} (14.021)

COCTC•QCK: 351.0 cm^{-1} (15.26), 971.5 cm^{-1} (13.557), 2358.8 cm^{-1} (12.677)

COCTCQCO•: 362.3 cm^{-1} (15.285), 970.7 cm^{-1} (13.79), 2314.0 cm^{-1} (12.922)

COCTCQ•CK: 352.2 cm^{-1} (16.004), 943.4 cm^{-1} (12.97), 2363.1 cm^{-1} (12.527)

Lennard-Jones parameters: $\sigma = 6.1414$A°, $\varepsilon/k = 678.63$ K

a. Estimated from CCC• + O_2 → CCCQ•

b. <MR>

c. A_r estimated using TST, $A = (\text{deg.})(ek_b/h)\, T^n \exp(\Delta S^{\neq}(T)/R)$, deg. = 3, $\Delta S^{\neq}(T)$ is estimated as loss of two rotors and gain one OI ($-4.3 \times 2 + 1.38$ cal mol^{-1} K^{-1}). $E_{a,f}$ = RS (10) + E_{abst} (8.2) + ΔU_{rxn} (13.64).

d. A_r estimated using TST, $A = (\text{deg.})(ek_b/h)\, T^n \exp(\Delta S^{\neq}(T)/R)$, deg. = 1, $\Delta S^{\neq}(T)$ is estimated as loss of three rotors and gain one OI ($-4.3 \times 3 + 1.38$ cal mol^{-1} K^{-1}). $E_{a,f}$ = E_{abst} (7..21) – 6 (H-Bond).

e. A_r estimated using TST, $A = (\text{deg.})(ek_b/h)\, T^n \exp(\Delta S^{\neq}(T)/R)$, deg. = 3, $\Delta S^{\neq}(T)$ is estimated as loss of three rotors and gain one OI ($-4.3 \times 3 + 1.38$ cal mol^{-1} K^{-1}). $E_{a,f}$ = E_{abst} (9.73) + ΔU_{rxn} (9.49).

f. k via <MR>; k_r estimated from rate constant of CH_3O + C*C(C)Q → C_2•CQOC which A estimated using canonical TST and B3LYP-determined entropies, Ea evaluated from CBS-q// B3LYP/6-31g(d) calculation. (Table6.4)

g. k via <MR>; k_r estimated from rate constant of HO_2 + C_2C*C → C_3•CQ which A estimated using canonical TST and B3LYP-determined entropies, Ea evaluated from CBS-q// B3LYP/6-31g(d) calculation. (chapter 5)

h. k via <MR>; k_r estimated from rate constant of CH_2O + C_2C•OC → (via transition state BT27) → C_2C(CO•)OC which A estimated using canonical TST and B3LYP-determined entropies, Ea evaluated from CBS-q// B3LYP/6-31g(d) calculation.

i. k via <MR>; k_r estimated from rate constant of CH_2O + C_2C•CQ → C_2CICQOC• which A estimated using canonical TST and B3LYP-determined entropies, Ea evaluated from CBS-q// B3LYP/6-31g(d) calculation. (chapter 2)

Table 5A.16 Input Parameters and High-Pressure Limit Rate Constants (k_∞) for QRRK Calculation: C_2·COHOC + O_2 → Products

Reaction	A (s-1 or cm^3/mol-s)	Ea (kcal/mol)	ref.
C_2•COHOC + O_2 → COCTCKCQ•	3.0×10^{12}	0.	a.
COCTCKCQ• → C_2•COHOC + O_2	3.92×10^{14}	31.41	b.
COCTCKCQ• → COCTCO•CQ	1.21×10^{11}	18.24	c.
COCTCKCQ• → COCTC•KCQ	3.60×10^{11}	21.84	d.
COCTCKCQ• → C•OCTCKCQ	4.14×10^{10}	19.17	e.
COCTCO•CQ → COCTCKCQ•	1.29×10^{11}	1.21	b.
COCTCO•CQ → CC*OCOOH + CH_3O	3.97×10^{13}	11.18	f.
COCTCO•CQ → CC*OOC + C•H_2OOH	5.56×10^{13}	7.39	g.
COCTC•KCQ → COCTCKCQ•	2.07×10^{10}	8.20	b.
COCTC•KCQ → C*COHCQ + CH_3O	4.86×10^{12}	24.27	h.
COCTC•KCQ → C*COHOC + C•H_2OOH	1.45×10^{13}	24.03	i.
C•OCTCKCQ → COCTCKCQ•	3.21×10^{9}	9.73	b.
C•OCTCKCQ → CC•(OH)CQ + CH_2O	1.53×10^{13}	17.93	j.

Geometric mean frequency
COCTCKCQ•: 370.6 cm^{-1} (15.29), 995.1 cm^{-1} (12.689), 2445.1 cm^{-1} (14.021)
COCTCO•CQ: 362.3 cm^{-1} (15.29), 970.7 cm^{-1} (13.793), 2314.0 cm^{-1} (12.922)
COCTC•KCQ: 351.0 cm^{-1} (15.265), 971.5 cm^{-1} (13.557), 2358.8 cm^{-1} (12.677)
C•OCTCKCQ: 352.2 cm^{-1} (16.004), 943.4 cm^{-1} (12.97), 2363.1 cm^{-1} (12.527)
Lennard-Jones parameters: σ = 6.1414A°, ε/k = 678.63 K

a. estimated from CCC• + O_2 → CCCQ•
b. <MR>
c. A_r estimated using TST, A = (deg.) (ek_b/h) T^n $\exp(\Delta S^*(T)/R)$, deg. = 3, $\Delta S^*(T)$ is estimated as loss of three rotors and gain one OI (-4.3 × 3 +1.38 cal mol^{-1} K^{-1}). $E_{a,f} = E_{abst}$ (7..21) – 6 (H-Bond).
d. A_r estimated using TST, A = (deg.) (ek_b/h) T^n $\exp(\Delta S^*(T)/R)$, deg. = 3, $\Delta S^*(T)$ is estimated as loss of three rotors and gain one OI (-4.3 ×3 +1.38 cal mol^{-1} K^{-1}). $E_{a,f} = E_{abst}$ (8.2) + ΔU_{rxn} (13.64).
e. A_r estimated using TST, A = (deg.) (ek_b/h) T^n $\exp(\Delta S^*(T)/R)$, deg. = 3, $\Delta S^*(T)$ is estimated as loss of four rotors and gain one OI (-4.3 × 4 +1.38 cal mol^{-1} K^{-1}). $E_{a,f} = E_{abst}$ (9.73) + ΔU_{rxn} (9.49).
f. k via <MR>; k_r estimated from rate constant of CH_3O + C_2C*O → (via transition state BT26) → C_2CO•OC which A estimated using canonical TST and B3LYP-determined entropies, Ea evaluated from CBS-q// B3LYP/6-31g(d) calculation.
g. k via <MR>; k_r estimated from rate constant of CH_3 + CO_2 → (via transition state BT38) → CC(O•)=O which A estimated using canonical TST and B3LYP-determined entropies, Ea evaluated from CBS-q// B3LYP/6-31g(d) calculation.
h. k via <MR>; k_r estimated from rate constant of C•H_2OOH + C=C(C)OC → C_2•ClCQOC which A estimated using canonical TST and B3LYP-determined entropies, Ea evaluated from CBS-q// B3LYP/6-31g(d) calculation.
i. k via <MR>; k_r estimated from rate constant of CH_3O• + C=C(C)CQ → C_2•ClOCCQ which A estimated using canonical TST and B3LYP-determined entropies, Ea evaluated from CBS-q// B3LYP/6-31g(d) calculation.
j. k via <MR>; k_r estimated from rate constant of CH_2O + C_2C•CQ → C_2ClCQOC• which A estimated using canonical TST and B3LYP-determined entropies, Ea evaluated from CBS-q// B3LYP/6-31g(d) calculation. (chapter 2)

Table 5A.17 Input Parameters and High-Pressure Limit Rate Constants (k_∞) for QRRK Calculation C*C(C)OC + HO_2 → Products

Reaction	A (s-1 or cm^3/mol-s)	Ea (kcal/mol)	ref.
C*C(C)OC + HO_2 → COC(C)CQ•	1.91×10^9	0.	a.
COC(C)CQ• → C*C(C)OC + HO_2	7.88×10^{10}	23.46	b.
COC(C)CQ• → COC•(C)CQ	1.05×10^{12}	28.03	c.
COC(C)CQ• → COC(C•)CQ	3.61×10^{11}	21.84	d.
COC(C)CQ• → C•OC(C)CQ	4.14×10^{10}	19.16	e.
COC• (C)CQ → COC(C)CQ•	9.93×10^{10}	19.80	b.
COC• (C)CQ → C*C(C)OC + HO_2	2.12×10^{11}	9.54	f.
COC(C•)CQ → COC(C)CQ•	2.08×10^{10}	8.20	b.
COC(C•)CQ → C*COC + C•H_2OOH	9.53×10^{12}	26.34	g.
COC(C•)CQ → C*CCQ + CH_3O	5.13×10^{12}	22.74	h.
C•OC(C)CQ → COC(C)CQ•	3.24×10^9	9.73	b.
C•OC(C)CQ → CC•CQ + CH_2O	4.80×10^{12}	18.64	i.

Geometric mean frequency
COC(C)CQ•: 282.2 cm^{-1} (9.583), 894.3 cm^{-1} (16.029), 2443.1 cm^{-1} (13.887)
COC• (C)CQ: 252.2 cm^{-1} (11.058, 915.0 cm^{-1} (13.772), 2316.1 cm^{-1} (14.170)
COC(C•)CQ: 250.1 cm^{-1} (9.507), 879.9 cm^{-1} (17.016), 2359.9 cm^{-1} (12.477)
C•OC(C)CQ: 250.5 cm^{-1} (9.892), 850.4 cm^{-1} (16.826), 2366.5 cm^{-1} (12.282)
Lennard-Jones parameters: $\sigma = 5.5471 A^\circ$, $\varepsilon/k = 584.86$ K

a. Estimated from $C_2C*C + HO_2 \rightarrow C_2CCQ\bullet$
b. <MR>
c. A_r estimated using TST, A = (deg.) (ek_b/h) T^n exp($\Delta S^{\neq}(T)/R$), deg. = 1, $\Delta S^{\neq}(T)$ is estimated as loss of two rotors and gain one OI (-4.3 × 2 +1.38 cal mol^{-1} K^{-1}). $E_{a,f}$ = RS (10) + E_{abst} (9.8) + ΔU_{rxn} (8.23).
d. A_r estimated using TST, A = (deg.) (ek_b/h) T^n exp($\Delta S^{\neq}(T)/R$), deg. = 3, $\Delta S^{\neq}(T)$ is estimated as loss of three rotors and gain one OI (-4.3 ×3 +1.38 cal mol^{-1} K^{-1}). $E_{a,f}$ = E_{abst} (8.2) + ΔU_{rxn} (13.64).
e. A_r estimated using TST, A = (deg.) (ek_b/h) T^n exp($\Delta S^{\neq}(T)/R$), deg. = 3, $\Delta S^{\neq}(T)$ is estimated as loss of four rotors and gain one OI (-4.3 × 4 +1.38 cal mol^{-1} K^{-1}). $E_{a,f}$ = E_{abst} (9.73) + ΔU_{rxn} (9.43).
f. k via <MR>; k_r estimated from rate constant of $C_2C*C + HO_2 \rightarrow C_2C\bullet CQ$ which A estimated using canonical TST and B3LYP-determined entropies, Ea evaluated from CBS-q// B3LYP/6-31g(d) calculation. (chapter 5)
g. k via <MR>; k_r estimated from rate constant of C•H_2OOH + C*COH → (via transition state BT66) → C•C(CQ)OH which A estimated using canonical TST and B3LYP-determined entropies, Ea evaluated from CBS-q// B3LYP/6-31g(d) calculation.
h. k via <MR>; k_r estimated from rate constant of CH_3O + C*CC → (via transition state BT59) → C_2•COC which A estimated using canonical TST and B3LYP-determined entropies, Ea evaluated from CBS-q// B3LYP/6-31g(d) calculation.
i. k via <MR>; k_r estimated from rate constant of CH_2O + CC•C → (via transition state BT51) → C_2COC• which A estimated using canonical TST and B3LYP-determined entropies, Ea evaluated from CBS-q// B3LYP/6-31g(d) calculation.

Table 5A.18 Input Parameters and High-Pressure Limit Rate Constants (k_∞) for QRRK Calculation: C·C*OOC → C*C*O + CH_3O

Reaction	A (s-1 or cm^3/mol-s)	n	Ea (kcal/mol)	ref.
C•C*OOC → C*C*O + CH_3O	3.75×10^{16}	-0.76471	52.10	a.

Geometric mean frequency
C•C*OOC: 250.1 cm^{-1} (5.877), 990.6 cm^{-1} (9.430), 2236.0 cm^{-1} (7.193)
Lennard-Jones parameters: σ = 5.1983A°, ε/k = 533.08 K

a. k via <MR>; k_r estimated from rate constant of CH_3O + C*C*C → (via transition state BT1) → C*C(C•)OC which A estimated using canonical TST and B3LYP-determined entropies, Ea evaluated

Reaction	A (s-1 or cm^3/mol-s)	Ea (kcal/mol)	Ref.
C•C*OOC + O_2 → Q•CC*OOC	1.5×10^{11}	0.	b.
Q•CC*OOC → C•C*OOC + O_2	2.25×10^{12}	26.95	c.
Q•CC*OOC → QCC*OOC•	4.14×10^{10}	19.15	d.
Q•CC*OOC → COC*OCO• + O	1.26×10^{14}	58.70	e.
QCC*OOC• → Q•CC*OOC	3.26×10^{9}	9.737	c.
QCC*OOC• → QCC•*O + CH_2O	7.15×10^{13}	29.53	f.

Geometric mean frequency
Q•CC*OOC: 100.2 cm^{-1} (1.537), 472.3 cm^{-1} (13.926), 2023.9 cm^{-1} (12.536)
QCC*OOC•: 407.3 cm^{-1} (10.45), 419.1 cm^{-1} (6.004), 1868.3 cm^{-1} (11.043)
Lennard-Jones parameters: σ = 5.8569A°, ε/k = 632.06 K

b. Estimated from O*CC• + O_2 → O*CCQ•
c. <MR>
d. A_r estimated using TST, A = (deg.) (ek_b/h) T^n exp($\Delta S^\ne(T)/R$), deg. = 3, $\Delta S^\ne$(T) is estimated as loss of four rotors and gain one OI (-4.3 × 4 +1.38 cal mol^{-1} K^{-1}). $E_{a,f} = E_{abst}$ (9.73) + ΔU_{rxn} (9.42).
e. Estimate from O + CH_3O
f. k via <MR>; k_r estimated from rate constant of CH_2O + CC•*O → (via transition state BT11A) → CC*OOC• which A estimated using canonical TST and B3LYP-determined entropies, Ea evaluated from CBS-q// B3LYP/6-31g(d) calculation.

Input Parameters and High-Pressure Limit Rate Constants (k_∞) for QRRK Calculation: QCC*OOC• +O_2 → Products

Reaction	A (s-1 or cm^3/mol-s)	Ea (kcal/mol)	Ref.
QCC*OOC• + O_2 → QCCOOCQ•	4.82×10^{12}	0.	g.
QCCOOCQ• → QCC*OOC• + O_2	4.47×10^{14}	33.68	c.
QCCOOCQ• → QC•COOCQ	2.76×10^{10}	15.93	h.
QC•COOCQ → QCCOOCQ•	2.45×10^{11}	11.57	c.
QC•COOCQ → QC*C*O + O•COOH	3.36×10^{16}	54.90	i.

Geometric mean frequency
QCCOOCQ•: 361.5 cm^{-1} (12.733), 402.3 cm^{-1} (6.664), 1826.4 cm^{-1} (13.603)
QC•COOCQ: 345.0 cm^{-1} (12.593), 402.9 cm^{-1} (5.790), 1377.8 cm^{-1} (14.117)
Lennard-Jones parameters: σ = 6.4008A°, ε/k = 720.52 K

g. Estimated from COC• + O_2 → COCQ•
h. A_r estimated using TST, A = (deg.) (ek_b/h) T^n exp($\Delta S^\ne(T)/R$), deg. = 2, $\Delta S^\ne$(T) is estimated as loss of four rotors and gain one OI (-4.3 × 4 +1.38 cal mol^{-1} K^{-1}). $E_{a,f} = E_{abst}$ (11.57) + ΔU_{rxn} (4.36)
i. k via <MR>; k_r estimated from rate constant of CH_3O + C*C*C→ (via transition state BT1) → C*C(C•)OC which A estimated using canonical TST and B3LYP-determined entropies, Ea evaluated

Table 5A.19 Input Parameters and High-Pressure Limit Rate Constants (k_∞) for QRRK Calculation: CC*OOC· → CC·*O + CH_2O

Reaction	A (s-1 or cm^3/mol-s)	n	Ea (kcal/mol)	ref.
CC*OOC• → CC•*O + CH_2O	1.35×10^{15}	-0.24879	30.437	a.

Geometric mean frequency
CC*OOC•: 251.1 cm^{-1} (6.954), 1056.0 cm^{-1} (8.246), 2312.2 cm^{-1} (7.301)
Lennard-Jones parameters: σ = 5.1983A°, ε/k = 533.08 K

a. Fit with three parameter modified Arrhenius equation; A estimated using canonical TST and B3LYP-determined entropies, Ea evaluated from CBS-q// B3LYP/6-31g(d) calculation.

Input Parameters and High-Pressure Limit Rate Constants (k_∞) for QRRK Calculation CC*OOC• +O_2 → Products

Reaction	A (s-1 or cm^3/mol-s)	Ea (kcal/mol)	ref.
CC*OOC• + O_2 → CC*OOCQ•	4.82×10^{12}	0.	b.
CC*OOCQ• → CC*OOC• + O_2	6.56×10^{14}	37.32	c.
CC*OOCQ• → C•C*OOCQ	4.14×10^{10}	17.87	d.
CC*OOCQ• → CC*OOC• + O	8.60×10^{13}	58.33	e.
C•C*OOCQ → CC*OOCQ•	3.67×10^{10}	10.43	c.
C•C*OOCQ → C*C*O + O•COOH	2.68×10^{14}	51.72	f.

Geometric mean frequency
CC*OOCQ•: 150.9 cm^{-1} (7.436), 758.0 cm^{-1} (8.880), 2031.2 cm^{-1} (11.684)
C•C*OOCQ: 433.4 cm^{-1} (10.881), 409.1 cm^{-1} (4.699), 1704.2 cm^{-1} (11.920)
Lennard-Jones parameters: σ = 5.8569A°, ε/k = 632.06 K

b. Estimated from COC• + O_2 → COCQ•
c. <MR>
d. A_r estimated using TST, A = (deg.) (ek_b/h) T^n exp($\Delta S^{\neq}(T)/R$), deg. = 3, $\Delta S^{\neq}(T)$ is estimated as loss of four rotors and gain one OI (-4.3 × 4 +1.38 cal mol^{-1} K^{-1}). $E_{a,f} = E_{abst}$ (10.43) + ΔU_{rxn} (7.44).
e. Estimate from O + CH_3O
f. k via <MR>; k_r estimated from rate constant of CH_3O + C*C*C → (via transition state BT1) → C*C(C•)OC which A estimated using canonical TST and B3LYP-determined entropies, Ea evaluated from CBS-q// B3LYP/6-31g(d) calculation.

Input Parameters and High-Pressure Limit Rate Constants (k_∞) for QRRK Calculation: C•C*OOCQ +O_2 → Products

Reaction	A (s-1 or cm^3/mol-s)	Ea (kcal/mol)	Ref.
C•C*OOCQ + O_2 → Q•CCOOCQ	1.50×10^{11}	0.	g.
Q•CCOOCQ → CC*OOCQ• + O_2	1.05×10^{12}	22.95	c.
Q•CCOOCQ → QCCOOC•Q	2.76×10^{10}	18.46	h.
QCCOOC•Q → Q•CCOOCQ	2.43×10^{9}	9.90	c.
QCCOOC•Q → QCC•*O + QCHO	5.16×10^{12}	27.56	i.

Geometric mean frequency
Q•CCOOCQ: 361.5 cm^{-1} (12.733), 402.3 cm^{-1} (6.664), 1826.4 cm^{-1} (13.603)
QCCOOC•Q: 345.0 cm^{-1} (12.593), 402.9 cm^{-1} (5.790), 1377.8 cm^{-1} (14.117)
Lennard-Jones parameters: σ = 6.4008A°, ε/k = 720.52 K

g. Estimated from O*CC• + O_2 → O*CCQ•
h. A_r estimated using TST, A = (deg.) (ek_b/h) T^n exp($\Delta S^{\neq}(T)/R$), deg. = 2, $\Delta S^{\neq}(T)$ is estimated as loss of four rotors and gain one OI (-4.3 × 4 +1.38 cal mol^{-1} K^{-1}). $E_{a,f} = E_{abst}$ (9.9) + ΔU_{rxn} (8.56)
i. k via <MR>; k_r estimated from rate constant of HOC*O + CC•*O → (via transition state BT47) → CC*OOC•OH which A estimated using canonical TST and B3LYP-determined entropies, Ea evaluated from CBS-q// B3LYP/6-31g(d) calculation.

Table 5A.20 Input Parameters and High-Pressure Limit Rate Constants (k_∞) for QRRK Calculation: C$_2$·CC*O + O$_2$ → Products

Reaction	A (s-1 or cm^3/mol-s)	n	Ea (kcal/mol)	ref.
C$_2$•CC*O → C*CC + HCO	3.52×10^{11}	0.48959	22.97	a.

Geometric mean frequency
C$_2$•CC*O: 393.5 cm^{-1} (8.45), 1269.9 cm^{-1} (13.429), 2935.6 cm^{-1} (6.618)
Lennard-Jones parameters: σ = 5.1983A°, ε/k = 533.08 K

a. Fit with three parameter modified Arrhenius equation; A estimated using canonical TST and B3LYP-determined entropies, Ea evaluated from CBS-q// B3LYP/6-31g(d) calculation.

Reaction	A (s-1 or cm^3/mol-s)	Ea (kcal/mol)	ref.
C$_2$•CC*O + O$_2$ → Q•CC(C)O	3.0×10^{12}	0.	b.
Q•CC(C)O → C$_2$•CC*O + O$_2$	3.82×10^{14}	31.76	c.
Q•CC(C)O → QCC•(C)CO	1.05×10^{12}	24.55	d.
Q•CC(C)O → QCC(C)C•O	1.20×10^{11}	13.76	e.
Q•CC(C)O → QCC(C•)CO	3.66×10^{11}	21.83	f.
Q•CC(C)O → C*ClCC*O+ HO$_2$	5.31×10^{10}	22.74	g.
QCC•(C)CO → Q•CC(C)O	1.27×10^{12}	21.97	c.
QCC•(C)CO → C*ClCC*O+ HO$_2$	1.43×10^{12}	16.43	h.
QCC(C)C•O→ Q•CC(C)O	4.45×10^{10}	12.23	c.
QCC(C)C•O→ CC*C*O+ C•H$_2$OOH	5.22×10^{13}	38.3	i.
QCC(C)C•O→CC•CQ + CO	6.87×10^{13}	10.22	j.
QCC(C•)CO→ Q•CC(C)O	2.09×10^{10}	8.20	c.
QCC(C•)CO→ C*CCQ + HCO	6.89×10^{12}	22.11	k.
QCC(C•)CO→ C*CC*O+ C•H$_2$OOH	1.66×10^{12}	21.87	l.

Geometric mean frequency
Q•CC(C)O: 251.2 cm^{-1} (8.887), 995.9 cm^{-1} (147346), 2492.6 cm^{-1} (10.379)
QCC(C)C•O: 250.2 cm^{-1} (10.113), 925.8 cm^{-1} (13.182), 2227.1 cm^{-1} (10.205)
QCC(C•)CO: 250.6 cm^{-1} (9.6593), 1017.5 cm^{-1} (15.228), 2407.9 cm^{-1} (8.612)
Lennard-Jones parameters: σ = 6.1414A°, ε/k = 678.63 K

b. Estimated from CC• + O$_2$ → CCQ•

c. <MR>

d. A_r estimated using TST, A = (deg.) (ek_b/h) T^n exp($\Delta S^{\neq}$(T)/R), deg. = 1, $\Delta S^{\neq}$(T) is estimated as loss of two rotors and gain one OI (-4.3 × 2 +1.38 cal mol^{-1} K^{-1}). $E_{a,f}$ = RS (10) + E_{abst} (11.97) + ΔU_{rxn} (2.58).

e. A_r estimated using TST, A = (deg.) (ek_b/h) T^n exp($\Delta S^{\neq}$(T)/R), deg. = 1, $\Delta S^{\neq}$(T) is estimated as loss of three rotors and gain one OI (-4.3 × 3 +1.38 cal mol^{-1} K^{-1}). $E_{a,f}$ = E_{abst} (12.23) + ΔU_{rxn} (1.53).

f. A_r estimated using TST, A = (deg.) (ek_b/h) T^n exp($\Delta S^{\neq}$(T)/R), deg. = 3, $\Delta S^{\neq}$(T) is estimated as loss of three rotors and gain one OI (-4.3 × 3 +1.38 cal mol^{-1} K^{-1}). $E_{a,f}$ = E_{abst} (8.2) + ΔU_{rxn} (13.63).

g. k via <MR>; k_r estimated from rate constant of HO$_2$ + C2C*C → C$_2$CCQ• which A estimated using canonical TST and B3LYP-determined entropies, Ea evaluated from CBS-q// B3LYP/6-31g(d) calculation. (chapter 3)

h. k via <MR>; k_r estimated from rate constant of HO$_2$ + C2C*C → C$_2$C•CQ which A estimated using canonical TST and B3LYP-determined entropies, Ea evaluated from CBS-q// B3LYP/6-31g(d) calculation. (chapter 5)

i. k via <MR>; k_r estimated from rate constant of C•H$_2$OH + C*C*O → (via transition state BT80) → C•C*OCOH which A estimated using canonical TST and B3LYP-determined entropies, Ea evaluated from CBS-q// B3LYP/6-31g(d) calculation.

j. k via <MR>; k_r estimated from rate constant of CO + CC•C → (via transition state BT52) → C$_2$CC•*O which A estimated using canonical TST and B3LYP-determined entropies, Ea evaluated from CBS-q// B3LYP/6-31g(d) calculation.

k. k via <MR>; k_r estimated from rate constant of HCO + C*CC → (via transition state BT62) → C$_2$•CC*O which A estimated using canonical TST and B3LYP-determined entropies, Ea evaluated from CBS-q// B3LYP/6-31g(d) calculation.

l. k via <MR>; k_r estimated from rate constant of C•H$_2$OH + C*CC → C$_2$•COH which A estimated using canonical TST and B3LYP-determined entropies, Ea evaluated from CBS-q// B3LYP/6-31g(d) calculation. (in C2C*C + OH reaction system)

Table 5A.21 Input Parameters and High-Pressure Limit Rate Constants (k_∞) for QRRK Calculation: $C_2C{\cdot}C{*}O + O_2 \rightarrow$ Products

Reaction	A (s-1 or cm^3/mol-s)	Ea (kcal/mol)	ref.
$C_2C{\bullet}C{*}O + O_2 \rightarrow C_2CQ{\bullet}C{*}O$	1.5×10^{11}	0.	a.
$C_2CQ{\bullet}C{*}O \rightarrow C_2C{\bullet}C{*}O + O_2$	5.1×10^{12}	17.64	b.
$C_2CQ{\bullet}C{*}O \rightarrow C_2{\bullet}CQC{*}O$	6.28×10^{12}	31.86	c.
$C_2CQ{\bullet}C{*}O \rightarrow C_2CQC{\bullet}{*}O$	1.05×10^{12}	20.70	d.
$C_2CQ{\bullet}C{*}O \rightarrow C{*}ClCC{*}O + HO_2$	5.92×10^{11}	13.25	e.
$C_2CQ{\bullet}C{*}O \rightarrow C_2C{*}C{*}O + HO_2$	7.42×10^{12}	54.51	f.
$C_2{\bullet}CQC{*}O \rightarrow C_2CQ{\bullet}C{*}O$	3.26×10^{11}	18.20	b.
$C_2{\bullet}CQC{*}O \rightarrow C{*}C(C)Q + HCO$	5.69×10^{12}	21.92	g.
$C_2{\bullet}CQC{*}O \rightarrow C{*}ClCC{*}O + HO_2$	3.09×10^{11}	5.24	h.
$C_2CQC{\bullet}{*}O \rightarrow C_2CQ{\bullet}C{*}O$	3.82×10^{11}	19.15	b.
$C_2CQC{\bullet}{*}O \rightarrow C_2C{*}O + CO + OH$	5.36×10^{13}	2.02	i.
$C_2CQC{\bullet}{*}O \rightarrow C_2C{*}C{*}O + HO_2$	7.32×10^{11}	42.83	j.

Geometric mean frequency
$C_2CQ{\bullet}C{*}O$: 250.5 cm^{-1} (8.768), 1053.5 cm^{-1} (16.206), 2758.4 cm^{-1} (9.027)
$C_2{\bullet}CQC{*}O$: 250.4 cm^{-1} (9.459), 1059.9 cm^{-1} (16.729), 2720.9 cm^{-1} (7.312)
$C_2CQC{\bullet}{*}O$: 317.0 cm^{-1} (11.903), 1100.5 cm^{-1} (13.887), 2631.9 cm^{-1} (7.710)
Lennard-Jones parameters: σ = 6.1414A°, ε/k = 678.63 K

a. Estimated from $O{*}CC{\bullet} + O_2 \rightarrow O{*}CCQ{\bullet}$
b. <MR>
c. A_r estimated using TST, A = (deg.) (ek_b/h) T^n exp($\Delta S^{\neq}(T)/R$), deg. = 6, $\Delta S^{\neq}(T)$ is estimated as loss of two rotors and gain one OI (-4.3 × 2 +1.38 cal mol^{-1} K^{-1}). $E_{a,f}$ = RS (10) + E_{abst} (8.2) + ΔU_{rxn} (13.66).
d. k via <MR>; k_r estimated from rate constant of $Q{\bullet}CC{*}O \rightarrow QCC{\bullet}{*}O$ which A estimated using canonical TST and B3LYP-determined entropies, Ea evaluated from CBS-q// B3LYP/6-31g(d) calculation.
e. k via <MR>; k_r estimated from rate constant of HO_2 + C2C*C $\rightarrow$ $C_3CQ{\bullet}$ which A estimated using canonical TST and B3LYP-determined entropies, Ea evaluated from CBS-q// B3LYP/6-31g(d) calculation. (chapter 3)
f. k via <MR>; k_r estimated from rate constant of $HO_2 + C{*}C{*}O$ $\rightarrow$ (via transition state TCQJCHOE) $\rightarrow$ $Q{\bullet}CC{*}O$ which A estimated using canonical TST and B3LYP-determined entropies, Ea evaluated from CBS-q// B3LYP/6-31g(d) calculation.
g. k via <MR>; k_r estimated from rate constant of HCO + C*C(C)OH $\rightarrow$ (via transition state BT45) $\rightarrow$ $C_2{\bullet}COHC{*}O$ which A estimated using canonical TST and B3LYP-determined entropies, Ea evaluated from CBS-q// B3LYP/6-31g(d) calculation.
h. k via <MR>; k_r estimated from rate constant of HO_2 + C2C*C $\rightarrow$ $C_3{\bullet}CQ$ which A estimated using canonical TST and B3LYP-determined entropies, Ea evaluated from CBS-q// B3LYP/6-31g(d) calculation. (chapter 5)
i. k via <MR>; k_r estimated from rate constant of CO + $C_2C{\bullet}OH$ $\rightarrow$ (via transition state BT30) $\rightarrow$ $C_2COHC{\bullet}{*}O$ which A estimated using canonical TST and B3LYP-determined entropies, Ea evaluated from CBS-q// B3LYP/6-31g(d) calculation.

Table 5A.22 Input Parameters and High-Pressure Limit Rate Constants (k_∞) for QRRK Calculation: C_2CC·*O + O_2 → Products

Reaction	A (s-1 or cm^3/mol-s)	n	Ea (kcal/mol)	ref.
C_2CC•*O → CC•C + CO	4.70×10^{13}	0.20957	13.02	a.

Geometric mean frequency
C_2CC•*O: 390.4 cm^{-1} (8.38), 1275.9 cm^{-1} (13.645), 2955.9 cm^{-1} (6.475)
Lennard-Jones parameters: σ = 5.1983A°, ε/k = 533.08 K

a. Fit with three parameter modified Arrhenius equation; A estimated using canonical TST and B3LYP-determined entropies, Ea evaluated from CBS-q// B3LYP/6-31g(d) calculation.

Reaction	A (s-1 or cm^3/mol-s)	Ea (kcal/mol)	ref.
C_2CC•*O + O_2 → C_2CCQ•*O	6.0×10^{12}	0.	b.
C_2CCQ•*O → C_2C•C*O + O_2	1.94×10^{15}	30.62	c.
C_2CCQ•*O → C_2•CCQ*O	7.21×10^{11}	15.18	d.
C_2CCQ•*O → C_2C•CQ*O	1.05×10^{12}	19.70	e.
C_2CCQ•*O → C_2C*C*O + HO_2	6.16×10^{16}	24.41	f.
C_2•CCQ*O → C_2CCQ•*O	4.13×10^{10}	11.53	c.
C_2•CCQ*O → C*CC +C•QO	2.88×10^{13}	29.76	g.
C_2C•CQ*O → C_2CCQ•*O	1.25×10^{12}	27.1	c.
C_2C•CQ*O → C_2C*C*O + HO_2	5.59×10^{13}	36.52	h.

Geometric mean frequency
C_2CCQ•*O: 250.5 cm^{-1} (8.768), 1053.5 cm^{-1} (16.206), 2758.4 cm^{-1} (9.027)
C_2•CCQ*O: 250.4 cm^{-1} (9.459), 1059.9 cm^{-1} (16.729), 2720.9 cm^{-1} (7.312)
C_2C•CQ*O: 317.0 cm^{-1} (11.903), 1100.5 cm^{-1} (13.887), 2631.9 cm^{-1} (7.710)
Lennard-Jones parameters: σ = 6.1414A°, ε/k = 678.63 K

b. Estimated from C*C• + O_2 → C*CQ•

c. <MR>

d. A_r estimated using TST, $A = (\text{deg.}) (ek_b/h) T^n \exp(\Delta S^{\ne}(T)/R)$, deg. = 6, $\Delta S^{\ne}(T)$ is estimated as loss of three rotors and gain one OI (-4.3 × 3 +1.38 cal mol^{-1} K^{-1}). $E_{a,f} = E_{abst}$ (11.53) + ΔU_{rxn} (3.65).

e. A_r estimated using TST, $A = (\text{deg.}) (ek_b/h) T^n \exp(\Delta S^{\ne}(T)/R)$, deg. = 1, $\Delta S^{\ne}(T)$ is estimated as loss of two rotors and gain one OI (-4.3 × 2 +1.38 cal mol^{-1} K^{-1}). $E_{a,f}$ = RS (10) + E_{abst} (9.7)

f. k via <MR>; k_r estimated from rate constant of HO_2 + C*C*O → (via transition state TCQJCHOE) → Q•CC*O which A estimated using canonical TST and B3LYP-determined entropies, Ea evaluated from CBS-q// B3LYP/6-31g(d) calculation.

g. k via <MR>; k_r estimated from rate constant of HOC•*O + C*CC → (via transition state BT50)→ C_2•CC*OOH which A estimated using canonical TST and B3LYP-determined entropies, Ea evaluated from CBS-q// B3LYP/6-31g(d) calculation.

h. k via <MR>; k_r estimated from rate constant of HO_2 + C*C*O → (via transition state TCJCOXQ) → C•CQ*O which A estimated using canonical TST and B3LYP-determined entropies, Ea evaluated from CBS-q// B3LYP/6-31g(d) calculation.

Table 5A.23 Input Parameters and High-Pressure Limit Rate Constants (k_∞) for QRRK Calculation: C*CIC·C*O → Products

Reaction	A (s-1 or cm^3/mol-s)	n	Ea (kcal/mol)	ref.
C*CIC•C*O → C*C*C +HCO	1.08×10^{16}	-0.2757	52.04	a.

Geometric mean frequency
C*CIC•C*O: 490.7 cm^{-1} (10.084), 1223.9 cm^{-1} (8.782), 2973.7 cm^{-1} (4.634)
Lennard-Jones parameters: σ = 5.1983A°, ε/k = 533.08 K

a. Fit with three parameter modified Arrhenius equation; A estimated using canonical TST and B3LYP-determined entropies, Ea evaluated from CBS-q// B3LYP/6-31g(d) calculation.

Input Parameters and High-Pressure Limit Rate Constants (k_∞) for QRRK Calculation: C*CIC•C*O +O_2 → Products

Reaction	A (s-1 or cm^3/mol-s)	n	Ea (kcal/mol)	ref.
C*CIC•C*O +O_2 → C*CICQ•CO	3.0×10^{11}	0.	0.	b.
C*CICQ•CO → C*CIC•C*O +O_2	4.51×10^{12}	0.	18.01	c.
C*CICQ•CO → C*CICQC•O	2.06×10^{7}	1.3458	10.28	d.
C*CICQ•CO → C•*CICQCO	2.09×10^{12}	0.	28.76	e.
C*CICQ•CO → C*CICO•CO + O	1.27×10^{14}	0.	58.71	f.
C*CICQC•O → C*CICQ•CO	4.15×10^{9}	0.6506	15.78	c.
C*CICQC•O → C*C•CQ + CO	1.05×10^{15}	0.	28.28	g.
C*CICQC•O → C*C*C*O + C•H_2OOH	1.10×10^{14}	0.	51.15	h.
C•*CICQCO → C*CICQ•CO	5.70×10^{11}	0.	4.83	c.
C•*CICQCO → C#CC*O + C•H_2OOH	1.11×10^{13}	0.	30.25	i.
C•*CICQCO → C#CCQ + HCO	2.65×10^{13}	0.	25.85	j.

Geometric mean frequency
C*CICQ•CO: 307.9 cm^{-1} (9.839), 936.8 cm^{-1} (10.464), 2390.7 cm^{-1} (8.198)
C*CICQC•O: 285.2 cm^{-1} (10.24), 897.9 cm^{-1} (10.879), 2298.4 cm^{-1} (6.877)
C•*CICQCO: 317.0 cm^{-1} (11.903), 1100.5 cm^{-1} (13.887), 2631.9 cm^{-1} (7.710)
Lennard-Jones parameters: σ = 5.8564A°, ε/k = 632.06 K

b. Estimated from C*CC• + O_2 → C*CCQ• and C_2•C*C + O_2 → C*CICQ•C
c. <MR>
d. Fit with three parameter modified Arrhenius equation; A estimated using canonical TST and PM3-determined entropies, Ea evaluated from $E_a = E_{abst} + \Delta U_{rxn}$
e. A_r estimated using TST, A = (deg.) (ek_b/h) T^n exp($\Delta S^{\neq}$(T)/R), deg. = 2, $\Delta S^{\neq}$(T) is estimated as loss of two rotors and gain one OI (-4.3 × 2 +1.38 cal mol^{-1} K^{-1}). $E_{a,f} = E_{abst}$ (4.83) + ΔU_{rxn} (23.95).
f. Estimated from O + CH_3O
g. k via <MR>; k_r estimated from rate constant of C*C•COH + CO → (via transition state BT62) → C*CICOHC•*O which A estimated using canonical TST and B3LYP-determined entropies, Ea evaluated from CBS-q// B3LYP/6-31g(d) calculation
h. k via <MR>; k_r estimated from rate constant of C•OH + C*C*C*O → (via transition state BT64) → O*CC•CCOH which A estimated using canonical TST and B3LYP-determined entropies, Ea evaluated from CBS-q// B3LYP/6-31g(d) calculation.
i. k via <MR>; k_r estimated from rate constant of C•OH + C*CC → C_2•COH which A estimated using canonical TST and B3LYP-determined entropies, Ea evaluated from CBS-q// B3LYP/6-31g(d) calculation. (in C2C*C + OH reaction system)
j. k via <MR>; k_r estimated from rate constant of HCO + C*CC → (via transition state BT61) → C_2•CC*O which A estimated using canonical TST and B3LYP-determined entropies, Ea evaluated from CBS-q// B3LYP/6-31g(d) calculation

Table 5A.24 Input Parameters and High-Pressure Limit Rate Constants (k_∞) for QRRK Calculation: C*CICC·*O → Products

Reaction	A (s-1 or cm^3/mol-s)	n	Ea (kcal/mol)	ref.
C*CICC•*O → C*C*C*O +CH3	9.21×10^{13}	0	56.52	a.
C*CICC•*O → CC•*C +CO	3.52×10^{11}	0.48959	22.97	b.

Geometric mean frequency
C*CICC•*O: 481.7 cm^{-1} (11.001), 1443.5 cm^{-1} (7.933), 3430.9 cm^{-1} (4.566)
Lennard-Jones parameters: σ = 5.1983A°, ε/k = 533.08 K

a. Estimated from CH3 + C*C*C → C2.C*C (73 TSA)
b. Fit with three parameter modified Arrhenius equation; A estimated using canonical TST and B3LYP-determined entropies, Ea evaluated from CBS-q// B3LYP/6-31g(d) calculation.

Input Parameters and High-Pressure Limit Rate Constants (k_∞) for QRRK Calculation: C*CICC•*O + O$_2$ → Products

Reaction	A (s-1 or cm^3/mol-s)	Ea (kcal/mol)	ref.
C*CICC•*O +O$_2$ → C*CICCQ•O	1.0×10^{12}	0.	c.
C*CICCQ•O → C*CICC•*O +O$_2$	7.37×10^{12}	26.83	d.
C*CICCQ•O → C2DCCO•*O+O	9.64×10^{13}	9.71	e.
C*CICCQ•O → C*CIC•CQO	3.60×10^{11}	25.46	f.
C*CIC•CQO → C*CICCQ•O	3.73×10^{10}	20.48	d.
C*CIC•CQO → C•QO+C*C*C	1.49×10^{14}	52.58	g.
C*CIC•CQO → C•*CICCQO	2.09×10^{12}	28.78	h.
C•*CICCQO → C*CIC•CQO	5.65×10^{11}	4.83	d.
C•*CICCQO → C•QO+C#CC	5.52×10^{14}	31.35	i.

Geometric mean frequency
C*CICCQ•O: 326.6 cm^{-1} (10.004), 1054.5 cm^{-1} (11.073), 2735.2 cm^{-1} (7.423)
C*CIC•CQO: 322.2 cm^{-1} (9.929), 969.0 cm^{-1} (12.586), 2459.5 cm^{-1} (5.485)
C•*CICCQO: 317.0 cm^{-1} (11.903), 1100.5 cm^{-1} (13.887), 2631.9 cm^{-1} (7.710)
Lennard-Jones parameters: σ = 6.1414A°, ε/k = 678.63 K

c. Estimated from C*C• + O$_2$ → *CCQ and C*CC• + O$_2$ → C*CCQ•
d. <MR>
e. Estimated from O + CH$_3$O
f. A_r estimated using TST, A = (deg.) (ek_b/h) T^n exp($\Delta S^{\neq}$(T)/R), deg. = 3, $\Delta S^{\neq}$(T) is estimated as loss of three rotors and gain one OI (-4.3 × 3 +1.38 cal mol^{-1} K^{-1}). $E_{a,f} = E_{abst}$ (9.17).
g. A_r estimated using TST, A = (deg.) (ek_b/h) T^n exp($\Delta S^{\neq}$(T)/R), deg. = 2, $\Delta S^{\neq}$(T) is estimated as loss of two rotors and gain one OI (-4.3 × 2 +1.38 cal mol^{-1} K^{-1}). $E_{a,f} = E_{abst}$ (4.83) + ΔU_{rxn} (23.95).
h. k via <MR>; k_r estimated from rate constant of Q•C*O + C*C → (via transition state BT13)→ C•CCQ*O which A estimated using canonical TST and B3LYP-determined entropies, Ea evaluated from CBS-q// B3LYP/6-31g(d) calculation.
i. k via <MR>; k_r estimated from rate constant of HO•C*O + C#C → (via transition state BT70)→ C•*CCOH*O which A estimated using canonical TST and B3LYP-determined entropies, Ea evaluated from CBS-q// B3LYP/6-31g(d) calculation.

Table 5A.25 Input Parameters and High-Pressure Limit Rate Constants (k_∞) for QRRK Calculation: C*CICC*O + OH → C_2·CIOHCO →Products

Reaction	A (s-1 or cm^3/mol-s)	n.	Ea (kcal/mol)	ref.
C*CICC*O +OH → C_2•CIOHCO	1.81×10^{13}	0.	0.	a.
C_2•CIOHCO → C*CICC*O +OH	2.24×10^{14}	0.	21.63	b.
C_2•CIOHCO → C_2C(O•)CO	3.21×10^{12}	0.	27.98	c.
C_2•CIOHCO → C*C(C)OH + HCO	3.26×10^{12}	0.14607	22.46	d.
C_2C(O•)CO → C_2•CIOHCO	6.01×10^{13}	0.	24.59	b.
C_2C(O•)CO → C_2C*O + HCO	5.19×10^{14}	-0.21122	4.70	e.

Geometric mean frequency
C_2•CIOHCO: 431.6 cm^{-1} (12.21), 1412.1cm^{-1} (15.266), 3486.6 cm^{-1} (4.027)
C_2C(O•)CO: 431.6 cm^{-1} (12.21), 1412.1 cm^{-1} (15.266), 3486.6 cm^{-1} (4.027)
Lennard-Jones parameters: σ = 5.1983A°, ε/k = 533.08 K

a. Estimated from OH + C*CC → C2•COH (90TSA)
b. <MR>
c. k via <MR>; k_r estimated from rate constant of C_3CO• → C_3•COH which A estimated using canonical TST and B3LYP-determined entropies, Ea evaluated from CBS-q// B3LYP/6-31g(d) calculation. (in C2C*C + OH reaction system)
d. k via <MR>; k_r estimated from rate constant of HCO + C_2C*O → (via transition state BT46) → C_2CO•C*O which A estimated using canonical TST and B3LYP-determined entropies, Ea evaluated from CBS-q// B3LYP/6-31g(d) calculation.
e. k via <MR>; k_r estimated from rate constant of HCO + C*C(C)OH→ (via transition state BT45) → C_2•COHC*O which A estimated using canonical TST and B3LYP-determined entropies, Ea evaluated from CBS-q// B3LYP/6-31g(d) calculation.

Input Parameters and High-Pressure Limit Rate Constants (k_∞) for QRRK Calculation: C*CICC*O + OH → CCI•COHCO → Products

Reaction	A (s-1 or cm^3/mol-s)	Ea (kcal/mol)	ref.
C*CICC*O +OH → CCI•COHCO	1.80×10^{13}	0.	a.
CCI•COHCO → C*CICC*O +OH	7.62×10^{14}	29.21	b.
CCI•COHCO → CC(CO•)CO	1.63×10^{12}	36.27	c.
CC(CO•)CO → CCI•COHCO	7.33×10^{11}	21.84	b.
CC(CO•)CO → CC•C*O + CH_2O	2.89×10^{13}	9.351	d.

Geometric mean frequency
CCI•COHCO: 432.1 cm^{-1} (12.93), 1419.8 cm^{-1} (11.690), 2998.7 cm^{-1} (6.385)
CC(CO•)CO: 392.3 cm^{-1} (10.257), 1270.1 cm^{-1} (14.560), 2975.3 cm^{-1} (6.683)
Lennard-Jones parameters: σ = 5.1983A°, ε/k = 533.08 K

a. Estimated from OH + C*CC → CC•COH (90TSA)
b. <MR>
c. k via <MR>; k_r estimated from rate constant of C_2CCO•C_2C•COH which A estimated using canonical TST and B3LYP-determined entropies, Ea evaluated from CBS-q// B3LYP/6-31g(d) calculation.(in C_2C*C + OH reaction system)
f. k via <MR>; k_r estimated from rate constant of C•C*O + CH_2O → (via transition state BT40)→ O*CCCO• which A estimated using canonical TST and B3LYP-determined entropies, Ea evaluated from CBS-q// B3LYP/6-31g(d) calculation.

Table 5A.26 Input Parameters and High-Pressure Limit Rate Constants (k_∞) for QRRK Calculation: C_2·CIOHCO + O_2 → Products

Reaction	A (s-1 or cm^3/mol-s)	Ea (kcal/mol)	ref.
C_2•CIOHCO+O_2 → CCTCQ•KCO	3.0×10^{12}	0.	a.
CCTCQ•KCO → C_2•CIOHCO+O_2	13.89×10^{14}	31.19	b.
CCTCQ•KCO → C•CTCQKCO	3.61×10^{11}	21.85	c.
CCTCQ•KCO → CCTCQO•CO	1.20×10^{11}	18.25	d.
CCTCQ•KCO → CCTCQKC•O	1.20×10^{11}	14.04	e.
C•CTCQKCO → CCTCQ•KCO	2.08×10^{10}	8.20	b.
C•CTCQKCO → C*C(OH)CHO + C•H_2OOH	1.36×10^{12}	21.23	f.
CCTCQO•CO → CCTCQ•KCO	1.28×10^{11}	1.21	b.
CCTCQO•CO → CC*OC*O + C•H_2OOH	1.01×10^{13}	7.25	g.
CCTCQKC•O → CCTCQ•KCO	4.42×10^{10}	12.50	b.
CCTCQKC•O → CC(OH)*CO+ C•H_2OOH	1.16×10^{13}	31.04	h.

Geometric mean frequency
CCTCQ•KCO: 284.4 cm^{-1} (12.427), 1102.8 cm^{-1} (15.555), 2617.8 cm^{-1} (8.518)
C•CTCQKCO: 265.5 cm^{-1} (12.695), 1091.2 cm^{-1} (16.380), 2529.8 cm^{-1} (6.925)
CCTCQO•CO: 279.2 cm^{-1} (12.697), 1093.5 cm^{-1} (16.792), 2462.2 cm^{-1} (7.011)
CCTCQKC•O: 263.8 cm^{-1} (12.683), 1100.0 cm^{-1} (16.555), 2544.5 cm^{-1} (6.761)
Lennard-Jones parameters: σ = 6.1414A°, ε/k = 678.63 K

a. Estimated from CC• + O_2 → CCQ•
b. <MR>
c. A_r estimated using TST, A = (deg.) (ek_b/h) T^n exp($\Delta S^{\neq}$(T)/R), deg. = 3, $\Delta S^{\neq}$(T) is estimated as loss of three rotors and gain one OI (-4.3 × 3 +1.38 cal mol^{-1} K^{-1}). $E_{a,f} = E_{abst}$ (8.2) + ΔU_{rxn} (13.65).
d. A_r estimated using TST, A = (deg.) (ek_b/h) T^n exp($\Delta S^{\neq}$(T)/R), deg. = 1, $\Delta S^{\neq}$(T) is estimated as loss of three rotors and gain one OI (-4.3 × 1 +1.38 cal mol^{-1} K^{-1}). $E_{a,f} = E_{abst}$ (7.21) + ΔU_{rxn} (17.04) – H-Bond (6).
e. A_r estimated using TST, A = (deg.) (ek_b/h) T^n exp($\Delta S^{\neq}$(T)/R), deg. = 1, $\Delta S^{\neq}$(T) is estimated as loss of three rotors and gain one OI (-4.3 × 1 +1.38 cal mol^{-1} K^{-1}). $E_{a,f} = E_{abst}$ (12.5) + ΔU_{rxn} (1.54).
f. k via <MR>; k_r estimated from rate constant of C•OH + C*C(OH)C*O→ (via transition state BT56)→ C•C(OH)(COH)C*O which A estimated using canonical TST and B3LYP-determined entropies, Ea evaluated from CBS-q// B3LYP/6-31g(d) calculation.
g. k via <MR>; k_r estimated from rate constant of C•OH + CC*OC*O→ (via transition state BT44)→ CC(COH)(O•)C*O which A estimated using canonical TST and B3LYP-determined entropies, Ea evaluated from CBS-q// B3LYP/6-31g(d) calculation.
h. k via <MR>; k_r estimated from rate constant of C•OOH + C*C(C)OC→ C2•C(OOH)OC which A estimated using canonical TST and B3LYP-determined entropies, Ea evaluated from CBS-q// B3LYP/6-31g(d) calculation. (in C3•COC + O2 reaction system)

Table 5A.27 Input Parameters and High-Pressure Limit Rate Constants (k_∞) for QRRK Calculation CCl·COHCO + O_2 → Products

Reaction	A (s-1 or cm^3/mol-s)	Ea (kcal/mol)	ref.
CCl•COHCO+O_2 → CCTCKQ•CO	3.0×10^{11}	0.	a.
CCTCKQ•CO → CCl•COHCO+O_2	1.199×10^{13}	23.61	b.
CCTCKQ•CO → CCTCO•QCO	1.20×10^{11}	18.25	c.
CCTCKQ•CO → C•CTCKQCO	3.15×10^{12}	31.73	d.
CCTCKQ•CO → CCTCKQC•O	1.05×10^{12}	23.77	e.
CCTCO•QCO → CCTCKQ•CO	3.05×10^{12}	2.21	b.
CCTCO•QCO → CC• (Q)CHO + CH_2O	6.94×10^{14}	7.13	f.
C•CTCKQCO → CCTCKQ•CO	1.46×10^{11}	18.20	b.
C•CTCKQCO → CC*ClQCC*O + C•H_2OH	1.57×10^{13}	26.28	g.
CCTCKQ•CO → CCTCKQ•CO	3.86×10^{11}	22.23	b.
CCTCKQ•CO → CC(Q)*C*O+ C•H_2OH	3.61×10^{13}	36.02	h.

Geometric mean frequency
CCTCKQ•CO: 284.4 cm^{-1} (12.427), 1102.8 cm^{-1} (15.555), 2617.8 cm^{-1} (8.518)
CCTCO•QCO: 279.2 cm^{-1} (12.697), 1093.5 cm^{-1} (16.792), 2462.2 cm^{-1} (7.011)
C•CTCKQCO: 269.9 cm^{-1} (12.992), 1080.2 cm^{-1} (15.427), 2504.8 cm^{-1} (7.581)
CCTCKQ•CO: 263.8 cm^{-1} (12.683), 1100.0 cm^{-1} (16.555), 2544.5 cm^{-1} (6.761)
Lennard-Jones parameters: σ = 6.1414A°, ε/k = 678.63 K

a. Estimated from C*CC• + O_2 → C*CCQ•
b. <MR>
c. A_r estimated using TST, A = (deg.) (ek_b/h) T^n exp($\Delta S^{\neq}$(T)/R), deg. = 1, $\Delta S^{\neq}$(T) is estimated as loss of three rotors and gain one OI (-4.3 × 3 +1.38 cal mol^{-1} K^{-1}). $E_{a,f} = E_{abst}$ (1.21) + ΔU_{rxn} (17.04)) – H-Bond (6).
d. A_r estimated using TST, A = (deg.) (ek_b/h) T^n exp($\Delta S^{\neq}$(T)/R), deg. = 3, $\Delta S^{\neq}$(T) is estimated as loss of two rotors and gain one OI (-4.3 × 2 +1.38 cal mol^{-1} K^{-1}). $E_{a,f} = E_{abst}$ (18.2) + ΔU_{rxn} (13.53).
e. A_r estimated using TST, A = (deg.) (ek_b/h) T^n exp($\Delta S^{\neq}$(T)/R), deg. = 1, $\Delta S^{\neq}$(T) is estimated as loss of two rotors and gain one OI (-4.3 × 2 +1.38 cal mol^{-1} K^{-1}). $E_{a,f} = E_{abst}$ (1.54) + ΔU_{rxn} (22.23).
f. k via <MR>; k_r estimated from rate constant of C•C*O + CH_2O → (via transition state BT40)→ O*CCCO• which A estimated using canonical TST and B3LYP-determined entropies, Ea evaluated from CBS-q// B3LYP/6-31g(d) calculation.
g. k via <MR>; k_r estimated from rate constant of C• H_2OH + C*C(OH)C*O→ (via transition state BT56)→ CC(OH)COH)C*O which A estimated using canonical TST and B3LYP-determined entropies, Ea evaluated from CBS-q// B3LYP/6-31g(d) calculation.
h. k via <MR>; k_r estimated from rate constant of C•H_2OOH + C*C(C)OC→ C_2•C(OOH)OC which A estimated using canonical TST and B3LYP-determined entropies, Ea evaluated from CBS-q// B3LYP/6-31g(d) calculation. (in C3•COC + O2 reaction system)

Table 5A.28 Input Parameters and High-Pressure Limit Rate Constants (k_∞) for QRRK Calculation: CC*OC·*O → CC·*O + CO

Reaction	A (s-1 or cm^3/mol-s)	n	Ea (kcal/mol)	ref.
CC*OC•*O → CC•*O + CO	1.00×10^{14}	0.6814	7.8311	a.

Geometric mean frequency
CC*OC•*O: 414.7 cm^{-1} (6.847), 1254.2 cm^{-1} (5.933), 2393.4 cm^{-1} (4.220)
Lennard-Jones parameters: σ = 5.1983A°, ε/k = 533.08 K

a. Fit with three parameter modified Arrhenius equation; A estimated using canonical TST and B3LYP-determined entropies, Ea evaluated from CBS-q// B3LYP/6-31g(d) calculation.

Input Parameters and High-Pressure Limit Rate Constants (k_∞) for QRRK Calculation CC*OC•*O +O_2 → Products

Reaction	A (s-1 or cm^3/mol-s)	Ea (kcal/mol)	ref.
CC*OC•*O + O_2 → CC*OCQ•*O	3.12×10^{12}	0.	b.
CC*OCQ•*O → CC*OC•*O + O_2	1.59×10^{13}	36.53	c.
CC*OCQ•*O → C•C*OCQ*O	3.61×10^{11}	12.5	d.
CC*OCQ•*O → CC*OCO•*O + O	7.69×10^{13}	35.36	e.
C•C*OCQ*O → CC*OCQ•*O	1.43×10^{11}	13.04	c.
C•C*OCQ*O → C•QO + C*C*O	2.09×10^{13}	40.26	f.

Geometric mean frequency
CC*OCQ•*O: 327.0 cm^{-1} (6.942), 802.6 cm^{-1} (6.269), 1962.5 cm^{-1} (9.289)
C•C*OCQ*O: 335.5 cm^{-1} (7.761), 401.2 cm^{-1} (1.690), 1443.0 cm^{-1} (12.549)
Lennard-Jones parameters: σ = 5.8569A°, ε/k = 632.06 K

b. Estimated from C*C• + O_2 → C*CQ•

c. <MR>

d. A_r estimated using TST, A = (deg.) (ek_b/h) T^n exp($\Delta S^{*}(T)/R$), deg. = 3, $\Delta S^{*}(T)$ is estimated as loss of three rotors and gain one OI (-4.3 × 3 +1.38 cal mol^{-1} K^{-1}). $E_{a,f} = E_{abst}$ (12.5) + ΔU_{rxn} (0.54).

e. Estimate from O + CH_3O

f. k via <MR>; k_r estimated from rate constant of HOC•*O + C*C*O → (via transition state BT48)→ C•C(*O)C*OOH which A estimated using canonical TST and B3LYP-determined entropies, Ea evaluated from CBS-q// B3LYP/6-31g(d) calculation.

Table 5A.29 Input Parameters and High-Pressure Limit Rate Constants (k_∞) for QRRK Calculation C·C*OC*O → CC·*O + CO

Reaction	A (s-1 or cm^3/mol-s)	N	Ea (kcal/mol)	ref.
C•C*OC*O → C*C*O + HCO	1.60×10^{14}	0.	24.87	a.

Geometric mean frequency
C•C*OC*O: 410.1 cm^{-1} (5.879), 1024.8 cm^{-1} (6.269), 2047.9 cm^{-1} (4.852)
Lennard-Jones parameters: σ = 5.1983A°, ε/k = 533.08 K

a. Fit with two parameter modified Arrhenius equation; A estimated using canonical TST and B3LYP-determined entropies, Ea evaluated from CBS-q// B3LYP/6-31g(d) calculation.

Input Parameters and High-Pressure Limit Rate Constants (k_∞) for QRRK Calculation C•C*OC*O +O_2 → Products

Reaction	A (s-1 or cm^3/mol-s)	Ea (kcal/mol)	Ref.
C•C*OC*O + O_2 → Q•CC*OC*O	3.10×10^{11}	0.	b.
Q•CC*OC*O → C•C*OC*O + O_2	2.13×10^{12}	20.16	c.
Q•CC*OC*O → QCC*OC•*O	1.20×10^{11}	10.77	d.
Q•CC*OC*O → O•CC*OCO*O + O	9.35×10^{13}	58.42	e.
QCC*OC•*O → Q•CC*OC*O	1.43×10^{11}	13.04	c.
QCC*OC•*O → QCC•*O + CO	6.17×10^{15}	8.51	f.

Geometric mean frequency
Q•CC*OC*O: 437.7 cm^{-1} (8.793), 447.3 cm^{-1} (4.253), 1934.9 cm^{-1} (9.454)
QCC*OC•*O: 408.9 cm^{-1} (8.673), 419.7 cm^{-1} (5.052), 1768.3 cm^{-1} (8.275)
Lennard-Jones parameters: σ = 5.8569A°, ε/k = 632.06 K

b. Estimated from C*CC• + O_2 → C*CCQ•
c. <MR>
d. A_r estimated using TST, A = (deg.) $(ek_b/h)\ T^n \exp(\Delta S^{\neq}(T)/R)$, deg. = 1, $\Delta S^{\neq}(T)$ is estimated as loss of three rotors and gain one OI (-4.3 × 3 +1.38 cal mol^{-1} K^{-1}). $E_{a,f} = E_{abst}$ (10.77).
e. Estimate from O + CH_3O
f. k via <MR>; k_r estimated from rate constant of CC•*O + CO → (via transition state BT21)→ CC*OC•*O which A estimated using canonical TST and B3LYP-determined entropies, Ea evaluated from CBS-q// B3LYP/6-31g(d) calculation.

Table 5A.30 $\Delta H^0_{f,298}$ of C*C(C)OC, CC*OOC, C_2CC*O, C*ClCC*O, And CC*OC*O Stable Molecules And Corresponding Radicals

Bond Energies (kcal/mole)	molecule	$\Delta H^0_{f,298}$ (kcal/mole)	Isodesmic Reaction	ΔH_{rxn} (kcal/mole)
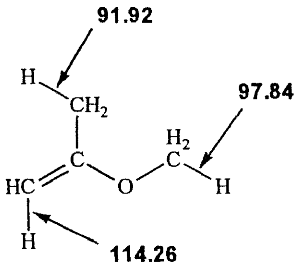	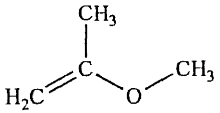	-36.03	C*C(C)OC + C=COH + CCOH ⇔ C*C(OH)C + C=COCC + COH	1.70
	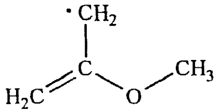	3.79	C*C(C)OC + CC• ⇔ C*C(C•)OC + CC•	-9.18
	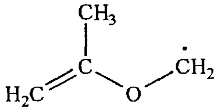	9.71	C*C(C)OC + COC• ⇔ C*C(C)OC• + COC•	1.15
	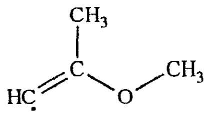	26.13	C*C(C)OC + CC• ⇔ C•*C(C)OC + CC•	13.16
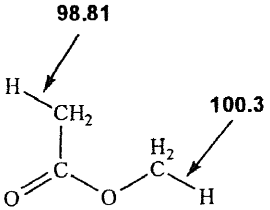	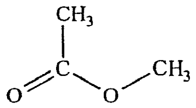	-98.26	CC*OOC + COH ⇔ COC*O + COC	1.02
	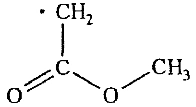	-51.55	CC*OOC + COC• ⇔ CC*OOC• + COC	-2.29
	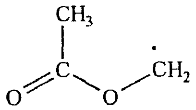	-50.26	CC*OOC + CC• ⇔ C•C*OOC + CC	3.61

Table 5A.30 (Continued)

Bond Energies (kcal/mole)	molecule	ΔH^0_{f298} (kcal/mole)	Isodesmic Reaction	ΔH_{rxn} (kcal/mole)
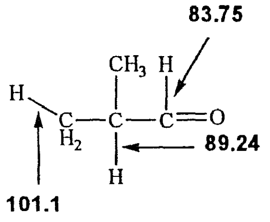	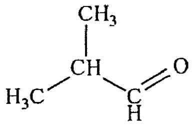	-51.11	C2CC*O + CC ⇔ CCHO + C3C	-0.85
	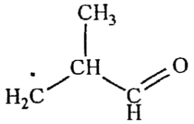	-1.61	C2CC*O + CC• ⇔ C2•CC*O + CC	0.0
	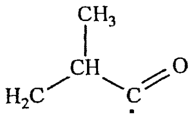	-13.97	C2CC*O + CC• ⇔ C2CC•*O + CC	-11.86
	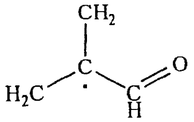	-19.46	C2CC*O + CC• ⇔ C2C•C*O + CC	-17.35
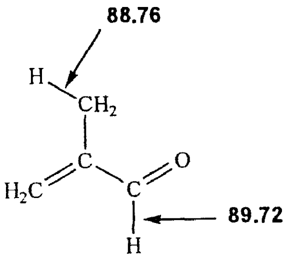	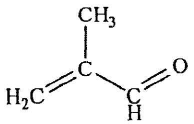	-28.12	C=C(C)C=O+ C=C ⇔ C=C-C + C=C-C=O	2.23
	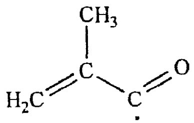	10.28	C=C(C)C=O + CC• ⇔ C=C(C)C•=O + CC	-11.38
	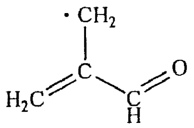	9.32	C=C(C)C=O + CC• ⇔ C=C(C•)C=O + CC	-12.34

Table 5A.30 (Continued)

Bond Energies (kcal/mole)	molecule	$\Delta H^0_{f,298}$ (kcal/mole)	Isodesmic Reaction	ΔH_{rxn} (kcal/mole)
	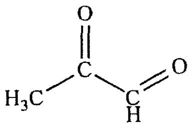	-64.8 (Expt.)		
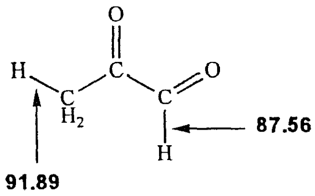	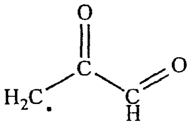	-25.01	CC*OC*O + CC• ⇔ C•C*OC*O + CC	-9.21
	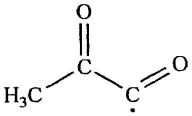	-29.34	CC*OC*O + CC• ⇔ CC*OC•*O + CC	-13.6

Table 5A.31 Reference High-Pressure Rate Constants Calculated from CBS-q//B3LYP/6-31g(d)

				TS				$\Delta H^{\neq}$	A	n	Ea	A(800K)
$CH_3O\bullet$	+	CO	->	**BT35** 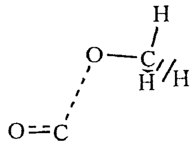	->	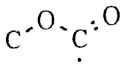 C•*C(C)OC	Forward	5.26	$1.65*10^6$	2.09	3.22	$5.38*10^{12}$
							Reverse	20.67	$5.92*10^6$	0.17	23.12	$7.88*10^{12}$
$CH_3O\bullet$	+	$H_2C=O$	->	**AT2** 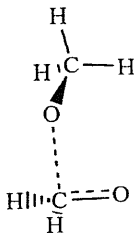	->	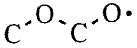 C*C(C•)OC	Forward	6.92	$1.57*10^6$	1.83	5.91	$7.13*10^{13}$
							Reverse	17.43	$1.53*10^6$	-0.07	19.02	$3.12*10^{13}$
$CH_3O\bullet$	+	C=C	->	**AT1** 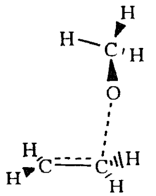	->	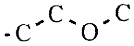 C•COC	Forward	5.33	$4.66*10^6$	1.80	5.15	$1.73*10^{12}$
							Reverse	21.94	$2.06*10^6$	0.02	22.90	$9.00*10^{12}$
$CH_3O\bullet$	+	C=C-C	->	**BT59** 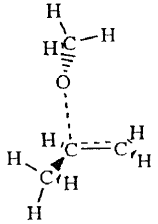	->	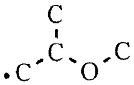 $C_2\bullet COC$	Forward	3.55	$2.93*10^6$	1.59	3.64	$2.12*10^{11}$
							Reverse	19.94	$1.76*10^6$	-0.63	21.13	$5.00*10^{12}$

Table 5A.31 (Continued)

				TS				$\Delta H^{\neq}$	A	n	Ea	A(800K)
$CH_3O\bullet$	+	C≡C-C	->	**BT2** 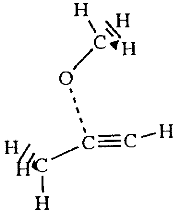	->	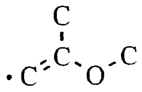 C•*C(C)OC	Forward	5.55	$6.06*10^{8}$	1.08	6.46	$9.20*10^{11}$
							Reverse	27.31	$6.46*10^{17}$	-1.24	28.62	$1.75*10^{13}$
$CH_3O\bullet$	+	C=C=C	->	**BT1** 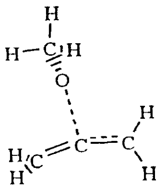	->	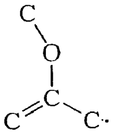 C*C(C•)OC	Forward	5.75	$5.14*10^{6}$	1.75	5.71	$1.36*10^{12}$
							Reverse	50.63	$3.75*10^{6}$	-0.76	52.10	$4.08*10^{13}$
O=C-C•		$H_2C=O$	->	**BT40** 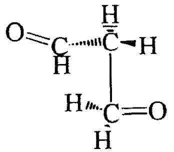	->	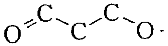 O*CCCO•	Forward	7.57	$9.39*10^{4}$	2.29	2.27	$1.42*10^{12}$
$C.H_2OH$	+	C=C	->	**AT3** 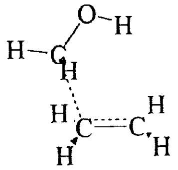	->	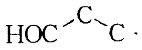 C•CCOH	Forward	5.98	$5.70*10^{5}$	1.77	5.71	$1.51*10^{11}$
							Reverse	26.55	$4.78*10^{11}$	0.50	27.18	$8.45*10^{12}$

Table 5A.31 (Continued)

				TS				$\Delta H^{\ddagger}$	A	n	Ea	A(800K)
C.H$_2$OH	+	CC(=O)C=O	->	**BT44** 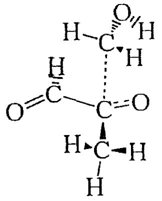	->	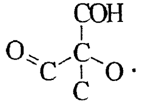 CC(COH)(O•)C*O	Forward	-3.15	$1.11*10^5$	1.50	0.27	$3.93*10^9$
C.H$_2$OH	+	O=C(OH)$_2$	->	**BT43A** 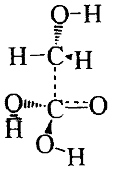	->	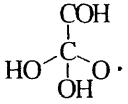 C(OH)$_2$(O•)COH	Forward	19.36	1.61*104	1.91	19.42	1.3810^{10}
C.H$_2$OH	+	C=C-C=O	->	**BT64** 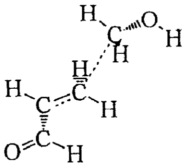	->	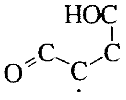 O*CC•CCOH	Forward	0.18	$2.46*10^5$	1.68	0.17	$3.35*10^{10}$
C.H$_2$OH	+	C=C=O	->	**AT7B (BT80)** 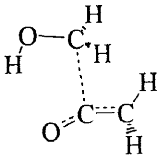	->	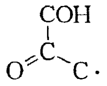 C•C*OCOH	Forward	3.13	$4.06*10^4$	1.91	2.90	$2.98*10^{10}$

Table 5A.31 (Continued)

				TS				ΔH$^{\neq}$	A	n	Ea	A(800K)
C.H$_2$OH	+	C$_2$C=O	->	**BT85** 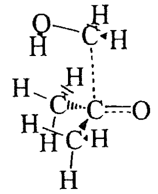	->	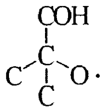 C$_2$C(COH)O•	Forward	4.06	$3.19*10^{2}$	2.28	3.88	$5.12*10^{9}$
C.H$_2$OOH	+	CO	->	**TCQXCJO** 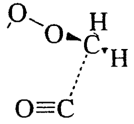	->	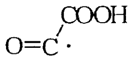 O*C•COOH	Forward	4.23	$7.80*10^{4}$	2.46	2.71	$4.21*10^{12}$
							Reverse	10.07				
C.H$_2$OOH	+	C=C	->	**AT5** 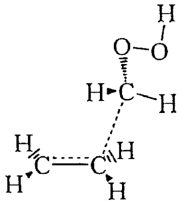	->	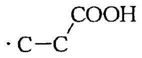 C•CCOOH	Forward	5.04	$1.13*10^{3}$	2.83	2.89	$9.60*10^{11}$
							Reverse	26.17	$4.34*10^{9}$	1.28	27.20	$2.83*10^{13}$
C.H$_2$OOH	+	H$_2$C=O	->	**AT6** 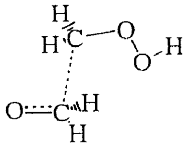	->	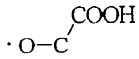 O•CCOOH	Forward	0.51	$4.21*10^{5}$	1.92	0.29	$3.78*10^{10}$

Table 5A.31 (Continued)

				TS				$\Delta H^{\neq}$	A	n	Ea	A(800K)
$C.H_2OH$	+	C=C(OH)C=O	->	**BT56** 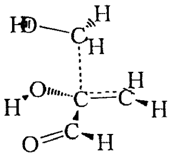	->	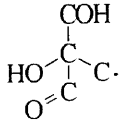 C•C(OH)(COH)C*O	Forward	3.48	$7.36*10^{3}$	1.93	3.30	$6.93*10^{9}$
$C.H_2OOH$	+	C=C=O	->	**AT7A** 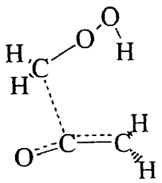	->	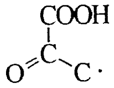 C•C(COOH)*O	Forward	1.3	$6.57*10^{4}$	1.72	1.12	$1.15*10^{10}$
$C.H_2OOH$	+	C=COH	->	**BT66** 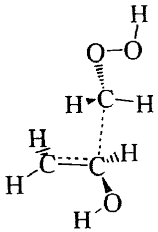	->	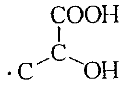 C•CC(Q)OH	Forward	6.39	$1.25*10^{4}$	2.09	6.10	$3.88*10^{10}$
$C.H_2OOH$	+	C=C(C)OC	->	**TS4** 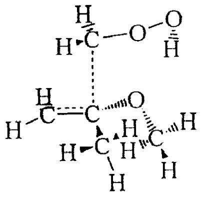	->	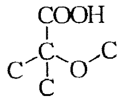 C_2•C(COOH)OC	Forward	7.63	$1.42*10^{1}$	2.69	6.60	$4.91*10^{9}$
							Reverse	21.17	$1.67*10^{12}$	0.13	22.04	$1.59*10^{12}$

Table 5A.31 (Continued)

				TS				$\Delta H^{\ddagger}$	A	n	Ea	A(800K)
CH_3	+	O=C=O	->	**BT36** 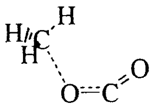	->	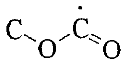 COC•*O	Forward	36.02	$1.76*10^{7}$	1.68	33.12	$2.39*10^{12}$
							Reverse	12.79	$3.24*10^{12}$	0.15	16.25	$4.02*10^{12}$
CH_3	+	O=C=O	->	**BT38** 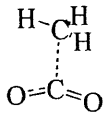	->	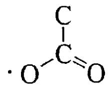 CCO•*O	Forward	14.69	$1.84*10^{7}$	1.62	14.68	$1.58*10^{12}$
									$3.69*10^{12}$	0.41	7.39	
$C_2H_5\cdot$	+	$H_2C=O$	->	**AT8** 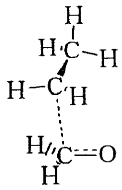	->	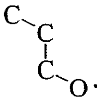 CCCO•	Forward	1.45	$1.14*10^{4}$	2.38	0.53	$3.71*10^{11}$
								11.91	$1.99*10^{13}$	0.26	13.09	$5.60*10^{13}$
$C_2H_5\cdot$	+	$H_2C=O$	->	**AT9** 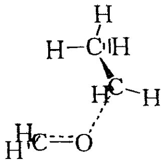	->	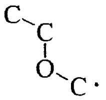 CCOC•	Forward	15.20	$5.45*10^{3}$	2.55	13.96	$6.66*10^{11}$
							Reverse	23.23	$3.79*10^{12}$	0.28	24.59	$1.21*10^{13}$
CC•C	+	CO		**BT52** 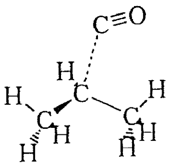		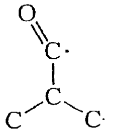 C_2CC•*O	Forward	4.1311.78	$7.44*10^{3}$	2.42	3.47	$3.48*10^{11}$
									$4.70*10^{13}$	0.21	13.02	$9.81*10^{13}$

Table 5A.31 (Continued)

				TS				$\Delta H^{\neq}$	A	n	Ea	A(800K)
CC•C	+	$H_2C=O$		**BT51** 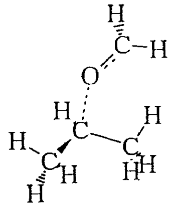		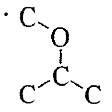 $C_2COC\bullet$	Forward	12.09	$7.44*10^{11}$	2.92	10.48	$1.68*10^{11}$
							Reverse	19.83	$3.49*10^{13}$	-0.08	21.67	$6.82*10^{12}$
CC•OC	+	$H_2C=O$	->	**BT74** 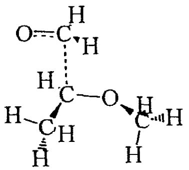	->	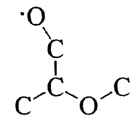 $COC(C)CO\bullet$	Forward	-2.13	$1.62*10^{3}$	2.38	-0.20	$5.34*10^{10}$
$C_2C\bullet OC$	+	$H_2C=O$	->	**BT27** 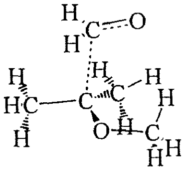	->	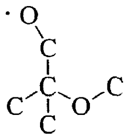 $C_2C(CO\bullet)OC$	Forward	-5.94	$5.37*10^{1}$	2.46	-0.39	$3.16*10^{9}$
$C_2C\bullet OH$	+	CO	->	**BT30** 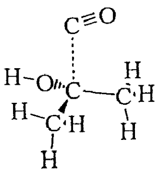	->	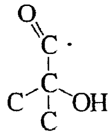 $C_2COHC\bullet{*}O$	Forward	1.77	$1.48*10^{2}$	2.74	1.12	$7.02*10^{10}$

Table 5A.31 (Continued)

				TS				ΔH$^{\neq}$	A	n	Ea	A(800K)
$C_2C{\bullet}OH$	+	$H_2C{=}O$	->	**BT72** 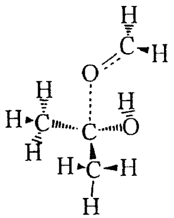	->	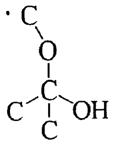 $C_2COHOC{\bullet}$	Forward	6.42	$1.11*10^{1}$	3.00	4.60	$4.40*10^{10}$
							Reverse	16.81	$6.09*10^{12}$	0.14	18.68	$6.92*10^{12}$
CC.COH		$H_2C{=}O$	->	**BT73** 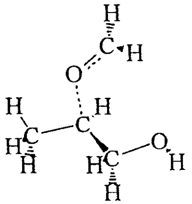	->	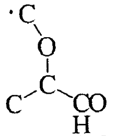 CC(COH)OC•	Forward	12.96	$2.12*10^{1}$	3.12	11.67	$2.22*10^{11}$
							Reverse	22.42	$8.28*10^{12}$	0.14	23.95	$9.19*10^{12}$
H	+	CO_2	->	**BT84** 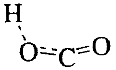	->	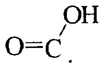 HOC•*O	Forward	5.07	$1.24*10^{11}$	0.98	4.21	$8.41*10^{13}$
							Reverse	5.22	$1.22*10^{9}$	1.16	6.40	$3.18*10^{12}$
H	+	$C_2C{=}O$	->	**BT81** 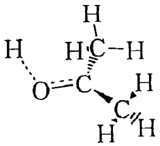	->	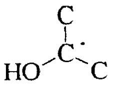 $C_2C{\bullet}OH$	Forward	8.3	$6.84*10^{7}$	1.66	7.42	$9.36*10^{12}$
							Reverse	31.37	$1.18*10^{7}$	1.65	32.20	$1.53*10^{12}$
OH	+	$H_2C{=}O$	->	**TSCH2OXOH** 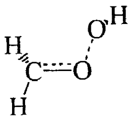	->	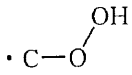 C•OOH	Forward		$4.40*10^{5}$	2.10	32.82	$1.57*10^{12}$
							Reverse		$2.74*10^{13}$	-0.23	0.66	$1.69*10^{12}$

Table 5A.31 (Continued)

				TS				$\Delta H^{\neq}$	A	n	Ea	A(800K)
OH	+	CO_2	->	**BT22** 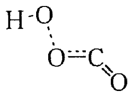	->	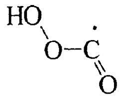 QC•*O	Forward	80.53	$2.61*10^{9}$	1.48	77.92	$8.39*10^{13}$
							Reverse	10.51	$5.46*10^{11}$	0.47	13.71	$7.47*10^{12}$
HCO	+	CO	->	**BT60** 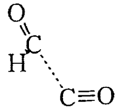	->	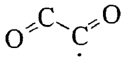 O*CC•*O	Forward	9.91	$7.54*10^{6}$	1.76	9.97	$2.03*10^{12}$
							Reverse		$1.50*10^{16}$	-0.38	14.57	
HCO	+	C=C	->	**BT20** 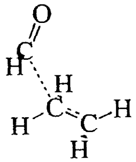	->	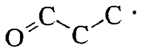 C•CC*O	Forward	6.02	$1.77*10^{4}$	2.49	5.51	$1.23*10^{12}$
HCO	+	C≡C	->	**BT69** 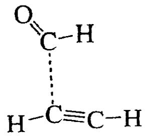	->	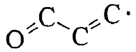 C•*CC*O	Forward	6.67	$1.08*10^{7}$	1.82	6.71	$4.61*10^{12}$
HCO	+	C=C-C	->	**BT61** 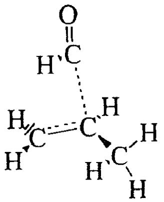	->	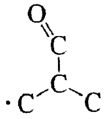 C_2•CC*O	Forward	5.93	$4.09*10^{3}$	2.34	5.56	$1.00*10^{11}$
							Reverse	22.25	$3.52*10^{11}$	0.49	22.97	$6.20*10^{12}$

Table 5A.31 (Continued)

				TS				$\Delta H^{\ddagger}$	A	n	Ea	A(800K)
HCO	+	C=C=C	->	**BT12** 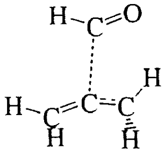	->	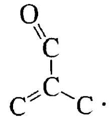 C*CIC•C*O	Forward	6.23	$6.32*10^{4}$	2.36	3.82	$1.60*10^{12}$
							Reverse	49.13	$1.08*10^{16}$	-0.28	52.04	$4.70*10^{14}$
HCO	+	C=C(OH)C	->	**BT45** 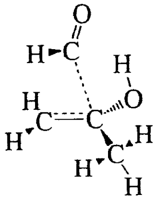	->	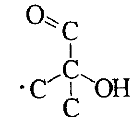 C_2•COHC*O	Forward	8.14	$8.14*10^{2}$	2.36	7.90	$2.38*10^{10}$
							Reverse		$3.26*10^{12}$	0.15	22.46	
HCO	+	$C_2C=O$	->	**BT46** 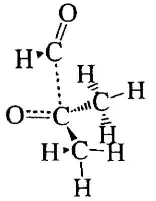	->	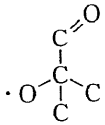 C_2CO•C*O	Forward	5.74	$4.91*10^{2}$	2.56	5.54	$7.13*10^{10}$
							Reverse		$5.19*10^{14}$	-0.21	4.70	
HOC•=O	+	C=C	->	**BT17** 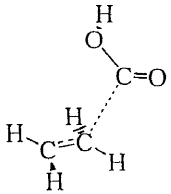	->	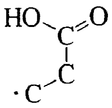 C•CC*OOH	Forward	4.81	$2.22*10^{3}$	2.66	4.15	$5.58*10^{11}$

Table 5A.31 (Continued)

				TS				$\Delta H^{\neq}$	A	n	Ea	A(800K)
HOC•=O	+	C=C-C	->	**BT50** 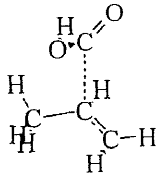	->	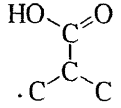 C_2•CC*OOH	Forward	5.19	$3.50*10^1$	2.72	4.612.90	$1.47*10^{10}$
HOC•=O	+	C_2C=C	->	**BT49A** 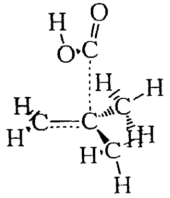	->	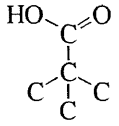 C3CC*OOH	Forward	4.29	$4.68*10^1$	2.64	3.77	$1.05*10^{10}$
HOC•=O	+	C≡C	->	**BT70** 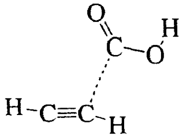	->	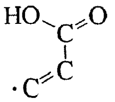 C•*CCOH*O	Forward	6.07	$1.10*10^5$	2.27	5.72	$1.39*10^{12}$
HOC•=O	+	C=C=O	->	**BT48** 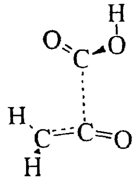	->	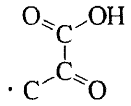 C•C(*O)C*OOH	Forward	7.17	$2.50*10^3$	2.34	6.86	$5.47*10^{10}$

Table 5A.31 (Continued)

				TS				$\Delta H^{\neq}$	A	n	Ea	A(800K)
HOC•=O	+	C_2C=O	->	**BT31** 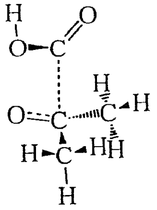	->	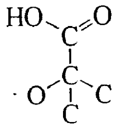 C_2C(O•)C*OOH	Forward	7.90	47.45	2.65	7.51	$1.28*10^{10}$
HOOC•=O	+	C=C	->	**BT13** 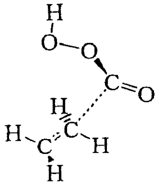	->	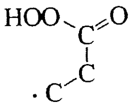 C•CCQ*O	Forward	3.08	$2.25*10^{1}$	3.13	2.28	$2.33*10^{11}$
C=C.	+	H_2C=O	->	**BT82** 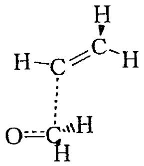	->	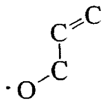 C*CCO•	Forward	0.12	$4.33*10^{4}$	2.50	-0.3042	$3.25*10^{12}$
C=C•-C	+	H_2C=O	->	**BT3** 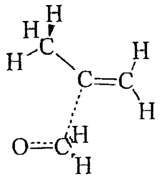	->	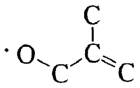 C_2*CCO•	Forward	-1.95	$4.08*10^{4}$	2.28	-0.24	$6.25*10^{11}$
							Reverse	17.92	$3.91*10^{14}$	-0.05	25.03	$9.86*10^{13}$

Table 5A.31 (Continued)

				TS				$\Delta H^{\neq}$	A	n	Ea	A(800K)
C=C•-C	+	$H_2C=O$	->	**BT3A** 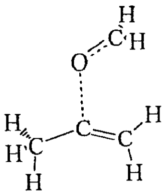	->	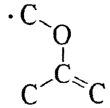 C*C(C)OC•	Forward	7.47	$2.81*10^{4}$	2.43	6.06	$1.34*10^{11}$
							Reverse	30.26	$1.48*10^{14}$	-0.51	32.37	$1.05*10^{13}$
C-C•=O	+	CO	->	**BT21** 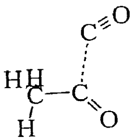	->	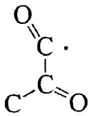 CC*OC•*O	Forward	7.21	$5.81*10^{4}$	2.72	6.6267	$2.51*10^{11}$
							Reverse	7.28	$1.00*10^{14}$	0.68	7.8311	$7.38*10^{13}$
C-C•=O	+	$H_2C=O$	->	**BT11** 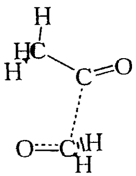	->	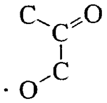 CC*OCO•	Forward	-1.45	$1.90*10^{4}$	2.35	-0.2896	$4.65*10^{11}$
C-C•=O	+	$H_2C=O$		**BT11A** 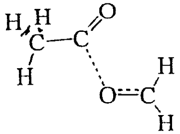		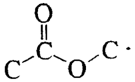 CC*OOC•	Forward	8.86	$1.90*10^{4}$	2.50	-0.3042	$5.31*10^{11}$
							Reverse	29.02	$1.35*10^{15}$	-0.25	30.44	$7.14*10^{13}$

Table 5A.31 (Continued)

				TS				$\Delta H^{\neq}$	A	n	Ea	A(800K)
C-C•=O	+	HO-C=O		**BT47** 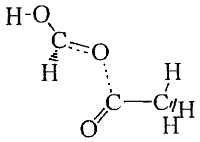		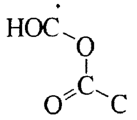 CC*OCOC•OH	Forward	18.88	49.49	2.53	18.62	$5.62*10^{9}$
C=C•COH	+	CO		**BT62** 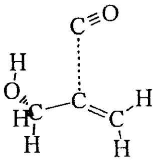		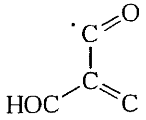 C*CICOHC•*O	Forward	0.06	$8.60*10^{4}$	2.32	-0.2244	$1.68*10^{12}$
HO_2	+	CO	->	**BT23** 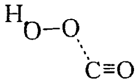	->	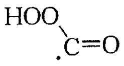 QC•*O	Forward	12.37	1.89×10^{4}	2.32	9.91	3.90×10^{11}
							Reverse	5.26	8.25×10^{9}	0.70	7.69	6.95×10^{11}
HO_2	+	C=C=O	->	**TCJCOXQ** 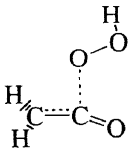	->	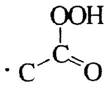 C•CQ*O	Forward	10.69	$4.10*10^{5}$	1.80	8.40	$1.46*10^{11}$
							Reverse	32.39				
HO_2	+	C=C=O	->	**TCXQCJO** 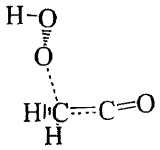	->	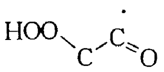 QCC•*O	Forward	16.80	$5.82*10^{5}$	1.92	14.30	$5.46*10^{11}$
							Reverse	23.17				

Table 5A.31 (Continued)

				TS				$\Delta H^{\neq}$	A	n	Ea	A(800K)
HO_2	+	C=C=O	->	**TCCOXQE** 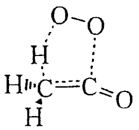	->	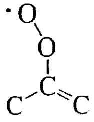 CCQ•*C	Forward	5.63	$5.25*10^{1}$	2.97	3.54	$1.30*10^{11}$
							Reverse	35.79				
HO_2	+	C=C=O	->	**TCQJCHOE** 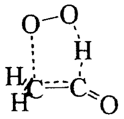	->	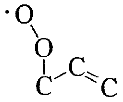 Q•CC*C	Forward	41.41	$8.65*10^{1}$	2.76	39.40	$4.73*10^{10}$
							Reverse	51.54				
HO_2	+	C=C=C	->	**BT25** 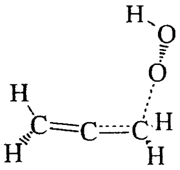	->	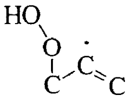 QCC•*C	Forward	11.05	$8.57*10^{4}$	2.38	10.76	$1.57*10^{12}$
HO_2	+	C=C=C	->	**BT24** 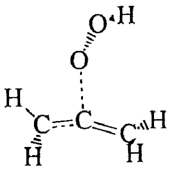	->	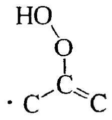 C•CQ*C	Forward	13.52	$3.80*10^{4}$	2.47	13.19	$2.53*10^{12}$

Table 5A.31 (Continued)

			TS			$\Delta H^{\neq}$	A	n	Ea	A(800K)
HO_2	+	$C_2C=C=O$	**BT67** 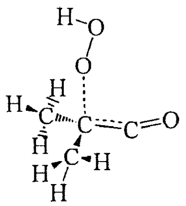	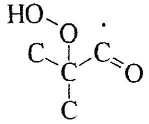 $C_2CQC\bullet*O$	Forward	31.64	$4.78*10^4$	1.81	31.42	$1.59*10^{10}$
HO_2	+	C≡C-C	**BT79A** 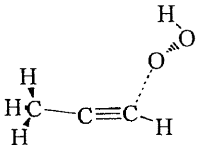	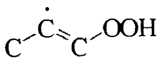 $CC\bullet*CQ$	Forward	15.68	$6.55*10^4$	2.35	15.47	$1.77*10^{12}$

Rate Constants in Form $AT^n \exp(-Ea/RT)$
Units: A factor: bimolecular: $cm^3\ mol^{-1}\ s^{-1}$; unimolecular: s^{-1}; Ea: kcal/mol

APPENDIX 5B

FIGURES IN THE METHYL *TERT*-BUTYL ETHER OXIDATION AND PYROLYSIS EXPERIMENT: COMPARISON WITH MODEL

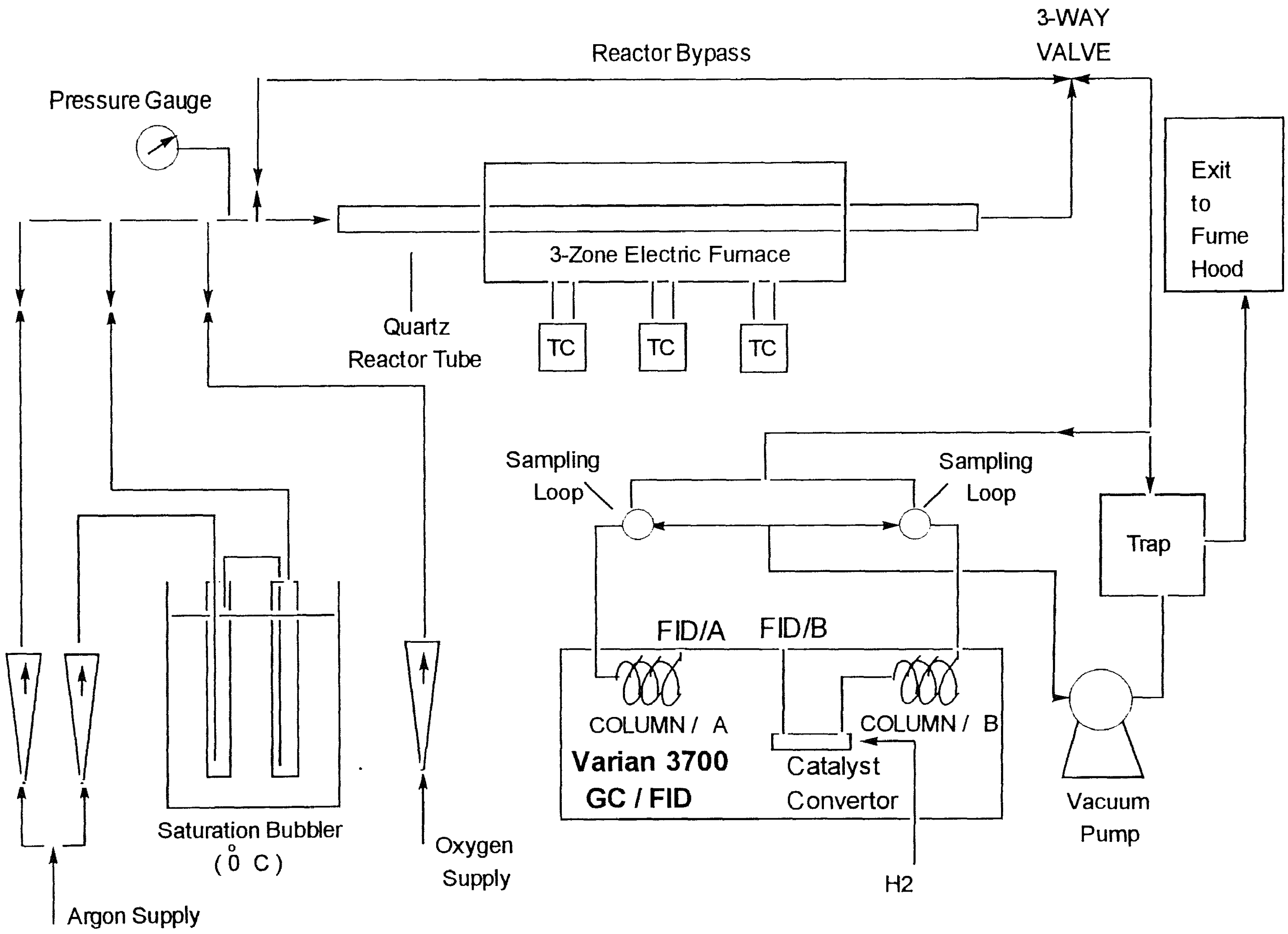

Figute 5B.1 Experimental system

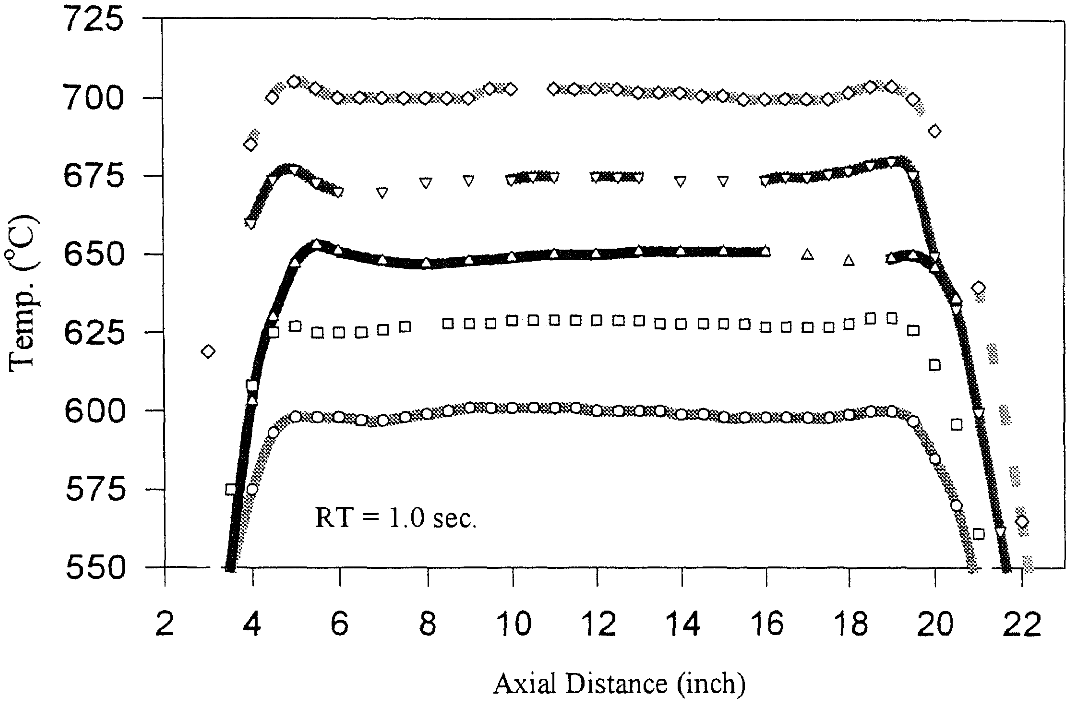

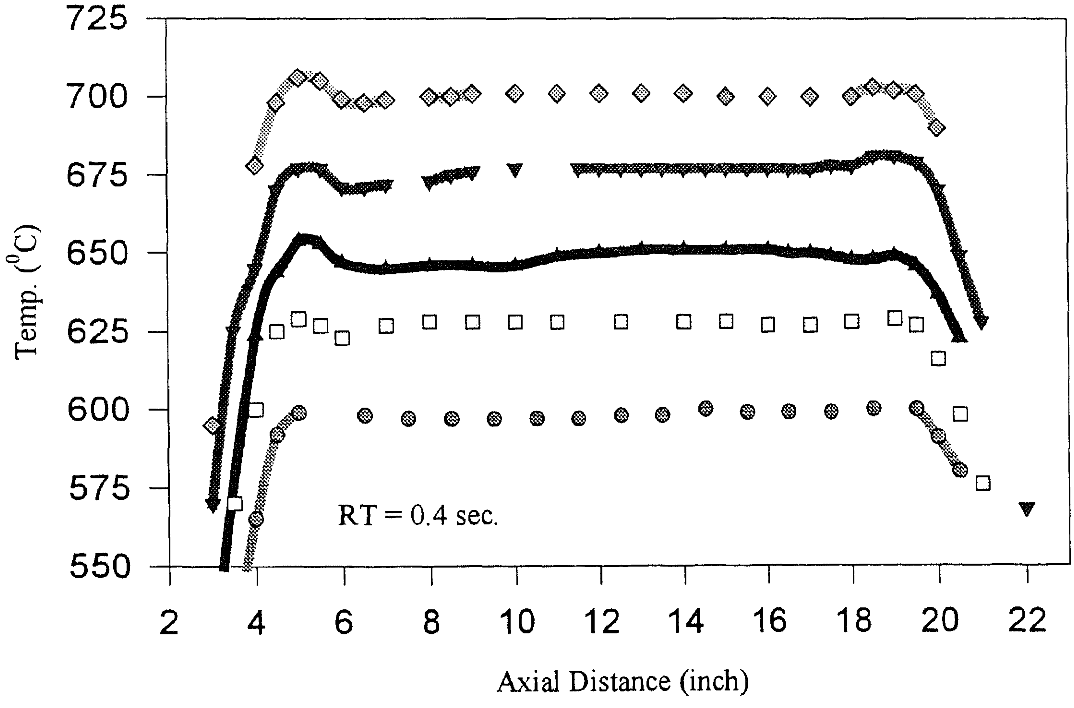

Figure 5B.2 Temperature profiles at RT=1.0 and RT=0.4 sec

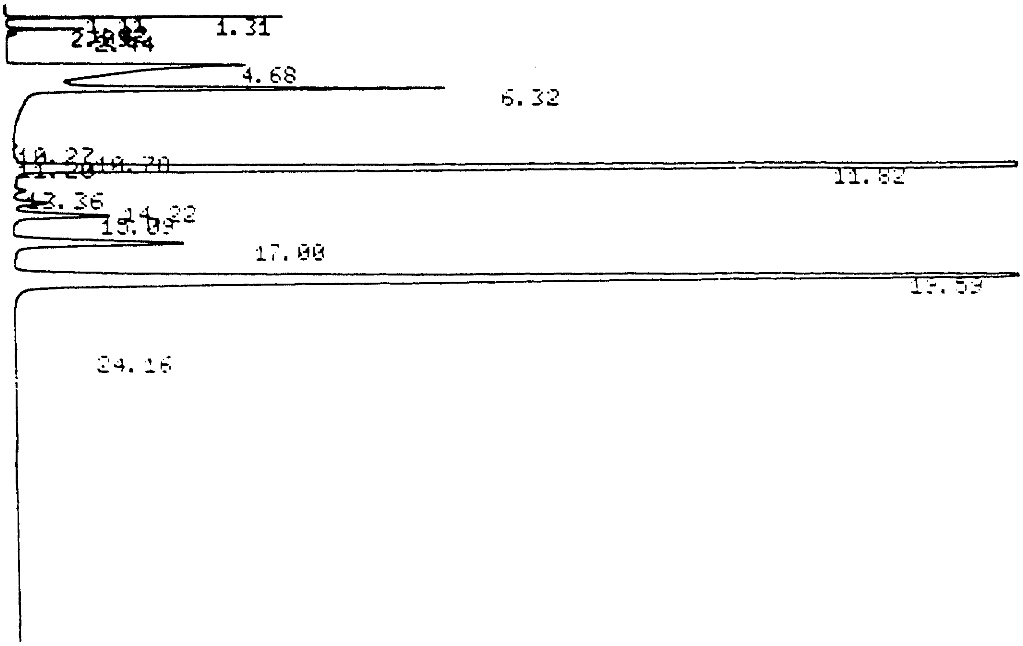

```
                              06/12/94 17:11:21      CH= "A"   PS=  1.

FILE  1.       METHOD  0.      RUN 105      INDEX 105

PEAK#       AREA%         RT        AREA BC

    1        0.003       1.11         205 02
    2        1.137       1.31       92486 03
    3        0.005       1.82         377 02
    4        0.381       2.09       31022 02
    5        0.056       2.44        4537 03
    6        6.674       4.68      542763 02
    7        6.007       6.32      488535 03
    8        0.03       10.27        2423 01
    9        0.017      10.78        1374 02
   10        0.035      11.2         2881 02
   11       53.372      11.82     4340657 03
   12        0.118      13.36        9616 01
   13        0.412      14.22       33490 02
   14        1.35       15.09      109811 03
   15        3.029      17.        246131 01
   16       27.344      19.59     2223928 01
   17        0.031      24.16        2491 01

TOTAL      100.                   8132869
```

Figure 5B.3 GC-FID results on MTBE oxidation

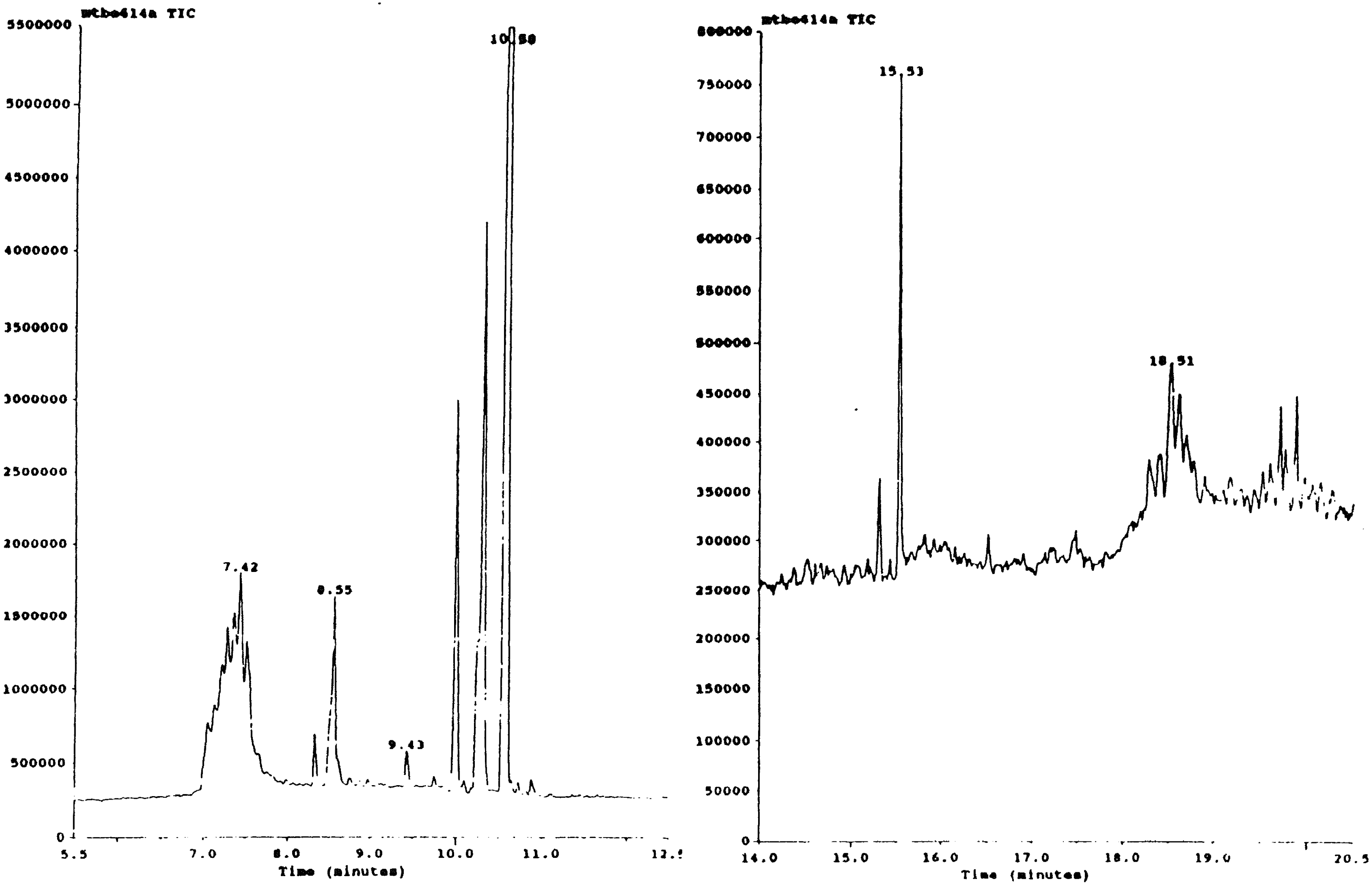

Figure 5B.4 GC-MS results on MTBE oxidation

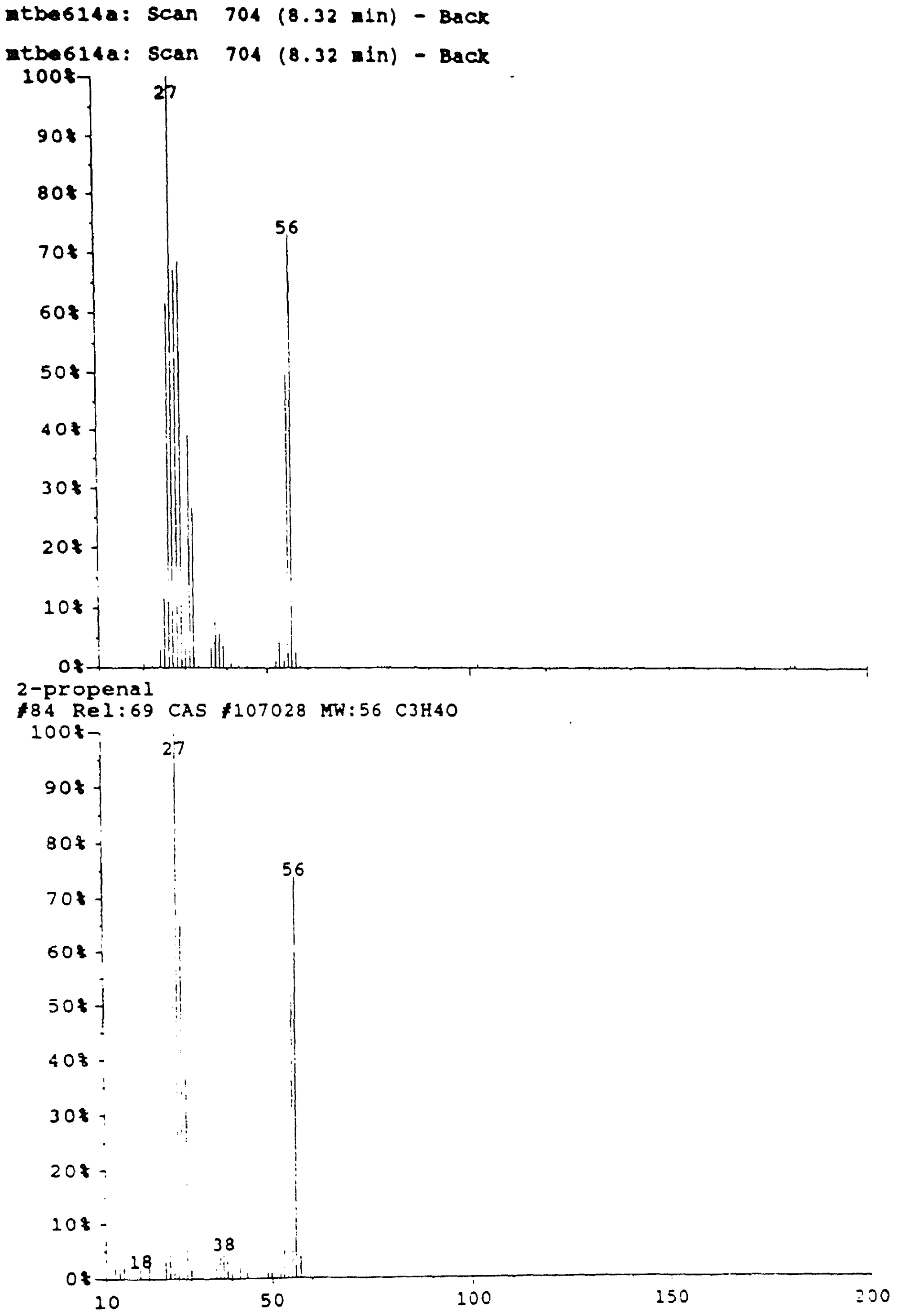

Figure 5B.5 GC/MS spectra at 8.32 min peck of MTBE oxidation gas sample and Acrolein (C=C-C=O) mass spectra

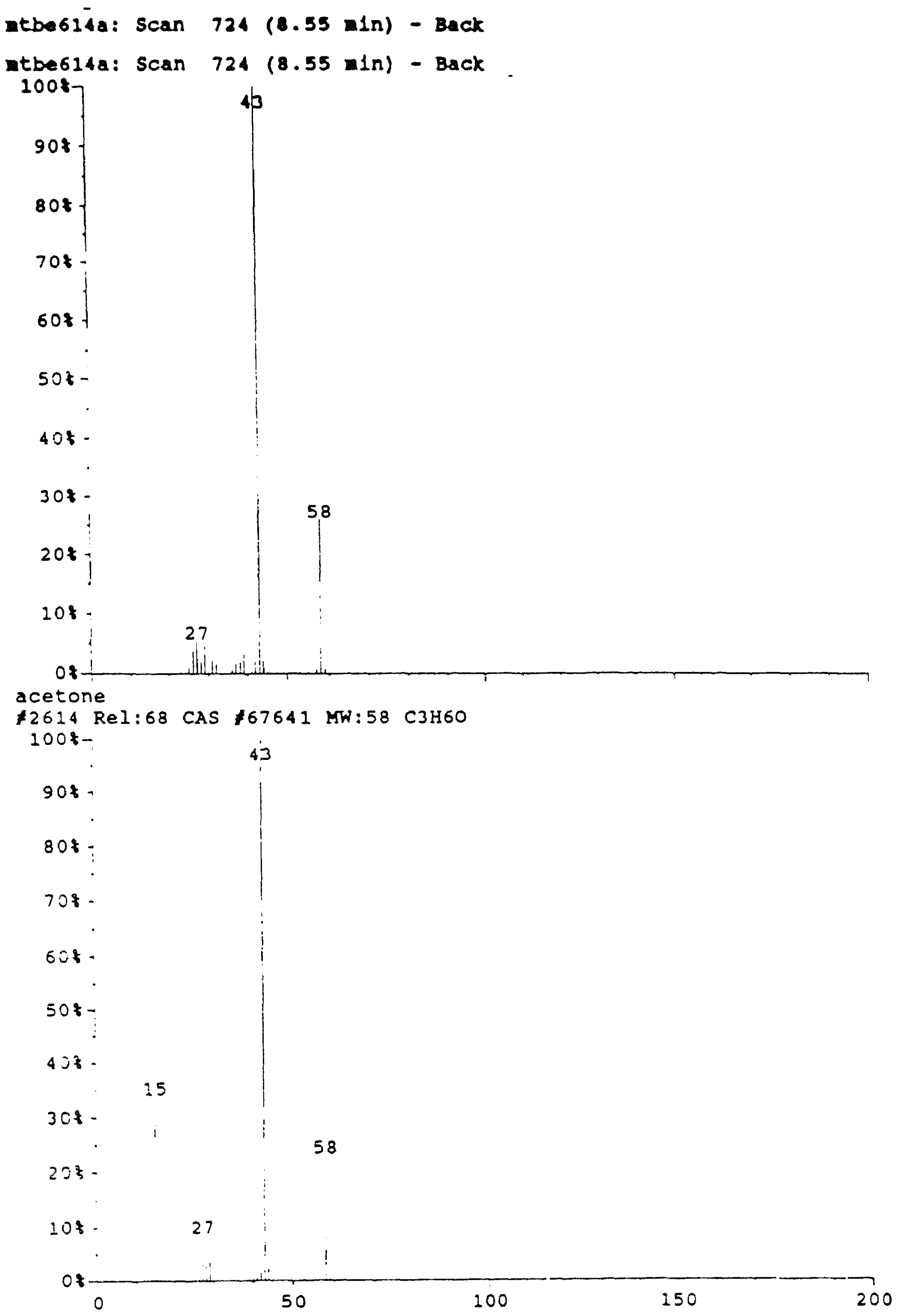

Figure 5B.6 GC/MS spectra at 8.55 min peck of MTBE oxidation gas sample and Acetone ($C_2C{=}O$) mass spectra

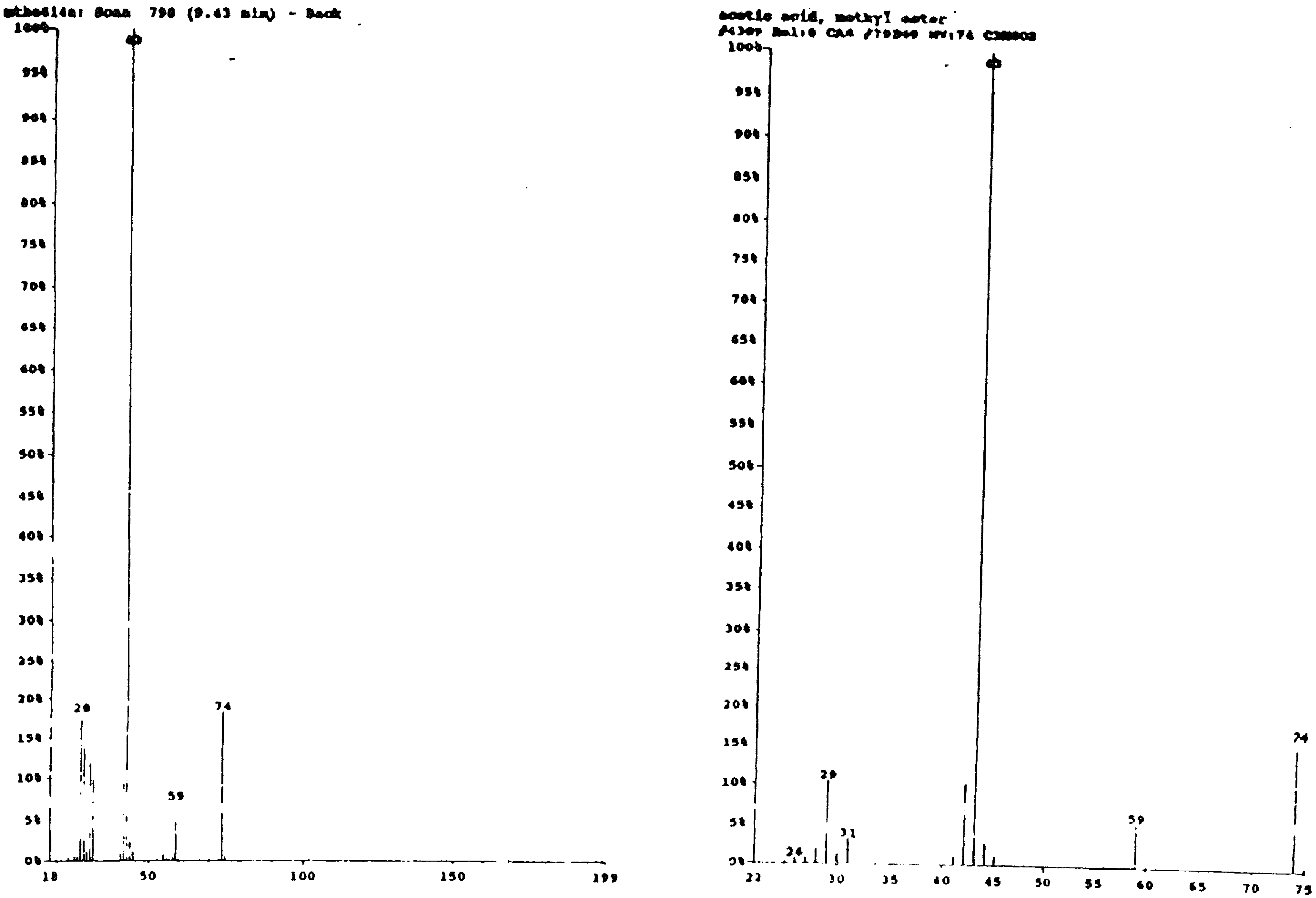

Figure 5B.7 GC/MS spectra at 9.43 min peck of MTBE oxidation gas sample and Methyl Acetate (CC(=O)OC) mass spectra

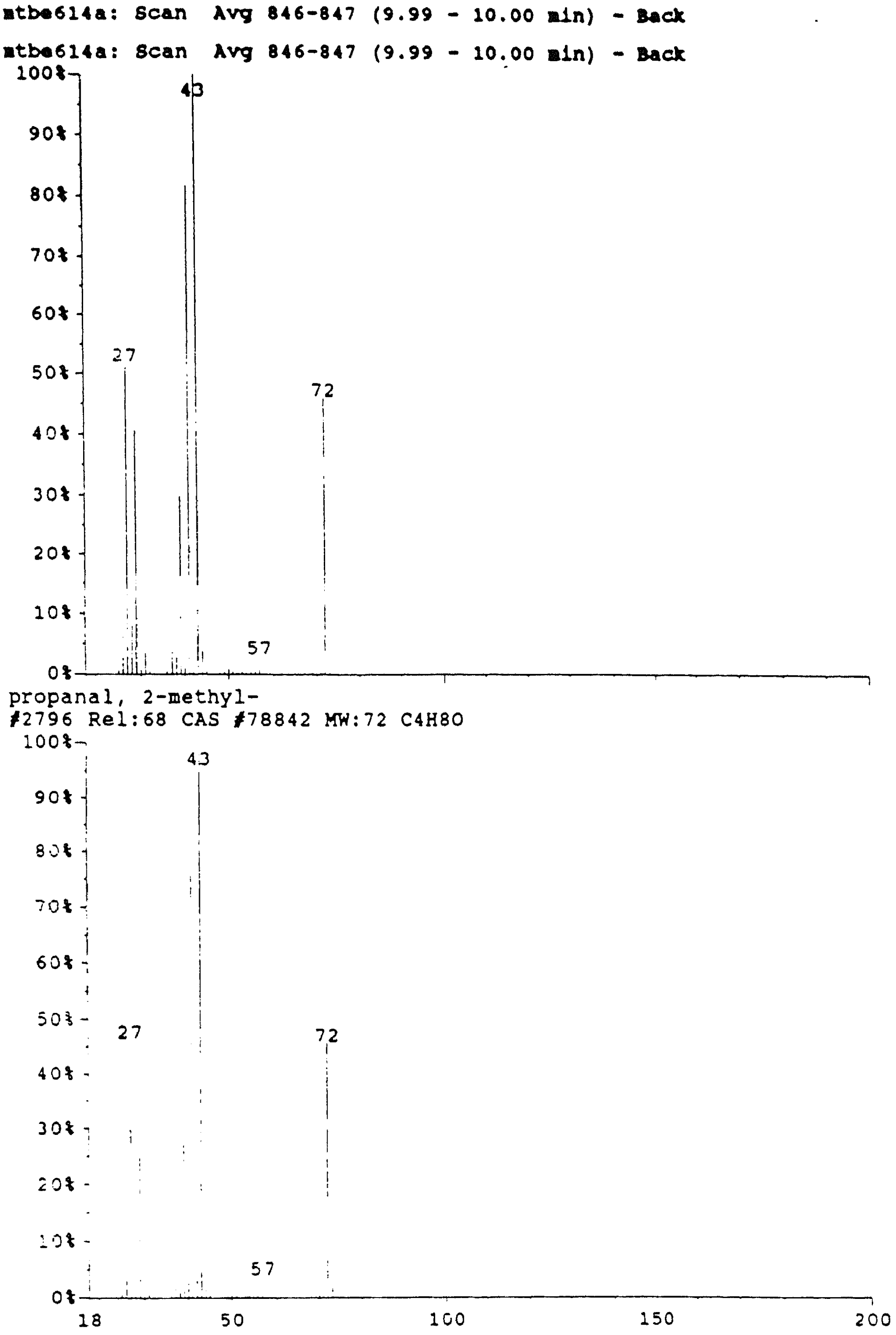

Figure 5B.8 GC/MS spectra at 9.99 min peck of MTBE oxidation gas sample and Isobutyraldehyde ($C_2CC{=}O$) mass spectra

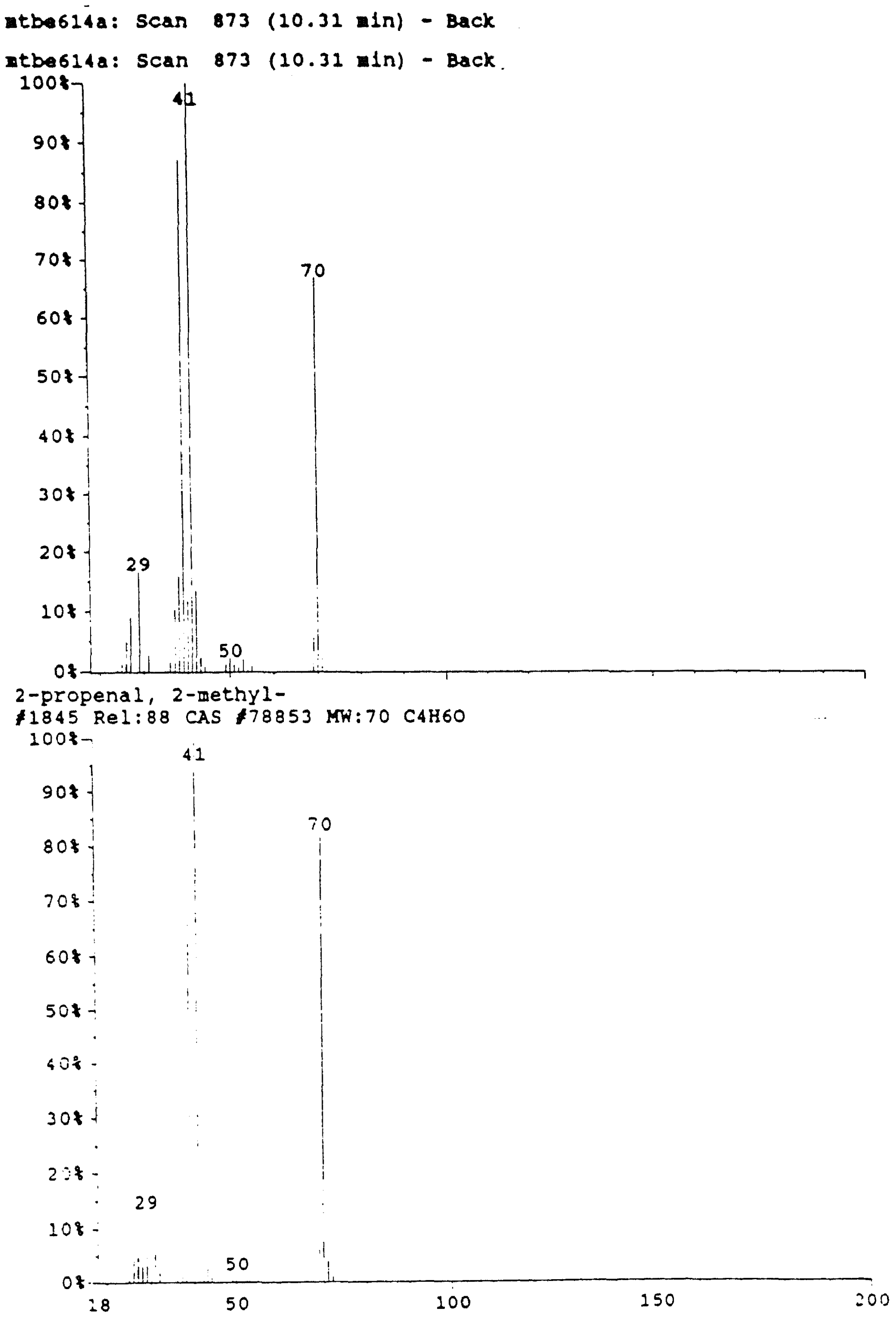

Figure 5B.9 GC/MS spectra at 10.31 min peck of MTBE oxidation gas sample and Methacrolein (C=C(C)C=O) mass spectra

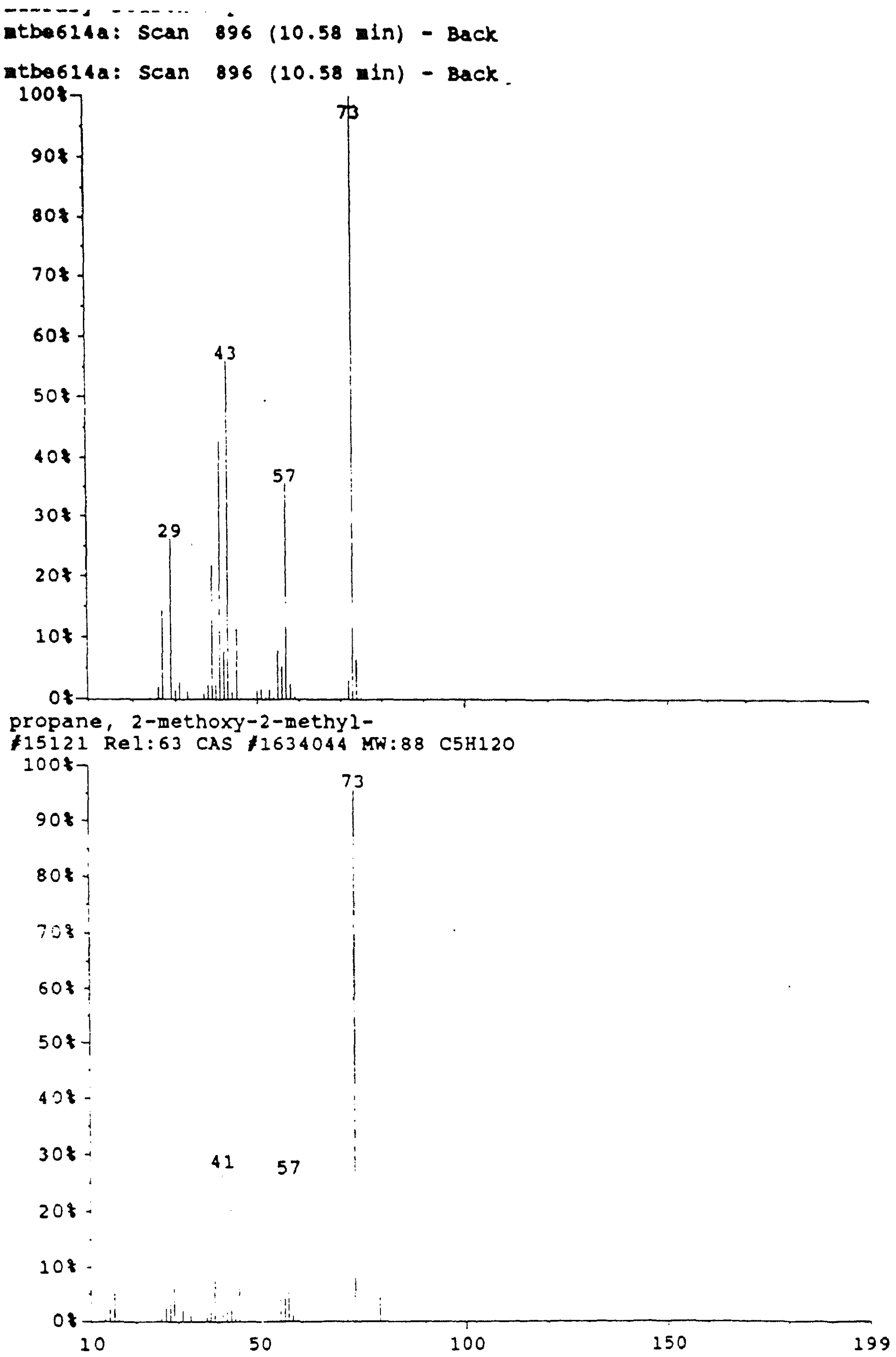

Figure 5B.10 GC/MS spectra at 10.58 min peck of MTBE oxidation gas sample and MTBE (C_3COC) mass spectra

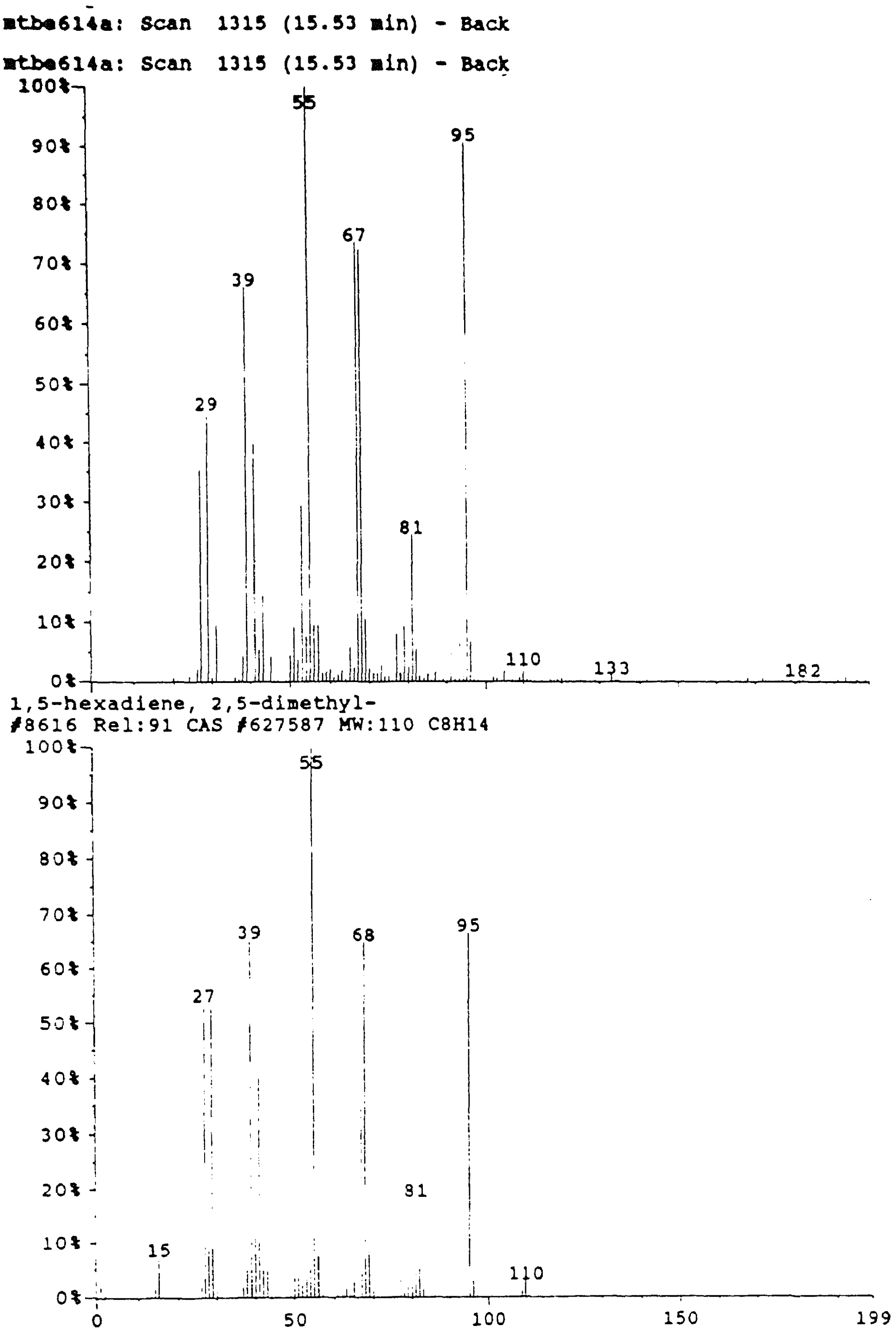

Figure 5B.11 GC/MS spectra at 15.53 min peck of MTBE oxidation gas sample and 2,5 Dimethylhexa-1,5-diene (DIC$_2$·C=C) mass spectra

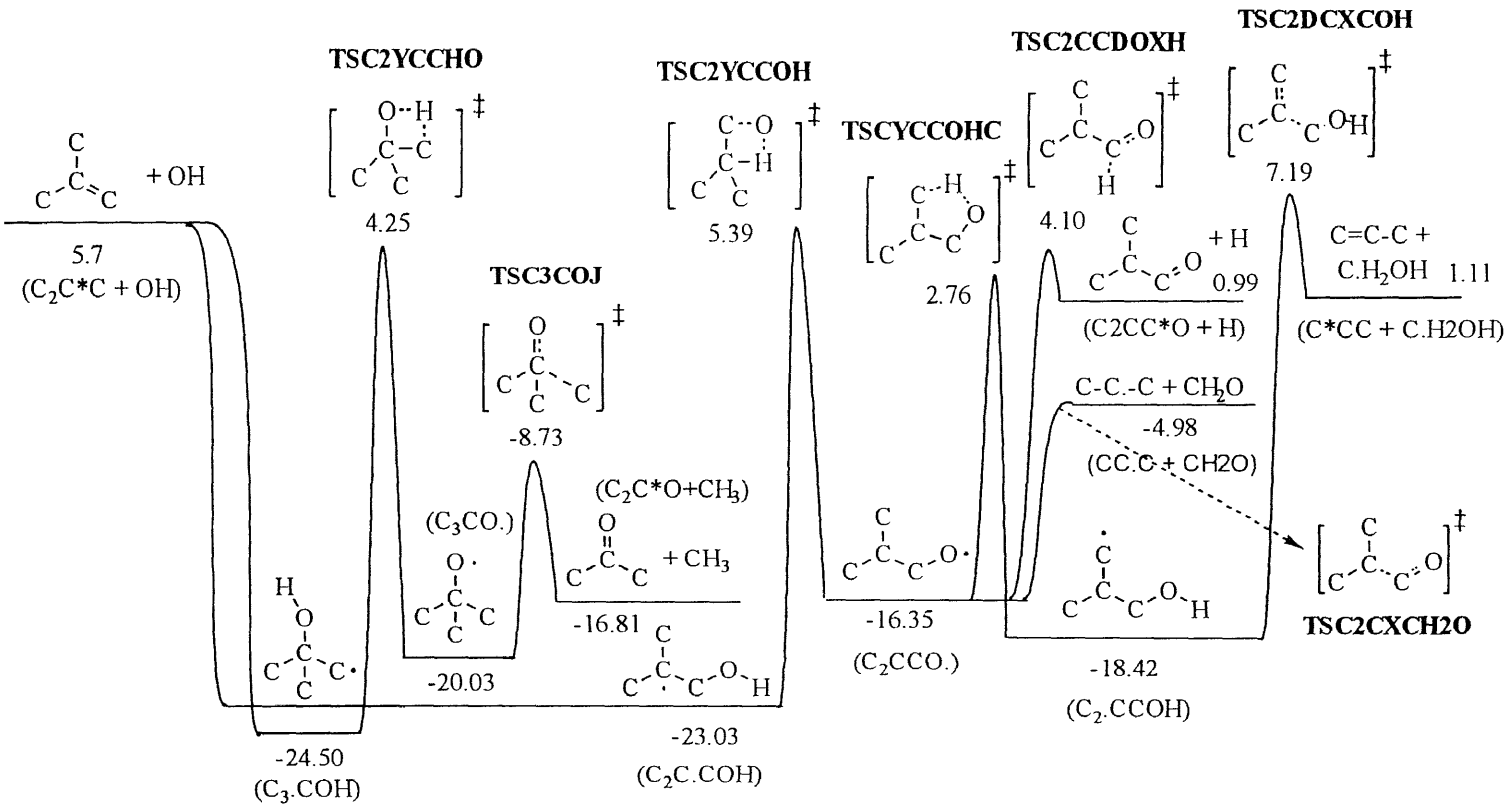

Figure 5B.12 The potential energy level diagram for C_2C^*C + OH -> products

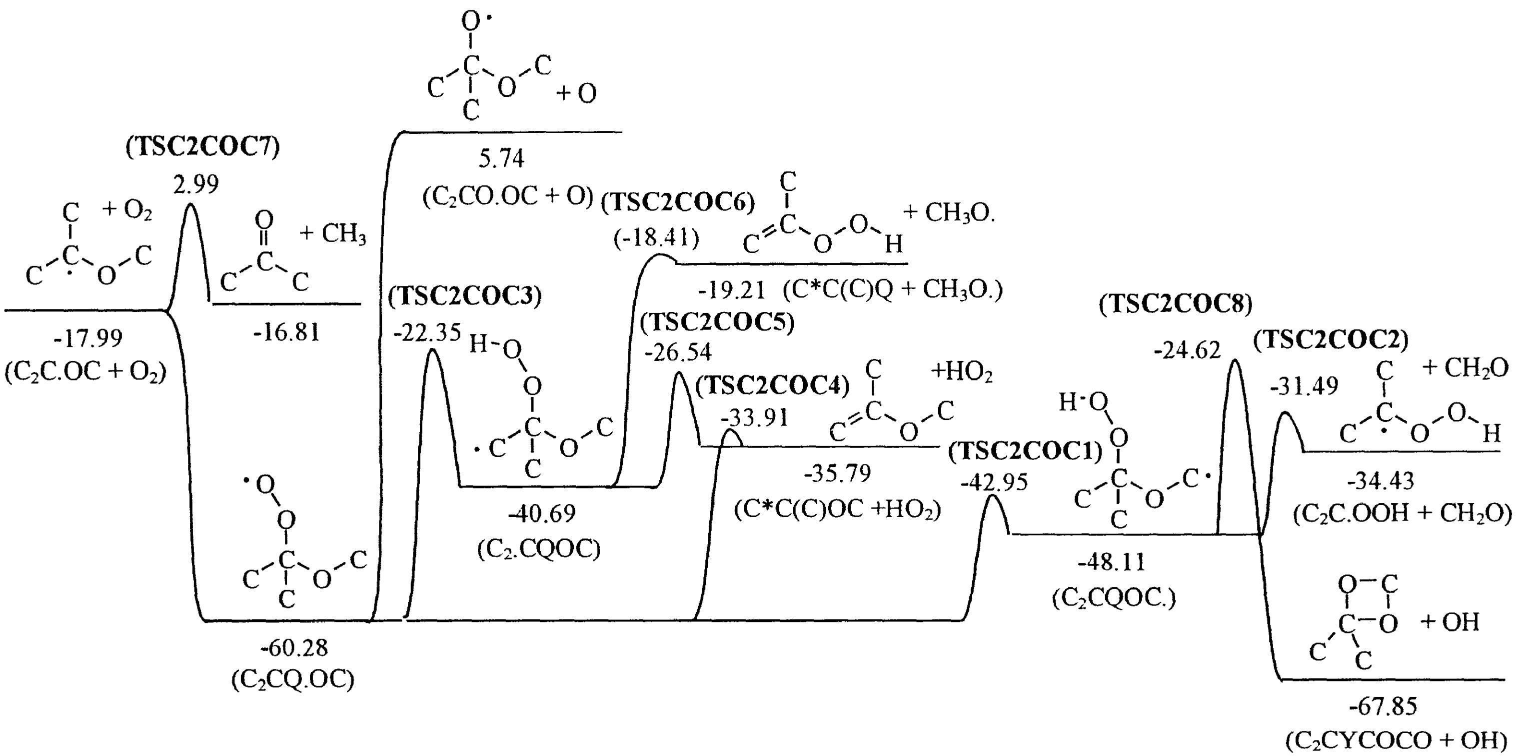

Figure 5B.13 The potential energy level diagram for $C_2C{\cdot}OC + O_2$ -> pProducts

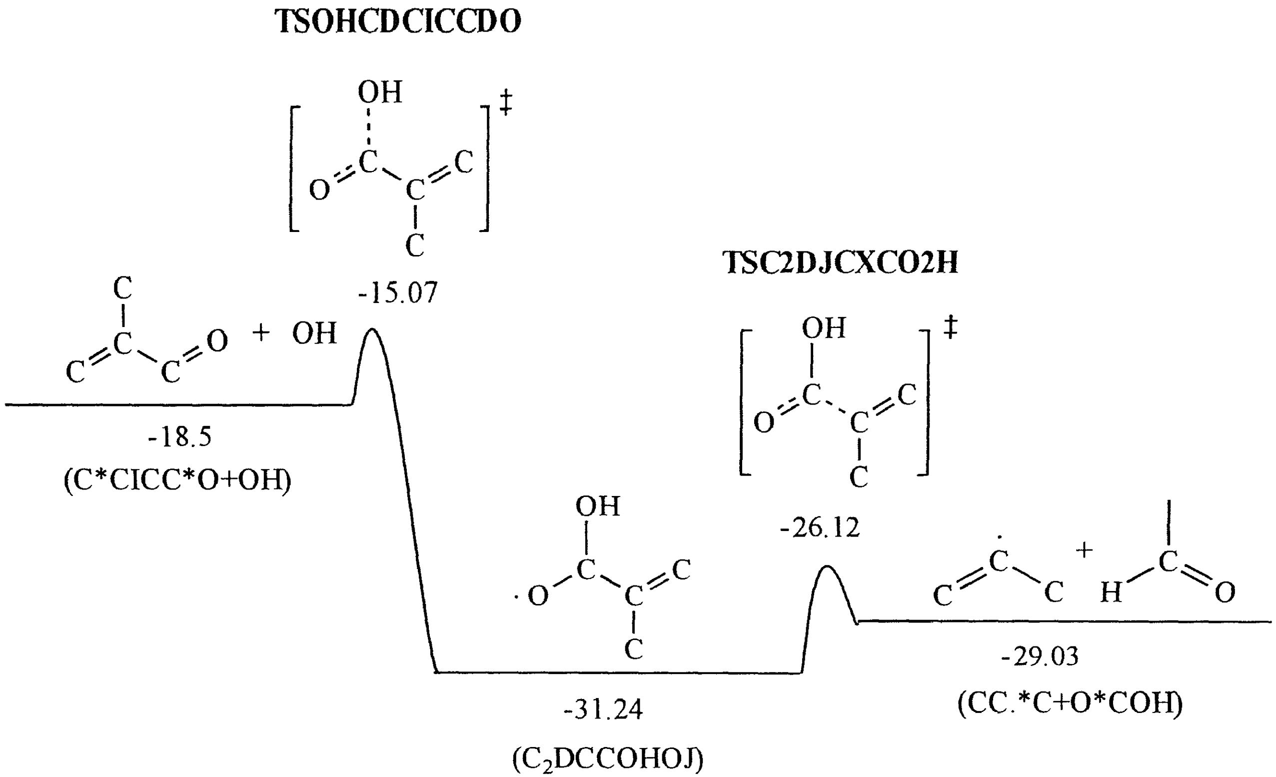

Figure 5B.14 The potential energy level diagram for C*CICC*O + OH -> products

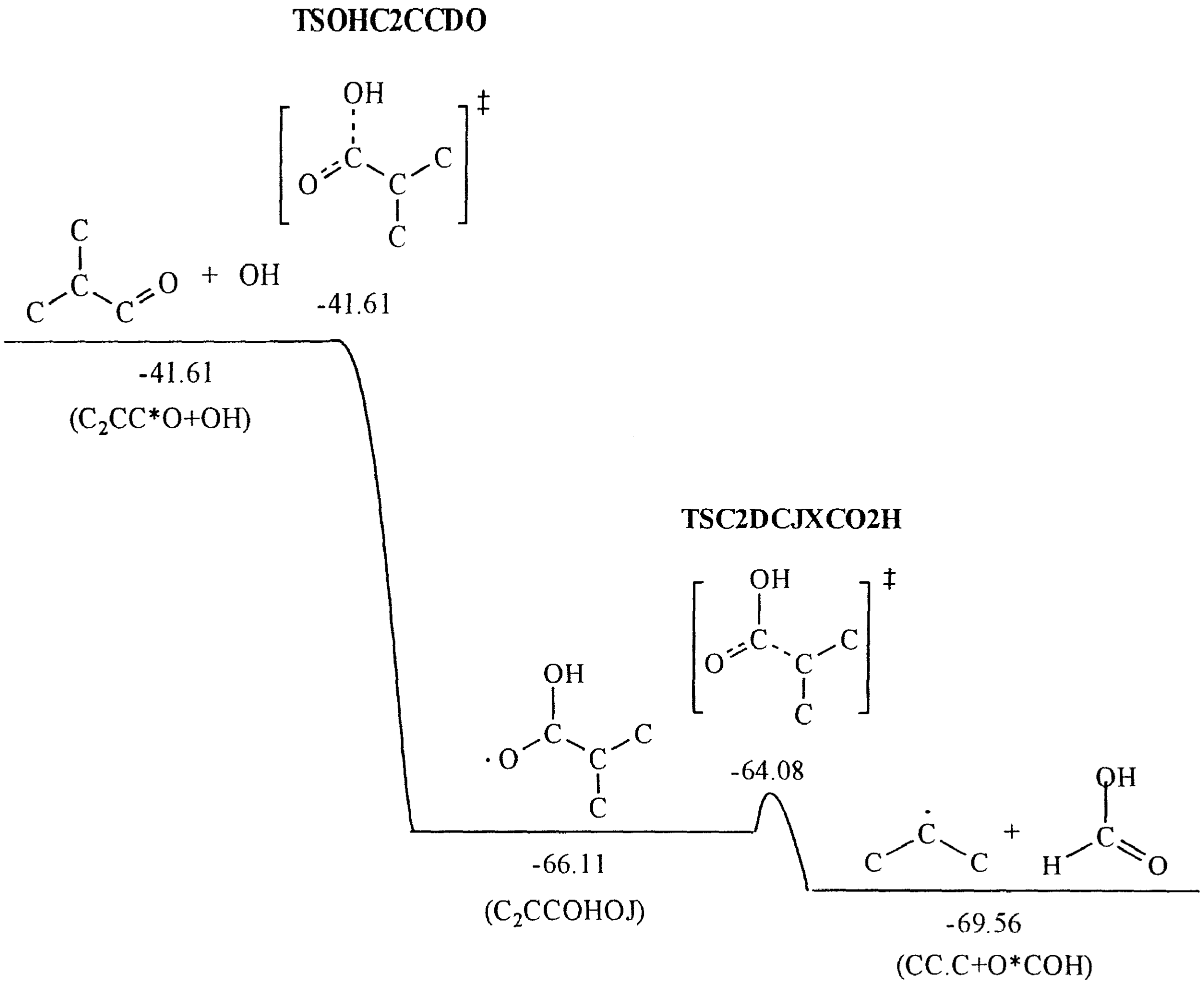

Figure 5B.15 The potential energy level diagram for $C_2CC{*}O + OH \rightarrow$ products

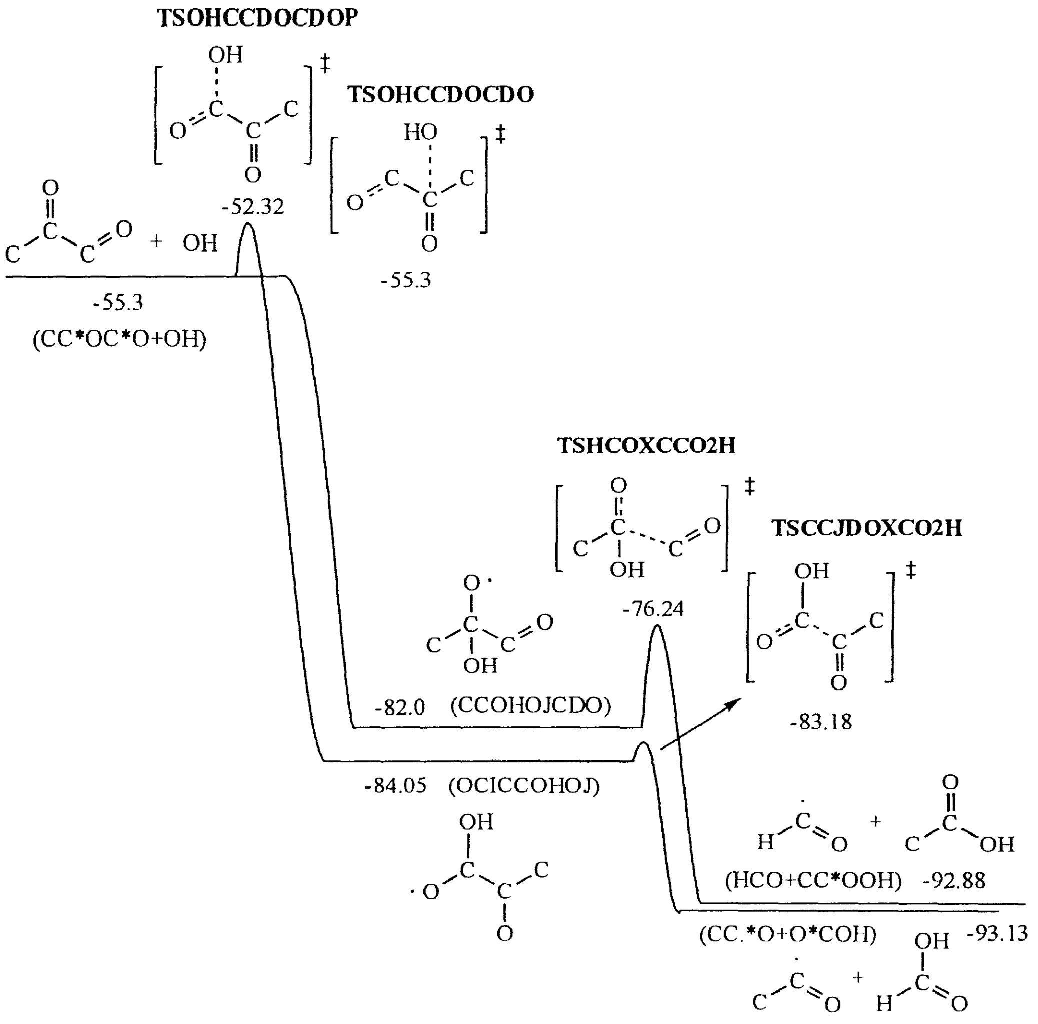

Figure 5B.16 The potential energy level diagram for CC*OC*O + OH -> products

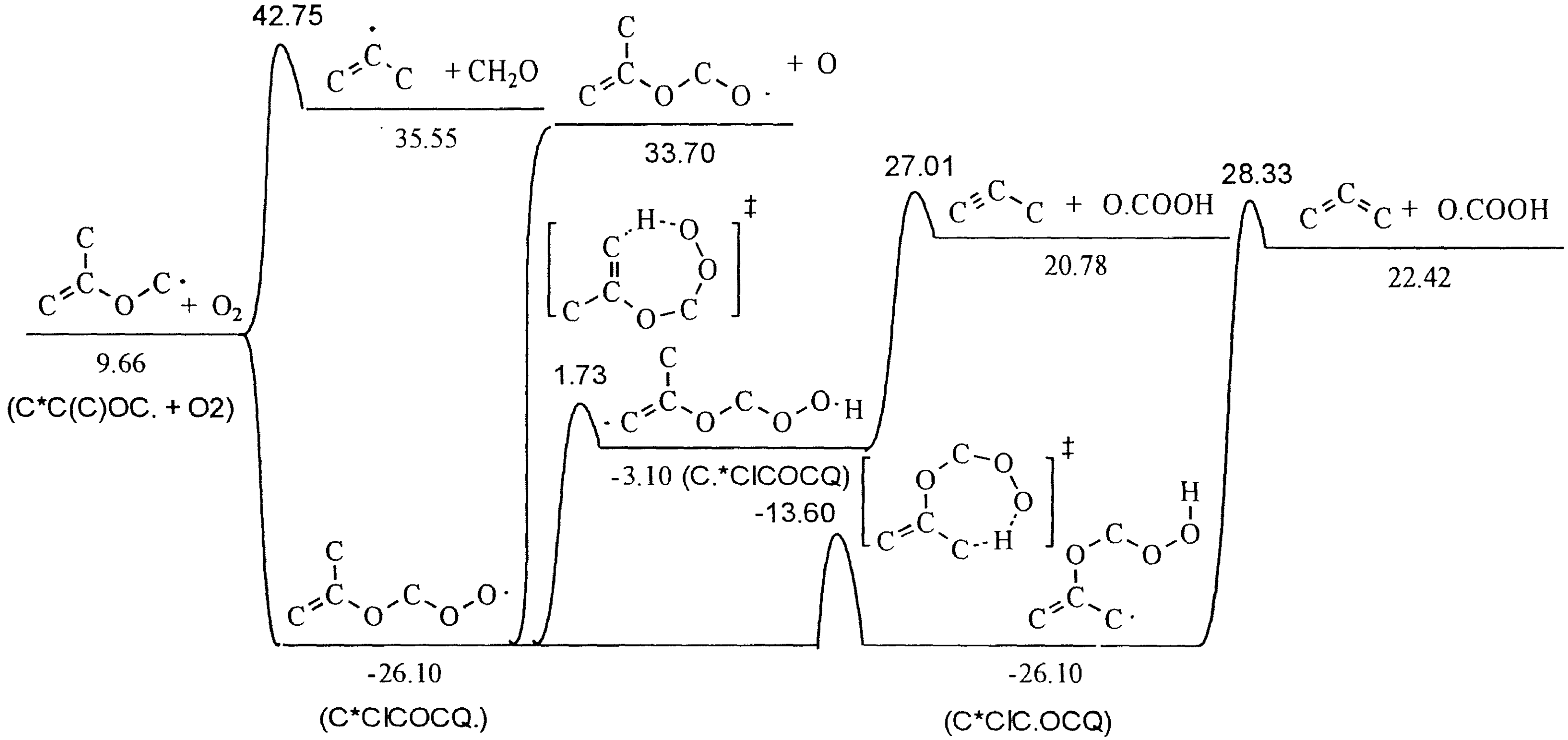

Figure 5B.17 The potential energy level diagram for C=C(C)OC· + O_2 -> products

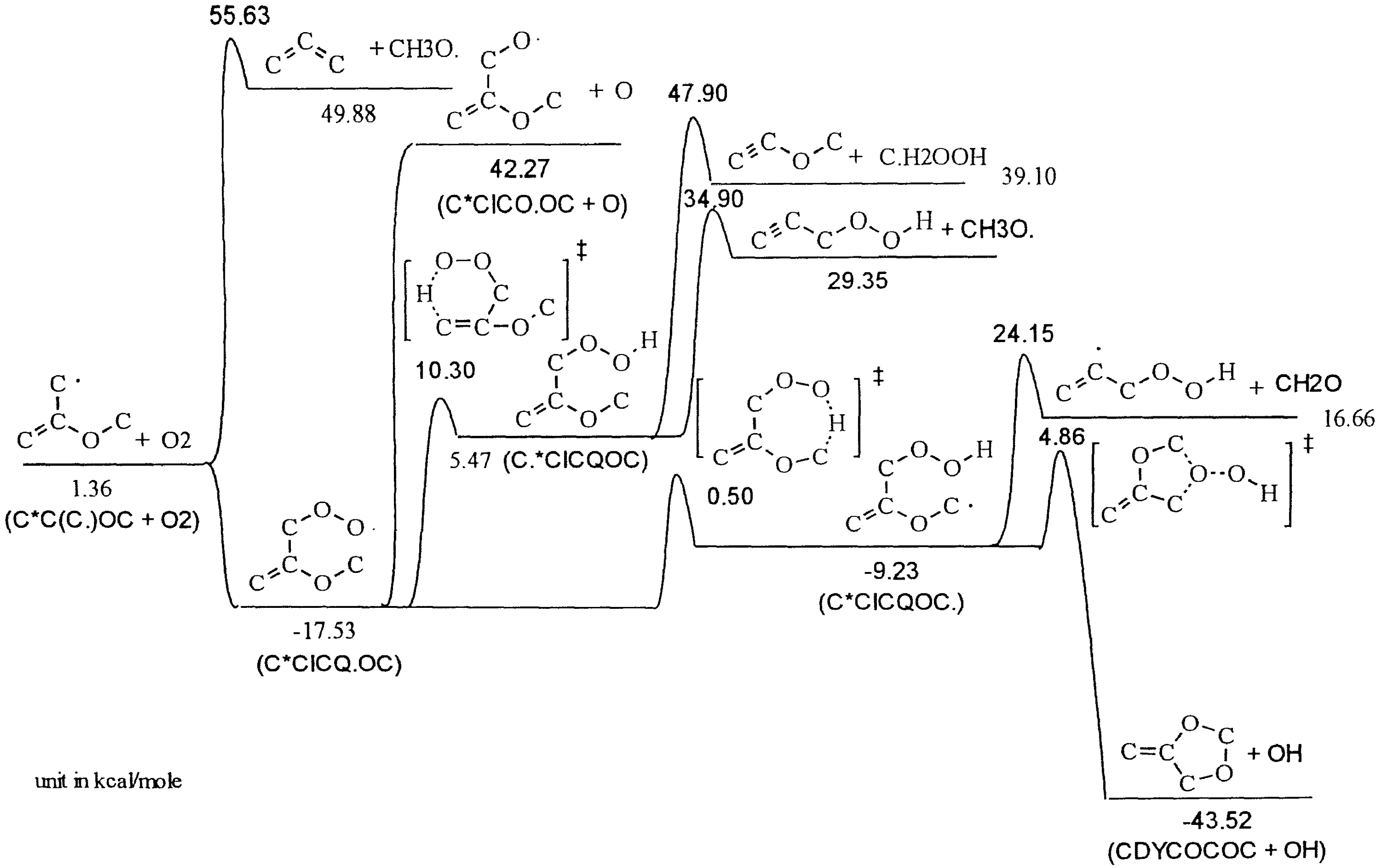

Figure 5B.18 The potential energy level diagram for C*C(C·)OC + O_2 -> products

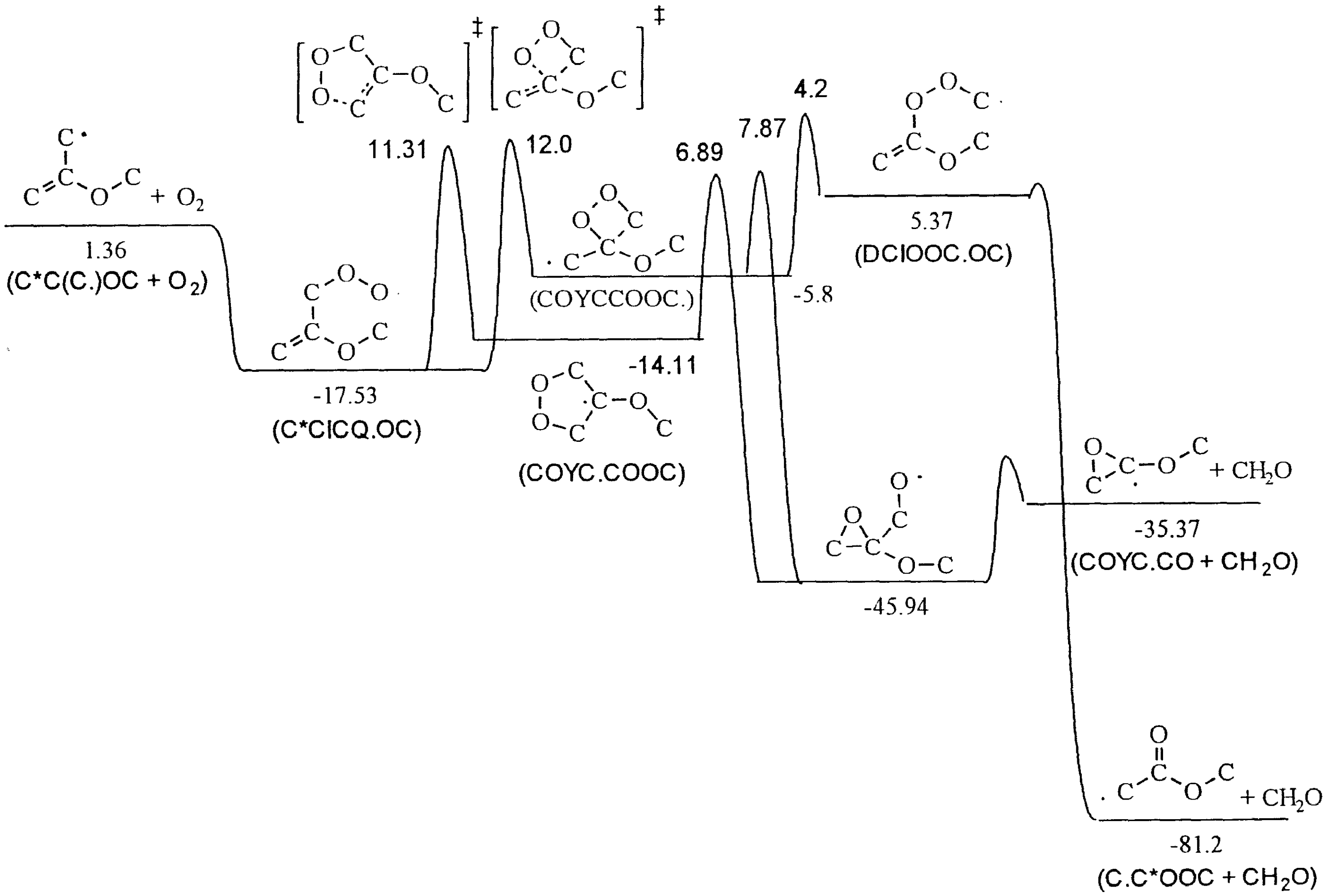

Figure 5B.19 The potential energy level diagram for C*C(C·)OC + O_2 -> products

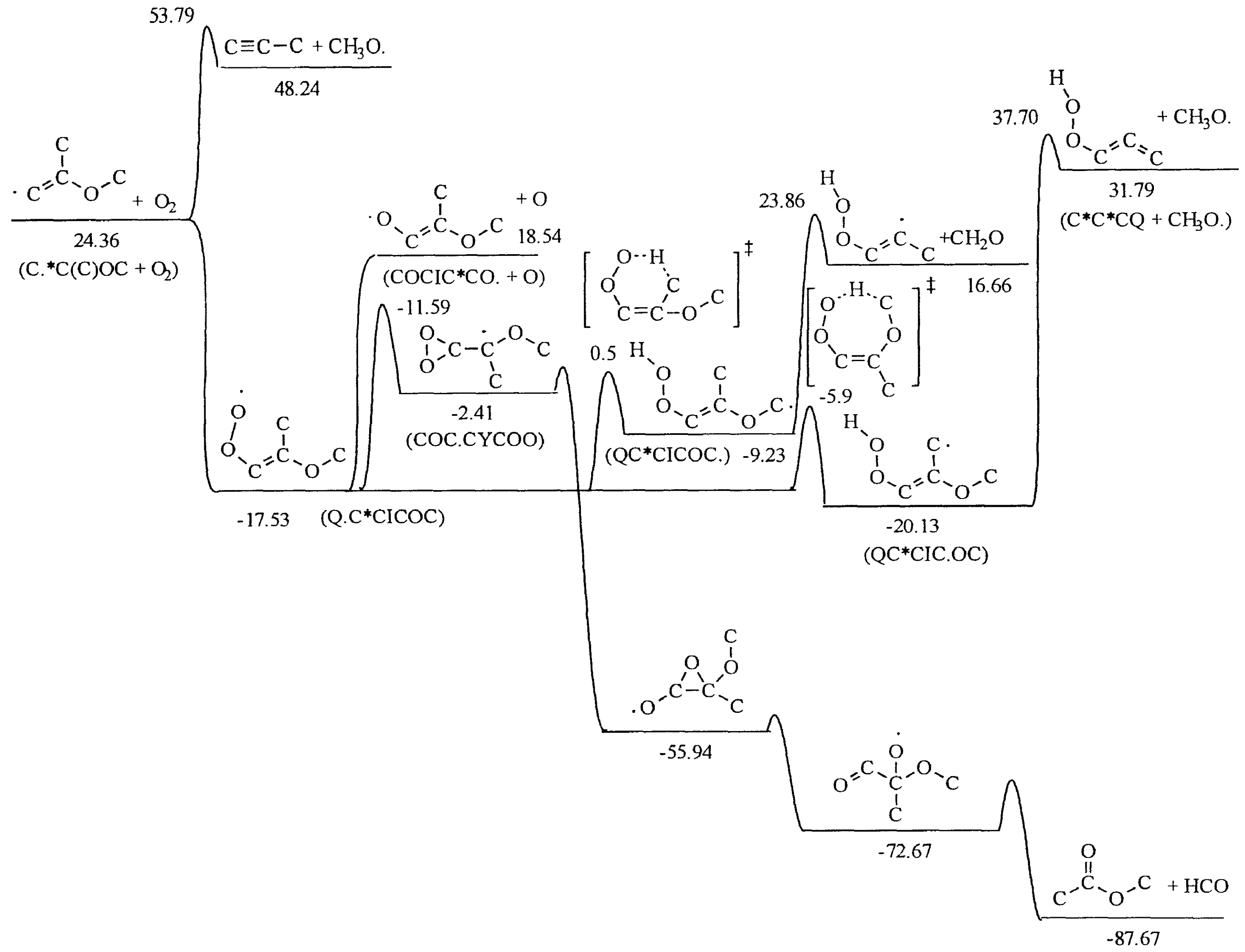

Figure 5B.20 The potential energy level diagram for C·*C(C)OC + O2 -> products

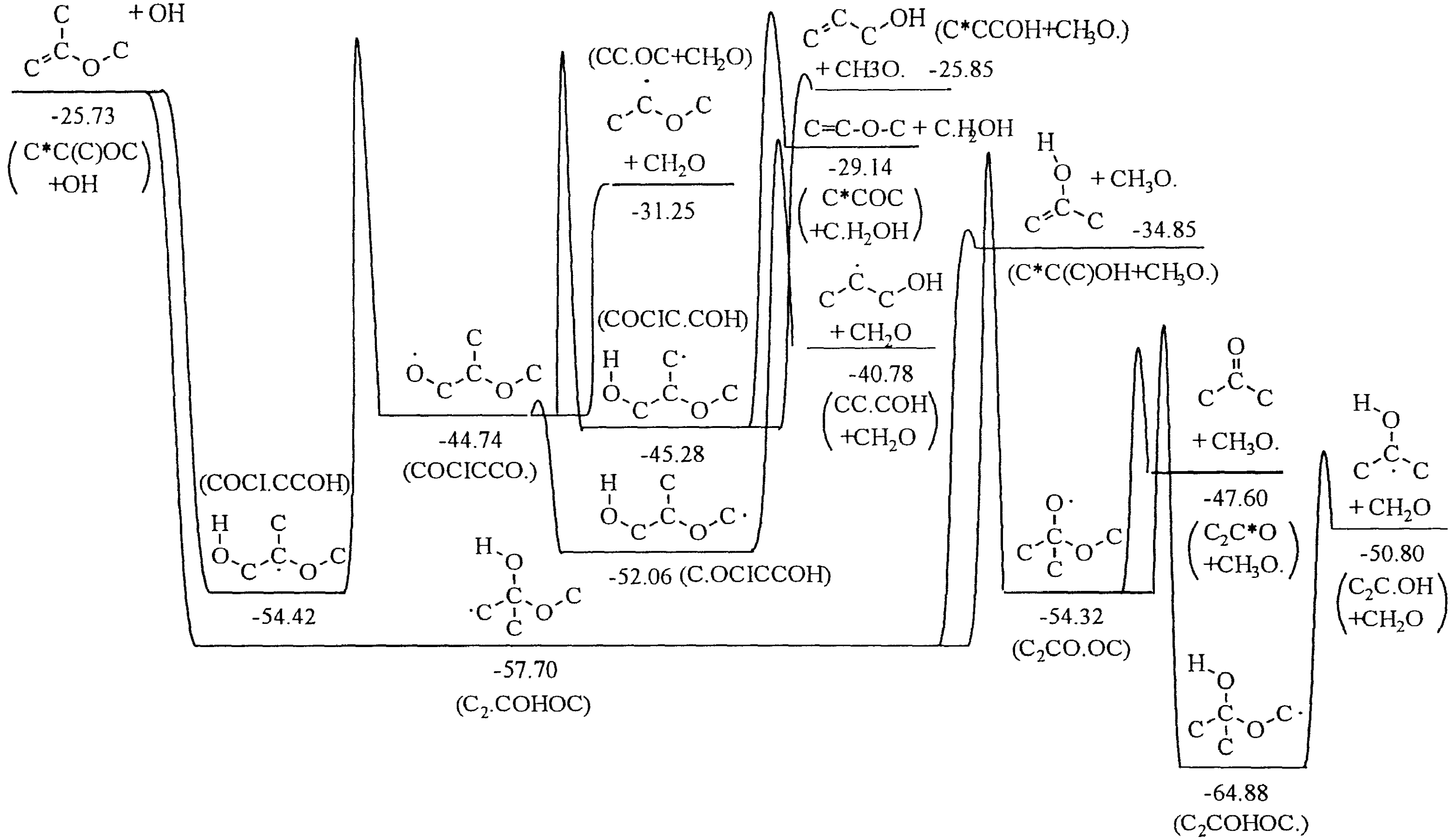

Figure 5B.21 The potential energy level diagram for C*C(C)OC + OH -> products

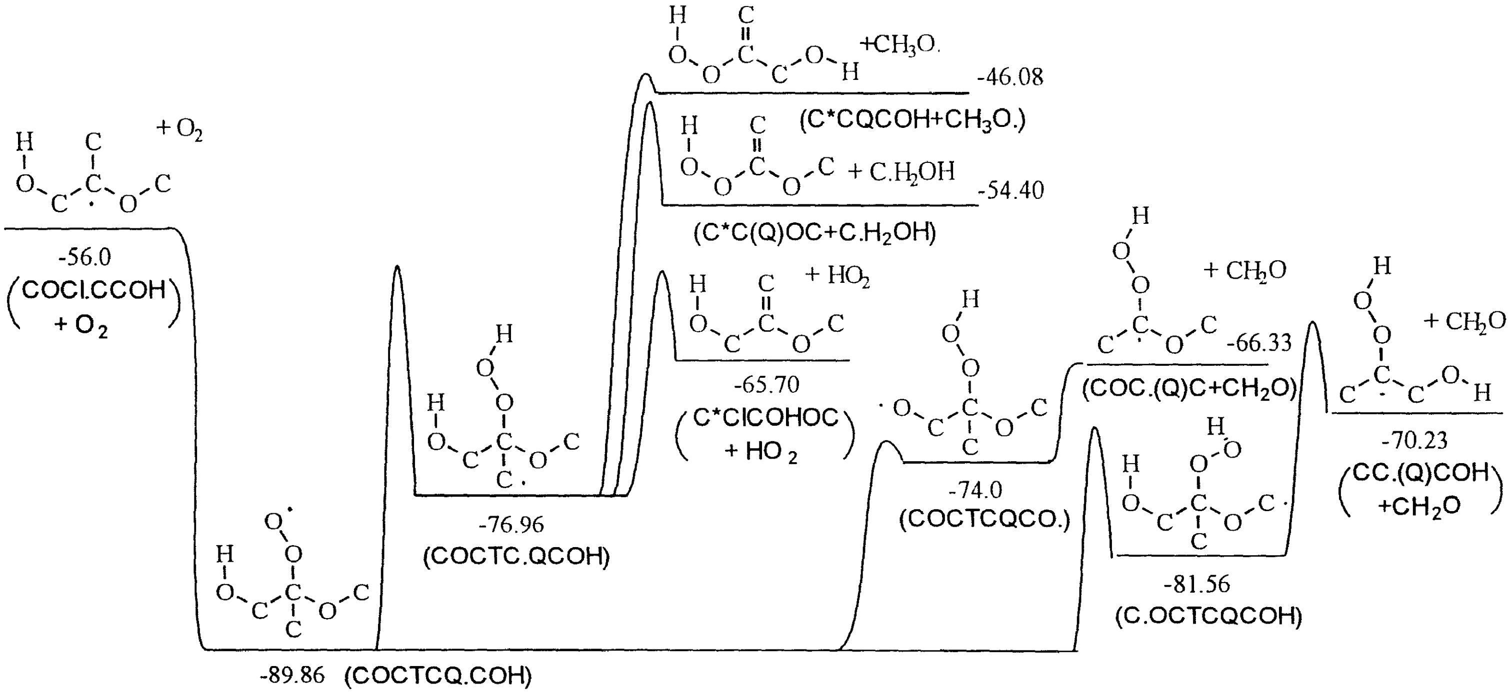

Figure 5B.22 The potential energy level diagram for COCI·CCOH + O_2 -> products

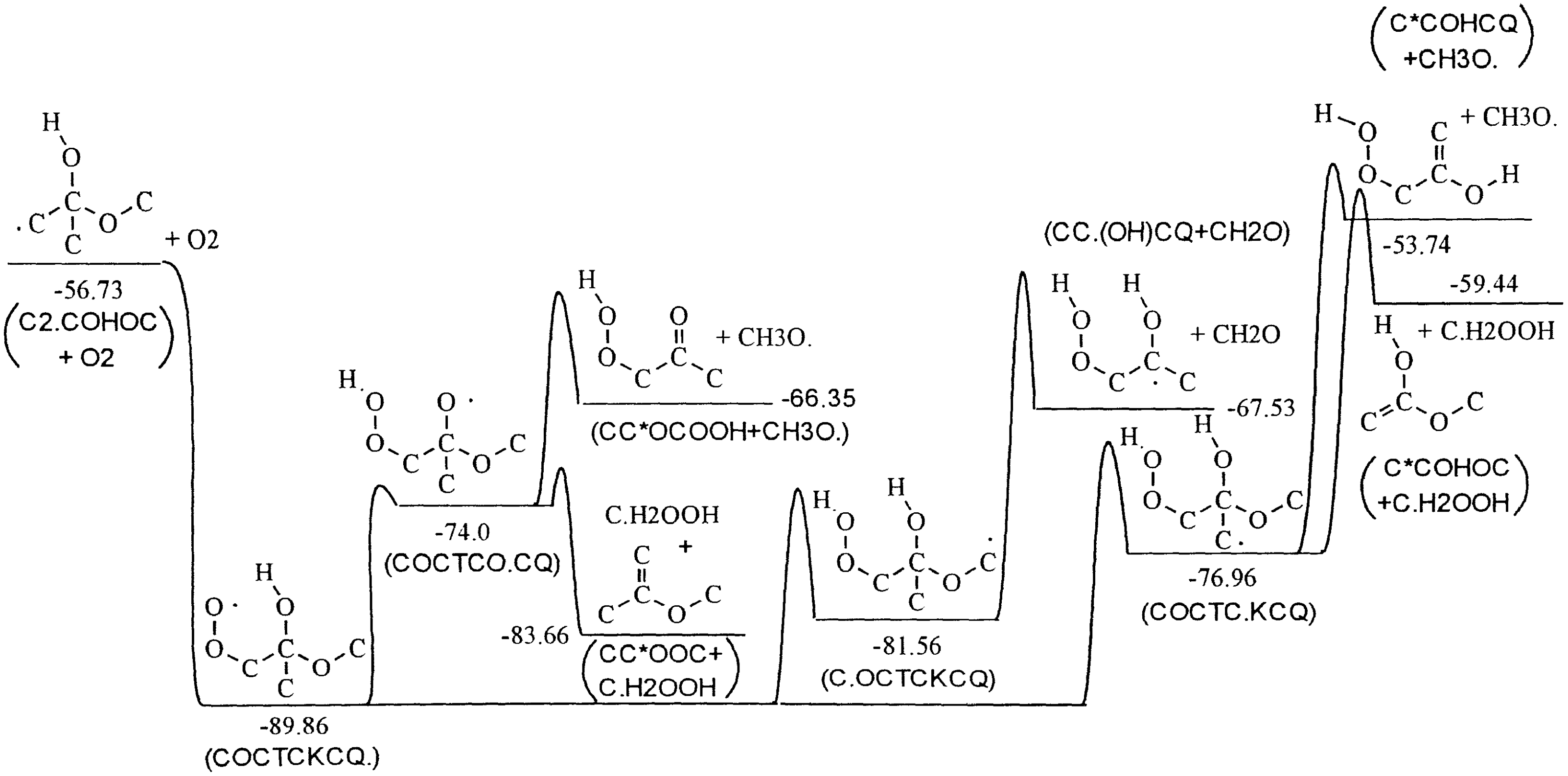

Figure 5B.23 The potential energy level diagram for $C_2{\cdot}COHOC + O_2 \rightarrow$ products

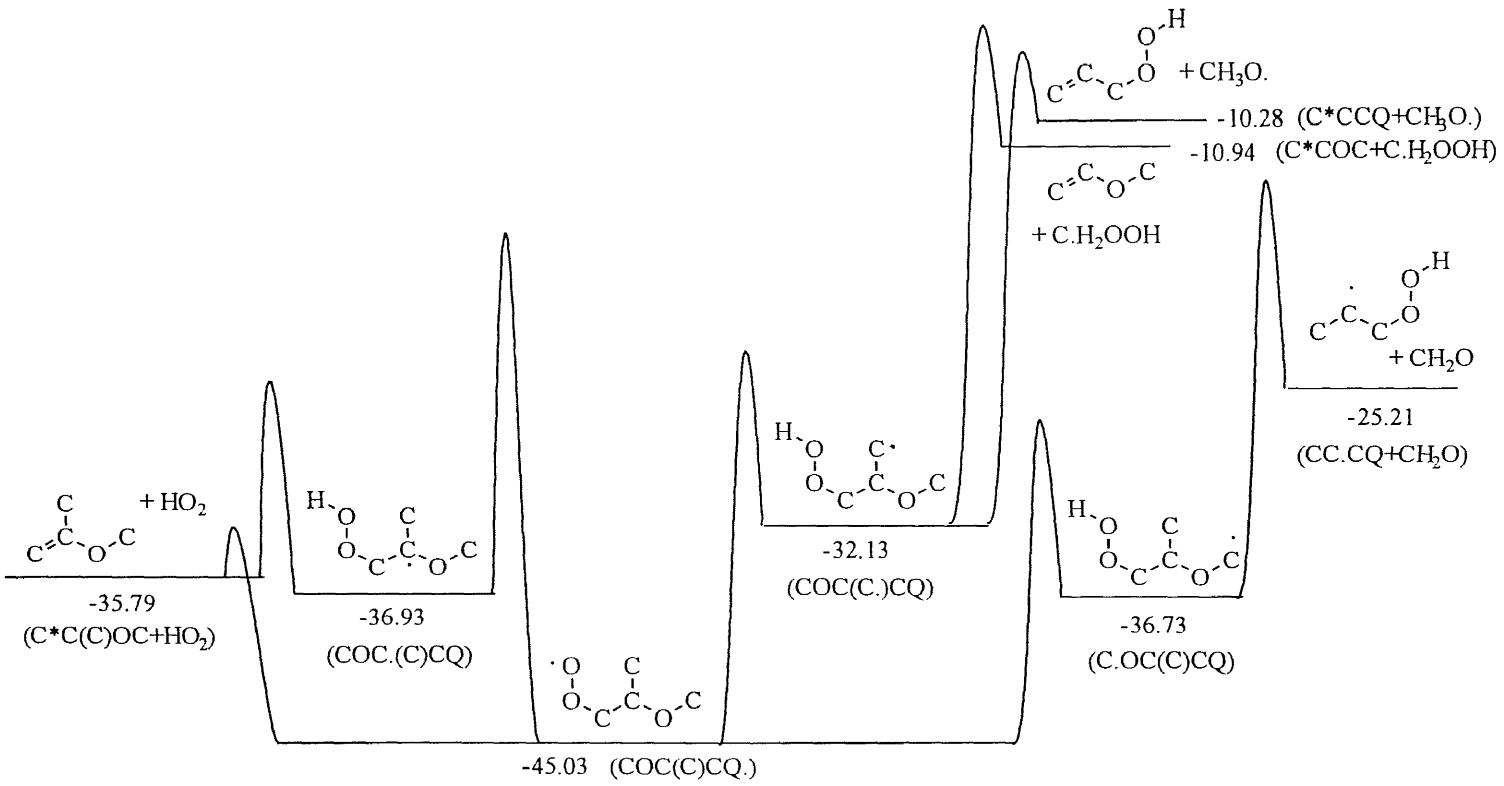

Figure 5B.24 The potential energy level diagram for C*C(C)OC + HO$_2$ -> products

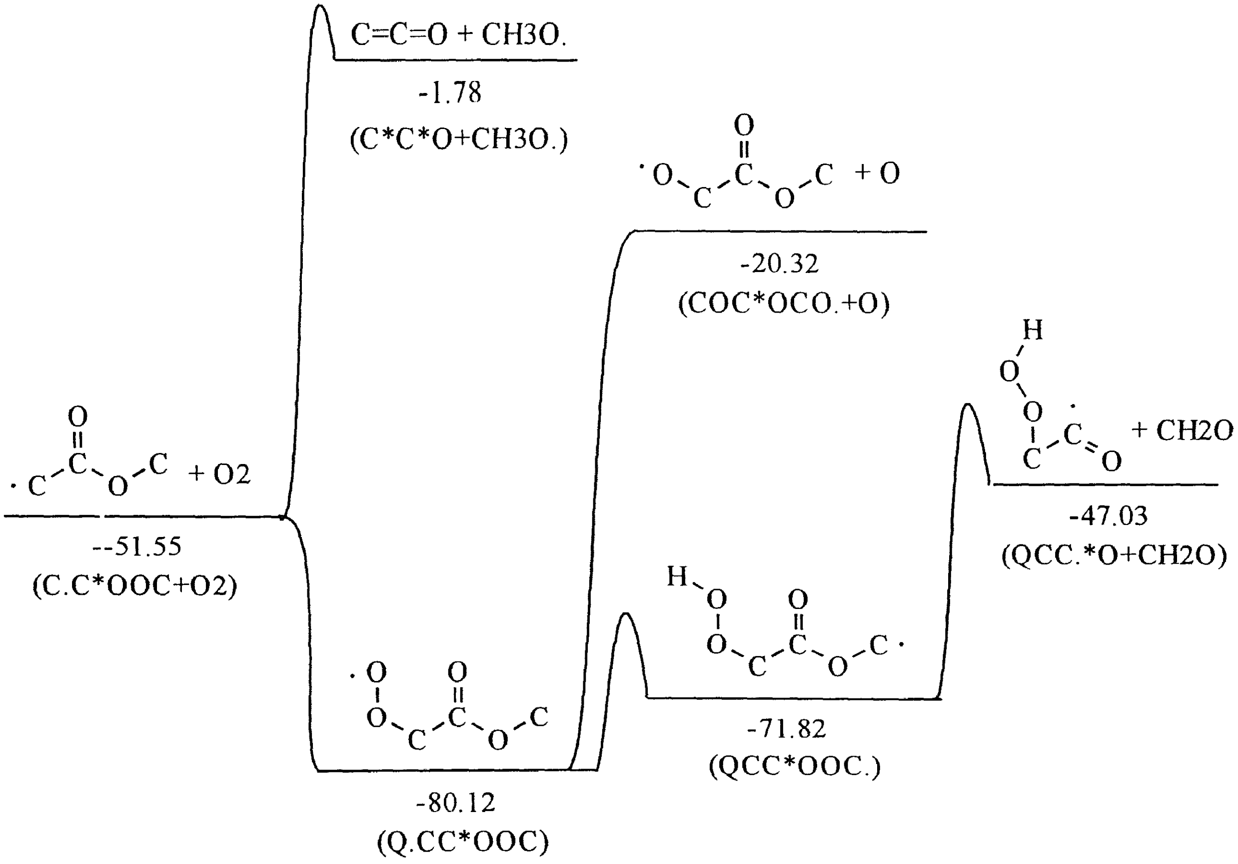

Figure 5B.25 The potential energy level diagram for C·C*OOC + O_2 -> products

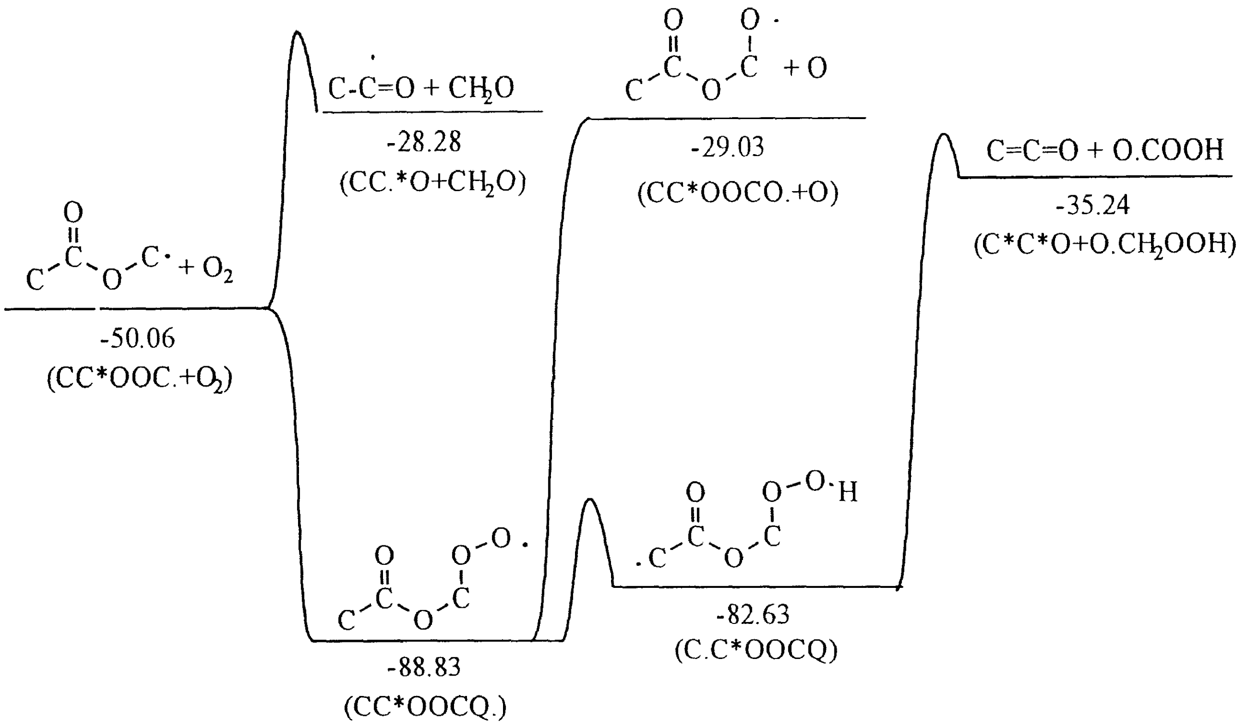

Figure 5B.26 The potential energy level diagram for CC*OOC· + O_2 -> products

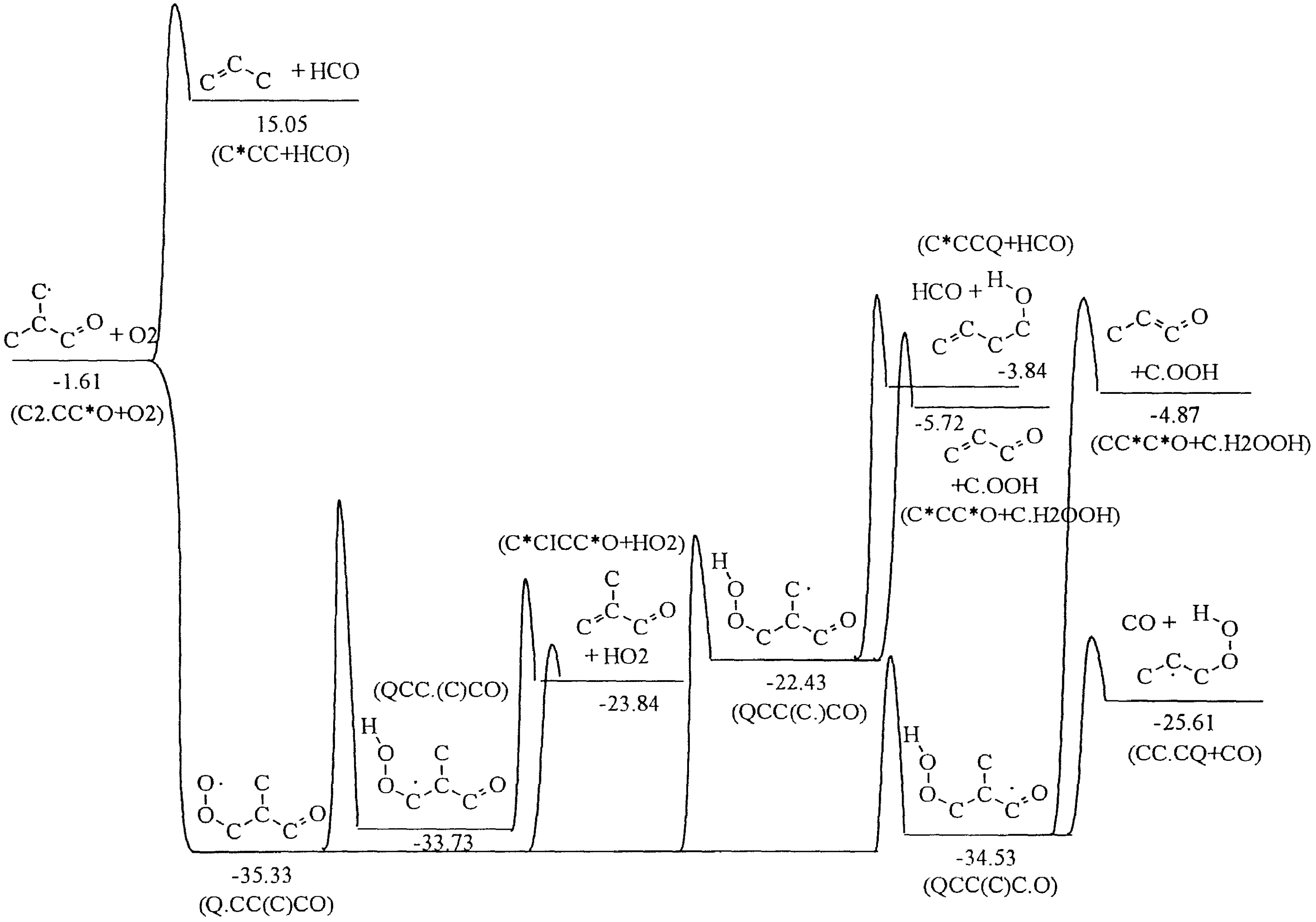

Figure 5B.27 The potential energy level diagram for $C_2 \cdot CC{*}O + O_2$ -> products

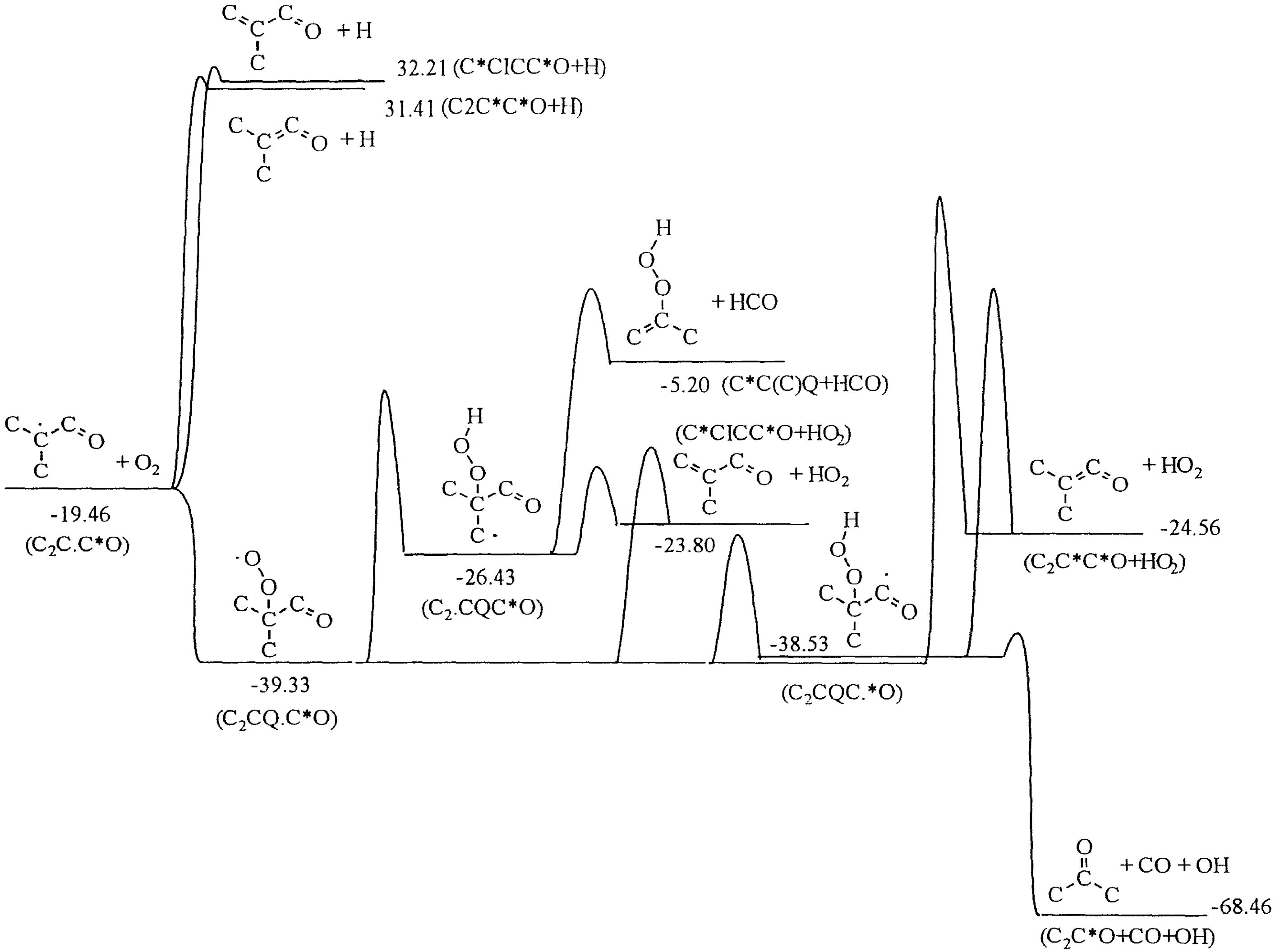

Figure 5B.28 The potential energy level diagram for $C_2C{\cdot}C{*}O + O_2$ -> products

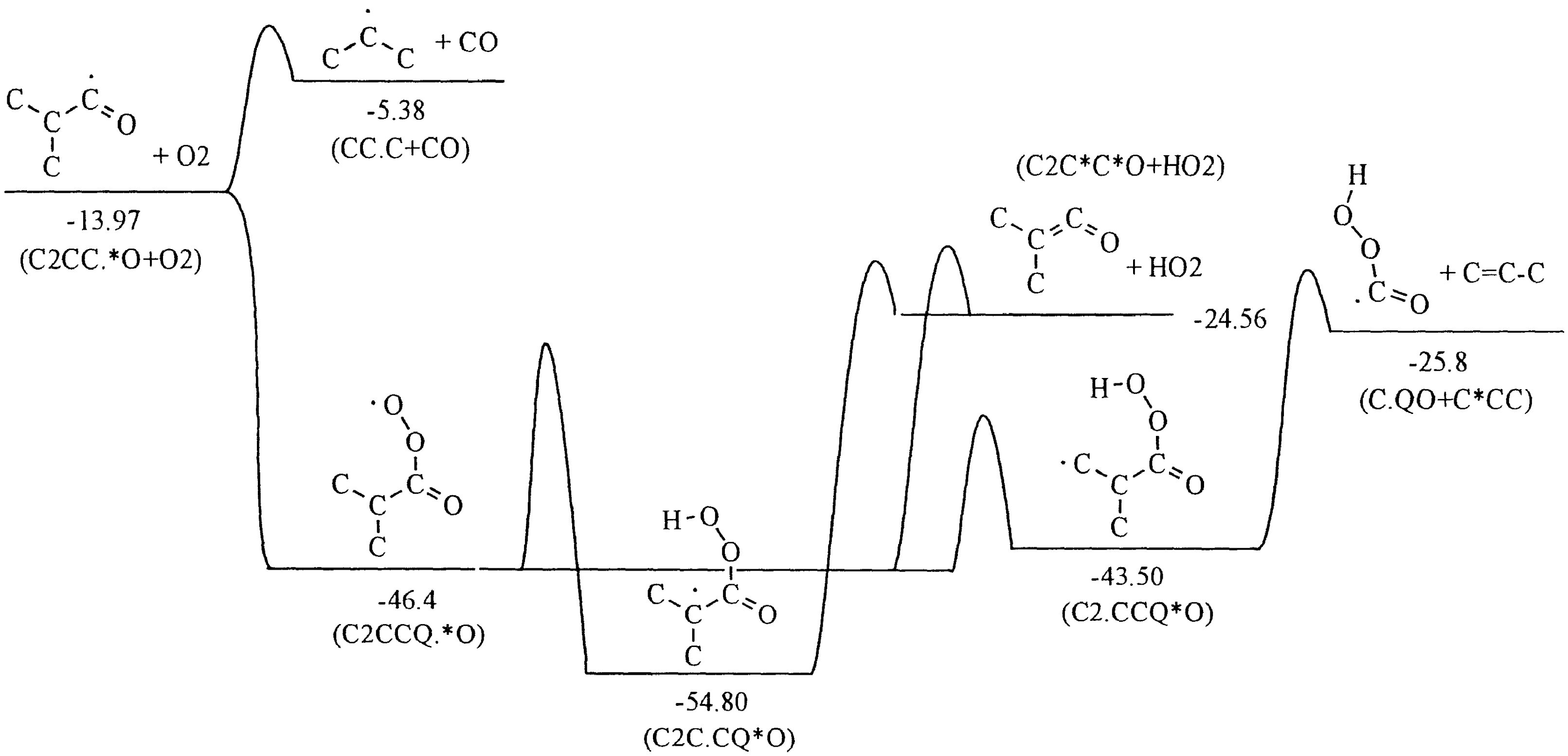

Figure 5B.29 The potential energy level diagram for $C_2CC{\cdot}{*}O + O_2$ -> products

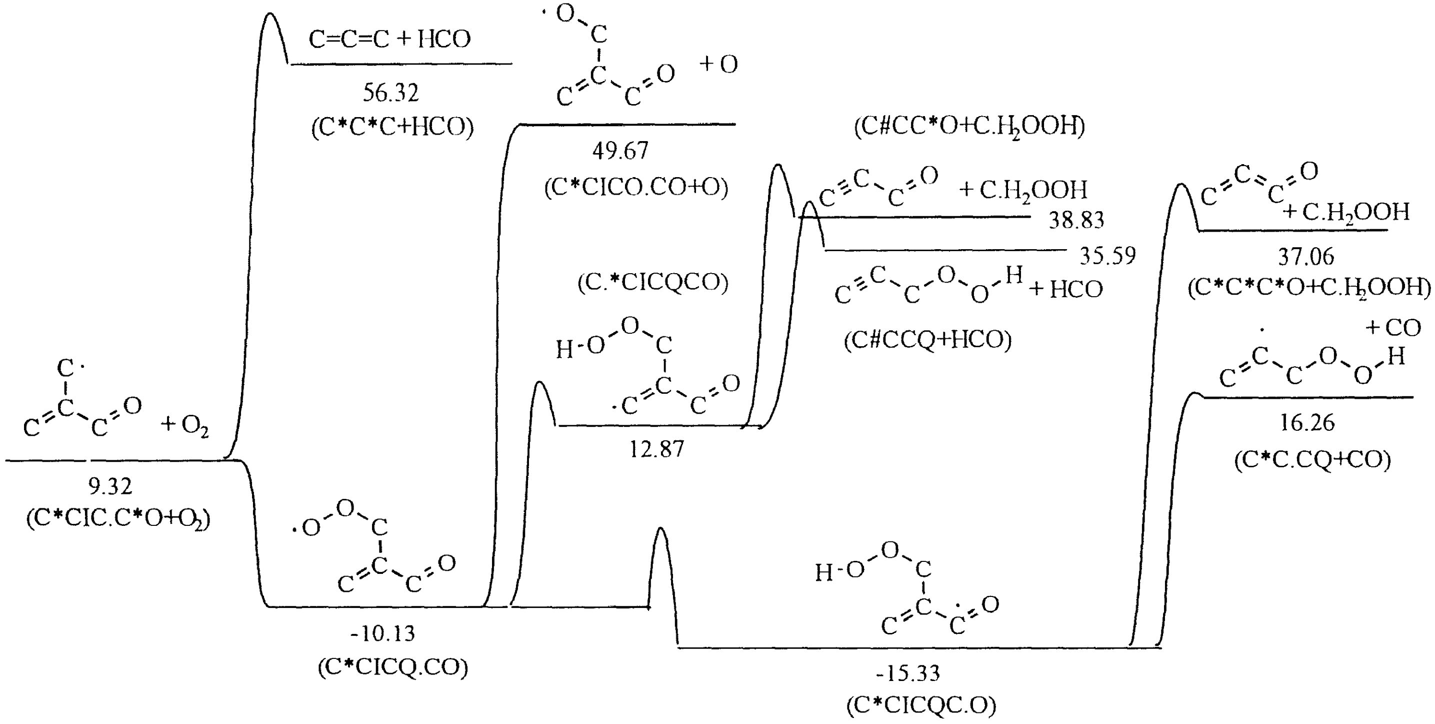

Figure 5B.30 The potential energy level diagram for C*CIC·C*O + O_2 -> products

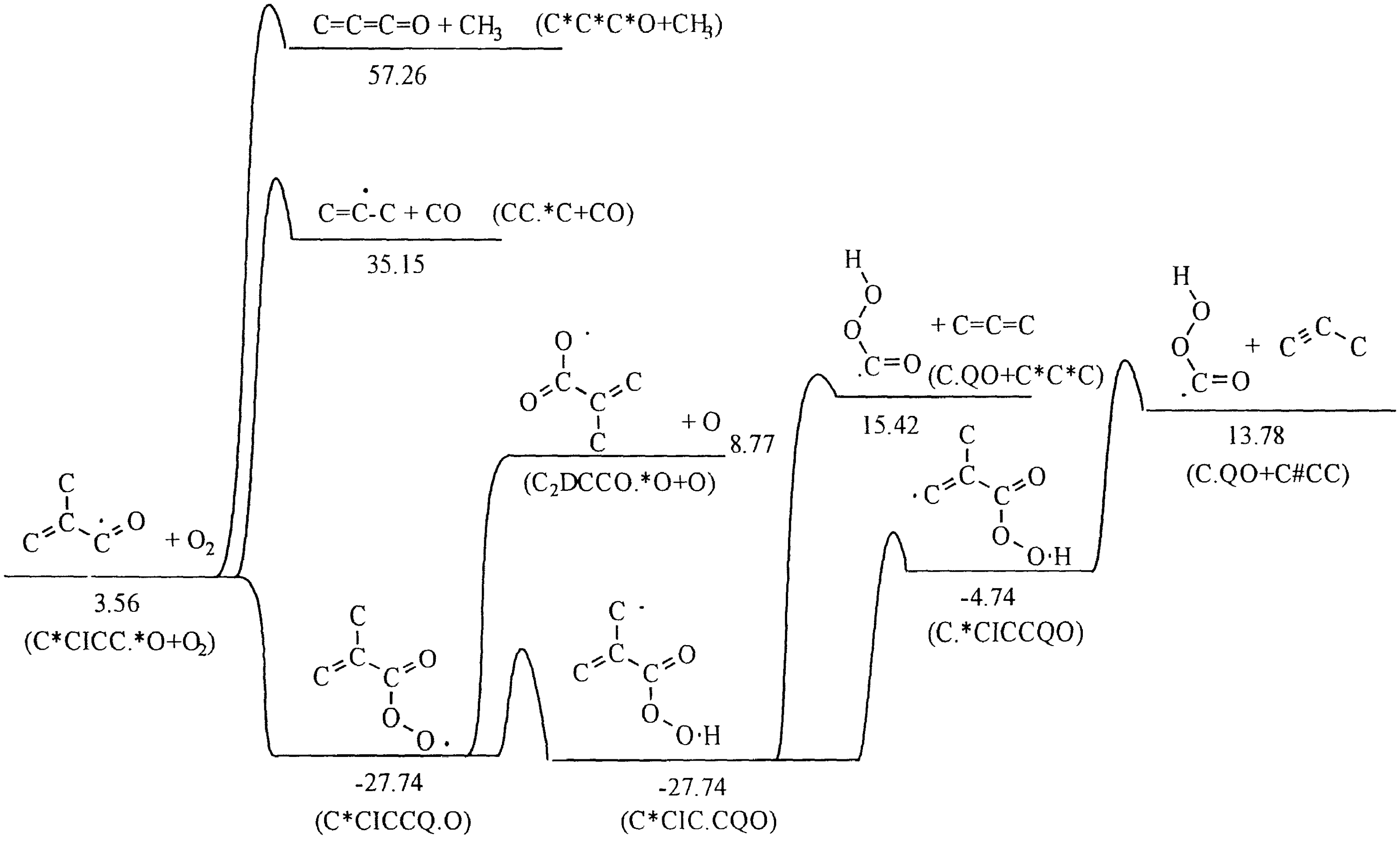

Figure 5B.31 The potential energy level diagram for C*CICC·*O + O_2 -> products

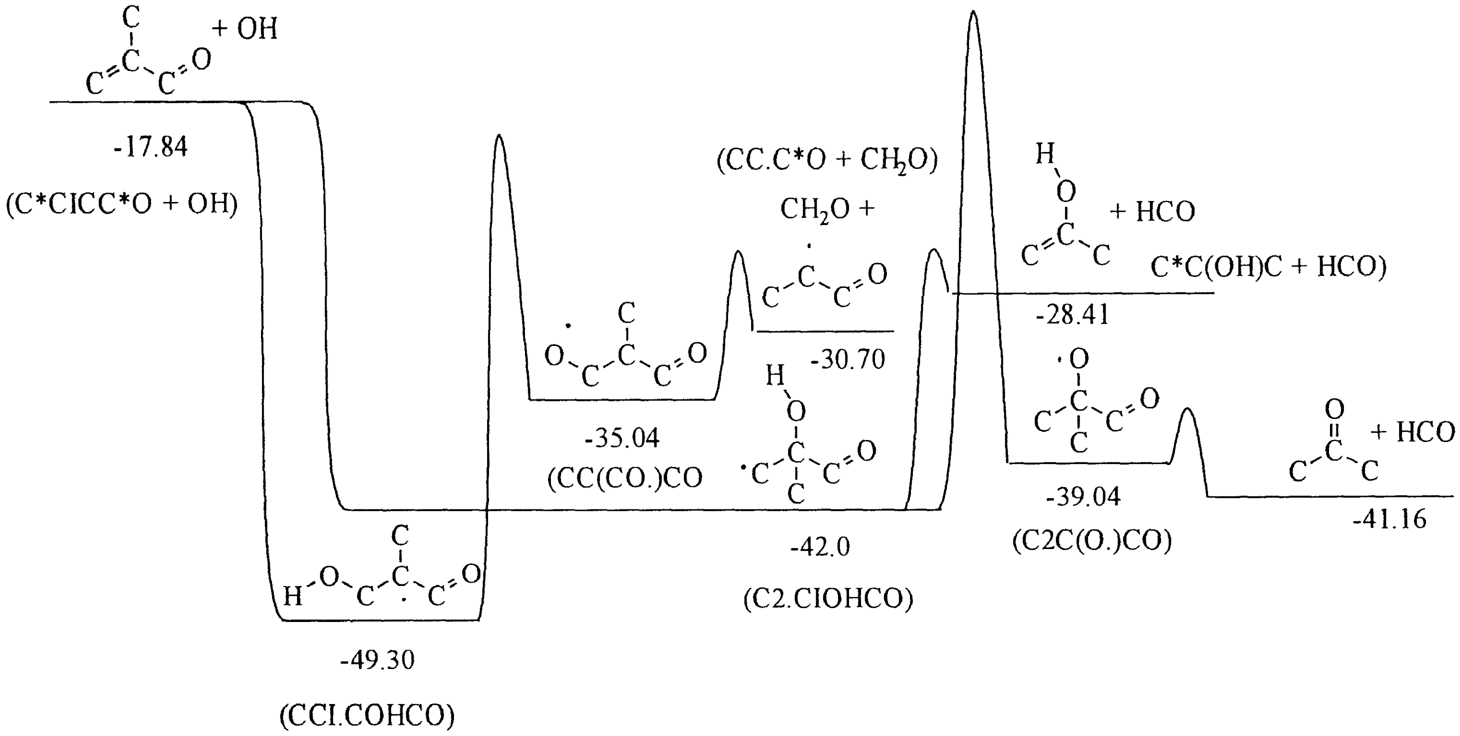

Figure 5B.32 The potential energy level diagram for C*CICC*O + OH -> products

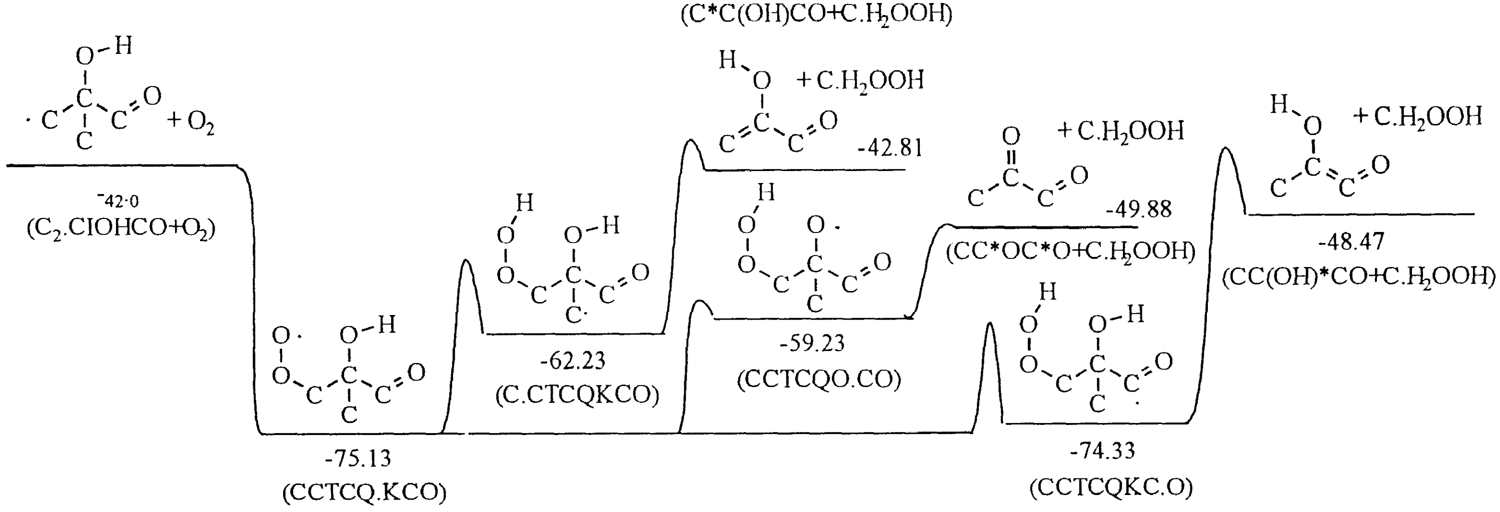

Figure 5B.33 The potential energy level diagram for C_2·CIOHCO + OH -> products

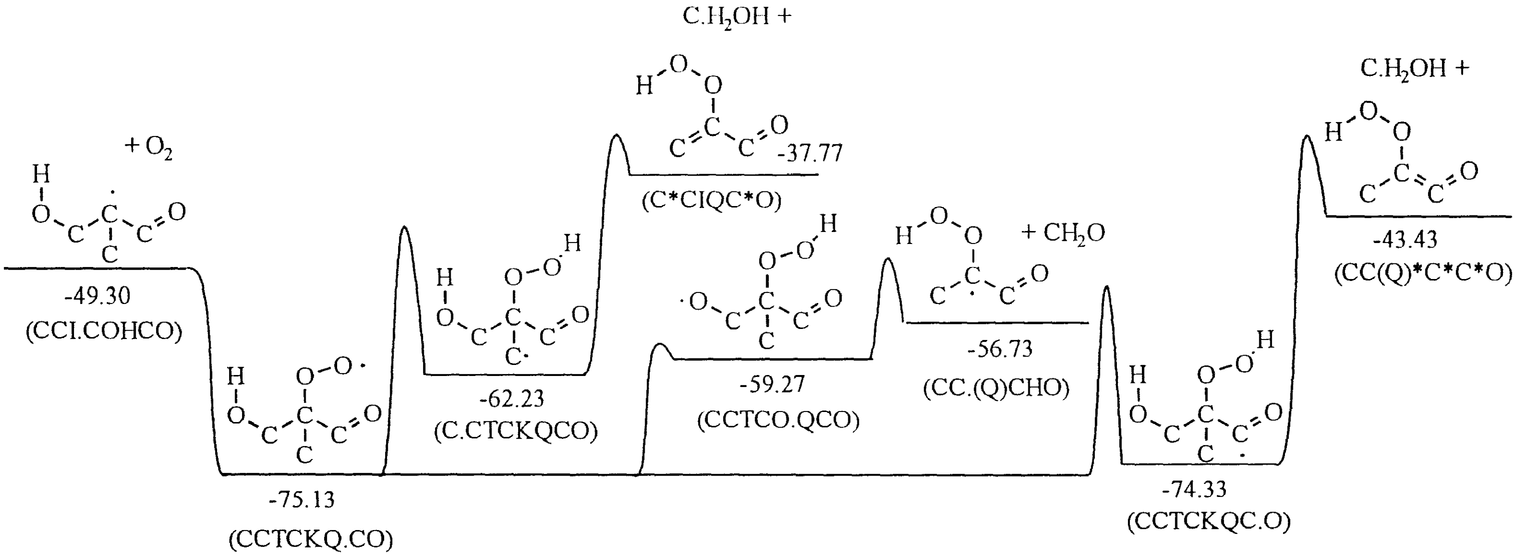

Figure 5B.34 The potential energy level diagram for CCI·COHCO + OH -> products

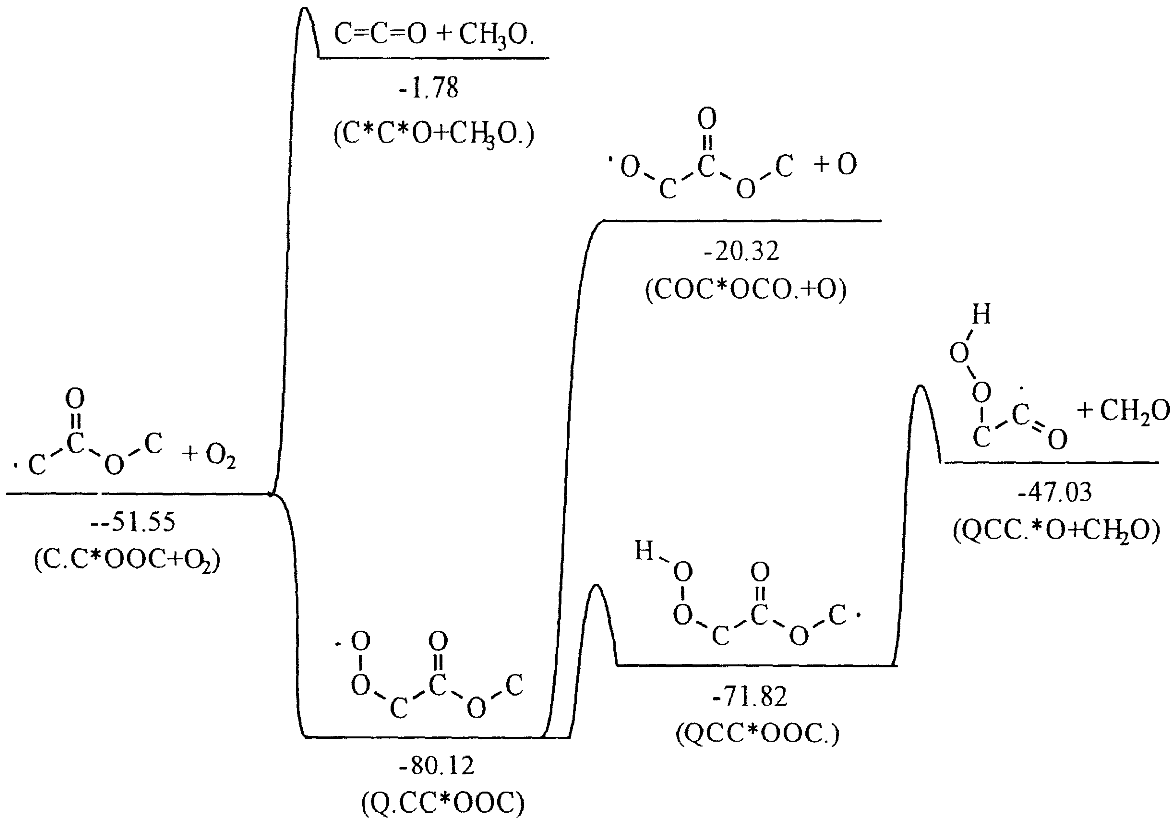

Figure 5B.35 The potential energy level diagram for C·C*OOC + O_2 -> products

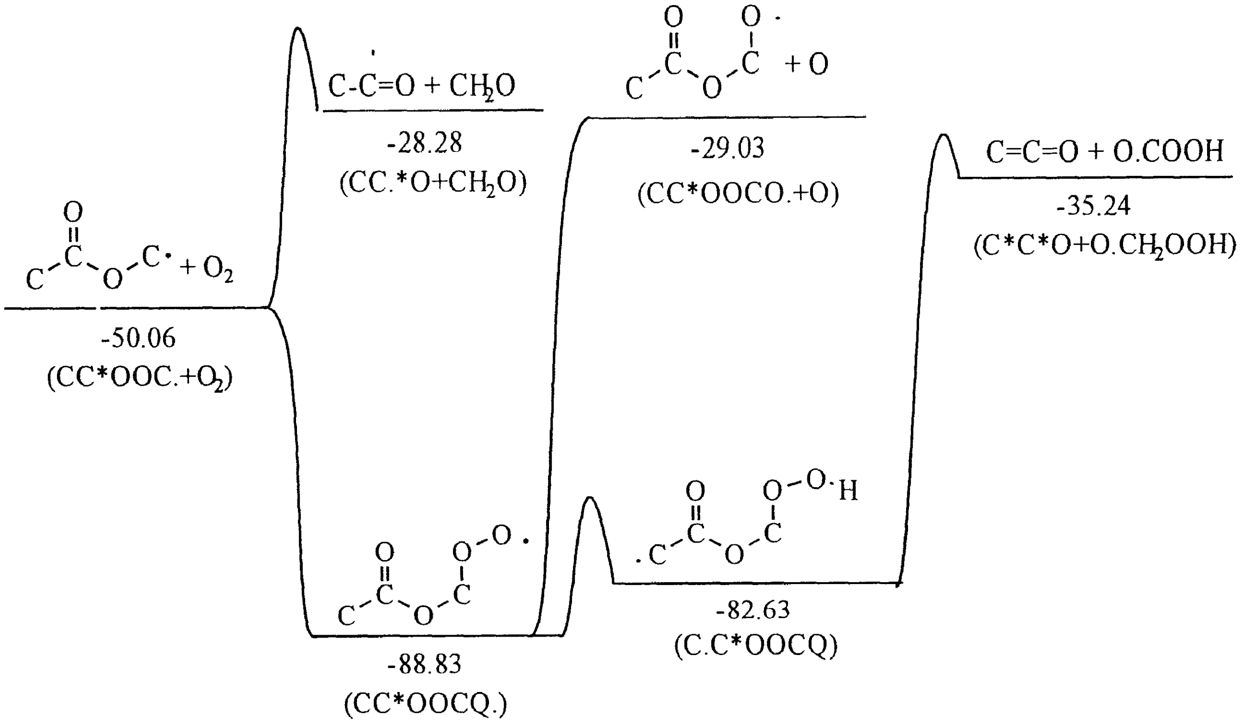

Figure 5B.36 The potential energy level diagram for $CC^*OOC\cdot + O_2 \rightarrow$ products

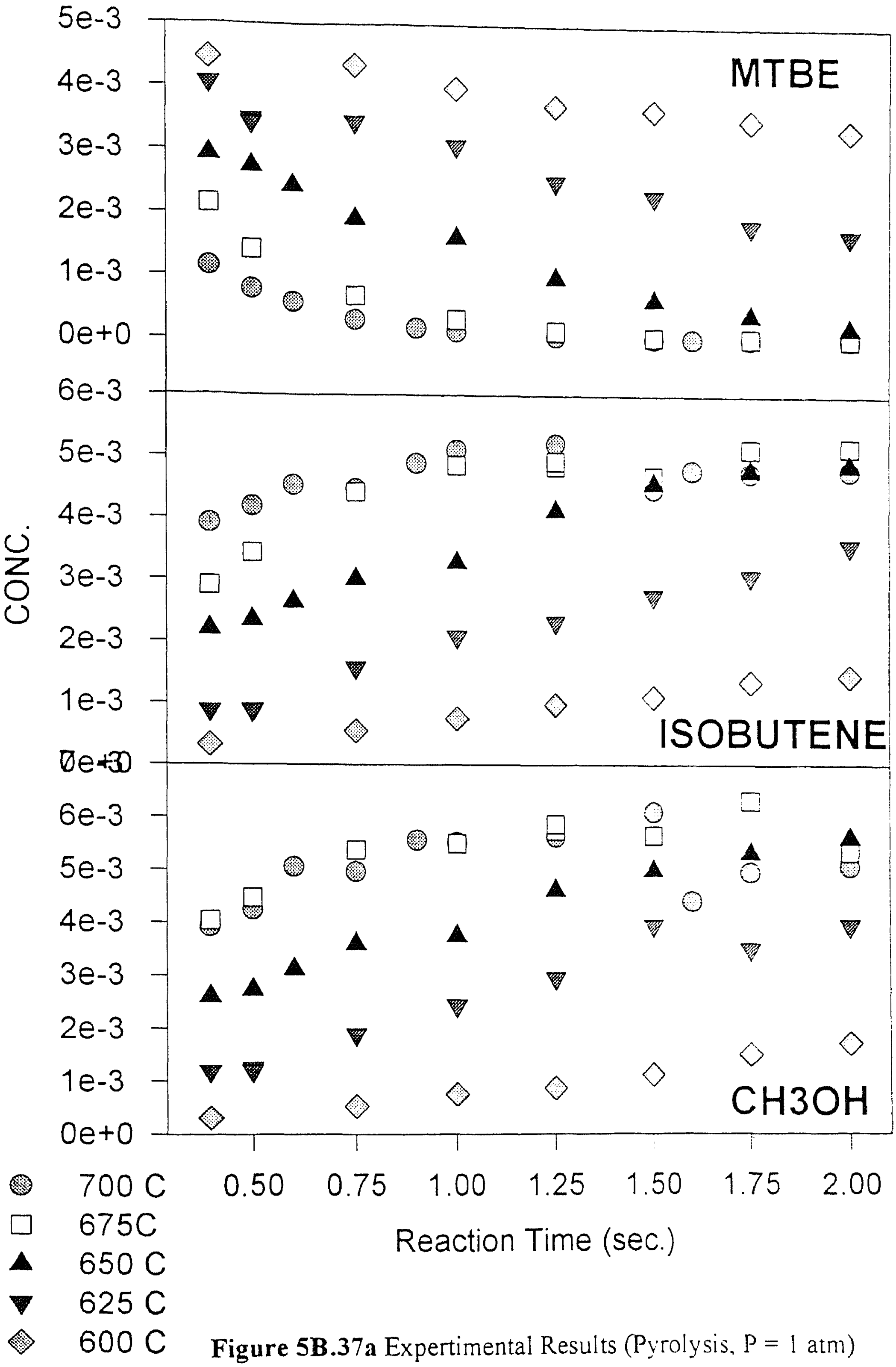

Figure 5B.37a Expertimental Results (Pyrolysis, P = 1 atm)

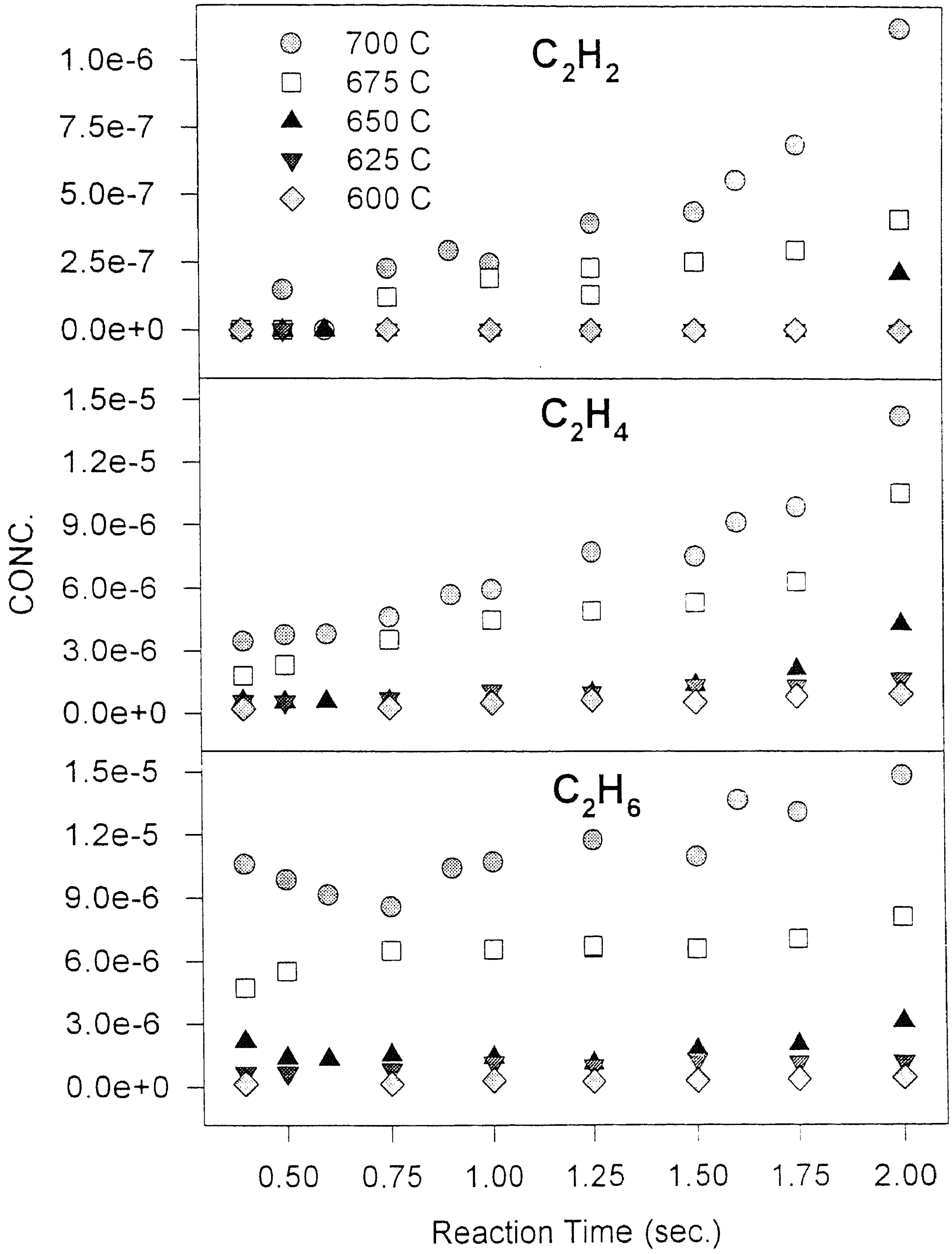

Figure 5B.37b Expertimental Results (Pyrolysis, P = 1 atm)

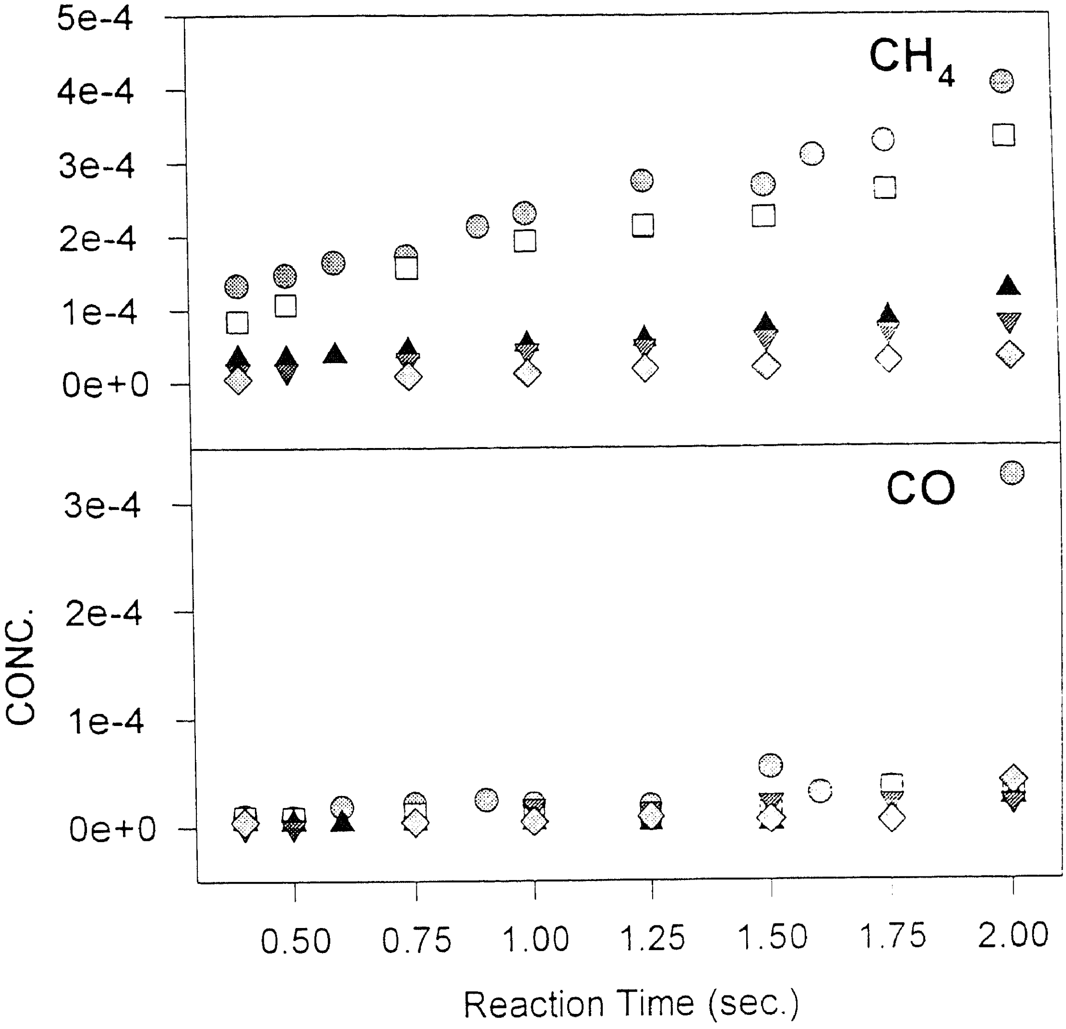

Figure 5B.37c Expertimental Results (Pyrolysis, P = 1 atm)

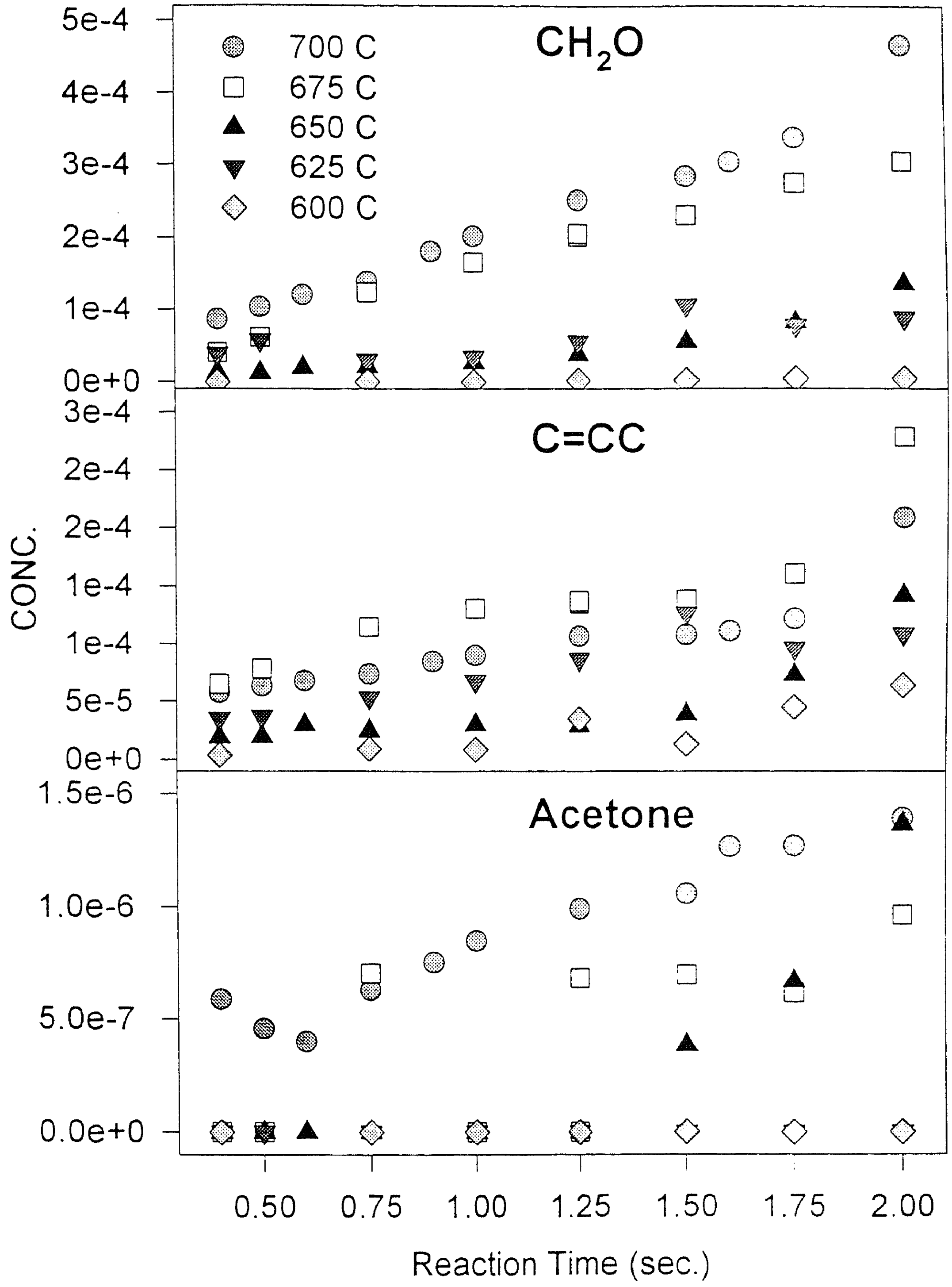

Figure 5B.37d Expertimental Results (Pyrolysis, P = 1 atm)

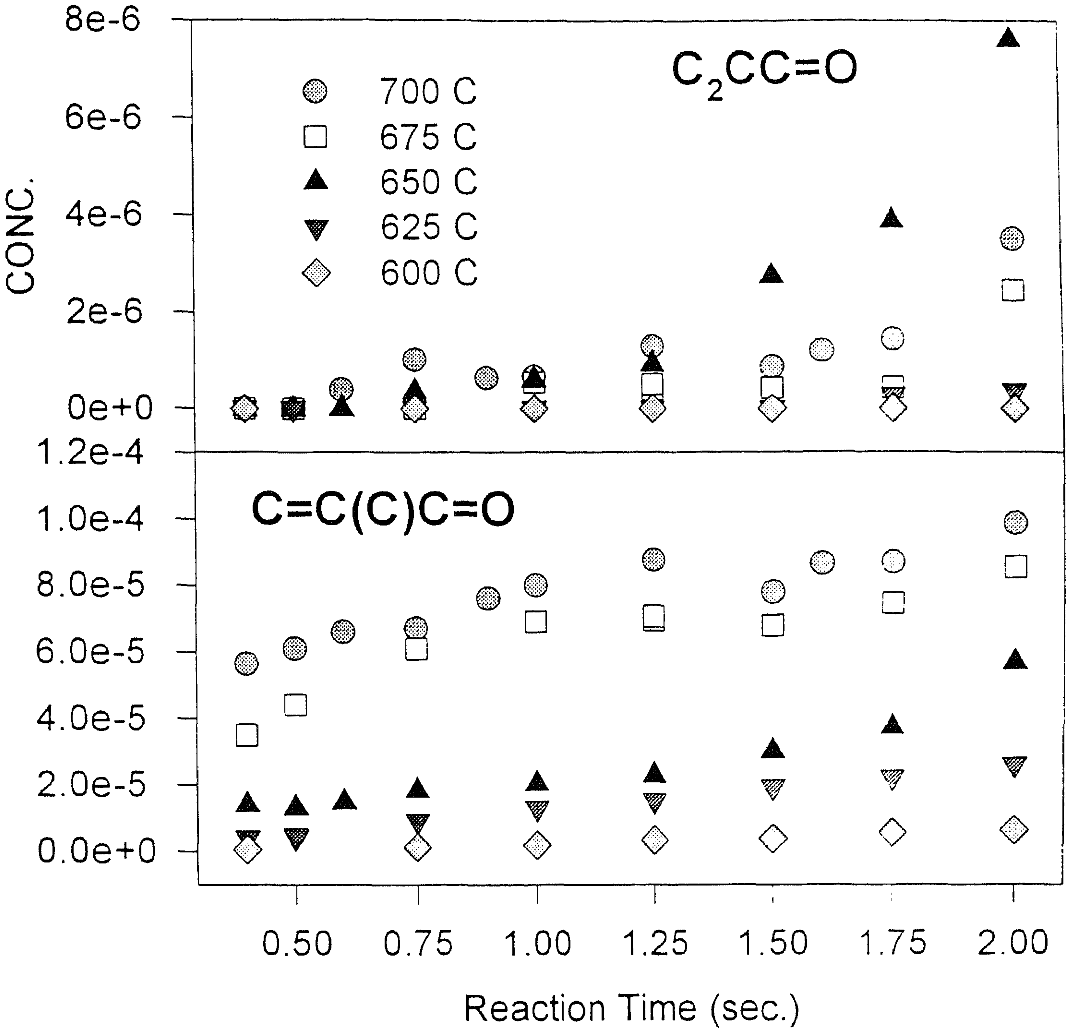

Figure 5B.37e Expertimental Results (Pyrolysis, P = 1 atm)

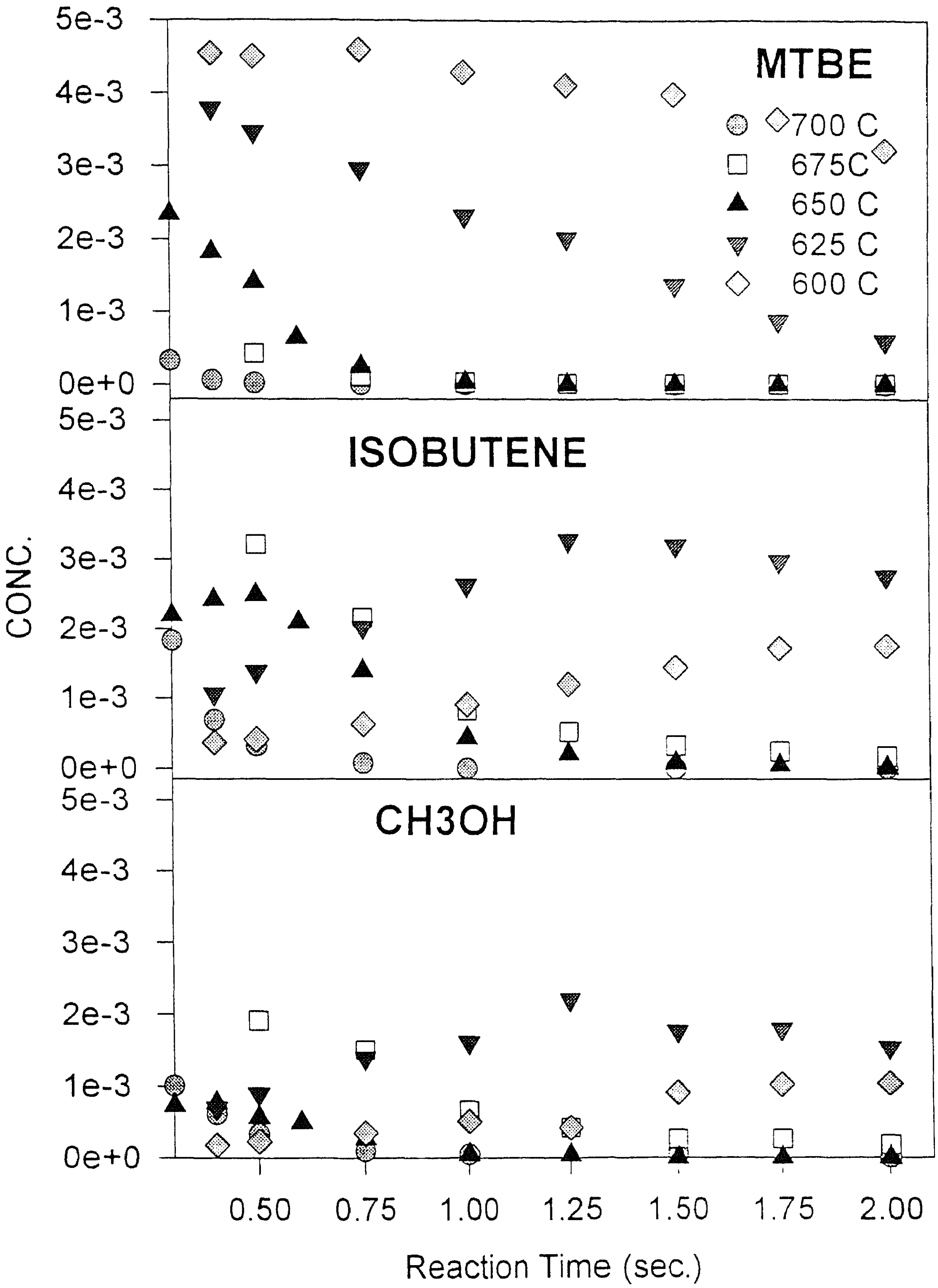

Figure 5B.38a Expertimental Results (Phi = 1.5, P = 1 atm)

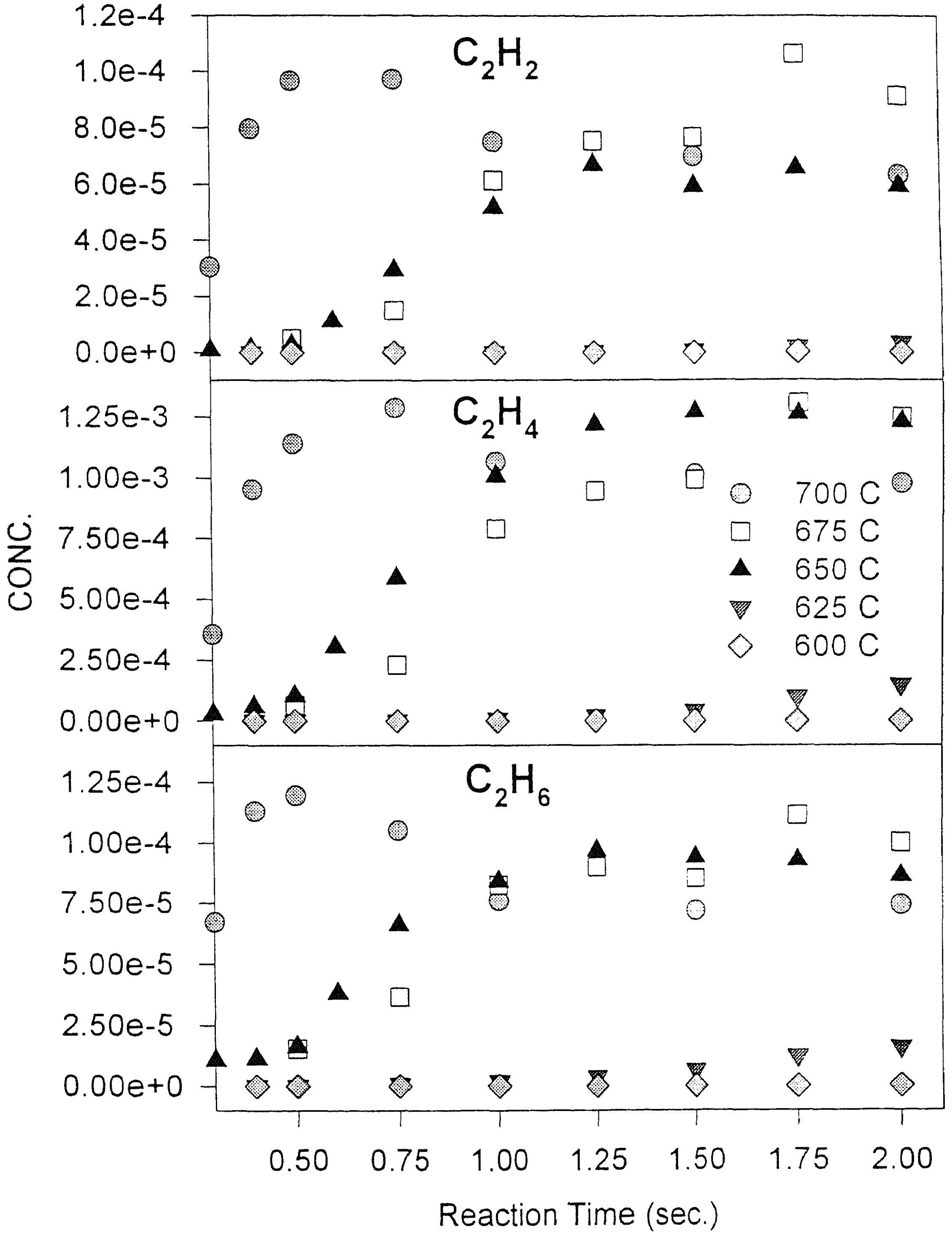

Figure 5B.38b Expertimental Results (Phi = 1.5, P = 1 atm)

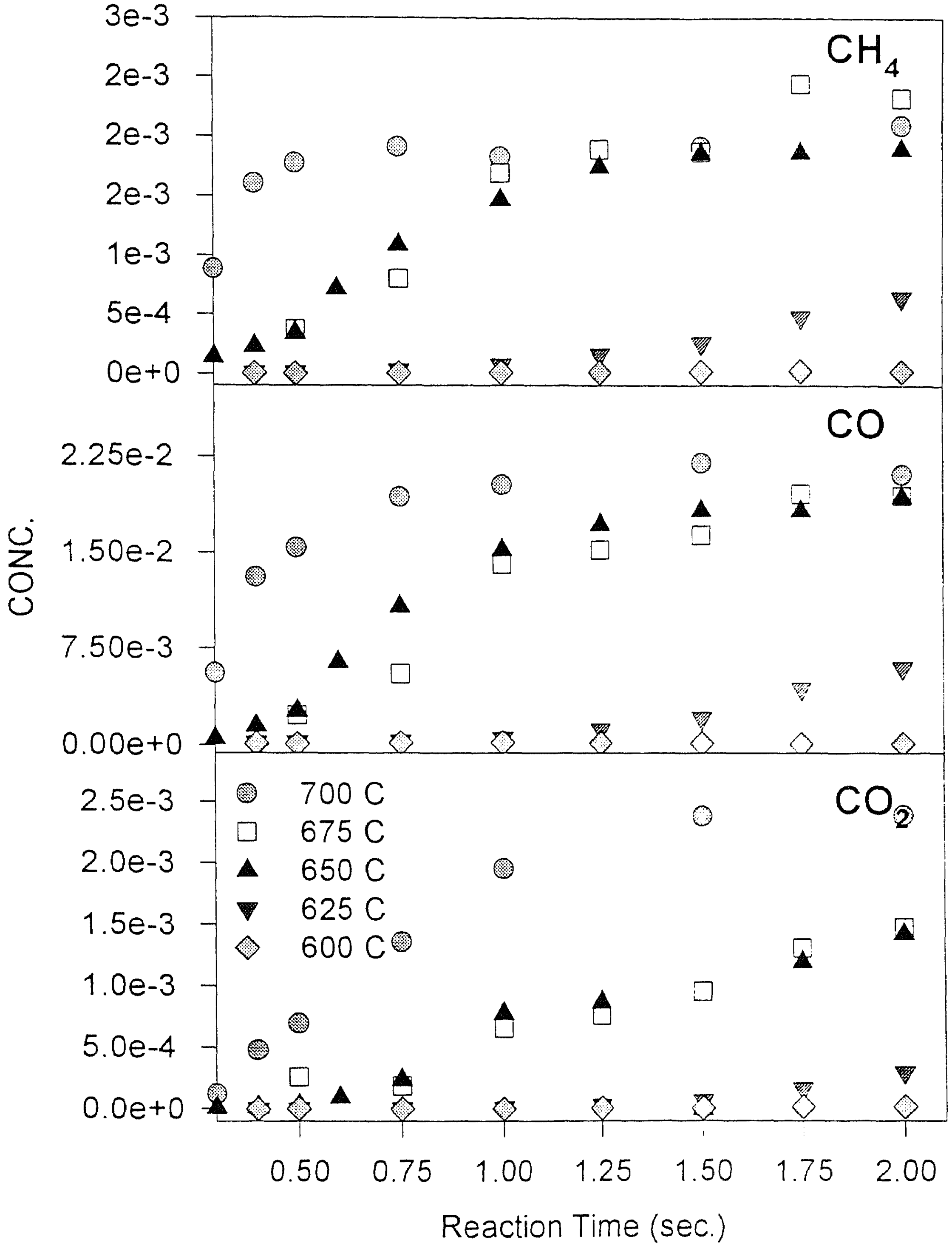

Figure 5B.38c Expertimental Results (Phi = 1.5, P = 1 atm)

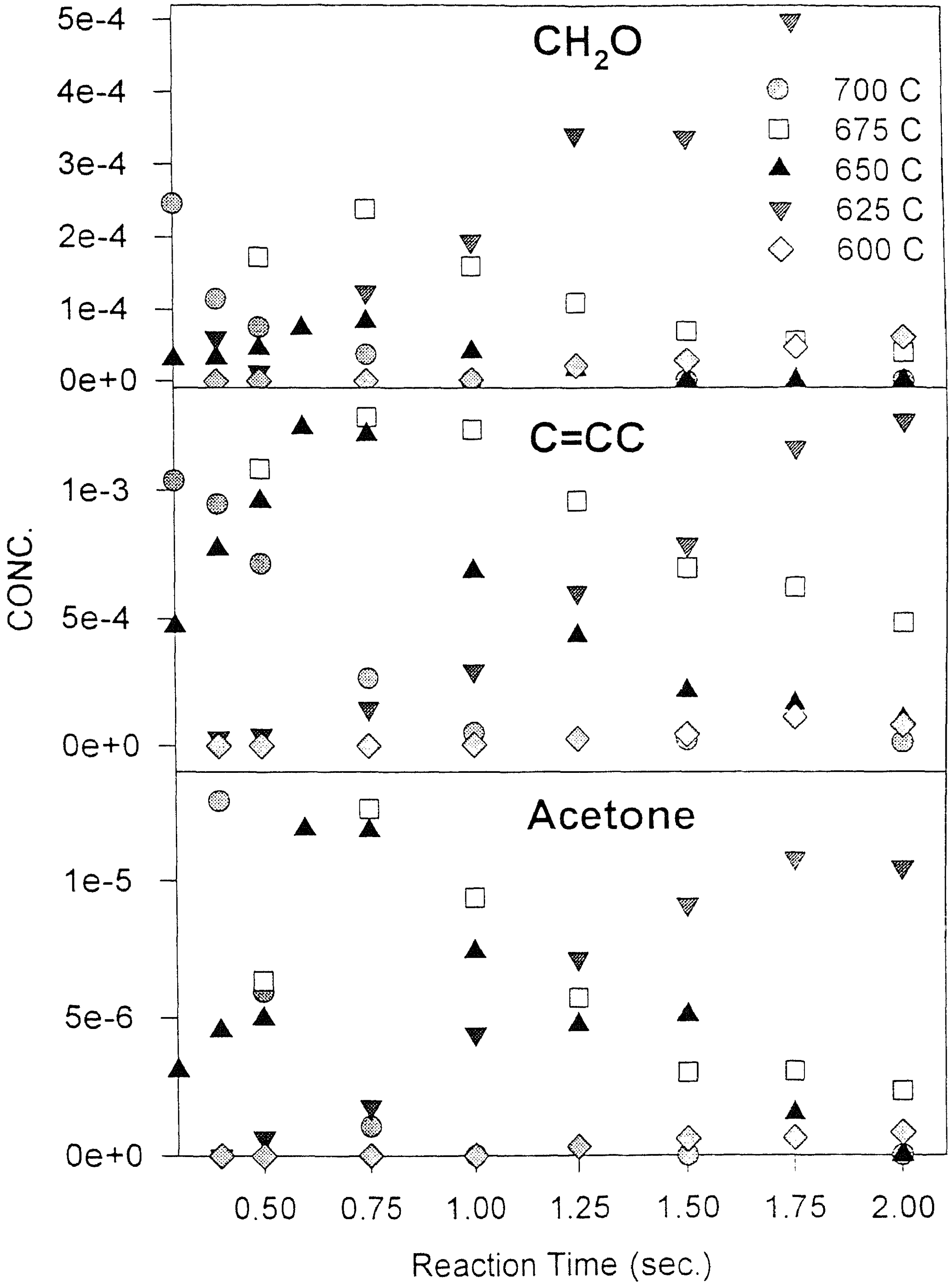

Figure 5B.38d Expertimental Results (Phi = 1.5, P = 1 atm)

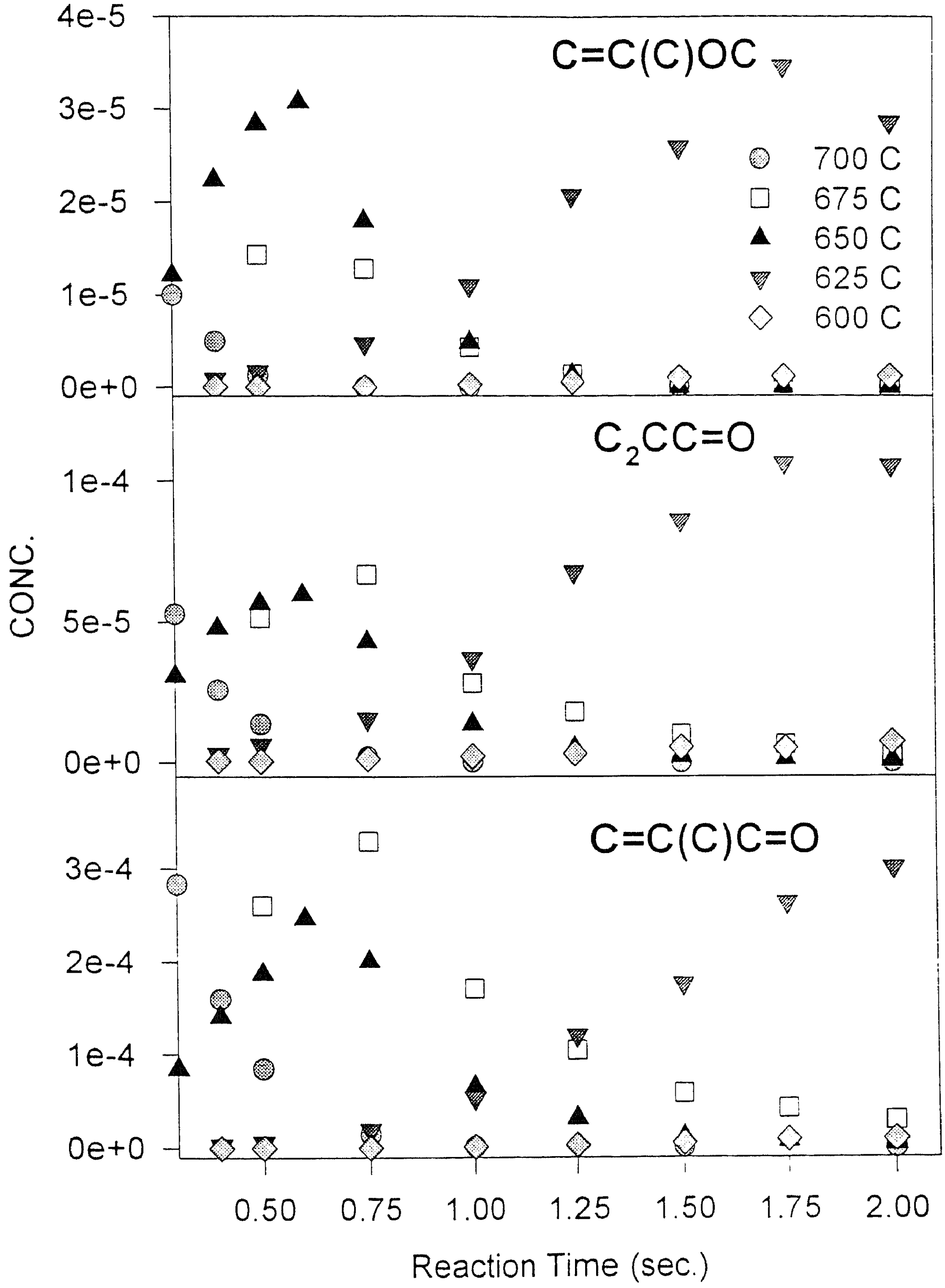

Figure 5B.38e Expertimental Results (Phi = 1.5, P = 1 atm)

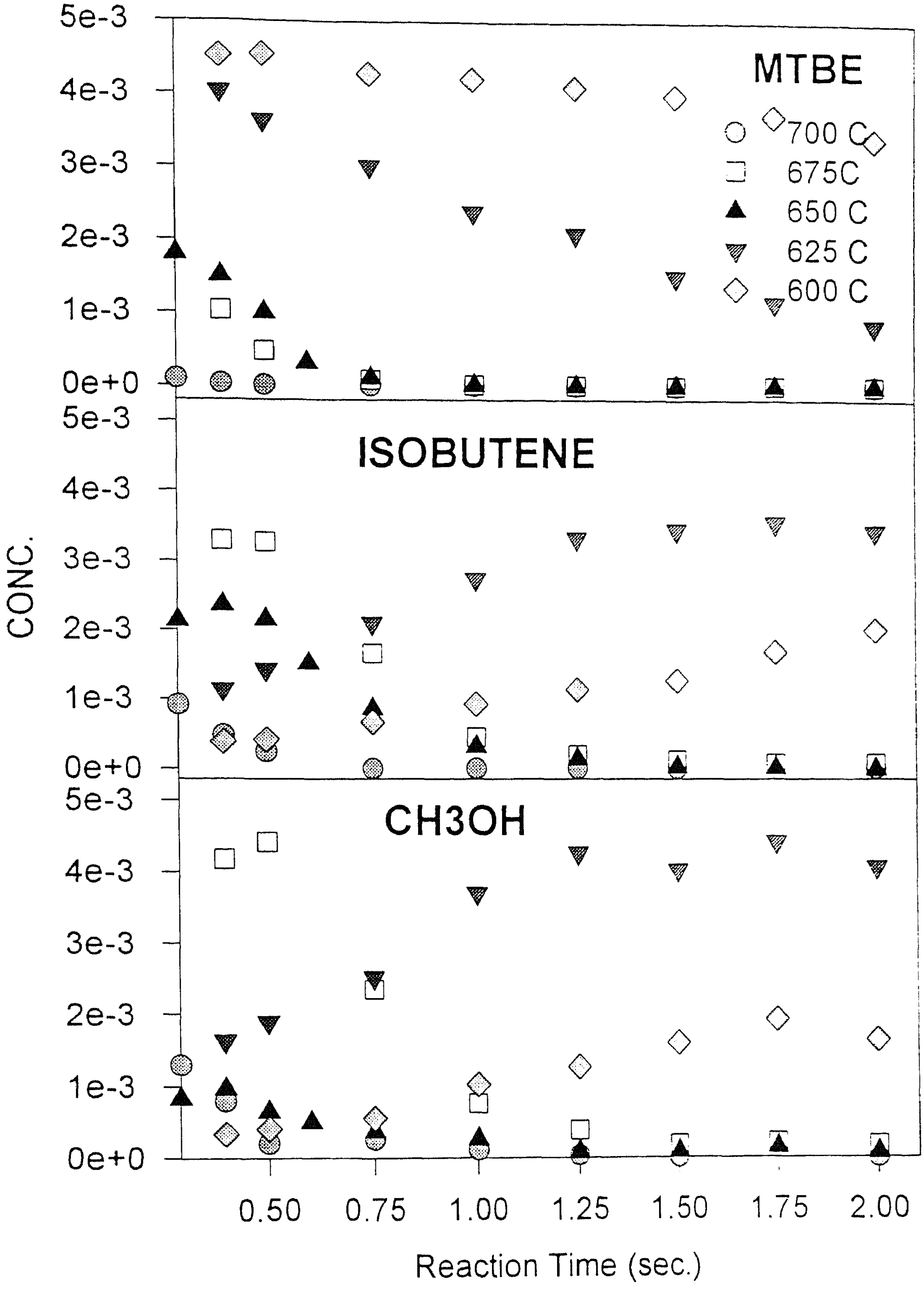

Figure 5B.39a Expertimental Results (Phi = 1.0, P = 1 atm)

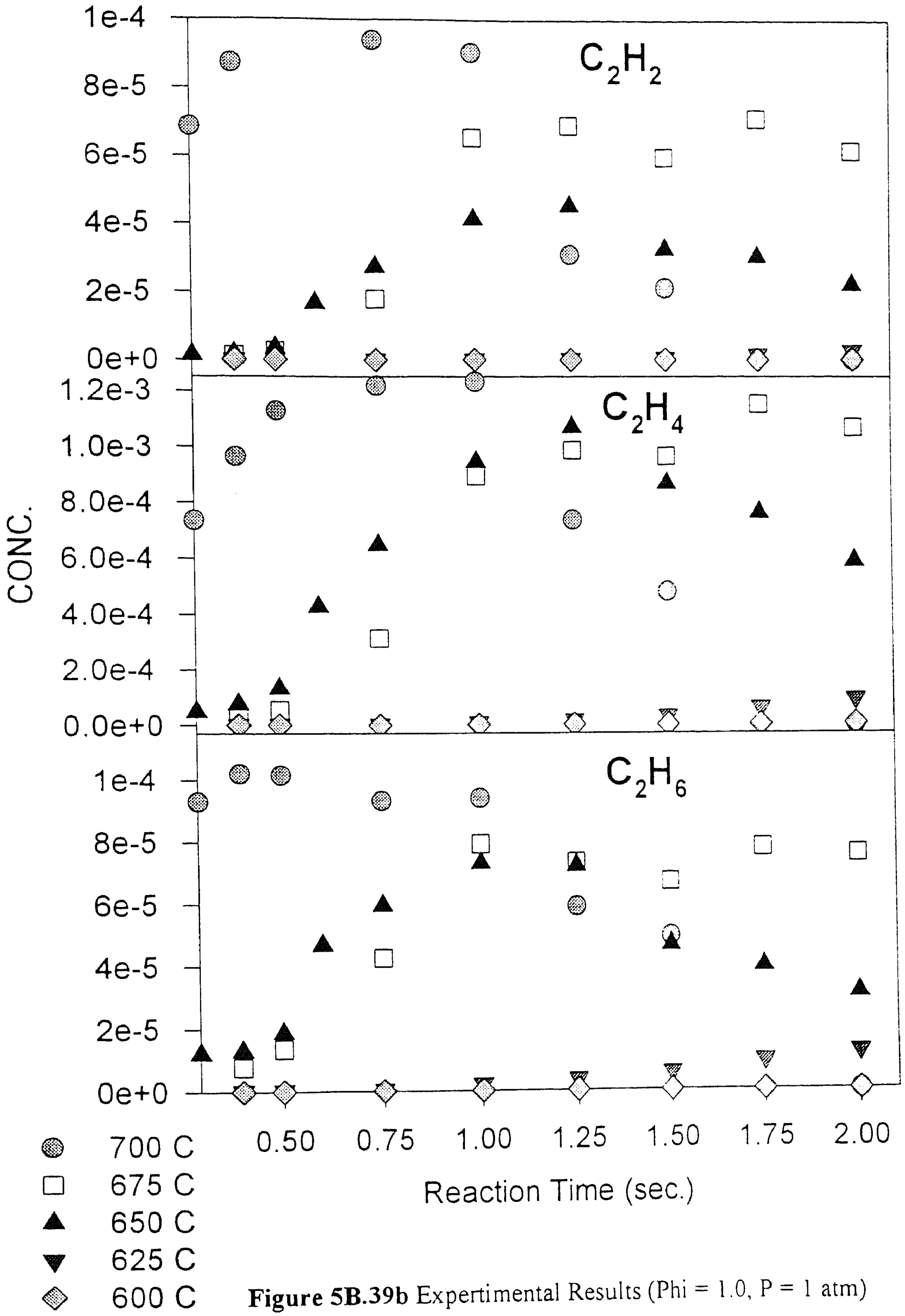

Figure 5B.39b Expertimental Results (Phi = 1.0, P = 1 atm)

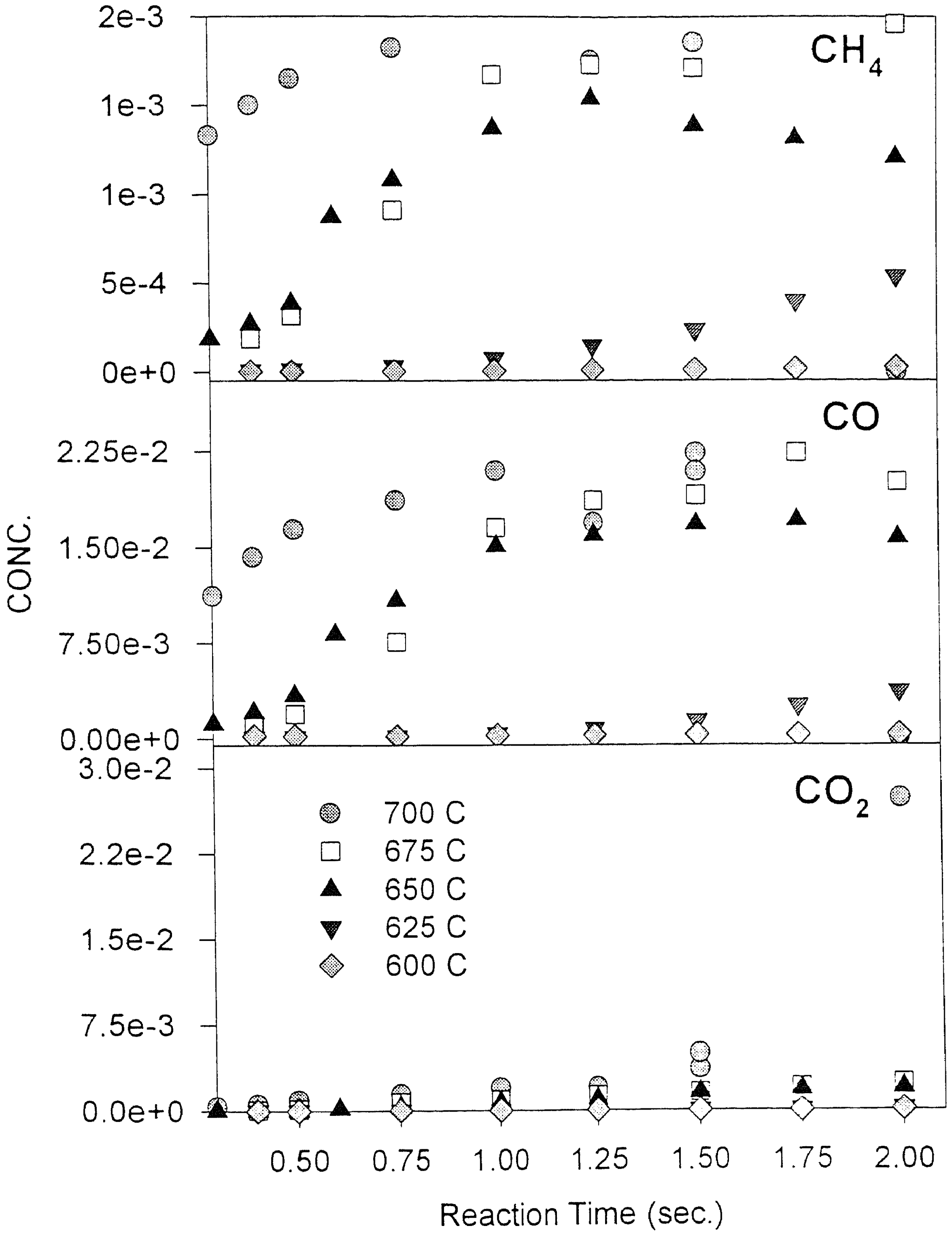

Figure 5B.39c Expertimental Results (Phi = 1.0, P = 1 atm)

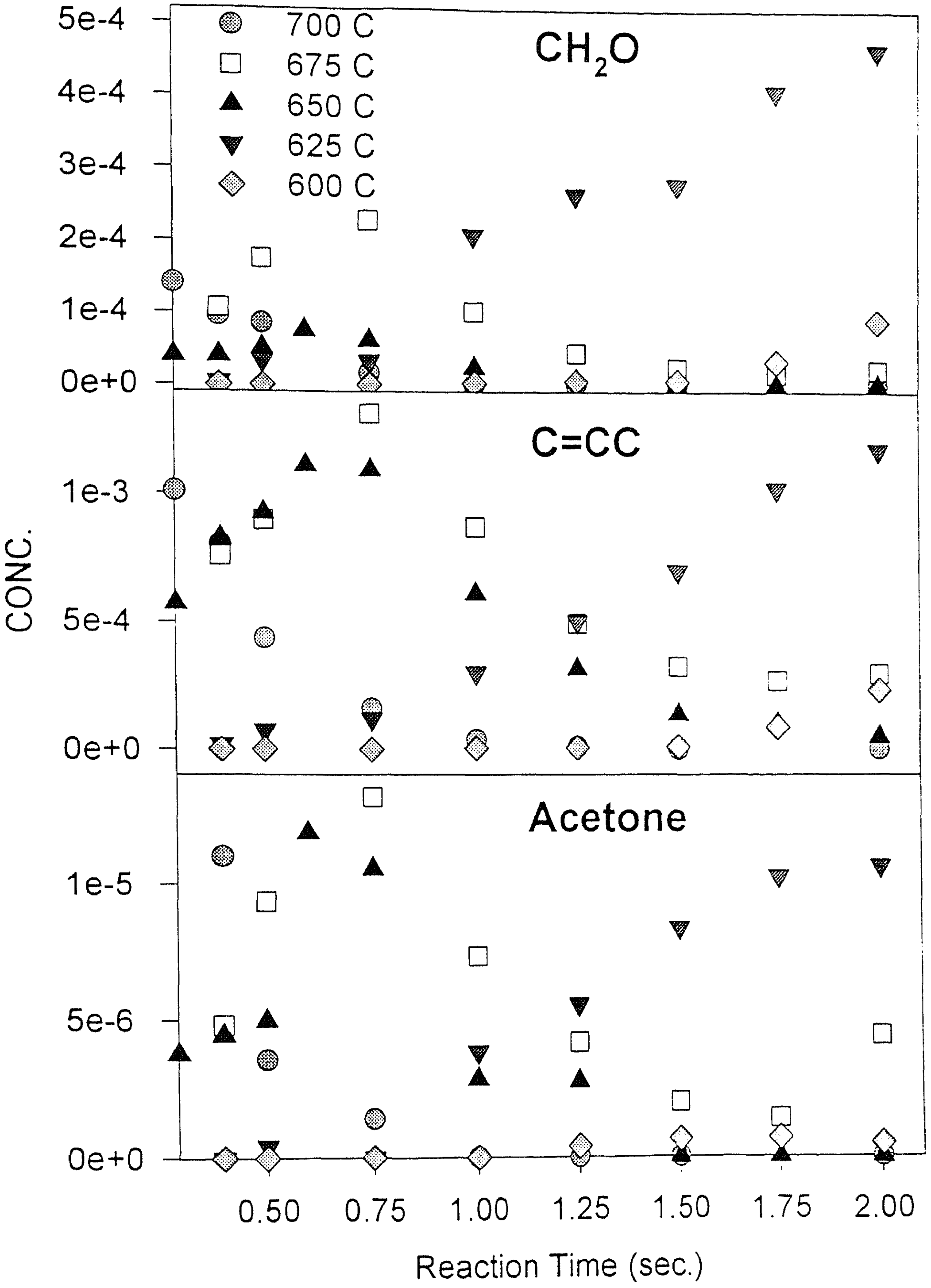

Figure 5B.39d Expertimental Results (Phi = 1.0, P = 1 atm)

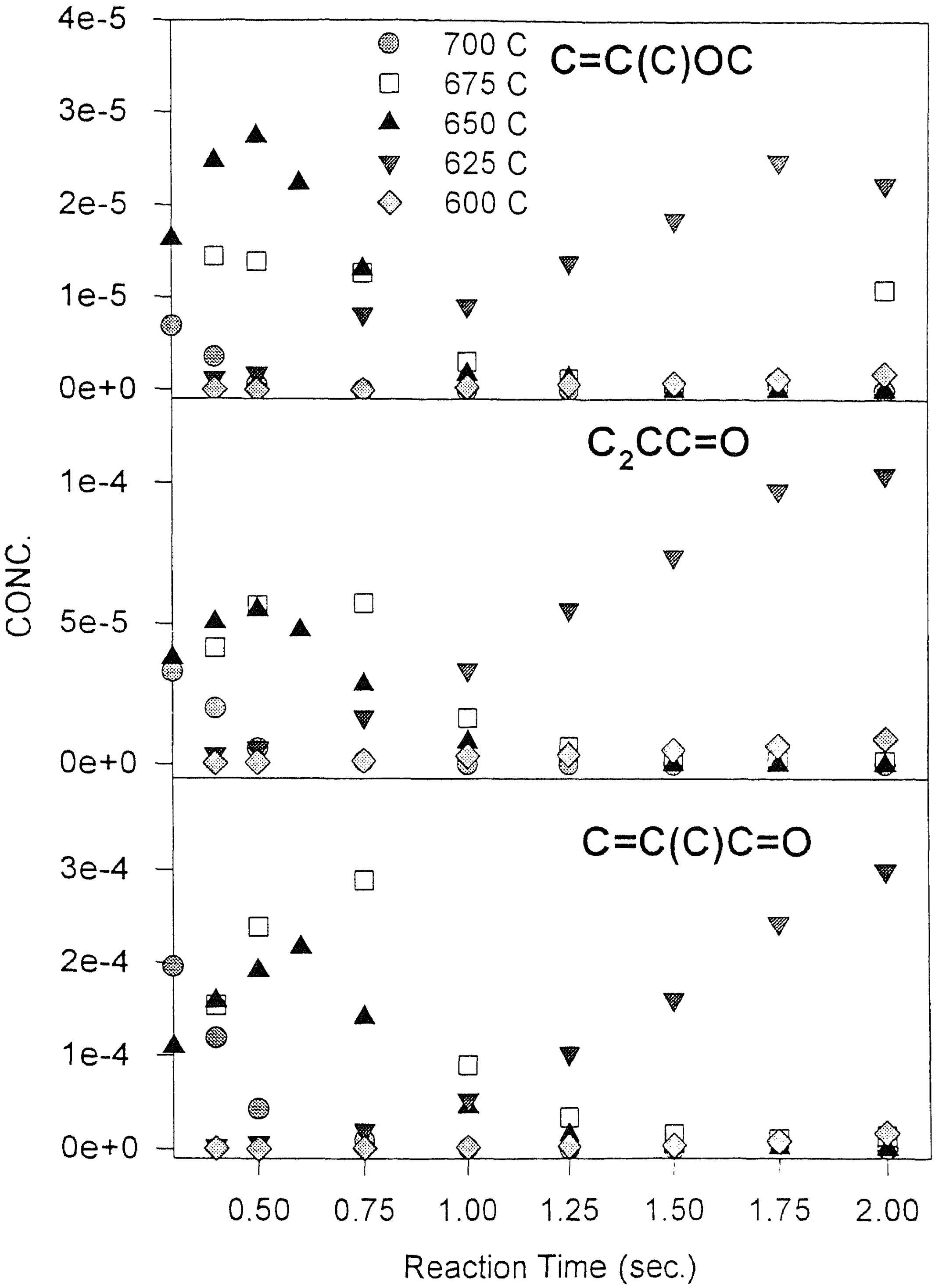

Figure 5B.39e Expertimental Results (Phi = 1.0, P = 1 atm)

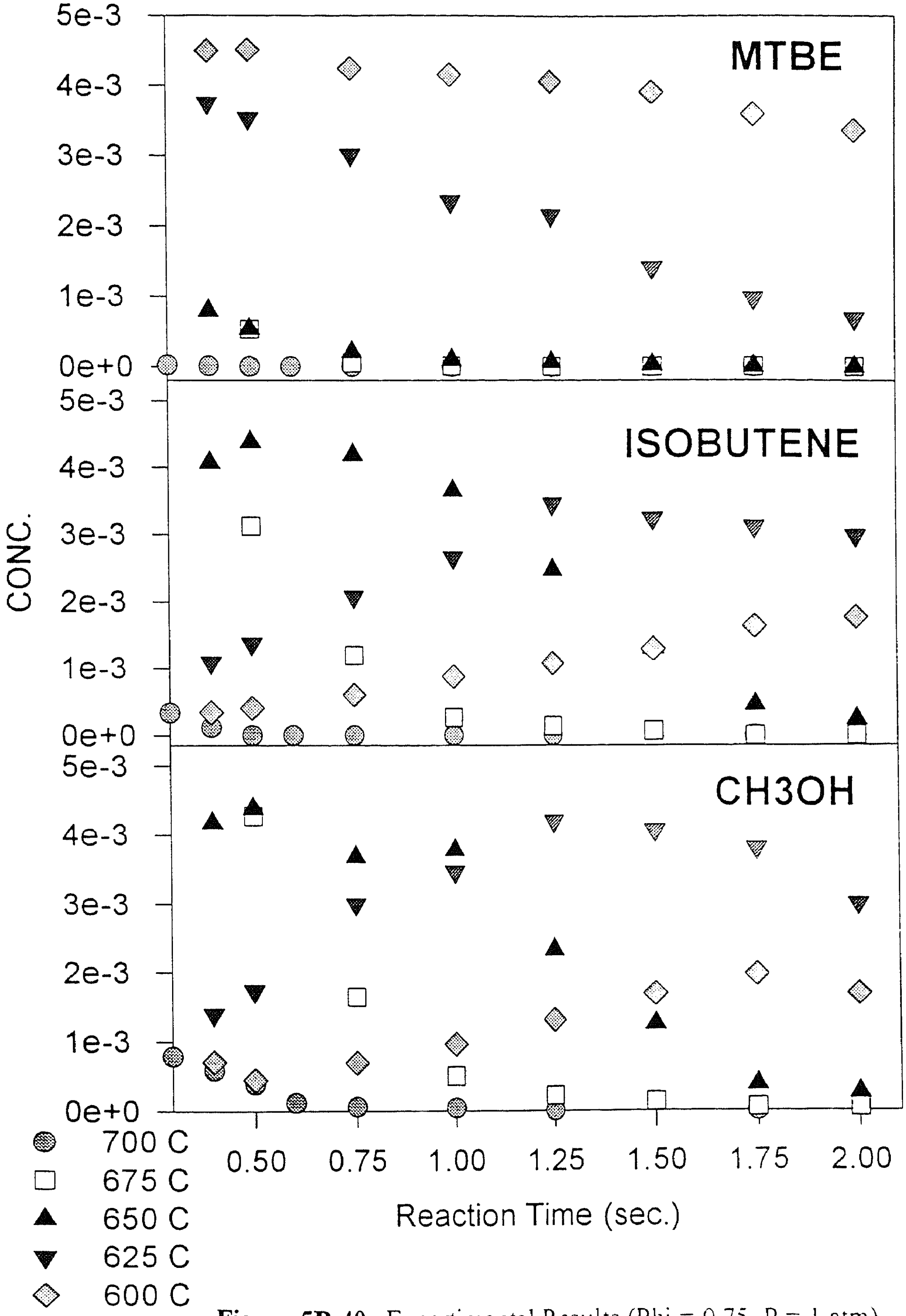

Figure 5B.40a Expertimental Results (Phi = 0.75, P = 1 atm)

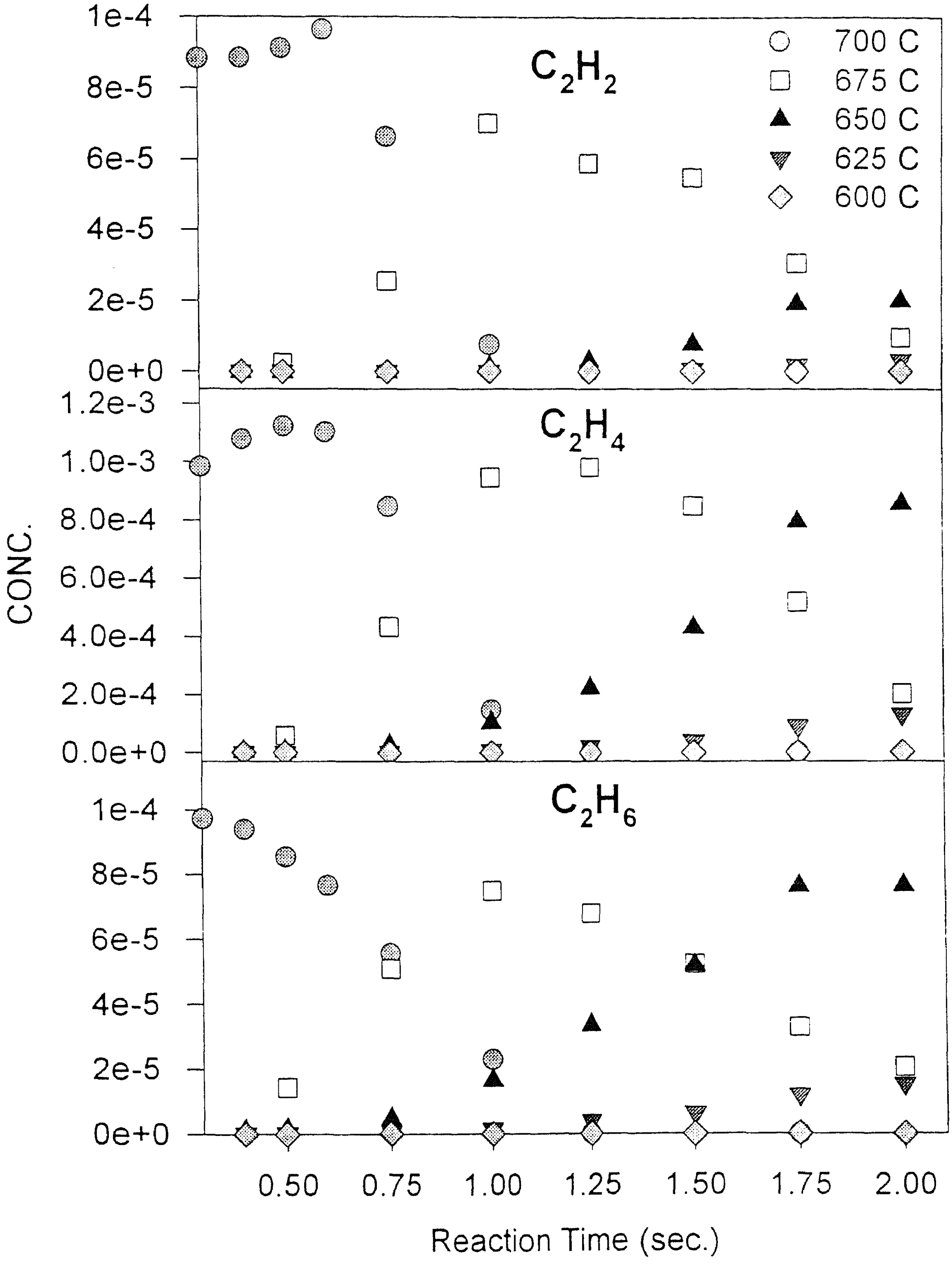

Figure 5B.40b Expertimental Results (Phi = 0.75, P = 1 atm)

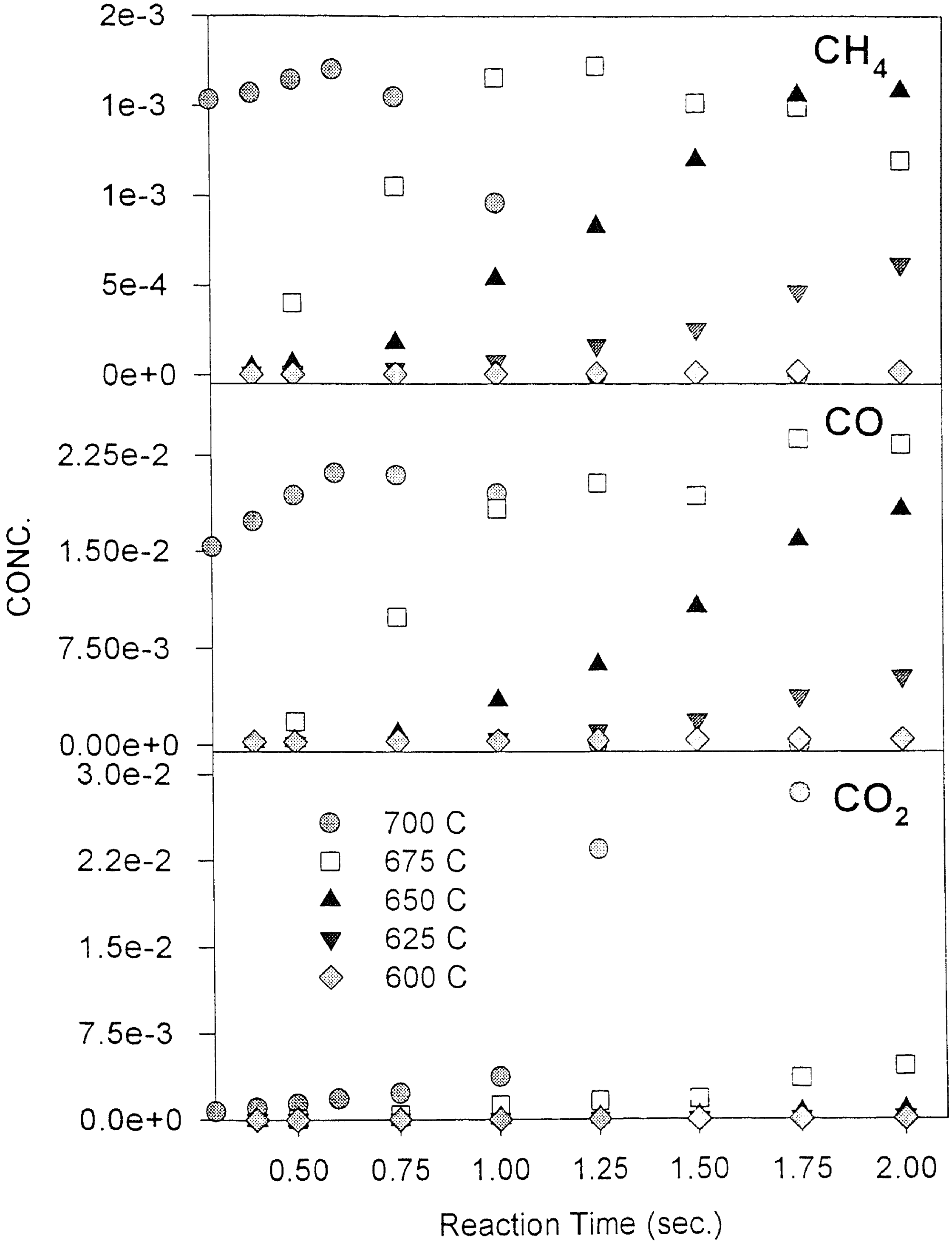

Figure 5B.40c Expertimental Results (Phi = 0.75, P = 1 atm)

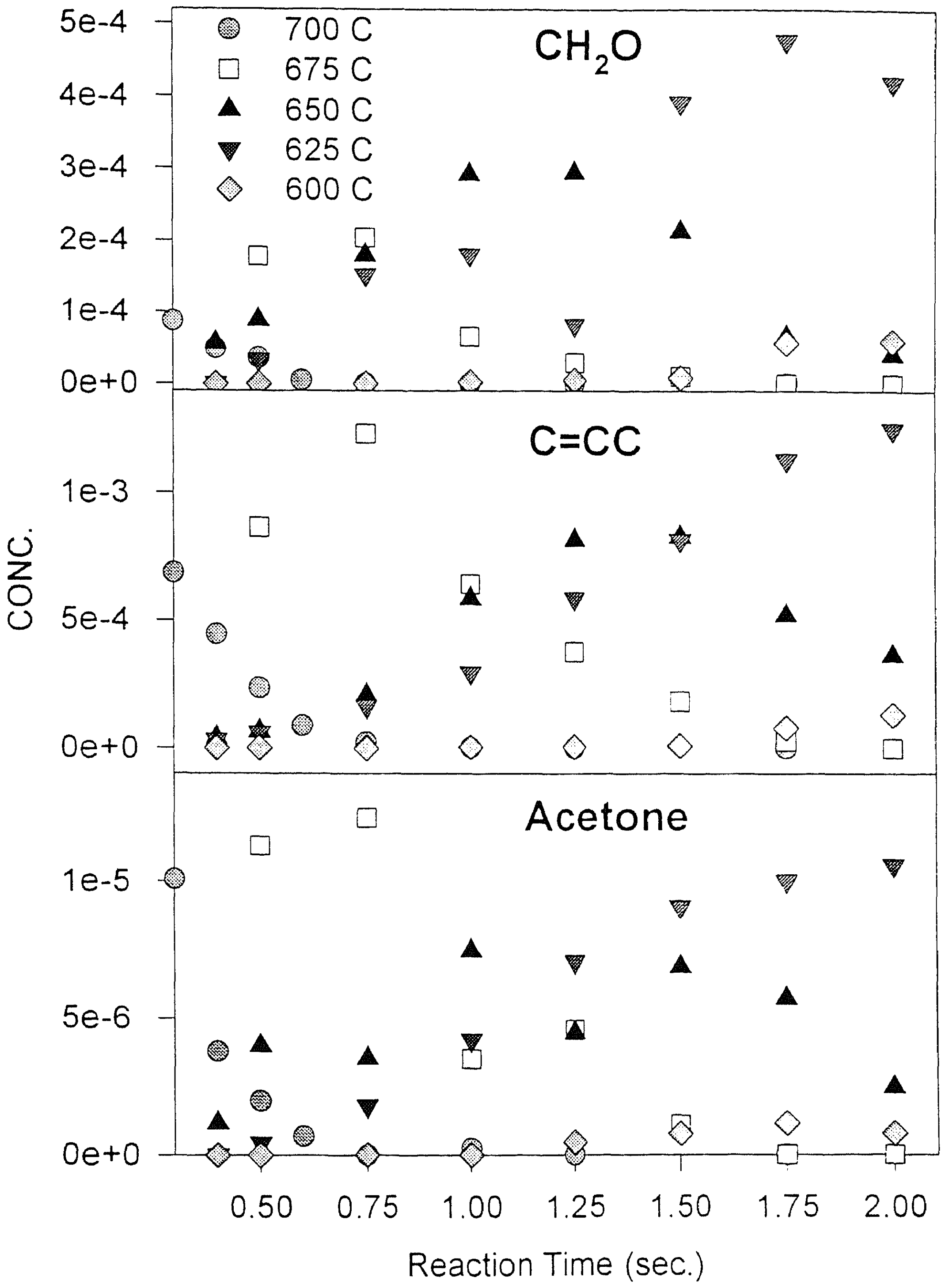

Figure 5B.40d Expertimental Results (Phi = 0.75, P = 1 atm)

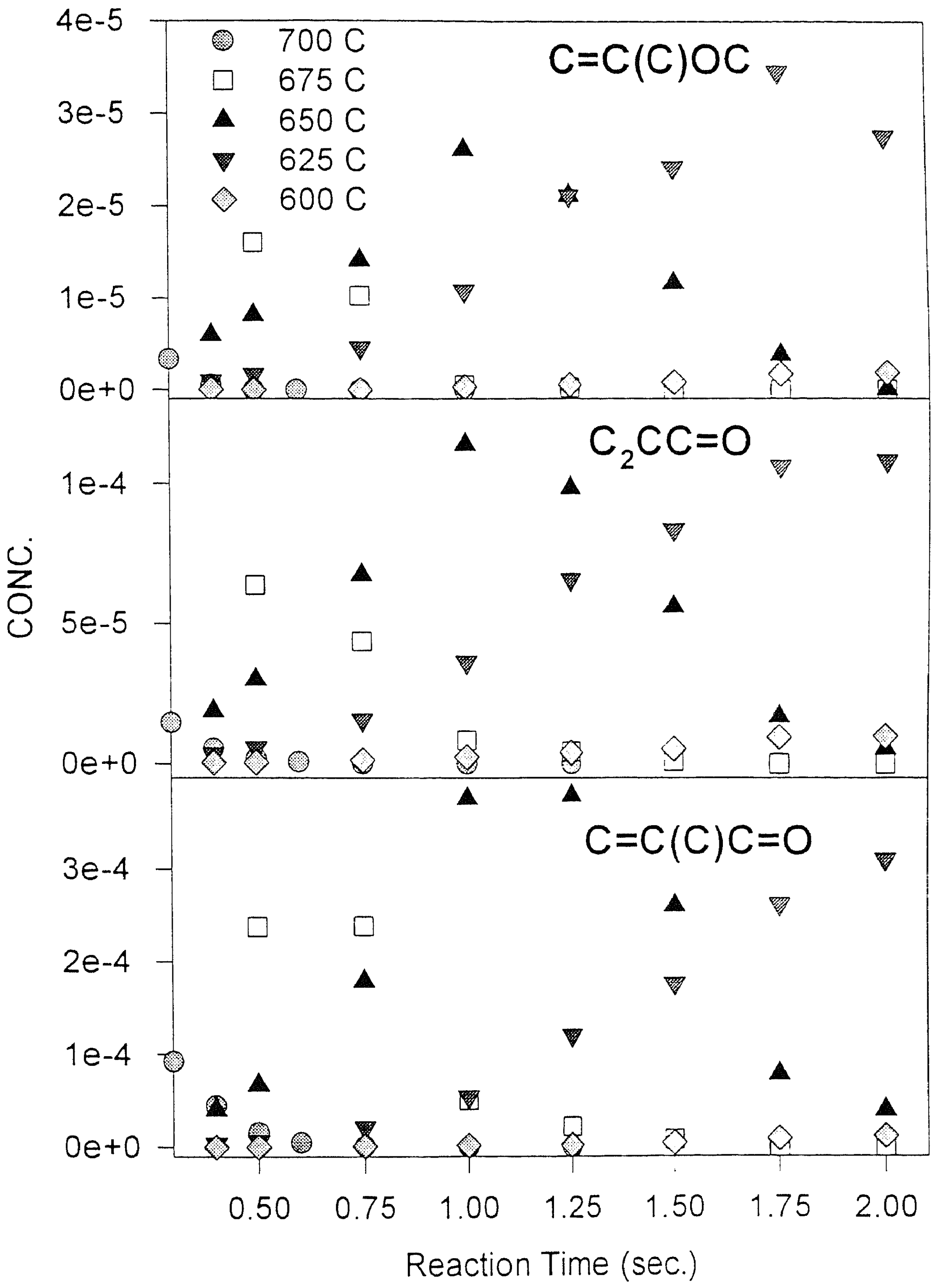

Figure 5B.40e Expertimental Results (Phi = 0.75, P = 1 atm)

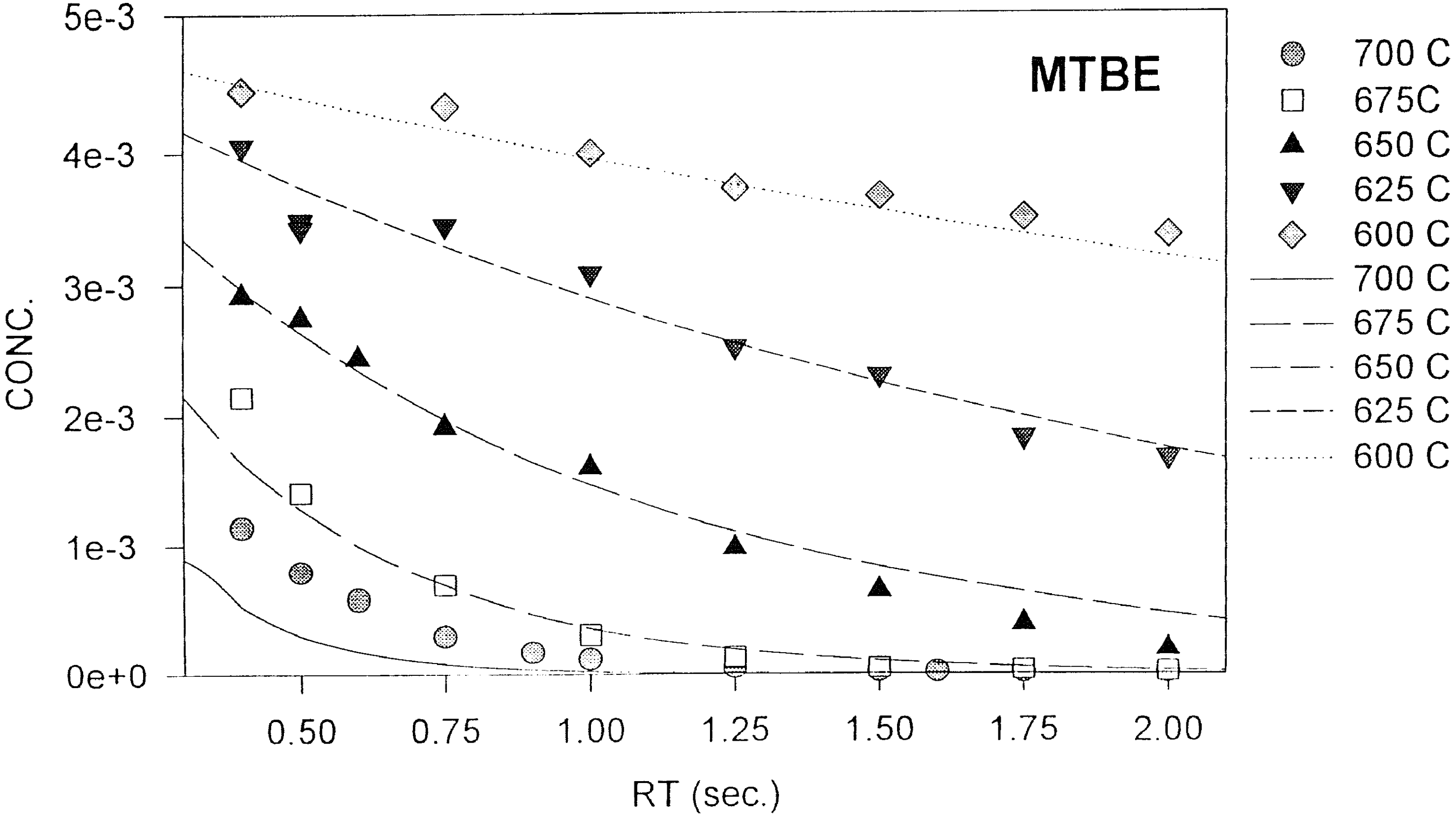

Figure 5B.41a Experimental results comparison with model (pyrolysis, P = 1 atm)

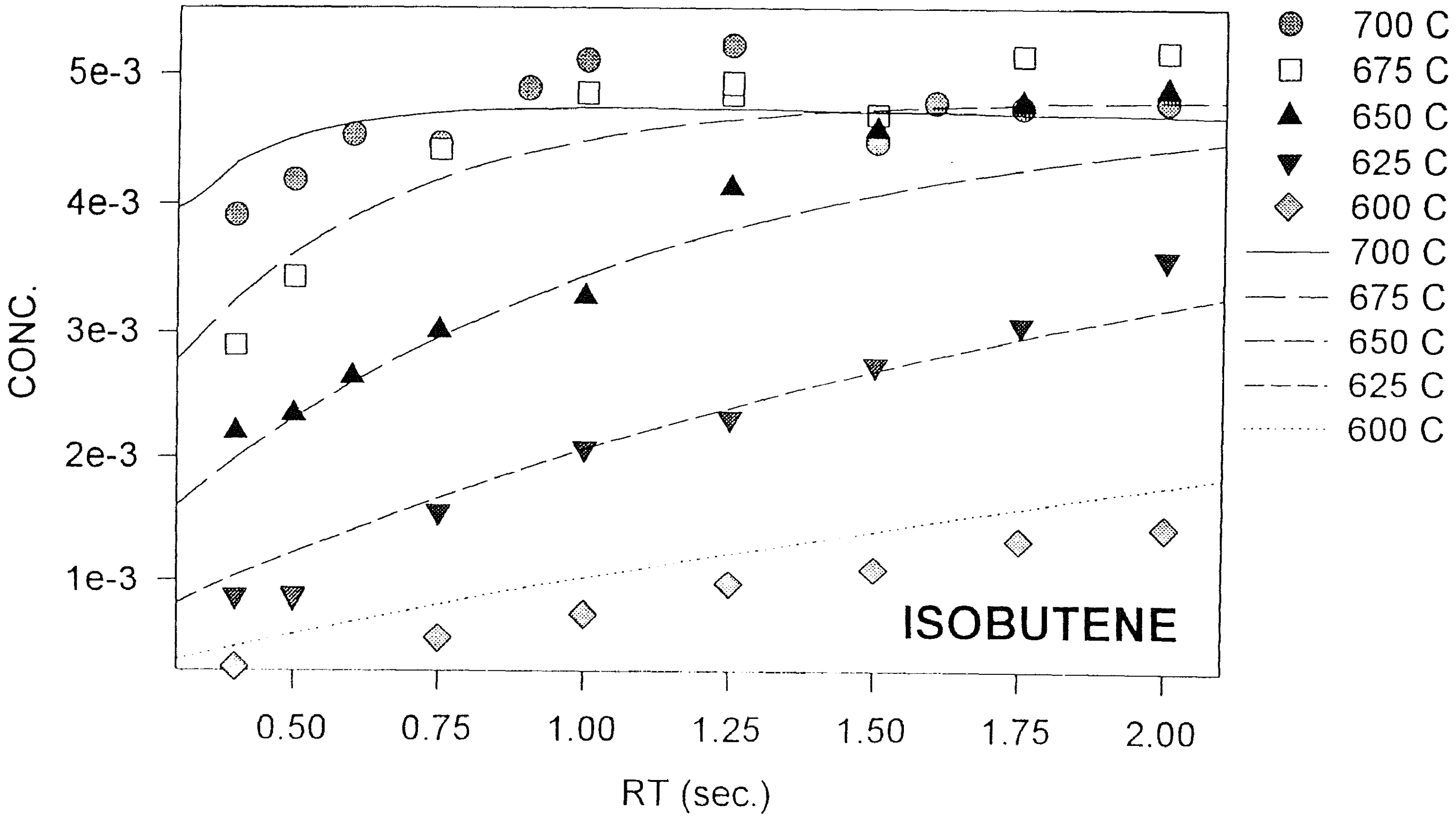

Figure 5B.41b Experimental results comparison with model (pyrolysis, P = 1 atm)

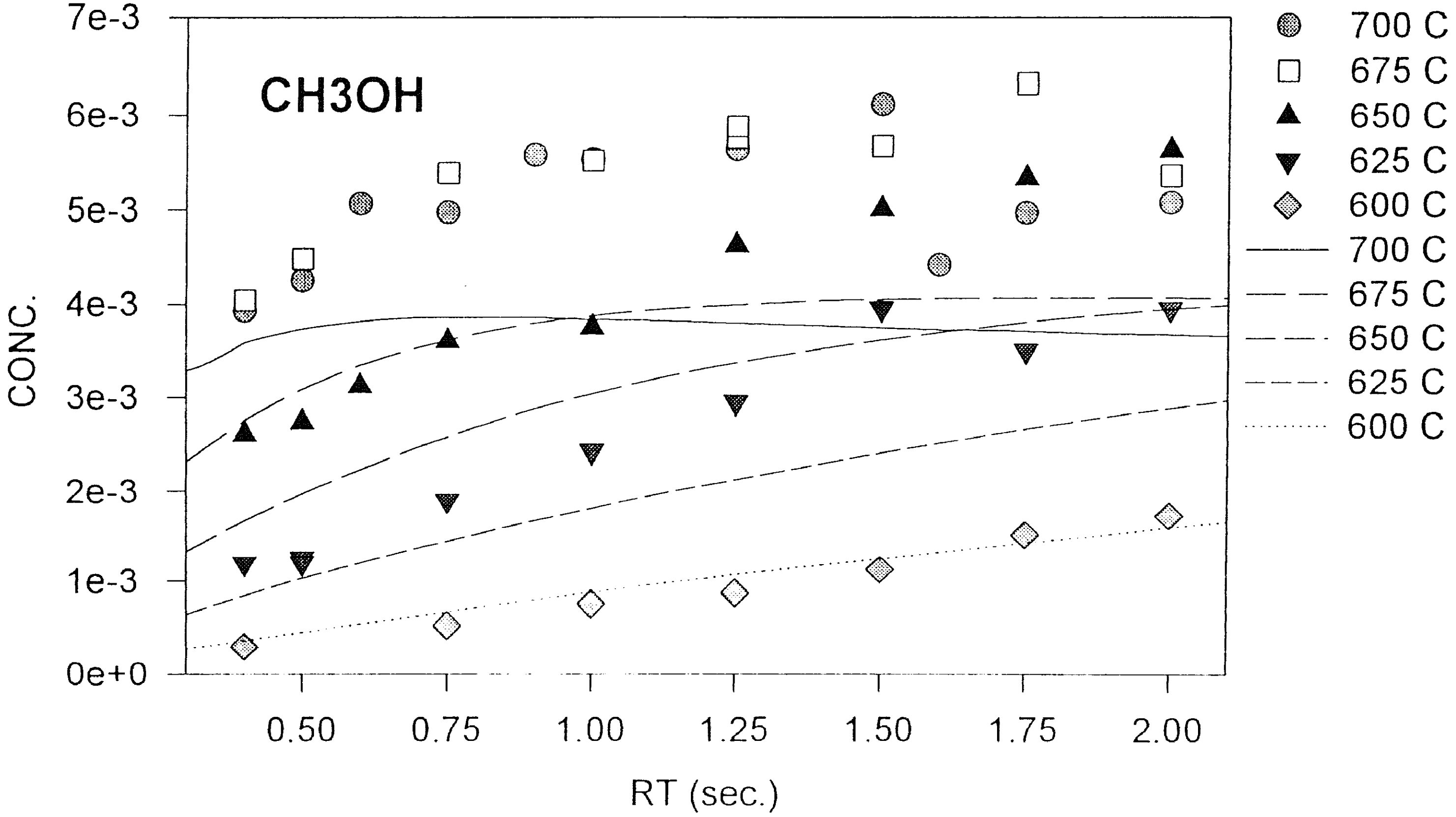

Figure 5B.41c Experimental results comparison with model (pyrolysis, P = 1 atm)

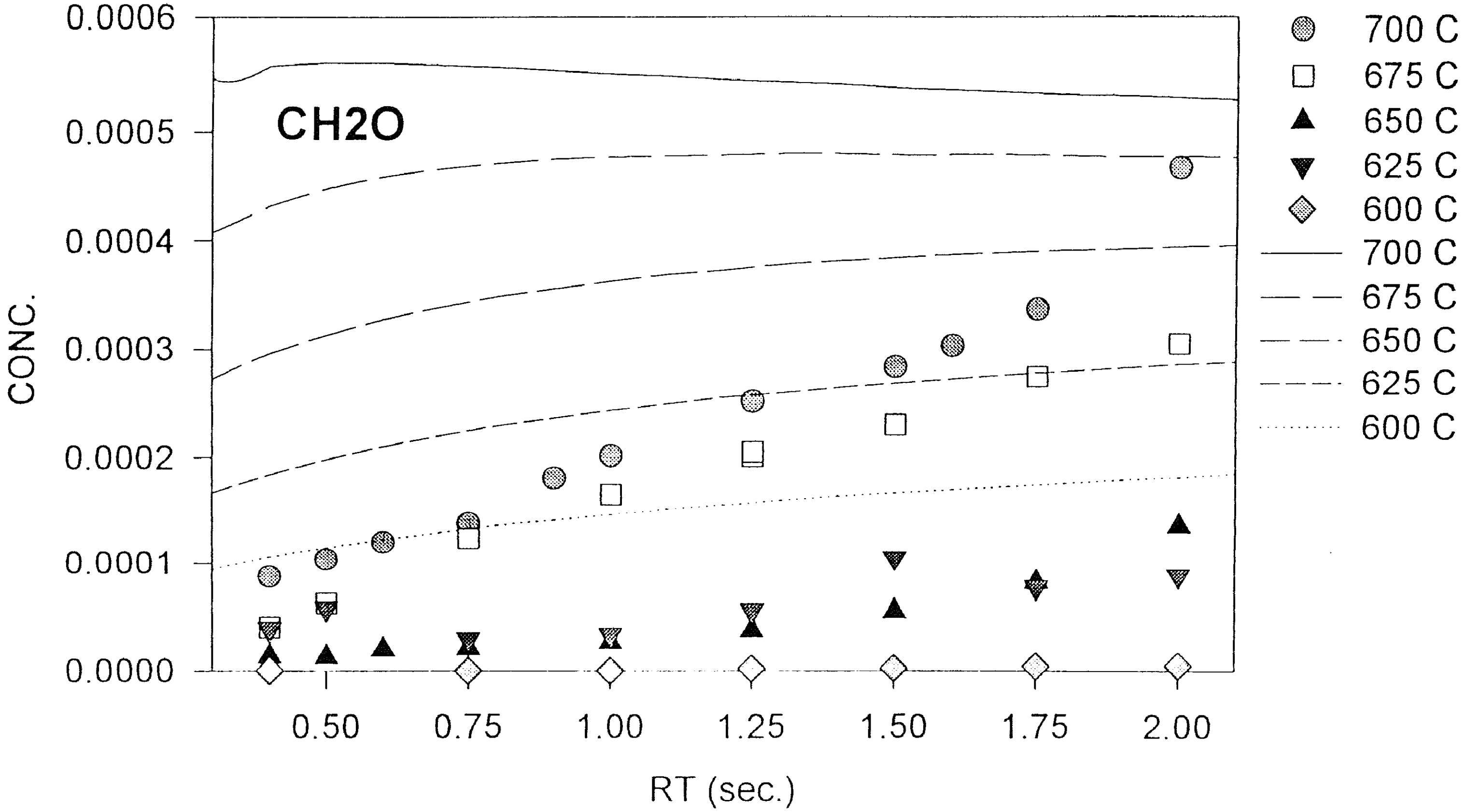

Figure 5B.41d Experimental results comparison with model (pyrolysis, P = 1 atm)

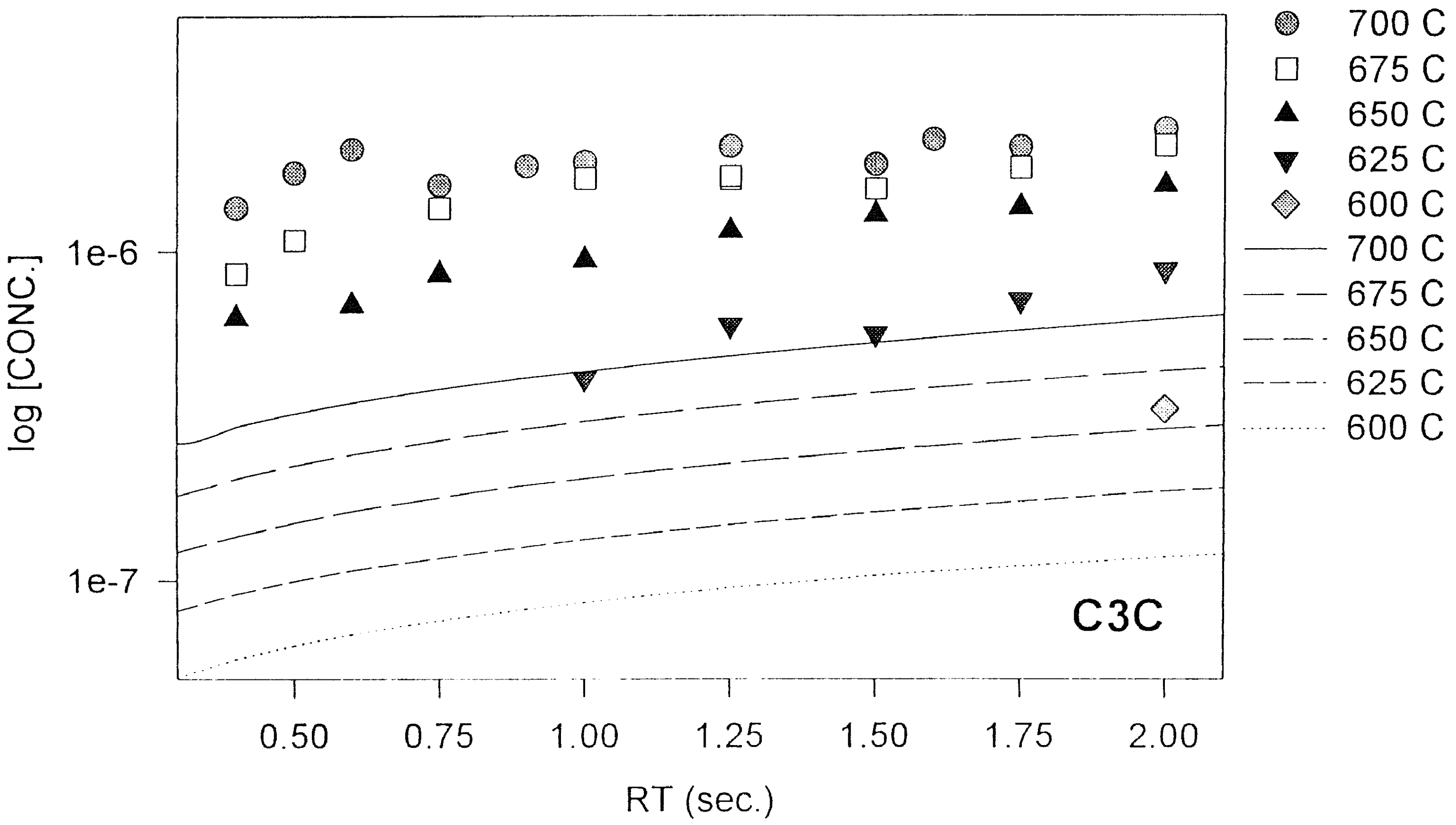

Figure 5B.41e Experimental results comparison with model (pyrolysis, P = 1 atm)

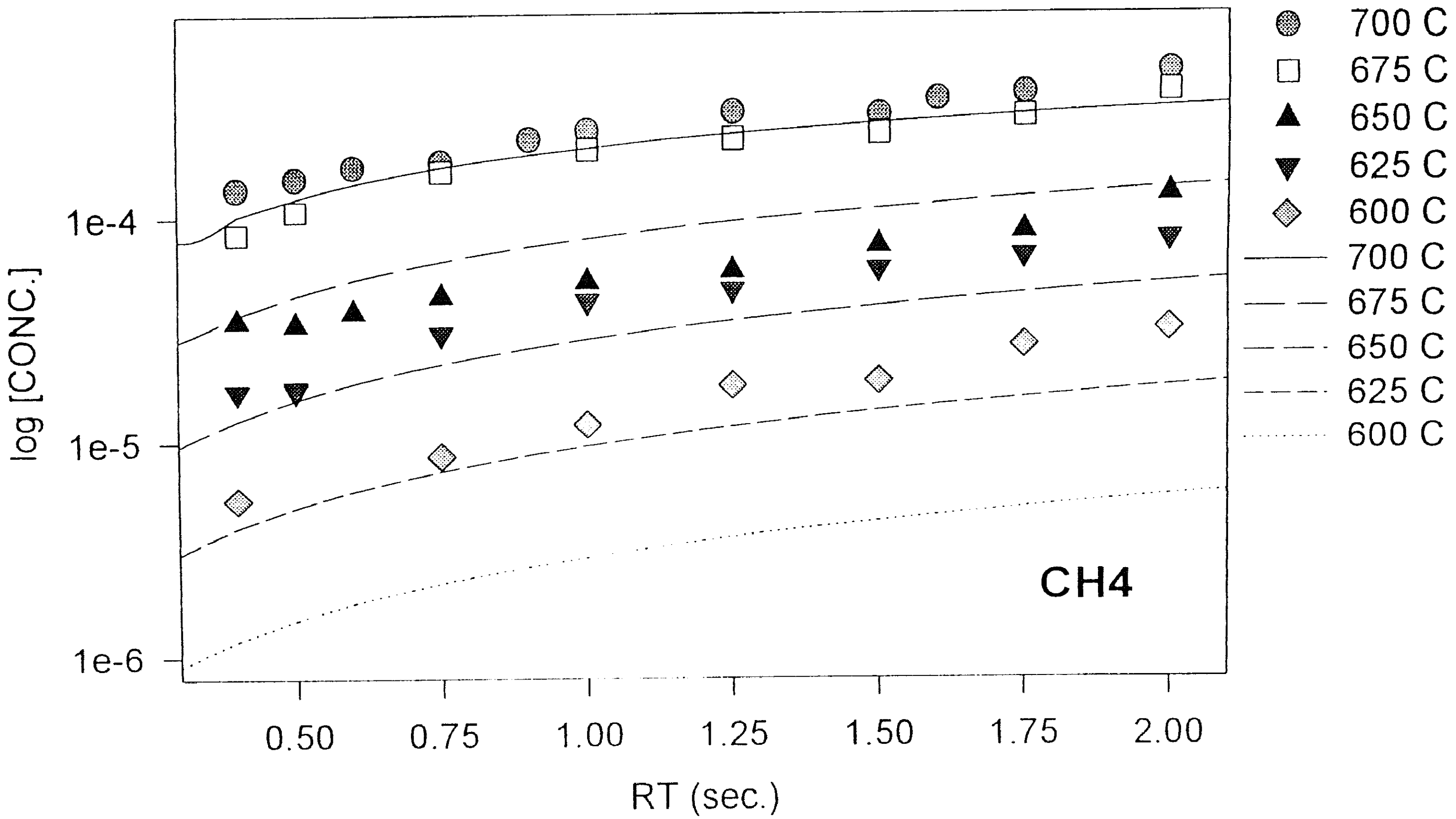

Figure 5B.41f Experimental results comparison with model (pyrolysis, P = 1 atm)

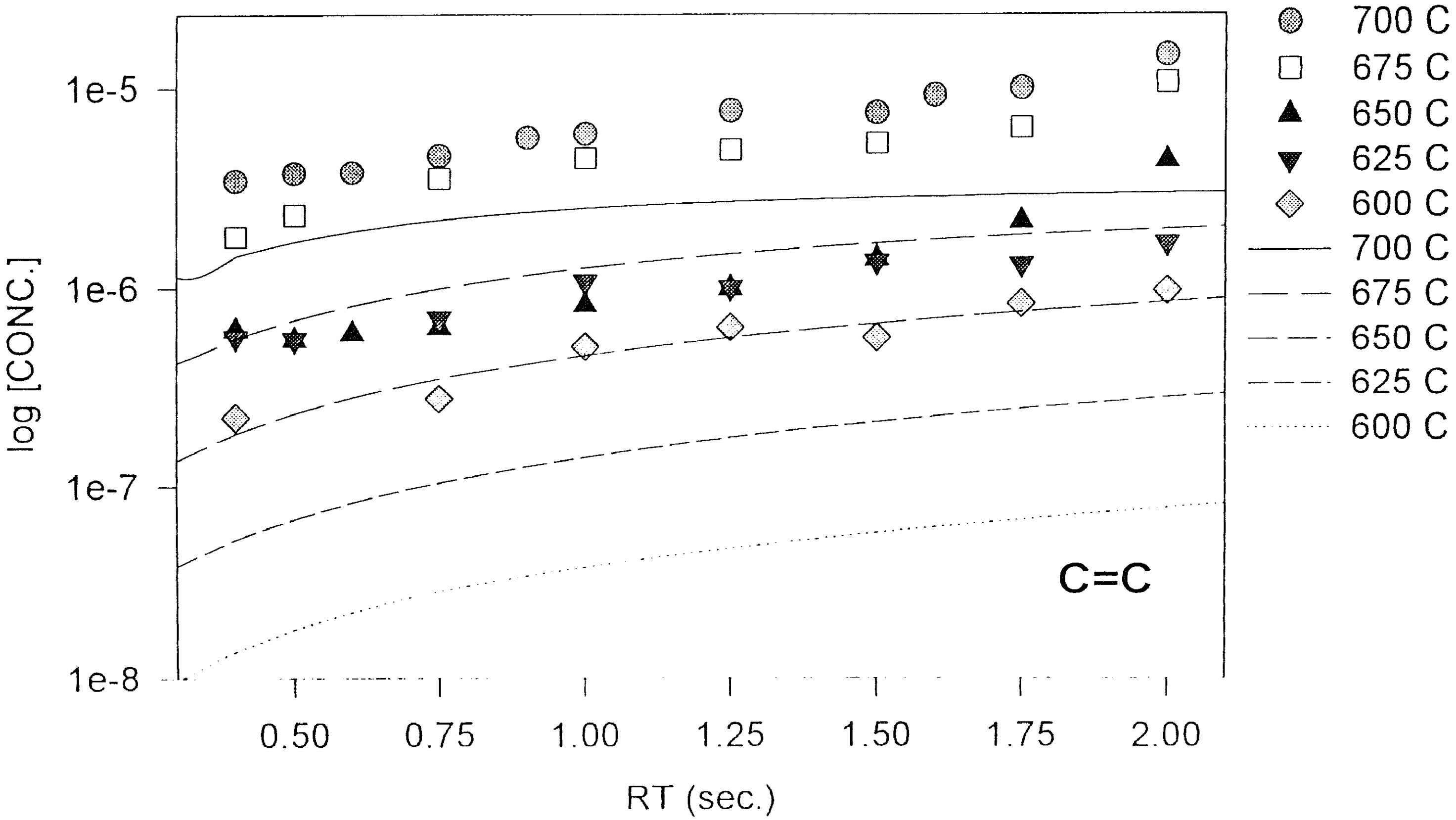

Figure 5B.41g Experimental results comparison with model (pyrolysis, P = 1 atm)

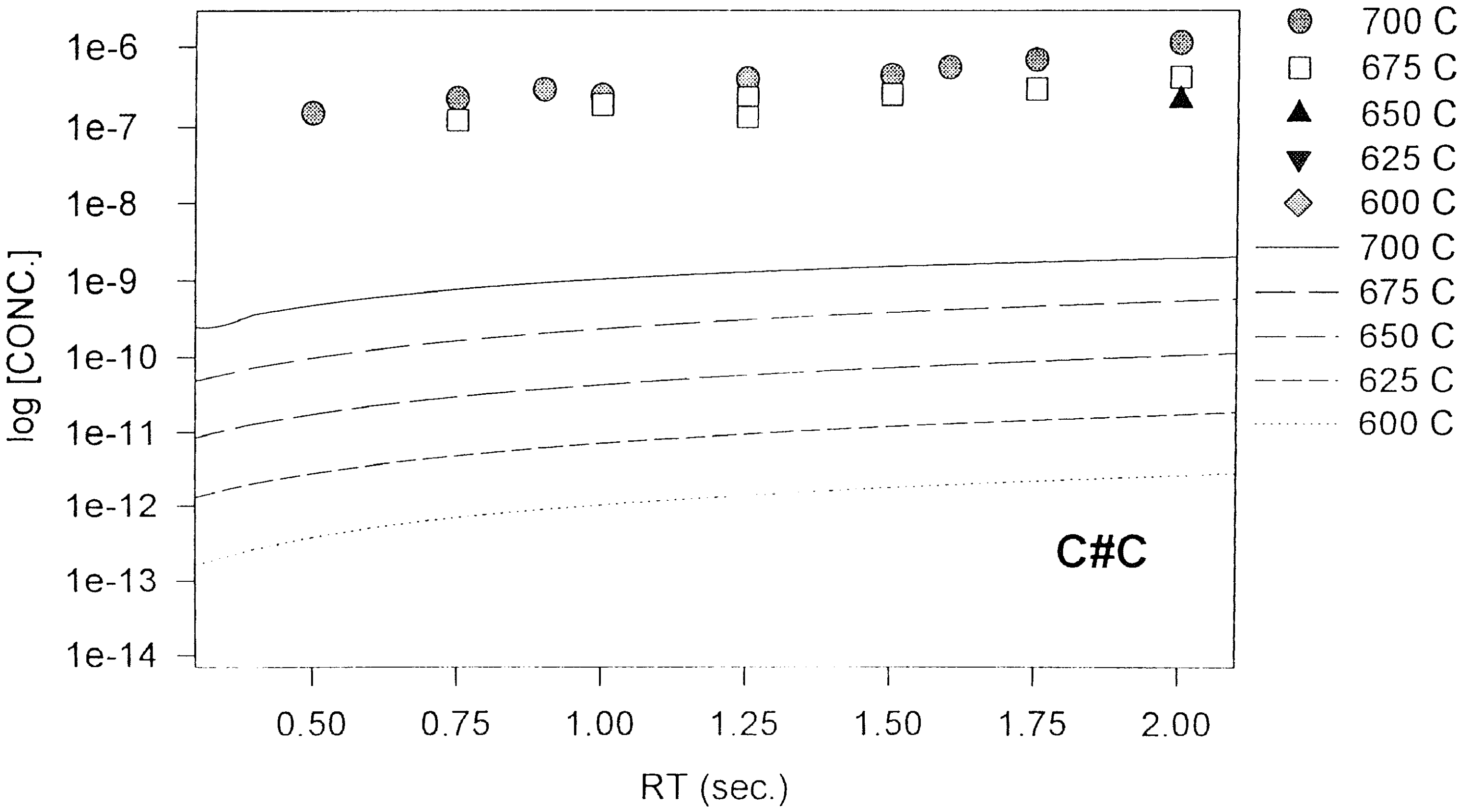

Figure 5B.41h Experimental results comparison with model (pyrolysis, P = 1 atm)

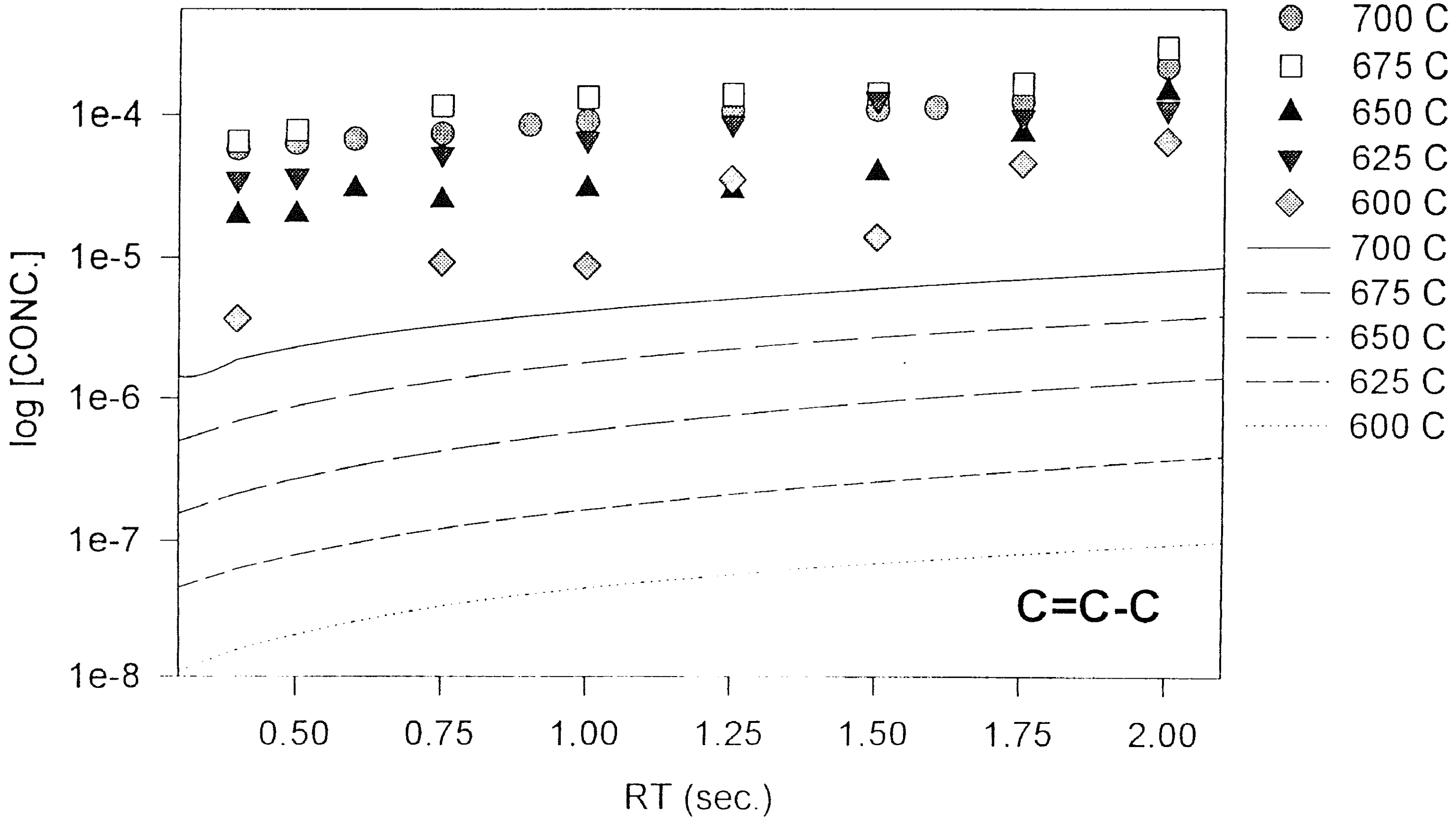

Figure 5B.41i Experimental results comparison with model (pyrolysis, P = 1 atm)

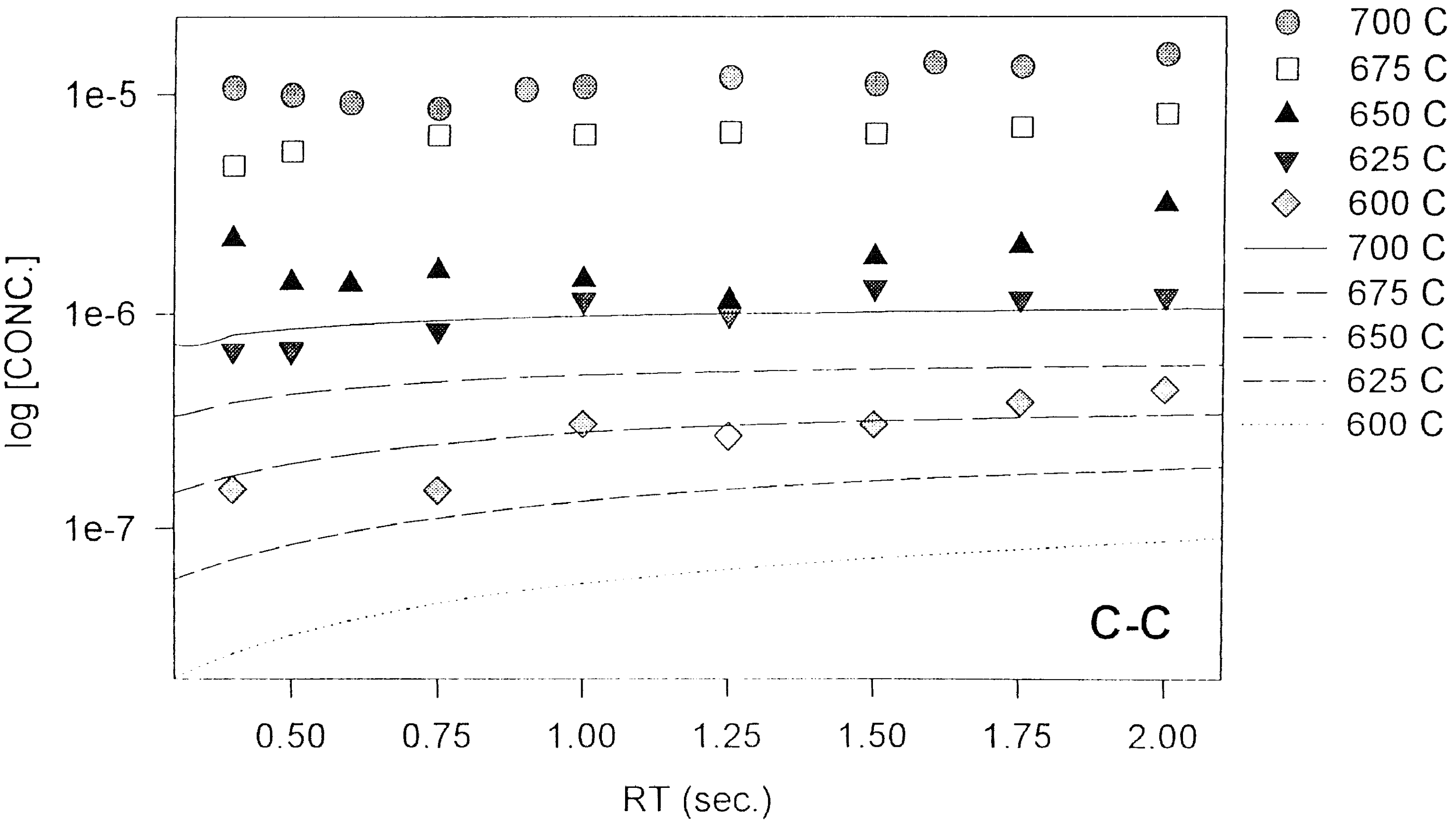

Figure 5B.41j Experimental results comparison with model (pyrolysis, P = 1 atm)

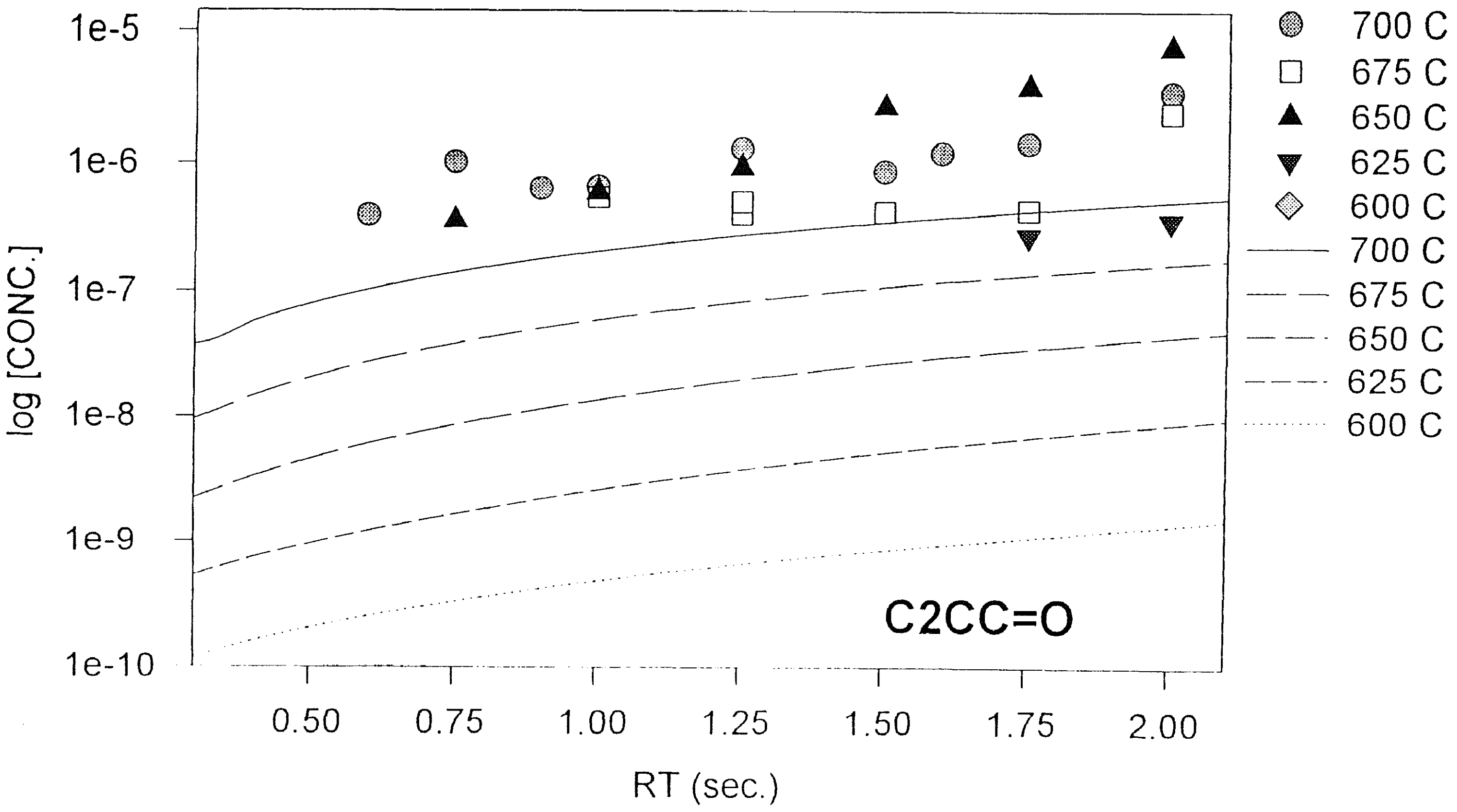

Figure 5B.41k Experimental results comparison with model (pyrolysis, P = 1 atm)

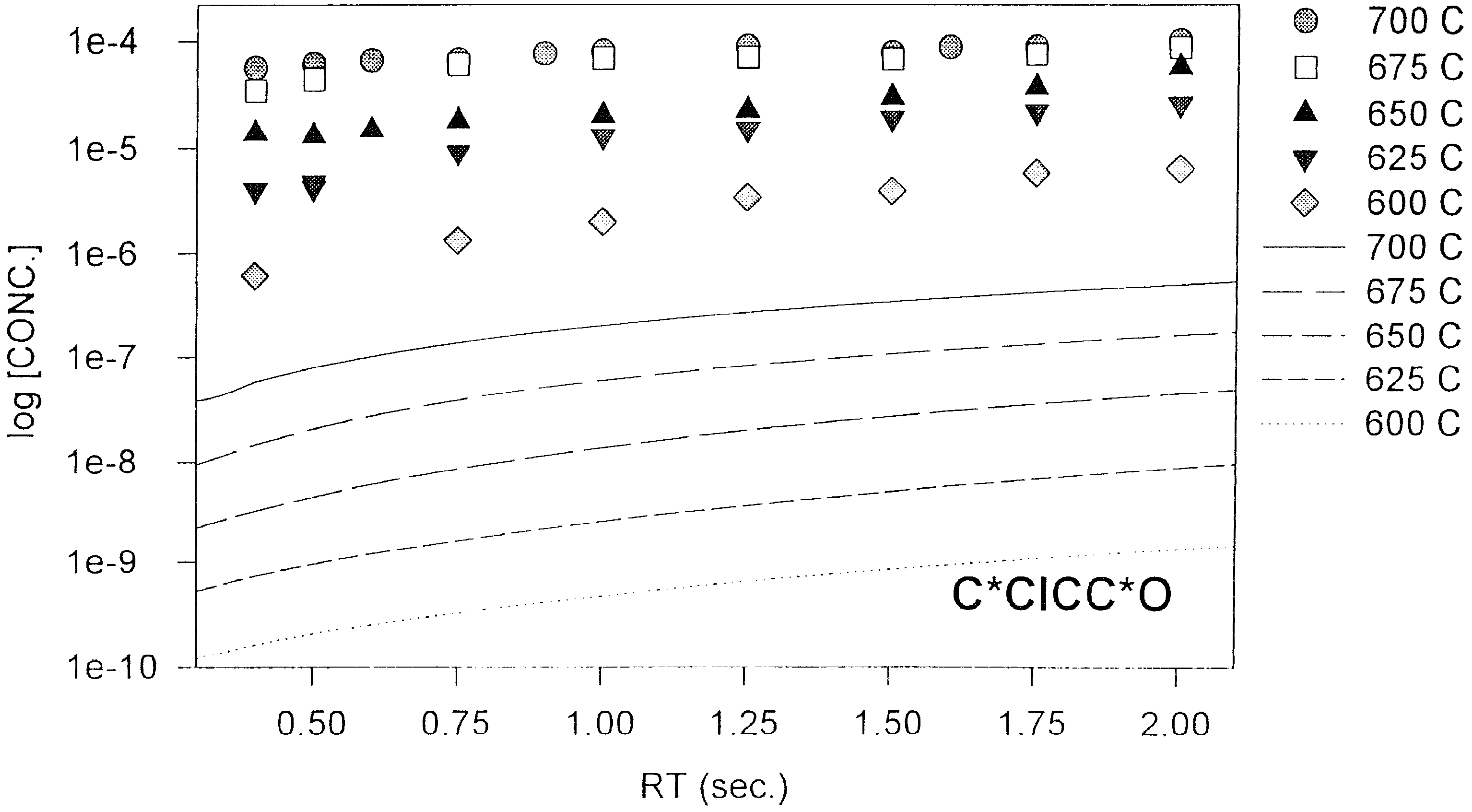

Figure 5B.41l Experimental results comparison with model (pyrolysis, P = 1 atm)

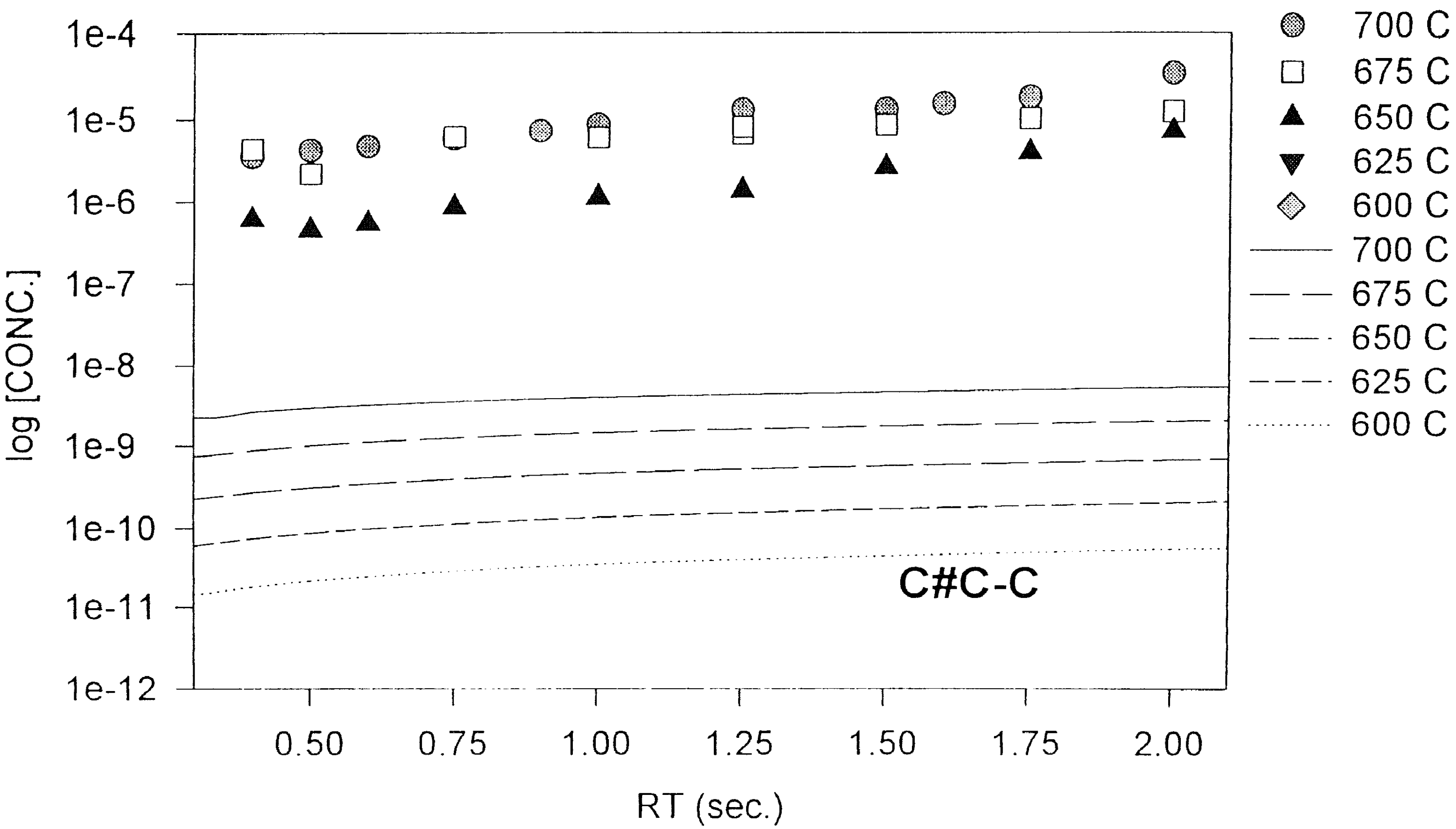

Figure 5B.41m Experimental results comparison with model (pyrolysis, P = 1 atm)

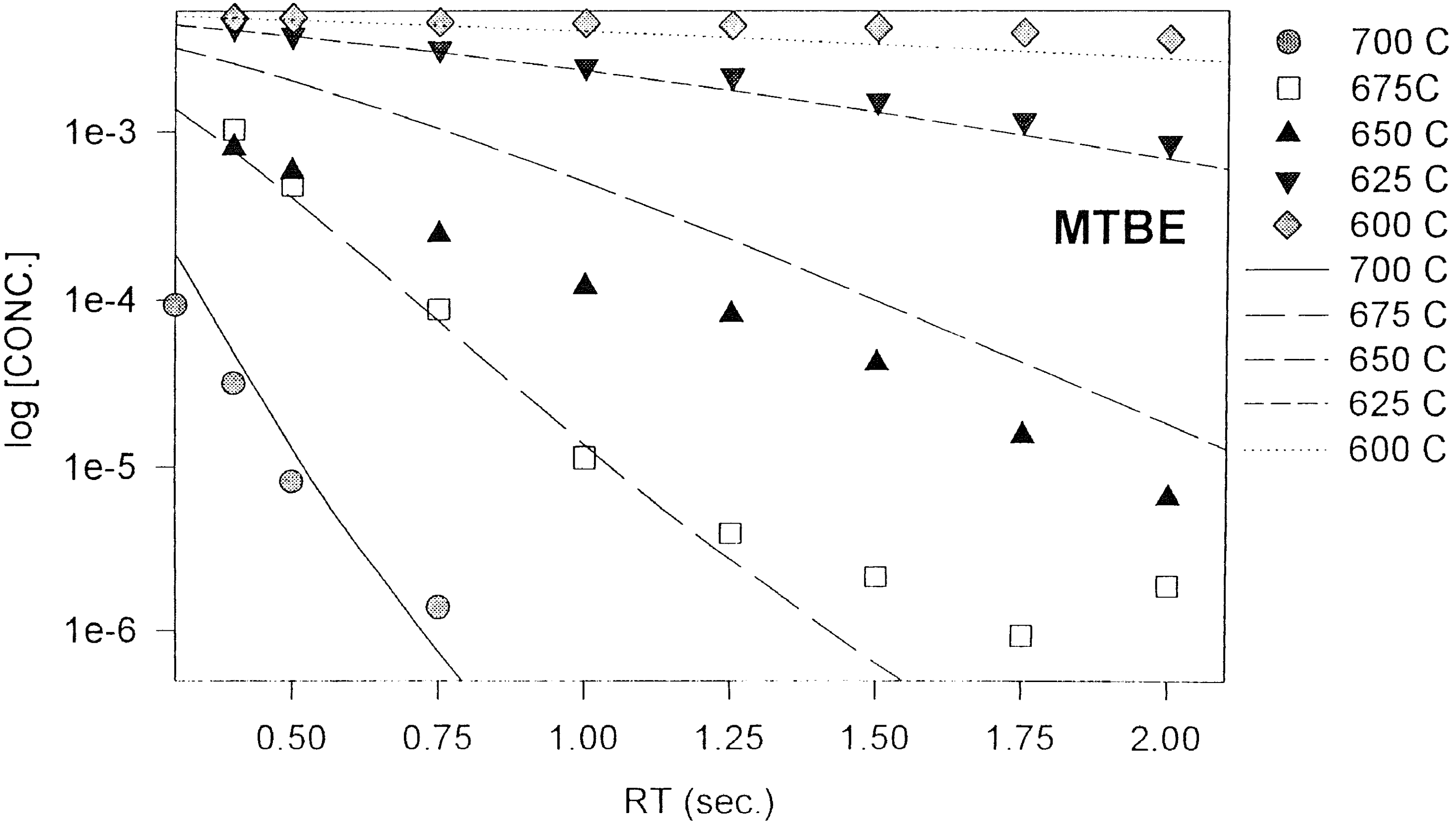

Figure 5B.42a Experimental results comparison with model (phi = 1.0, P = 1 atm)

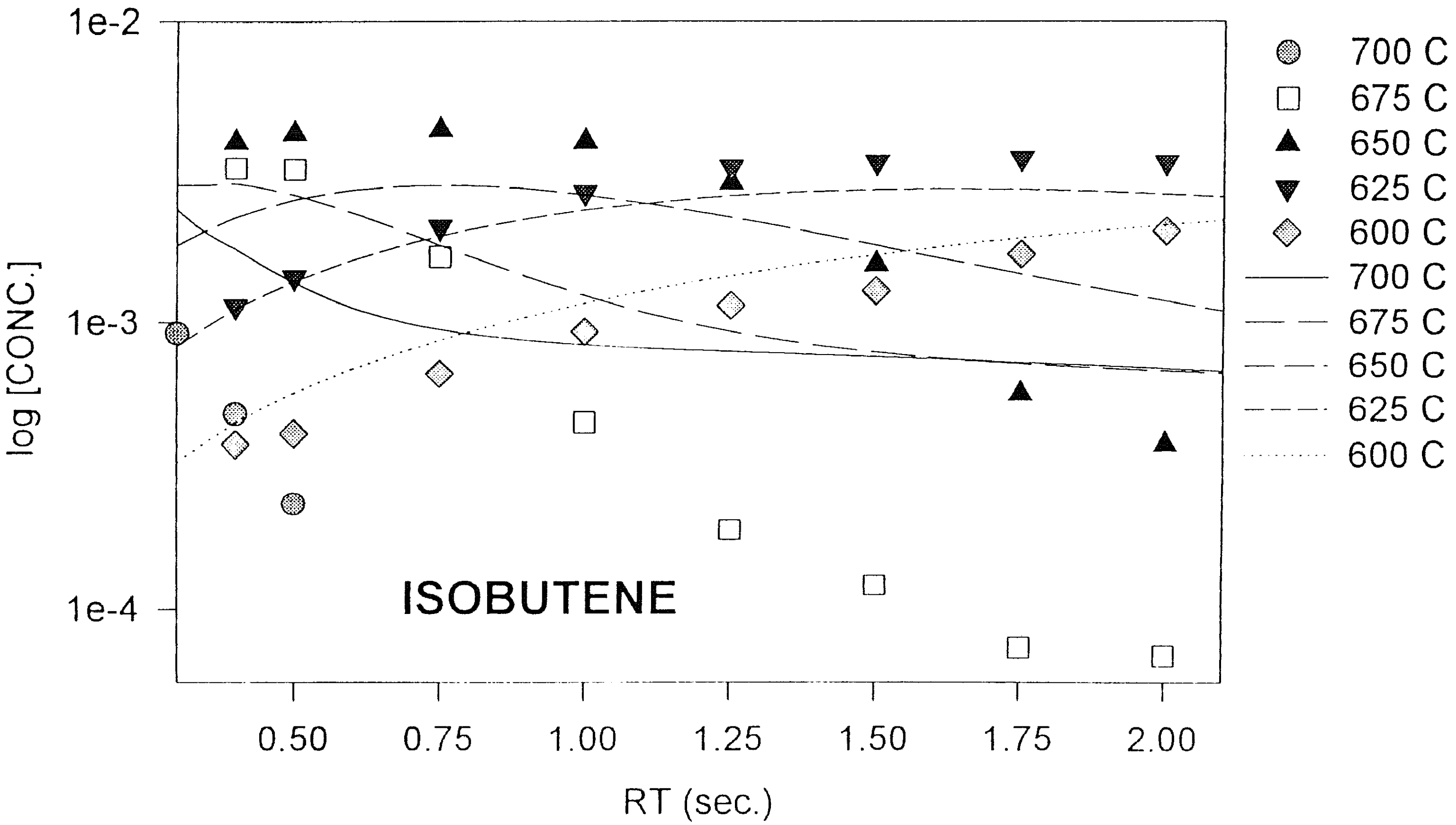

Figure 5B.42b Experimental results comparison with model (phi = 1.0, P = 1 atm)

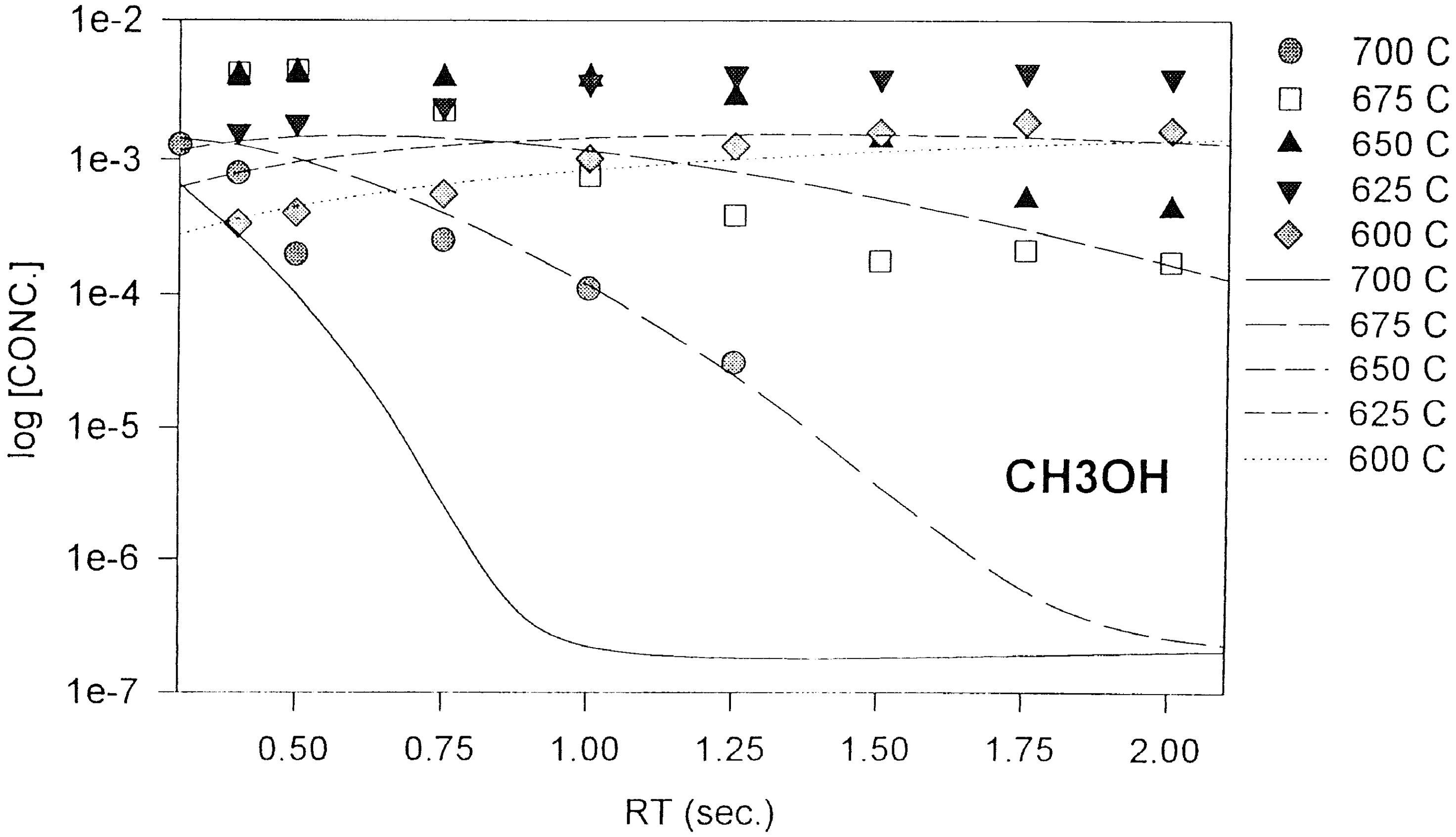

Figure 5B.42c Experimental results comparison with model (phi = 1.0, P = 1 atm)

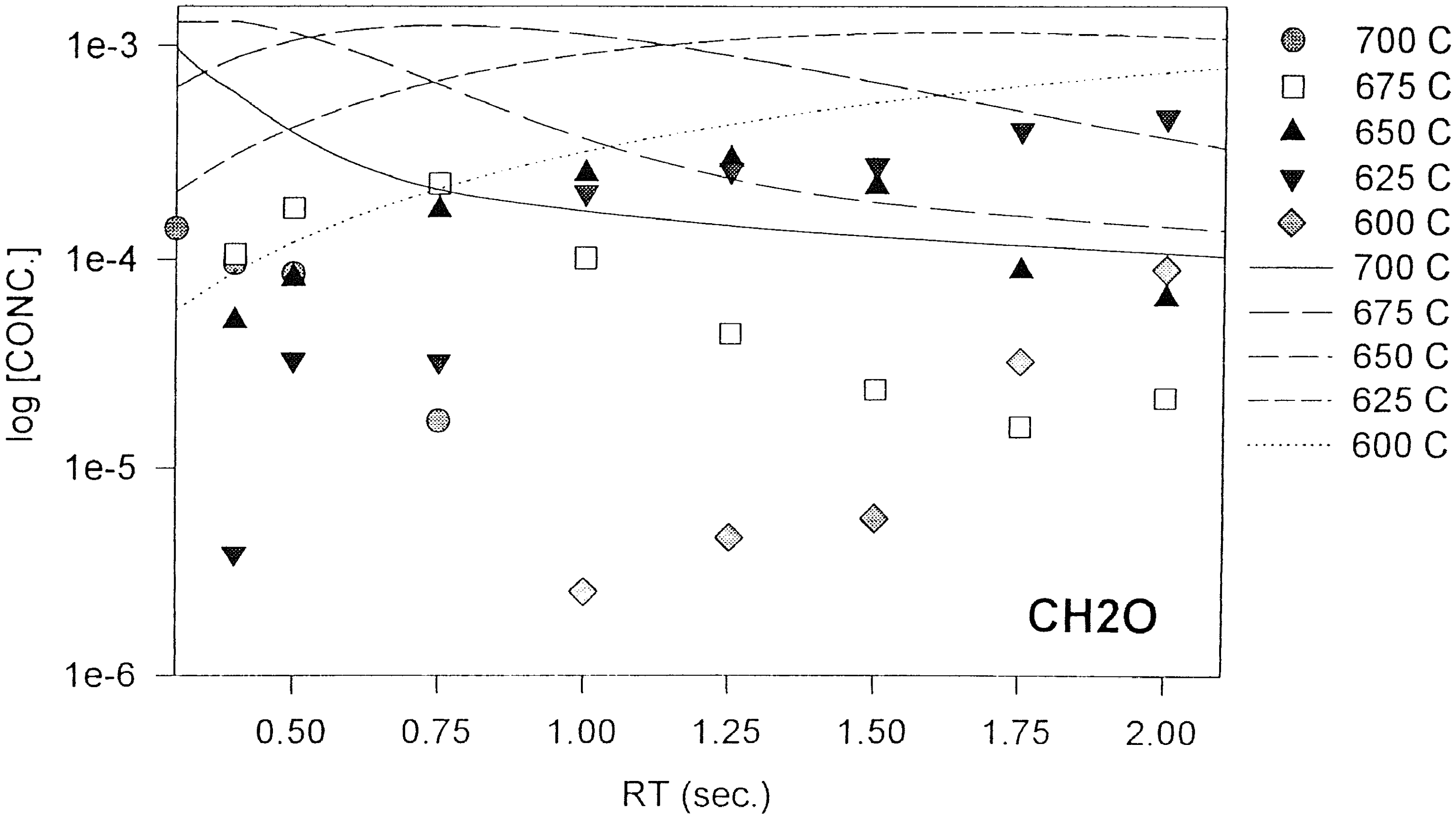

Figure 5B.42d Experimental results comparison with model (phi = 1.0, P = 1 atm)

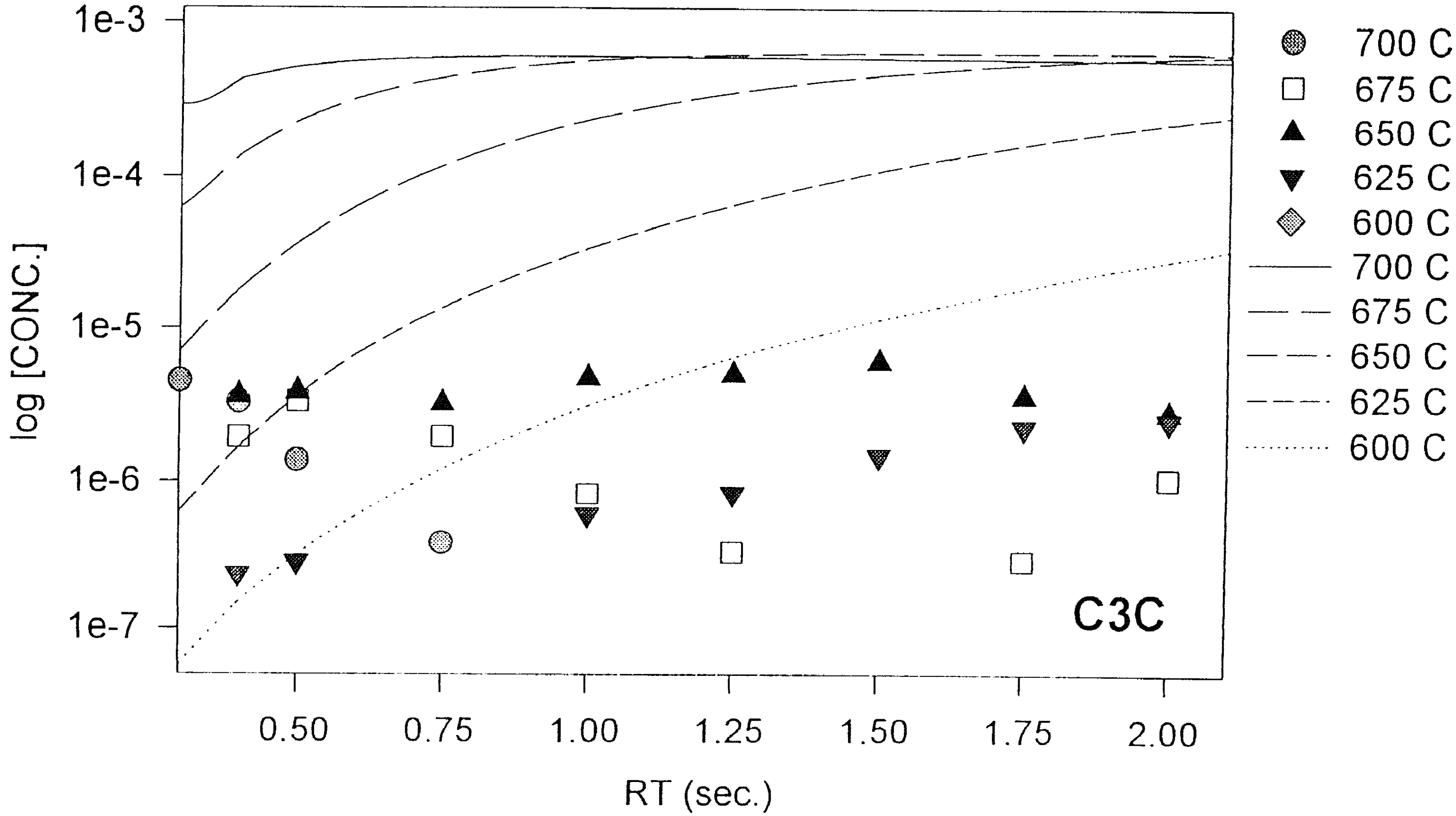

Figure 5B.42e Experimental results comparison with model (phi = 1.0, P = 1 atm)

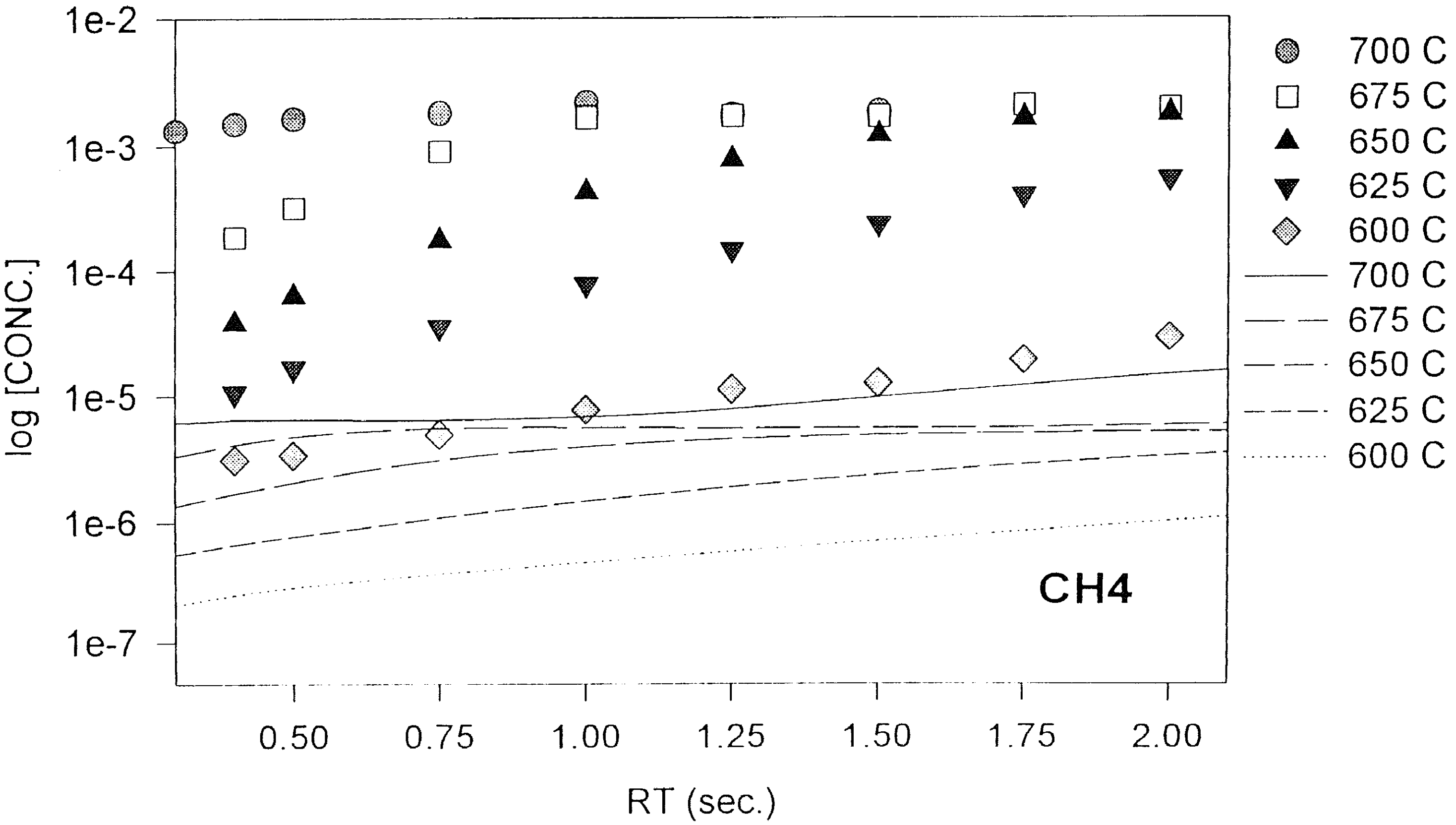

Figure 5B.42f Experimental results comparison with model (phi = 1.0, P = 1 atm)

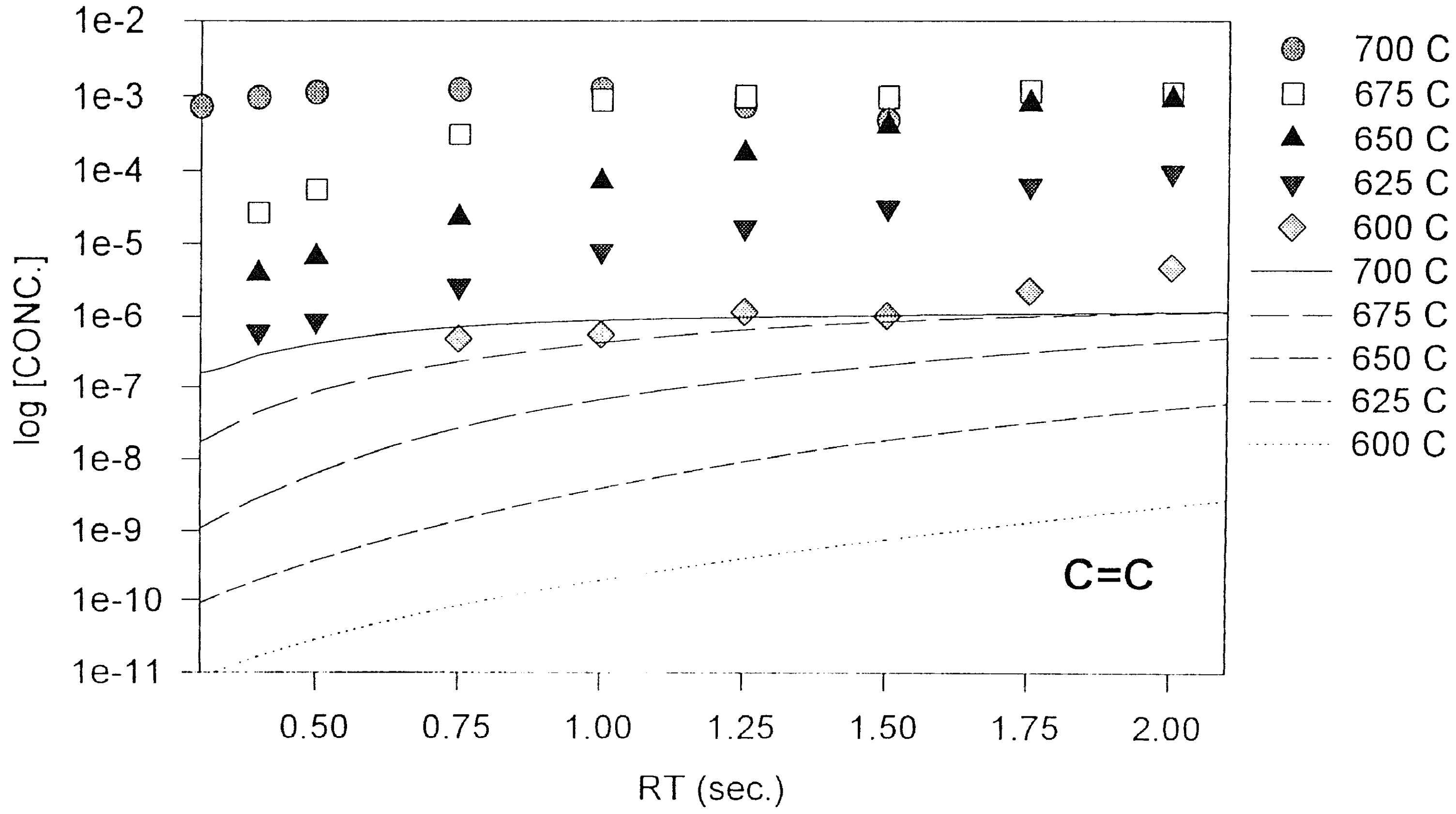

Figure 5B.42g Experimental results comparison with model (phi = 1.0, P = 1 atm)

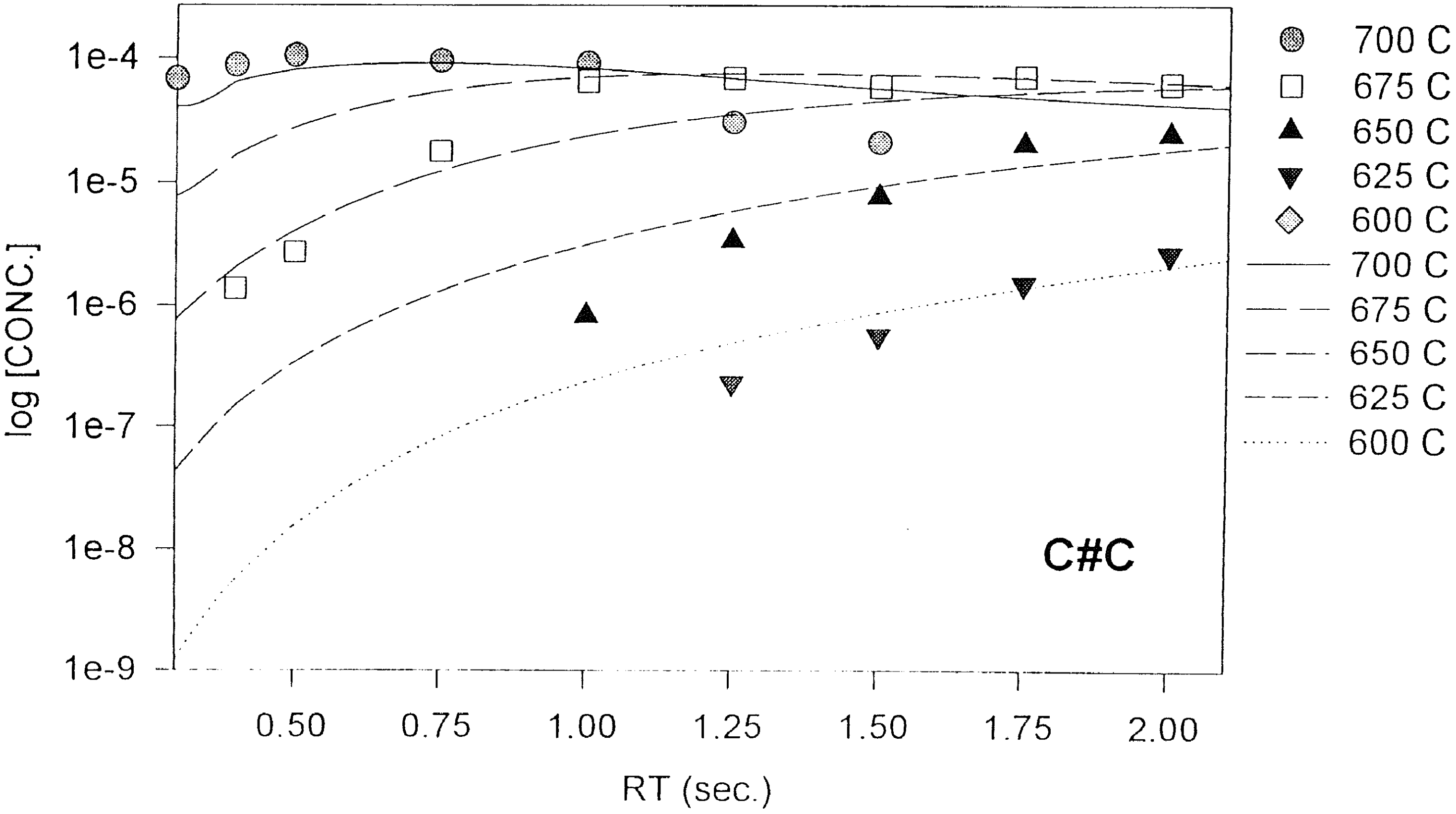

Figure 5B.42h Experimental results comparison with model (phi = 1.0, P = 1 atm)

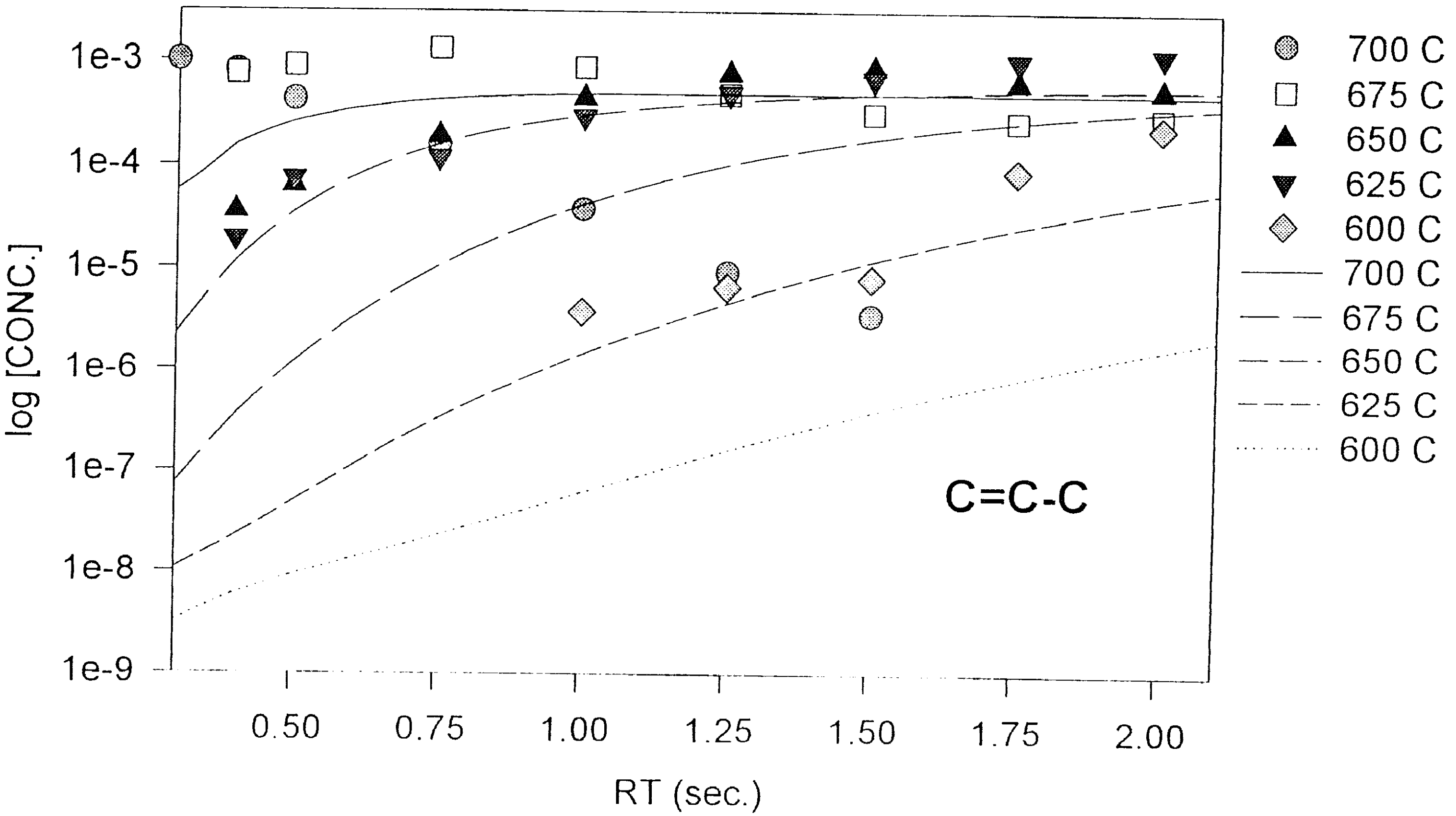

Figure 5B.42i Experimental results comparison with model (phi = 1.0, P = 1 atm)

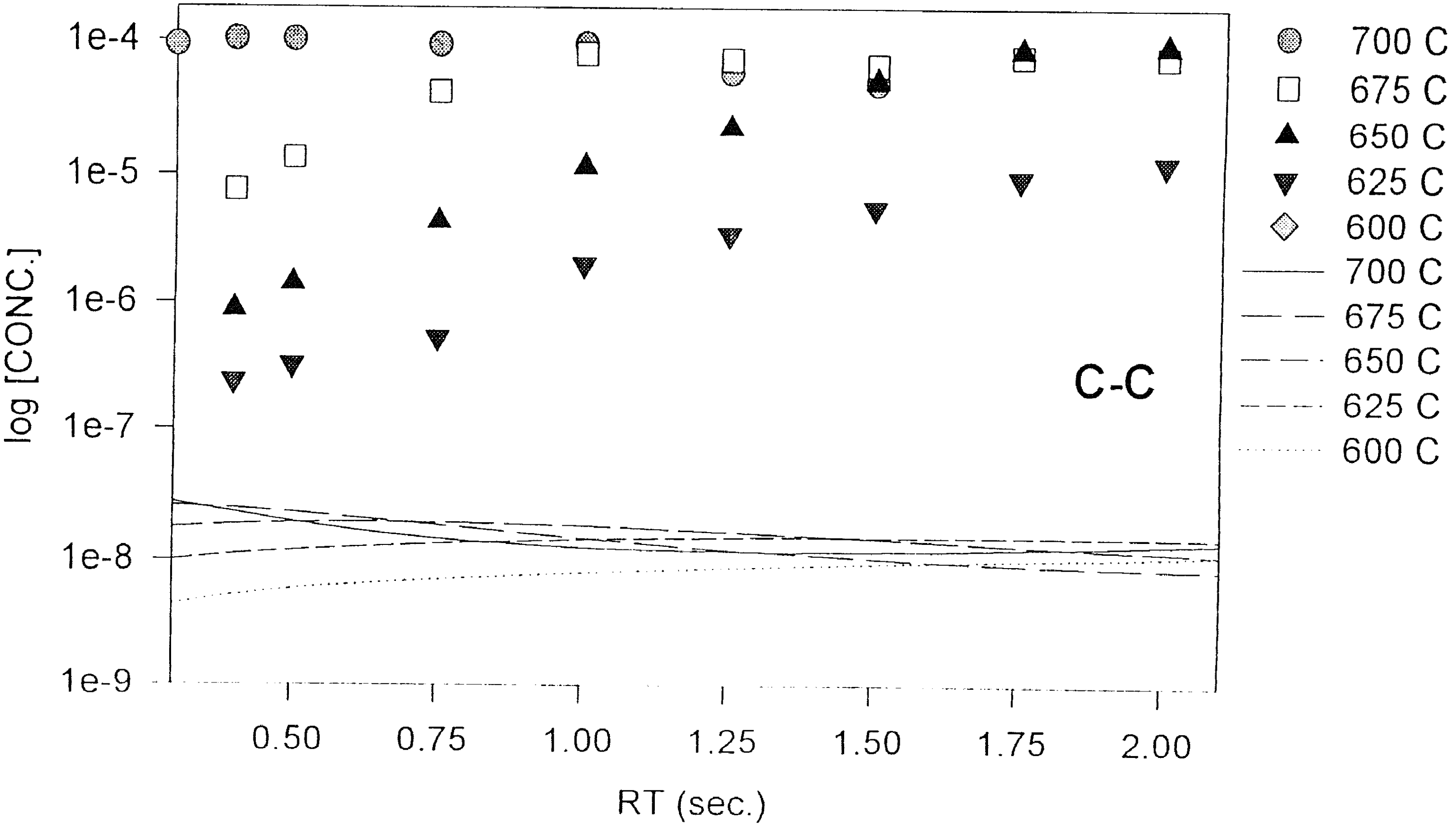

Figure 5B.42j Experimental results comparison with model (phi = 1.0, P = 1 atm)

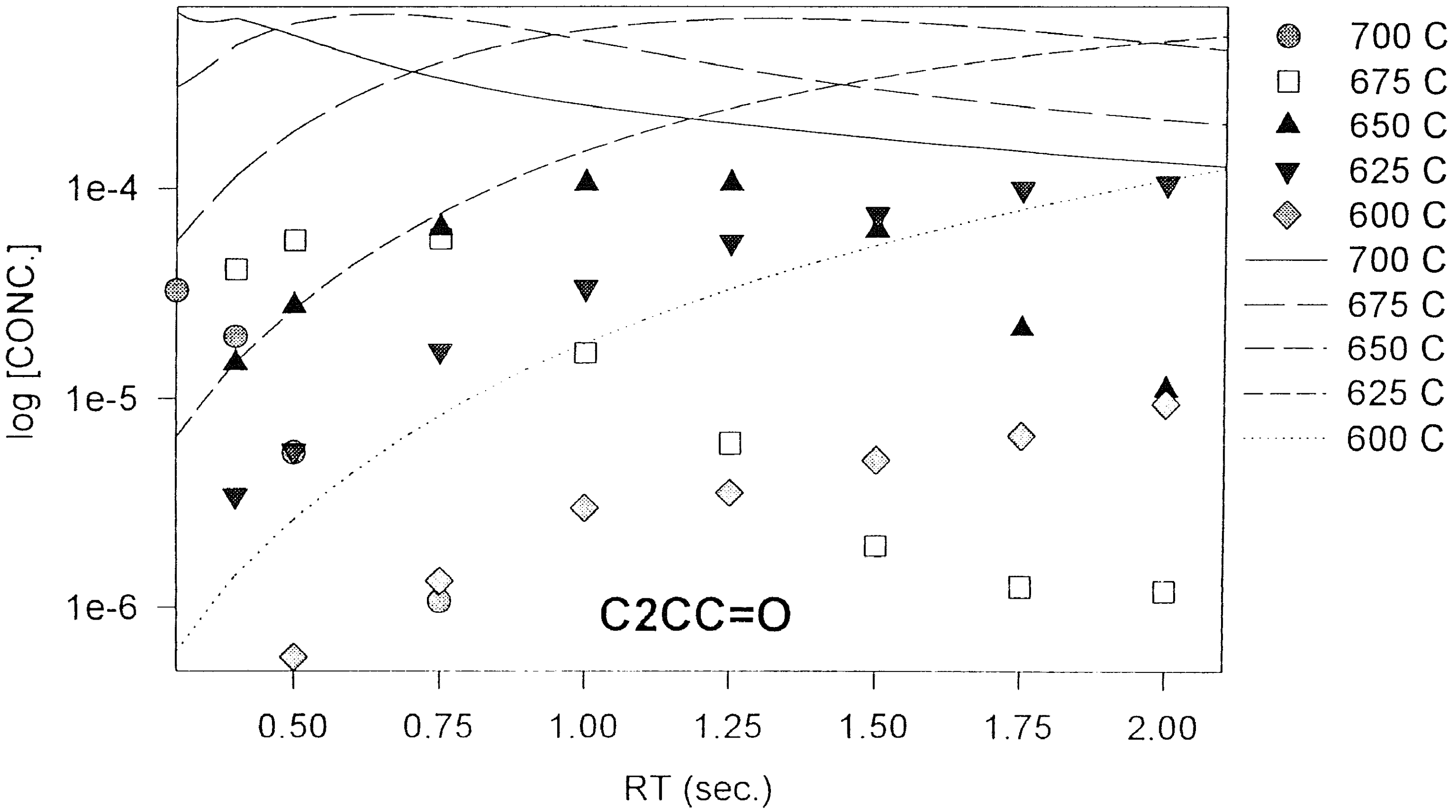

Figure 5B.42k Experimental results comparison with model (phi = 1.0, P = 1 atm)

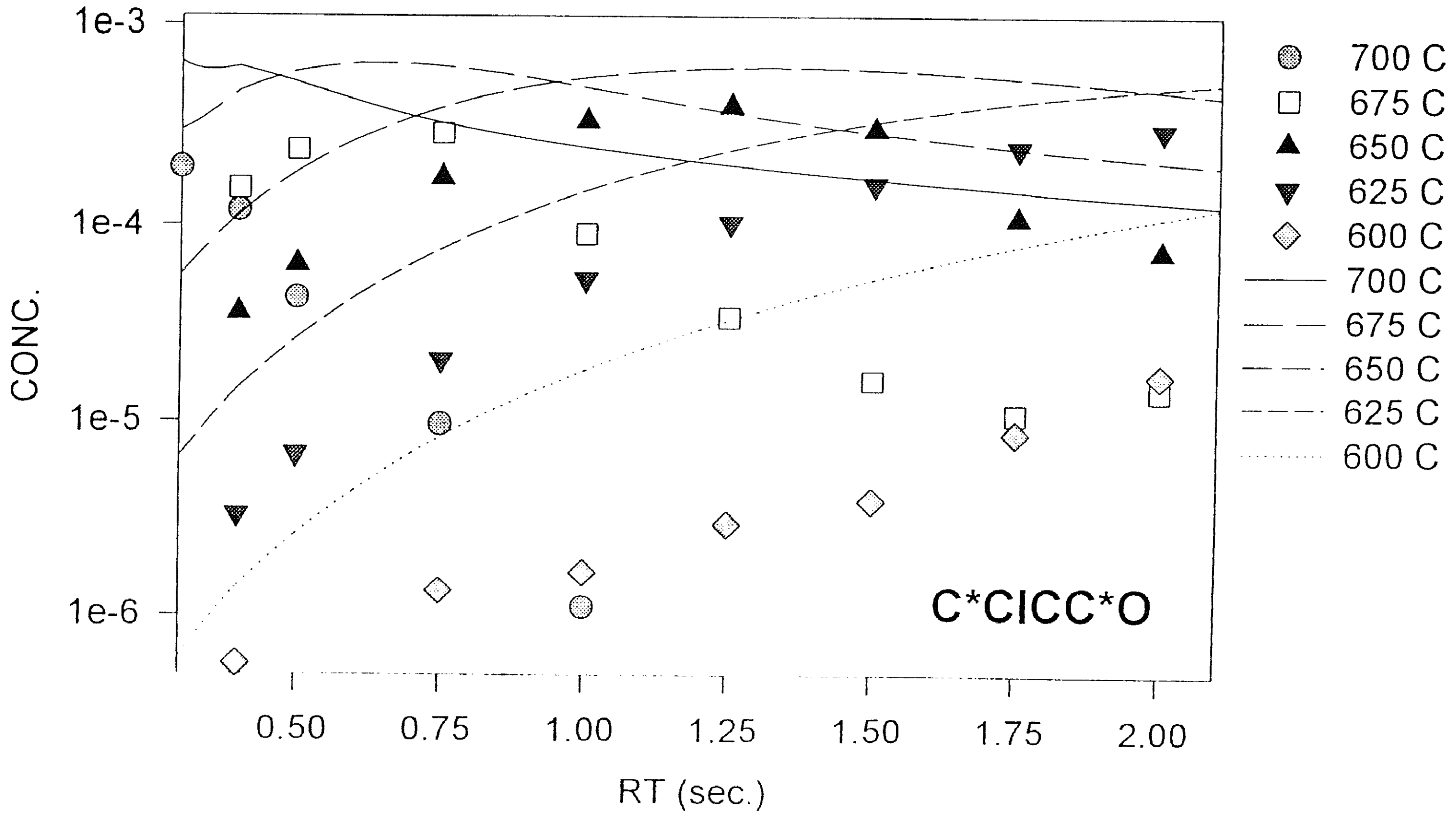

Figure 5B.421 Experimental results comparison with model (phi = 1.0, P = 1 atm)

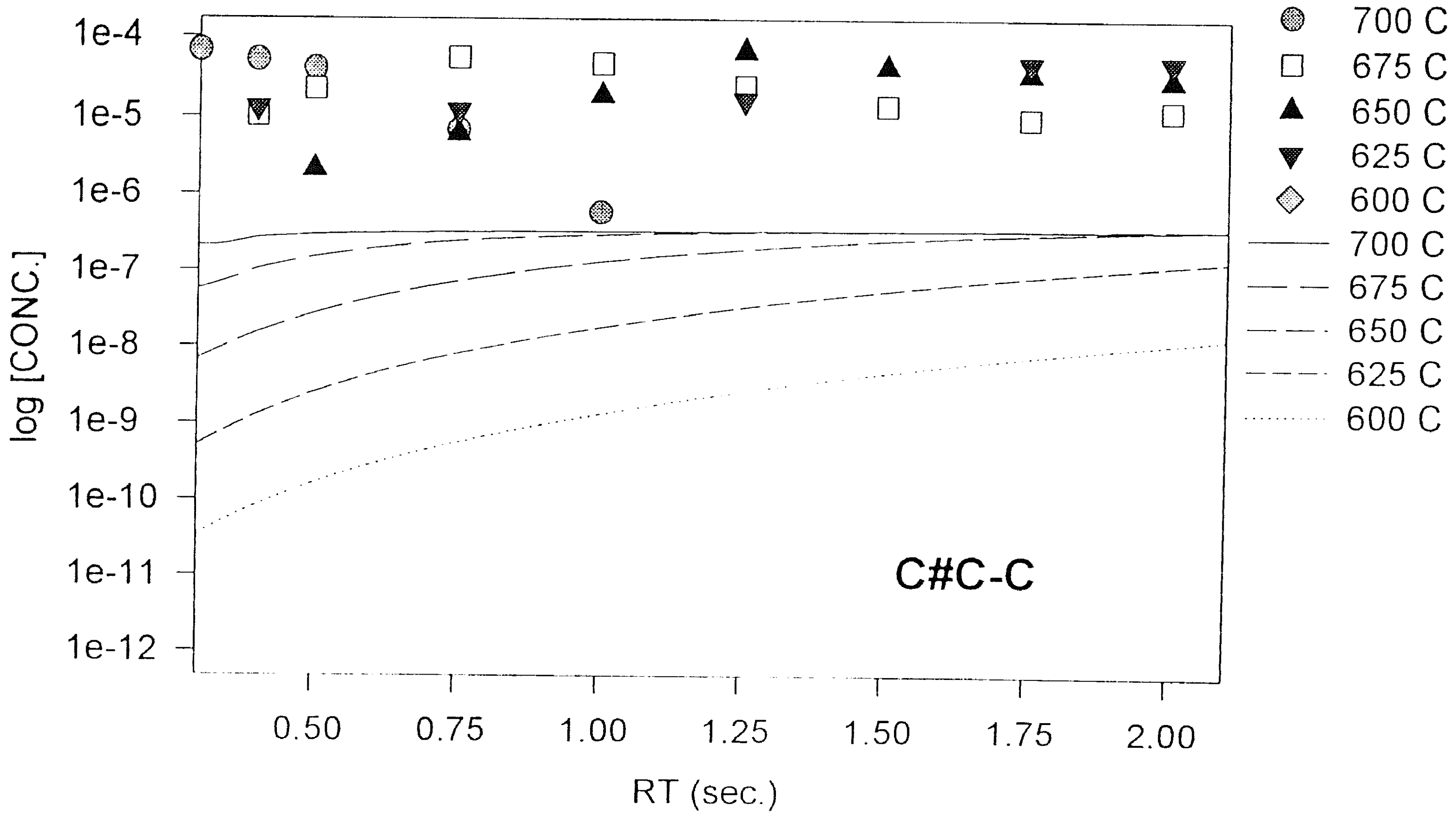

Figure 5B.42m Experimental results comparison with model (phi = 1.0, P = 1 atm)

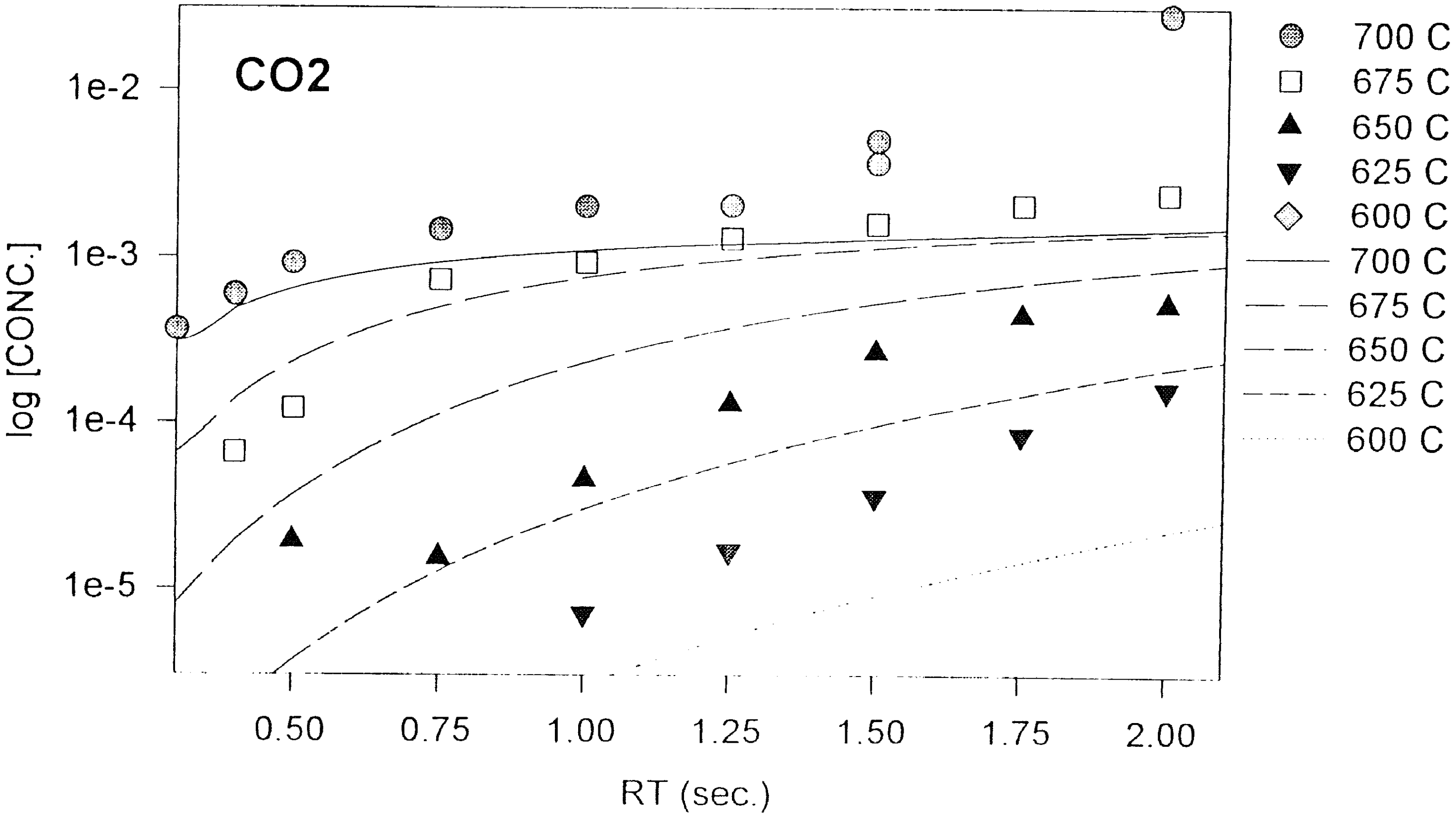

Figure 5B.42n Experimental results comparison with model (phi = 1.0, P = 1 atm)

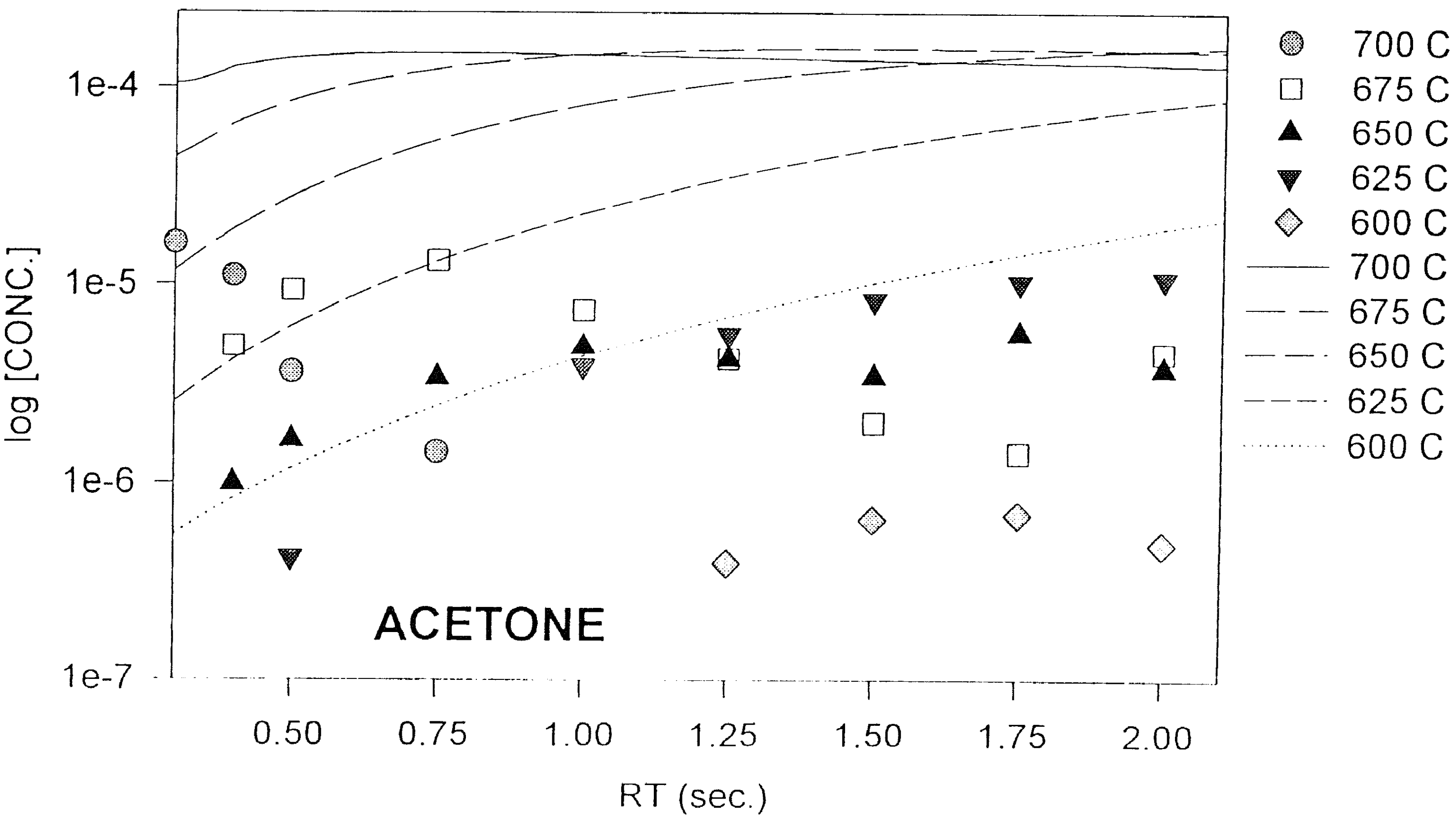

Figure 5B.42o Experimental results comparison with model (phi = 1.0, P = 1 atm)

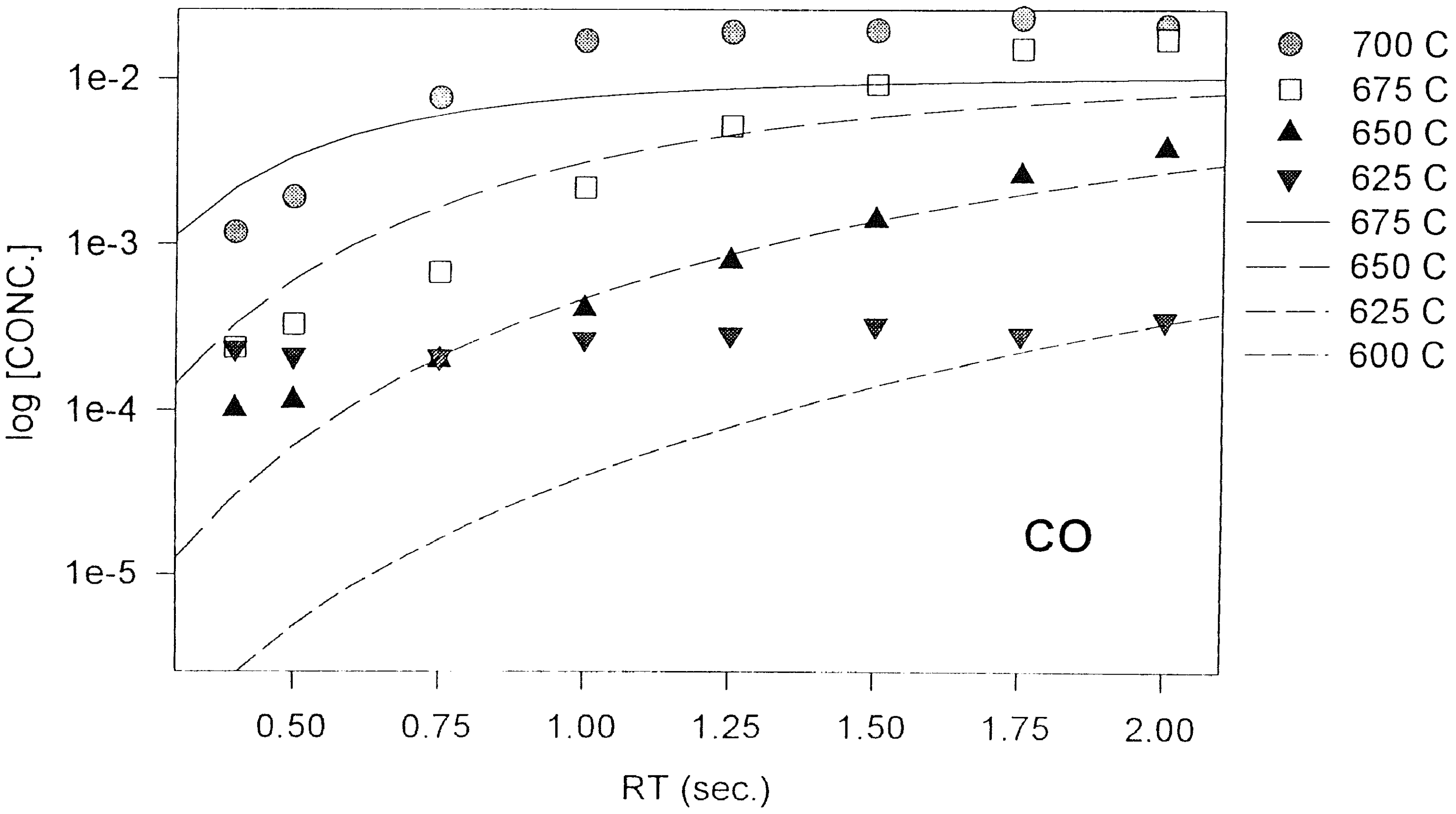

Figure 5B.42p Experimental results comparison with model (phi = 1.0, P = 1 atm)

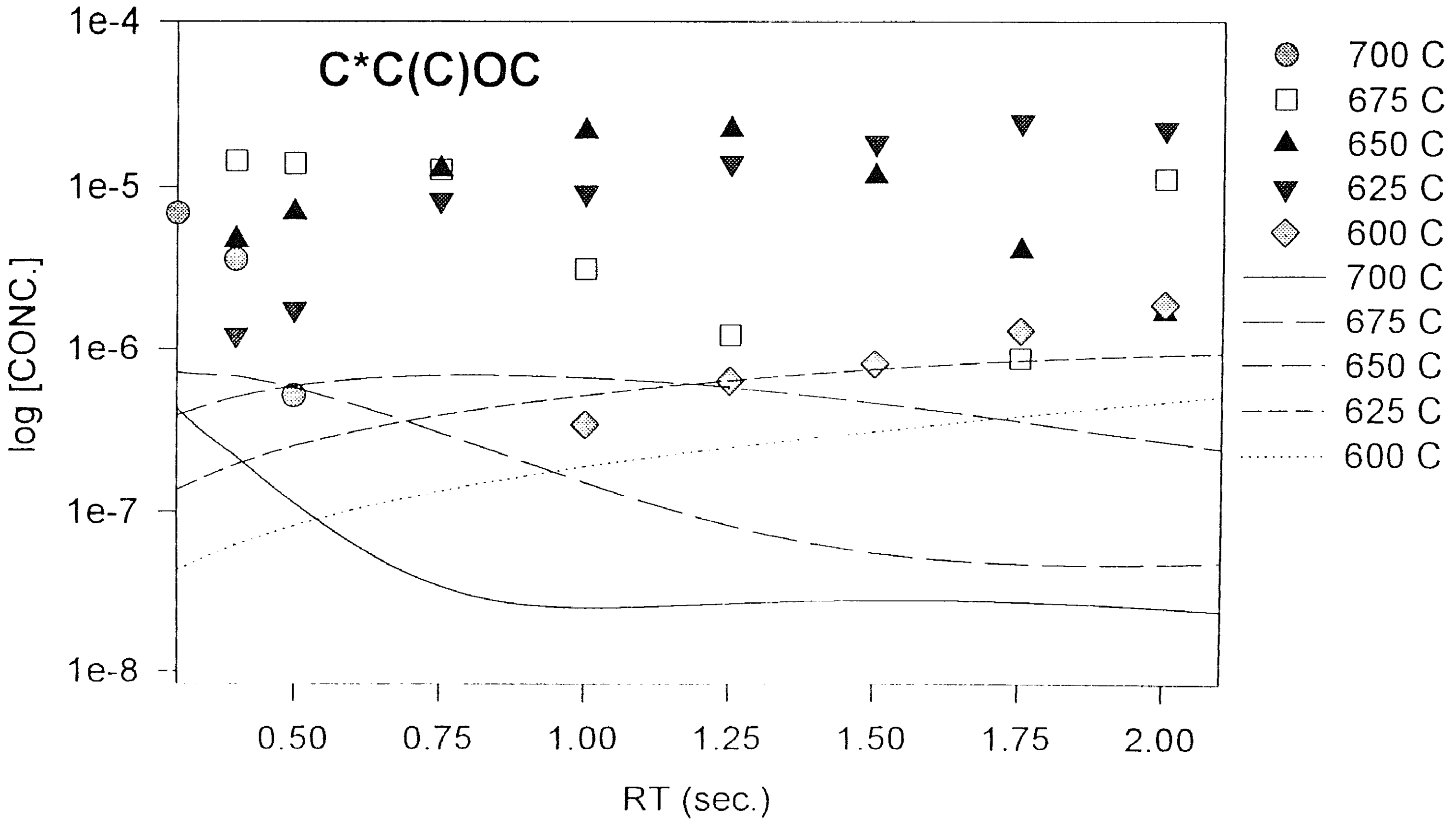

Figure 5B.42q Experimental results comparison with model (phi = 1.0, P = 1 atm)

APPENDIX 6A

TABLES IN STANDARD CHEMICAL THERMODYNAMIC PROPERTIES OF MULTI-CHLORO ALKANES AND ALKENES: A MODIFIED GROUP ADDITIVITY SCHEME

Table 6A.1 Comparison of Enthalpy of Formation and Entropy at 298 K Incorporating New Chlorocarbon Group Values

Group	Compounds	Stull[15]	TRC[16]	Pedley[17]	Group Calc.	
					Benson /Cohen	non-next-nearest neighbor (this work)[a]
		Enthalpies of Formation at 298 K				
C/C/Cl$_2$/H	1,1 dichloro-ethane	-31.05	-31.10	-30.52	-27.90	-31.04
	1,1 dichloro-propane		-36.03		-32.90	-36.04
	1,1 dichloro-butane		-40.96		-37.90	-41.04
	1,1 dichloro-pentane		-45.89		-42.90	-46.04
	1,1 dichloro-hexane		-50.82		-47.90	-51.04
	1,3 dichloro-propane	-38.60		-38.05	-38.40	*
C/C$_2$/Cl$_2$	2,2 dichloro-propane	-42.00		-41.40	-41.40	-42.00
C/C/Cl$_3$	1,1,1 trichloro-ethane		-34.01		-28.00	-33.84
	1,1,1 trichloro-propane		-38.94		-33.00	-38.84
	1,1,1 trichloro-butane		-43.88		-38.00	-43.84
	1,1,1 trichloro-pentane		-48.80		-43.00	-48.84
	1,1,1 trichloro-hexane		-53.73		-48.00	-53.84
CD/Cl$_2$	1,1 dichloro-ethylene	0.30	0.57	0.62	4.56	0.50
CD/CD/Cl	2 chloro-1,3-butadiene		6.64			5.56
	2,3 dichloro-1,3-butadiene		-12.98			-12.44
	1,1,2 trichloro-1,3-butadiene		-2.21			-1.39
INT/Cl$_2$	1,2 dichloro-ethane	-31.00	-30.30	-30.33	-33.40	-31.05
	1,2 dichloro-propane	-39.60		-38.91	-41.30	-38.72
INT/Cl$_3$	1,1,2 trichloro-ethane	-33.10	-34.56	-34.80	-34.60	-33.99
	1,2,3 trichloro-propane	-44.40		-43.71	-48.00	-44.22
INT/Cl$_4$	1,1,1,2 tetrachloro-ethane		-35.71		-34.70	-35.54
	1,1,2,2 tetrachloro-ethane	-36.50	-35.61	-35.66	-35.80	-36.98
INT/Cl$_5$	Pentachloro-ethane	-34.00			-35.90	-34.00
INT/Cl$_6$	Hexachloro-ethane	-33.80		-34.32	-36.00	-34.06
INT/CD/Cl$_2$	1,2 (Z) dichloro-ethylene	0.45	-0.67	1.10	1.2	0.30
	1,2 (E) dichloro-ethylene	1.00	-0.10	1.20	2.2	0.70
INT/CD/Cl$_3$	trichloro-ethylene	-1.40	-1.94	-2.30	-1.1	-1.88
INT/CD/Cl$_4$	tetrachloro ethylene	-3.40	-2.90		-3.4	-3.15
		Entropies of Formation at 298 K				
C/C/Cl$_2$/H	1,1 dichloro-ethane <3>[b]	72.89	72.91		71.82	73.03
	1,1 dichloro-propane <3>		82.39		81.22	82.43
	1,1 dichloro-butane <3>		91.87		90.62	91.83
	1,1 dichloro-pentane <3>		101.36		100.02	101.23
	1,1 dichloro-hexane <2>		110.85		109.42	110.63
	1,3 dichloro-propane <18>	83.91			83.62	*
C/C$_2$/Cl$_2$	2,2 dichloro-propane <3>	77.92			77.26	77.92
C/C/Cl$_3$	1,1,1 trichloro-ethane <9>		76.49		76.33	76.62
	1,1,1 trichloro-propane <9>		85.97		85.73	86.02
	1,1,1 trichloro-butane <9>		95.46		95.13	95.42
	1,1,1 trichloro-pentane <9>		104.95		104.53	104.82
	1,1,1 trichloro-hexane <9>		114.43		113.93	114.22
CD/Cl$_2$	1,1 dichloro-ethylene <1>	68.85	67.90		69.71	68.38
CD/CD/Cl	2 chloro-1,3-butadiene		74.91			76.07
	2,3 dichloro-1,3-butadiene		79.87			81.49
	1,1,2 trichloro-1,3-butadiene		92.70			90.73
INT/Cl$_2$	1,2 dichloro-ethane <1>	73.66	73.10		76.34	75.05
	1,2 dichloro-propane <3>	84.00			83.52	82.33
INT/Cl$_3$	1,1,2 trichloro-ethane <1>	80.57	79.69		81.50	81.22
	1,2,3 trichloro-propane <2>	91.52			91.82	90.43
INT/Cl$_4$	1,1,1,2 tetrachloro-ethane <3>		85.05		86.02	84.53
	1,1,2,2 tetrachloro-ethane <2>	86.69	84.84		86.02	86.29

Table 6A.1 (Continued)

Group	Compounds		Stull[15]	TRC[16]	Pedley[17]	Group Calc.	
						Benson /Cohen	non-next-nearest neighbor (this work)
			Entropies of Formation at 298 K				
INT/Cl_5	Pentachloro-ethane	<3>	90.95			91.92	90.95
INT/Cl_6	Hexachloro-ethane	<18>	94.77			95.06	94.77
INT/CD/Cl_2	1,2 (Z) dichloro-ethylene	<2>	69.20	69.22		69.42	69.21
	1,2 (E) dichloro-ethylene	<2>	69.29	69.28		69.42	69.29
INT/CD/Cl_3	trichloro-ethylene	<1>	77.63	77.70		77.50	77.67
INT/CD/Cl_4	tetrachloro ethylene	<4>	81.46	81.47		81.45	81.47

[a] Benson/Cohen hydrocarbon groups and corresponding chloroalkane and alkene groups

[b] <#> Symmetry

* No interaction term

Units: $\Delta H_f°$, kcal/mole; $S°$ and Cp, cal/(mole-K)

Table 6A.2 Group Values

Group	$\Delta H_f{}^\circ_{298}$	S°_{298}	Cp (T)						
			300 K	400 K	500 K	600 K	800 K	1000 K	1500 K
a.	**Benson/Cohen Hydrocarbon Groups (recommended[10, 11] values)**								
$C/C/H_3$	-10.00	30.30	6.19	7.84	9.40	10.79	13.02	14.77	17.58
$C/C_2/H_2$	-5.00	9.40	5.50	6.95	8.25	9.35	11.07	12.34	14.20
$C/C_3/H$	-2.14	-12.30	4.54	6.00	7.17	8.05	9.31	10.05	11.18
C/C_4	-0.10	-35.00	4.37	6.13	7.36	8.12	8.77	8.76	8.12
CD/H_2[a]	6.26	27.61	5.10	6.36	7.51	8.50	10.07	11.27	13.19
CD/CD/H[a]	6.78	6.38	4.46	5.79	6.75	7.42	8.35	9.11	
GAUCHE (Cohen)	0.80	0.00	0.00	0.00	0.00	0.00	0.00	0.00	0.00
b.	**Chlorocarbon groups for multi-chloro alkane and alkene groups[b]**								
$C/C/Cl/H_2$[c]	-16.80	38.17	8.74	10.54	12.08	13.31	15.15	16.47	18.46
$C/C_2/Cl/H$[c]	-14.47	17.33	8.47	10.20	11.68	12.76	14.29	15.38	16.21
$C/C_3/Cl$[c]	-14.03	-6.45	8.09	10.15	11.69	12.65	13.47	13.53	13.32
$C/C/Cl_2/H$	-21.04	44.91	11.99	13.98	15.53	16.62	18.09	18.80	19.43
$C/C_2/Cl_2$	-22.00	23.06	13.12	14.88	15.95	16.48	16.96	17.02	16.82
$C/C/Cl_3$	-23.84	50.69	15.83	17.86	19.25	20.10	21.06	21.21	21.42
CD/CD/Cl	-13.76	14.47	7.23	8.86	9.66	10.26	10.96	11.28	
CD/Cl_2	-5.76	40.77	10.97	12.42	13.33	13.92	14.63	15.01	15.44
CD/Cl/H[a]	-1.20	35.40	7.90	9.20	10.30	11.20	12.30	13.10	14.25
CD/C/Cl[d]	-2.10	15.0	8.00	8.40	8.50	9.00	9.20	9.40	
c.	**Interaction groups for multi-chloro alkane and alkene groups[b]**								
INT/Cl_2	2.54	-1.29	0.75	0.46	0.23	0.08	-0.05	-0.05	0.02
INT/Cl_3	3.85	-1.86	0.58	0.33	0.04	-0.12	-0.24	-0.24	0.2
INT/Cl_4	5.10	-2.15	0.05	-0.11	-0.26	-0.24	-0.10	0.43	0.73
INT/Cl_5	10.88	-2.47	0.45	0.02	-0.31	-0.44	-0.53	0.02	0.18
INT/Cl_6	13.62	-0.87	1.06	0.44	-0.15	-0.44	-0.73	-0.17	0.47
CIS/Cl/Cl	-0.4	-0.08	-0.37	-0.17	-0.09	-0.05	-0.01	-0.01	0.0
$Z/Cl/CD_3$	18.01	0.65	0.24	-0.76	-0.60	-0.47	-0.51	-0.40	
$INT/CD/Cl_2$	3.10	-0.13	0.16	0.15	0.03	-0.15	-0.02	0.02	0.13
$INT/CD/Cl_3$	5.08	1.50	0.39	0.18	0.04	-0.06	0.01	0.04	0.1
$INT/CD/Cl_4$	8.37	2.68	0.79	0.26	0.06	0.02	0.02	0.05	0.09
GAUCHE-Cl	1.3	0.0	0.0	0.0	0.0	0.0	0.0	0.0	0.0

[a] ref.5

[b] Use with the Benson/Cohen recommended[10, 11] values. Heat capacities are those of Benson for all cases.

[c] ref.14

[d] $\Delta H_f{}^\circ_{298}$ and S°_{298} are from ref.5. Heat capacities are from ref.8.

Units: $\Delta H_f{}^\circ$, kcal/mole; S° and Cp, cal/(mole-K)

Table 6A.3 Heat Capacity Comparison of TRC Recommended Heat Capacities to Group Data

Group	Compound	*Cp(T)* 300 K	400 K	500 K	600 K	800 K	1000 K	1500 K
		TRC Data						
$C/C/Cl_2/H$	1,1 dichloro-ethane	18.32	21.87	24.81	27.23	30.79	33.40	37.35
	1,1 dichloro-propane	23.75	28.78	33.11	36.64	42.02	45.82	51.72
	1,1 dichloro-butane	29.18	35.72	41.43	46.11	53.25	58.25	66.09
	1,1 dichloro-pentane	34.62	42.66	49.75	55.55	64.47	70.67	80.46
	1,1 dichloro-hexane	40.05	49.60	58.07	65.01	75.70	83.09	94.83
	1,3 dichloro-propane[a]	22.93	28.69	32.82	36.22	41.56	45.50	
$C/C_2/Cl_2$	2,2 dichloro-propane	25.40	30.56	34.75	38.06	43.00	46.56	
$C/C/Cl_3$	1,1,1 trichloro-ethane	22.14	25.71	28.51	30.68	33.75	35.81	38.80
	1,1,1 trichloro-propane	27.58	32.66	36.84	40.13	44.98	48.23	53.17
	1,1,1 trichloro-butane	33.01	39.60	45.16	49.59	56.20	60.66	67.54
	1,1,1 trichloro-pentane	38.45	46.53	53.48	59.05	67.43	73.09	81.91
	1,1,1 trichloro-hexane	43.88	53.48	61.80	68.51	78.65	85.51	96.28
CD/Cl_2	1,1 dichloro-ethylene	16.05	18.76	20.82	22.40	24.68	26.26	28.63
CD/CD/Cl	2 chloro-1,3-butadiene	22.21	27.35	31.44	34.70	39.52	42.98	
	2,3 dichloro-1,3-butadiene	25.25	30.50	34.49	37.57	41.96	45.03	
	1,1,2 trichloro-1,3-butadiene	29.40	33.84	37.31	40.04	43.98	46.67	
		Group Additivity Values, This Work						
$C/C/Cl_2/H$	1,1 dichloro-ethane	18.18	21.82	24.93	27.41	31.11	33.57	37.01
	1,1 dichloro-propane	23.68	28.77	33.18	36.76	42.18	45.91	51.21
	1,1 dichloro-butane	29.18	35.72	41.43	46.11	53.25	58.25	65.41
	1,1 dichloro-pentane	34.68	42.67	49.68	55.46	64.32	70.59	79.61
	1,1 dichloro-hexane	40.18	49.62	57.93	64.81	75.39	82.93	93.81
	1,3 dichloro-propane[a]	22.98	28.03	32.41	35.97	41.37	45.28	51.12
$C/C_2/Cl_2$	2,2 dichloro-propane	25.50	30.56	34.75	38.06	43.00	46.56	51.98
$C/C/Cl_3$	1,1,1 trichloro-ethane	22.02	25.70	28.65	30.89	34.08	35.98	39.00
	1,1,1 trichloro-propane	27.52	32.65	36.90	40.24	45.15	48.32	53.00
	1,1,1 trichloro-butane	33.02	39.60	45.15	49.59	56.22	60.66	67.40
	1,1,1 trichloro-pentane	38.52	46.55	53.40	58.94	67.29	73.00	81.60
	1,1,1 trichloro-hexane	44.02	53.50	61.65	68.29	78.36	85.34	95.80
CD/Cl_2	1,1 dichloro-ethylene	16.07	18.78	20.84	22.42	24.70	26.28	28.63
CD/CD/Cl	2 chloro-1,3-butadiene	21.89	27.37	31.43	34.70	39.44	42.92	
	2,3 dichloro-1,3-butadiene	25.41	30.90	34.57	37.6	42.01	45.05	
	1,1,2 trichloro-1,3-butadiene	28.15	33.61	37.29	40.04	44.02	46.71	

[a] No interaction term

UNITS: Cp, cal/(mol-K); temperature, K

Table 6A.4 Heat Capacity Comparison of TRC Recommended Heat Capacities to Group Data

Group	Compound	*Cp(T)* 300 K	400 K	500 K	600 K	800 K	1000 K	1500 K
				TRC Data				
INT/Cl_2	1,2 dichloro-ethane	18.77	21.98	24.83	27.18	30.78	33.39	37.64
	1,2 dichloro-propane	23.60	28.60	32.95	36.47	41.97	46.08	
INT/Cl_3	1,1,2 trichloro-ethane	20.87	24.75	27.83	30.21	33.57	35.78	39.29
	1,2,3 trichloro-propane	26.96	31.71	35.69	38.87	43.79	47.34	
INT/Cl_4	1,1,1,2 tetrachloro-ethane	24.69	28.36	31.16	33.28	36.24	38.17	40.70
	1,1,2,2 tetrachloro-ethane	23.95	27.79	30.71	32.90	35.92	37.89	40.66
INT/Cl_5	Pentachloro-ethane	28.27	31.86	34.47	36.28	38.62	40.03	42.00
INT/Cl_6	Hexachloro-ethane	32.72	36.16	38.35	39.76	41.39	42.25	43.31
INT/CD/Cl_2	1,2 (Z) dichloro-ethylene	15.59	18.37	20.53	22.20	24.57	26.20	28.63
	1,2 (E) dichloro-ethylene	15.95	18.54	20.62	22.25	24.59	26.21	28.63
INT/CD/Cl_3	trichloro-ethylene	19.26	21.80	23.67	25.06	26.94	28.15	29.79
INT/CD/Cl_4	tetrachloro ethylene	22.73	25.10	26.72	27.86	29.28	30.07	30.97
				Group Additivity Values, This Work				
INT/Cl_2	1,2 dichloro-ethane	18.23	21.54	24.39	26.70	30.25	32.89	36.94
	1,2 dichloro-propane	24.15	29.04	33.39	36.94	42.41	46.57	52.27
INT/Cl_3	1,1,2 trichloro-ethane	21.31	24.85	27.65	29.81	33.00	35.03	38.09
	1,2,3 trichloro-propane	26.53	31.61	35.88	39.26	44.35	48.08	53.33
INT/Cl_4	1,1,1,2 tetrachloro-ethane	24.62	28.29	31.07	33.17	36.11	38.11	40.61
	1,1,2,2 tetrachloro-ethane	24.03	27.85	30.80	33.00	36.08	38.03	39.59
INT/Cl_5	Pentachloro-ethane	28.27	31.86	34.47	36.28	38.62	40.03	41.03
INT/Cl_6	Hexachloro-ethane	32.72	36.16	38.35	39.76	41.39	42.25	43.31
INT/CD/Cl_2	1,2 (Z) dichloro-ethylene	15.59.	18.38	20.54	22.20	24.57	26.21	28.63
	1,2 (E) dichloro-ethylene	15.96	18.55	20.63	22.25	24.58	26.22	28.63
INT/CD/Cl_3	trichloro-ethylene	19.26	21.80	23.67	25.06	26.94	28.15	29.79
INT/CD/Cl_4	tetrachloro ethylene	22.73	25.10	26.72	27.86	29.28	30.07	30.97

UNITS: Cp, cal/(mol-K); temperature, K

Table 6A.5 Example Calculations of Thermodynamic Properties for More Complex Clorocarbons

	Gr #	GROUP ID	Quantity	CPINF	NROTORS	SYMMETRY
Hexachloro-1,3-butadiene						
C4Cl6	1	CD/CD/Cl	2	54.64	1	4
	2	CD/Cl2	2			
	3	INT/Cl2	1			
	4	INT/CD/Cl3	2			
	5	Z/Cl/CD3	1			
1,1,2,4,4-Pentachloro-1,3-butadiene						
C4HCl5	1	CD/Cl2	2	54.64	1	1
	2	CD/CD/H	1			
	3	CD/CD/Cl	1			
	4	INT/CD/Cl2	1			
	5	INT/CD/Cl3	1			
	6	Z/Cl/CD3	1			
trans,1,1,2,3,4-Pentachloro-1,3-butadiene						
C4HCl5	1	CD/Cl/H	1	54.64	1	1
	2	CD/Cl2	1			
	3	CD/CD/Cl	2			
	4	INT/Cl2	1			
	5	INT/CD/Cl2	1			
	6	INT/CD/Cl3	1			
	7	Z/Cl/CD3	1			
1,1,2,4,4-Pentachloro-2,3-butadiene						
C4HCl5	1	CD/Cl$_2$	1	54.64	1	1
	2	CA	1			
	3	CD/C/Cl	1			
	4	C/CD/Cl2/H	1			
	5	INT/Cl3	1			
	6	GAUCHE-Cl	1			
1,1,2,3,3,4,4-Heptachloro-butylene						
C4Cl7H	1	CD/Cl2	1	65.57	2	1
	2	CD/C/Cl	1			
	3	C/C/CD/Cl2	1			
	4	C/C/Cl2/H	1			
	5	INT/Cl3	1			
	6	INT/Cl4	1			
	7	INT/CD/Cl3	1			
	8	GAUCHE-Cl	1			
1,1,2,3,4,4,4-Heptachloro-butylene						
C4Cl7H	1	CD/Cl2	1	65.57	2	3
	2	CD/C/Cl	1			
	3	C/C/CD/Cl/H	1			
	4	C/C/Cl3	1			
	5	INT/Cl2	1			
	6	INT/Cl4	1			
	7	INT/CD/Cl3	1			
	8	GAUCHE-Cl	1			

	$H_f^{\circ}{}_{298}$	$S^{\circ}{}_{298}$	C_{p300}	C_{p400}	C_{p500}	C_{p600}	C_{p800}	C_{p1000}
Hexachloro-1,3-butadiene	-8.33	110.09	38.17	42.62	45.69	47.85	50.64	52.21
1,1,2,4,4-Pentachloro-1,3-butadiene	7.69	104.41	34.42	39.06	42.54	44.84	48.05	50.07
trans,1,1,2,3,4-Pentachloro-1,3-butadiene	-5.75	105.84	34.87	39.37	42.65	45.04	48.28	50.28
1,1,2,4,4-Pentachloro-2,3-butadiene	10.45	104.17	35.82	39.76	42.24	44.46	46.95	48.44
1,1,2,3,3,4,4-Heptachloro-butylene	-34.03	120.33	45.48	50.45	53.48	55.82	58.64	60.54
1,1,2,3,4,4,4-Heptachloro-butylene	-30.61	120.95	44.84	49.78	53.12	55.78	59.13	61.50

Units: ΔH_f°, Kcal/mole; S° and Cp, cal/(mole-K)

Table 6A.6 Enthalpy Interaction Correction on a per Chlorine Base

Group	Enthalpy interaction per Cl, kcal/mole
INT/Cl_2	1.27
INT/Cl_3	1.28
INT/Cl_4	1.28
INT/Cl_5	2.18 (1.81[a])
INT/Cl_6	2.27 (1.51[b])
INT/CD/Cl_2	1.55
INT/CD/Cl_3	1.69
INT/CD/Cl_4	2.09

[a] multiplicative number of interactions = 6

[b] multiplicative number of interactions = 9

APPENDIX 6B

FIGURES IN THE STANDARD CHEMICAL THERMODYNAMIC PROPERTIES OF MULTI-CHLORO ALKANES AND ALKENES: A MODIFIED GROUP ADDITIVITY SCHEME

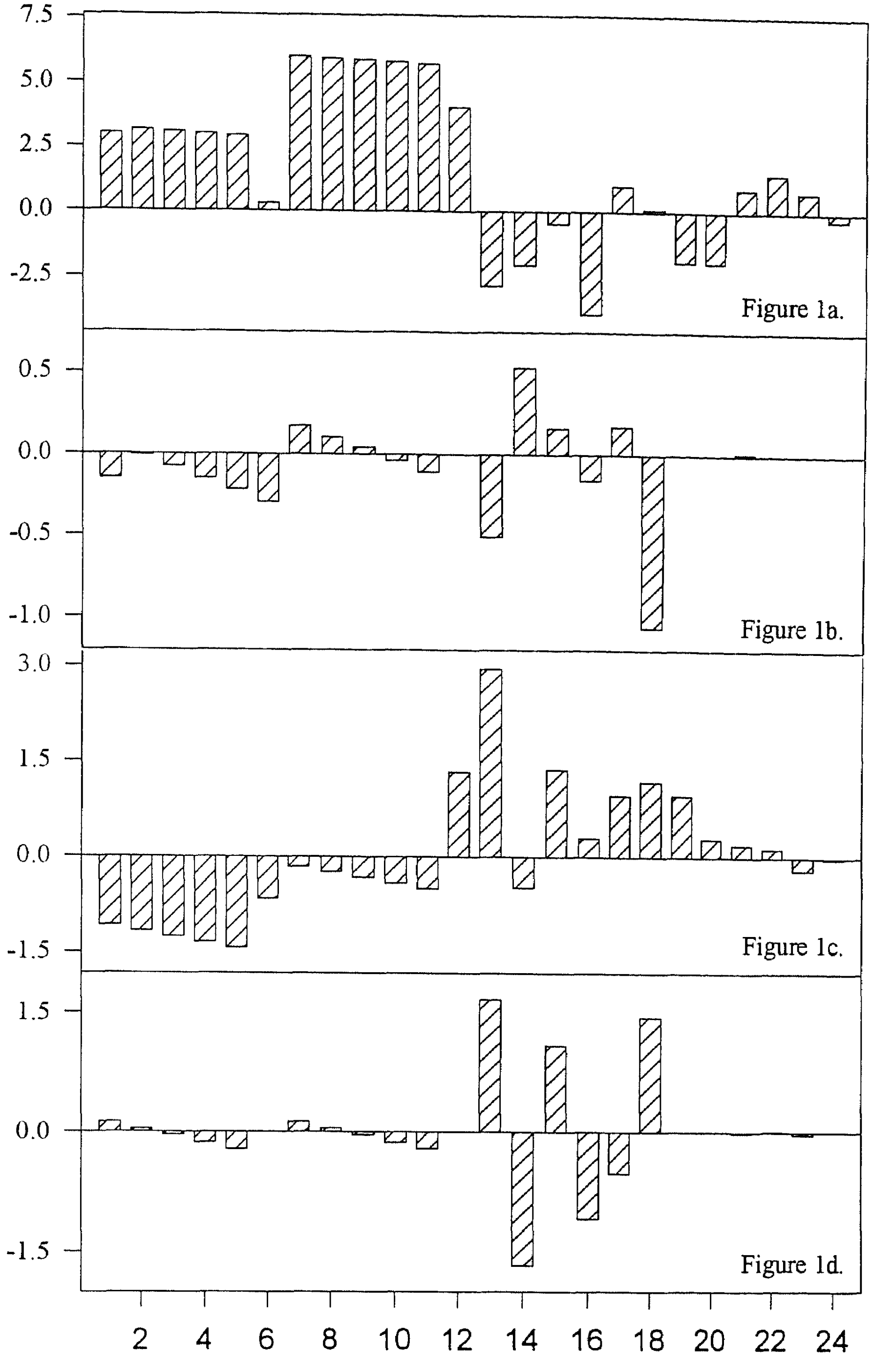

Figure 6B.1 Enthalpy deviations between values calculated by using published Benson groups vs. literature values for $\Delta H_f°_{,298}$. b. Enthalpy deviations between values calculated by using newly derived (this work) groups with interaction terms verses literature values for $\Delta H_f°_{,298}$. c. Entropy deviations between

Figure 6B.1 (Continued) values calculated by using published Benson groups vs. literature values for entropy at 298 K d. Entropy deviations between values calculated by using newly derived (this work) groups and literature values for entropy at 298 K. Units: $\Delta H_f{}^{\circ}{}_{,298}$, kcal/mole; entropy, cal/(mole-K). Key: (1)1,1 dichloro-ethane, (2)1,1 dichloro-propane, (3)1,1 dichloro-butane, (4)1,1 dichloro-pentane, (5)1,1 dichloro-hexane, (6)2,2 dichloro-propane, (7)1,1,1 trichloro-ethane, (8)1,1,1 trichloro-propane, (9)1,1,1 trichloro-butane, (10)1,1,1 trichloro-pentane, (11)1,1,1 trichloro-hexane, (12)1,1 dichloro-ethylene, (13)1,2 dichloro-ethane, (14)1,2 dichloro-propane, (15)1,1,2 trichloro-ethane, (16)1,2,3 trichloro-propane, (17)1,1,1,2 tetrachloro-ethane, (18)1,1,2,2 tetrachloro-ethane, (19)Pentachloro-ethane, (20)Hexachloro-ethane, (21)1,2 (E) dichloro-ethylene, (22)1,2 (Z) dichloro-ethylene, (23)trichloro-ethylene, (24)tetrachloro ethylene.

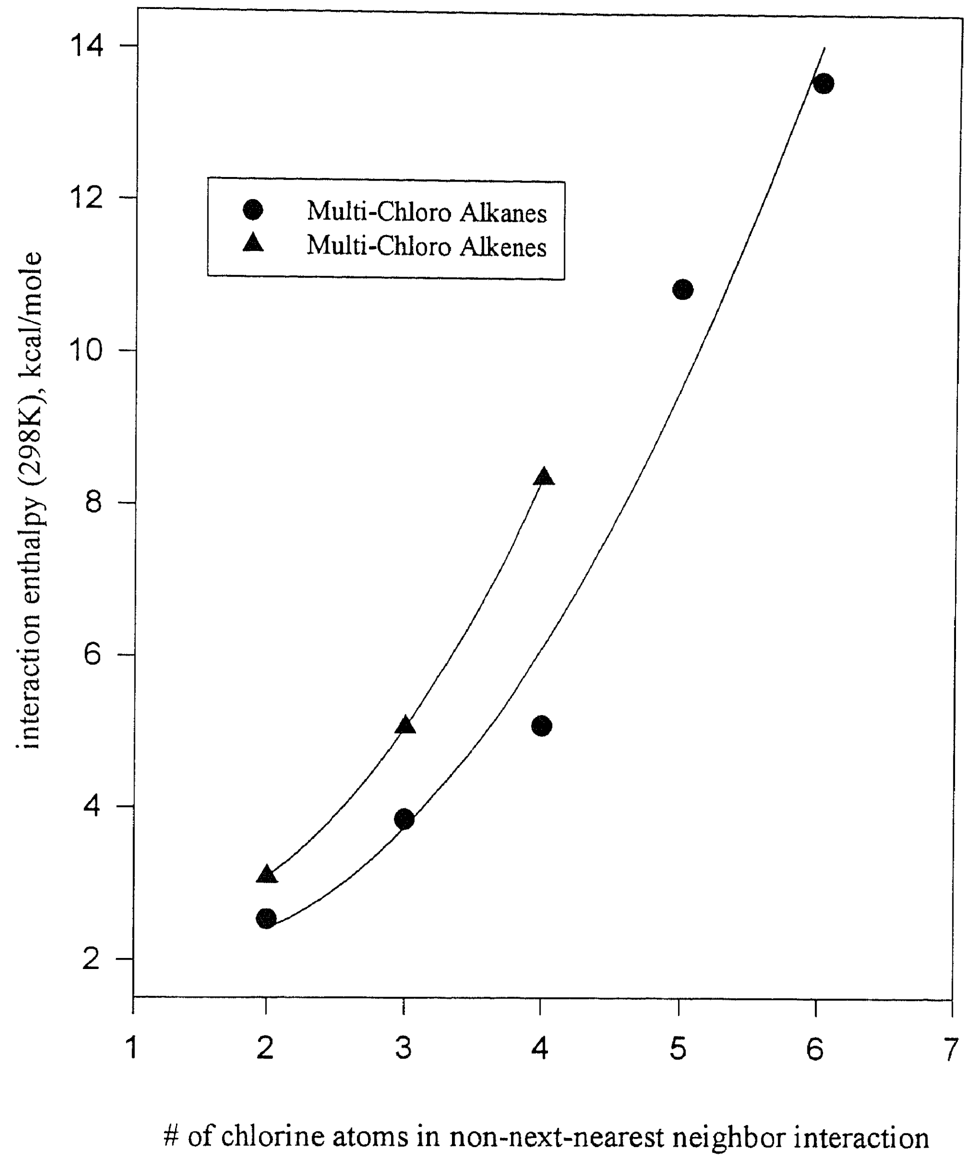

Figure 6B.2 Interaction enthalpies as a function of number of interactions for multi-chloro alkanes and alkenes.

REFERENCES

1. Becke, A. D. *Phys. Rev. A* **1988**, 38, 3098.

2. Slater, N. B. *Theory of Unimolecular Reactions*, Methuen, London, **1959**.

3. Lindemann, F. A. *Trans. Faraday Soc.* **1922**, 17, 598.

4. Christiansen, J. A. *Ph.D. Thesis*, Dept. of Chemistry, Copenhagen, **1921**.

5. Hinshelwood, C. N. *Proc. Roy. Soc. A* **1927**, 113, 230.

6. Rice, O. K.; Ramsperger, H. C. *J. Am. Chem. Soc.* **1927**, 49, 1617.

7. Kassel, L. S. *J. Phys. Chem.* **1928**, 32, 225.

8. Kassel, L. S. *J. Phys. Chem.* **1928**, 32, 1065.

9. Kassel, L. S. *Kinetics of Homogenous Gas Reaction*, Chemical Catalog Co., NY, **1932**.

10. Chang, A. Y.; Bozzelli, J. W.; Dean, A. M. submitted to *J. Phys. Chem.* **1999**.

11. Dean, A. M. *J. Phys. Chem.* **1985**, 89, 4600.

12. Dean, A. M.; Bozzelli, J. W.; Ritter, E. R. *Combust. Sci. and Tech.* **1991**, 80, 63.

13. Gilbert, R. G.; Smith, S. C. *Theory of Unimolecular and Recombination Reactions,* Black Scientific Publications, Mass, **1990**.

14. Gilbert, R. G.; Smith, S. C.; Jordan, M. J. T., *UNIMOL program suite (calculation of falloff curves for unimolecular and recombination reactions)* (1993). Available from the authors: School of Chemistry, Sydney University, NSW 2006, Australia or by email to: gilbert_r@summer.chem.su.oz.au.

15. Personal communication Dean, A. M.; Chang, A. Y., Exxon Corp. Res., Annandale NJ.

16. Steinfeld, J. I.; Franciso, J. S.; Hase, W. L. *Chemical Kinetics and Dynamics*, Prentice Hall, NJ, **1989**.

17. Ritter, E. R. *J. Chem. Info. Comput. Sci.* **1991**, 31, 400.

18. Bozzelli J. W.; Chang, A. Y.; Dean, A. M. *Int. J. Chem. Kinet.* **1997**, 29, 3, 161.

REFERENCES
(Continued)

19. Hirschfelder, J. O.; Curtiss, C. F.; Bird, R. B. *Molecular Theory of Gases and Liquids*, 2nd Ed., Wiley, London, **1963**.

20. Reid, R. C.; Prausnitz, J. M.; Sherwood, T. K. *Properties of Gases and Liquids*, 2nd Ed., McGraw Hill, NY, **1997**.

21. Westmoreland, P. R.; Howard, J.B.; Longwell, J. P.; Dean, A.M., *AICHE Annual meeting*, **1986**, 32.

22. Westmoreland, P. R. *Combust. Sci. and Tech.* **1992**, 82, 1515.

23. Dean, A. M.; Westmoreland, P. R. *Int. J. Chem. Kinet.* **1987**, 19, 207.

24. Bozzelli, J. W.; Dean, A. M. *J. Phys. Chem.* **1990**, 94, 3313.

25. Bozzelli, J. W.; Dean, A. M. *J. Phys. Chem.* **1993**, 97, 4427.

26. Sengupta, D.; Chandra, A. K. *J. Chem. Phys.* **1994**, 101, 3906.

27. Nguyen, M. T.; Sengupta, D.; Vanquickenborne, J. *J. Phys. Chem.* **1996**, 100, 10956.

28. Nguyen, M. T.; Sengupta, D.; Vanquickenborne, J. *J. Phys. Chem.* **1996**, 100, 9730.

29. Wooldridge, P.; Hanson, R. *25th Symposium (Intern'l) on Combustion, The Combustion Inst.*, Pittsburgh, PA, **1994**; 983.

30. Nguyen, M. T.; Sengupta, D. *J. Chem. Phys.* **1997**, 106, 9703.

31. Biggs, P.; C.; Mas, C. E.; Frachebourd, J. M.; Pan, A.; Shallcross, D. E.; Wayne, R. P. *J. Chem. Soc. Faraday Trans.* **1993**, 89, 4163.

32. Craig, S. L.; Zhong, M.; Choo, B.; Brauman, J. L. *J. Phys. Chem.* **1997**, 101, 19.

33. Zhong, M.; Brauman, J. L. *J. Am. Chem. Soc.* **1996**, 118, 636.

34. Dunphy, M.; Simmie, J. M. *Combust. Sci. and Tech.* **1989**, 66, 157.

35. Daly, N. J.; Wentrup, C. *Aust. J. Chem.* **1968**, 21, 2711.

36. Choo, K. Y.; Golden, D. M.; Benson, S. W. *Int. J. Chem. Kinet.* **1974**, 6, 631.

REFERENCES
(Continued)

37. Brocard, J. C.; Baronnet, F. *Oxidation Commun.* **1980**, 1, 321.

38. Brocard, J. C.; Baronnet, F. *J. Chim. Phys. Biol.* **1987**, 84, 19.

39. Wallington, T. J.; Andino, J. M.; Skewes, L. M.; Siegl, W. O.; Japar, S. M. *Int. J. Chem. Kinet.* **1989**, 21, 993.

40. Wallingtom, T. J.; Dagant, P.; Liu, R.; Kurylo, M. *Combust. Sci. and Tech.* **1988**, 22, 842.

41. Bennett, P. J.; Kerr, J. *J. A. Atoms. Chem.* **1990**, 10, 29.

42. Wallington, T. J; Skewes, L. M.; Siegl, W. O.; Wu, C. H.; Japar, S. M. *Int. J. Chem. Kinet.* **1988**, 20, 867.

43. Langer, S.; Ljungstrom, E. *Int. J. Chem. Kinet.* **1994**, 26, 367.

44. Atkinson, R. *J. Phys. Chem. Ref. Data* **1994**, Monograph 2, 65.

45. Brocard, J. C.; Baronnet, F.; O'Neal, H. E. *Combust. Frame* **1983**, 52, 25

46. Norton, T. S.; Dryer, F. L. *23th Symposium (Intern'l) on Combustion, The Combustion Inst.*, Pittsburgh, PA, **1990**, 179.

47. Jungkamp T. P. W.; Smith J. N.; Seinfeld, J. H. *J. Phys. Chem.* **1997**, 101, 4392.

48. Jungkamp, T. P. W.; Seinfeld, J. H. *J. Chem. Phys.* **1997**, 107, 1513.

49. Ochterski, J. W.; Petersson, G. A. *J. Chem. Phys.* **1996**, 104, 2598.

50. Yamada, T.; Lay, T. H.; Bozzelli, J. W. *27th Symposium (Intern'l) on Combustion, The Combustion Inst.*, Boulder, CO, **1998**, 183.

51. Stewart, J. J. P., *MOPAC 6.0*, Frank J. Seiler Research Lab., US Air Force Academy, CO, **1990**.

52. Frisch, M.j.; Truck, G. W.; Head-Gordon, M.; Gill, P. M. W.; Wong, M. W.; Foresman, J. B.; Johnson, B. G.; Schelgel, H. B.; Robb, M. A.; Peplogle, E. S.; Gromperts, R.; Andres, J. L., Raghavachari, K.; Binkley, J, S., Gonzalez, C.; Martin, R. L.; Fox, D. J.; Defrees, D. J.; Baker, J.; Stewart, J. J. P.; Pople, J. A.; Eds., *Gaussian 94 Computer Program, Revision C 2*, Gaussian Inc., Pittsburgh, **1995**.

REFERENCES
(Continued)

53. Scott, A. P.; Radom, L. *J. Phys. Chem.* **1996**, 100, 16502.

54. Montgomery, J. A.; Ochterski, J. W.; Petersson, G. A. *J. Chem. Phys.* **1994**, 101, 5900.

55. Ochterski, J. W.; Petersson, G. A.; Wiberg, K. B. *J. Am. Chem. Soc.* **1995**, 117, 11299.

56. Ochterski, J. W.; Petersson, G. A.; Montgomery, J. A. *J. Chem. Phys.* **1996**, 104, 2598.

57. Pitzer, K. S.; Gwinn, W. D. *J. Chem. Phys.* **1942**, 10, 428.

58. Atri, M. G.; Baldwin, R. R.; Evans, G. A.; Walker, R. W. *J. Chem. Soc. Faraday Trans.* **1978**, 74, 366.

59. Slagle, I. R.; Feng, Q.; Gutman, D. *J. Phys. Chem.* **1984**, 88, 3648.

60. Gutman, D. *J. Chem. Phys.* **1987**, 84, 409.

61. Kaiser, E. W.; Rimai, L.; Wallington, T. J. *J. Phys. Chem.* **1989**, 93, 4094.

62. Kaiser, E. W.; Wallington, T. J.; Andino, J. M. *Chem. Phys. Lett.* **1990**, 186, 309.

63. Kaiser, E. W.; Lorkovic, I. M.; Wallington, T. J. *J. Phys. Chem.* **1990**, 94, 3352.

64. Kaiser, E. W. *Int. J. Chem. Kinet.* **1992**, 24, 179.

65. Kaiser, E. W. *J. Phys. Chem.* **1993**, 97, 11681.

66. Kaiser, E. W. *J. Phys. Chem.* **1995**, 99, 771.

67. Brouard, M.; Lightfoot, P. D.; Pilling, M. J. *J. Phys. Chem.* **1986**, 90, 445.

68. Bozzelli, J. W.; Dean, A. M. *J. Phys. Chem.* **1990**, 94, 3313.

69. Wagner, A. F.; Slagle, I. R.; Sarzynski, D.; Gutman, D. *J. Phys. Chem.* **1990**, 94, 1858.

70. Baldwin, R. W.; Dean, C. E.; Walker, R. W. *J. Chem. Soc. Faraday Trans.* **1986**, 82, 1445.

REFERENCES
(Continued)

71. Gulati, S. K.; Mather S.; Walker, R. W. *J. Chem. Soc. Faraday Trans.* **1987**, 83, 2171.

72. Ignatyev, I. S.; Xie, Y.; Allen, W. D.; Schaefer, H. F. *J. Chem. Phys.* **1997**, 107, 141.

73. Baldwin, R. R.; Hisham, M. W.; Keen, A.; Walker, R. W. *J. Chem. Soc. Faraday Trans.* **1982**, 78, 1165.

74. Evans, G. A.; Walker, R. W. *J. Chem. Soc. Faraday Trans.* **1979**, 75, 1458.

75. Lenhardt, T. M.; McDade, C. E.; Bayes, K. D. *J. chem. Phys.* **1990**, 94, 8.

76. Slagle, I. R.; Ratajczak, E.; Gutman, D. *J. Phys. Chem.* **1986**, 90, 402.

77. Knyazev, V. D.; Dubinsky, I. A.; Slagle, I. R.; Gutman D. *J. Phys. Chem.* **1994**, 98, 5279

78. Ritter, E. R.; Bozzelli, J. W. *Int. J. Chem. Kinet.* **1991**, 23, 767.

79. Lay, T. H.; Krasnoperov, L. N.; Venanzi, C. A.; Bozzelli, J. W. *J. Phys. Chem.* **1996**, 100, 8240.

80. Lay, T. H.; Yamada, T.; Bozzelli, J. W. *J. Phys. Chem.* **1997**, 101, 13, 2471.

81. Lay, T. H.; Bozzelli, J. W. *Chem. Phys. Lett.* **1997**, 268,175.

82. Lay, T. H.; Bozzelli, J. W.; Dean, A. M.; Ritter, E. R. *J. Phys. Chem.* **1995**, 99, 14514.

83. Troe, J. *Gas-Phase Combustion Chemistry*; Gardiner W. C., Jr., Ed.; Springer-Verlag, NY, **1984**.

84. Knyazev, V. D. *J. Phys. Chem.* **1996**, 100, 5318.

85. Baldwin, R. R.; Pickering, I. A.; Walker, R. W. *J. Chem. Soc. Faraday Trans.* **1980**, 76, 2374.

86 Tsang, W. *Int. J. Chem. Kinet.* **1978**. 10. 821.

87. Tsang, W. *J. Phys. Chem. Ref. Data* **1990**, 19, 1.

REFERENCES
(Continued)

88. Lay, T. H.; Bozzelli, J. W. *J. Phys. Chem.* **1997**, 101, 9505.

89. Schwartz, M.; Marshall, P.; Berry, R. J.; Ehlers, C. J.; Petersson, G. A. *J. Phys. Chem.* **1998**, 102, 10074.

90 Gulati, S. K.; Mather, S.; Walker, R. W. *J. Chem. Soc. Faraday Trans.* **1987** 83, 2171.

91. Mallard, W. G.; Westley, F.; Herron, J. T.; Hampson, R. F. *NIST Chemical Kinetics Database, Version 6.0*, NIST Standard Reference Data, Gaithersburg, MD, **1994**.

92. Dean, A. M.; Bozzelli, J. W. In *Gas-Phase Combustion Chemistry II, Chapter 2 Combustion Chemistry of Nitrogen*, Gardiner W. C., Jr., Ed., Springer-Verlag, NY, **1999**.

93. Curtiss, L. A.; Raghavachari, K.; Redferm, P. C.;Pople, J. A., *J. Chem. Phys.* **1997**, 106, 1063.

94. Durant, J. L. *Chem. Phys. Lett.* **1996**, 256, 595.

95. Durant, J. L.; Rohlfing, C. M. *J. Chem. Phys.* **1993**, 98, 8031.

96. Malick, D. K.; Petersson, G. A. *J. Chem. Phys.* **1998**, 108, 5704.

97. Personal communication Fox, D., Gaussian Inc.

98. Personal communication Petersson, G. A., Wesleyan University, Middletown, Connecticut.

99. Jungkamp, T P. W.; Seinfeld, J. H. *J. Chem. Phys.* **1997**, 107, 1513.

100. Mebel, A. M.; Diau, E. W. G.; Lin, M. C.; Morokuma, K. *J. Am. Chem. Soc.* **1996**, 118, 9759.

101. Yamada, T.; Bozzelli, J. W. "Kinetic and Thermodynamic Analysis on Dimethyl-ether + O2 Reaction (Application of *ab initio* Calculation, CBS-q and G2)" *J. Phys. Chem*, in press.

102. Yamada, T.; Bozzelli, J. W. "Kinetic and Thermodynamic Analysis on OH Addition to Ethylene: Adduct Stabilization, Isomerization, and Isomer Dissociations" *J. Phys. Chem*, in press

REFERENCES
(Continued)

103. Wang, H.; Brezinsky, K. *J. Phys. Chem.* **1998**, 102, 1530.

104. Benassi, R.;Taddie, F. *J. Molecular Structure (Theochem)* **1994**, 3.3, 101.

105. Jonsson, M. *J. Phys. Chem.* **1996**, 100, 6814.

106. Bach, R. D.; Ayala, P. Y.; Schlegel, H. B. *J. Am. Chem. Soc.* **1996**, 118, 12758.

107. Raiti, M. J.; Sevilla, M. D. *J. Phys. Chem.* **1999**, 103, 1619.

108. Benassi, R.; Folli, U.; Sbardellati, S.; Taddei, F. *J. Comput. Chem.* **1993**, 4, 379.

109. Brezinsky, K.; Dryer, F. L. *Combust. Sci. and Tech.* **1986**, 45, 225.

110. Ingham, T.; Walker, R. W.; Woolford, R. E. *25th Symposium (Intern'l) on Combustion, The Combustion Inst.*, Pittsburgh, PA, **1994**, 783.

111. Bauge, J. C.; Battin-Leclerc, F.; Baronnet, F. *Int. J. Chem. Kinet.* **1998**, 30, 629.

112. Personal communication Knyazev, V. D., The Catholic University of American, Washington, D.C.

113. Douhou, S.; Perrin, D.; Martin, R. *J. Chim. Phys.* **1994**, 91, 1597.

114. Tsang, W. *J. Phys. Chem. Ref. Data* **1991**, 20, 221.

115. Jenkin, M. E.; Murrells, T. P.; Shalliker, S. J.; Hayman, G. D. *J. Chem. Soc. Faraday Trans.* **1993**, 89, 433.

116. Slagle, I. R.; Park, J. Y.; Heaven, M. C.; Gutman, D. *J. Am. Chem. Soc.* **1984**, 106, 4356.

117. Ruiz, R. P.; Bayes, K. D.; Macpherson, M. T.; Pilling, M. J. *J. Phys. Chem.* **1981**, 85, 1622.

118. Mallard, W. G.; Westley, F.; Herron, J. T.; Hampson, R. F.; Frizzell, D. H. *NIST Chemical Kinetics Database, Version 2Q98*, NIST Standard Reference Data, Gaithersburg, MD, **1998**.

119. Chen, C. J.; Bozzelli, J. W. *J. Phys. Chem.* **1999**, 103, 9731.

REFERENCES
(Continued)

120. Chen, C. J.; Bozzelli, J. W. "Reaction Pathways and Kinetic Analysis on Methyl *tert*-Butyl Ether Pyrolysis and Oxidation Reactions", *Chemical and Physical Processes in Combustion*, Proceedings of Eastern Section Combustion Institute Fall Technical Meeting, 2, pp. 37-40, North Carolina State University, Raleigh, NC, October 10-13, **1999**.

121. Baldwin R. R.; Stout, D. R.; Walker, R. W. *J. Chem. Soc. Faraday Trans.* **1991**, 87, 2147.

122. Stothard, N. D.; Walker, R. W. *J. Chem. Soc. Faraday Trans.* **1990**, 86, 2115.

123. Gulati, S. K.; Mather S.; Walker, R. W. *J. Chem. Soc. Faraday Trans.* **1987**, 83, 2171.

124. Baldwin R. R.; Dean, C. E.; Walker, R. W. *J. Chem. Soc. Faraday Trans.* **1986**, 82, 1445.

125. Baldwin R. R.; Stothard, N. D.; Walker, R. W. *J. Chem. Soc. Faraday Trans.* **1984**, 80, 3481.

126. Lay, T. H.; Krasnoperov, L. N.; Venanzi, C. A.; Bozzelli, J. W. *J. Phys. Chem.* **1996**, 100, 8240.

127. McQuarrie, D. A. *Statistical Mechanics*, Haper & Row. NY. **1976**.

128. Benson, S. W.; Buss, J. H. *J. Chem. Phys.* **1958**, 29, 546.

129. Hehre, W. J.; Radom, L.; Schleyer. P. v.R.; Pople, J. A. *AB Initio Molecular Orbital Theory*, John Wiley & Sons, NY **1986**

130. Marshall, P. *J. Phys. Chem.* **1999**, 103, 4560.

131. Ho, W.; Yu, Q. R.; Bozzelli, J. W. C*ombust. Sci. and Tech.* **1992**, 85, 23.

132. Westbrook, C. K. *19th Symposium (Intern'l) on Combustion, The Combustion Inst.*, Pittsburgh, PA, **1982**, 382.

133. Karra, D.; Senkan, S. M. C*ombust. Sci. and Tech.* **1987**, 54, 333.

134. Chang, W. D.; Karra, S. D.; Senkan, S. M. C*ombust. Sci. and Tech.* **1986**, 49, 107.

REFERENCES
(Continued)

135. Dewar, M. J. S.; Thiel, W. *J. Am. Chem. Soc.* **1977**, 99, 4899.

136. Zhu, L., Bozzelli, J. W., Lay, T. H. "Comparison of AM1, PM3 in MOPAC6 with Literature for the Thermodynamic Parameters of C_1, C_2 Chlorocarbons" (to be submitted)

137. Benson, S. W. *Thermodynamic Kinetics,* 2nd Ed., Wiley-Interscience, NY, **1976**.

138. Cohen, N. A. *J. Phys. Chem.* **1992**, 96, 9052.

139. Reid, R. C.; Prausnitz, J. M.; Sherwood, T. K. *The Properties of Gases and Liquids*, 3rd Ed., McGraw Hill, NY, **1979**.

140. Cohen, N. *J. Phys. Chem. Ref. Data* **1996**, 25, 6, 1411.

141. Cohen, N.; Benson, S. W. *Chem. Rev.* **1993**, 93, 2419.

142. Wu, Y. G.; Patel, S. N.; Ritter, E. R. *Thermochimica Acta.* **1993**, 222, 2, 153.

143. Wong, D. K.; Kretkowki, D. A.; Bozzelli, J.W., *Industrial & Engineering Chemistry Research* **1993**, 32, 3184.

144. Rodgers, A. S. Selected Values for Properties of Chemical Compounds; Thermodynamic Research Center(TRC), Texas A&M University: College Station, TX **1982**.

145. Pedley, J. B.; Naylor, R. O.; Kirby, S. P. *Thermodynamic Data of Organic Compounds*, Chapman and Hall, NY, **1986**.

146. Stull, D. R.; Westrum, E. F.; Sinke, G. C. *The Chemical Thermodynamics of Organic Compounds,* Robert E. Krieger Publishing, Malibar, FL, **1987**.

147. Atkinson, R.; Baulch, D. L.; Cox, R. A.; Hampson, R. F., Jr.; Kerr, J. A.; Troe, J. *J. Phys. Chem. Ref. Data* **1989**, 18, 881.

148. Baulch, D. L.; Cobos, C. J.; Cox, R. A.; Esser, C.; Frank, P.; Just, Th.; Kerr, J. A.; Pilling, J.; Troe, J.; Walker, R. W.; Warnatz, J. *J. Phys. Chem. Ref. Data* **1992**, 21, 411.

150. Atkinson, R.; Baulch, D. L.; Cox, R. A.; Hampson, R. F., Jr.; Kerr, J. A.; Troe, J. *J. Phys. Chem. Ref. Data* **1992**, 21, 1125.

REFERENCES
(Continued)

149. Tsang, W.; Hampson, R. F. *J. Phys. Chem. Ref. Data* **1986**, 15, 1087.

151. Chase, M. W. Jr., *NIST-JANAF Themochemical Tables, Fourth Edition*, *J. Phys. Chem. Ref. Data* **1998**, Monograph 9, 1.

152. Baulch, D. L.; Cobos, C. J.; Cox, R. A.; Frank, P.; Hayman, G.; Just, Th.; Kerr, J. A.; Murrells, T.; Pilling, M. J.; Troe, J.; Walker, R. W.; Warnatz, J. *J. Phys. Chem. Ref. Data* **1994**, 23, 847.

153. Lightfoot, P. D.; Roussel, P.; Caralp, F.; Lesclaux, R. *J. Chem. Soc. Faraday Trans.* **1991**, 87, 3213.

154. Kirk, A. D.; Knox, J. H. *J. Chem. Soc. Faraday Trans.* **1960**, 56, 1296.

155. Sahetchian, K. A.; Rigny, R.; Tardieu de Maleissye, J.; Batt, L.; Anwar Khan, M.; Mathews, S. *Symp. Int. Combust. Proc.* **1992**, 24, 637.

156. Mulder, P.; Louw, R. *Recl. Trav. Chim. Pays-Bas* **1984**, 103, 148.